



Past Present *Future*



# GEOMÜNSTER 2019

22–25 September 2019 | Münster | Germany

## Book of Abstracts



Supported by



# Content

<b>Plenary Lectures</b> .....	<b>21</b>
Building Earth's highest topography: lessons learned from the Indo-Asia mega-orogeny.....	21
Fluids in the Lower Crust: Deep is Different.....	21
50 Years Since Apollo: The Earth in the Context of Solar System Exploration.....	22
Und dann verschwand ein Ozean – wie die geologische Geschichte der Erde unsere Zivilisation ermöglicht.....	23
<b>1) Understanding Early Earth processes using novel geochemical approaches and methods</b> .....	<b>24</b>
<b>1a) The Present is the Key to the Past – Reconstructing Early Earth Environments through Modern Analogues</b> .....	<b>24</b>
Stable isotope biosignatures: from modern analogue to ancient ecosystem.....	24
The influence of microbial sulfate reduction on the sulfur isotopic composition of CAS in modern Mg-rich carbonates from Lagoa Vermelha and Brejo do Espinho, Brazil .....	25
The stable W isotope composition of Fe/Mn-rich sediments from the Baltic Sea.....	25
Applicability of the Ge/Si ratio in BIFs as a source proxy for silica in the Early Earth's ocean – insights from modern marine ferromanganese oxyhydroxides .....	26
Insights on the Archean environment from the oldest sediments on Earth .....	26
Mon: 1: Surviving the ferruginous Archean ocean – Assessing the potential toxicity of Fe <sub>2</sub> + on basal Cyanobacteria in anaerobic conditions.....	27
Mon: 2: Triple oxygen isotope study of manganese formations as a proxy for the triple oxygen isotope composition of Precambrian air O <sub>2</sub> .....	28
<b>1b) Early Earth Processes: Constraints from the Rock Record</b> .....	<b>29</b>
Archean lithospheric change and the start of modern-style plate tectonics .....	29
A new Titanium excess phase saturation thermometer for silicate melts with implications for conditions of Archean crust formation .....	30
In-situ identification of Archean high Th and U zircons in Jack Hills metasediment .....	30
Constraints on Earth's Paleoproterozoic crustal evolution by bulk Lu-Hf isotope analysis of single zircon grains .....	31
Formation of charnockitic silicic rocks in the Archean: a case study from Coorg, S. India.....	32
182W isotope patterns in mantle derived and crustal rocks from the Pilbara Craton, NW Australia .....	32
Hafnium and Nd isotope constraints on Archean mantle-depletion processes from the Pilbara Craton, NW Australia .....	33
PGE and Re-Os isotope systematics of 3.46 Ga meta-komatites from the Dwalile Greenstone Remnant, Swaziland.....	34
Inferences on crustal growth and mantle heterogeneity from open system models of the Earth .....	34
<b>2) Structure and evolution of planetary bodies</b> .....	<b>35</b>
<b>2a) Petrology, volcanism and surface processes on terrestrial bodies</b> .....	<b>35</b>
Building the volcanic crust of Mercury .....	35
Infrared Spectroscopy of Synthetic Planetary Analogs for Mercury for the BepiColombo Mission.....	36
A shock recovery experiment: Tracing Spectral Fingerprints of Impact Melt, npFe and Element Migration in Shocked Porous Materials .....	36
Present-day Activity of Slope Streaks on Mars.....	37
A volcanic ash layer in the Miocene Nördlinger Ries impact structure (Germany): Indication of crater fill geometry and long-term crater floor sagging.....	38

Isotopic and Trace Element Geochemistry of Karliova-Varto volcanism (Eastern Turkey): Deciphering the mantle source, crustal contributions and its tectonic controls .....	38
Prebiotic synthesis in volcanic discharges: exposing porous ash to volcanic gas atmospheres .....	39
Mon: 3: Formation of sulfide phases on the surface of Mercury by reactions with reducing high temperature gases .....	40
Mon: 4: Excimer Laser Experiments on Mixed Silicates Simulating Space Weathering .....	40
Mon: 5: Mineralogy of the weigelt-scholle .....	41
<b>2b) High-spatial resolution studies of small-scale and complex extraterrestrial and terrestrial samples .....</b>	<b>42</b>
Finding a piece of Earth on the Moon? .....	42
High-resolution Mg-isotope investigation of presolar silicates: New implications for the stardust inventory of the Solar System .....	43
Graphite in Meteorites – Occurrence, Abundance and Origin.....	43
Xenolithic C1 Clasts and their Relation to the Host Rocks Revealed by Chromium Isotopes and Trace Element Concentrations .....	44
Dynamic Deformation of Meteoritic Iron in a Diamond Anvil Cell: In-situ Observation of the $\epsilon$ -Iron Phase Transition and the Formation of Shock Defects.....	45
Shock History of the Metal-rich CB Chondrite Quebrada Chimborazo (QC) 001 .....	45
The incomplete amorphization of natural and experimentally shocked plagioclase investigated by optical and electron microscopy, and various spectroscopic techniques .....	46
Exploring radiation damage on near-Earth asteroid 25143 Itokawa by TEM.....	47
Nanoscale compositional segregation and structure in complex In-bearing sulfides: Results from transmission kikuchi diffraction and atom probe tomography .....	48
Halogen analysis of sulphide minerals at the ultratrace level – first applications of the Dresden Super-SIMS.....	48
Mon: 6: Modal abundances of coarse-grained (>5 $\mu\text{m}$ ) components within CI-chondrites and their individual clasts .....	49
Mon: 7: Sorted stone circles on Svalbard – An analog study for Mars.....	49
Mon: 8: The Multi-Temporal Database of Planetary Image Data (MUTED): A Web-Based Tool to Study Surface Changes and Processes on Dynamic Mars .....	50
Mon: 9: Classification of 13 CM Chondrite Breccias .....	50
Mon: 10: A Chondrule Formation Experiment Aboard the ISS: Experimental Set-up and Test Experiments .....	51
<b>2c) Planetary Accretion and Impact Processes .....</b>	<b>52</b>
The triple oxygen isotope composition of lunar rocks .....	52
An outer solar system origin of the Moon-forming impactor .....	53
Mechanics and conditions for devolatilising the Moon .....	53
Modeling partitioning of SVEs during Earth’s core formation.....	54
Chalcophile Element Accretion from the Late Veneer .....	54
Tellurium stable isotopic constraints on the nature of late accretion.....	55
Tue: 1 : A History of Outhouse Rock.....	56
<b>2e) Recent advances in lunar science .....</b>	<b>57</b>
Dating Lunar Surface Features With Crater Size-Frequency Distribution Measurements: A Review ....	57
Ages of the geological events around the Apollo 17 landing site .....	58

Complex Copernican Geology at the Apollo 17 Landing Site .....	58
The light plains of the lunar northern hemisphere .....	59
Lunar Basaltic Volcanic Eruptions:	
New Discoveries and Insights from Modeling and Observations.....	59
Experimental simulation of Apollo 16 “rusty rock” alteration by a fumarolic metal bearing gas .....	60
Origin of Granular Zircon in Lunar Impactites .....	61
Mon: 11: Exploration of Icelandic lava caves and extrapolation to a semi-permanent Lunar habitat.....	62
Mon: 12: The ESA-JAXA-CSA-NASA Joint Study HERACLES on Returning to the Moon.....	62
Mon: 13: Geology and ages of the landing sites: Apollo 11, Apollo 12 and Apollo 17 .....	63
Mon: 14: Mare Moscoviense: A site for future lunar missions .....	64
Mon: 15: Lunar gravity: Impact processes inform the density structure of the mare crust .....	64
Mon: 16: Geological Mapping of the South Pole-Aitken Basin - A Progress Report .....	65
<b>3) Orogenesis .....</b>	<b>66</b>
<b>3b) Tectono-Metamorphic Evolution of the Cyclades, Greece.....</b>	<b>66</b>
Tectonic and geodynamic evolution of the Aegean region, from mantle dynamics to crustal evolution. ....	66
Dating white micas in the blueschist-greenschist domain: pointless or worthwhile? .....	67
Extracting metamorphic time scales using fluid inclusions.....	67
Sr and Ar diffusion systematics in polygenetic white micas from Naxos.....	68
Metasomatic sulfur-driven redox reactions: A case study of Syros, Greece .....	69
Fabric-forming amphiboles in the Cycladic Blueschists and their tectonic implications.....	69
The age, origin and emplacement of the Tsiknias Ophiolite, Tinos, Greece .....	70
Tue 2: Exhumation patterns in a bivergent metamorphic core complex:	
The central Menderes Massif (western Turkey).....	71
Tue 3: The evolution of Vari Detachment (Syros, Cyclades).....	71
<b>3c) Assembly of Pangea: What do we know about the Variscan orogen and its Avalonian-Cadomian precursors? .....</b>	<b>72</b>
How did Pangea behave? Rethinking some tectonic processes in a superplate world.....	72
From a bipartite Gondwanan shelf to an arcuate Variscan belt: The early Paleozoic evolution of northern Peri-Gondwana .....	73
Beyond the Bohemian Massif: search for Cadomian and Variscan correlatives in the Balkans .....	73
Petrochronology by EPMA and automated SEM in the Saxothuringian high pressure nappes of the central and western Erzgebirge .....	74
U-Pb LA-ICP MS Zircon Ages of Devonian felsic volcanic Rocks in the Rheinsh Massif (North Rhine-Westphalia) .....	75
New U-Pb ages of detrital zircon from the central Variscan orogen and its Avalonian-Cadomian precursors .....	76
Tue: 4: New insights into the Sierra de Juárez Mylonitic Complex, southern Mexico: constraints on its pre-Mesozoic history and regional implications.....	76
Tue: 5: Longlived pulsed magmatic intrusions along the Northern Gondwana margin revealed by Ordovician to Early Permian LA U-Pb geochronology of Central Pyrenean gneiss domes .....	77
Tue: 6: U–Pb zircon dating of Paleozoic volcanic rocks from the Rheno-Hercynian Zone: new age constraints for the Steinkopf formation, Lahn-Dill area, Germany .....	78

<b>4) Continents, oceans and global change .....</b>	<b>79</b>
<b>4a) Limnogeology and paleolimnology including lagoon systems .....</b>	<b>79</b>
Heterocyst glycolipids: Novel tools for reconstructing continental climate change using lacustrine deposits .....	79
The Early Eocene of Schöningen - Testing effects of climate variations on coastal wetlands under greenhouse conditions .....	80
Terrestrial archives from the Eocene greenhouse of Central Europe: Palynological studies of lacustrine sediments on the Spendlinger Horst (Southwest Germany) .....	80
Assessing the Late Quaternary climatic and environmental history of the Russian Arctic – keys results of the Russian-German PLOT (Paleolimnological Transect) project.....	81
The Holocene lacustrine record of the Layla Lakes (central Saudi Arabia): The use of phytolith analysis for the reconstruction of paleoenvironment and paleoclimate .....	82
A 8.5 kyr high-resolution multi-proxy paleoclimate record from lake Voëlvlei, Southern Cape, South Africa.....	82
Heavy metals in surface sediments of Richards Bay Harbour: anthropogenic impact on the former Mhlatuze estuary, South Africa .....	83
Geometals in sediment from Densu estuary, Ghana: potential proxy's for reconstructions .....	84
Tue: 7: Ostracod fauna associated with <i>Cyprideis torosa</i> – a tool to differentiate brackish environments.....	84
Tue: 8: The Middle Eocene maar lake “Groß Zimmern” (Hesse, Southwest Germany): Vegetation dynamics in a disturbed lacustrine record.....	85
<b>4d) Latest Achievements in Scientific Ocean and Continental Drilling.....</b>	<b>86</b>
The ICDP Oman Drilling Project: a status report .....	86
Geological Research through Integrated Neoproterozoic Drilling (GRIND): The Ediacaran-Cambrian Transition .....	86
Permeability estimation in sedimentary sequences: a comparison between inferences from wireline resistivity logs and computations from porosity distributions in CT scans of drillcore .....	87
CO <sub>2</sub> -induced natural deformation structures in well HJB-1 (Cheb Basin, Czech Republic).....	88
Temperate rain forests at 77°S palaeolatitude during the Late Cretaceous.....	89
Paleoclimate, Paleoenvironment, and Paleoecology of Neogene Central America: Bridging Continents and Oceans (NICA-BRIDGE) .....	88
Paleoenvironmental indications and cyclostratigraphic studies of sediments from tropical Lake Towuti obtained from downhole logging.....	90
Mon: 17: Feather feature orientations in shocked granitic rocks of the Chicxulub crater: Implications for the formation of peak rings.....	91
Mon: 18: Deep Lake Sediment Sampling on Lake Constance using Hipercorig.....	91
<b>4e/f) Archives of environmental changes throughout Earth history: bio- and authigenic mineralization to paleoenvironmental reconstruction.....</b>	<b>92</b>
The expression of global Oceanic Anoxic Events (OAE) in continental interiors: An example from the Early Jurassic Toarcian OAE.....	93
Carbonates with spherulites and cone-in-cone structures from the Precambrian of Arctic Norway, and their palaeoenvironmental significance.....	93
Coral geochemistry: a window into the biomineralisation process .....	94
Understanding the Interaction between Glaciers and Volcanoes through Glacier Cave Research. ....	94
The geosphere and the climate system: A new dimension of Earth system interaction.....	95

Preliminary data from short sediment drill cores beneath the Ekström Ice Shelf, Antarctica .....	96
Mon: 19: The distribution of rare earth elements and yttrium (REY) between the truly dissolved, nanoparticulate/colloidal and suspended loads during high and low discharge in the Kalix and Råne Rivers, Northern Sweden .....	96
Mon: 20: Calcification, skeletal structure and composition of the cold-water coral <i>Desmophyllum dianthus</i> . .....	97
Mon: 21: The relation between $\Delta^{17}O$ and bodymass for bioapatite .....	98
Mon: 22: Palynofacies as an indicator for transgressive-regressive trends in offshore marine mudstones – a critical evaluation .....	98
Mon: 23: Distribution patterns of some ‘rhenotypic’ faunal elements related to a sea-level rise during the Emsian/Eifelian transition in the eastern Rhenish Massif (Sauerland and Bergisches Land). .....	99
<b>4g) Advances in geochronology from modern to deep time .....</b>	<b>100</b>
High-resolution calibration of Earth system processes with precise and accurate U-Pb geochronology .....	100
Challenges for the accuracy of U-Th systematics in marine carbonate archives of extreme environments: identifying and overcoming limitations of early diagenesis.....	101
Advances in rutile petrochronology.....	101
Towards in-situ U-Pb dating of sulphates.....	102
In-situ U-Pb garnet dating. Strengths and weaknesses.....	103
Tue: 9: Radiation damage in zircon - A Raman multi-band approach .....	103
Tue: 10: Insights into Fe-duricrust evolution in French Guiana using (U-Th-Sm)/He dating of supergene iron oxides and oxyhydroxides.....	104
Tue: 11: U-Th-total Pb geochronology of uraninite and its secondary phases (Evje-Iveland Pegmatite Field, Norway) .....	104
Tue: 12: Aqueous alteration events in silicified wood from Escalante, Utah, USA.....	105
<b>5) Magmatic systems and experimental petrology .....</b>	<b>106</b>
<b>5a) Volatiles in the Earth’s Mantle – Elemental Budgets &amp; Cycles .....</b>	<b>106</b>
Identifying the mineralogy of a metasomatised mantle source by halogen partitioning experiments: A new approach .....	106
Initial CO <sub>2</sub> content in parental arc magmas estimated using micro-Raman spectroscopy and mass-balance calculations: a case study of Karymsky volcano (Kamchatka, Russia) .....	107
Dissolution of graphite in high-pressure aqueous fluids: the roles of crystallinity and of coexisting silicates and carbonates .....	107
Redox control on nitrogen isotope fractionation during planetary core formation.....	108
The role of C-O-H fluids on partial melting of eclogite and lherzolite under reducing conditions.....	109
Amorphous precursor phase observed at mantle conditions during hydration of clinoenstatite to 3.65 Å phase, MgSi(OH) <sub>6</sub> .....	109
Experimental evidence and implications of coupled silica and water loss from melt inclusions in olivine.....	110
Al, Fe and H incorporation in natural rutile.....	111
Electrical conductivity of forsterite aggregates containing H <sub>2</sub> O-NaCl fluids at 800 °C and 1 GPa: implications for the high electrical conductivity anomalies in subduction zones .....	111
Tue: 13: NMR analysis on fluorine defects in forsterite and wadsleyite .....	112

Tue: 14: A preliminary density model for carbonate-rich melts based on high pressure experimental data.....	113
<b>5b) Volcanic geology.....</b>	<b>114</b>
Integration of SAR and Seismic Interferometry imaging techniques to investigate volcanism at Campi Flegrei caldera.....	114
Lava dome growth monitoring at Nevado del Ruiz using high-resolution TerraSAR-X amplitude imagery .....	115
Mediterranean S1 Tephra as a Marker Horizon for the Fertile Crescent: Source Evidence and Characterization of the 9 ka Dikkartin Dome (Mt. Erciyes, Turkey) Eruption .....	115
Parameters controlling the cyclic activity of silicic volcanic systems: evidence from Milos (Greece). 116	116
Physical volcanology of Quaternary ignimbrites in the Aragats Volcanic Province (Lesser Caucasus): a lithofacies-based approach .....	116
Understanding the 1888 sector collapse of Ritter Island (Papua New Guinea) by integrating 3D seismic data and Discrete Element Models .....	117
Rejuvenated volcanism at a Cretaceous seamount off El Hierro (Canary Islands).....	117
Facies analysis, depositional style and geochemistry of Ediacaran volcano-sedimentary successions at the NE Edge of Saghro inlier (Eastern Anti-Atlas, Morocco) .....	118
Cambrian alkaline submarine to emergent volcanism near Ouinguigui (Ougnat inlier, eastern Anti-Atlas, Morocco).....	119
Volcanic evolution and petrology of a late- to post-Variscan volcanic system: The Carboniferous Altenberg-Teplice Caldera (Germany-Czech Republic) .....	120
The Lower Permian Rochlitz caldera: A supervolcano in Central Europe.....	120
A competition between magma mingling and mixing: The monotonous intermediates of the Late Paleozoic North Saxon Volcanic Complex in Central Germany.....	121
Timescales and processes within transcrustal magmatic systems.....	122
Mon: 24: Alkaline volcanism on Patmos (Aegean Sea) – constraints from new radiogenic isotope data and $^{40}\text{Ar}/^{39}\text{Ar}$ dating.....	122
Mon: 25: The Pliocene pyroclastic succession of Ani, Armenian-Turkish border: geochronology, geochemistry and paleomagnetic constraints.....	123
<b>5c) Intraplate volcanism, mantle plumes and continental breakup .....</b>	<b>124</b>
Did Gondwana breakup trigger the formation of a(nother) Large Igneous Province in the southwestern Indian Ocean? .....	124
What geology tells about the role of mantle plumes in Pangea dispersal.....	125
New constraints on the evolution of Mesozoic rifting in the Eastern Cordillera of Colombia .....	125
The evolution of intraplate volcanoes in extensional tectonic environments: constraints from João de Castro Seamount, Azores.....	126
Geochemical and isotopic characterization of single olivine-hosted melt inclusions .....	126
Formation of Megacryst Phases by Interaction of Aillikite Melts with Lithospheric Mantle– Evidence from HP-HT Experiments and Natural Samples from the Arkhangelsk Province, Russia.....	127
Experimental melting of mixed Iherzolite + kaersutite-rich metasome in the garnet stability field .....	128
Tue: 15: Demenitskoy Smt. (East Atlantic) and the importance of small, isolated intraplate seamounts in the ocean basins.....	128
Tue: 16: Double Age progressive hotspot tracks – Primary EM I-type and secondary HIMU mantle plumes in the South Atlantic.....	129
Tue: 17: Geochemical evolution of the Main Deccan Volcanic Province, NW-India .....	130

Tue: 18: Storage, Transport and Emplacement of Low-ti Dacites in the Southern Paraná-Etendeka LIP: Geochemical Characterization and Implications for Trans-Atlantic Correlations .....	130
<b>5d) The role of subduction zones on Earth’s dynamic evolution .....</b>	<b>131</b>
Mantle controls on the variability of chalcophile elements in subduction-related magmas .....	131
Deserpentinization is not the reverse of serpentinization: implications for redox budget transfer and the oxidation of arc-magma source zones.....	132
Tracing atmospheric oxygenation with selenium isotopes in mantle melts .....	132
Simulating mantle metasomatism by reacting carbonate-rich sediment with peridotite at forearc mantle P-T conditions .....	133
Preliminary experimental results on phase relations in the system $K_2O$ - $MgO$ - $Al_2O_3$ - $SiO_2$ - $H_2O$ at 7-12 GPa to understand phase relations after deep subduction of continental crust .....	134
Alternation of shoshonitic and calc-alkaline magmatism during subduction migration – a cross section through Aegean magmatism .....	134
Tue: 19: Molybdenum isotope systematics at convergent plate margins – the effect of deep sea pelagic sediments .....	135
Tue: 20: Variations in $Fe^{3+}/Fe^T$ ratios in igneous amphiboles as a function of oxygen fugacity in hydrous arc magmas .....	135
Tue: 21: Variably depleted mantle wedge sections beneath Tonga – insights from stable Zn isotope systematics in arc lavas.....	136
Tue: 23: Crustal recycling within the mantle: reaction experiments on the origin of ultrapotassic magma .....	137
<b>5e) Stable isotope fractionation at high temperatures .....</b>	<b>138</b>
Tue: 24: Chromium isotope fractionation during magma differentiation .....	138
Tue: 25: Sulfur isotope measurements of reference materials using MC-ICP-MS.....	138
Tue: 26: An experimental approach to determine Calcium isotope fractionation between minerals and melts.....	139
Tue: 28: Molybdenum isotope fractionation between melt, exsolved fluid and hydrothermal minerals at the magmatic-hydrothermal transition.....	140
Tue: 29: Lithium chemical and isotope diffusion in natural olivines and its implications on the timing of magmatic events.....	140
<b>5f) The distribution and influence of volatile elements in the Earth’s interior and their exchange with the surface.....</b>	<b>142</b>
Role of high pressure hydrous phase in lower mantle dynamics.....	142
Formation of diamond from methane-rich fluids .....	143
Formation of diamonds from reduced COH fluids and their genetic link to pyroxenite/eclogite in the Earth’s upper mantle .....	143
Understanding the redox conditions during diamond anvil cells experiments.....	144
The oxygen fugacity of sublithospheric diamond formation and the conditions encountered during their ascent to the surface.....	145
Mantle thermometry using sulphide inclusions in diamonds.....	145
Water partitioning between upper mantle minerals and melts .....	146
Tue: 30: The effect of F on the stability of antigorite and the transfer of halogens in the deep mantle.....	147
Tue: 31: The role of oxygen fugacity on the stability of serpentinites in subduction zones.....	147
Tue: 32: Pargasite stability in the upper mantle at $H_2O$ -undersaturated conditions.....	148

Tue: 33: Tracing redox evolution of arc magmas during amphibole fractionation in the deep crust: Constraints from cumulate xenoliths from Ichinomegata Maar, NE Japan .....	148
Tue: 34: Trace element partitioning between Cl- and S-bearing aqueous fluid and basaltic melt.....	149
<b>5g) Reconstructing the evolution (P-T-t-X) of magmatic processes.....</b>	<b>150</b>
On the formation of oceanic layered gabbros: drillcore GT1 of the ICDP Oman Drilling Project.....	150
Tracing heterogeneous intercumulus processes by rutile: examples from the Bushveld Complex ....	151
Soufflé collapse: Vesicle shrinkage in hydrous silicate melts during quench .....	151
Advances in high-temperature rheometry methods: a silicate melt case study.....	152
Rheological and Thermal Evolution of Magmatic Systems: Insights into the Volcanic Past on Earth and other Planets and Moons in our Solar System.....	153
<b>5h) Processes and timescales in the evolution of transcrustal magma systems: from field and geochemical observations, through experiments to modelling.....</b>	<b>154</b>
Ignimbrites and silicic magmatism in the Central Andes: Sources, timing and processes of magma generation .....	154
Towards 3D geodynamic modelling of the Altiplano-Puna magma system .....	155
Deep crust hot zone: the control of depth on magmatic differentiation .....	155
Evolution of transcrustal magmatic systems investigated by petrological-geodynamical models.....	155
First steps in linking melt-matrix-two-phase flow with fast melt transport via dykes in a continental crust scenario.....	156
Evolution of magmatic systems at different temporal and spatial scales – what did we learn from zircon U/Pb dating?.....	157
Quantitative magma plumbing studies: Accessing the dynamic evolution of transcrustal magmatic systems in space and time.....	158
Constraining pre-eruptive history by diffusion chronometry: Laacher See (Germany) and Taapaca volcano (Chile).....	159
Timescales of magmatic processes during the eruptive cycle 2014-2015 at Piton de la Fournaise, La Réunion, obtained by Mg-Fe diffusion modelling in olivine .....	159
Halogen diffusion in dry rhyodacitic melt .....	160
Antecrysts – angels or devils in <sup>40</sup> Ar/ <sup>39</sup> Ar geochronology? Examples from Cape Verde seamounts....	161
Millennial to decadal magma evolution in an arc volcano from zircon and tephra of the 2016 Santiaguito eruption (Guatemala) .....	161
Mon: 26: Geodynamic constraints on the initiation of mélange diapirs from subducting slabs.....	162
Mon: 27: Times of magma ascent and residence reflected in Mg/Fe and Ni diffusion in olivine from arc lavas in Kamchatka.....	162
Mon: 28: Variations of Fo and Ni in the centres of olivine cores reflect processes of crystallization and diffusion .....	163
Mon: 29: Divergent compositional domains in the shallow plume mantle beneath the West Eifel volcanic field, W Germany.....	164
Mon: 30: U/Th disequilibrium dating of Late Quaternary perovskite .....	165
<b>6) Metamorphic systems .....</b>	<b>166</b>
<b>6a) Metamorphic processes.....</b>	<b>166</b>
Early Paleozoic blueschists from the Scandinavian and Svalbard Caledonides – what can they tell us? .....	166
Evolution of a suture zone (Baie Verte Line; W Newfoundland, Canada) during a “hard” continent-arc collision: evidence from conditions and timing of metamorphism .....	167

Subduction Initiation & metamorphosis sole formation from the Lycian ophiolites, SW Turkey: Evidence for timing of plate boundary magmatism and metamorphism .....	168
Low pressure-high temperature metamorphism and migmatization in the Proterozoic Epupa Complex, NW Namibia .....	168
Reconstitution of mineral compositions reflecting peak-metamorphic conditions: Ti-in-quartz thermobarometry applied to ultrahigh-temperature granulites .....	169
Grain and phase boundaries in rocks of the upper crust and at the earth's surface .....	170
Tue: 36: A Barrovian-type overprint of high pressure rocks: PTT-evolution in the Ordovician Corner Brook Complex (W-Newfoundland, Canada) .....	171
Tue: 37: Investigation of U-Pb ages from the Bantimala Complex, SW Sulawesi, Indonesia: Protolith ages and an unusual zircon population.....	171
Tue: 38: Structural and petrographic description of an ultramafic complex in the north of the Fjällfjäll-window (North Sweden).....	172
Tue: 39: Contradictory in-situ U-Pb ages from major and accessory metamorphic phases.....	173
Tue: 40: Petrological and Lu-Hf age constraints for eclogitic rocks from the Pam Peninsula, New Caledonia .....	173
<b>6b) Reaction and deformation .....</b>	<b>174</b>
Deformation facilitated by transformative processes: mineral reactions and diffusion creep in the mafic system .....	174
Growth related defect microstructures in replacement reactions.....	175
Wall-rock damage and alteration in orthogneisses from Lofoten as revealed by CL imaging, EBSD, and TEM analyses .....	176
Quantifying non-hydrostatic, reaction-induced stresses during metamorphic hydration reactions...	176
Magnetic signatures of rock deformation.....	177
Variations of magnetic Verwey transition: New insights through magnetic susceptibility of magnetite-rich rocks deformed under laboratory seismic-related fatigue loadings.....	177
Chemical effects in stressed systems: think global, act local .....	178
Metamorphic Pressures from Elastic Geobarometry: A novel formalism with application to the Rhodope Metamorphic Province, Greece.....	179
What's Next? Exploring the future of metamorphic geology .....	180
Chemically induced recrystallization: Implications for grain recycling and diffusion chronometry ....	180
Mon: 31: The role of chemically induced stresses in the mechanisms of element exchange between minerals – an experimental study based on pyroxenes .....	181
Mon: 33: Episodic deformation and metamorphic reactions at decreasing distances to the tip of a seismic active fault zone – the record of mylonites from the DAV, Eastern Alps .....	182
<b>6c) Fluid-rock interaction: from mechanisms to rates – from atoms to plates.....</b>	<b>182</b>
Dissolution rate variability of the four different etch pit steps of the 104 calcite crystal face.....	183
Mesoscale Calcite Dissolution Modelling – Parametrization and Data Analysis .....	184
Experimental Constraints on Hydrothermal Indium Transport .....	184
Extreme W enrichment in highly serpentinised abyssal peridotites from IODP Leg 209.....	185
The influence of a nanophase on mineral equilibration in the system $Al_2O_3-SiO_2-H_2O$ .....	186
Coupling 2D numerical modelling of microscale dehydration to fully quantitative automated mineralogy mapping .....	186
Mon: 34: Chemical controls of the aqueous environment on mineral growth and dissolution. ....	187

Mon: 35: Tectonometamorphic and hydraulic processes along a fossil subduction plate interface in the northern Mirdita Ophiolites (Bajram Curri, Albania) .....	187
Mon: 36: Sulfide mineralogy as a tracer for fluid-rock interaction in serpentinites .....	188
Mon: 37: Solubility of forsterite, enstatite and magnesite in redox-buffered high-pressure COH fluids .....	189
<b>7) Earth Surface Processes and Basin Analysis.....</b>	<b>190</b>
<b>7a) Quaternary Geochronology .....</b>	<b>190</b>
OSL and ESR thermochronometry of the Japanese Alps.....	190
Reconstructing production, mixing and erosion of soils using single-grain OSL methods .....	191
Mass movements: can they be dated using luminescence from rock surfaces? .....	191
Direct dating of faulting in the absence of overlying sediments.....	192
The cosmogenic $^{10}\text{Be}$ (meteoric)/ $^9\text{Be}$ ratio as a tracer of weathering and erosion in lithologies with and without quartz .....	193
Geomagnetic field reconstructions as late Quaternary dating tools.....	193
Dynamics and evolution of carbonate landscapes inferred from cosmogenic nuclides .....	194
Reconstruction of the Landscape Evolution of South Central Africa: A Case Study on Waterfalls of Northern Zambia and South-Eastern D.R. Congo.....	194
Can cosmogenic nuclide exposure dating help to solve the existing controversy about the evolution of hyperaridity in the Atacama Desert?.....	195
Using TCN to decipher a steep erosional gradient in the hyperarid core of northern Chile over multiple time scales .....	196
Mon: 38: A constant slip rate for the western Qilian Shan frontal thrust during the last 200 ka consistent with GPS-derived and geological shortening rates .....	196
Mon: 39: Spatial patterns of erosion and landscape evolution in a bivergent metamorphic core complex revealed by cosmogenic $^{10}\text{Be}$ : The central Menderes Massif (Western Turkey) .....	197
Mon: 40: A global geomagnetic field reconstruction of the past 100 ka .....	197
Mon: 41: An engineering geomorphologic characterization of the Kaju River near Qasr-e-qand city	198
Mon: 42: Glacial evolution using $^{36}\text{Cl}$ moraine dating in the Krnica Valley, Julian Alps, Slovenia .....	198
Mon: 43: The evolution of low relief landscapes in the Eastern Alps constrained by a multi-system approach .....	199
Mon: 44: Quantifying river incision into low-relief surfaces using local and catchment-wide $^{10}\text{Be}$ denudation rates.....	200
<b>7b) Sediment generation and quantitative provenance analysis .....</b>	<b>200</b>
Studies on the Marinoan tillite of the Port Nolloth Zone in southern Namibia: zircon analyses on matrix and pebbles and their significance for provenance studies of glacial deposits .....	201
The evolution of the southern Namibian Karoo aged basins – Implications from detrital zircon data.....	201
OH defects in quartz as monitor for igneous, metamorphic, and sedimentary processes .....	202
OH defects in quartz as a provenance tool: Application to fluvial and deep marine sediments from SW Japan .....	202
Dispersed occurrence of mafic and felsic ultrahigh-pressure rocks in the central Saxonian Erzgebirge (Germany) revealed by diamond and coesite inclusions in detrital garnet.....	203
Pangea and the Lower Mantle.....	204
Relative importance of palaeogeography versus solid Earth degassing rate in the Phanerozoic climatic evolution .....	204

Meanders Displacement Due to Implementation of Organizing Plans in the Bahokalal River, South East of Iran .....	205
Provenance analysis of carbonate and radiolarite pebbles of Jurassic sedimentary mélanges in the Circum Pannonian orogens (Western Tethys) .....	206
Provenance of central Arctic Ocean ice-rafted debris: the first U-Pb zircon ages for Lomonosov Ridge during the late Quaternary .....	206
Provenance, facies, geochronology and tectonic evolution of continental extensional basins: a case study of the Permotriassic Mitu Group (Central Andes, Peru) .....	207
The missing link of Rodinia break up in western South America: A zircon U-Pb and Hf isotope study of the volcanosedimentary Chilla beds (Altiplano, Bolivia) .....	208
Tue: 41: Late Palaeozoic and Early Mesozoic evolution of the Palaeotethys: new insights from sandstone provenance (Karaburun Peninsula and Konya Complex, Turkey) .....	208
Tue: 42: Crustal growth history of the Iberian Peninsula constrained by detrital zircon in modern rivers .....	209
Tue: 43: OH defects in detrital quartz: a proxy for reconstructing the tectonic environment of sedimentary deposits? .....	210
Tue: 44: Preliminary study on stratigraphy, facies analysis and petrography of Neoproterozoic meta-sediments, magmatic bodies and volcanoclastic deposits in Skoura inlier (Central High Atlas, Morocco). .....	210
Tue: 45: Mineralogy, geochemistry and U-Pb zircon ages of diverse Tonian orthogneisses of the Pearya Terrane, northern Ellesmere Island, Canada .....	211
Tue: 46: Genesis and petrography of the “Mammendorfer Sandstone” .....	212
Tue: 47: The ‘life cycle’ of coesite-bearing garnet: From inclusion entrapment over exhumation, surface weathering, erosion and sedimentary transport, to its deposition .....	212
Tue: 48: Paleozoic accretionary orogens along the Western Gondwana margin .....	213
Tue: 49: High-n sample comparison of detrital age spectra from pre-orogenic units of the Variscan-Appalachian belt .....	214
Tue: 50: Trace element inventory of detrital garnet: a case study from the Central Alps .....	214
<b>7c) Rock and fluid dynamics in deep sedimentary systems .....</b>	<b>215</b>
Geochemical and petrographical analysis of the Mesozoic Birkhead and Murta source rock formations, Eromanga Basin, Central Australia .....	215
Bound gas in near-surface sediment from the Barents Sea and North East Greenland Shelf .....	216
Kinetic modeling of Westphalian coals:	
Insights from artificial heating experiments on a maturity sequence .....	217
Thermal effects of magmatism on surrounding sediments and petroleum systems in the northern offshore Taranaki Basin, New Zealand: a numerical basin modelling study .....	217
3D basin and petroleum system modelling in the North Sea Central Graben:	
a cross-border Dutch, German and Danish pilot study .....	218
Petroleum Systems Modeling in the Northwestern Part of the Persian Gulf, Iranian sector:	
3D Basin Modeling .....	218
Reservoir quality controls in deeply buried Rotliegend sandstones and their outcrop analogs .....	219
Tue: 51: Reservoir quality controls in deeply buried Rotliegend sandstones and their outcrop analogs .....	220
Tue: 52: Carnian outer continental shelf successions in the Western Tethys realm .....	221
<b>7d) The stable isotope toolbox in sedimentary systems: From water-rock-biosphere interactions to (palaeo-) environmental reconstructions .....</b>	<b>222</b>

Early microbial impact on carbonate diagenesis in lagoon sediments on Aldabra, Western Indian Ocean.....	222
Impact of ambient conditions on the Si isotope fractionation in marine pore fluids during early diagenesis .....	223
Alexander von Humboldt, Paleoaltimetry and Geobiodiversity.....	224
Radiogenic and stable Strontium isotopic fingerprints of ecosystem nutrition. ....	224
High-precision triple oxygen isotopes of Archean carbonates.....	225
Characterization and differentiation of two different marbles as possible reservoir rocks in geothermal systems by stable isotope investigations – An example from Western Anatolia, Turkey.....	226
Hydrochemistry and isotope hydrology of thermal springs in the Alps.....	226
Mon: 45: Biological and lithological controls on Mg isotope fractionation in a forested watershed (the Black Forest, Germany).....	227
Mon: 46: Reconstruction of multimillennial changes in Eastern Tropical Pacific oxygen-minimum zones.....	228
Mon: 47: Boron isotopes by femtosecond LA-ICP-MS with application to pH reconstruction in biogenic carbonates. ....	228
Mon: 48: Sediments of the supposed Ries impact ejecta-dammed “Rezat-Altmühl-Lake” (Miocene, Southern Germany) .....	229
<b>8) Applied and Environmental Geosciences .....</b>	<b>230</b>
<b>8a) Geological and hydrogeological characterisation of reservoir rocks.....</b>	<b>230</b>
Coal as a Natural Archive: New Implications from the Miocene Lignites of the Lower Rhine Basin.....	230
Deep Geothermal Energy Potential at Weisweiler, Germany: 3D-Modelling of Subsurface Mid-Palaeozoic Carbonate Reservoirs.....	231
Geothermal potential of Dinantian carbonates in the subsurface of North Rhine-Westphalia, Germany .....	232
Thermo-Hydraulic Heterogeneity Assessment Across First-Order Hiatal Surfaces – A Case Study from the Post-Variscan Nonconformity. ....	232
Towards a better understanding of the central German Buntsandstein aquifer system: Combined study of petrological, facial and petrophysical observations .....	233
Log derived permeability estimation of Valanginian (Lower Cretaceous) sandstone units of the Lower Saxony Basin.....	234
Thickness distribution and sequence stratigraphy of the late Jurassic Malm reservoir in Bavaria: implications for geothermal exploration.....	234
Tue: 54: Buntsandstein (Lower Triassic) reservoirs in Northeast Germany: perspectives for geothermal use.....	235
Tue: 55: 4D Geo-Positron-Emission-Tomography (GeoPET) in situ fluid flow channel visualization in an unaltered granite fracture from Soultz-sous-Forêts (France).....	235
<b>8b) Deep subsurface groundwater systems.....</b>	<b>236</b>
The thermal provinces of Hesse, Germany .....	237
Reservoir rocks for geothermal applications in the North German Basin: Hydraulic characterization of Dogger sediments. ....	237
3D numerical modeling of cross-boundary flow in the subsurface of Berlin (Germany) .....	238
Mon: 49: Krypton-81 feasibility study on deep thermal groundwaters in the karstified Upper Jurassic limestone of the Molasse basin (Germany-Austria).....	239
Mon: 50: Geothermal potential and thermal energy storage of Buntsandstein and Keuper aquifers in NE Bavaria .....	239

Mon: 51: Developing a three-dimensional hydrogeological model based on the Konrad-site as an example to calculate the density-driven flow in deep groundwater systems.....	240
Mon: 52: Reactive Reservoir Systems - Crystal Nucleation and Filter Processes in Geothermal Systems.....	241
<b>8c) Geosciences and safe nuclear waste disposal – current status and future directions.....</b>	<b>241</b>
Geosciences and safe nuclear waste disposal – current status and future directions .....	242
The Mont Terri Project: Research in a generic underground research rock laboratory .....	242
VerSi - A method for comparing repositories for radioactive waste in different host rocks .....	243
Finding a suitable site for a high-level nuclear waste repository - insights into the work of the site selection team at the BGE .....	243
How does burial history influence the petrophysical properties of Jurassic shales? – Implications for radioactive waste storage in the Lower Saxony Basin .....	244
Investigation of porewater in bedrocks – important tools for the geohydrological characterisation and safety assessment of potential deep radioactive waste deposits .....	245
Fluid propagation, swelling pressure and cation exchange in sandwich sealing system.....	245
Numerical modelling of fracture stability of a proposed site for a spent nuclear fuel repository in Forsmark, Sweden.....	246
First in situ and real time observation of the alteration behaviour of Chernobyl “lava” studied by fluid-cell Raman spectroscopy .....	246
Tue: 56: SpannEnD – Modelling the 3D stress state of Germany.....	247
Tue: 57: Application of High Performance Computing to evaluate effects of system heterogeneity in coupled reactive transport simulations at various scales .....	248
Tue: 58: Method development for pore water extraction from consolidated clays: optimization for dissolved short-chain organic acids .....	248
Tue: 59: Transmission X-ray microscopy as a novel tool to study corroded silicate waste glasses.....	249
Tue: 60: A unifying mechanistic model for borosilicate glass corrosion .....	250
Tue: 61: Would you like stress?.....	250
<b>9) The geological signatures of natural hazards and extrem events .....</b>	<b>251</b>
<b>9a) Natural Hazards like earthquakes, landslides, floods and sea-level changes .....</b>	<b>251</b>
Paleoseismology in continental interiors and seismic hazard assessments - what have we learned? ...	251
Recent advances in qualitative and quantitative lacustrine paleoseismology.....	252
Palaeoseismic structures in Quaternary sediments of Hamburg (NW Germany) .....	253
Modeling the Holocene slip history of the Wasatch fault (Utah): Coseismic and postseismic Coulomb stress changes and implications for paleoseismicity and seismic hazard .....	253
The geological legacy of typhoons in the Philippines .....	254
The varved sediment package of the Great Blue Hole, Lighthouse Reef, Belize (Central America), a high-resolution archive of Atlantic hurricane activity throughout the entire Common Era.....	254
Tsunami hazard under rising sea levels and other climate change impacts.....	255
Precursors and processes culminating in the Anak Krakatau December 2018 sector collapse and tsunami .....	256
Project “Mass Movements in Germany (MBiD)”: A methodical approach for surveying areas prone to shallow translational landslides at regional scale.....	256
Landslide Hazard Assessment at Sorkhab Basin Using Fuzzy Logic and GIS.....	257
Mon: 53: Quaternary Tectonics of the Kalabagh fault, Sub Himalayas- insights from field studies, GPR and topographic analysis.....	257

Mon: 54: AD 1755 tsunami backwash deposits offshore – the biomarker perspective (METEOR cruise M152) .....	258
Mon: 55: Calculation for the transport of dust by the wind: from what particle size is this not possible, any longer? .....	258
Mon: 56: Organic geochemical signatures of the 2011 Tohoku-oki tsunami deposits (Northern Japan) .....	259
Mon: 57: Earthquake damage recorded along the Roman Eifel Aqueduct (Lower Rhine Embayment, Germany) .....	260
<b>10) Mineral Physics and Mineral Chemistry .....</b>	<b>261</b>
<b>10a) Minerals in the depths: an experimental approach .....</b>	<b>261</b>
Ferropericlase and diamond crystallization at upper mantle conditions: implications for the origin of ferropericlase inclusions in diamond .....	261
Microstructures across phase transitions in SiO <sub>2</sub> and the origin of seismic scatterers in the mantle	262
When history is written in sample heterogeneity .....	262
The kinetics of the glass transition of silicate glass measured by fast scanning calorimetry .....	263
Grain Size Dependency of Ge-Olivine/Spinel on Phase Transformational Faulting Mechanism for Deep-focus Earthquakes .....	263
Petredunnite, a high-pressure indicator: Influence of Fe & f <sub>O<sub>2</sub></sub> on the stability of zinc bearing clinopyroxenes .....	264
Earth's lower mantle elasticity from mineral-physics constraints .....	265
Towards studying kinetics of structural and electronic phase transitions at variable strain rates using diamond anvil cells. ....	265
Mon: 58: Atomic structure and theoretical IR spectra of amorphous SiO <sub>2</sub> at high pressures from first-principles molecular dynamics simulations .....	266
Mon: 59: Goethite decomposition at the lower mantle conditions .....	266
Mon: 60: The effect of carbon and silicon on the strength of iron alloys: Implications for anisotropy in the Earth's inner core .....	267
Mon: 61: Phase stabilities and elemental redistribution processes between magnesite and mantle silicate at conditions of the lower mantle .....	267
Mon: 62: Towards a systematic interpretation of Mg L-edge X-ray Raman scattering spectra of compressed amorphous magnesiosilicates .....	268
Mon: 63: Phase relations of Al-bearing MgFe <sub>2</sub> O <sub>4</sub> : Implications for natural occurrences in diamond .....	269
<b>10b) Detailed insights into geodynamic processes and geotechnical applications through neutron and synchrotron X-ray diffraction .....</b>	<b>269</b>
Progress in texture analysis of rocks and sediments using synchrotron, neutron and electron beams .....	270
Non-invasive investigation of concrete deterioration in aggressive aqueous environments by means of neutron diffraction .....	271
In situ – strain investigations for reservoir conditions using neutron time-of-flight diffraction .....	271
Transport of electrolyte solutions and interfacial layer in silica nanoconfinement – case of plane and parallel surfaces (nanochannels) .....	272
Quartz texture development in exhumation channel related shear zones of the Erzgebirge: The interplay of Grain Boundary Migration and Sub Grain Rotation .....	273
Determining elastic properties of rocks for a representative cross section through the Western Alps .....	273

Mon: 87: Dynamic compression of baddeleyite in membran-driven diamond anvil cells as an analogue experiments for impact events.....	274
Mon: 88: EPSILON - the neutron time-of-flight strain/stress diffractometer and its sample environment for strain investigations in rocks .....	275
Mon: 89: Pressure-induced crystallographic changes of dynamically compressed quartz by X-ray diffraction and electron microscopy.....	275
Synchrotron diffraction as a tool for the texture analysis of mid-ocean ridge serpentinites.....	276
<b>11) Crystallography.....</b>	<b>277</b>
<b>11a) Structural properties of minerals and materials .....</b>	<b>277</b>
In situ synchrotron studies of open-framework silicates at non-ambient temperature and pressure .....	277
Crystal Chemistry of the Ion Conducting Li-Oxide Garnet doped with Al, Ga, and Fe .....	278
Composition dependency of the temperature-driven structural changes in (1-x)PbTiO <sub>3</sub> -xBiNi <sub>0.5</sub> Ti <sub>0.5</sub> O <sub>3</sub> .....	278
Comparison of polarizability approach with Gladstone-Dale concept in mineral optics .....	279
High-pressure phases of feldspars with five- and six-fold coordinated aluminium.....	280
Dauphiné twin in a naturally deformed quartz: Characterization by electron channelling contrast imaging and large-angle convergent-beam diffraction .....	280
First-principles calculations elucidate the dynamics of extra-framework species in zeolites .....	281
Tue: 62: Crack-enhanced weathering in engraved marble: a possible application in epigraphy.....	282
Tue: 63: Characterization of heat-treated ceramics consisting of zoned acicular crystals with two mullite phases of different compositions.....	282
Tue: 64: Polarized mapping Raman spectroscopy: Identification of particle orientation in biominerals .....	283
Tue: 65: Thermoelastic properties of rare-earth scandates SmScO <sub>3</sub> , TbScO <sub>3</sub> and DyScO <sub>3</sub> .....	283
Tue: 66: Studies on Labradorescence.....	284
Tue: 67: The diagenetic loop of the opal-A to opal-CT transformation.....	284
Tue: 68: Structural modulations in malayaite, CaSnOSiO <sub>4</sub> .....	285
Tue: 69: Structural control of thermomechanical properties of monoclinic rare-earth calcium oxoborates .....	285
Tue: 70: Ceramic transformations during firing of ancient Japanese stone ware (Sueki): insights from firing experiments .....	286
Tue: 71: Thermal stability and oxidation processes in actinolite studied by Raman spectroscopy.....	287
Tue: 72: Radiation induced lattice disordering in monazite and xenotime from Namibia .....	287
Tue: 73: Comparison of the thermal expansivity of transition metal olivines .....	288
Tue: 74: Insights into the stability of 5-fold coordinated Si in MgSiO <sub>3</sub> -melts at pressures of the Earth's upper mantle.....	288
Tue: 75: Nanoindentation to evaluate the mechanical properties of geopolymers: first steps .....	289
Tue: 76: Characterization of a badly crystalline phyllosilicate, Ca <sub>2</sub> xMn <sub>1-x</sub> O <sub>2</sub> ·1.5-2 H <sub>2</sub> O (Lagalyite).....	290
Tue: 77: Mineralogical study of a pair of Bronze Age plaques from the Erlitou culture, China.....	290
Tue: 78: Hand-coloured maps – An interdisciplinary study of cartographers' historical pigments.....	291
<b>12) Mineral deposits and mining .....</b>	<b>292</b>
<b>12a) New Models for Old Deposits .....</b>	<b>292</b>
New models for old districts - The Erzgebirge Metallogenic Province .....	292

Mineralogy of the polymetallic Waschleithe Zn-Pb-(W) skarn – implications for skarn genesis in the Schwarzenberg district, western Erzgebirge, Germany .....	293
Unravelling the geological structure and mineralizing vectors using detailed petrographic investigations – a case study from the Delitzsch tungsten skarn occurrence, Central Germany.....	293
Epithermal Ag-(Au)-Zn-Pb mineralisation in the northern part of the Freiberg District, Germany.....	294
Mineralogical and geochemical zonation in five-element (Ag-Bi-Co-Ni-As±U) veins of the Annaberg district, Erzgebirge (Germany) .....	295
The Niederschlag fluorite-barite deposit, Erzgebirge, Germany – a fluid inclusion study .....	296
New vents and extensive sulfide fields off-axis the Southeast Indian Ridge, Indian Ocean: Results from seafloor sulfide exploration .....	296
The Historic Copper Mines of Southwest Ireland – A New Chronological Evaluation on Vein-hosted Mineral Deposits.....	297
Explaining metal zonation at the Lisheen Zn-Pb deposit, Ireland .....	298
Genetic processes and source components in submarine iron ores: Insights from the Lahn-Dill-type iron ores, Rhenish Massif, Germany .....	298
Rare metal partitioning in a metamorphosed SHMS system: the Austroalpine polymetallic ore district.....	299
Regional scale geochemical investigation of precious and base metal-rich deposits in the Cyclades, Greece.....	300
Mon: 65: Exploration, deposit evaluation and first economic information about a spodumene pegmatite in Canada Ontario .....	300
<b>12b) Mineral deposits of societal relevance for Europe .....</b>	<b>301</b>
Decarbonisation, circular economy and deindustrialisation – a Vision for the European minerals industry?.....	301
Historical mine sites revisited .....	302
The Path to European Rare Earth Element Security.....	302
Extraction of lithium from geothermal brines of the Upper Rhine Graben using manganese oxide adsorbents – A first approach .....	303
Tellurium a strategic metal for green energy technologies: Insights into ore-forming processes.....	304
Mon: 66: GeoERA – Geological Survey Organisations contribution to Europe’s raw materials sustainability .....	304
<b>12c) Mineralogy of Ore Deposits – Genesis, Characterization, and Applications .....</b>	<b>305</b>
Using LIBS to detect REE-rich areas in Storkwitz drill cores – A new method for rapid and spatially detailed analysis of geological samples .....	306
The use of muscovite for B-isotope studies of hydrothermal ores .....	306
Making space for giant Zn deposits in Palaeozoic carbonaceous mudstones: the role of diagenesis.....	307
Properties of mineralizing fluids at high-temperature (200 < T < 600 °C): Insights from in-situ spectroscopy .....	307
From seawater to black smoker vents: Hydrothermal fluids that leach metals from the oceanic crust and generate VMS deposits .....	308
Giant Carlin-type Au deposits formed by coupled partitioning of Au and As into pyrite.....	308
The importance of magmatic processes on the formation of orogenic Au deposits: insight from the Central Lapland Greenstone Belt, Finland .....	309
Tue: 79: Thorium-poor monazite and columbite-(Fe) mineralization in the Gleibat Lafhouda carbonatite and its associated iron-oxide-apatite deposit of the Ouled Dlim Massif, South Morocco....	309

Tue: 80: As-rich VMS Mineralization at Niuva South, Tonga Arc.....	310
Tue: 81: Detection, distribution and speciation of chemical elements with fast XRF mapping and micro X-ray absorption spectroscopy demonstrated for a TI containing ore .....	311
Tue: 82: High resolution mineral-chemical analysis of scheelite from the Felbertal tungsten deposit, Austria .....	311
Tue: 83: Quantification of minerals and valuable metals in drill cores from orogenic gold deposits by LIBS and $\mu$ -EDXRF .....	312
Tue: 84: Lower Group and Middle Group chromitites of the Bushveld Complex – the effect of weathering on the distribution of platinum-group elements.....	313
Tue: 85: Field observations and mineralogical characterization of magnetite-skarn-occurrences in Isfahan Province, Central Iran .....	314
Tue: 86: Geochemical analyses of stream sediments and morphological studies of gold micro-nuggets from the Carnon River Mining District, Cornwall .....	314
Tue: 87: Granitic pegmatites and Nb-, Y-REE- and F-mineralization in the Las Chacras Batholith, Argentina.....	315
Tue: 88: Fluid-melt partitioning of Sn and W as function of the alumina saturation index of the granitic melt .....	316
Tue: 89: Spectral X-ray CT: A potential new analytical method for a 3-dimensional chemical characterization of ores .....	316
Tue: 90: Mn-mineralization in the iron ores from West-Crete (Greece) .....	317
Tue: 91: New insights on Ag-Hg mineralization in the Anti-Atlas Precambrian belt: Case study of the Tassafta ore deposit, NE of the Saghro inlier (Eastern Anti-Atlas, Morocco).....	318
Tue: 92: Impact of IRUP on mineralogy and mineral chemistry of the UG2 chromitite in the Thaba mine, Bushveld Complex .....	318
<b>12d) Reuse Potential of Mining Residues .....</b>	<b>319</b>
Sourcing of critical elements and minerals from mine waste .....	319
Re-mining of mine wastes in Germany: Challenges and opportunities .....	320
Innovative exploration of mine tailings based on core scanner applications.....	321
Next Generation of Tailing Exploration Technologies: XRF-CPT Probe as Real-Time High Resolution Tool for Low Invasive Tailing Characterization.....	321
Novel approaches to Scandium-species investigation in Bauxite residues by X-ray adsorption near edge structure spectroscopy - Looking for the needle in a haystack .....	322
Bioleaching of Cu/Co-rich mine tailings from the polymetallic Rammelsberg mine, Germany .....	322
Microbe-mineral interactions during chalcopyrite bioleaching .....	323
Tue: 93: Interdisciplinary study of mining residues and implications for secondary mining.....	324
<b>13) Open Session .....</b>	<b>325</b>
<b>13a) 3D Geological Modelling and subsurface potentials .....</b>	<b>325</b>
An overview of current geological modelling activities in the German North Sea by the BGR.....	325
3D geological modelling in Saxony-Anhalt - documentation, methods, results and applications towards modern subsurface information systems.....	326
Producing an improved geological 3D model of Lower Saxony (TUNB) from the 3D tectonic atlas (GTA3D) .....	327
Towards a velocity model of the deep subsurface of Schleswig-Holstein for geological 3D modeling – A part of the joint project TUNB .....	327
3D-Deutschland: a three-dimensional lithospheric-scale density and thermal model of Germany ...	328

A multimodal and multitemporal assessment of mud volcanism in Azerbaijan by drone and remote sensing.....	328
Mon: 67: Step by step: The 3D subsurface model of Mecklenburg-Vorpommern is growing .....	329
Mon: 68: Tectonic 3D-model of the Berga antiform – Saxo-Thuringian Zone .....	330
Mon: 69: More data - more Model. Experiences within the project TUNB. ....	330
Mon: 70: Experience with the construction of a volumetric model in the German North Sea Sector ...	331
Mon: 71: On the visualization of 3D geological models and their uncertainty .....	331
<b>13c) Tectonic Systems (TSK open session) .....</b>	<b>332</b>
Rheology of evaporites at slow deformation rates: integrated understanding of Salt tectonics, Salt caverns and Nuclear waste repositories .....	332
Microfabrics and composition of brittle faults and veins in Lower Cretaceous claystones (Lower Saxony Basin, Germany): Constraints on the barrier behaviour of clay-rich rock formations.....	333
Two regional tectonic structures - The intersection of Elbe Zone and Eger Rift .....	333
The near surface structure of rift systems .....	334
Challenges to unravel an abandoned Oligocene rift segment along the River Nile in Egypt .....	334
High-angle normal faulting at the Tangra Yumco graben (southern Tibet) since ~15 Ma.....	335
The Adriatic slab gap: Regional-scale surface uplift in the Dinarides fold-thrust belt validated by geomorphologic indices .....	336
Forearc growth through background seismicity in Peru-Chile .....	336
Hydrothermal monazite dating in the Lepontine Dome between exhumation and shear zone activity .....	337
The problem of misconceptions for understanding Phanerozoic collisional orogens.....	337
Mon: 72: Seismic reflection study of a regional lines in the Western Desert of Iraq.....	338
Mon: 73: Retrograde tectonic activity in the Mont Blanc and Aiguilles Rouges Massifs dated through hydrothermal monazite .....	339
Mon: 74: Elements of the Osning Fault Zone (NW-Germany) – Key Structures of a Strike-Slip Zone .....	339
Mon: 75: The boundary between Eastern and Western Alps as seen from a foreland perspective – an example from the Miocene Molasse Basin.....	340
Mon: 76: Structural geological study of a shear zone at the Stora Le Marstrand formation, island Arndorsholmen (SW Sweden).....	341
Mon: 77: Slab hydration: combining constraints from oceanic plate structure and intraslab seismicity.....	341
Mon: 78: Pre-Alpine tectonic and sedimentary contacts in the southeastern Ötztal Nappe (Austroalpine, Italy).....	342
Mon: 79: Exhumation of a metamorphic core complex: The journey from mid-crust to surface.....	342
Mon: 80: The Altmark Swell – sedimentary high or uplifted graben shoulder? .....	343
Mon: 81: Stress rotation due to discontinuities and material transitions.....	344
Mon: 82: Salt pillow growth in the Bay of Mecklenburg, SW Baltic Sea: Timing and regional tectonic link.....	344
Mon: 83: Strain analysis of the Zervreila Orthogneiss of the northern Adula Nappe, eastern Switzerland, Central Alps .....	345
Mon: 84: On the indispensability of haptic sensations with hand specimens – a plea for integrating rock collections into structural geology and tectonics teaching in the digital era .....	345
Mon: 85: Extensional continental basins: Feedbacks between the tectonic and thermal history.....	346

<b>13d) Communicating (geo-)science .....</b>	<b>347</b>
More Geosciences in German Schools: Opportunities for Geoscientists to Support the Training and Selection of Students for the Annual Competition „International Earth Science Olympiad (IESO)“ .....	347
Der Mineralogische Lehrkoffer im MINT-Unterricht – eine Brücke von Natur zu Naturwissenschaft und Technik .....	348
Geology in a nutshell – A rock-cycle game created during a geology course for elementary school students .....	348
Teaching Science Communication to Geoscience students .....	349
Minerals in Thin Section (‘MINTS’): An open-access, interactive website for transmitted-light petrographic microscopy.....	350
OutcropWizard - A modern access to the classic themes of geoscience .....	350
Why PDFs are not suitable for communicating (geo)scientific results .....	351
Asteroid Day: Communicating the danger from impacts on Earth and the relevance of meteorites and their parent bodies .....	352
<b>13e) Building a Global Network of Geochemical Data .....</b>	<b>353</b>
Big Data in Geochemistry? Examples, needs and outlook .....	353
An online research platform for cosmochemistry.....	354
Medusa: A Metadata System for Samples analysed in the Geo- and Environmental Sciences.....	354
EPOS Multi-scale laboratories: a network of European laboratories .....	355
GEOROC - a Global Geochemical Database.....	356
Building on the Success of Geochemical Databases: Toward a Global Research Infrastructure of Geochemical Data.....	356
<b>13f) Research data and software management in times of FAIR and Open Data .....</b>	<b>357</b>
Wasn’t “open” FAIR enough? The future of data and software publication .....	357
Increasing the visibility of data and samples: publishing services of GFZ Data Services.....	358
Visual Project Summary, Bull-Eye Chart, Task Bingo and Work Package Chess - graphical tools for a data management workshop within the Horizon 2020 MEET project .....	359
Publication of the Content of BGR’s Information Systems to the Semantic Web .....	359
A Roadmap for Research Data Management in the Geosciences: Responding to Community Needs .....	360
Enhancing FAIRness of global air quality data: The Tropospheric Ozone Assessment Report database .....	360
NFDI4Earth: current state and goals for the future .....	361
Next Generation of Interoperable Information Systems for Spatial Data .....	361
Research software - landscape and actors .....	362
Promoting cultural change in data publishing .....	362
Computational reproducibility in the geoscientific publication cycle .....	363
Tue: 94: Building a Portal for Interdisciplinary Planetary Data.....	364
Tue: 95: V-FOR-WaTer – a virtual research environment to access and process environmental data.....	364
Tue: 96: The Metadata Editor of GFZ Data Services.....	365

## Plenary Lectures

Monday 23 September

Location: Lecture hall building H 1

Opening Ceremony, 3:00pm - 3:45pm

### Building Earth's highest topography: lessons learned from the Indo-Asia mega-orogeny

**Marin K. Clark**

*University of Michigan, United States of America*

Insights into geodynamic processes are gained from an understanding of how topography in orogens develops. Whether created on individual fault blocks or by more distributed processes involving the deep crust and mantle lithosphere, topographic growth reflects how continents accommodate convergent plate motion and redistribute continental material. Wide, diffuse deformation zones and long-distance flow of crustal material can extend high orogenic topography over great distances from the plate boundary. Nowhere on Earth is topography related to orogenesis more dramatic in both height and breadth than the Indo-Asian continental collision. Largely resulting from nearly 50 million years of continued plate convergence since collision, the terrain of central Asia is dominated by the broad, high Tibetan Plateau, which is surrounded by nearly impenetrable mountains flanked by curiously low gradient plateau margins. The topographic history of the Indo-Asian orogen continues to be an area of active study as we struggle to understand competing ideas of how the proxy record for elevation change is interpreted and whether or not specific geodynamic processes can be uniquely interpreted by topographic change.

Much new information about how Tibet has grown outward and upward in time has emerged in the past decade owing to greater access to Tibet's remote interior, new methods for understanding surface change and large-scale integration of datasets. These details have challenged previous concepts of orogenic growth, namely by redefining the timing and geographic extent of topographic growth and its relationship to plate motion, crustal mass balance and surface deformation. With these new histories, exciting new questions have emerged that highlight the role of rheology and deformation mechanisms of mega-orogens in setting expansive high topography on Earth.

Tuesday 24 September

Location: Lecture hall building H 1

2:00pm

### Fluids in the Lower Crust: Deep is Different

**Craig Manning**

*University of California at Los Angeles (UCLA), USA*

Deep fluids are important for the evolution and properties of the lower crust and upper mantle in tectonically active settings. Uncertainty about their chemistry has led past workers to use upper crustal fluids as analogues. However, recent results show that fluids at >15 km differ fundamentally from shallow fluids and help explain high-pressure metasomatism and resistivity patterns. Deep fluids are comprised of four components: H<sub>2</sub>O, non-polar gases (chiefly CO<sub>2</sub>), salts (mostly alkali chlorides), and rock-derived solutes (dominated by aluminosilicates and related components). The first three generally define the solvent properties of the fluid, and models must account for observations that H<sub>2</sub>O activity may be quite low. The contrasting behavior of H<sub>2</sub>O-gas and H<sub>2</sub>O-salt mixtures yields immiscibility in the ternary system, which can lead to separation of two phases with fundamentally different chemical and transport properties. Thermodynamic modeling of equi-

librium between rocks and H<sub>2</sub>O using simple ionic species known from shallow-crustal systems yields solutions possessing total dissolved solids and ionic strength that are too low to be consistent with experiments and resistivity surveys. Addition of CO<sub>2</sub> further lowers bulk solubility and conductivity. Therefore, additional species must be present in H<sub>2</sub>O, and H<sub>2</sub>O-salt solutions likely explain much of the evidence for fluid action in high-P settings. At low salinity, H<sub>2</sub>O-rich fluids are powerful solvents for aluminosilicate rock components that are dissolved as previously unrecognized polymerized clusters. Experiments show that, near H<sub>2</sub>O-saturated melting, Al-Si polymers comprise >80% of solutes. The stability of these species facilitates critical mixing in rock-H<sub>2</sub>O systems. Addition of salt (e.g., NaCl) changes solubility patterns, but aluminosilicate contents remain high. Thermodynamic models indicate that the ionic strength of fluids with X<sub>salt</sub> = 0.05 to 0.4 and equilibrated with model crustal rocks have predicted bulk conductivities of 10-1.5 to 100 S/m at porosity of 0.001. Such fluids are thus consistent with conductivity anomalies commonly observed in the lower crust (e.g., the “G” anomaly), and are capable of the mass transfer commonly seen in metamorphic rocks exhumed from the lower crust and subduction zones.

## Wednesday 25 September

**Location: Lecture hall building H 1**

**11:00am**

### 50 Years Since Apollo: The Earth in the Context of Solar System Exploration

**Jim Head**

*(Brown University, USA)*

50 years ago, the Apollo lunar exploration missions began the transformation of astronomical objects, the Moon, terrestrial planets and outer planet satellites, into objects of geologic exploration and characterization. The Apollo missions resolved fundamental questions about the Moon (origin of the Moon-hot or cold; origin of its craters-volcanic or impact; age and origin of the dark maria-young or old, dust or lava; origin of basins-endogenous or exogenous; etc.). Apollo also provided a fundamental framework and paradigm for understanding the history and evolution of the terrestrial planets, including Earth. What have we learned about planetary formation and evolution in the ensuing five decades from this Moon-based comparative planetology?

- 1) Ejecta from a large Mars-sized projectile impacting into early Earth appears to have formed the Moon.
- 2) Impact cratering plays a fundamental role in initial impact heating and melting to create a molten magma ocean whose thermal and chemical evolution dictates much of subsequent history.
- 3) Planetary internal heating, melting and extrusion of molten rock (lava) to the surface supplies additional volatiles to the primordial atmospheres and resurfaces significant areas.
- 4) Earth loses heat through plate tectonics, but smaller bodies lose heat primarily by conduction and rapidly become “one-plate planets”.
- 5) Planets lose atmospheres as a function of time and Mars is a laboratory for this change, perhaps evolving from warm and wet to today’s sub-freezing desert.
- 6) The current position of planets relative to their stars is not necessarily where they originated.
- 7) Abundant planetary environments have the ingredients for life, but life has thus far only been detected on Earth.
- 8) The themes in the geological and thermal planetary evolution revealed by solar system exploration provide a basis for an improved understanding of the nature and evolution of our own Home Planet, Earth.
- 9) Our new neighborhood, the Solar System is but one of many dozens of exoplanetary systems and thousands of exoplanets.

10) Today astronomers and planetary scientists are teaming up to tackle fundamental questions in comparative planetary systems: How can we use our knowledge about our Solar System and the characteristics and histories of its planets and satellites to interpret the nature of exoplanets? Where does the Solar System fit in the menagerie of exoplanetary systems? Is our Solar System typical or anomalous? What does this mean about the future eons of Earth history?

**Tuesday, 24/Sep/2019**

**Location: Lecture hall building H 1**

**8:00pm - 9:00pm** Public Evening Lecture

**Und dann verschwand ein Ozean – wie die geologische Geschichte der Erde unsere Zivilisation ermöglicht**

**Colin Devey**

*GEOMAR Helmholtz Centre for Ocean Research Kiel, Germany*

Wo wir leben, wie wir leben, wovon wir leben - alles wird von dem Aufbau der Erde bestimmt. Dieser Aufbau ist im Laufe der Jahrmilliarden durch Bewegungen der tektonischen Platten zur Stande gekommen. Dabei sind es oft Ozeanbecken, die entstehen und verschwinden und dadurch Rohstoffe, Landschaften und wetterbeeinflussenden Gebirgen hinterlassen, die unser Leben massgeblich prägen. Im Vortrag wird darauf eingegangen, was wir über die Prozesse der Plattenbewegungen kennen, welche dieser Prozesse wir heute vor allem in den Ozeanen beobachten können und wie sie die Erde geformt haben.

## 1) Understanding Early Earth processes using novel geochemical approaches and methods

Tuesday, 24/Sep/2019: 3:45pm - 5:30pm

### 1a) The Present is the Key to the Past – Reconstructing Early Earth Environments through Modern Analogues

**Session Chair: Sümeyya Eroglu** (University of Münster)

**Session Chair: Harald Strauß** (WWU Münster)

**Location: Schlossplatz 7 Hof: SP 7**

#### Session Abstract

Earth's litho-, bio-, hydro-, and atmosphere experienced major changes throughout its history, which are still partly preserved in the rock record. The reconstruction of environmental conditions of ancient marine and terrestrial settings is based on deciphering these rock records. A major obstacle hereby is that all of these archives experienced diagenetic or even metamorphic overprint and, hence, do not necessarily preserve the original (bio-)geochemical signatures. Studies on modern environments can improve our understanding of formation and preservation processes of these (bio-)geochemical signatures. Thereby, settings with a redox-stratified water column or unique parameters, e.g. high temperatures, acidity or Fe content are of particular interest as they can serve as modern analogues of Early Earth and the Precambrian. We invite contributions focusing on new insights into reconstructing Precambrian conditions based on (isotope) geochemical, mineralogical, and microbiological insights of these modern analogues. Furthermore, we encourage submissions on experimental approaches under lab conditions as well as novel applications on Precambrian sedimentary rocks.

#### Lecture Presentations

**3:45pm - 4:15pm** *Session Keynote*

#### **Stable isotope biosignatures: from modern analogue to ancient ecosystem**

**Paul Mason**

*Utrecht University, The Netherlands*

Defining the nature and evolution of the early biosphere on Earth remains a major scientific challenge. Over recent decades, much work has been done to attempt to find robust biosignatures that can be used to interrogate the ancient rock record. Isotope fraction has become a widely used tool for identifying the traces of past life in the absence of a fossil record and for tracking the evolution of redox conditions and metabolism across geological timescales. Any reliable tracer must fulfil the two criteria of antiquity and biogenicity. These requirements are challenging to fulfil and the issue of biological origin requires robust calibration against modern experimental data or field settings. Here I review how modern data from two different stable isotope systems (S, Se) have been used for tracing past changes in global redox conditions and microbiological evolution. Sulfur isotope fractionation has been studied experimentally since the 1950s and is well-established for investigating sulfur-based metabolisms. Selenium isotopes in contrast are a very new proxy, that respond in a very different way to S during biosphere and redox evolution. Both systems rely on a wealth of data from modern analogue systems for the interpretation of geological data. Isotope fractionation has been studied in abiotic experiments as well as in a range of different microbial laboratory culture experiments and in situ in field sites. I will outline currently-accepted fractionation models and how they are linked to environmental parameters such as substrate availability, temperature and type of electron donor. I will discuss how analogous model organisms/ modern microbial consortia can be for ancient populations and review how confident we can be in interpreting the ancient record using modern data. I will conclude by discussing the variable preservation of biogenic isotope signals into minerals and the rock record.

**4:15pm - 4:30pm**

### **The influence of microbial sulfate reduction on the sulfur isotopic composition of CAS in modern Mg-rich carbonates from Lagoa Vermelha and Brejo do Espinho, Brazil**

**Simon L. Schurr<sup>1</sup>, Vanessa Fichtner<sup>2</sup>, Harald Strauss<sup>1</sup>, Adrian Immenhauser<sup>3</sup>, Crisogono Vasconcelos<sup>4</sup>, Sabrina Hänsch<sup>1</sup>, Vera Heßeler<sup>1</sup>, Camila Areias de Oliveira<sup>5</sup>, Catia Fernandes-Barbosa<sup>1</sup>**

<sup>1</sup>Institut für Geologie und Paläontologie, Westfälische-Wilhelms-Universität Münster, Corrensstr. 24, 48149 Münster, Germany; <sup>2</sup>Department of Earth & Environmental Sciences, University of Kentucky, Lexington, KY 40506, USA; <sup>3</sup>Institute of Geology, Mineralogy and Geophysics, Ruhr-University Bochum, Universitätsstraße 150, 44801 Bochum, Germany; <sup>4</sup>Geological Institute, ETH-Zürich, Sonneggstrasse 5, 8092 Zürich, Switzerland; <sup>5</sup>Departamento de Geoquímica, Universidade Federal Fluminense, RJ-24020-141 Niterói, Brazil

Dolomite is an important carbonate archive in the early Earth's history that allows to reconstruct the global marine sulphur cycle through the  $\delta^{34}\text{S}$  value of carbonate associated sulphate (CAS) and pyrite (py). However, studies of both proxies in environments characterized by modern dolomite precipitation are limited. Here we present  $\delta^{34}\text{S}$  data for CAS and pyrite from Mg-rich carbonate sediments of two hypersaline lagoons (Lagoa Vermelha and Brejo do Espinho) in Brazil. Both lagoons are ideal locations to study the microbial influence on Mg-rich carbonate precipitation with the possibility to compare archived sedimentary sulphur isotopic compositions with the ambient porewater as well as surface water.

In Lagoa Vermelha  $\delta^{34}\text{S}$  values of sedimentary pyrite reveal a variation from 17 to 5‰ and up to 27‰ for dissolved porewater sulphide.  $\delta^{34}\text{S}_{\text{CAS}}$  values at 28‰ for carbonate associated sulphate are isotopically heavier than the respective surface water with 20.5‰. However,  $\delta^{34}\text{S}_{\text{CAS}}$  values are comparable to the porewater sulphate  $\delta^{34}\text{S}$  composition, which is increasing from 20.5‰ at the sediment surface to 28‰ at 0.4m depth.

The carbonates of Brejo do Espinho display increasing  $\delta^{34}\text{S}_{\text{CAS}}$  values from 24‰ at the sediment surface to 43‰ at 0.4m depth despite a constant porewater sulphate  $\delta^{34}\text{S}$  value of 23‰. There the  $\delta^{34}\text{S}_{\text{py}}$  data show an average value of 12‰, comparable to porewater sulphide  $\delta^{34}\text{S}$  values of 20‰.

Both,  $\delta^{34}\text{S}_{\text{CAS}}$  and  $\delta^{34}\text{S}_{\text{py}}$  values reveal a strong influence of microbial sulphate reduction during Mg-rich carbonate precipitation, which indicates the necessity of a careful assessment if ancient dolomites will be used as a marine  $\delta^{34}\text{S}_{\text{CAS}}$  proxy.

**4:30pm - 4:45pm**

### **The stable W isotope composition of Fe/Mn-rich sediments from the Baltic Sea**

**Florian Kurzweil<sup>1</sup>, Martin Wille<sup>2</sup>, Olaf Dellwig<sup>3</sup>, Ronny Schoenberg<sup>4</sup>, Carsten Münker<sup>1</sup>**

<sup>1</sup>Universität zu Köln, Germany; <sup>2</sup>University of Bern, Switzerland; <sup>3</sup>Leibniz-Institute for Baltic Sea Research, Rostock, Germany; <sup>4</sup>Eberhard Karls Universität Tübingen, Germany

Manganese oxides represent a major sink for dissolved marine  $\text{WO}_4^{2-}$  as well as for other oxyanions such as  $\text{MoO}_4^{2-}$ . During the adsorption of  $\text{WO}_4^{2-}$  and  $\text{MoO}_4^{2-}$  onto Mn oxides the coordination of W and Mo changes from tetrahedral to octahedral. Due to the weaker bonding structure in octahedral coordination light isotopes are preferentially adsorbed. In contrast to Mo, however, W forms these octahedral inner sphere complexes not only on Mn oxides, but also on Fe hydroxides. Thus, changes in the W isotopic composition of dissolved  $\text{WO}_4^{2-}$  and sedimentary W are already expected, when the local marine redox potential is still too low to form Mn oxides but already high enough to form Fe hydroxides (e.g. in oldest Superior Type iron formations). Tungsten stable isotope measurements in Archean sediments, thus, represent an additional and complementary redox proxy to the well-studied Mo isotope system. In comparison to Mo isotopes, tungsten stable isotope measurements allow for a more distinct investigation of earliest and even slight changes in the marine redox state.

We will present the first stable W isotope data of modern sapropels and Mn-rich sedimentary layers from the Landsort Deep, Baltic Sea. The funnel-shaped sub-basin exhibits a distinct vertical stratification with respect to  $\text{O}_2$  and  $\text{H}_2\text{S}$ . Due to well-documented occasional inflows of oxic waters from the North Sea, the Landsort Deep represents an ideal setting to investigate the impact of temporally changing redox conditions

on the geochemical cycling of W from the water column into the sediment. We observe resolvable variations in sedimentary stable W isotope compositions with  $\delta^{186/184}\text{W}$  values between 0.086 and 0.226 ‰ (external reproducibility of 0.018 ‰). These  $\delta^{186/184}\text{W}$  values show smooth trends with depth. Our investigation might therefore contribute to the understanding of stable W isotope systematics in modern marine sedimentary settings, which is required to establish stable W isotopes as a potential tracer for Early Earth environmental reconstructions.

**4:45pm - 5:00pm**

### **Applicability of the Ge/Si ratio in BIFs as a source proxy for silica in the Early Earth's ocean – insights from modern marine ferromanganese oxyhydroxides**

**Katharina Schier<sup>1</sup>, David M. Ernst<sup>1</sup>, Dieter Garbe-Schönberg<sup>2</sup>, Michael Bau<sup>1</sup>**

<sup>1</sup>Jacobs University Bremen gGmbH, Germany; <sup>2</sup>Christian-Albrechts-Universität zu Kiel

Germanium and Si show coherent behavior in igneous and clastic rocks, but are fractionated during weathering and hydrothermal water-rock interaction. This results in slightly lower Ge/Si in river waters and significantly higher Ge/Si in marine hydrothermal fluids compared to their respective source rocks. Modern siliceous precipitates show little fractionation of Ge and Si relative to ambient seawater, whereas experimental studies show preferential scavenging of Ge onto ferric hydroxides. While pure (meta)chert bands of BIFs show low Ge/Si ratios similar to those of modern seawater, Fe-dominated bands show high Ge/Si ratios similar to those of modern marine hydrothermal fluids. Hence, Fe-rich BIF bands are considered to have formed during times of intense marine hydrothermal activity, while (meta)chert bands precipitated during times of hydrothermal quiescence and dominant riverine input into the ocean. This general model, however, is based on the fundamental assumption that no Ge-Si fractionation occurs during formation of Fe-dominated BIF bands. Since this has recently been questioned, there is need for verification/falsification of this assumption. As a first step, we here report results of an investigation of Ge-Si behaviour during formation of *modern* marine ferromanganese oxides. *In situ* microscale analyses by Laser Ablation High-Resolution ICP-MS of a fast growing hydrogenetic ferromanganese crust from the Clarion-Clipperton Fracture Zone (CCZ) in the Pacific Ocean reveal Ge/Si ratios that are an order of magnitude higher ( $19 \times 10^{-6}$  to  $76 \times 10^{-6}$ ) than those of modern seawater ( $1.86 \times 10^{-6}$ ; Mortlock & Froelich, 1996), revealing preferential scavenging of Ge relative to Si during the formation of modern marine hydrogenetic ferromanganese oxide precipitates, providing evidence from a natural system for the preferential Ge scavenging as observed in experimental studies. Hence, Ge-Si relationships in alternating Fe- and Si-dominated BIF layers *alone* cannot be used as source proxy for the origin of Si in the Early Earth's ocean but need to be complemented by additional evidence from other geochemical proxies.

[1] Mortlock, R.A. & Froelich, P.N. (1996), *Analytica Chimica Acta* 332, 277-284.

**5:00pm - 5:15pm**

### **Insights on the Archean environment from the oldest sediments on Earth**

**Joanna Lea Claire Brau**

Ludwig Maximilians Universität München, Germany

Joanna Brau (Geoscience, LMU Munich) joanna.brau@min.uni-muenchen.de, Marion Garçon (Geochemistry, ETH Zurich) marion.garcon at erdw.ethz.ch

The Archean age was a turning point during the early Earth evolution. Water was present on the planet and oceans spread around the world, continents start to form. Earth starts to be geodynamically active and eventually, life emerges. Due to recycling processes, it is hard to find evidence from this early stage. However relics called cratons still remain at the surface of the Earth, and are disseminated all around the world. In this study we focused on two cratons in particular, the biggest one known so far, the Superior craton located

in Canada in the region of Saglek, and the well-known Pilbara craton located in Australia. In this project we aim to use Archean sediments in order to find more information about the Archean environment. Knowing that detritic and chemical sediments are respectively products of continental weathering and seawater precipitation, we analysed Archean detritic and chemical sediments such as: quartzites, cherts and BIF from the Canadian and Australian cratons. In order to characterize those samples we separated Pb, HREE, Sm, Nd, Lu, Hf elements by using geochemical processes such as chromatography. We measured trace elements with ICP-MS and Sm-Nd isotopic ratios with a Multi collector ICP-MS NEPTUNE PLUS. We found out given their age, (3.45 Ga for Pilbara samples and 3.4-3.6 Ga for Saglek samples), the samples are not cogenetic and some of them have been disturbed after their formation by external events. Both batches of sediments originated from a source mixture between two end members. BIFs and quartzites from Pilbara were formed from the erosion mixture between old mafic and felsic crusts (4Ga), whereas Saglek BIFs derived from a mixture between two felsic crusts of about 4 and 3.4-3.6 Ga. Each chemical and detrital sediment from both locations, records respectively the composition of seawater and continental crusts, and shows that hydrothermalism was important during the Archean period.

## Poster Presentations

Mon: 1

### **Surviving the ferruginous Archean ocean – Assessing the potential toxicity of Fe<sup>2+</sup> on basal Cyanobacteria in anaerobic conditions.**

**Achim Jan Herrmann, Michelle M. Gehringer**

*Technische Universität Kaiserslautern, Germany*

The oxygenation of early Earth's atmosphere ~2.4 Ga ago, known as the Great Oxygenation Event (GOE) was presumably caused by oxygenic photosynthesis from (proto-) Cyanobacteria. Previous the Archean oceans were anoxic with high levels of Fe<sup>2+</sup> (40-120 μM Fe<sup>2+</sup>). However recent studies suggest that Fe<sup>2+</sup> concentrations of >100 μM are toxic to modern, marine Cyanobacteria. This would have modulated their expansion in the ferruginous Archean oceans, necessary for the GOE. Studies to date have focused on closed systems with elevated CO<sub>2</sub>, allowing the build-up of O<sub>2</sub>. This study investigated the potential toxicity of Fe<sup>2+</sup> on two basal strains of cyanobacteria in an atmosphere representing the Archean, in both a closed and open culture system.

*Pseudanabaena* PCC7367 and *Synechococcus* PCC7336, were incubated under an anoxic, elevated CO<sub>2</sub> atmosphere in buffered ASNIII Media with increasing Fe<sup>2+</sup> concentrations (15 μM, 120 μM and 600 μM). The cultures were monitored for chlorophyll *a* and Fe<sup>2+</sup>/ Fe<sup>3+</sup> concentrations for 21 days. Additionally the production of O<sub>2</sub> in the closed system was measured at the beginning and middle of the light cycle. Mid and late logarithmic cultures were assessed for respiration (CTC), viability (SYTOX Green) and Fe<sup>3+</sup> precipitation using fluorescence microscopy. Media was assessed for dissolved CO<sub>2</sub>, nitrate and phosphate content.

While the closed system controls indicated a similar Fe<sup>2+</sup> toxicity response to that seen in the literature, the cultures grown in an open system showed interesting deviations in Fe<sup>3+</sup> accumulation and growth morphologies.

This study emphasises the influence of experimental design and importance of using different strains in investigating ecological trends, especially during the period leading up to the GOE.

**Mon: 2**

**Triple oxygen isotope study of manganese formations as a proxy for the triple oxygen isotope composition of Precambrian air O<sub>2</sub>**

**Sukanya Sengupta<sup>1</sup>, Andreas Pack<sup>1</sup>, Sebastian Viehmann<sup>2</sup>**

<sup>1</sup>Department of Isotope Geology, Georg-August-Universität-Göttingen, Germany; <sup>2</sup>Department of Geodynamics und Sedimentology, Universität Wien, Austria

The great oxidation event, recorded by the absence of mass independent fractionation of sulphur isotopes in marine sediments, sets the time for the advent of biologically mediated free oxygen in the oceans and the atmosphere [1]. The triple oxygen isotope composition of molecular O<sub>2</sub> in the atmosphere is a tracer for global bio-productivity [2] and ancient pCO<sub>2</sub> in the atmosphere [3]. Here, we attempt to reconstruct the triple isotope composition of Precambrian atmospheric O<sub>2</sub> by means of analysis of Mn-rich iron formations.

Only few lithospheric materials bear signatures of atmospheric O<sub>2</sub>. Sedimentary sulphates [3] and cosmic spherules [4] contain oxygen originally derived from air O<sub>2</sub>. Also aqueous Mn-IV-oxides can contain a portion of oxygen originally derived from air O<sub>2</sub> [5]. Laboratory experiments showed that 30-50% of oxygen in laboratory precipitated manganese-IV-oxides derived from molecular O<sub>2</sub> dissolved in water.

We study the detrital-poor iron formation of the Neoproterozoic Urucum iron and manganese formation in the Santa Cruz Formation, Brazil [6]. Drill core samples from neither the Mn-rich nor the Fe-rich layers have evidence of metamorphic or hydrothermal overprints [6]. We will analyze triple oxygen isotope compositions of the shallow water Mn-oxides in the Urucum Fe-Mn-formation and compare these data to modern analogues. Our results will be discussed with respect to Precambrian pCO<sub>2</sub> and global bioproduction rates. We will highlight the use of triple oxygen isotopes in Precambrian Mn-oxides for calculating the triple oxygen isotope of Precambrian air O<sub>2</sub>.

[1] Farquhar et al. (2000) *Science* 289, 756-758; [2] Luz et al. (1999) *Nature* 400, 547-550; [3] Bao et al. (2008) *Nature* 453, 504-506; [4] Pack et al. (2017) *Nat. Comm.* 8, 15702; [5] Mandernack et al. (1995) *GCA* 59, 4404-4425; [6] Viehmann et al. (2016) *Precamb. Res.* 282, 74-96.

## 1b) Early Earth Processes: Constraints from the Rock Record

Tuesday, 24/Sep/2019: 9:15am - 10:00am

**Session Chair: Erik E. Scherer** (WWU Münster)

**Session Chair: Axel Gerdes** (Goethe-University Frankfurt)

**Session Chair: Armin Zeh** (KIT Karlsruhe)

**Location: Schlossplatz 7 Hof: SP 7**

### Session Abstract

The silicate Earth differentiated early in its history into a variety of mantle and crustal reservoirs. The degree and style of interaction among these reservoirs is recorded in the chemical and isotopic signatures of Archean rocks and even older minerals, offering clues to their linked evolution in the context of a changing geodynamic setting. We encourage contributions that employ tools such as fieldwork, petrology, geochemistry, geochronology, and geodynamic modelling to illuminate early Earth processes ranging from the earliest silicate differentiation, through the evolution of continents and oceans, to the onset of plate tectonics.

### Lecture Presentations

9:15am - 9:45am *Session Keynote*

#### Archean lithospheric change and the start of modern-style plate tectonics

**Matthijs Smit**

*University of British Columbia, Canada*

The continental crust underwent growth and compositional maturation between 3.5 and 2.8 Ga. Ancient sediments indicate that the crust changed from mafic to andesitic compositions [1-3]. Much of the subcontinental lithospheric mantle (SCLM) stabilized during this same time period. Post-majoritic pyrope from the SCLM, now dated by Lu-Hf chronology [4], capture the extreme asthenospheric decompression and melting that allowed the SCLM to form. These changes had a drastic and long-lasting effect on the Earth system, and its emerging oxygen and nutrient cycles. Nevertheless, causes and driving mechanism remain enigmatic.

A link to the development of plate tectonics has long been proposed [2,5-7]. Much of the crust made during this time indeed comprises juvenile tonalite-trondhjemite-granodiorite (TTG) rocks, which could be considered as arc analogues. Nevertheless, magmatic differentiation of the lower crust can equally produce TTGs [8-10] and mechanisms other than plate tectonics can explain the wide range of observations made so far [8]. The interpretation of TTGs and the implied occurrence or absence of Archean global plate tectonics remain debated [7,11].

Boron isotope analysis—a powerful method in magmatic provenance analysis [12]—could provide the test needed to progress in this field. We used this method in conjunction with age dating and trace-element analysis on TTG samples from different Archean cratons. All samples show low B concentrations and  $^{11}\text{B}/^{10}\text{B}$  values—inconsistent with arc magmatism, yet symptomatic for magmas produced by lower-crustal melting. The data indicate that Archean TTGs did not form in subduction zones, but instead were produced by partial melting within a thickened lithospheric pile [8,10]. This mechanism dominated crustal growth and differentiation at least until 2.8 Ga. With other arc analogues lacking in the Archean rock record, it appears that modern-style plate tectonics was the consequence, rather than the cause, of Archean lithospheric change.

[1] Konhauser et al. (2009) *Nature* 458, 750-753; [2] Tang et al. (2016) *Science* 22, 372-375; [3] Smit & Mezger (2017) *Nature Geosci.* 10, 788–792; [4] Cutts et al. (in revision) *Earth Planet. Sci. Lett.*; [5] Dhuime et al. (2012) *Science* 335, 1334-1336; [6] Næraa et al. (2012) *Nature* 485, 627-30; [7] Moyen and Martin (2014) *Lithos* 148, 312-336; [8] Kamber (2015) *Prec. Res.* 258, 48-82; [9] van Kranendonk et al. (2007) *Terra Nova* 19, 1-38; [10] Johnson et al. (2017) *Nature* 543, 239-242; [11] van Hunen & Moyen (2012) *Ann. Rev. Earth Planet. Sci.* 40, 195-219; [12] Ryan, J.G., Chauvel, C. (2014) *Treatise Geochem.* 3, 479-508.

9:45am - 10:00am

### A new Titanium excess phase saturation thermometer for silicate melts with implications for conditions of Archean crust formation

Alexander Wellhäuser<sup>1,2,3</sup>, Tracy Rushmer<sup>1</sup>, John Adam<sup>1</sup>, Gerhard Wörner<sup>2</sup>

<sup>1</sup>Macquarie University, Australia; <sup>2</sup>Georg August University, Germany; <sup>3</sup>Nanjing University, P.R. China

We have calibrated a new titanium excess phase (rutile, ilmenite) saturation thermometer via regression with an extensive experimental literature database of 375 experiments. Based on statistical analysis, we find temperature and melt polymerisation, expressed as NBO/T (non-bridging oxygens per tetrahedral cation; Mysen et al., 1981) significant for the solubility of Ti in silicate melts. Additional parameters, such as pressure, H<sub>2</sub>O and Oxygen fugacity are insignificant for solubility below the liquidus. The thermometer is calibrated on mafic to felsic compositions and over a temperature range of 675 to 1450°C. The calculated temperature is the liquidus temperature at which a composition is saturated with a Ti excess phase. Our model results in following solubility relation:

$$\log_{10}(\text{Ti}) = -2.83 \pm 0.05 + 0.00241 * T \pm 0.00006 + 2.4 * \text{NBO/T} \pm 0.1 - 1.9 * (\text{NBO/T})^2 \pm 0.2$$

Ti concentration is given in mol%, temperature (T) in °C and NBO/T is the parameter describing melt polymerisation .

We apply the Ti excess phase saturation thermometer to tonalite-trondhjemite-granodiorite (TTG) compositions, which are the characteristic granitoids of Archean cratons to better constrain conditions of their formation. By comparing natural TTG compositions with experimental melts that are saturated in a Ti-excess phase, we can distinguish between TTGs that are Ti excess phase saturated from those that are undersaturated. Less evolved compositions are more commonly undersaturated. The calculated temperatures of Ti-saturated compositions using our new calibration are between 750 and 900°C. TTGs that are at the liquidus over this temperature range should be hydrous melts with 10 to 15 wt% dissolved H<sub>2</sub>O. This is either due to low degrees of melting, fluid presence during melting and/or crystal fractionation. Undersaturated TTGs most likely formed from higher degree melting, at higher temperatures.

The TTG database also allows us to consider the potential role the Ti-excess phases may have in controlling their Nb and Ta depletion. We find that – contrary to expectation, all TTG are relatively depleted in Nb, i.e. have superchondritic La/Nb ratios, irrespective of whether they are saturated in a Ti-excess phase or not. This can be explained only if (1) the Nb depletion is inherited from the TTG source or (2) that TTGs were once Ti-phase saturated but lost this condition by mixing with low-Ti more mafic magmas.

Mysen, B. O., Virgo, D., & Kushiro, I. (1981). The structural role of aluminium in silicate melts—a Raman spectroscopic study at 1 atmosphere. *American Mineralogist*, 66(7-8), 678-701.

10:45am - 11:00am

### In-situ identification of Archean high Th and U zircons in Jack Hills metasediment

Martina Menneken<sup>1</sup>, Alexander Nemchin<sup>2</sup>, Thorsten Geisler<sup>1</sup>, Martin Whitehouse<sup>3</sup>

<sup>1</sup>University of Bonn, Department of Geosciences, Germany; <sup>2</sup>Curtin University, Faculty of Science and Engineering, Perth, Australia; <sup>3</sup>Swedish Museum of Natural History, Department of Geosciences, Stockholm, Sweden

Since the first 500 Million years of Earth's geological history are inaccessible for direct analyses with respect to whole rock samples, detrital zircon grains with ages of up to about 4.4 Ga from the Jack Hills greenstone belt, in Western Australia, have been the focus of many studies. However, conclusions drawn from these studies do not completely concur. Some data seem to indicate conditions were quite similar to conditions found on modern Earth, while other data suggest long term isolation of the Hadean proto-crust, which cannot be achieved with a fully operating “conveyer belt” process. Most of these studies focus solely on “zircon concentrates”, which are obtained by crushing and processing a whole rock sample and then separating the

detrital zircon grains. With this method a large amount of zircon grains can be obtained and analysed. However, all information related to deposition and potential alteration inside the meta-sediment is lost. Since it has already been shown by inclusion and  $\delta^{18}\text{O}$  data that some grains have been altered after deposition, we identified and characterised 17 zircon grains in-situ, i.e., in thin sections of the Jack Hills meta-conglomerate. Their Pb-Pb-age distribution, obtained by SIMS analyses, appears to be similar to conventionally separated zircons with ages between 3 and > 4 Ga, indicating that they are from a similar aged source region to those zircon grains. However, all of the zircons identified in this study have Th and U concentrations that are by a factor of up to 100 higher than zircon grains obtained by conventional methods, typical for zircon crystals that formed during late stages in felsic magmas, and have accordingly accumulated a significant amount of radiation damage as shown by Raman spectroscopy. These results emphasise very stable conditions throughout the first billion years of Earth's history in the Yilgarn craton region, where (felsic?) material was generated in a repeated cyclic process between 4.4 and about 3.0 Ga. More importantly, we are able to show that conventional zircon separation methods, involving crushing and grinding, not only skew the results by particularly losing small-sized grains, but the process of crushing and grinding also destroys information about the local paragenesis as well as those zircons that are strongly metamict and thus less resistant against physical forces.

**11:00am - 11:15am**

### **Constraints on Earth's Paleoproterozoic crustal evolution by bulk Lu-Hf isotope analysis of single zircon grains**

**Alessandro Maltese<sup>1</sup>, Klaus Mezger<sup>1</sup>, Dewashish Upadhyay<sup>2</sup>, Erik Scherer<sup>3</sup>**

<sup>1</sup>University of Bern, Switzerland; <sup>2</sup>Indian Institute of Technology, Kharagpur, India; <sup>3</sup>Westfälische Wilhelms-Universität, Münster

Constraining the evolution of Earth's crust-mantle system using geochemical tracers requires robust age information and high precision determination of initial radiogenic isotope ratios. In-situ isotope investigations of individual growth zones in zircon are a common approach for obtaining U-Pb ages and initial Hf isotope compositions for the same spot or at least for the same grain. This has the potential to more reliably constrain the differentiation history of the silicate Earth as compared to bulk analyses of ancient whole rocks, whose isotopic signatures 1) may be more readily disturbed and 2) may not have been set at the time given by the U-Pb zircon (or other) age of the rock. However, in-situ methods produce  $\epsilon\text{Hf}$  data of only modest precision ( $\geq 1$   $\epsilon$ -unit), albeit at high spatial resolution. In particular, inaccurate corrections of Yb isobaric interference commonly generate scatter among calculated initial Hf isotope ratios, making it difficult to distinguish among the early terrestrial reservoirs.

An alternative approach is to select individual zircon grains from populations where the U-Pb systematics, measured by LA-ICP-MS, are intact and the crystallization age can be well constrained. For this study on early Archean rocks, the best preserved zircon grains were selected for determination of their bulk Hf-isotope composition by MC-ICP-MS after chemical purification of Hf. This yields high precision Hf isotope measurements with uncertainties of better than 0.3  $\epsilon$ -units. In addition, data scatter is drastically reduced as compared to in-situ analyses. Thus, the results provide a much higher resolution for differentiation processes recorded by early Archean rocks.

We applied this bulk Lu-Hf method to single zircon grains from TTGs of the Archean Bastar Craton, India. The oldest sample, with an age of 3.58 Ga, yields  $\epsilon\text{Hf} = +1.60 \pm 0.14$ . Younger samples progressively yield lower  $\epsilon\text{Hf}$  values down to  $\epsilon\text{Hf} = -3.06 \pm 0.18$ . These data are similar to Hf isotope signatures from other Paleoproterozoic terranes that imply near-chondritic reservoirs for TTGs. This, together with the global Hf isotope record, suggests that only moderate amounts of continental crust formed by the Paleoproterozoic. Furthermore, the results highlight the potential for bulk single zircon Hf analysis as an alternative to in-situ investigations.

**11:15am - 11:30am**

### **Formation of charnockitic silicic rocks in the Archean: a case study from Coorg, S. India**

**Sampriti Basak<sup>1</sup>, Aitor Cambeses<sup>2</sup>, Sumit Chakraborty<sup>3</sup>**

<sup>1</sup>*Institut für Geologie, Mineralogie und Geophysik, Ruhr-Universität Bochum, Bochum, Germany;* <sup>2</sup>*Institut für Geologie, Mineralogie und Geophysik, Ruhr-Universität Bochum, Bochum, Germany;* <sup>3</sup>*Institut für Geologie, Mineralogie und Geophysik, Ruhr-Universität Bochum, Bochum, Germany*

Studies on Archean silica-rich rocks provides insight into the continental crust forming processes. In the Coorg Block in S. India huge exposures of orthopyroxene bearing granitoids (enderbites) are preserved. The enderbites and mafic granulites are spatially, compositionally and temporally related. We have used bulk compositional data of the enderbitic and mafics rocks for thermodynamic phase equilibria modelling (Perple\_X software [1] with thermodynamic data from [2,3] to geochemically model different pathways for the generation of the observed enderbitic rocks. Two processes are critical and common to all pathways: (1) To produce a significant amount of melt (15-30 vol. %) from the mafic granulite, the presence of water (2-6 wt %) at pressures between 6-20 kbar and a temperature range of 850°C to 1000°C is necessary to facilitate the depression of melting point. (2) The ascent of the melt to shallower depths and crystallization, accompanied by gradual dehydration is essential for producing Opx-bearing granitoids. We use measured geochemical data from the rocks to show that the calculated trends are compatible with observations. The global prevalence of these unique set of enderbitic rocks mostly to the late Archean-Proterozoic eon is possibly the consequence of early 'peeling off' style of plate tectonics [4]. This geodynamic scenario provides the necessary setting for deep burial and hydration of mafic crust to initiate melting, as well as shallow hot regions where melt could ascend, pool, and crystallize. In special tectonic settings where these conditions are obtained, enderbitic rocks may also be generated at later times in the history of the Earth.

[1] Connolly, J.A.D. (1990) American Journal of Science. 290, 666-718; [2] Holland and Powell (2011) J. Metamorph. Geol. 29, 333-383; [3] Green et al. (2016) J. Metamorph. Geol. 34, 845-869; [4] Chowdhury et al. (2017) Nat. Geosci. 10, p. 698

**11:30am - 11:45am**

### **182W isotope patterns in mantle derived and crustal rocks from the Pilbara Craton, NW Australia**

**Jonas Tusch<sup>1</sup>, Carsten Münker<sup>1</sup>, Mike Jansen<sup>1</sup>, Eric Hasenstab<sup>1</sup>, Chris S. Marien<sup>1</sup>, Florian Kurzweil<sup>1</sup>, Martin van Kranendonk<sup>2</sup>**

<sup>1</sup>*Universität zu Köln, Germany;* <sup>2</sup>*Australian Center for Astrobiology, University of New South Wales, Australia*

The record of <sup>182</sup>W isotope anomalies in terrestrial rocks has recently been expanded from the Archean to the Phanerozoic. Unfortunately, most <sup>182</sup>W isotope studies only provide "snapshots" of the early terrestrial rock record and do not consider elemental W redistribution by secondary processes that would also affect <sup>182</sup>W isotope systematics. This might obscure the original W isotope composition of parental mantle sources and can complicate the reconstruction of the secular <sup>182</sup>W isotope evolution.

Here, we attempt to assess the long-term evolution of <sup>182</sup>W isotope patterns during the Archean by studying mantle-derived and crustal rocks from the Pilbara Craton, NW Australia. Mantle-derived rocks provide snapshots of the ambient mantle composition, whereas the crustal rocks provide a long-term average of crust-mantle evolution. By combining <sup>182</sup>W isotope analyses with high-precision isotope dilution measurements for HFSE, U, and Th, we demonstrate the preservation of primary geochemical signatures in our sample selection, which allows for the reconstruction of the <sup>182</sup>W isotope composition of the ambient mantle in NW Australia. Mantle-derived rocks from the oldest Warrawoona Group display uniform excesses and define a mean  $m^{182}\text{W}$  of  $+12.1 \pm 2.1$  ppm (95% CI). Younger rocks from the the Kelly and Soanesville groups document that <sup>182</sup>W isotope anomalies decrease between 3465 and 3340 Ma to ca +5 ppm and vanish by c. 3190 Ma. Diminishing <sup>182</sup>W isotope anomalies in the Pilbara Craton are also archived in shales and granitoid rocks, which provide an integration of the lithosphere. These rocks are characterized by a lower <sup>182</sup>W isotope

anomaly of  $+8.0 \pm 1.2$  ppm (95% CI). Similar to the evolution of mantle-derived rocks, anomalies in granitoids slightly decrease with decreasing age and are higher in less evolved rocks. The origin of elevated  $^{182}\text{W}$  isotope compositions in Pilbara rocks, and their decline to modern mantle values, is consistent with a progressive in-mixing of late veneer material, as previously suggested by decreasing PGE depletions in rocks from the same lithostratigraphic units [1].

[1] Maier et al. (2009) *Nature* **460**, 620-623.

**11:45am - 12:00pm**

## **Hafnium and Nd isotope constraints on Archean mantle-depletion processes from the Pilbara Craton, NW Australia**

**Eric Hasenstab<sup>1</sup>, Jonas Tusch<sup>1</sup>, Christiane Schnabel<sup>1</sup>, Christian S. Marien<sup>1</sup>, Vera Schmitt<sup>1</sup>, Martin Van Kranendonk<sup>2</sup>, Carsten Münker<sup>1</sup>**

<sup>1</sup>Universität zu Köln, Germany; <sup>2</sup>Australian Centre for Astrobiology

Hafnium and Nd isotope patterns of mafic to ultramafic samples have become an excellent tool for investigating the depletion history of the Archean mantle. The Pilbara Craton in NW Australia is particularly suitable for Archean mantle studies due to its weak metamorphic overprint and the long time of volcanic activity (ca. 3.6 - 2.7 Ga). Hence, we analyzed 45 basalts, komatiites and felsic rocks from the Pilbara Craton for their trace element and their initial Hf and Nd isotope compositions.

Our Hf and Nd data are consistent with the small amount of previously published Hf and Nd data from the Pilbara Craton [1–3]. All Paleoarchean metabasalts and komatiites are characterized by positive initial  $\epsilon\text{Nd}(i)$  (+0.2 to +2.0) and  $\epsilon\text{Hf}(i)$  values (0.0 to +4.6), suggesting that these rocks were derived from a long-term depleted mantle reservoir. The  $\epsilon\text{Hf}(i)$  and  $\epsilon\text{Nd}(i)$  values decrease with increasing crystallization age, which is in accordance with an origin from an isolated depleted mantle domain that likely started to differentiate in the Hadean. Furthermore, covariations between  $\text{La}/\text{Yb}_{\text{CN}}$  and  $\epsilon\text{Hf}(i)$  and  $\epsilon\text{Nd}(i)$  values are observed which imply that these melts have interacted with a second component that was isotopically more enriched, likely reflecting crustal contamination. However, all of the studied Paleoarchean samples lack pronounced negative Nb-Ta anomalies that would be expected if felsic crust was assimilated. Rather, AFC-modelling suggests that mafic crust was assimilated which is also in accordance with generally low Th/Yb (0.10-0.67) ratios observed in our samples.

Between ca. 3.35-3.25 Ga, radiogenic isotope patterns change, and  $\epsilon\text{Hf}(i)$  and  $\epsilon\text{Nd}(i)$  values first decrease and eventually increase sharply at 3.18 Ga, which is also confirmed by previously published Nd data [3]. The decrease in  $\epsilon\text{Hf}(i)$  and  $\epsilon\text{Nd}(i)$  values is best explained by a partial convective overturn of mafic crust [4] that became gravitationally unstable and re-enriched the mantle. The sudden shift towards radiogenic composition can then be explained by influx of more depleted asthenospheric material. The key implication of our study is that mantle-crust differentiation had likely already begun in the Hadean, whereas two different processes (crustal contamination and partial convective overturn of mafic crust) affected the composition of the basalts and komatiites to various degrees.

[1] Smithies et al. (2007) GSWA, open file report 104, 48; [2] Gardiner et al. (2017) *Precambrian Res.* 297, 56-76; [3] Arndt et al. (2001) *Geological Society of America*, 359–387; [4] Collins et al. (1998) *J. Struct. Geol.* 20, 1405–1424.

**12:00pm - 12:15pm**

## **PGE and Re-Os isotope systematics of 3.46 Ga meta-komatiites from the Dwalile Greenstone Remnant, Swaziland**

**J. Elis Hoffmann<sup>1</sup>, Patrick Gans<sup>1</sup>, Alfred Kröner<sup>2</sup>**

<sup>1</sup>Freie Universität Berlin, Germany; <sup>2</sup>Universität Mainz, Germany

Based on the PGE abundances of high degree mantle melts, it has been proposed that chondritic material was mixed into the Earth's mantle throughout the Archean [1]. In contrast, Eoarchean mantle peridotites show almost the full inventory of PGE [2], suggesting either a heterogeneous mantle or the full inclusion of late veneer by c. 3.8 Ga. Here we measured geochemically well-characterized serpentinized meta-komatiites and meta-komatiitic basalts from the 3.46 Ga Dwalile greenstone remnant in SW Swaziland for their Re-Os isotope composition and PGE abundances to place constraints on the PGE contents of their mantle sources. Primitive mantle-normalized PGE patterns are flat and show ca. 0.3 to 2 times depletion and enrichment compared to the primitive mantle estimate as well as a strong Re depletion. The measured <sup>187</sup>Os/<sup>188</sup>Os isotope compositions of mafic to ultramafic samples vary from 0.1041 to 0.5473, indicating crustal contamination by older felsic crust as is also supported by Sm-Nd and Lu-Hf isotope and trace element systematics. The least contaminated samples yielded initial <sup>187</sup>Os/<sup>188</sup>Os isotope compositions of 0.1034, close to the chondritic composition at 3.46 Ga. Meta-komatiites with primary melt-like MgO concentrations of ca. 28 wt.% yield partly lower PGE abundances than modern BSE. However, others of these samples have strongly enriched PGE abundances, arguing heterogeneous PGE abundances in the sources. This contrasts to the PGE inventory of the 3.48 Ga Komati Fm. and 3.5 Ga Schapenburg Fm., which both are in close areal proximity to the Dwalile greenstone remnant, indicating large heterogeneities within the Palaeoarchean mantle.

**12:15pm - 12:30pm**

## **Inferences on crustal growth and mantle heterogeneity from open system models of the Earth**

**Seema Kumari<sup>1,2</sup>, Andreas Stracke<sup>2</sup>, Debajyoti Paul<sup>1</sup>**

<sup>1</sup>Department of Earth Sciences, Indian Institute of Technology, Kanpur, India; <sup>2</sup>Institut für Mineralogie, Westfälische Wilhelms-Universität, Münster, Germany

We use an open system geochemical model for the Earth, comprising Earth's major silicate reservoirs (bulk continental crust (CC), depleted upper mantle (UM), lower non-chondritic mantle (LM) and an isolated reservoir (IR)), to simulate the Nd-Hf isotope evolution through Earth's history. Various crustal growth scenarios, e.g., continuous versus episodic and early versus late crustal growth, and their effect on the evolution of the Hf-Nd isotope systematics in the silicate reservoirs have been evaluated. The most plausible model-derived solution is the one that produces the present-day concentrations as well as isotopic ratios in terrestrial reservoirs, constrained from published data. Modeling results suggest that a whole mantle that is compositionally similar to the present-day MORB source is not consistent with observational constraints. However, a heterogeneous mantle model, in which the present-day UM is ~60% of the total mantle mass and a lower non-chondritic mantle, reproduces the estimated isotopic ratios and abundances in Earth's silicate reservoirs.

Our results show that the mode of crustal growth strongly affects the isotopic evolution of the silicate Earth; only an exponential crustal growth pattern satisfactorily explains the chemical and isotopic evolution of the crust-mantle system. The exponential crustal growth model requires early differentiation of mantle to form 30% of present-day CC mass by the end of Hadean and 75% by the end of the Archean. The complementary depletion of the UM is diminished by crustal recycling and efficient mixing in the initial 900 Myr. A primitive composition of the LM is maintained due to limited mass exchange with other silicate reservoirs and long-term isolation of recycled crustal material in the IR. Over time, the Ga-long isolation of recycled crustal relics in the IR leads to a flux of isotopically different material into the LM, and may have some similarity to transient reservoirs (such as Large Low Shear Velocity Provinces) near the core-mantle boundary.

## 2) Structure and evolution of planetary bodies

### 2a) Petrology, volcanism and surface processes on terrestrial bodies

Tuesday, 24/Sep/2019: 8:30am - 10:00am & 10:45am - 11:15am

**Session Chair: Christian J. Renggli** (Universität Münster)

**Session Chair: Andreas Markus Morlok** (Westfälische Wilhelms-Universität Münster)

**Session Chair: Iris Weber** (Westfälische Wilhelms Universität)

**Location: Schloss: Aula**

#### Session Abstract

In this session, we look for contributions from the fields of experimental petrology and volcanology, observational geology, remote sensing planetology, and the development of planetary analogue materials for the study of rocky bodies including the Moon, Mercury, Venus, Mars, the Galilean moons of Jupiter, Titan, asteroids and also comets. We invite contributions from experimentalists who use laboratory based methods to test processes in planetary interiors and on their surfaces, and results from the investigation of analogue materials to provide standards for remote observations. Remote observations from planetary missions provide information on the scale, dynamics and relative ages of volcanic and geologic processes from bodies where direct samples and landing missions are limited or not available. Additionally, a number of spectroscopic methods (IR, UV, X-rays, gamma rays or neutrons) provide information on the chemistry and mineralogy of planetary surfaces.

#### Lecture Presentations

**8:30am - 9:00am Session Keynote**

#### Building the volcanic crust of Mercury

**Bernard Charlier<sup>1</sup>, Mikael Beuthe<sup>2</sup>, Olivier Namur<sup>3</sup>, Attilio Rivoldini<sup>2</sup>, Tim Van Hoolst<sup>2</sup>**

<sup>1</sup>University of Liege, Belgium; <sup>2</sup>Royal Observatory of Belgium, Belgium; <sup>3</sup>KU Leuven, Belgium

Unique physical and chemical characteristics of Mercury have been recently revealed by measurements from NASA's MESSENGER spacecraft. The closest planet to our Sun is made up of a large metallic core that is partially liquid, a thin mantle thought to be formed by solidification of a silicate magma ocean, and a relatively thick crust. The crust of Mercury was built over the first billion years of the planet by intense volcanic activity. Mantle melting and emplacement of lava to the surface produced a secondary magmatic crust varying spatially and over time in composition and mineralogy. We have made calculations of the thickness of the crust using the MESSENGER gravity and topography data and taking into account lateral variations of crustal density. The mineralogy at the surface translates to pore-free crustal densities of 2,800-3,150 kg.m<sup>-3</sup>. Maximum crustal density (3,100-3,150 kg.m<sup>-3</sup>) is found in High-Mg regions that are forsterite-dominated and plagioclase-poor. The lightest crust (2,750-2,800 kg.m<sup>-3</sup>) is found in Al-rich regions such as the North Volcanic Plain that are plagioclase-dominated. We find that the calculated local thickness of the crust is correlated with the degree of mantle melting calculated using surface compositions obtained by X-ray spectrometry on board MESSENGER. Low-degree melting of the mantle below the Northern Volcanic Plains produced a thin crust while the highest melting degree in the ancient High-Mg region produced the thickest crust, excluding mantle excavation by an impact in that region.

9:00am - 9:15am

## Infrared Spectroscopy of Synthetic Planetary Analogs for Mercury for the BepiColombo Mission

**Andreas Markus Morlok<sup>1</sup>, Bernard Charlier<sup>2</sup>, Christian Renggli<sup>3</sup>, Stephan Klemme<sup>3</sup>, Oliver Namur<sup>4</sup>, Cristian Carli<sup>5</sup>, Martin Sohn<sup>6</sup>, Iris Weber<sup>1</sup>, Aleksandra N. Stojic<sup>1</sup>, Maximilian Reitze<sup>1</sup>, Harald Hiesinger<sup>1</sup>, Joern Helbert<sup>7</sup>**

<sup>1</sup>Institut für Planetologie, Westfälische Wilhelms-Universität Münster, Germany; <sup>2</sup>University of Liege, Sart-Tilman, Belgium; <sup>3</sup>Institut für Mineralogie, Westfälische Wilhelms-Universität Münster, Germany; <sup>4</sup>Department of Earth and Environmental Sciences, KU Leuven, Leuven, Belgium; <sup>5</sup>IAPS-INAF, Rome, Italy; <sup>6</sup>Hochschule Emden/Leer, Emden, Germany; <sup>7</sup>Institute for Planetary Research, DLR, Berlin, Germany

The purpose of the IRIS (Infrared and Raman for Interplanetary Spectroscopy) laboratory is to produce spectral data for the comparison with results from the ongoing ESA/JAXA BepiColombo mission to Mercury [1]. The mid-infrared spectrometer MERTIS (Mercury Radiometer and Thermal Infrared Spectrometer) will map the surface mineralogy in the 7-14  $\mu\text{m}$  range (resolution  $\sim$  500 meters) [2-5].

Impact cratering, lava extrusion and explosive volcanic eruptions are processes which played a central part in the formation of the surface of Mercury [e.g. 6]. This led to the formation of glasses whose ordered microstructures are missing and which were rapidly quenched from high temperature melts [7].

We produce synthetic analog glasses with compositions determined by remote sensing to obtain infrared spectra of materials, which are not available in our collections [8-10]. Furthermore, we use synthetic analog material to investigate the gas-solid reaction between S-rich gases produced in early volcanism and in impacts with silicate minerals on early Mercury and its effect on the mineralogy [11].

We measured FTIR diffuse reflectance spectra of powder size fractions 0-25  $\mu\text{m}$ , 25-63  $\mu\text{m}$ , 63-125  $\mu\text{m}$ , and 125-250  $\mu\text{m}$ . We used a Bruker Vertex 70 infrared system with a MCT detector at the IRIS laboratories at the Institut für Planetologie in Münster. We conducted the analyses at low pressure (10-3bar) to reduce atmospheric bands from 2-18  $\mu\text{m}$ . For additional FTIR microscope analyses of polished thick sections, we applied a Bruker Hyperion 1000/2000 System at the Hochschule Emden/Leer with a 250 $\times$ 250  $\mu\text{m}$  sized aperture.

This work was partly supported by DLR grant 50 QW 1701 in the framework of the BepiColombo mission.

[1]Weber I. et al. (2018) 49th LPSC Abstract #1430; [2]Maturilli A. (2006) Planetary and Space Science 54, 1057–1064; [3]Helbert J. and Maturilli A. (2009) Earth and Planetary Science Letters 285, 347-354; [4]Benkhoff J. et al. (2010) Planetary and Space Science 58, 2-20; [5]Hiesinger H. et al. (2010) Planetary and Space Science 58, 144–165; [6]Fasset C.I.(2016) Journal of Geophysical Research: Planets 121, 1900-1926; [7]Lee et al. (2010) Journal of Geophysical Research 115 1-9; [8]Namur and Charlier (2017) Nature Geoscience 10, 9-15; [9]Namur O. et al. (2016) Earth and Planetary Science Letters 448, 102-114; [10]Namur O. et al. (2016) Earth and Planetary Science Letters 439, 117-128; [11]Renggli C. and King P. (2018) Rev.Min.Geochem 84, 229-255

9:15am - 9:30am

## A shock recovery experiment: Tracing Spectral Fingerprints of Impact Melt, npFe and Element Migration in Shocked Porous Materials

**Aleksandra N. Stojic<sup>1</sup>, Andreas Morlok<sup>1</sup>, Martin Sohn<sup>2</sup>, Harald Hiesinger<sup>1</sup>, Tomas Kohout<sup>3</sup>, Hagen Aurich<sup>4</sup>, Iris Weber<sup>1</sup>, Joern Helbert<sup>5</sup>**

<sup>1</sup>WWU Muenster, Germany; <sup>2</sup>Hochschule Emden/Leer, Germany; <sup>3</sup>University of Helsinki, Finland; <sup>4</sup>Ernst - Mach Institut, Germany; <sup>5</sup>DLR Berlin, Germany

Here we present Micro FTIR data from ongoing work on shocked olivine (San Carlos) and pyroxene (Bamblé) powders that will complement the mid-infrared database for the next ESA/JAXA mission BepiColombo to Mercury [1,2].

Apart from “classic” mineral mixtures that will comprise the database, also Mercury’s specific surface conditions and their various effects on the exposed planetary regolith have to be taken into account. This is important, when it comes to the qualitative and quantitative interpretation of spectral information that we will obtain from the MERTIS instrument once BepiColombo reaches the Hermean orbit. Mercury lacks a shielding atmosphere and its peculiar magnetic field allows for cosmic radiation, solar wind and (micro-)

meteorite impactors to hit the planetary surface to full extent in vast areas. These processes are commonly known as space weathering (SW) [3], which is a considerable factor, altering unshielded planetary regolith significantly. Not only in terms of structural decay of the regolith comprising minerals, melt production, solar wind implantation and the numerous intermediate states, but also in terms of their spectral signature that such a “re-worked” surface will give us. Considering the long exposure times, these changes (extreme discrepancy of day – and night time temperatures, proton implantation, impactors, etc.) can probably obscure characteristic mineral spectra as we know them under terrestrial conditions to the point of no recognition. In order to interpret the awaited MERTIS data correctly and quantitatively, our intention is to incorporate “Mercury-adjusted” analog material in our MERTIS database. We therefore conducted classic shock recovery experiments to account for impact events that cause interstitial melt or complete melting of regolith grains.

[1] Benkhoff, J., et al., *Planetary and Space Science*, 58.1-2, pp. 2-20, 2010; [2] Hiesinger, H., J. Helbert, and MERTIS Co-I. *Planetary and Space Science* 58.1-2, pp. 144-165, 2010; [3] Domingue, D. L., et al., *Space Science Reviews*, 181.1-4, pp. 121-214, 2014.

**9:30am - 9:45am**

### **Present-day Activity of Slope Streaks on Mars**

**Thomas Heyer<sup>1</sup>, Misha Kreslavsky<sup>2</sup>, Harald Hiesinger<sup>1</sup>, Dennis Reiss<sup>1</sup>, Hannes Bernhardt<sup>3</sup>, Ralf Jaumann<sup>4</sup>**

<sup>1</sup>Institut für Planetologie, Westfälische Wilhelms-Universität, Münster, Germany; <sup>2</sup>Earth and Planetary Sciences, University of California, Santa Cruz, USA; <sup>3</sup>School of Earth and Space Exploration, Arizona State University, USA;

<sup>4</sup>German Aerospace Center (DLR), Berlin, Germany.

Slope streaks are gravity-driven dark or light-toned features that form throughout the martian year in high-albedo and low-thermal inertia equatorial regions on Mars [e.g., 1, 2]. These distinctive features have never been observed in a terrestrial environment or laboratory. However, morphologically similar features on Earth are formed by avalanches of dry, loose snow [3] or by percolation of meltwater in the subsurface above the ice table in the Antarctic Dry Valleys [4]. Based on diverse orbital observations, a number of mechanisms including granular [e.g., 1] and aqueous flows [e.g., 4] have been proposed to explain their formation on Mars. Using multi-temporal images taken by the Context Camera (CTX) [5] aboard the Mars Reconnaissance Orbiter (MRO), we identified newly formed streaks in multiple martian years and estimated seasonal streak formation rates at intermediate latitudes, as well as at the equator. We found seasonal variations in streak activity in multiple consecutive martian years, including high formation rates during autumn (solar longitude  $L_s \sim 190^\circ$ ). During this time, slope streak activity exceeds the long-term formation rate multiple times. The highest seasonal formation rate of 0.16% per streak per martian day was observed in the Olympus Mons aureole in autumn ( $L_s \sim 210^\circ$ ) of Mars year 30. In some sites, slope streak formation rate at slopes of opposite orientation peaks at different seasons. The seasonal variations of the formation rate are inconsistent with sporadic trigger mechanisms and revealed that changing conditions at the slopes affect the formation of the streaks throughout the martian year. Modelled environmental parameters at the streak-bearing slopes indicate a correlation between seasonal streak activity and surface temperature, as well as wind velocity. Seasonal variations of streak activity could be a result of varying intensities of both dry and wet mechanisms or could be explained by the interaction of multiple mechanisms. The strong year-to-year variability in the seasonal cycle of slope streak formation suggests a strong effect of changing climate conditions on slope streak formation potential and/or triggering, regardless of the specific formation mechanism.

[1] Sullivan et al. (2001) *JGR*, 106, 23607–33; [2] Schorghofer and King (2011) *Icarus*, 216, 159–68; [3] Baratoux et al. (2006) *Icarus*, 183, 30–45; [4] Kreslavsky and Head (2009) *Icarus*, 201, 517–27; [5] Malin et al. (2007) *JGR*, 112, E05S04.

9:45am - 10:00am

### **A volcanic ash layer in the Miocene Nördlinger Ries impact structure (Germany): Indication of crater fill geometry and long-term crater floor sagging**

**Gernot Arp<sup>1</sup>, István Dunkl<sup>1</sup>, Gerald Hartmann<sup>1</sup>, Dietmar Jung<sup>2</sup>, Volker Karius<sup>1</sup>, Réka Lukács<sup>3</sup>, Andreas Reimer<sup>1</sup>, Michael Wolff<sup>4</sup>, Jim Head<sup>5</sup>**

<sup>1</sup>Georg-August-Universität Göttingen, Germany; <sup>2</sup>Bayerisches Landesamt für Umwelt, Hof/Saale, Germany; <sup>3</sup>MTA-ELTE Volcanology Research Group, Budapest, Hungary; <sup>4</sup>Münchshecke 1B, Siegburg, Germany; <sup>5</sup>Brown University, Providence, USA

Since its recognition as an astrobleme, volcanic rocks were not expected to occur in the Nördlinger Ries impact structure. Here, we describe for the first time a strongly altered, zeolitized volcanic ash layer composed mostly of clinoptilolite, heulandite and buddingtonite within the 330 m thick Miocene lacustrine crater fill of the 26-km-sized impact structure. Single grain zircon U-Pb ages of 14 Ma and trace element characteristics of allanite crystals point to the Bükkalja Volcanic Field in the Pannonian Basin, 760 km east of the Nördlinger Ries, as the source of the volcanic ash. The diagenetically derived zeolite-feldspar bed is intercalated in laminated claystones of the soda lake stage and represents the first unequivocal stratigraphic marker bed in this basin, traceable from marginal surface outcrops to 218 m below surface in the crater centre. Thereby, it demonstrates a deeply bowl-shaped geometry of crater fill sediments, not explainable by sediment compaction and corresponding stratigraphic backstripping alone. Since most of the laminated claystones apparently formed at shallow water depths, the bowl-shaped geometry of the crater fill must reflect a long-term sagging of the deeply fractured and brecciated crater floor during sedimentation. As a result, the outcrop pattern of the lithostratigraphic crater fill units at its present erosional plain appears concentric, reminiscent of, but genetically different from crater fills with rhythmic layering on Mars. The apparent lack of similar sagging features in Martian lacustrine crater fills may point to a significant time lag between impact crater formation during cold and dry phases and aquatic sedimentation for most of the asteroid impacts.

10:45am - 11:00am

### **Isotopic and Trace Element Geochemistry of Karlıova-Varto volcanism (Eastern Turkey): Deciphering the mantle source, crustal contributions and its tectonic controls**

**Özgür Karaoğlu<sup>1</sup>, Fatma Gülmez<sup>2</sup>, Gönenç Göçmengil<sup>3</sup>, Samuele Agostini<sup>4</sup>, Michele Lustrino<sup>5</sup>, Paolo Di Giuseppe<sup>6</sup>, Piero Manetti<sup>7</sup>, Mehmet Yılmaz Savaşçın<sup>8</sup>**

<sup>1</sup>Eskişehir Osmangazi University, Turkey; <sup>2</sup>Institute of Geosciences, University of Mainz, Germany; <sup>3</sup>Faikbey Mescidi Sokak, No:20, Kadıköy, İstanbul; <sup>4</sup>Istituto di Geoscienze e Georisorse, Consiglio Nazionale delle Ricerche, Pisa; <sup>5</sup>Dipartimento di Scienze della Terra, Sapienza Università di Roma; <sup>6</sup>Dipartimento di Scienze della Terra, Università degli Studi di Pisa, Italy; <sup>7</sup>Istituto di Geoscienze e Georisorse, Consiglio Nazionale delle Ricerche, Italy; <sup>8</sup>Tunceli Üniversitesi, Jeoloji Mühendisliği Bölümü, Tunceli

Eastern Anatolia High Plateau (EAHP) is characterised by numerous volcanoes produced a large volume of lavas of Late Miocene to Quaternary in a wide compositional range, i.e. from basalts to rhyolites those of displaying an affinity variation calcalkaline to alkaline products. The enigmatic aspect of EAHP is the absence of widespread extension to trigger voluminous magma production, especially between late Miocene and recent when magmatism reached a maximum peak. This volcanism has been interpreted as related with the intense deformation of the region, following the Arabia-Eurasia collision. The complex mechanical interaction between colliding plates resulted in the formation of Karlıova Triple Junction (KTJ), which is one of the best provinces where different mantle sources are observed under the control of complex tectonics in the world. The early phase volcanism (~7.4-4.4 Ma) in KTJ consisting of mildly Na-alkali basalts and trachytic lavas developed along with East Anatolia Fault-related fractures. Middle phase volcanism (mostly ~3.6-2.6 Ma) characterised by volcanic products consisting of basalts to rhyolites with slightly subalkaline as well as mildly Na-alkaline affinity, emplacing as polygenetic volcanoes along Varto Fault (the east continuum of North Anatolian Fault Zone) and producing the most voluminous eruptions of the KTJ. Late Phase (1.96-0.5 Ma) within the

Muş depression represented by mostly basaltic and basaltic andesitic lavas with Na-sodic alkaline affinity. The most mafic lava samples ( $\text{SiO}_2$  wt % < 52) of early phase tend to reveal similar flattened patterns with slight enrichment of LREE relative to HREE which is evident by low La/Yb ratios on chondrite normalized REE diagram. On the contrary, the middle and late phase samples display both flattened and concave upward patterns resulted from enrichment in Light Rare Earth Element (LREE), although showing identical Heavy Rare Earth Element (HREE) depletions. These difference between these two-magma compositions is more striking in terms of Nb and Ta depletions on the primitive mantle-normalised incompatible element.

Late phase volcanic rocks are similar to coeval volcanism produced in Muş Basin and Anatolian microcontinent-west of KTJ, represented mostly by high  $^{143}\text{Nd}/^{144}\text{Nd}$  (0.51269-0.51277) and low  $^{87}\text{Sr}/^{86}\text{Sr}$  (0.70413-0.705) plotting in the depleted quadrant on Sr vs. Nd isotope diagram. However, early and middle phases have similar  $^{87}\text{Sr}/^{86}\text{Sr}$  (0.70426-0.706367), and  $^{143}\text{Nd}/^{144}\text{Nd}$  (0.51268-0.51280) showing broader variation could result from the combination of crystallization processes and source heterogeneity — the least differentiated volcanic rocks from all series mostly likely derived from an amphibole-spinel peridotitic mantle source. Possible “garnet-facies” geochemical characters can be derived from multi-step metasomatic processes developed within the lithospheric during the complex geodynamic history of the Eastern Anatolia. Anyhow, possible infiltration of the deep seated metasomatic melts possibly imprints a deep-sourced character for the most mafic volcanic rocks.

It should be noted that the Na-alkaline magma source below the KTJ, represented by the last volcanic phase, is likely affected by the asthenosphere ascending. However, the source domain hybridization and the assimilation fractional crystallization processes have completely masked the presence of this Na-Alkaline source throughout entire eastern Turkey. The rifting process since 6 Ma appears to trigger the lithospheric thinning, then resulting in mixing of melts derived from garnet-bearing sources with lithospheric melts and use the tectonic pathways for magma propagation in the KTJ region.

**11:00am - 11:15am**

### **Prebiotic synthesis in volcanic discharges: exposing porous ash to volcanic gas atmospheres**

**Christina Springsklee<sup>1</sup>, Thomas Steiner<sup>2</sup>, Thomas Geisberger<sup>2</sup>, Bettina Scheu<sup>1</sup>, Claudia Huber<sup>2</sup>, Wolfgang Eisenreich<sup>2</sup>, Corrado Cimarelli<sup>1</sup>, Donald Bruce Dingwell<sup>1</sup>**

<sup>1</sup>Ludwig Maximilian University of Munich, Germany; <sup>2</sup>Technical University of Munich, Germany

The question about the origin of life and the emergence of the first organic molecules is still unraveled. Lightning has been considered as a potential energy source for the emergence of life or alternatively as a potential energy source for the synthesis for first organic molecules. One of the most prominent abiotic synthesis experiments are the discharge experiments performed 1953 by Miller and Urey [1] under simulated reducing atmosphere conditions. The presence of volcanic ash has been largely neglected in this early study and in addition new theories about the composition of the Early Earth's atmosphere have been developed.

Volcanism associated with volcanic lightning provides a possible energy source, a variety of different, including reducing volcanic gases and possible catalysts to synthesize a variety of primitive organic molecules. Volcanic ash particles are known for their porosity, high surface area and high surface reactivity. During explosive volcanic eruptions, the occurrence of volcanic lightning has frequently been observed. Recent laboratory studies successfully recreated volcanic lightning under laboratory conditions [2,3]. As main mechanisms for the electrification of ash particles within volcanic plumes and laboratory experiments triboelectrification and fractoemission were identified [2,3,4]. Volcanic plumes themselves provide a high variety of volcanic gases including, but not limited to reducing ones, and therefore may enlarge the spectrum for possibly available gas compositions in the Early Earth exposed to volcanic lightning.

Over the last decades new theories about the composition of the Early Earth's atmosphere have been developed. This calls for a new series of discharge experiments including more oxidizing or slightly reducing atmosphere conditions in the presence of volcanic ash.

We will present first insights from volcanic discharge experiments under different atmosphere compositions, varying in CH<sub>4</sub>, H<sub>2</sub>S, CO<sub>2</sub>, CO and H<sub>2</sub>O composition to mimic some first Early Earth conditions. Special focus is given to the role of ash particles as catalysts and compartment provider and the variety and influence of gas composition on the yield of organic compounds.

[1] Miller, S.L. (1953). A production of amino acids under possible primitive earth conditions. *Science*, 117, 528-529; [2] Cimarelli, C., Alatorre-Ibargüengoitia, M.A., Kueppers, U., Scheu, B. and Dingwell, D.B. (2014). Experimental generation of volcanic lightning. *Geology*, 42, 79-82; [3] Gaudin, D. and Cimarelli, C. (2019). The electrification of volcanic jets and controlling parameters: A laboratory study. *EPSL*, 513, 69-80; [4] James, M.R., Wilson, L., Lane, S.J., Gilbert, J.S., Mather, T.A., Harrison, R.G. and Martin, R.S. (2008). Electrical charging of volcanic plumes. *Space Science Reviews*, 137, 399-418.

## Poster Presentations

### Mon: 3

#### Formation of sulfide phases on the surface of Mercury by reactions with reducing high temperature gases

**Christian J. Renggli<sup>1</sup>, Stephan Klemme<sup>1</sup>, Andreas Morlok<sup>2</sup>, Iris Weber<sup>2</sup>, Harald Hiesinger<sup>2</sup>**

<sup>1</sup>Institut für Mineralogie, Universität Münster, Germany; <sup>2</sup>Institut für Planetologie, Universität Münster, Germany

Sulfur is abundant on the surface of Mercury with average concentrations of 4 wt. % [1]. The sulfur on Mercury's surface has likely volcanic origins and may have been redistributed by explosive eruptions and impact events. In these processes, silicate materials were exposed to a hot S-rich gas phase at a very low oxygen fugacity of 4-5  $f_{O_2}$  log units below the iron-wüstite (IW) buffer [2].

We conduct experiments reacting a reducing sulfur-rich gas with synthetic basalt glasses. These glasses have compositions representative of Mercury terranes, including the high-Mg and high-Al regions, as well as the low-Mg northern volcanic plains [3]. We expose polished glass chips to a gas mixture of CO and SO<sub>2</sub> at 800 °C for 24 h, corresponding to a  $f_{O_2}$  of IW-2 to IW-5. This gas-solid reaction results in the formation of a coating similar to the reaction between SO<sub>2</sub> and basaltic glasses [4]. In addition to conventional mineralogical and chemical analysis (SEM, Raman), the resulting coatings are characterized using diffuse reflectance FTIR spectroscopy in the mid-infrared from 2.5-18 μm. The obtained spectral data will be used to interpret remote sensing data from the MERTIS spectrometer (Mercury Radiometer and Thermal Infrared Spectrometer) onboard the BepiColombo (ESA/JAXA) mission to Mercury [5]. The comparison of the spectra will allow testing of our hypothesis on high-temperature gas-solid alteration of the surface of Mercury by reduced S-rich gases.

In addition to the experiments, we conduct Gibbs free energy minimization calculations. The dominant S-bearing gas species in a C-O-S gas mixture at Mercury conditions are CS<sub>2</sub> and COS. The rock forming minerals forsterite, anorthite and diopside react in such a gas phase at 800 °C and IW-5 to form the sulfides CaS and MgS. Similarly, Na-bearing silicates react to form Na<sub>2</sub>S and Na<sub>2</sub>S<sub>2</sub>. We suggest that proposed sulfides on the surface of Mercury formed via gas-solid reactions.

[1] Nittler et al. (2011) *Science* 333, 1847-1850; [2] Zolotov M.Y. (2011) *Icarus* 212, 24-41; [3] Vander Kaaden et al. (2017) *Icarus* 285, 155-168; [4] Renggli et al. (2018) *Rev. Mineral. Geochem.* 84; [5] Hiesinger et al. (2010) *Planet. Space Sci.* 58, 144-165.

### Mon: 4

#### Excimer Laser Experiments on Mixed Silicates Simulating Space Weathering

**Iris Weber<sup>1</sup>, Andreas Morlok<sup>1</sup>, Marcel Heeger<sup>2</sup>, Thorsten Adolphs<sup>2</sup>, Maximilian P. Reitze<sup>1</sup>, Hiesinger Harald<sup>1</sup>, Karin E. Bauch<sup>1</sup>, Aleksandra N. Stojic<sup>1</sup>, Heinrich F. Arlinghaus<sup>2</sup>, Jörn Helbert<sup>3</sup>**

<sup>1</sup>Westfälische Wilhelms Universität, Institut für Planetologie, 48149 Münster, Germany; <sup>2</sup>WWU, Physikalisches Institut, 48149 Münster, Germany; <sup>3</sup>DLR, Institut für Planetenforschung, 12489 Berlin, Germany

Here we present near and mid-infrared spectra of olivine-pyroxene mineral mixtures irradiated with a pulsed ArF UV excimer laser. Our experimental set-up simulates micrometeorite bombardment as one possible source of space weathering [1,2]. The subdued transparency feature of the irradiated samples indicates grain

coarsening upon irradiation. Furthermore, the obvious darkening of the irradiated sample surface might be caused by agglutinate formation.

Petrographic and light microscope images confirmed the pure character of the sample crystals used for laser experiments. Reflectance infrared (IR) spectra obtained of olivine (Ol), pyroxene (Px), and mixtures of olivine and pyroxene with 70/30 and 30/70 (in weight %, grain size fractions: 63 – 125 µm) were compared with data of a spectral unmixing program for silicates of the same chemical composition. Results for these mixtures is in good agreement with the original sample mixtures [3]. Olivine and pyroxene show typical Christiansen Feature (CF) and Reststrahlen bands (RB) for these silicates [4]. The Ol70/Px30 mixture shows a significant blue shift of the CF. We observe a new RB shoulder at 9 µm and a peak split of the original olivine RB at 10.6 µm. The RB shoulder at 11.3 µm morphs into a separate RB feature. The CF of the Px70/Ol30 mixture shifted to higher wavelengths similar to the former pyroxene RB at 10.4 µm with a red shift to 10.5 µm and a significantly higher reflectance. It is remarkable that the olivine rich mixture exhibits more of the genuine olivine RBs than pyroxene in the pyroxene rich mixture. Results of IR investigations in vacuum on the same mineral mixtures but on pressed powder pellets before laser irradiation show a strong transparency feature (TF). After irradiation this TF disappears. The absence of this feature is indicative of grain coarsening. The TF could be used as a grain size tracer. The darkening of the sample surface is possibly also an effect of agglutination [5]. This work was partly supported by DLR grant 50 QW 1701 in the framework of the BepiColombo mission.

[1] Brunetto R. et al. *Icarus* 180, 546–554, 2006; [2] Loeffler et al. *Meteoritics & Planetary Science*, 51(2), 261-275, 2016; [3] Bauch K.E. et al. *LPSC* 50th, #2521, 2019; [4] Salisbury J. W. in: *Topics in Remote Sensing* 4, 79 – 98, 1993; [5] Stojic A. et al. *LPSC* 49th, #2083, 2018.

## Mon: 5

### Mineralogy of the weigelt-scholle

#### Patrick Winkler

*Martin-Luther-Universität, Germany*

The „Weigelt-Scholle“ is a sedimentary block with a size of 14 x 3 m, which lays in the rhyolitic porphyry of the small mountain Galgenberg in Halle (Saale) Germany. The Weigelt-Scholle was a interesting objekt for many generations of scientists over 100 years. It was first discovered by Johannes Weigelt in 1906, who then became the eponym of the Weigelt-Scholle. Other scientists such as Ernst Haase, Max Schwab und Günter Krumbiegel also did researches with the block in the first half of the 20<sup>th</sup> century. They focused on the formation of the subvolcanos in Halle and the surrounding areas.

The rhyolith of the Galgenberg takes place for 300 Ma ago, as the supercontinent Pangäa began to falling into pieces. This resulted in crustal deformations in Europe, and hot magma began to rise into the upper continental crust. This hot magma intruded into sedimentary layers, which were formed in central Europe. During this time, central Europe was divided into two regions; The Northern Perm Basin and the Southern Perm Basin. The today's Galgenberg and Halle are now located, where Southern Perm Basin used to be. As the magma rose the sedimentary layers above it got assimilated, however some parts of the layers – such as the block of the Weigelt-Scholle - broke off and fell into the magma. The block of the Weigelt-Scholle strikes SE-NW and has a dipangle of ca. 35° to the north. It is generally made of fine klastica like fine sandstone and siltstone. Furthermore, it also contains tuff breccia. The content of the bachelor thesis is to take some samples and create some thin sections to determine the mineralogy of the Weigelt-Scholle. Additionally, the thesis aims to create some profiles as well as to illustrate the genesis of the Weigelt-Scholle.

The Weigelt-Scholle consists of three different lithologies. The first lithology was an arcogenic sandstone with ca. 85% xenomorphic quartz, ca. 10% plagioclase and lots of exogenous inclusions. There were also orthoclases that were sericitized, thus, a lot of opaque dispersed hematite.

The second lithology is a reddish siltstone with lots of bright reddish round inclusions. These inclusions were once roots. In this sample, there was also a lot of dispersed hematite.

The third lithology is a red tuff with a porphyritic texture. The fourth sample is the porphyritic rhyolith, which is called *Hallescher Porphyry*.

## 2b) High-spatial resolution studies of small-scale and complex extra-terrestrial and terrestrial samples

Tuesday, 24/Sep/2019: 11:30am – 12:30pm & 3:45pm - 5:30pm

**Session Chair: Christian Vollmer** (Universität Münster)

**Session Chair: Dennis Harries** (Friedrich-Schiller-Universität Jena)

**Session Chair: Julia Roszjar** (Natural History Museum Vienna)

**Location: Schloss: Aula**

### Session Abstract

Investigations of heterogeneous samples like meteorites, interplanetary dust particles, or returned mission samples require the application of high-spatial resolution analytical techniques to minimize sample destruction and maximize contextual information. This also applies to a wide variety of terrestrial rocks and experimental analogues that document the evolution of planetary bodies (e.g., impact-generated lithologies, shocked minerals, fluid/mineral inclusions, high-pressure/high-temperature experiments, synthetic nanomaterials). In this session, we welcome contributions from geo-cosmochemistry-material sciences disciplines that make use of high-spatial resolution methods (e.g., electron microscopy, laser-ablation and secondary ion mass spectrometry, atom probe tomography, Raman spectroscopy, and synchrotron radiation techniques) that improve our understanding of small-scale chemical, isotopic and structural properties and processes. Cross-disciplinary contributions giving possible new insights into old problems are particularly encouraged.

### Lecture Presentations

**11:30am - 12:00pm** *Session Keynote*

#### **Finding a piece of Earth on the Moon?**

**Jeremy Bellucci**

*Swedish Museum of Natural History, Sweden*

A feldspar clast in lunar breccia Apollo sample 14321 has petrographic and chemical features that are consistent with formation conditions commonly assigned to both lunar and terrestrial environments. Results from Secondary Ion Mass Spectrometry trace element analyses indicate that zircon grains recovered from this clast have positive Ce/Ce\* anomalies corresponding to an oxygen fugacity +2 to +4 log units higher than that of the lunar mantle, with crystallization temperatures of  $771 \pm 88$  to  $810 \pm 37^\circ\text{C}$  ( $2\sigma$ ) that are unusually low for lunar magmas. Additionally, Ti-in-quartz and zircon calculations indicate a pressure of crystallization of  $6.9 \pm 1.2$  kbar, corresponding to a depth of crystallization of  $167 \pm 27$  km on the Moon. Such low- $T$ , high- $f_{\text{O}_2}$ , and high- $P$  have not been observed for any other lunar clasts, are not known to exist on the Moon, and are broadly similar to those found in terrestrial magmas. The terrestrial-like redox conditions inferred for the parental magma of these zircon grains and other accessory minerals in the feldspar contrasts with the presence of Fe-metal, bulk clast geochemistry, and the Pb isotope composition of K-feldspar grains within the clast, all of which are consistent with a lunar origin. The dichotomy between redox conditions recorded in the clast necessitates a multi-stage petrogenesis. Two, currently unresolvable hypotheses for the origin and history of the clast are allowed by these data. The first suggests that the relatively oxidizing conditions were developed in a lunar magma, possibly by fractional crystallization and enrichment of incompatible elements in a fluid-rich, phosphate-saturated magma, at the base of the lunar crust to form the zircon grains and their host feldspar. Subsequent excavation by the Imbrium impact introduced more typical lunar features to the clast but preserved primary chemical characteristics in zircon and some other accessory minerals. However, this hypothesis fails to explain the high  $P$  of crystallization. Alternatively, the feldspar and its zircon crystallized on Earth at a modest depth of  $19 \pm 3$  km in the continental crust where oxidizing, low- $T$ , fluid-rich conditions are common. Subsequently, the clast was ejected from the Earth during a large impact, entrained in the lunar regolith as a terrestrial meteorite with the evidence of reducing conditions introduced during its incorporation into the Imbrium ejecta and host breccia.

12:00pm - 12:15pm

## High-resolution Mg-isotope investigation of presolar silicates: New implications for the stardust inventory of the Solar System

**Jan Leitner, Peter Hoppe, János Kodolányi**

*Max-Planck-Institute for Chemistry, Germany*

A minor, but important component of primitive solar system materials are isotopically anomalous dust grains that formed in the outflows of evolved stars or in the ejecta of stellar explosions. Silicates constitute the most abundant type of such “presolar” dust available for single grain analyses [1]. The stellar sources of these grains are typically identified based on the grains’ O-isotopic compositions. In this classification scheme [2], the vast majority (~90 %) of presolar silicates with sizes of  $\geq 200$  nm are attributed to low-mass ( $1.2\text{--}2.2 M_{\text{sun}}$ ) asymptotic giant branch (AGB) stars of sub-solar to solar metallicities. An alternative source for some of these grains could be intermediate-mass ( $4\text{--}8 M_{\text{sun}}$ ) AGB stars experiencing hot bottom burning [3]. Most of the remaining grains (~10 %) come from core-collapse supernovae, while a few silicates and oxides might have formed in nova outbursts. Other than refractory phases, presolar silicates cannot be chemically extracted from their meteoritic hosts, but have to be identified *in situ* by secondary ion mass spectrometry (SIMS) at high lateral resolutions. Isotope measurements for major elements in presolar silicates other than oxygen, e.g., magnesium, require measurements with an  $\text{O}^+$  primary ion source, which were limited to 200–300 nm spatial resolution. This hindered precise systematic Mg isotopic analysis of presolar silicates until recently. The new Hyperion RF plasma  $\text{O}^+$  primary ion source installed on the MPIC’s Cameca NanoSIMS 50 allows measurements of Mg-isotopes with a spatial resolution of  $<100$  nm [4]. The isotopic composition of Mg is not expected to be modified significantly by nucleosynthesis in low-mass AGB stars when O-rich dust forms [4]; thus, they generally represent the initial isotopic compositions of their parent stars, mainly reflecting Galactic chemical evolution (GCE).

We found that a fraction of these presumed low-mass AGB star grains displayed large  $^{25}\text{Mg}$ -excesses and only small  $^{26}\text{Mg}$  excesses, incompatible with such an origin, indicating core-collapse supernovae as their sources [5]. Additionally, we identified two  $^{25}\text{Mg}$ -depleted silicates that are potential pre-supernova condensates of massive stars, and several silicate stardust grains with Mg- and O-isotopic signatures indicating formation around intermediate-mass AGB stars.

[1] Floss C. & Haenecour P. (2016) *Geochem. J.* **50**, 3–25; [2] Nittler L. R. et al. (1997) *ApJ* **483**, 475–495; [3] Lugaro M. et al. (2017) *Nat. Astron.* **1**, 0027; [4] Hoppe P. et al. (2018) *ApJ* **869**, 47–59; [5] Leitner J. & Hoppe P. (2019) *Nat Astron.*, in press.

12:15pm - 12:30pm

## Graphite in Meteorites – Occurrence, Abundance and Origin

**Jakob Storz<sup>1</sup>, Addi Bischoff<sup>1</sup>, Markus Patzek<sup>1</sup>, Surya Snata Rout<sup>2</sup>, Thomas Ludwig<sup>3</sup>, Mario Trieloff<sup>3</sup>**

<sup>1</sup>*Institut für Planetologie, WWU Münster, 48149 Münster, Germany;* <sup>2</sup>*Betriebseinheit Elektronenmikroskopie, TU Hamburg, 21073 Hamburg, Germany;* <sup>3</sup>*Klaus-Tschira-Labor für Kosmochemie, Institut für Geowissenschaften, Universität Heidelberg, 69120 Heidelberg, Germany*

Carbon, the 4<sup>th</sup> most abundant element in our solar system, is a key element for tracing Earth’s volatile element inventory. Meteorites, considered to be analogues for building blocks of terrestrial planets, exhibit several carbon-bearing phases including graphite. Therefore, the characterization of meteoritic graphite and its understanding as a carbon carrying phase is crucial. In the last decades, research on meteoritic graphite has mainly focused on isotopically anomalous presolar grains. However, larger graphite aggregates ( $>5 \mu\text{m}$ ) were rarely addressed in previous studies. Here, we report the results of the investigation of 130 graphite-bearing meteorites including ureilites, enstatite chondrites, and ordinary chondrites.

Graphite, a carbon allotrope, tends to form distinct morphologies linked to specific meteorite groups. Ureilites, the most carbon-rich meteorites (up to 7 wt% [1]), were studied extensively accounting for 62% of all investigated specimens. In ureilites, graphite occurs along silicate grain boundaries, whereas its preservation

is heavily dependent upon secondary processing of the parent body. Since the nature of the ureilite parent body (UPB) and the origin of diamond inclusions in graphite are highly controversial, the characterization of these inclusions was of particular interest. Although, enstatite chondrites generally do not exceed bulk carbon contents of 0.7 wt% [1], graphite grains have been frequently reported. Graphite predominantly occurs as subhedral to euhedral laths in association with silicate minerals and as aggregates surrounded by metal. In unequilibrated ordinary chondrites (UOCs), the carbon content is generally below 0.6 wt% [1] with no dominant carbon-bearing phase. However, well-crystallized graphite grains are present in carbon-bearing clasts as remnants of impact processing on meteoritic parent bodies. Only recently, Bischoff et al. (2018) reported graphite-bearing clasts having an O-isotopic compositions close to ureilitic material [2].

In conclusion, diverse graphite morphologies were reviewed, reflecting various formation mechanisms such as crystallization from a melt or graphitization of carbonaceous matter. Additional SIMS investigations are scheduled to further unravel the origin of these phases.

[1] Grady, M. M. & Wright, I. P. (2003) Elemental and Isotopic Abundances of Carbon and Nitrogen in Meteorites. *Space Science Reviews* **106**, 231–248; [2] Bischoff, A., Schleiting, M., Wieler, R. & Patzek, M. (2018) Brecciation among 2280 ordinary chondrites – Constraints on the evolution of their parent bodies. *Geochimica et Cosmochimica Acta* **238**, 516–541.

**3:45pm - 4:00pm**

### **Xenolithic C1 Clasts and their Relation to the Host Rocks Revealed by Chromium Isotopes and Trace Element Concentrations**

**Markus Patzek<sup>1</sup>, Yogita Kadlag<sup>2</sup>, Addi Bischoff<sup>1</sup>, Robbin Visser<sup>2</sup>, Harry Becker<sup>2</sup>, Timm John<sup>2</sup>**

<sup>1</sup>Westfälische Wilhelms-Universität, Institut für Planetologie Münster, Wilhelm-Klemm-Str. 10, D-48149 Münster, Germany; <sup>2</sup>Freie Universität Berlin, Institut für Geologische Wissenschaften, Malteserstr. 74-100, 12249 Berlin, Germany

Xenolithic CI- and CM-like clasts can be found in various chondrite and achondrite breccias including ordinary and CR chondrites as well as ureilites and HEDs [1-3]. CI-like clasts from different host meteorites and CI chondrites exhibit different H and O isotope signatures as well as different S isotopic distributions of their sulfide grains, although they have a very similar mineralogy [4-6]. Thus, these clasts are more C1 clasts rather than CI- (Ivuna)-like clasts. We obtained Cr isotope data and trace element concentrations of one C1 clast from the DaG 1064 ureilite (C1a) and of one from the CR chondrite Acfer 311 (C1b). Additional data on a CM-like clast from the polymict eucrite NWA 7542 will be discussed.

The C1a clast in the ureilite show nearly chondritic REE concentrations and are enriched in <sup>54</sup>Cr ( $\epsilon^{54}\text{Cr}$  of  $2.84 \pm 0.12$ ). Also considering the O and H isotope data [4,5], this material is certainly of very primitive nature. The <sup>54</sup>Cr value of C1a clast is clearly higher compared to similar samples from the Almahata Sitta strewnfield [7] and may result from a heterogeneous distribution of the carrier phase of <sup>54</sup>Cr.

The C1b clast in the CR chondrite Acfer 311 is similarly enriched in <sup>54</sup>Cr ( $1.43 \pm 0.36$ ) when compared to CR chondrites. Also O and H isotope data of the C1b clast indicating a genetic relationship between the clast and its host. REE concentrations of clasts C1a and C1b are nearly chondritic showing a slightly decreasing trend from La to Lu.

Based on petrology, O, H, and partly their Cr isotopes, CM-like clasts in HEDs are clearly related to “common” CM chondrites. The REE data of CM-like clast NWA 7542-G show a pattern similar to those of group II Ca,Al-rich inclusions, which may dominate the pattern in the sample aliquot. REE and Cr isotope data of clasts from different meteorite groups confirm the late accretion of CM and C1 parent bodies on the differentiated asteroids.

[1] Bischoff A. et al. (1993) *Geochim. et Cosmochim. Acta* 57:2631-2648; [2] Zolensky M.E. et al. (1996) *Meteorit. & Planet. Sci.* 31:518-537; [3] Patzek M. et al. (2018) *Meteorit. & Planet. Sci.* 53:2519-2540; [4] Patzek M. et al. (2018) *Meteorit. & Planet. Sci.* 53 #6254; [5] Patzek M. et al. (2019) LPSC, Abstract 1779; [6] Visser R. et al. (2018) *Meteorit. & Planet. Sci.* 53, #6190; [7] Goodrich et al. (2019) LPSC, Abstract 1312.

4:00pm - 4:15pm

### Dynamic Deformation of Meteoritic Iron in a Diamond Anvil Cell: In-situ Observation of the $\epsilon$ -Iron Phase Transition and the Formation of Shock Defects

**Doreen Schmidt<sup>1</sup>, Dennis Harries<sup>1</sup>, Agnese Fazio<sup>1</sup>, Hanns-Peter Liermann<sup>2</sup>, Kilian Pollok<sup>1</sup>, Falko Langenhorst<sup>1</sup>**

<sup>1</sup>Friedrich Schiller University Jena, Institute for Geosciences, Carl-Zeiss-Promenade 10, 07745 Jena, Germany;

<sup>2</sup>Deutsches Elektronen Synchrotron (DESY), Notkestraße 85, 22607 Hamburg, Germany

Iron meteorites originate from differentiated asteroids and reveal insights in the processes of early core formation and subsequent impacts. The latter is expected to result in phase transitions of the iron polymorphs. These are in general studied comprehensively [1], such as the  $\alpha$ - to  $\epsilon$ -transformation, which is known to occur in the low temperature regime at a pressure around 13 GPa in both static and shock experiments [2, 3]. In iron meteorites, there is also textural evidence for the transformation of kamacite to the hexagonal structured  $\epsilon$ -phase [4], but to our knowledge  $\epsilon$ -kamacite has so far not been directly detected in iron meteorites. In this work, we present an experimental approach to simulate the effects of impacts by dynamic compression in a diamond anvil cell (DAC). Simultaneous in-situ synchrotron X-ray diffraction (XRD) is used to detect the phase transitions and to unravel their mechanisms and kinetics.

Dynamic, non-hydrostatic DAC experiments were performed at room temperature at the Extreme Conditions Beamline P02.2 at PETRA III at DESY in Hamburg, Germany. As starting material, we used the Muonionalusta iron meteorite and crushed it with a rasp to swarf. This powder was then loaded with gold for internal pressure calibration in membrane-driven DACs. Time-resolved in-situ XRD patterns were acquired during the compression with a rate of 17 GPa/min to a peak pressure of 60 GPa and during subsequent decompression. The XRD pattern of the uncompressed material shows dominantly the peaks of the body-centered cubic (bcc) kamacite and a weak signal of the face-centered cubic (fcc) taenite. During compression the formation of hexagonal  $\epsilon$ -iron starts at 10 GPa, which is 3 GPa lower than in other room temperature experiments on iron [2] and even about 6 GPa lower than in experiments on natural kamacite [3]. At 15 GPa most of the kamacite is transformed. On decompression the reverse transition begins around 25 GPa. At the final experimental pressure of 10 GPa there is still a strong signal of the hexagonal  $\epsilon$ -structure. The experiments provide evidence for a rapid transformation mechanism of kamacite. Scanning (SEM) and Transmission Electron Microscopy (TEM) investigation are currently under way to characterize the defect microstructure of recovered samples.

[1] Boehler, R. (2000) *Reviews of Geophysics*, 38(2): 221-245; [2] Bundy, F. (1965) *Journal of Applied Physics*, 36(2): 616-620; [3] Sears, D.W. et al. (1984) *Geochimica et Cosmochimica Acta*, 48(2): 343-360; [4] Jaeger, R. and M. Lipschutz (1967) *Nature*, 213(5080): 975.

4:15pm - 4:30pm

### Shock History of the Metal-rich CB Chondrite Quebrada Chimborazo (QC) 001

**Tamara E. Koch<sup>1</sup>, Frank E. Brenker<sup>1,2</sup>, Emilia Götz<sup>3</sup>, Ute Kolb<sup>3,4</sup>, Dave J. Prior<sup>5</sup>, Kat Lilly<sup>5</sup>, Alexander N. Krot<sup>2</sup>, Anja Schreiber<sup>6</sup>, Martin Bizzarro<sup>7</sup>**

<sup>1</sup>Institute of Geosciences, Goethe University Frankfurt, Germany; <sup>2</sup>Hawai'i Institute of Geophysics and Planetology, University of Hawai'i at Mānoa, USA; <sup>3</sup>Institute of Applied Geosciences, Technische Universität Darmstadt, Germany; <sup>4</sup>Centre for High Resolution Electron Microscopy, Johannes Gutenberg University Mainz, Germany; <sup>5</sup>Department of Geology, University of Otago, New Zealand; <sup>6</sup>GFZ German Research Centre for Geosciences, Helmholtz Centre Potsdam, Germany; <sup>7</sup>Centre for Star and Planet Formation, Natural History Museum of Denmark

The Quebrada Chimborazo (QC) 001 meteorite belongs to the rare group of CB (Bencubbin type) chondrites, metal-rich carbonaceous chondrites with mineralogical, chemical and isotopic characteristics that sharply distinguish them from other chondrites [1]. Furthermore, most CB chondrites reached higher shock stages (S3–S4) than other carbonaceous chondrite groups and contain high-pressure phases such as wadsleyite, ringwoodite, majorite, majorite-pyrope solid solution, and coesite [1–5]. Previous studies described high-pressure minerals in QC 001 and estimated  $P$ - $T$  conditions of shock metamorphism ( $\geq 19$  GPa and  $\sim 2100$  K); similar to those predicted for the Earth's transition zone. So far, the QC 001 meteorite is one of two geological samples which contain asimowite, the Fe-analog of wadsleyite [5]. It is likely that asimowite crystal-

lized from a Fe-enriched melt produced by a mixture of partially molten Fe,Ni-metal and silicate at  $> 2000$  K  $\geq 15$  GPa [5]. The purpose of this study is to expand the previous knowledge about the  $P$ - $T$  conditions of the shock event experienced by QC 001.

Transmission electron microscopy on several focused ion beam (FIB) sections from shock melted regions of QC 001 was performed to obtain detailed high-resolution images, elemental maps and detailed chemical analysis. For a more detailed structural characterization some high-pressure phases were investigated by electron diffraction. Cell parameter, space group determination and crystal structure solution were conducted based on data obtained with Automated Electron Diffraction Tomography (ADT) and direct methods implemented in SIR2014.

One of the FIB sections was cut from a  $10 \times 10$   $\mu\text{m}$ -sized silicate melt droplet within the metal matrix. This melt droplet consists mostly of wadsleyite grains with unusual high Fe-contents ( $\text{Fa}_{30}$  to  $\text{Fa}_{40}$ ) associated with ringwoodite ( $\text{Fa}_{50}$ ), olivine ( $\text{Fa}_{35-42}$ , one with  $\text{Fa}_{10}$ ) and pyroxene.

Another FIB section was cut from a  $68 \times 110$   $\mu\text{m}$ -sized chondrule fragment. It consists of an assemblage of olivine ( $\text{Fa}_{1.4}$ ) and low-Ca pyroxene with interstitial garnets. The garnets have either a composition of majorite-pyroxene solid solution or a composition similar to the Al-rich diopsides of this meteorite what implies that they represent high-pressure polymorphs. The results from this study propose peak shock conditions of  $\sim 15 \pm 2$  GPa and  $\sim 2100 \pm 200$  K for QC 001.

[1] Weisberg M. K. et al. 2006. *MAPS* 36; [2] Weisberg M. K. et al. 2010. *MAPS* 45; [3] Koch T. E. et al. 2016. *Ann. Meet. Met. Soc. LXXIX*, Abstract #6287; [4] Brenker F. E. et al. 2017. *LPSC XLVIII*, Abstract #1967; [5] Bindi L. et al. 2019. *Am. Min.* 104.

## 4:30pm - 4:45pm

### The incomplete amorphization of natural and experimentally shocked plagioclase investigated by optical and electron microscopy, and various spectroscopic techniques

Lidia Pittarello<sup>1</sup>, Julia Roszjar<sup>2</sup>, Luke Daly<sup>3</sup>, Christoph Lenz<sup>4</sup>, Chutimun Chanmuang N.<sup>4</sup>, Ludovic Ferrière<sup>2</sup>, Joerg Fritz<sup>5</sup>, Peter Chung<sup>3</sup>, Annemarie E. Pickersgill<sup>3</sup>, Martin R. Lee<sup>3</sup>, Christian Koeberl<sup>1,2</sup>

<sup>1</sup>Universität Wien, Vienna, Austria; <sup>2</sup>Naturhistorisches Museum, Vienna, Austria; <sup>3</sup>School of Geographical and Earth Sciences, University of Glasgow, United Kingdom; <sup>4</sup>Institut für Mineralogie und Kristallographie, Universität Wien, Vienna, Austria; <sup>5</sup>Saalbau Weltraum Projekt, Heppenheim, Germany

The process of mineral amorphization in response to shock metamorphism is not yet fully constrained, especially in plagioclase, even though this mineral is quite abundant on the surface of terrestrial planets, rocky asteroids, and in some stony meteorites. The best opportunity to investigate the progression of amorphization is provided in cases of incomplete transformation of crystalline plagioclase into amorphous material. In this work, we focus on experimentally and naturally shocked plagioclase, showing incomplete amorphization. The selected samples derive from both a shock recovery experiment, performed at 28 GPa with a troctolite, and a shatter cone from the Manicouagan impact structure, Québec, Canada, formed in a garnet-bearing metagranite. Apart from the incomplete amorphization, shock conditions, chemical composition, mineral paragenesis, and shock effects are different between the two cases.

Transmitted light optical microscopy of petrographic thin sections, whenever available, provides a first evaluation of the distribution of amorphous domains in shocked plagioclase. Further information on the degree of amorphization is provided by spectroscopic techniques, such as Raman spectroscopy, cathodoluminescence, and photoluminescence. Such spectroscopic techniques, although limited to the top few  $\mu\text{m}$  from the surface, allow the evaluation of shock effects in plagioclase on polished mounts without requiring the preparation of a petrographic thin section. Similarly, electron back-scatter diffraction (EBSD), which collects crystallographic information from the top 20-40 nm of the sample surface, provides information on the abundance, distribution, and orientation of shock effects in plagioclase, but requires special sample polishing/preparation.

The amorphization of plagioclase in the investigated experimentally shocked sample is irregularly distributed within individual crystals and among the lithic clasts recovered after the experiment, and its occurrence is

likely affected by (i) the crystallographic orientation of each grain with respect to the shock wave reflection in the used experimental set up, (ii) the presence of crystal anisotropies, such as inclusions, cracks, and cleavage and their orientation, and (iii), the nature of neighboring phases (size, orientation, mineralogy, and corresponding physical properties, such as shock impedance). On the other hand, the degree of amorphization of the naturally shocked plagioclase from the Manicouagan impact structure is controlled by the formation of microtwins. Our observations imply that the formation of microtwins is the first response to shock compression, followed by amorphization of those previously formed twins conveniently oriented with respect to the locally scattered shock wave.

**4:45pm - 5:00pm**

### **Exploring radiation damage on near-Earth asteroid 25143 Itokawa by TEM**

**Dennis Harries<sup>1</sup>, Agnese Fazio<sup>1</sup>, Falko Langenhorst<sup>1</sup>, Toru Matsumoto<sup>2</sup>**

<sup>1</sup>Friedrich Schiller University, Jena, Germany; <sup>2</sup>Kyushu University, Fukuoka, Japan

Atmosphere-less bodies in the solar system are irradiated by energetic ions of the solar wind and solar flares (1 keV/nucleon to 100 MeV/nucleon). Century-long exposure to this radiation and meteoroid impacts leads to significant changes in the spectral reflectance of their surfaces, summarily referred to as space weathering. In 2005 the Hayabusa spacecraft of the Japan Aerospace Exploration Agency (JAXA) touched down of near-Earth asteroid 25143 Itokawa and collected dust-sized particles of its surface regolith. In 2010 the spacecraft re-entered Earth's atmosphere and the samples collected were successfully retrieved.

The Hayabusa collection has provided a unique insight into space weathering on small, dynamically evolving bodies, which contrasts with observations made on the lunar surface. Most notably, it was expected that mineral surfaces irradiated by ions of the solar wind will become amorphous down to a few tens of nanometres. However, using transmission electron microscopy (TEM) this has been observed consistently only for plagioclase – olivine and pyroxenes instead develop polynanocrystalline rims with very little if any amorphous material [1]. Also, radiation damage appears to develop at much slower rates than predicted by numerical simulations [2]. This behaviour appears to be related to thermally driven annealing that competes with ionization damage and the implantation of hydrogen and helium of the solar wind.

Nanophase metallic iron (npFe<sup>0</sup>) and iron sulphide (npFeS), the main agents of spectral changes during space weathering, have been observed in rims with significant amounts of amorphous material [3]. Such chemically distinct rims were probably produced by vapour-deposition after meteoroid impacts, which are evident by sub-micrometre-sized craters on many Itokawa particles [4, 5]. In purely radiation damaged rims or rims of low exposure age npFe<sup>0</sup> and npFeS appear to be largely absent. However, a large unknown is still how the superposition of ionization damage and vapour deposition effectively alter the surfaces of regolith particles and their spectral properties.

References: [1] Harries D. and Langenhorst F. (2014) *Earth, Planets and Space* 66:163; [2] Keller L.P. et al. (2016) 47th LPSC, Houston, USA, abstract #2525; [3] Noguchi T. et al. (2014) *Meteoritics & Planetary Science* 49:188-214; [4] Harries D. et al. (2016) *Earth and Planetary Science Letters* 450:337-345; [5] Matsumoto et al. (2018) *Icarus* 303:22-33. JAXA is acknowledged for providing Hayabusa-returned samples. The FIB-TEM facility at FSU Jena is supported by DFG grant LA 830/14-1.

**5:00pm - 5:15pm**

### **Nanoscale compositional segregation and structure in complex In-bearing sulfides: Results from transmission kikuchi diffraction and atom probe tomography**

**Joachim Krause<sup>1</sup>, Steven M. Reddy<sup>2</sup>, William D.A. Rickard<sup>2</sup>, David W. Saxey<sup>2</sup>, Denis Fougereuse<sup>2</sup>, Matthias E. Bauer<sup>3</sup>**

<sup>1</sup>Helmholtz-Zentrum Dresden-Rossendorf, Helmholtz-Institute Freiberg for Resource Technology, Germany;

<sup>2</sup>Geoscience Atom Probe, ARCF, John de Laeter Centre, Curtin University, Perth, Australia; <sup>3</sup>TU Bergakademie Freiberg, Institute of Mineralogy, Brennhaugasse 14, D-09599 Freiberg, Germany

Indium-bearing sphalerites from the Hämmerlein skarn deposit, located in the western Erzgebirge (Germany), show complex distribution patterns of major and minor elements on a micrometer to sub-micrometer

scale. However, with the spatial resolution of traditional analytical methods, such as SEM-based image analysis and field emission electron probe microanalysis (FE-EPMA), many features in these samples cannot be resolved. It remains unclear whether Cu, In and Fe are in solid solution in the sphalerite or form discrete phases.

Atom probe tomography combined with transmission kikuchi diffraction has been used to resolve the compositional heterogeneity and the nanostructure of these complex In-Cu-Fe-sphalerites. The obtained data indicate a complex structure with micro- to nanometer sized, plate-shaped inclusions of chalcopyrite in the sphalerite. In addition, a nanometer scale In-Cu-sulfide phase forms plate-like segregations in the sphalerite. All types of segregations have similar crystal structure and record the same crystal orientation indicating that they likely formed by exsolution.

The results indicate that complex sulfides containing cations of more than one element as minor or major constituents may represent discrete, exsolved phases, rather than solid solutions. This heterogeneous nature will affect the nanoscale properties of the sphalerite, which may have implications for the economic extraction of precious elements such as In. Furthermore these nanoscale properties will open up new perspectives on formation processes of In-Cu-Fe-sphalerites, which might be relevant for other chemically complex minerals as well.

**5:15pm - 5:30pm**

### **Halogen analysis of sulphide minerals at the ultratrace level – first applications of the Dresden Super-SIMS**

**Axel D. Renno<sup>1</sup>, Georg Rugel<sup>2</sup>, Michael Wiedenbeck<sup>3</sup>, René Ziegenrücker<sup>2</sup>**

<sup>1</sup>Helmholtz-Zentrum Dresden-Rossendorf, Helmholtz Institute Freiberg for Resource Technology, Germany;

<sup>2</sup>Helmholtz-Zentrum Dresden-Rossendorf, Institute of Ion Beam Physics and Materials Research; <sup>3</sup>Deutsches GeoForschungsZentrum GFZ

The integration of an ion source having very high spatial resolution with a tandem accelerator is a long-standing concept for improving analytical selectivity and sensitivity by orders of magnitude [1]. Translating this design concept into reality has its challenges [e.g. 2,3], meaning this approach has seldom been employed for mineralogical and geochemical research [e.g. 4].

Supporting a strong focus on natural, metallic and mineral resources, the Helmholtz Institute Freiberg for Resource Technology installed a so-called Super-SIMS at the Ion Beam Center at HZDR in Dresden-Rossendorf; this highly novel tool is devoted to the characterization of minerals and ores. The secondary ion beam from a CAMECA IMS 7f-auto is injected into the 6MV Dresden Accelerator Mass Spectrometry [5] facility, which effectively eliminates all molecular species from the ion beam.

We will present the current status of this initiative and will report our first results from halogen determinations (F, Cl, Br, I) in both sphalerite and galena. These data demonstrate a systematic and significant change in the counting rates of all halogens in mineralogically distinct areas of both minerals. Furthermore, we will describe our concepts for the quantification of these data at ultratrace levels.

[1] Matteson (2008) *Mass Spec Rev* **27**, 470-484; [2] Ender *et al.* (1997) *NIMB* **123**, 575-578; [3] Fahey *et al.* (2016) *Anal Chem* **88**, 7145-7153; [4] Sie *et al.* (2000) *NIMB* **172**, 228-234; [5] Rugel *et al.* (2016) *NIMB* **370**, 94-100.

## Poster Presentations

Mon: 6

### Modal abundances of coarse-grained (>5 µm) components within CI-chondrites and their individual clasts

**Julian Alfig<sup>1,2</sup>, Markus Patzek<sup>1</sup>, Addi Bischoff<sup>1</sup>**

<sup>1</sup>Institut für Planetologie, Westfälische Wilhelms-Universität Münster, Wilhelm-Klemm Str. 10, D-48149 Münster, Germany; <sup>2</sup>Institut für Mineralogie, Westfälische Wilhelms-Universität Münster, Corrensstr. 24, D-48149 Münster, Germany

The CI chondrites are complex breccias and their degree of brecciation among the studied rocks is decreasing in the sequence: Orgueil > Ivuna > Alais ~ Tonk. Considering the CI chondrite bulk rocks in general, various values for the modal abundance of matrix (95-100 vol% [1-3]) and the accompanied mineral constituents are given. Here, we discuss the determined modal abundance of phases >5 µm in the CI chondrites Orgueil, Ivuna, Alais, and Tonk. If this cut-off grain-size is used to distinguish between matrix and coarse-grained constituents, then, the modal abundance of the minor phases magnetite, pyrrhotite, carbonate, olivine, and pyroxene is 6 vol% in total. These phases are embedded within the fine-grained, phyllosilicate-rich matrix making up 94 vol%. The values vary slightly from meteorite to meteorite. Considering the four studied chondrites the most abundant phase is magnetite (4.3 vol%) followed by pyrrhotite (~1.1 vol%) and carbonates (~0.5 vol%). Phosphate, olivine, and pyroxene are also rare constituents. However, the CI-breccias contain clasts with highly-variable modal abundances. Therefore, we also studied individual clasts with the highest abundance of specific coarse-grained phases. In this respect, in Orgueil a fragment with 21.5 vol% of magnetite was found. We also detected a phosphate-rich fragment in the same meteorite having 31.8 vol% phosphate, whereas in Ivuna an individual clast with 21.5 vol% carbonates was detected. Such a heterogeneity of CI chondrites was earlier described (e.g. [4,5]). Thus, since the CI-composition is used as a standard for comparison in geochemistry, one has to consider that sufficiently large sample masses are required to obtain a representative CI-composition. Small aliquots with one dominating lithology may deviate significantly from the suggested CI-composition used as a standard.

[1] Weisberg M. K. et al. 2006. Meteorites and the Early Solar System II. Univ. of Arizona, Tucson, 19–52; [2] Scott E. R. D. and Krot A. N. 2014. Treatise on Geochemistry (Second Edition), Elsevier, 65-137; [3] Alexander C.M. O'D. 2019. Geochim. Cosmochim. Acta 254, 277-309; [4] Endress M. et al. 1996. Science 379, 701–703; [5] Morlok A. et al. 2006. Geochim. Cosmochim. Acta 70, 5371-5394.

Mon: 7

### SORTED STONE CIRCLES ON SVALBARD – AN ANALOG STUDY FOR MARS

**Sandra Buer<sup>1</sup>, Harald Hiesinger<sup>1</sup>, Dennis Reiss<sup>1</sup>, Ernst Hauber<sup>2</sup>, Andreas Johnsson<sup>3</sup>, Hannes Bernhardt<sup>4</sup>**

<sup>1</sup>Institut für Planetologie, Westfälische Wilhelms-Universität, Wilhelm-Klemm-Str. 10, 48149 Münster, Germany; <sup>2</sup>DLR-Institut für Planetenforschung, Rutherfordstr. 2, 12489 Berlin, Germany; <sup>3</sup>Univ. of Gothenburg, Box 100 SE-405 30 Gothenburg, Sweden; <sup>4</sup>Arizona State University, School of Earth and Space Exploration, 550 East Tyler Mall Bateman Physical Sciences Center F-Wing Room F506 Tempe, AZ 85287-1404, USA

**Introduction:** On Mars, sorted stone circles (SSC), one type of patterned ground, were observed in several locations [1-4]. Balme et al. [2] proposed that these Martian SSCs might share the same origin as SSCs on Earth, i.e. sorting by repeated freeze-thaw cycles due to an active layer. To decipher the formation mechanisms of SSCs on Mars, we studied analog SSCs on Earth.

Western Spitsbergen in the high-arctic archipelago of Svalbard was chosen as study area, because there are well-developed SSCs that formed in a cold-climate environment that display a wide range of Mars-analogue periglacial landforms [3]. The study area is located north-west of the research station Ny Ålesund at the tip of the Brøggerhalvøya peninsula called Kvadehuksletta [1].

**Methods:** To investigate the SSCs on Svalbard, we measured the topography (only 2016) and the soil temperatures, sampled vertical profiles and took areal pictures [4]. The grain size distribution, the soil moisture and the soil organic carbon (SOC) were analyzed in the laboratory [4].

**Results:** Three SSCs were examined during the field work in 2016 (16SC2 and 16SC4) and 2017 (17SC1). The grain size analyses show that the walls (type 1) have coarser material than the inner domain (type 2–4). At the surface, soil moisture in the fine material is higher than in the coarser walls. In the circles sampled in 2014 [1] and 2016, we do not observe a pattern of SOC values that is reminiscent of a convection-like movement of particles in the inner domain as found by [5].

**Discussion/Conclusions:** We hypothesize that in fall, thawed stone circles likely freeze top-down. In such a scenario, the cooler, drier and permeable coarser-grained walls might conduct cold air downwards, so that the walls and the parts adjacent and beneath the walls freeze before the more wet central interior of the SSC. If this working hypothesis is correct, a convection-like movement of soil as proposed by [5] might be an oversimplification. Neither the distribution of grain size and soil moisture, nor the SOC strongly support a convection-like movement.

[1] Hiesinger H. et al. (2017) *LPSC 48th*, Abstract #1164; [2] Balme M. R. et al. (2009) *Icarus*, 200, 30-38; [3] Hauber E. et al. (2011) *Geol. Soc. London Spec. Pub.* 356, 111-131; [4] Buer S. et al. (2019) *LPSC 50th*, Abstract #2313; [5] Hallet B. and Prestrud S. (1986) *Quat. Res.*, 26, 81-99.

## Mon: 8

### The Multi-Temporal Database of Planetary Image Data (MUTED): A Web-Based Tool to Study Surface Changes and Processes on Dynamic Mars

Thomas Heyer<sup>1</sup>, Harald Hiesinger<sup>1</sup>, Dennis Reiss<sup>1</sup>, Jan Raack<sup>1</sup>, Ralf Jaumann<sup>2</sup>

<sup>1</sup>Institut für Planetologie, Westfälische Wilhelms-Universität, Münster, Germany; <sup>2</sup>German Aerospace Center (DLR), Berlin, Germany

The Multi-Temporal Database of Planetary Image Data (MUTED) is a web-based tool to support the identification of surface changes and time-critical processes on Mars. The database enables scientists to quickly identify the spatial and multi-temporal coverage of orbital image data of all major Mars missions. Since the 1970s, multi-temporal spacecraft observations have revealed that the martian surface is very dynamic [e.g., 1]. The observation of surface changes and processes, including eolian activity [e.g., 2], mass movement activities [e.g., 3], the growth and retreat of the polar caps [e.g., 4], and crater-forming impacts [5] became possible by the increasing number of repeated image acquisitions of the same surface areas. Today more than one million orbital images of Mars are available [6]. This increasing number highlights the importance of efficient and comprehensive tools for planetary image data management, search, and access. MUTED is accessible at <http://muted.wwu.de> and will assist and optimize image data searches to support the analysis and understanding of short-term, long-term, and seasonal processes on the surface and in the atmosphere of Mars. In particular, images can be searched in temporal and spatial relation to other images on a global scale or for a specific region of interest. Additional information, e.g., data acquisition time, the temporal and spatial context, as well as preview images and raw data download links are available. Due to continuous data acquisition by spacecraft, the amount of image data is steadily increasing and enables further comprehensive analyses of martian surface changes.

[1] Sagan et al. (1972) *Icarus*, 17, 346-372; [2] Reiss et al. (2011) *Icarus*, 215, 358-369; [3] Dundas et al. (2015) *Icarus*, 251, 244-263; [4] Calvin et al. (2017) *Icarus*, 292, 144-153; [5] Daubar et al. (2013) *Icarus*, 225, 506-516; [6] Heyer et al. (2018) *PSS*, 159, 56-65.

## Mon: 9

### Classification of 13 cm chondrite breccias

Sarah Lentfort, Addi Bischoff, Samuel Ebert

WWU Münster, Germany

CM chondrites are complex impact (mostly regolith) breccias, in which lithic clasts show various degrees of aqueous alteration. These fragments are mixed together and lithified in a fine-grained matrix; however, the conditions of aqueous alteration are still controversial (e.g., [1-6]). In particular, this is the case considering

the chronological relationship between aqueous alteration and brecciation. To quantify the degree of alteration, different classification schemes have been suggested (e.g., [5-6]).

In this study, individual fragments of 13 CM chondrite breccias have been investigated in detail. The alteration index of 90 fragments was determined based on the optical appearance and chemistry of their PCPs using the procedure suggested by [6]. An accurate subclassification can only be performed by obtaining the chemical composition of the PCPs considering the “FeO”/SiO<sub>2</sub>- and S/SiO<sub>2</sub>-ratios and the SiO<sub>2</sub>, FeO, and MgO contents. For certain clasts “FeO”/SiO<sub>2</sub>-ratios were significantly above the values of  $2.9 \pm 0.6$  (subtype CM2.6 by [6]) and lead to the definition of some new subtypes (CM2.7-2.9). Samples free of well-defined clasts were also classified by the analyses of PCP objects randomly distributed throughout the sample (e.g., NWA 10907). On this basis the CM chondrites are classified as follows: LON 94101 (CM2.0-2.8, also containing CI clasts), ALH 85013 (CM2.0-2.8), ALHA 77306 (CM2.0-2.6), Banten (CM2.4-2.9), NWA 10907, 10908 (CM2.3-2.4), Maribo (CM2.4-2.6), Jbilet Winselwan (CM2.3-2.9), Cold Bokveld (CM2.0-2.8), Nogoya CM2.0-2.6), Murchison (CM2.4-2.9), Y-791198 (CM2.4-2.8), Santa Cruz (CM2.4-2.8). The study shows that the degree of aqueous alteration can vary from clast to clast within a single thin section and between thin sections. Consequently, the CM subtype classification based on the most abundant fragment-type as used by [6] is not appropriate for the classification of complex CM chondrite breccias. Therefore, an extended classification scheme from 2.0-2.9 that takes the brecciation and the degree of alteration into account is more precise and preferable.

[1] Fuchs L.H. et al. (1973) *Smiths. Contrib. Earth Sci.* 10:1-39; [2] Metzler K. et al. (1992) *Geochim. Cosmochim. Acta* 56: 2873-2897; [3] Bischoff A. (1998) *Meteoritics & Planet. Sci.* 33: 1113-1122; [4] Metzler K. (2004) *Meteoritics & Planet. Sci.* 39:1307-1319; [5] Browning L. et al. (1996) *Geochim. Cosmochim. Acta* 60: 2621-2633; [6] Rubin A.E. et al. (2007) *Geochim. Cosmochim. Acta* 71: 2361-2382.

**Acknowledgement:** We thank the DFG for support within the SFB-TRR 170 (subproject B05) and the Meteorite Working Group and Mike Zolensky (both Houston) and the NIPR (Tokio) for the loan of meteorite samples.

## Mon: 10

### A Chondrule Formation Experiment Aboard the ISS: Experimental Set-up and Test Experiments

**Dominik Spahr<sup>1</sup>, Tamara E. Koch<sup>1</sup>, David Merges<sup>1</sup>, Anna A. Beck<sup>1</sup>, Oliver Christ<sup>1</sup>, Shintaro Fujita<sup>2</sup>, Philomena-T. Genzel<sup>1</sup>, Jochen Kerscher<sup>2</sup>, Miles Lindner<sup>1</sup>, Diego Menderos-Leber<sup>1</sup>, Fabian Wilde<sup>3</sup>, Wolfgang Morgenroth<sup>1</sup>, Frank E. Brenker<sup>1</sup>, Björn Winkler<sup>1</sup>**

<sup>1</sup>Goethe University Frankfurt, Germany; <sup>2</sup>HackerSpace FFM e. V., Oberursel, Germany; <sup>3</sup>Helmholtz-Zentrum Geesthacht, HZG Outstation at DESY in Hamburg, Hamburg, Germany

The formation of chondrules is one of the most enigmatic processes in planetary science. The EXCISS experiment (**Experimental Chondrule formation aboard the ISS**) was developed in order to investigate if chondrule formation via “nebular lightning” [1–5] is a viable process. At conditions of long-term micro gravity synthetic forsterite (Mg<sub>2</sub>SiO<sub>4</sub>) particles were repeatedly exposed to electrical discharges with the aim to observe if these particles melt and fuse under these conditions. EXCISS was launched with Cygnus NG-10 on November 17<sup>th</sup>, 2018 and was carried in December 2018 and January 2019 aboard the ISS. Here, we will present the experimental set-up of the ISS based experiment together with the first results of the experiments in space.

The experimental set-up is mounted in a 1.5 U NanoRacks NanoLab with a size of approx. 10 × 10 × 15 cm<sup>3</sup>. Forsterite particles (80 – 120 μm) were levitating in a glass sample chamber, filled with Ar at 100 mbar pressure, where they were subjected to electrical arcs. The behavior of the particles in micro gravity was documented with a video camera. We complemented these experiments by laboratory-based discharge experiments on Earth.

The experiments aboard the ISS were successfully completed. We performed about 80 arc discharges. The video documentation shows that some dust particles initially stuck on the walls and the electrode. Furthermore, many particles formed irregular shaped agglomerates levitating in the sample chamber and thus became precursors well suited for the discharge experiments. These agglomerates were attracted by the charged electrodes. After the discharge experiments, we observe that the arc discharges led to changes in the particle size and shape. The capsule return is planned with SpaceX CRS17 scheduled for end of May 2019 and after sample return, we will analyze these experimental products in detail.

## 2) Structure and evolution of planetary bodies

[1] Whipple F. L. (1966) *Science* **153**:54–56; [2] Horányi, M. et al. (1995) *Icarus* **114**:174–185; [3] Desch S. J. and Cuzzi, J. N. (2000) *Icarus* **143**:87–105; [4] Johansen A. and Okuzumi A. (2018) *Astronomy & Astrophysics* **A31**:1–22; [5] Güttler C. et al. (2008) *Icarus* **195**:504–510.

**Acknowledgments:** We gratefully acknowledge the HackerSpace FFM, Rainer Haseitl, Solveigh Matthies and the IAP Frankfurt for technical support. We are grateful for financial support by the DFG (Wi1232), the Dr. Rolf M. Schwiete Stiftung, the BMBF (05K16RFB), the German Aerospace Center (DLR), BIOVIA, ZEISS, DreamUp, NanoRacks and Nordlicht GmbH. We acknowledge DESY. Parts of this research were carried out at PETRA III.

## 2c): Planetary Accretion and Impact Processes

Wednesday, 25/Sep/2019: 1:00pm - 3:00pm

**Session Chair: Thomas Haber** (Westfälische Wilhelms-Universität Münster)

**Session Chair: Gregory Jude Archer** (University of Münster)

**Session Chair: Emily Anne Worsham** (University of Münster)

**Location: H2**

### Session Abstract

Impact events of all sizes were crucial for the growth of the terrestrial planets and continue shaping their surfaces today. Thus, studying the nature of the impactors and the effects of the impacts themselves helps us to understand how the four terrestrial planets and related, smaller bodies (e.g., the Moon) formed and evolved. The goal of this session is to present and discuss research on the characteristics and origin of the material delivered to the terrestrial planets, the large-scale consequences of the addition of these materials for the isotopic and elemental compositions of terrestrial bodies, and the impact processes themselves, including the effects of giant impacts and the structures and materials generated by non-disruptive impacts. For this interdisciplinary session we invite contributions from the fields of planetary sciences, geophysics, petrology, and geochemistry.

### Lecture Presentations

1:00pm - 1:15pm

#### The triple oxygen isotope composition of lunar rocks

**Meike B. Fischer<sup>1,2</sup>, Stefan T. M. Peters<sup>1</sup>, Paul Hartogh<sup>2</sup>, Andreas Pack<sup>1</sup>**

<sup>1</sup>Department of Isotope Geology, Georg-August-Universität Göttingen, Germany; <sup>2</sup>Department of Planets and Comets, Max Planck Institute for Solar System Research, Germany

According to the original giant impact hypothesis the Moon formed due to a catastrophic collision of proto-Earth with the impactor Theia. Debris of both bodies were thrown in the Earth's orbit and this material formed the Moon. In such a scenario Theia is expected to have a triple oxygen isotope composition ( $\Delta^{17}\text{O}$ ) distinct from the proto-Earth. The Moon should also differ in its  $\Delta^{17}\text{O}$  from Earth, because the original giant impact hypothesis implies that the Moon accreted a higher portion (70-90%) of Theia than the Earth [1-3].

The triple oxygen isotope composition of the Moon vs. Earth was investigated in several studies [4-12]. These studies reported differences in  $\Delta^{17}\text{O}$  (Moon-Earth) between 0 and 12 ppm. We reassess the composition of lunar rocks in comparison to terrestrial rocks by means of improved high-precision  $^{18}\text{O}/^{16}\text{O}$  and  $^{17}\text{O}/^{16}\text{O}$  measurements.

Oxygen was extracted from the samples by  $\text{BrF}_5$  laser fluorination and measured using a gas source stable isotope ratio mass spectrometer (MAT 253). A new laser fluorination line was constructed and an analytical protocol with longer measurement sessions was developed.

We present new triple oxygen isotope data on lunar rocks from 5 different Apollo missions. Mare basalts/gabbros, anorthosites, breccias, soil, and pyroclastic glasses were studied. We analysed typical terrestrial mantle materials for an Earth-Moon comparison.

## 2) Structure and evolution of planetary bodies

[1] Cameron (2000) *Origin of the Earth and Moon* (eds. K. Righter and R. Canup), University Arizona Press, Tucson, 133-144; [2] Canup and Asphaug (2001) *Nat.* **412**, 708–712; [3] Canup (2004) *Icarus* **168**, 433-456; [4] Clayton and Mayeda (1975) *Proc. Lunar Sci. Conf. Sixth*, 1761-1769; [5] Clayton and Mayeda (1996) *Geochim. Cosmochim. Acta* **60**, 1999-2017; [6] Wiechert *et al.* (2001) *Science* **294**, 345–348; [7] Spicuzza *et al.* (2007) *Earth Planet. Sci. Lett.* **253**, 254–265; [8] Hallis *et al.* (2010) *Geochim. Cosmochim. Acta* **74**, 6885–6899; [9] Herwartz *et al.* (2014) *Science* **344**, 1146–1150; [10] Young *et al.* (2016) *Science* **351**, 493–496; [11] Greenwood *et al.* (2018) *Sci. Adv.* **4**, 1–8; [12] Cano *et al.* (2019) *Lunar Planet. Sci. Conf.* **50**, abstract #2132.

**1:15pm - 1:30pm**

### **An outer solar system origin of the Moon-forming impactor**

**Thorsten Kleine, Gerrit Budde, Christoph Burkhardt**

*University of Münster, Germany*

The Moon is thought to have formed from debris ejected by a giant impact on the early Earth, but the origin of the impactor and whether it derives from the same or a distinct reservoir as the Earth are unknown. The striking isotopic similarity between the Earth and Moon indicates either that the Moon largely consists of proto-Earth material or that the Earth and Moon isotopically equilibrated in the aftermath of the giant impact. Either way, the isotopic composition of the Moon provides no information on the nature of the impactor. Here we show, however, that the isotopic composition of siderophile elements in the Earth's mantle allows constraining the origin of the Moon-forming impactor. This is because siderophile elements in the present-day Earth's mantle predominantly derive from the late stages of accretion and their isotopic composition is, therefore, strongly influenced by that of the last giant impactor. Based on the Mo isotopic dichotomy between non-carbonaceous and carbonaceous meteorites, which represent inner and outer solar system materials, respectively, we show that about half of the Mo in Earth's mantle derives from outer solar system objects. Given that most of the Mo in Earth's mantle derives from the Moon-forming impactor, these results imply that this impactor originally formed in the outer solar system. This object may have been scattered into the inner solar system during the early migration and growth of Jupiter, and may have been later destabilized during the orbital instability of the gas giant planets about 100 Ma after formation of the solar system.

**1:30pm - 2:00pm Session Keynote**

### **Mechanics and conditions for devolatilising the Moon**

**Paolo A. Sossi**

*Institute of Geochemistry and Petrology, ETH Zürich, Sonneggstrasse 5, CH-8092, Zürich, Switzerland*

Chemical measurements of the first lunar basalts returned from the Moon revealed that, although they share similar abundances of refractory lithophile elements with respect to terrestrial basaltic rocks, they are impoverished in volatile metals, such as K and Zn [1-3]. More recently, the heavy isotopic composition of these volatile elements in lunar rocks has been cited as evidence of an evaporation process that stripped the Moon of its volatiles [4, 5]. However, the timing, conditions and mechanisms that could have resulted in volatile depletion of the Moon, whilst maintaining Earth's mantle-like refractory element abundances and isotopic compositions, remain poorly known. Here, thermodynamic calculations, based on new experimental work of the evaporation of silicate melts, are used to predict the expected depletion patterns of moderately volatile elements due to vaporisation. It is found that, in order to match the measured lunar volatile element abundances and isotope compositions, rather low ( $\approx 1500$  K) temperatures are required. These temperatures are far too low for the atmosphere to have been lost by Jeans escape given escape velocities for the present-day Moon. However, because the accretion of the Moon occurred at the Earth's Roche Limit (at 2.5 Earth radii), the strong gravitational well of the Earth would have significantly assisted volatile escape from the Moon, in which particles are lost when they cross its Hill sphere radius. In this case, the lunar atmosphere can escape hydrodynamically over a period of  $10^4$  years, and the particles are re-accreted to the Earth. Volatile loss is then arrested over a similar timescale due to *i)* a rapid cooling of the Moon and *ii)* its outward orbital migration, which increases the Hill sphere radius. This process is therefore akin to that occurring for double stars and star-proximal exoplanets, and may be effective in causing the widespread volatile depletion observed in small rocky bodies.

## 2) Structure and evolution of planetary bodies

[1] Ringwood, A.E., & Essene, E. (1970). *Science*, 167, 607-610; [2] O'Hara, M. J *et al.* (1970). *Geochim. Cosmochim. Acta Suppl.*, 1, 695; [3] Wolf, R., & Anders, E. (1980). *Geochim. Cosmochim. Acta Suppl.*, 44(12), 2111-2124; [4] Paniello, R. C., Day, J. M., & Moynier, F. (2012). *Nature*, 490(7420), 376-379; [5] Wang, K., & Jacobsen, S. B. (2016). *Nature*, 538, 487-490.

**2:00pm - 2:15pm**

### **Modeling partitioning of SVEs during Earth's core formation**

**Dominik Loro**ch, Sebastian Hackler, Arno Rohrbach, Stephan Klemme

*Universität Münster, Germany*

That Earth's mantle is depleted in numerous elements as a result of accretion and core-mantle differentiation is known and intensely studied for more than four decades now. However, siderophile but volatile elements (SVEs), potentially very important has received considerably less attention in this context. For SVEs especially the partitioning between metal/sulfide melt and silicate melt ( $D^{\text{metal/silicate}}$ ,  $D^{\text{sulfide/silicate}}$ ) at core formation conditions is poorly constrained, nevertheless these elements are very important for most of the core formation models.

The hypothesis that we are testing uses the accretion of major portions of volatile elements while the core formation was still active. This study is using new metal-silicate partitioning data for a wide range of SVEs (S, Se, Te, Tl, Ag, As, Au, Cd, Bi, Pb, Sn, Cu, Ge, Zn, In and Ga), from internally consistent experiments, with a focus on sulfur dependencies.

We performed high pressure (1 to 20 GPa), high temperature (1400 to 2300 °C) metal/silicate partitioning experiments where we vary the sulfur content from sulfur-free to stoichiometric sulfide melt compositions. For trace element analysis we are using a Photon Machines Analyte G2 Excimer laser (193 nm) ablation system coupled to a Thermo Fisher Element 2 single-collector ICP-MS (LA-ICP-MS) to determine  $D^{\text{metal/silicate}}$  values.

We will present the results for a suite of elements, similar in terms of volatility (i.e. 50% condensation temperature and depletion in the bulk silicate Earth (BSE) relative to CI chondrite). This dataset was used to model the compositional evolution of the BSE, the segregating metal diapirs and the Earth's core. The data has been compiled in a step-wise accretion model assuming continuous core formation and heterogeneous impactor compositions.

The modeling results are showing not only the necessity of HP, HT partitioning data for most of the elements, due to the limitations and possible extensive high errors on the extrapolation. But importantly, model outcome is suggesting that the core formation due to metal/silicate partitioning, on its own, is not reproducing the observed depletion trend for the PM values (c.f. [1]) for various SVEs.

[1] Lodders K. (2003) *Astrophys. J.* 591, 1220–1247.

**2:15pm - 2:30pm**

### **Chalcophile Element Accretion from the Late Veneer**

**Sebastian Hackler**, Loroch Dominik, Arno Rohrbach, Stephan Klemme, Jasper Berndt

*Westfälische Wilhelms-Universität Münster, Institut für Mineralogie, Corrensstraße 24, 48149 Münster, Germany*

The arrival of volatile elements to the Earth is one of the most important aspects for the development of life, however, the timing of volatile delivery and its carrier materials to Earth are still poorly constrained. Processes of accretion and core formation that established the chemical budgets of the Earth's mantle and core are still matter of debate. Several competing theories have been developed over the last decades. Either the Earth accreted mostly from refractory building blocks and volatile elements were delivered late after core formation had ceased or volatile rich material accreted during the main stages of accretion with core formation being active.

Understanding the partitioning behavior of volatile elements that are also siderophile and/or chalcophile (S, Se, Te, Tl, Ag, Au, Cu, Bi, Sn, Cu, Ge and In) may provide key information in this regard. We tested if the

chalcophile element concentrations in the bulk silicate Earth (In, Cd, S, Se, Sn, Te, Pb, Cu, Bi) were established solely by a late segregation of a sulfide melt (“Hadean Matte”) or if an additionally a chondritic late veneer event is needed.

To examine the influence of sulfur on siderophile volatile element partitioning between sulfide/metal- and silicate melts ( $D^{\text{sul-sil}} / D^{\text{met-sil}}$ ), we performed experiments from sulfur free to sulfur rich-melts (~35 wt.% S). Partitioning experiments were carried out under various P-T-fO<sub>2</sub> conditions with a 600 t walker-type multi-anvil press (1-20 GPa, 1400-2100 °C). The run products were analyzed via FEG-EMPA and LA-ICP-MS.

Our results show that Te ( $D^{\text{sul-sil}} = 200$ ) is considerably more chalcophile than Se and S ( $D^{\text{sul-sil}} = 50$ ) which implies that Te should appear more depleted in the bulk silicate Earth compared to Se and S. Commonly referred chalcophile elements with similar volatility (In, Cd, Sn, Pb, Cu, Bi) show lower  $D^{\text{sul-sil}}$  compared to  $D^{\text{met-sil}}$ , arguing for a less effective “Hadean Matte” depletion effect. We observe that various mass fractions of different meteorites is needed during a possible late veneer event to explain the bulk silicate Earth element abundances. Therefore, we propose, that a late sulfide segregation in combination with a late veneer event is unable to explain the mantle concentrations of the studied elements.

**2:30pm - 2:45pm**

### **Tellurium stable isotopic constraints on the nature of late accretion**

**Jan L. Hellmann, Timo Hopp, Christoph Burkhardt, Thorsten Kleine**

*University of Münster, Germany*

Late accretion, or late veneer, is defined as the addition of broadly chondritic material to Earth’s mantle after core formation ceased. However, the origin and nature of the late-accreted material remains controversial. Nucleosynthetic Ru isotope anomalies for meteorites indicate that this material was most similar to enstatite and distinct from carbonaceous chondrites [1], consistent with prior conclusions based on the Os isotope composition of Earth’s mantle [2]. By contrast, the Se/Te ratio of Earth’s mantle is similar to that of volatile-rich carbonaceous chondrites, and distinct from enstatite and ordinary chondrites [3], suggesting that the late veneer contained some material from carbonaceous chondrites.

To resolve these disparate observations, and to better constrain the nature and origin of the late-accreted material, we obtained mass-dependent Te isotopic data for terrestrial samples and a comprehensive set of chondrites. Tellurium stable isotope variations may arise as a result of nebular processes, leading to distinct isotopic compositions among chondrites, which allow to distinguish between different chondrite groups as potential sources of the late veneer. To this end, we developed a <sup>123</sup>Te-<sup>125</sup>Te double spike method for the precise measurements of Te isotope variations by multi-collector ICP-MS. The Te stable isotopic composition of the bulk silicate Earth was precisely defined by analyses of several peridotites, which have been well characterized in previous studies [*e.g.*, 3]. Samples from the major chondrite classes display a range in Te isotopic compositions, and combined with their Se/Te ratios only some carbonaceous chondrite group overlap with the composition determined for the Earth’s mantle in this study. Our new data therefore indicate that the late veneer cannot have solely consisted of enstatite chondrite-like material, but also included volatile-rich carbonaceous chondrite-like material. When combined with the Ru and Os isotopic evidence for an enstatite chondrite-like composition of the late veneer, our new Te isotopic data indicate that the late accretionary assemblage was a mixture of volatile-rich carbonaceous and volatile-poor non-carbonaceous material.

[1] Fischer-Gödde M. and Kleine T. (2017) *Nature* **541**, 525–527; [2] Meisel T. et al. (2001) *GCA* **65**, 1311–1323; [3] Wang Z. and Becker H. (2013) *Nature* **499**, 328–331.

## Poster Presentation

Tue: 1

### A History of Outhouse Rock

**Thomas Haber, Erik E. Scherer**

*Westfälische Wilhelms-Universität Münster, Institut für Mineralogie, Corrensstr. 24, D-48149 Münster, Germany*

Outhouse Rock, a boulder at the rim of North Ray Crater, records several events that are important for understanding the lunar impact chronology. The matrix of the boulder is a KREEP-rich impact melt rock (Apollo 16 samples 67935, -36, and -37), in which brecciated feldspathic clasts (sampled as 67915 and -55) are embedded. Previous dating of the boulder matrix (Re-Os), as well as a feldspathic clast (Sm-Nd), yielded  $\sim 4.2$  Ga for both [1, 2]. However, different impactor signatures, textural characteristics, chemical compositions, and the clast-matrix relationship itself point to the clast and the matrix recording two distinct impact events, likely of basin-size [1, 2].

For this study, we are analysing the Lu-Hf, Sm-Nd, Rb-Sr, and Pb-Pb systematics of samples 67935 and -55 to better understand and constrain the events recorded by the boulder. For 67955, we determined a Sm-Nd isochron date of  $4202 \pm 45$  Ma (6 of 6, MSWD = 1.5), precisely confirming the  $4200 \pm 70$  Ma date reported by [2]. The Rb-Sr data of [2] for 67955 suggest a possible  $\sim 900$  Ma date, which suggests a possible link to Copernicus crater [3]. However, our Rb-Sr results and Sm-Nd neutron flux data indicate a more recent ejection, consistent with an excavation of the boulder during the formation of North Ray Crater at  $\sim 50$  Ma [e.g., 4].

For 67935, we obtained a Sm-Nd isochron date of  $3903 \pm 160$  Ma (5 of 7, MSWD = 1.3). This is considerably younger than the Re-Os date ( $4210 \pm 130$  Ma) of [1] for the same sample and coincides with the age of the Imbrium basin impact (3.91–3.94 Ga, [5]), which has been proposed to be the source for many of the KREEP-rich impact melt rocks at the Apollo landing sites [e.g., 6].

Overall, our data suggest that Outhouse Rock formed  $\sim 3.9$  Ga (instead of  $\sim 4.2$  Ga) from KREEP-rich Imbrium ejecta melt, which incorporated  $\sim 4.2$  Ga feldspathic material as clasts. The boulder most likely was excavated to the surface by North Ray Crater.

[1] Fischer-Gödde M. and Becker H. (2012) *GCA* 77, 135–156; [2] Norman M. D. et al. (2016) *GCA* 172, 410–429; [3] Norman M. D. et al. (2007) *LPS XXXVIII*, Abstract #1991; [4] Drozd R. J. (1974) *GCA* 38, 1625–1642; [5] Bottke W. F. and Norman M. D. (2017) *Annu. Rev. Earth Planet. Sci.* 45, 619–647; [6] Haskin L. A. et al. (1998) *MAPS* 33, 959–975.

## 2e) Recent advances in lunar science

Monday, 23/Sep/2019: 11:15am - 1:00pm

Session Chair: Harald Hiesinger (Westfälische Wilhelms-Universität Münster)

Location: Schloss: Aula

### Session Abstract

The Moon is a fundamentally important object for our understanding of the solar system. In the last decade, several space missions visited the Moon and returned information on its internal structure, thermal evolution, chemical and mineralogical composition, physical properties, and morphology in unprecedented detail. We invite contributions that utilized these new data sets, as well as older Apollo-era data sets, to decipher the geologic history and evolution of the Moon.

### Lecture Presentations

11:15am - 11:30am

#### Dating Lunar Surface Features With Crater Size-Frequency Distribution Measurements: A Review

Harald Hiesinger

*Westfälische Wilhelms-Universität Münster, Germany*

Astronauts carefully selected samples on the Moon and characterized their geologic context. Together with the samples of the Luna missions, they allow us to ground truth remote-sensing data of the landing sites with samples that have been investigated in detail in terrestrial laboratories [e.g., 1]. One particularly important outcome was the lunar chronology, which links CSFDs of the landing sites with their sample ages [e.g., 2,3]. The lunar chronology function (CF) and its extrapolation is crucial for understanding the history and evolution of other planetary bodies. From high-resolution imagery we can determine the size-frequency distribution of impact craters on the Moon across a wide range of diameters, i.e., the lunar production function (PF). Similar to the CF, the PF is crucially important because it describes the expected crater size-frequency measured on a geologic unit at a specific time [e.g., 4]. Although the CSFD dating method generally yields robust results, several critical questions remain, including the exact shapes of the PF and CF [e.g., 5], the existence of a lunar cataclysm [e.g., 6], whether the lunar derived PF and CF functions can be extrapolated to the asteroid belt [e.g., 7] or the outer Solar System [e.g., 8], and on the effects of (self-)secondary cratering and target properties [e.g., 9,10].

Applying the CSFD method allowed us to better understand the volcanic record of the Moon [e.g., 11, indicating that the Moon was volcanically active for more than 3 Ga until about 1.2 Ga ago although irregular mare patches might be as young as <100 Ma old [12] or as old as 3.5 Ga [13]. The distribution and recent ages of lobate scarps imply that the Moon was deformed by tidal forces and shrinking within the last <100 Ma [14]. Dating impact craters yields insight into the local/regional stratigraphy by defining important stratigraphic benchmarks.

[1] Nyquist et al., 2001, Kluwer; [2] Hartmann, 1970a, Icarus 13; [3] Neukum, 1983, Habilitation, Munich; [4] Ivanov, 2001, SSR 96; [5] Robbins, 2014, EPSL 403; [6] Zellner, 2017, Orig. Life Evol. Biosph. 47; [7] Hiesinger et al., 2016, Science 33; [8] Bierhaus et al., 2018, Meteoritics 53; [9] Zanetti et al., 2017, Icarus 298; [10] van der Bogert et al., 2017, Icarus 298; [11] Hiesinger et al., 2011, Geol. Soc. Am. Spec. Pap. 477; [12] Braden et al., 2014, Nat. Geosci. 7; [13] Qiao et al., 2017, Geology 45; [14] Watters et al., 2015, Geology 43.

11:30am - 11:45am

**Ages of the geological events around the Apollo 17 landing site****Wajiha Iqbal, Harald Hiesinger, Carolyn van der Bogert***Institut für Planetologie, Westfälische Wilhelms-Universität Münster, Germany*

The Apollo 17 landing site in Taurus Littrow valley shows a diverse geological history [1]. We used Lunar Reconnaissance Orbiter (LRO) Narrow-Angle Camera (NAC) and Wide-Angle Camera (WAC) images, the LOLA/SELENE merged digital terrain model (DTM), as well as Clementine, M3, and Kaguya Mineral Imager spectral data, to produce new high-resolution geological maps around the landing site. Furthermore, we used LRO NAC-derived DTMs and other products to measure the absolute model ages (AMAs) of the mapped geological units using crater size-frequency distribution (CSFDs) measurements.

The geological history of the Taurus-Littrow valley can be divided into the Copernican, post-Imbrian, Imbrian, and pre-Imbrian periods. The Copernican-aged events include the formation of the Lee-Lincoln lobate scarp, light mantle deposit (LMD) landslides, central cluster (Cc) interpreted as secondaries from Tycho crater, and a light debris feature called the Paint-splatter. Post-Imbrian mare basalt flows and pyroclastics fill the floor of the valley. The overlying dark pyroclastic materials also appear to fill the troughs in the surrounding highlands. The extent of the flows and mantling deposits were mapped through albedo and spectral contrasts. Patches of light Imbrian plains are also mapped in highlands. Although the highlands around the valley are mostly covered by ejecta from Imbrium basin, the massifs probably represent the remnants of the crater wall or ejecta material of Serenitatis basin.

We used LRO WAC and NAC data as well as Kaguya Terrain Camera data to measure CSFDs on the various geological units in the mapping area. The Copernican units mainly show AMAs from ~75 Ma to 102 Ma [2]. The AMA for the mare basalt flows and pyroclastics cluster around ~3.70 Ga [3,4]. The Imbrian plains material in the highlands shows an AMA of ~3.80 Ga. These measured AMAs are consistent with the Apollo 17 sample ages. The ages of the samples [5] are currently being compared with the new geological map and CSFD measurements to test and improve the lunar cratering chronology [6], which allows the dating of unsampled surfaces across the Moon, and is extrapolated for use on other planetary bodies.

[1] Schmitt et al (2016) *Icarus* 298, 2-33; [2] van der Bogert et al. (2019) *LPSC* 50, 1527; [3] van der Bogert et al. (2016) *LPSC* 47, 1616; [4] Hiesinger et al. (2000) *JGR* 105, 29239-29275; [5] Stöffler et al. (2006) *Rev. Min. Geochem.* 60, 519-596; [6] Neukum (1983) *Habil. thesis*, U. of Munich.

11:45am - 12:00pm

**Complex Copernican Geology at the Apollo 17 Landing Site****Carolyn H. van der Bogert<sup>1</sup>, Harald J. Hiesinger<sup>1</sup>, Wajiha Iqbal<sup>1</sup>, Jaclyn D. Clark<sup>2</sup>, Mark S. Robinson<sup>2</sup>, Bradley L. Jolliff<sup>3</sup>, Timothy M. Hahn Jr.<sup>3</sup>, Thomas R. Watters<sup>4</sup>, Maria E. Banks<sup>4,5</sup>, Harrison H. Schmitt<sup>6</sup>***<sup>1</sup>Westfälische Wilhelms Universität Münster, Germany; <sup>2</sup>Arizona State University, USA; <sup>3</sup>Washington University in St. Louis, USA; <sup>4</sup>Smithsonian Institution, USA; <sup>5</sup>NASA Goddard Space Flight Center; <sup>6</sup>University of Wisconsin-Madison, USA*

The Apollo 17 landing site exhibits complex geology partly characterized by several recent features: the Lee Lincoln lobate scarp (LLS), a light mantle deposit (LMD), and a secondary crater cluster called the Central Cluster (CC). The latter two were previously linked to Tycho crater [e.g., 1], and exposure ages from these features were used to calibrate the lunar cratering chronology for Tycho [2]. However, recent work dating the LLS found an age similar to Tycho [3], raising the possibility that the LMD was instead triggered by seismic shaking from an LLS event [1,3,4]. We review and discuss the origins and ages of these recent events.

Exposure ages of samples from the CC and LMD led [5] to conclude that both formed ~100 Ma ago. Additional exposure ages were determined for the CC and Sculptured Hills areas [6]. In sum, the results from [6] indicated an age of ~109±4 Ma for the CC and LMD, which [6] interpreted as the age of Tycho crater.

The paucity of >~100 m diameter craters on the LLS, along with its morphological freshness, indicates that it is young [e.g., 1,8]. CSFD measurements suggest that the last significant activity on the LLS occurred ~75 Ma ago [3,9]. CSFDs on the LMD and CC are consistent with CSFDs at Tycho crater [7]. New ages for the LMD using recent NAC data (~86 Ma) match NAC measurements on Tycho ejecta (85+15/-18 Ma) [10].

The similarity of the CSFDs and exposure ages of samples from the CC and LMD suggest a common origin. However, our work dating the LLS indicates it is statistically coeval with the LMD and Tycho. As such, the spread in the exposure and CSFD ages is plausibly explained by the occurrence of multiple events ~75-110 Ma. Given that Tycho secondaries and LLS are unrelated, the question remains – which event triggered the formation of the LMD?

[1] Lucchitta (1977) *Icarus* 30, 80; [2] Wolfe et al. (1975) *PLPSC* 6, 2463; [3] van der Bogert et al. (2012) *LPSC* 43, 1847; [4] Schmitt et al. (2017) *Icarus* 298, 2; [5] Arvidson et al. (1976) *PLPSC* 7, 2817; [6] Drozd et al. (1977) *PLPSC* 8, 3027; [7] König (1977) PhD Thesis, Univ. Heidelberg, NASA TM-75023; [8] Watters et al. (2010) *Science* 329, 936; [9] van der Bogert et al. (2018) *Icarus* 306, 255; [10] Hiesinger et al. (2012) *JGR* 117, E00H10.

**12:00pm - 12:15pm**

## **The light plains of the lunar northern hemisphere**

**Claudia M. Pöhler, Harald Hiesinger, Carolyn H. van der Bogert**

*WWU Münster, Germany*

The appearance of light plains is morphologically similar to dark mare plains. Due to the morphological similarity, a volcanic origin for light plains was proposed [1]. However, the Apollo 16 mission revealed light plains consisting mostly of impact breccias [2]. This led to several new hypotheses proposing an origin by one or two basin-forming events or several local impact events [e.g., 3,4]. Meanwhile, other lines of evidence still seem to support a volcanic origin [5,6]. To investigate whether light plains have common ages and/or origins, we determined the absolute model ages (AMAs) of light plains in the northern hemisphere to expand on existing data for light plains close to the equator [7], in the southern hemisphere [8], on the northern nearside [6], and around Orientale basin [9]. On the basis of Lunar Reconnaissance Orbiter Wide Angle Camera image data (100 m/pixel) [10], we identified and characterized the light plains in our study area extending from the north pole to 45°N. We performed crater size-frequency distribution (CSFD) measurements and determined absolute model ages (AMAs) using the production and chronology functions of [11,12,13]. We carefully examined the light plains units chosen for CSFD measurements for homogenous surfaces and gave special care to exclude secondary craters. We determined AMAs for 24 light plains occurrences. The light plains show AMAs ranging from  $3.43 \pm 0.096 / -0.28$  to  $3.98 \pm 0.019 / -0.022$  Ga. We observe a peak in ages around 3.8 Ga that could potentially correlate to the Orientale basin-forming event. The large timeframe for light plains formation excludes an origin solely by a single basin-forming event. In addition, we could not find morphological evidence for a volcanic origin of the light plains. The results of this study are in agreement with an origin by local impact events covering mare units and hence resulting in flat surfaces with highland like properties.

[1] Wilhelms and McCauley (1971) *USGS I-703*; [2] Muehlenberger et al. (1972) *Apollo 16 PSR*, 6-1–6-8; [3] Head (1974) *Moon* 11, 327-356; [4] Oberbeck et al. (1974) *PLPSC* 5, 111-136; [6] Neukum (1977) *Moon* 17, 383-393; [7] Köhler et al. (2000) *LPSC* 31, 1822; [8] Hiesinger et al. (2013) *LPSC* 44, 2827; [9] Meyer et al. (2016) *Icarus* 273, 135-145; [10] Robinson et al. (2010) *Space Sci. Rev.* 150, 81-124; [11] Neukum et al. (2001) *Space Sci. Rev.* 96, 55-86; [12] Hiesinger et al. (2000) *JGR* 105, 29239-29276; [13] Crater Analysis Working Group (1979) *Icarus* 37, 467-474.

**12:15pm - 12:30pm**

## **Lunar Basaltic Volcanic Eruptions: New Discoveries and Insights from Modeling and Observations**

**James Head<sup>1</sup>, Lionel Wilson<sup>1,2</sup>**

*<sup>1</sup>Brown University, United States of America; <sup>2</sup>Lancaster University, United Kingdom*

Recent advances in lunar science have revolutionized our view of basaltic magma generation, ascent and eruption. New insights from: 1) sample analysis (discovery of increased volatile content in lunar magmas), 2) magmatic volatiles and reactions (synthesis of the production of volatiles during magma ascent), 3) experimental petrology (magma source regions and their depths), 4) theory (models of magma generation, ascent and eruption), 5) eruption dynamics (modeling of eruptions in the lunar environment), 6) rates of extrusion and degassing (the Moon may have had transient atmospheres for tens of millions of years): 7) observations

(discovery and documentation of Irregular Mare Patches, IMPs, and Ring Moat Dome Structures, RMDS), 8) chronology (interpretation of IMPs as erupting in the last 100 Ma of lunar history), have all combined to radically alter our vision of lunar basaltic volcanism. We use the basic principles of magma generation, ascent, and eruption to examine the range of dike volumes, effusion rates, volatile species, and release patterns as a function of time and eruption duration, subdividing eruptions into four sequential phases with specific individual characteristics and predictions. Giant 50- to 90-km-long, 30- to 100-m-wide dikes transfer magma volumes of up to  $\sim 1,000 \text{ km}^3$  to the lunar surface, rising from the mantle at speeds of tens of m/s, and initially delivering magma volume fluxes of up to  $\sim 10^6 \text{ m}^3/\text{s}$  to the surface. The absence of an appreciable atmospheric pressure caused eruptions to have a vigorously explosive nature, despite the low magmatic volatile content by Earth standards. Assessment of mare basalt gas release patterns during individual eruptions provides the basis for predicting the effect of vesiculation processes on the structure and morphology of associated features, subdividing typical lunar eruptions into four phases: Phase 1, dike penetrates to the surface, transient gas release phase; Phase 2, dike base still rising, high-flux hawaiian eruptive phase; Phase 3, dike equilibration, lower flux hawaiian to strombolian transition phase; and Phase 4, dike closing, strombolian vesicular flow phase. We show how these four phases of mare basalt volatile release, together with total dike volumes, initial magma volatile content, vent configuration, and magma discharge rate, can help relate the wide range of apparently disparate lunar volcanic features (pyroclastic mantles, small shield volcanoes, compound flow fields, sinuous rilles, long lava flows, pyroclastic cones, summit pit craters, IMPs, and RMDS) to a common set of eruption processes. We outline implications for the history of lunar basaltic volcanism.

**12:30pm - 12:45pm**

### **Experimental simulation of Apollo 16 “rusty rock” alteration by a fumarolic metal bearing gas**

**Christian J. Renggli, Stephan Klemme**

*Institut für Mineralogie, Universität Münster, Germany*

The volatile rich Apollo 16 melt breccia 66095 is an exception to the otherwise volatile depleted lunar rock record. The sample named “rusty rock” is enriched in the volatile elements S and Cl, and the moderately volatile metals Zn, Cd, Pb and Tl [1]. The mineralogy includes lawrencite ( $\text{FeCl}_2$ ), sphalerite ( $\text{ZnS}$ ), troilite ( $\text{FeS}$ ), Fe metal as well as Fe-hydroxides [2]. Previous work on the isotopic composition of the “rusty rock”, including the isotopic systems of Zn, Fe and Cl, suggests that the source of the volatile enrichment was a fumarolic gas phase [2,3,4]. Lunar volcanic gas was reducing at 1-2  $\log f\text{O}_2$  units below the iron-wüstite buffer (IW) and the primary gas species were  $\text{CO}$ ,  $\text{S}_2$  and  $\text{H}_2$  [5].

We explore the conditions at which the “rusty rock” sulfide and chloride minerals formed and deposited from a lunar fumarolic gas. We mixed  $\text{ZnO}$ ,  $\text{FeS}$  and  $\text{MgCl}_2$  in relative molar abundances of 1:1:2, pressed the powder into a pellet and placed it in a 30 cm long evacuated silica tube [6]. We suspended the silica tube in a vertical tube furnace for 24 h, such that the source material was at 1260 °C and the tube extended to 320 °C at the top of the furnace. The calculated  $f\text{O}_2$  of the experimental gas mixture at 1250 °C is at IW-1. After the experiment, we quenched the silica tube and cut it in 1 cm long sections to investigate the deposited phases using SEM/EDS.

The source materials  $\text{ZnO}$ ,  $\text{FeS}$  and  $\text{MgCl}_2$  decompose at 1260 °C and react to form a Fe-Zn-Cl-S gas mixture and refractory  $\text{MgO}$ . We observe metals deposited as sulfides and chlorides at temperatures below 700 °C. The four phases observed are  $\text{FeCl}_2$ ,  $\text{FeS}$ ,  $\text{ZnCl}_2$  and  $\text{ZnS}$ . The phases  $\text{ZnS}$  and  $\text{FeCl}_2$  occur together at 500-580 °C. This assemblage of  $\text{ZnS}$  and  $\text{FeCl}$  suggests that the temperature range of 500-580 °C reflects the alteration conditions of the Apollo 16 “rusty rock”.

[1] Krahenbuhl et al. (1973) LPSC 4, 1325-1348; [2] Shearer et al. (2014) GCA 139, 411-433; [3] Day et al. (2017) PNAS 114, 9457-9551; [4] Day et al. (2019) GCA, in press; [5] Renggli et al. (2017) GCA 206, 296-311; [6] King et al. (2018) RIMG 84

12:45pm - 1:00pm

**Origin of Granular Zircon in Lunar Impactites****Dennis M. Vanderliek<sup>1</sup>, Monika A. Kusiak<sup>2,3</sup>, Richard Wirth<sup>4</sup>, Harry Becker<sup>1</sup>, Alexander Rocholl<sup>5</sup>**<sup>1</sup>*Freie Universität Berlin, Institute for Geological Sciences, Malteserstr. 74 - 100, 12249 Berlin, Germany;*<sup>2</sup>*GeoForschungs Zentrum Potsdam, Section 3.<sup>6</sup>Chemistry and Physics of Earth Materials, Telegrafenberg 1, 14473**Potsdam, Germany;* <sup>3</sup>*Polish Academy of Sciences, Institute of Geophysics, Ksiecia Janusza 64, 01-452 Warsaw, Poland;*<sup>4</sup>*GeoForschungs Zentrum Potsdam, Section 3.<sup>5</sup>Interface Geochemistry, Telegrafenberg 1, 14473 Potsdam, Germany;*<sup>5</sup>*GeoForschungs Zentrum Potsdam, Section 3.<sup>1</sup>Inorganic and Isotope Geochemistry, Telegrafenberg 1, 14473**Potsdam, Germany*

In Apollo 15 breccia 15455, a pristine cataclastic norite cross-cut by an impact melt vein, granular zircon ( $\text{ZrSiO}_4$ ) aggregates of 5 – 20  $\mu\text{m}$  occur in  $\text{SiO}_2$ -diopside enriched domains. The latter are interpreted as representing late stage igneous crystallization products within the norite. All zircons show a granular texture consisting of aggregates of euhedral 1 – 2  $\mu\text{m}$  sized zircon neoblasts. Although these textures are important to tie their U-Pb ages to impact heating, the formation mechanisms of these aggregates are still poorly understood. Locally, zircons formed between  $\text{SiO}_2$  and relict baddeleyite (partially recrystallized to zircon), suggesting a reaction relationship. Using a focused ion beam, a section was cut through a granular zircon to study the internal properties using transmission electron microscopy (TEM). The cores of the granules were found to be amorphous whereas their rims are crystalline. Triple junctions between the granules form nearly perfect angles of  $120^\circ$  and are filled with amorphous silica containing minor concentration of Mg and Fe as analyzed by EDX analysis. The silica glass occasionally contains relict bubbles and obviously represents melt trapped in-between the zircon neoblasts. Previous studies interpret aggregates of granular zircon neoblasts as indicators of impact-induced recrystallization of zircon, presumably in bedrock adjacent to large impact melt sheets [1,2]. Based on textures and petrography, the mechanism of recrystallization or new crystallization of zircon appears to be the mobilization of silica by highly localized shock-induced (?) melting of silicates along grain boundaries and Zr release from existing zircon and/or baddeleyite. The bubbles found in some of the interstitial glass imply a volatile rich nature of the melt. Granular zircon aggregates appear to represent a robust texture for identification of impact-related zircon growth. *In-situ* U-Pb ages produced at the GFZ Potsdam using the CAMECA IMS 1280 HR suggest that the granules formed at  $\sim 4.2$  Ga. Previous dating of granular zircon in the same sample yield ages of  $\sim 4.3$  Ga [2]. Our study supports that impact-induced localized melting can lead to spatially confined recrystallization and complete resetting of the U-Pb system in previously existing Zr phases.

[1] Grange, M. L., Nemchin, A. A., & Pidgeon, R. T. (2013). *JGR:P*, 118(10), 2180-2197; [2] Crow, C. A., McKeegan, K. D., & Moser, D. E. (2017). *GCA*, 202, 264-284.

## Poster Presentations

Mon: 11

### Exploration of Icelandic lava caves and extrapolation to a semi-permanent Lunar habitat

**Marjolein Daeter<sup>1</sup>, Marc Heemskerck<sup>1</sup>, Bernard Foing<sup>1,2,3</sup>**

<sup>1</sup>VU Amsterdam, The Netherlands; <sup>2</sup>ESTEC, ESA; <sup>3</sup>ILEWG/EuroMoonMars

For the testing and planning of Lunar missions, it is important to find terrestrial locations comparable to The Moon. Current Moon-analogue bases, like HiSeas (Hawaii) and LunAres (Poland) rely on vast, man-made structures. Because bringing this much material to The Moon to build a semi-permanent settlement might not be feasible, a possible alternative is to use already existing structures in the Lunar subsurface. An example of these structures is lava caves.

Lava caves are long stretched, cylindrical cave structures, formed by the crystallization of a layer of rock around a lava flow. These cave systems have sporadic openings to the surface, making them relatively easy to access. But what makes the lava caves the most convenient, is that the temperature inside the caves is roughly the average surface temperature. For The Moon this would mean that the temperature is stable around -20°C. This is much less extreme and more stable than possible temperature variations on the Lunar surface, meaning less temperature adjustments would need to be made to create a habitable living environment. Secondly, caves also give protection against radiation and (micro)meteorites.

The reason that lava caves in Iceland would be a good analogue site, is that the Icelandic basalts are geochemically similar to basalts on The Moon. The low weathering rate on Iceland due to the cold climate also makes the geomorphology of the caves similar to what we expect of Lunar lava caves. Furthermore, the remoteness of the lava caves (1.5 hour drive from Reykjavik) and the difficult weather conditions, especially in winter, add to the suitability of this location to be a Moon-analogue site.

In September 2018, a team of researchers visited three cave systems in Iceland. The Stefanshellir lava cave was selected for a Lunar analogue base, because of its remote location and long lava tubes. A campaign to Iceland in August this year will cover exploration of the cave systems with drones and mapping of the surrounding area. Furthermore, the first simulations of analogue Lunar missions will be conducted. This will include equipment testing, geological and glaciological research as well as evaluation of psychological and protocol factors.

A Moon-analogue habitat in lava caves in Iceland can be a real addition to already existing analogue-sites because it is very possible that our first semi-permanent base will be using already existing structures in or on the (sub)surface of The Moon, and perhaps in the future, even Mars.

Mon: 12

### The ESA-JAXA-CSA-NASA Joint Study HERACLES on Returning to the Moon

**Harald Hiesinger<sup>1</sup>, Markus Landgraf<sup>2</sup>, William Carey<sup>2</sup>, Yuzuru Karouji<sup>3</sup>, Tim Haltigin<sup>4</sup>, Gordon Osinski<sup>5</sup>, Urs Mall<sup>6</sup>, Ko Hashizume<sup>7</sup>**

<sup>1</sup>Westfälische Wilhelms-Universität Münster, Germany; <sup>2</sup>European Space Agency (ESA), Directorate of Human Spaceflight and Robotic Exploration Programmes; <sup>3</sup>Japan Aerospace Exploration Agency (JAXA), Space Exploration System Technology Unit; <sup>4</sup>Canadian Space Agency (CSA); <sup>5</sup>University of Western Ontario, Centre for Planetary Science and Exploration; <sup>6</sup>Max-Planck Institut für Sonnensystemforschung; <sup>7</sup>Ibaraki University, Dept. of Earth Science

**Introduction:** Several space agencies have recognized the scientific (and strategic) benefits of returning to the Moon as well as the opportunities the Moon offers for testing hardware and operational procedures for the exploration and utilization of space beyond Low Earth Orbit. In this context, the Human Enhanced Robotic Architecture Capability for Lunar Exploration and Science (HEREACLES) is an ESA-led international effort to prepare for the return of humans to the Moon and to provide opportunities for unprecedented science utilizing the lunar Gateway. HERACLES is a joint phase-A study of the European Space Agency (ESA), the Japan Aerospace Exploration Agency (JAXA), the Canadian Space Agency (CSA), and NASA.

**Mission Concept:** The key objectives of HERACLES include: (1) Preparing the return of humans by implementing, demonstrating, and certifying technologies for human lunar landing, surface operations, and return; (2) Create opportunities for science, including sample return; (3) Gain scientific and exploration knowledge, particularly on potential resources; and (4) Create opportunities to demonstrate and test technologies and operational procedures for future Mars missions. HERACLES will consist of the Lunar Descent Element (LDE), which will be provided by JAXA, the ESA-built Interface Element that will house the Canadian rover, and the European Lunar Ascent Element (LAE) that will return the samples to the lunar Gateway. The 330 kg rover will be powered by a radioisotope power system that will enable the rover to drive more than 100 km and to survive lunar night. The rover will collect samples along a ~35 km long traverse from about ten individual sampling stations and will return them to the LAE. The rover will be equipped with a suite of scientific instruments that will allow us to comprehensively study the sampling locations and the context of the samples, as well as the geology along the traverse. The international Science Definition Team (iSDT) is currently discussing an appropriate instrument suite, which will most likely include cameras, spectrometers, a laser reflector, and potentially some geophysical instruments. During the surface mobility demonstration phase, the rover will go on a >100 km long traverse. The iSDT is evaluating a suite of potential landing sites, guided by the recommendations of the 2007 NRC report and several subsequently published documents. The list of potential landing sites includes the Schrödinger basin, the Moscoviense basin, Copernicus crater, Jackson crater, and some young basalts in the Flamsteed region.

## Mon: 13

### Geology and ages of the landing sites: Apollo 11, Apollo 12 and Apollo 17

**Wajiha Iqbal, Harald Hiesinger, Carolyn van der Bogert**

*Institut für Planetologie, Westfälische Wilhelms-Universität Münster, Germany*

The lunar cratering chronology [1,2] is widely used to derive absolute model ages (AMAs) of geological units on the Moon [3], as well as other terrestrial planetary bodies throughout the Solar System. With new datasets, the accuracy of the chronology can be tested and updated via reexamination of the calibration points from the landing sites [4,5,6], which consist of both crater size-frequency distribution measurements and sample ages.

Using data including Lunar Reconnaissance Orbiter Camera (LRO) Narrow-angle Camera (NAC) and Wide Angle Camera (WAC) frames, digital terrain models (DTM) derived from LOLA/SELENE merged data, as well as spectral data collected by Clementine, M3, and Kaguya Mineral Imager, we are producing new detailed geological maps around the Apollo landing sites. The geological units are defined via albedo, relief, and spectral differences. The new geological maps were used to identify homogeneous areas with crater densities characteristic for the sampled materials. We also used high-resolution LROC NAC and the LRO NAC-derived DTMs, to measure crater size-frequency distributions (CSFD) and determine  $N(1)$  values (i.e. the cumulative number of craters with diameters  $\geq 1$  km) for the different geological units around the landing sites.

We correlated the updated radiometric ages of well-studied Apollo samples [7] with the newly measured  $N(1)$  values, to improve the calibration points for the lunar chronology curve [1]. We gained several calibration points representing the geological units including mare units, and crater materials around the landing sites Apollo 11, 12, and 17. The new, improved calibration points gained from the geological units around the landing sites supports the validity of the lunar chronology curve [1].

[1] Neukum(1983) Habil. thesis, U. of Munich; [2] Neukum et al. (2001) Space Sci. Rev. 96, 55; [3] Hiesinger, et al. (2000) JGR 105, 29239; [4] Iqbal, et al (submitted 2019) Icarus; [5] Iqbal, et al (2018) LPSC 49, 1002; [6] Iqbal, et al (2018) LPSC 50, 1005; [7] Stöffler, et al. (2006) RMG 60, 519.

**Mon: 14****Mare Moscoviense: A site for future lunar missions****Sascha Mikolajewski, Harald Hiesinger, Carolyn H. van der Bogert***Institut für Planetologie, Westfälische Wilhelms-Universität Münster, Wilhelm-Klemm-Str. 10, 48149 Münster, Germany*

**Introduction:** Exploration of the Moon has generated increasing international interest over the last few years. Several studies [1-11] have used multispectral data and images to gain insights into the timing and duration of mare volcanism on the Moon. Clementine [1, 2] and Kaguya [3-5] spectral data, have been used to document compositional differences in lunar rocks and regolith. In this work, we use recent lunar datasets for Mare Moscoviense, on the lunar farside, to generate a new geological map and examine possible landing locations for future missions.

**Data/Methods:** Within ArcGIS, we used Kaguya Mineral Maps [3], Clementine FeO and TiO<sub>2</sub> multispectral data [1], and Lunar Reconnaissance Orbiter Camera (LROC) datasets [7] to define morphological and compositional geological units within Mare Moscoviense. Using digital terrain models [8], slope maps, and LRO Diviner rock abundance values [6], we examined possible safe landing sites and select locations for scientific research.

**Results:** Inside Mare Moscoviense, there are three volcanic flows with different spectral compositions [9 and this work]. The slope map derived from the LROC image digital elevation model indicates that the basin floor is very flat. The rock abundance map of the targeted region indicates that the southeastern and eastern part of the basin has the lowest abundance of rocks.

**Discussion/Conclusions:** On the lunar farside, mare volcanism occurs on a smaller scale than compared to the nearside as shown by [10, 11, and this work]. The southeastern and eastern volcanic flows show the lowest abundance of rocks compared to the other flows. The eastern flow provides access to older impact craters that may be related to the original basin floor. The evaluation of the rock abundance values also showed that the eastern part of Mare Moscoviense is the most promising part for scientific research with respect to lander and rover safety.

[1] Lucey et al. (1998) *JGR*, 103, 3679-3699; [2] Chevrel. et al. (2000) *JGR*. 107, NO. E12, 5132; [3] Lemelin et al. (2016) 47<sup>th</sup> LPSC #2994; [4] Morota et al. (2009) *GRL*, 36, L21202; [5] Morota et al. (2011) *Earth Planets Space*, 63, 5-13; [6] Bandfield et al. (2011) *Icarus*, 116; [7] Sato et al. (2017) *Icarus*, 296, 216-238; [8] Scholten et al. (2012) *JGR*, 117(3); [9] Kramer et al. (2008) *JGR*, 113; [10] Pasckert et al. (2015) *Icarus*, 257, 336-354; [11] Pasckert et al. (2018) *Icarus*, 299, 538-562.

**Mon: 15****Lunar gravity: Impact processes inform the density structure of the mare crust****Gregory A. Neumann<sup>1</sup>, Sander J. Goossens<sup>2</sup>, Ariel N. Deutsch<sup>3</sup>, James W. Head<sup>3</sup>***<sup>1</sup>Solar System Exploration Division, NASA Goddard, Greenbelt, MD, United States of America; <sup>2</sup>CRESST, University of Maryland Baltimore County, USA; <sup>3</sup>Department of Earth, Environmental and Planetary Sciences, Brown University, Providence, RI, USA*

Recent improvements in Gravity Recovery and Interior Laboratory (GRAIL) modeling (Goossens et al., 2018; 2019 submitted) allow a closer look at the laterally variable density structure of the nearside lunar mare regions. Spectral analyses of gravity in highland regions exhibit nearly perfect correlation with topography at spherical harmonic degrees from 250 to beyond 900, corresponding to spatial scales < 12 km, but in most of the nearside mare and the interior regions of the farside South Pole-Aitken basin the correlations drop off substantially. Since these scales are only influenced by the shallow crustal density structure, we employ relatively fresh impact craters in the range of 3-5 km depth and 16-130 km diameter as probes of mare density. Modeled gravity anomalies of these craters suggest an increase in density of 25-30% averaged over the crater depths between the excavated mare flow layers and the surrounding highlands. We interpret these results in the light of enigmatic quasi-circular gravity anomalies, in the southwestern Procellarum region for example, that have been suggested to arise from some combination of buried craters, volcanic intrusion and/or mantle uplift and crustal thinning.

Mon: 16

## Geological Mapping of the South Pole-Aitken Basin - A Progress Report

**Claudia Pöhler<sup>1</sup>, Harald Hiesinger<sup>1</sup>, Mikhail A. Ivanov<sup>2</sup>, Cedric Rueckert<sup>1</sup>, Carolyn H. van der Bogert<sup>1</sup>**

<sup>1</sup>WWU Münster, Germany; <sup>2</sup>Vernadsky Institute, RAS, Russia

The South Pole-Aitken basin (SPA), situated on the lunar farside and centered at 53°S 169°W, is the largest and oldest basin [1,2] on the Moon. Due to its morphological appearance it is argued that the SPA basin formed within an already solidified lunar crust [3]. Therefore, the time of SPA formation gives valuable information on the evolution of the lunar crust. The large scale of the impact led to the hypothesis of it penetrating the crust, potentially exposing lunar mantle material within the SPA [e.g., 4]. Thus, it might be possible to observe lunar mantle material or lower crustal material excavated by the impact event [e.g., 5]. Recently, the SPA has been the focus of several ongoing and upcoming missions [6-9]. On January 2, 2019, Chang'e 4 performed the first ever soft-landing on the farside of the Moon in Von Kármán crater (175.9° E and 44.8° S) [7]. This project is part of the PLANetary MAPping project, a Horizon2020-COMPET4 project, aiming to develop a professional European network for geological mapping. In the scope of PLANMAP we are creating a geological map of the SPA based on photogeology and absolute model ages derived by crater size-frequency distribution measurements. In the study area two major classes of landforms can be observed: (1) impact craters and related materials and (2) plains forming material. Impact craters and their related material are divided into further classes by different stages of degradation, allowing for relative age determinations. The plains forming material can represent volcanic activity as well as impact cratering e.g. by emplacement of distal ejecta from impact craters/basins. This map is an extension of the map by [8].

[1] Wilhelms (1987) USGS SP-1348, 302; [2] Hiesinger et al. (2012) LPSC 43, 2863; [3] Stuart-Alexander (1978) USGSMapi-1047, 1978; [4] Melosh et al. (2017) *Geology* 45, 1063-1066; [5] Yamamoto et al. (2010) *Nature Geoscience* 3, 533-536; [6] Hiesinger et al. (2018) LPSC 49, 2070; [7] Huang et al. (2018) *JGR* 123, 1684-1700; [8] Ivanov et al. (2018) *JGR* 123, 2585–2612; [9] Joliff et al. (2010) *LPI Cont* 1595, 3072.

## 3) Orogenis

### 3b) Tectono-Metamorphic Evolution of the Cyclades, Greece

Wednesday, 25/Sep/2019: 8:30am - 10:30am

**Session Chair: Michael Bröcker** (WWU Münster)

**Session Chair: Paris Xypolias** (University of Patras)

**Location: H4**

#### Session Abstract

The Attic-Cycladic Crystalline Belt represents a major tectonostratigraphic unit of the Hellenides and records a complex structural and metamorphic evolution that illustrates many aspects of subduction zone metamorphism and the exhumation of HP/LT rocks. Many decades of intensive research have unravelled the general geological and tectonic context, but in detail there are still significant knowledge gaps. We invite contributions focusing on the P-T-t and structural evolution of the Cyclades including the pre-subduction stratigraphy and paleogeography, and encourage submissions that integrate new advances in micro-analytical methods and modelling techniques.

#### Lecture Presentations

**8:30am - 9:00am** *Session Keynote*

#### **Tectonic and geodynamic evolution of the Aegean region, from mantle dynamics to crustal evolution**

**Laurent Jolivet**

*Sorbonne Université, France*

The tectonic history of back-arc region is intimately linked with the dynamics of subducting slabs at depth and associated mantle flow. The Mediterranean, and more specifically the Aegean-Anatolia region, has been at the forefront of studies of these relations between mantle and crustal processes. Starting in the Eocene with the subduction of oceanic and continental pieces of Apulia and construction of the Hellenic accretionary wedge with large-scale nappes and HP-LT metamorphism, the tectonic history of this region changed drastically at the turn of the Eocene-Oligocene. The regime of subduction changed when slab retreat accelerated and the Aegean Sea started to form by N-S extension and exhumation of MCC below the North Cycladic, West Cycladic, and Paros-Naxos detachment systems. Just above the retreating subduction zone the Cretan detachment exhumed the HP-LT tectonic units of Crete and the Peloponnese. At about 15 Ma, a slab tear formed below western Anatolia and eastern Aegean, permitting a faster retreat of the Hellenic arc and fast rotation of the Hellenides, until 8 Ma. This tear induced the emplacement of high-temperature gneiss domes (Naxos, Mykonos, Ikaria) and granitoids exactly during the same period. More recently a tear started to form farther west, below the Corinth Rift and the Peloponnese, and the North Anatolian Fault propagated in the Aegean Domain. The central part of the Aegean Sea and Crete were then flanked by two tears and slab retreat accelerated once more. This evolution can be modelled numerically in 3-D and slab retreat and associated mantle flow appear the main drivers of this evolution. An additional contribution of larger-scale mantle convection is likely, explaining the synchronous rifting of the Gulf of Aden and Red Sea. These interactions between mantle dynamics and crustal deformation have first-order consequences on the magmatic and metallogenic evolution of the Aegean-Anatolia region and the active geothermal activity of western Anatolia.

9:00am - 9:15am

**Dating white micas in the blueschist-greenschist domain: pointless or worthwhile?****Jan Wijbrans<sup>1</sup>, Bertram Uunk<sup>1</sup>, Manuel Alvarez Paz<sup>1,2</sup>, Fraukje Brouwer<sup>1</sup>**<sup>1</sup>Vrije Universiteit Amsterdam, The Netherlands; <sup>2</sup>University of Oviedo, Spain

White K-mica  $^{40}\text{Ar}/^{39}\text{Ar}$  dating is a powerful tool for constraining the timing and rates of metamorphism, deformation and exhumation. However, in the greenschist-blueschist-eclogite series dating may result in unexpectedly wide age ranges, which are not easily reconciled with constraints from other isotopic systems. The Cycladic Blueschist Unit (CBU) in Greece is has emerged as one of the focal areas in the discussion of the interpretation of such HP metamorphic  $^{40}\text{Ar}/^{39}\text{Ar}$  age series. Phengite multi-grain stepheating of CBU micas has yielded undulating 'crankshaft-shaped' age spectra ranging between 20-60 Ma. While some studies attempt to assign geological significance to ages seen in such spectra, others argue the ages are geologically meaningless and result from an interplay of partial diffusive resetting and continued crystallization.

By taking the alternative approach of multiple single grain fusion experiments, we demonstrate that we can quantify age heterogeneity within and between samples of variable metamorphic and overprinting grades, contrasting deformation mechanisms and intensities of deformation. The shape of single grain fusion age distribution patterns provide quantitative constraints on the homogeneity of samples and on the mechanism controlling  $^{40}\text{Ar}$  loss. Homogeneous age populations reflect the transition from effectively open to closed system conditions, heterogeneous populations indicate incomplete or heterogeneously acting processes. By comparing age distributions at the rock, outcrop and island scale, the scale at which different age-populations develop can be determined.

Results show clear evidence for both homogeneous and heterogeneous age populations. In the areas that preserve high pressure metamorphic assemblages in north Syros and north Sifnos, age results of 40-50 Ma are remarkably similar for different rocks within an outcrop (eclogite vs blueschist vs greenschist vs marble) while age variation occurs between different outcrops in the area. In the more pervasively overprinted domains of southern Syros and southern Sifnos, different rocks in an outcrop yield marked age contrasts, where age distributions are either heterogeneous spanning a larger part of the retrograde PT path (40-20 Ma) or homogeneously reflect the overprint (30-20 Ma).

The multiple single grain fusion ages are interpreted to reflect an interplay of diffusive resetting and (re) crystallisation, with variable relative contributions of these processes in the different domains and yields a more complete inventory of ages and thus leads to a better understanding of the processes responsible for age preservation during and after high pressure metamorphism.

9:15am - 9:30am

**Extracting metamorphic time scales using fluid inclusions****Bertram Uunk, Rosanne Huybens, Boris Versteegh, Onno Postma, Fraukje Brouwer, Jan Wijbrans***Vrije Universiteit Amsterdam, The Netherlands*

Metamorphic minerals trap ambient hydrous fluids in fluid inclusions. When sufficiently saline, dissolved KCl in the inclusion fluid will produce radiogenic  $^{40}\text{Ar}$  by radioactive decay, potentially allowing dating of fluid incorporation by the K/Ar system. Whilst primary fluid inclusions can date fluid incorporation during mineral growth, secondary fluid inclusions may provide age constraints on subsequent fluid flow events affecting the mineral.

At VU Amsterdam, a new *in-vacuo* crushing apparatus to determine the  $^{40}\text{Ar}/^{39}\text{Ar}$  age of fluid inclusions has been designed based on previous crushers<sup>1</sup>. Gas is released by crushing mineral separates inside a crusher tube connected to a quadrupole or multi-collector mass spectrometer. *In-vacuo* crushing occurs by lifting and dropping a steel pestle using an external coil. The new crusher design allows substantially improved control over individual crushing strokes. Step-wise crushing is achieved by increasing the number of strokes for each analysis, progressively sampling smaller and more isolated inclusions whilst reducing the grain size. A subsequent stepwise heating experiment can be conducted on the crushed powder by inserting the crusher tube into a resistance furnace.

Garnet samples from the high pressure (HP) metamorphic Cycladic Blueschist Unit in Greece were crushed to obtain fluid inclusion ages. In some cases, resulting fluid inclusions  $^{40}\text{Ar}/^{39}\text{Ar}$  ages overlap with the age of garnet growth as determined by Lu/Hf or Sm/Nd. This shows that the method is able to accurately date primary fluid inclusion incorporation during hosting crystal growth during peak blueschist to eclogite metamorphism (55-40 Ma). In other cases, fluid inclusions  $^{40}\text{Ar}/^{39}\text{Ar}$  ages postdate constraints on Lu/Hf and Sm/Nd, instead overlapping with the age of phengite (re)crystallisation. This indicates the method is also capable of constraining the age of fluid pulses during retrograde metamorphism, trapped as secondary fluid inclusions in garnet.

The stepwise crushing approach shows promise as an effective tool for dating fluid inclusions in minerals and thus provides a unique tool to actually date pulsed fluid flow during metamorphism. In HP metamorphic rocks the only potassium-bearing mineral is phengite, which is often plagued by incomplete resetting or multiple competing stages of mineral growth, resulting in ambiguous age results. Especially in these rocks, the method greatly expands our possibilities to accurately date metamorphic processes in the presence of fluids.

[1] Qiu, H.-N. & Wijbrans, J. R. Paleozoic ages and excess  $^{40}\text{Ar}$  in garnets from the Bixiling eclogite in Dabieshan, China: New insights from  $^{40}\text{Ar}/^{39}\text{Ar}$  dating by stepwise crushing. *Geochimica et Cosmochimica Acta* **70**, 2354-2370

**9:30am - 9:45am**

### **Sr and Ar diffusion systematics in polygenetic white micas from Naxos**

**Alexandre Jean Daniel Peillod<sup>1</sup>, Johannes Glodny<sup>2</sup>, Uwe Ring<sup>1</sup>, Alasdair Skelton<sup>1</sup>, Igor Maria Villa<sup>3,4</sup>**

<sup>1</sup>Dept of Geological Sciences, Stockholm University, 10691 Stockholm, Sweden; <sup>2</sup>German Research Centre for Geosciences GFZ, Telegrafenberg, 14473 Potsdam, Germany; <sup>3</sup>Universität Bern, Institut für Geologie, 3012 Bern, Switzerland; <sup>4</sup>Università di Milano Bicocca, Centro Universitario Datazioni e Archeometria, 20126 Milano, Italy

The metamorphic history of Naxos includes an Eocene blueschist event, Oligocene greenschist retrogression, and a Miocene high-temperature (HT) overprint. Age attributions for these events are inconsistent [1-3].

To resolve the contradictions we combined electron microprobe (EPMA) characterization of the white mica (WM) generations with multichronometry. WM samples analyzed by [2] consisted of “coarse” and “fine” sieve fractions (500-160  $\mu\text{m}$ , 90-160  $\mu\text{m}$ ). On three samples of that suite we obtained closely spaced microchemical analyses of WM. EPMA demonstrates that all three WM samples are strongly heterogeneous, each consisting of chemically distinct generations. This chemical disequilibrium explains [4] why Rb-Sr isochrons have MSWD >30 [2]. As in other polymetamorphic rocks [5], the two sieve sizes contain different WM generations.

Both sieve fractions of four WM samples were analyzed by  $^{39}\text{Ar}$ - $^{40}\text{Ar}$  stepheating. All eight age spectra are hump-shaped, as expected [1]. The “fine” sieve fractions are always Cl-rich than the “coarse” ones. The HT zone samples give linear arrays in Cl/K-age isotope correlation diagrams, proving that two WM generations predominate (one Cl-poor at ca. 38 Ma, one Cl-rich at 20-30 Ma). Low-grade sample Na0710 was less pervasively recrystallized, is older, and preserves  $\geq 3$  WM generations; its Cl-Si-rich, younger phengitic WM is preferentially enriched in the coarse fraction. In the HT zone, Rb-Sr ages [2] coincide with K-Ar ages. Ar diffuses  $4 \times 10^4$  times faster than Sr [6], therefore (i) K-Ar and Rb-Sr only can agree if both date mica crystallization, (ii) subsequent diffusive Ar loss from WM was negligible. Na0710 preserves a relict generation with a K-Ar age >62 Ma (cfr. [3]), consistent with the high Ar retentivity of WM [7]. The Rb-Sr 36 Ma isochron age of Na0710 [2] has high MSWD, as  $\geq 3$  non-cogenetic phases coexist in mutual disequilibrium.

The degassing rates of the fine and coarse WM fractions rule out “multidomain” diffusion (see the discussion of grain size dependence of degassing in [8]). As no sample is monomineralic, each degassing is controlled by the mass balance of the unrelated rate constants of its constituent phases. Major element heterogeneity suggests that all HP phengite grains are intergrown with retrograde muscovite, at a scale <1  $\mu\text{m}$  [5]. The HP event occurred around 38 Ma, relict mica survives in the low-grade zone.

[1] Contrib.Mineral.Petrol. 93(1986)187; [2] J.Metam.Geol. 35(2017)805; [3] Tectonophysics 745(2018)66; [4] Contrib.Mineral.Petrol. 156(2008)27; [5] Geol.Soc.LondonSpec.Pub. 378(2014)69; [6] Precamb.Res. 71(2019)76; [7] J. Petrol. 55(2014)803; [8] Contrib.Mineral.Petrol. 167(2014)1010

9:45am - 10:00am

**Metasomatic sulfur-driven redox reactions: A case study of Syros, Greece**Jesse B Walters<sup>1</sup>, Alicia Cruz-Urbe<sup>1</sup>, Horst Marschall<sup>2</sup><sup>1</sup>University of Maine, United States of America; <sup>2</sup>Goethe Universität Frankfurt, Germany

The mélange exposed on the island of Syros offers a unique opportunity to study the mobility of volatiles, such as sulfur, during subduction metamorphism and exhumation. One mole of sulfur may oxidize or reduce up to eight moles of iron. Therefore, reactions involving sulfur may drastically alter the mineralogy of rocks undergoing prograde metamorphism, and infiltration by sulfur-bearing fluids at the slab-mantle interface may aid in mélange formation. Fluid fractionation models generated by Perple\_X show that the oxidized sulfur species  $\text{HSO}_4^-$ ,  $\text{SO}_4^{2-}$ ,  $\text{HSO}_3^-$ , and  $\text{CaSO}_{4(\text{aq})}$  (from high to low concentration) become abundant in slab fluids following lawsonite breakdown along cold subducting slab-top geotherms. In addition, sulfur oxidation leads to ~60 % decrease in the initial  $\text{Fe}^{3+}/\text{SFe}$ .

Comparing thermodynamic model predictions to field and petrographic observations highlight a complex story of sulfide breakdown and reprecipitation in the mélange, such as during rind formation. Prograde sulfides are rare, occasionally preserved as inclusions in omphacite and garnet within the unaltered cores of metagabbroic blocks. These textural observations suggest that sulfide breakdown is largely complete as the rocks reach the eclogite facies. In contrast, sulfides associated with reaction-rind formation are relatively common. The innermost rinds of metagabbroic blocks in many cases show a replacement of the peak assemblage of garnet + omphacite + clinozoisite + rutile by the assemblage garnet + omphacite + chlorite + ilmenite + pyrite. This texture indicates that sulfide precipitation may have begun in the eclogite facies as blocks were first incorporated into the mélange. In one metagabbro block, pyrite is associated with the replacement of garnet + omphacite by glaucophane + chlorite. Pyrite is also commonly associated with outermost actinolite + chlorite + minor magnetite/ilmenite rinds in contact with the mélange matrix. In contrast, sulfides are absent from glaucophanite, omphacite, actinolite + talc, and magnetite + chlorite rinds. These textures suggest: 1. Sulfides are associated with mineralogical changes indicative of increasing  $f\text{O}_2$  (e.g., ilmenite after rutile), 2. Sulfide precipitation occurs intermittently, and 3. Sulfides formed during an earlier metasomatic phase may be removed during a later stage. These observations are consistent with the oxidized sulfur-bearing fluids predicted in our fluid fractionation models. Additionally, the occurrence of high  $f\text{O}_2$  sulfide-absent assemblages, such as chlorite + magnetite, suggest that other oxidation reactions may occur in addition to those involving sulfur.

10:00am - 10:15am

**Fabric-forming amphiboles in the Cycladic Blueschists and their tectonic implications**Paris Xypolias<sup>1</sup>, Nikolaos Gerogiannis<sup>1</sup>, Eirini Aravadinou<sup>1</sup>, Kostas Papapavlou<sup>2</sup>, Vasileios Chatzaras<sup>3</sup><sup>1</sup>Department of Geology, University of Patras, GR-26500, Patras, Greece; <sup>2</sup>GEOTOP, Université du Québec à Montréal, H2X 3Y7, Montréal, Canada; <sup>3</sup>The University of Sydney, School of Geosciences, New South Wales, Sydney, Australia

In this work, we present compositional and textural data of fabric-forming amphiboles from the Cycladic Blueschists exposed in Evia, Andros, and Sifnos islands.

The Cycladic Blueschists is characterized by two dominant phases of ductile deformation. The first phase is characterized by a locally well-preserved foliation. However, throughout the Cyclades, the early foliation is overprinted by structures formed during the second phase. The second phase is well-developed and is mainly expressed by a penetrative foliation and a well-developed ENE-trending stretching lineation associated with consistent ENE-directed ductile shearing. The intensity of the second foliation varies from a weakly-developed cleavage up to a mylonitic foliation. These mylonites commonly define thrust-sense shear zones, which restack the nappe pile established during the first phase.

Amphiboles defining the first foliation are compositionally characterized as glaucophane. Locally, these glaucophane grains display a compositional zoning from core to rim expressed by an increase in  $\text{Al}^{\text{VI}}$ ,  $\text{Fe}^{+2}$ , and  $\text{Na}_\text{B}$  content. The second foliation is defined by the shape-preferred orientation of acicular sodic, sodic-calcic

and calcic amphiboles. Sodic amphiboles are (ferro-)glaucophane and show a systematic decrease in  $\text{Fe}^{+3}/(\text{Fe}^{+3}+\text{Al}^{\text{VI}})$  ratio towards the grain rims. Sodic-calcic and calcic amphiboles are typically represented by (ferro-)winchite and actinolite, respectively. (Ferro-)winchite and actinolite occur either as isolated grains oriented parallel to the fabrics of the second phase or grow at the edges and necks of fractured (ferro-)glaucophane grains or on the outermost rims of (ferro-)glaucophane grains. Moreover, barroisite grows locally at the rims of sodic amphiboles (e.g., Sifnos).

Compositional data from amphiboles defining the first foliation indicate increase in metamorphic pressure during the syn-kinematic growth of glaucophane. Therefore, this phase is likely associated with the burial stage of the Cycladic Blueschists. Amphiboles defining the second-phase fabrics show that these rocks passed from the stability field of glaucophane to that of actinolite during progressive deformation. This deformation phase is associated with the main exhumation of the Cycladic Blueschists. Several studies suggest that exhumation was achieved by a mechanism of ductile extrusion. Our observations indicate that the ductile extrusion of the Cycladic Blueschists commenced under blueschist facies conditions and continued up to greenschist facies conditions. Therefore, the Cycladic Blueschists represent a natural example, which shows that ductile extrusion/exhumation can be accomplished during a single deformation phase.

**10:15am - 10:30am**

### **The age, origin and emplacement of the Tsiknias Ophiolite, Tinos, Greece**

**Thomas Neil Lamont<sup>1</sup>, Mike Searle<sup>2</sup>, Nick Roberts<sup>3</sup>, Phillip Gopon<sup>2</sup>, Dave Waters<sup>2</sup>**

<sup>1</sup>University of St Andrews, United Kingdom; <sup>2</sup>University of Oxford, United Kingdom; <sup>3</sup>Geochronology and Tracers Facility, British Geological Survey, Environmental Science Centre

The Tsiknias Ophiolite, exposed at the highest structural levels of Tinos, Greece, represents a thrust sheet of Tethyan oceanic crust and upper mantle emplaced onto the Attic-Cycladic Massif. We present new field observations and a new geological map of Tinos, integrated with petrology, THERMOCALC phase diagram modelling, U–Pb geochronology and whole rock geochemistry, resulting in a tectono-thermal model that describes the formation and emplacement of the Tsiknias Ophiolite and newly identified underlying metamorphic sole. The ophiolite comprises a succession of partially dismembered and structurally repeated ultramafic and gabbroic rocks that represent the Moho Transition Zone. A plagiogranite dated by U–Pb zircon at  $161.9 \pm 2.8$  Ma, reveals that the Tsiknias Ophiolite formed in a supra-subduction zone setting, comparable to the “East-Vardar Ophiolites”, and was intruded by gabbros at  $144.4 \pm 5.6$  Ma. Strongly sheared metamorphic sole rocks show a condensed and inverted metamorphic gradient, from partially anatectic amphibolites at P–T conditions of ca. 8.5 kbar 850–600 °C, down-structural section to greenschist-facies oceanic meta-sediments over ~250 m. Leucosomes generated by partial melting of the uppermost sole amphibolite, yielded a U–Pb zircon protolith age of ca. 190 Ma and a high-grade metamorphic-anatectic age of  $74.0 \pm 3.5$  Ma associated with ophiolite emplacement. The Tsiknias Ophiolite was therefore obducted ~90 Myrs after it formed during initiation of a NE-dipping intra-oceanic subduction zone to the northeast of the Cyclades that coincides with Africa’s plate motion changing from transcurrent to convergent. Continued subduction resulted in high-pressure metamorphism as the leading edge of the Cycladic continental margin attempted to subduct ~25 Myrs later.

## Poster Presentations

Tue: 2

**Exhumation patterns in a bivergent metamorphic core complex: The central Menderes Massif (western Turkey)****Nils-Peter Nilius<sup>1</sup>, Christoph Glotzbach<sup>2</sup>, Andreas Wölfler<sup>1</sup>, Andrea Hampel<sup>1</sup>, Cüneyt Akal<sup>3</sup>, Istvan Dunkl<sup>4</sup>, Ralf Hetzel<sup>5</sup>**

<sup>1</sup>Institut für Geologie, Leibniz Universität Hannover, Hannover, Germany; <sup>2</sup>Department for Geology and Geodynamics, Universität Tübingen, Tübingen, Germany; <sup>3</sup>Dokuz Eylül University, Department of Geological Engineering, Izmir, Turkey; <sup>4</sup>University of Göttingen, Geoscience Center, Sedimentology and Environment Geology, Göttingen, German; <sup>5</sup>Institut für Geologie und Paläontologie, Universität Münster, Münster, Germany

Metamorphic core complexes are commonly associated with an asymmetric exhumation pattern owing to a simple shear mode of extension along the core-bounding extensional detachment fault. In contrast, a symmetric exhumation pattern was proposed for the central Menderes Massif (western Turkey), because it comprises two detachment faults with opposite dip and shear sense, which accommodated N-S extension since the middle Miocene. However, available constraints on the evolution of the central Menderes Massif are mainly based on data from the northern part (Bozdağ Range) bounded by the north-dipping Gediz detachment. Exhumation of the southern part (Aydın Range) along the south-dipping Büyük Menderes detachment was assumed to occur more or less synchronously. New thermochronological and structural data (Wölfler et al., Tectonophysics, 2017; Nilius et al., JGSL, 2019) show, however, that extension in the southeastern Aydın Range was accommodated along the Büyük Menderes detachment during the middle Miocene and shifted in the Pliocene to the Demirhan detachment, which is situated in the hanging wall of the eastern Büyük Menderes detachment. Together with new zircon and apatite (U-Th)/He and fission track ages from the Gediz detachment, our data set allows constraining temporal and spatial variations in cooling and exhumation patterns in the entire central Menderes Massif. Our new data from the Gediz detachment imply that faulting commenced in the middle Miocene and continued until the late Pliocene. Exhumation rates in the detachments footwalls were constrained by 1D thermokinematic modelling. The results show that the Aydın Range was exhumed at rates of ~0.5 km/Ma in the middle Miocene and at ~0.4 km/Ma in the Pliocene. In contrast, the western Bozdağ Range was exhumed at rates of 0.3-1.0 km/Ma in the middle to late Miocene; the eastern part shows even higher exhumation rates of  $1.5 \pm 0.3$  km/Ma during the Pliocene. Faster exhumation of the Bozdağ Range compared to slower exhumation of the Aydın Range is also expressed in the slip rates derived from cooling ages in the footwalls of both detachments. As result, extension and exhumation along the Gediz detachment is higher than along the Büyük Menderes and Demirhan detachments.

Tue: 3

**The evolution of Vari Detachment (Syros, Cyclades)****Eirini Aravadinou, Nikolaos Gerogiannis, Paris Xypolias**

*Department of Geology, University of Patras, GR-26500, Patras, Greece*

In this work, we investigate the tectonic evolution of the Vari Detachment (Syros, Cyclades), which juxtaposes the Vari unit (Uppermost unit) and the underlying Cycladic Blueschists of the Cycladic massif. We present detailed (micro-)structural and quartz petrofabric data coupled with geological/structural mapping in southeast Syros focusing on the hanging-wall rocks of the Vari Detachment.

The early stages of deformation in Vari unit is characterized by distributed constrictional deformation expressed by transport-parallel upright folds and L-tectonites as well as by cleft girdles quartz c-axis fabrics, which indicate SW-directed shearing. Microstructural data show that these early deformation stages occurred at temperatures ca. 500 °C. Ductile deformation progressively localized at the lower structural levels of the Vari unit forming a greenschist-facies mylonitic zone. This mylonitic deformation occurred under plane strain conditions as indicated by cross-girdles quartz c-axis fabrics and is consistently associated with top-to-SW shear sense. The ongoing mylonitization is accompanied by progressive downward strain localization and

temporally increasing pure shear component of deformation coupled with cooling from ca. 500 °C to ca. 400 °C. All ductile structures associated with the Vari Detachment were overprinted by the Late Vari Detachment, which formed under brittle conditions. Our kinematic analyses show that the Late Vari Detachment is associated with SSW-directed sense of shear, similar to that recorded for the West Cycladic Detachment System. Thus, the Late Vari Detachment can be considered as a branch of this system.

We suggest that the ductile SW-directed Vari Detachment represents a passive normal-sense roof detachment, which was developed during the NE-directed ductile extrusion of the Cycladic Blueschists at middle Eocene – Oligocene times. The brittle SSW-directed Late Vari Detachment was formed at the middle Miocene and is responsible for the brittle exhumation of both the Cycladic Blueschists and the ductile Vari Detachment.

### **3c) Assembly of Pangea: What do we know about the Variscan orogen and its Avalonian-Cadomian precursors?**

**Tuesday, 24/Sep/2019: 3:45pm - 5:30pm**

**Session Chair: Ulf Linnemann** (Senckenberg Naturhistorische Sammlungen Dresden)

**Session Chair: Martin Salamon** (Geological Survey of North Rhine Westphalia)

**Location: H4**

#### **Session Abstract**

The Variscan orogen and its Avalonian-Cadomian precursors form the heart of the supercontinent Pangea. The Variscan orogen resulted from the continent-continent collision of the landmasses of Laurussia and Gondwana and its peripheral orogens. The Variscan mountain chain as the principal basement of Central and Western Europe is a target of intense geoscientific research since more than a century. During the last decades, numerous high quality data sets had been produced in the fields of mineralogical, geochemical, palaeontological, geological, and geophysical disciplines. Especially new robust geochronological data paved the way for new interpretation concerning the formation of the orogen and the architecture of the orocline. For this session we welcome presentations of all fields of geosciences which can contribute to answer our core question: What do we know about the Variscan orogen?

#### **Lecture Presentations**

**3:45pm - 4:15pm** *Session Keynote*

#### **How did Pangea behave? Rethinking some tectonic processes in a superplate world**

**Gabriel Gutierrez-Alonso**<sup>1,2</sup>

<sup>1</sup>University of Salamanca, Spain; <sup>2</sup>Tomsk State University, Russia

The Paleozoic Variscan-Alleghenian-Ouachita orogeny was a large-scale collisional event involving amalgamation of multiple continents and micro-continents leading to the amalgamation of the last known supercontinent, Pangea, together with other coeval collisional events. While the mechanisms that drive plate tectonics and the effects when different plates interact are well known, the behaviour of large superplates dominated by continental lithosphere is not yet well constrained. In this contribution, I speculate on the possible global processes involved in the lithospheric scale deformation of Pangea, including oroclines, lithospheric mantle replacement and rifts, and which may be the global driving mechanisms leading to such deformation. After the aforementioned continental collisions that led to the formation of Pangea, plate convergence may have continued in a large, wedge-shaped oceanic tract. Plate strain within and at the periphery of the supercontinent eventually resulted in self-subduction of the Pangean global plate, when the ocean margin of the continent subducted beneath the continental edge at the other end of the same plate. This scenario results

in a strain regime within Pangea that explains the development of a large vertical axis fold structure near the apex of the Palaeotethys Ocean, extensive lower crustal heating and continental magmatism at the core of the continent as well as the development of radially arranged continental rifts in more peripheral regions of the plate. The driving forces for such large deformations have to be looked for in the mantle dynamics re-organization as a consequence of the supercontinent formation and the possible change in the geoid shape caused by the accumulation of a large amount of subducted oceanic lithosphere at the core mantle boundary.

**4:15pm - 4:30pm**

### **From a bipartite Gondwanan shelf to an arcuate Variscan belt: The early Paleozoic evolution of northern Peri-Gondwana**

**Tobias Stephan<sup>1</sup>, Delia Rösel<sup>1</sup>, Rolf L. Romer<sup>2</sup>, Uwe Kroner<sup>1</sup>**

<sup>1</sup>TU Bergakademie Freiberg, Institut für Geologie, Freiberg, Germany; <sup>2</sup>Deutsches GeoForschungsZentrum GFZ, Potsdam, Germany

The Late Paleozoic Variscan Orogen of Europe and North Africa comprises reworked Neoproterozoic to Early Paleozoic crust of the northern Gondwanan shelf that collided with Laurussia. The orogen is characterized by an arcuate trend of the Rheic suture along two orthogonal orogenic arcs and an apparently arbitrary juxtaposition of contrasting paleogeographic proxies to the south of the suture.

In order to reconstruct the development and architecture of the Paleozoic shelf of northern Gondwana preceding the formation of Pangea, we compiled pre- and syn-Variscan constraints from the sedimentary, faunal, magmatic, and tectono-metamorphic record including ca. 70000 detrital zircon U–Pb ages from 780 Precambrian to Lower Paleozoic sedimentary rocks. The provenance data of the sedimentary rocks were filtered and statistically analyzed using multidimensional scaling coupled with density-based clustering revealing provenance endmembers and sedimentary mixing processes.

The comparison of the pre-Variscan paleogeographic proxies and Variscan structural implications demonstrates a contiguous but bipartite, i.e. a western and an eastern, shelf to the south of the Rheic Ocean. In the early Paleozoic both shelf segments were affected by heterogeneous extension whereby age and composition of extension-related magmatic rocks varies systematically from Cambrian alkaline and tholeiitic rocks in the western shelf to Ordovician calc-alkaline and peraluminous rocks in the eastern shelf. The regional variation in age and composition of the magmatic rocks reflects an eastward decreasing rate of extension along northern Gondwana. The higher extension in the western shelf culminated in the formation of the Armorican Spur. The subsequent intra-Ordovician compressional event(s), i.e. the “Sardic phase” and the “Cenerian orogeny”, exclusively affected the eastern shelf. Early Devonian collision of the Armorican Spur with Laurussia initiated the subduction accretion stage of the Variscan orogeny resulting in the formation of the Rheno-Hercynian–Moravo-Silesian Arc. At that time, the eastern shelf remained in a passive margin setting. Triggered by Late Devonian rifting along the eastern margin of Arabia, the eastern shelf decoupled from the Gondwanan plate and was displaced eastward, along to the northern margin of remaining mainland Gondwana. Early Carboniferous collision of the eastern shelf with the western shelf resulted in orogen wide transpressional tectonics and the formation of the Ibero-Armorican Arc. The tectonic interplay between the two segments of the Gondwana shelf is the underlying cause of the final patchwork pattern of paleogeographic markers and the arcuate shape of the Variscan orogenic belt.

4:30pm - 4:45pm

### Beyond the Bohemian Massif: search for Cadomian and Variscan correlatives in the Balkans

**Jiří Žák<sup>1</sup>, Ianko Gerdjikov<sup>2</sup>, Alexandre Kounov<sup>3</sup>, Dian Vangelov<sup>2</sup>, Jaroslava Hajná<sup>1</sup>, Martin Svojtka<sup>4</sup>, Lukáš Ackerman<sup>4</sup>**  
<sup>1</sup>*Institute for Geology and Paleontology, Charles University, Prague, Czech Republic;* <sup>2</sup>*Department of Geology, Paleontology and Fossil Fuels, Sofia University 'St. Kliment Ohridski', Bulgaria;* <sup>3</sup>*Department of Environmental Sciences, University of Basel, Switzerland;* <sup>4</sup>*Institute of Geology of the Czech Academy of Sciences, Prague, Czech Republic*

Most of the plate tectonic reconstructions of the Variscan belt and its Cadomian to Early Paleozoic precursors in Europe end at the eastern margin of the Bohemian Massif (BM), assuming that the southeasterly continuation of the orogen has been thoroughly reworked within the Alpine collision zone. This view, however, has been challenged by recent studies and mapping projects, showing that large portions of the Variscan belt have been exceptionally well preserved in the Balkans (BA). Furthermore, restoring the Jurassic–Cretaceous rifting and seafloor spreading in oceanic basins (Magura, Ceahlău–Severin) brings the BA terranes to the close proximity of the Bohemian Massif. The goal of this contribution is to review the possible similarities and differences in relevant, now distant lithotectonic units and to compare their geodynamic evolution during the late Neoproterozoic to Carboniferous times. In the BM, recent studies documented the 620–560 Ma Davle volcanic arc complex and the Blovice accretionary wedge with well-preserved polygenetic mélanges and dismembered Ocean Plate Stratigraphy (OPS). While the migmatized orthogneisses with ~560 Ma protolith ages in the high-grade Serbo–Macedonian Massif correspond well to the former, the structurally overlying low-grade pre-520 Ma Vlasina volcano-sedimentary complex, composed of interlayered basaltic volcanic–volcaniclastic and siliciclastic sequences, lacks the block-in-matrix fabric and abundant fragments of exotic oceanic material. It likely represents an intra-arc to back-arc basin similar to the 560–530 Ma Štěchovice Group in the BM. The Cadomian basement is intruded by 520–505 Ma Cambrian plutons and is unconformably overlain by middle to late Cambrian continental alluvial fan deposits in the BM. Deformed quartz-pebble conglomerates found within the Vlasina may represent correlative relics of the latter. The Early Paleozoic passive successions are also remarkably similar in the BM and BA, including the Armorican quartzite, Hirnantian diamictites, and Silurian graptolite black shales, but differ in the dominant Lower Devonian carbonate facies in the BM. The Variscan part of the story has been largely fragmented in the BA, preserving mostly the late stages of the orogeny including the 340–337 Ma anatexis, 339–337 Ma ultrapotassic rocks, subsequent foreland-directed nappe stacking, and latest Carboniferous granitic plutonism and post-collisional basins. In summary, slices of the former Cadomian active margin, variably reworked during the Variscan orogeny may well be traced from the BM to the BA. Still open issues to be addressed include the Neoproterozoic terrane provenance and better constraining the early Variscan processes in the BA.

4:45pm - 5:00pm

### Petrochronology by EPMA and automated SEM in the Saxothuringian high pressure nappes of the central and western Erzgebirge

**Bernhard Schulz<sup>1</sup>, Joachim Krause<sup>2</sup>, Manuel Lapp<sup>3</sup>**

<sup>1</sup>*TU Bergakademie Freiberg/Sachsen, Germany;* <sup>2</sup>*Helmholtz-Zentrum Dresden-Rossendorf, Helmholtz Institut Freiberg für Ressourcentechnologie, Chemnitzer Str. 40, 09596 Freiberg/Sachsen;* <sup>3</sup>*Sächsisches Landesamt für Umwelt, Landwirtschaft und Geologie (LfULG), Halsbrücker Strasse 31a, 09599 Freiberg/Sachsen*

The Saxothuringian Zone of the Variscan orogen is composed of autochthonous and allochthonous domains. Dating of metamorphic events in the domains of the Saxonian Granulite Massiv, and the Münchberg, Frankenberg, and Erzgebirge nappe units is critical to resolve the multiphase geodynamic evolution during Variscan orogeny. In-situ chemical Th-U-Pb monazite (Th, U, Si, LREE, Y, Ca)PO<sub>4</sub> dating by electron probe microanalysis (EPMA) has demonstrated its high potential to resolve polyphase metamorphism. The method is based on the premise that monazite inherits negligible amounts of common Pb and that the radiogenic Pb is retained due to very low diffusion rates at high T [1]. A monazite dating routine, enclosing the analysis of HREE, was

performed with a JEOL-JXA-8530F, producing 100 - 200 single analyses per sample. Also, energy dispersive x-ray mapping (GXMAP) by automated SEM was used for semiquantitative identification of garnet zonation patterns. Quantitative chemical compositions of garnet and related plagioclase, biotite and muscovite were then measured by EPMA for geothermobarometric estimates by cation exchange and net transfer reactions. Monazite is abundant in lenses of granulitic garnet gneisses ("saidenbachites") in the central Erzgebirge UHP unit. The monazite  $\text{ThO}_2^*$ -PbO data straightly define isochrons at around  $335\pm 3$  Ma. High pyrope (27 mol%) garnet crystallised at  $830^\circ\text{C}/19$  kbar [2]. Despite such high temperatures, the monazite Y contents are low. In the intercalated MP micaschists, the monazite  $\text{ThO}_2^*$ -PbO isochrones appear more diverse, between  $344\pm 5$  and  $334\pm 4$  Ma. Furthermore, monazite has been studied in the micaschists and related phyllites of the western Erzgebirge. The monazite data define isochrones between  $360\pm 10$  and  $323\pm 10$  Ma, with most samples around 340 Ma, interpreted as the ages of Variscan regional metamorphism at  $T_{\text{max}}$  of  $550^\circ\text{C}$ . Several samples bear an older minor monazite population with ages between 415 to 432 Ma. Special regard has been dedicated to metapelites within the Pöhla mineralisation. The Eibenstock granite Th-U-Pb monazite isochrone is  $321\pm 2$  Ma. In non-mineralised micaschists older monazites ( $329\pm 8$  Ma), and in mineralised parts younger ( $309\pm 6$  Ma) and hydrothermal low-Th monazites are observed.

- [1] Montel, J.-M., Foret, S., Veschambre, M., Nicollet, C., Provost, A. (1996): Electron microprobe dating of monazite. - *Chem. Geol.*, 131: 37-51;  
 [2] Tichomirowa, M., Whitehouse, M., Gerdes A., Schulz, B. (2018): Zircon (Hf, O isotopes) as melt indicator: Melt infiltration and abundant new zircon growth within melt rich layers of granulite-facies lenses versus solid-state recrystallization in hosting amphibolite-facies gneisses (central Erzgebirge, Bohemian Massif). - *Lithos* 302–303.

**5:00pm - 5:15pm**

### **U-Pb LA-ICP MS Zircon Ages of Devonian felsic volcanic Rocks in the Rhenish Massif (North Rhine-Westphalia)**

**Martin Salamon<sup>1</sup>, Ulf Linnemann<sup>2</sup>, Piecha Matthias<sup>1</sup>, Steuerwald Klaus<sup>1</sup>, Andreas Gärtner<sup>2</sup>, Johannes Zieger<sup>2</sup>, Mandy Hofmann<sup>2</sup>**

<sup>1</sup>*Geological Survey of North Rhine Westphalia, Germany;* <sup>2</sup>*Senckenberg Naturhistorische Sammlungen Dresden, DE*

Most of the southern part of North Rhine-Westphalia forms part of the Rhenish Massif. The geology of this area is mainly dominated by deformed Devonian sedimentary rocks. The entire succession ranges from the Ordovician to the Upper Carboniferous. The area is part of the Rhenohercynian-Zone of the Central European Variscides. The Devonian rocks are mainly marine, seldom terrestrial deposits on the shelf of the Old Red Continent. From the Lower Devonian to the Carboniferous, there are several volcanic events, mainly documented by effusive volcanic rocks or volcanic tuffs, but also intrusive subvolcanic rocks occur. Mafic volcanism occurred during the Devonian and Carboniferous. There are three main phases of mafic volcanism, two in the middle and upper Devonian and one in the Lower Carboniferous. In addition, a number of felsic volcanics occur within the sedimentary sequence. These are mainly rhyodacites or rhyodacitic tuffs. Their deposition started in the Lower Devonian and continued up into the Upper Carboniferous. The Lower Devonian felsic volcanic deposits are massive and reach in part thicknesses of up to 200 m. The rocks of the intense volcanic events cover an area of ca. 2000 km<sup>2</sup>. Such deposits are known in the old German literature such as "Keratophyre", "Quarzkeratophyre", "Keratopyrtuffe", or "Quarzkeratophyrtuffe". During Devonian and Carboniferous times, the felsic volcanic deposits became more distal. Only thin volcanic ash tuffs are documented, which became thinner during time. Our work concentrates on U-Pb zircon-dating of the massive felsic volcanic rocks intercalated into the shallow-marine sedimentary successions of the Emsian (Lower Devonian) to the Eifelian (Middle Devonian). These volcanic products form important geological marker horizons in the sedimentary succession. Main volcanic horizon is the "Hauptkeratophyr, K4" derived from a Lower Devonian "supervolcano", reaching a thickness of up to 200 m and covering an area of 2000 km<sup>2</sup>. Also samples from the famous "Bruchhauser Steine", the second National Monument of Germany, had been investigated. They are mainly effusive volcanics, embedded in middle Devonian marine sedimentary rocks. Further, also samples from the K3 -, K5 -, K6 - keratophyre, and two massive ash layers in Eifelian deep marine deposits were investigated.

5:15pm - 5:30pm

### New U-Pb ages of detrital zircon from the central Variscan orogen and its Avalonian-Cadomian precursors

Ulf Linnemann<sup>1</sup>, Martin Salamon<sup>2</sup>, Matthias Piecha<sup>2</sup>, Andreas Gärtner<sup>1</sup>, Mandy Hofmann<sup>1</sup>, Johannes Zieger<sup>1</sup>

<sup>1</sup>Senckenberg Naturhistorische Sammlungen Dresden, Germany; <sup>2</sup>Geologischer Dienst Nordrhein-Westfalen, Krefeld, Germany

New datasets from the Variscan Orogen of Central Europe, especially enormous huge masses of U-Pb ages of detrital zircon, allow new insights into Pangea's history. Roots of Pangea go back to the assembly of the Gondwana supercontinent, which was formed the collision of West and East Gondwana accompanied by Pan-African orogenic processes culminating at c. 600 Ma. Gravitational collapse of the Pan-African collisional orogens in the Late Ediacaran, their lateral extrusion, and subsequent onset of subduction zones at the margins of northern Gondwana led to the formation of several peri-Gondwanan terranes (c. 580 – 540 Ma). Roll-back induced tension caused enormous thinning of West African cratonic crust and the origin of arc and back-arc systems on stretched continental crust in a style of the recent Western Pacific. Collision of Baltica with NW-Gondwana at c. 540 Ma closed the Avalonian - Cadomian arc and back-arc system and formed prominent peri-Gondwanan terranes such as Avalonia and Cadomia. Early Cambrian rift-off of Baltica initiated the separation of Avalonia during the Lower Cambrian and a larger part of Cadomia in Lower to Middle Ordovician time. The Tornquist sea and the Rheic ocean became opened. Avalonia collided at c. 450 Ma with Baltica by closure of the Tornquist sea. Related to this is a jump of the subduction zone from the southern margin of Baltica to the southern margin of Avalonia (Rhenohercynia) where a Silurian magmatic arc over a northward dipping subduction zone (c. 440-420 Ma) was developed. The latter one was terminated under closure of the Rheic ocean by the arrival of Cadomia (Saxothuringia, part of the Armorican Terrane collage) at c. 420-400 Ma. A jump of the subduction zone to the southern margin of Saxothuringia opened the short-existing Rhenish seaway between Rhenohercynia and Saxothuringia during Eifelian-Givetian time (c. 393-383 Ma). The Rhenish seaway became closed by a southeastward subduction beneath Saxothuringia. The Mid-German Crystalline zone became formed by arc-related intense magmatism (c. 360-330 Ma). The main Variscan deformation and the final emplacement of Variscan nappes occurred during Viséan and Sepukhovian time.

## Poster Presentations

Tue: 4

### New insights into the Sierra de Juárez Mylonitic Complex, southern Mexico: constraints on its pre-Mesozoic history and regional implications

Guillermo Espejo-Bautista<sup>1</sup>, Luigi A. Solari<sup>1</sup>, Fernando Ortega-Gutiérrez<sup>2</sup>, Roberto Maldonado<sup>1</sup>, Yuly T. Valencia-Morales<sup>3</sup>

<sup>1</sup>Centro de Geociencias, Universidad Nacional Autónoma de México, Campus Juriquilla, Santiago de Querétaro 76001, Querétaro, México; <sup>2</sup>Instituto de Geología, Universidad Nacional Autónoma de México, Ciudad Universitaria, Ciudad de México 04510, México; <sup>3</sup>División de Ciencias de la Tierra, Centro de Investigación Científica y de Educación Superior de Ensenada (CICESE), Ensenada 22860, Baja California, México

The Sierra de Juárez Mylonitic Complex (SJMC) is located between the Cuicateco and Zapoteco tectonostratigraphic terranes in southern Mexico and essentially consists of a Precambrian to Paleozoic metamorphic complex with overprinted mylonitic textures of early-to middle-Jurassic age, occurred during the opening of the Gulf of Mexico. However, the origin of these metamorphic units before the Jurassic mylonitization event is poorly understood.

We present petrological analysis with a thermobarometric approach and U-Pb geochronology data from igneous and detrital zircon grains of the units belonging to the SJMC. The more extensive lithological unit consists in a gabbroic-anorthositic orthogneisses unit that yielded <sup>207</sup>Pb/<sup>Pb</sup><sup>206</sup> protolith crystallization ages of 1004 ± 21, 1015 ± 30 and 1017 ± 38 Ma, which are related to the Mexican AMCG suite and confirms the pres-

ence of Rodinian-type basement into the SJMC. We also report for the first time a rutile and garnet-bearing Paleozoic supracrustal sequence, named Etna unit, which has Silurian maximum deposit ages, as well as the crystallization age of a metagranitic-sill ( $195.3 \pm 4.3$  Ma) that is syntectonic to the Jurassic mylonitic event. Both the gabbroic-anorthositic and Etna units exhibit a medium-to high-pressure metamorphic peak of ca. 592 to 678 °C and 6.5 to 12 kbar.

These data allow us to interpret the supracrustal rocks of the SJMC as originated in a volcanosedimentary environment at the NW corner of Gondwana during Silurian-Devonian times in a pre-Pangean scenario. The pre-Jurassic metamorphic event can be constrained between the maximum deposit age of the Etna unit (Silurian) and the Jurassic age of the mylonitic metagranitic-sill, and is interpreted as formed in a collisional tectonic setting that juxtaposed the Yucatan block or the NW corner of Gondwana against the eastern border of Oaxaquia during the Pangea amalgamation in the late Paleozoic.

**Tue: 5**

### **Longlived pulsed magmatic intrusions along the Northern Gondwana margin revealed by Ordovician to Early Permian LA U-Pb geochronology of Central Pyrenean gneiss domes**

**Stephan Schnapperelle<sup>1</sup>, Jochen. E. Mezger<sup>2</sup>, Michael Stipp<sup>1</sup>, Mandy Hofmann<sup>3</sup>, Andreas Gärtner<sup>3</sup>, Ulf Linnemann<sup>3</sup>**

<sup>1</sup>Martin-Luther-Universität Halle-Wittenberg, Germany; <sup>2</sup>University of Alaska Fairbanks, United States of America;

<sup>3</sup>Senckenberg-Museum Dresden, Germany

Igneous rocks within gneiss domes of the Axial Zone of the Central Pyrenees preserve a record of Variscan magmatism, northern Gondwana margin rifting and earlier Cadomian intrusions. The cores of the gneiss domes are Ordovician granitic laccolith intrusions in Neoproterozoic-Ordovician metasedimentary rocks which also experienced significant syn- and post-tectonic Variscan magmatism. The objective of this study is to gain a better understanding of the exact timing and significance of individual magmatic events that previously have been poorly constrained. In this study we present laser ablation U-Pb zircon geochronology of peraluminous, alkaline granite dykes and small intrusions within the orthogneiss cores of the Aston and Hospitalet gneiss domes in the central Pyrenees. The majority of samples yield a wide range of U-Pb ages. Inherited zircon cores record Neoarchean to Mesoproterozoic ages, as well as Neoproterozoic and Cadomian ages. Zircon rims, and some of the cores show Ordovician (478-450 Ma) and Devonian (415-402 Ma and 385-383 Ma) ages. Most abundant, however, are Carboniferous ages that occur in three age clusters, 357-350 Ma, 336-325 Ma and the most frequent 306-303 Ma. This high-frequency cluster is followed by late Carboniferous to early Permian younger zircon ages ranging of 301-297 Ma and 287 Ma.

The wide range of Carboniferous ages suggests a multiphase pluton emplacement during the Variscan orogeny. Structural analysis at outcrop and microscopic scale displays syn- and post-tectonic relationships for the intrusions. Based on this relative timing a differentiation of the deformation phases is possible. The compressive  $D_1$  phase was active before ca. 336 Ma. Transpressive  $D_2$  occurred between 336 Ma to 299 Ma. It might be possible to subdivide further into  $D_{2-a}$  and  $D_{2-b}$ , based on two younger U-Pb zircon age clusters, although time brackets are not fully defined. During the transpressive  $D_3$  E-W oriented folds and mylonitic shear zones, like the Mérens-shear zone between the Aston and Hospitalet domes, were formed. A penetrative deformation of the young granitoids has not been observed. The beginning of  $D_3$  is determined at 299 Ma and can be confirmed up to 287 Ma.

The diversity of Ordovician, Devonian and Carboniferous up to Permian magmatic ages suggests a multiphase pluton emplacement along that section of the northern Gondwana margin predating and lasting throughout the complete Variscan orogeny. A possible origin of this prolonged magmatic activity since the late Devonian could be the TUZO mantle plume.

Tue: 6

**U–Pb zircon dating of Paleozoic volcanic rocks from the Rheno-Hercynian Zone: new age constraints for the Steinkopf formation, Lahn-Dill area, Germany****Jan Schulz-Isenbeck<sup>1,2</sup>, Michael Bröcker<sup>1</sup>, Jasper Berndt<sup>1</sup>**<sup>1</sup>*Institut für Mineralogie, Westfälische Wilhelms-Universität Münster, Corrensstr. 24, 48149 Münster, Germany;*<sup>2</sup>*Institut für Mineralogie, Technische Universität Bergakademie Freiberg, Brennhausgasse 14, 09599 Freiberg, Germany*

The Rheno-Hercynian Zone records extensive, predominantly mafic and minor felsic intraplate volcanism on the southern shelf of Laurussia throughout Devonian and Lower Carboniferous time. Small and volumetrically subordinate outcrops of alkali-rhyolitic to trachytic metavolcanic rocks as well as metavolcaniclastic rocks are widespread in the Lahn-Dill paleobasin, SE Rheinisches Schiefergebirge, Germany. These occurrences are related either to late Early Devonian or to Middle Devonian episodes of volcanic activity. An ambiguous age assignment for the time of eruption could not be established so far by biostratigraphic constraints due to an incomplete record of the local rock sequence. Most volcanic rocks of the study area are not suitable for application of U–Pb geochronology. A notable exception is the Steinkopf rock suite in the SW Lahn-Dill area, which comprises various zircon-bearing volcanic rock types (e.g. metatrachytes, metavolcaniclastic rocks). However, a straightforward interpretation of the U–Pb age data is hampered by complex zircon populations recording crystallization from newly formed melt, inheritance, assimilation of country rocks, variable degrees of Pb-loss and fluid-assisted Zr-mobility. A plausible evaluation of the combined LA-ICP-MS U–Pb zircon data of two metatrachytes and a metavolcaniclastic rock document a coherent age group at ca. 390–384 Ma, interpreted to date zircon crystallization in the Steinkopf magma chamber. The new age data suggest that the felsic volcanic rocks from the SW Lahn-Dill area can be linked with the Middle Devonian (Givetian) phase of volcanism affecting the Rheno-Hercynian Zone. Zircon-bearing veinlets in a metatrachyte document infiltration of external fluids and/or internal Zr-redistribution. However, such processes are of rather limited importance and not responsible for formation of the main zircon population. LA-ICP-MS U–Pb dating of secondary zircon indicate a Late Devonian to Early Carboniferous age ( $364 \pm 10$  Ma).

## 4) Continents, oceans and global change

### 4a): Limnogeology and paleolimnology including lagoon systems

Wednesday, 25/Sep/2019: 8:30am - 10:30am

Session Chair: Torsten Haberzettl (University of Greifswald)

Session Chair: Thomas Kasper (Friedrich-Schiller-University Jena)

Location: H2

#### Session Abstract

Understanding and quantifying the processes that modify and shape the surface of the Earth requires the determination of accurate dates and rates. Thus, the improvement and development of existing and new dating methods is essential for a better understanding of Earth's surface processes and their relation to climate and tectonics. Currently employed geochronological methods include, for example, exposure and burial dating with cosmogenic nuclides, luminescence, radiocarbon, and paleomagnetic dating. This session invites contributions on developments and applications of all dating methods relevant to decipher Late Cenozoic landscape evolution, climate change, and active tectonics. The keynote speakers Georgina King (Lausanne) and Vincent Godard (Aix-Marseille) will give talks on luminescence thermochronometry and the use of  $^{36}\text{Cl}$  in carbonate landscapes. Interested participants are invited to visit the cosmogenic nuclide laboratory in Münster and discuss all aspects of  $^{10}\text{Be}$  separation and target preparation with R. Hetzel and T. Dunai.

#### Lecture Presentations

8:30am - 8:45am

#### Heterocyst glycolipids: Novel tools for reconstructing continental climate change using lacustrine deposits

Thorsten Bauersachs<sup>1</sup>, James Russell<sup>2</sup>, Lorenz Schwark<sup>1</sup>

<sup>1</sup>Christian-Albrechts-University, Institute of Geosciences, Department of Organic Geochemistry; <sup>2</sup>Brown University, Department of Earth, Environmental and Planetary Sciences

Lacustrine sequences are high-resolution archives of paleoclimate and paleoenvironmental change. Obtaining qualitative and quantitative information on past climate variability from such sequences, however, proves troublesome as many tools that e.g. are routinely applied in the oceans, such as lipid paleothermometers ( $\text{TEX}_{86}$ ,  $\text{U}^{\text{K}}_{37}$ , LDI) or oxygen isotopes, cannot or only inadequately be applied to lake archives. A novel tool, which may fill this gap is provided by heterocyst glycolipids (HGs). These components, specific to  $\text{N}_2$ -fixing heterocystous cyanobacteria, are ubiquitously distributed in modern freshwater environments and previous investigations of lacustrine water column profiles have demonstrated that changes in HG distribution patterns are significantly correlated with variations in lake surface water temperatures (SWT). The sedimentary distribution of HGs may thus offer the exciting possibility to reconstruct SWTs in lacustrine settings.

In this study, the potential of HGs to serve as a novel proxy in continental climate research was, for the first time, investigated. We studied the distribution of HGs in surface sediments of 48 tropical East African lakes located on an altitudinal transect from 615 to 4237 masl and SWTs varying from 5.8 to 27.9 °C. HGs were omnipresent in all studied lakes and their relative distribution changed gradually along the investigated transect. In form of the  $\text{HDI}_{26}$  (heterocyst diol index of 26 carbon atoms), HGs showed a significant positive correlation with SWT ( $r^2 = 0.93$ ;  $p < 0.001$ ) with values of this proxy ranging from 0.55 in Lake Speke (4235 masl; 5.8°C) to 0.97 in Lake Albert (615 masl; 27.9°C), providing first proof for a temperature controlled distribution of HGs in lacustrine surface sediments. Application of this proxy to a 37,000 years-covering sediment record from tropical Lake Tanganyika (East Africa) evidenced an increase in  $\text{HDI}_{26}$  values from 0.88 at ~20,000 years BP to 0.96 at the core top. This change in  $\text{HDI}_{26}$  values corresponds to a SWT increase by about 3-4°C from the

last glacial period to the present-day, which is in agreement with previous estimates of tropical East African climate change.

Our results demonstrate that sedimentary HG distribution patterns capture modern and past SWT signals in lacustrine systems. Given that HGs are ubiquitously distributed in polar to tropical lake sediments, this suggests that the HDI<sub>26</sub> may represent a novel proxy for the reconstruction of past continental climate change using lacustrine archives with a potential global perspective.

**8:45am - 9:00am**

### **The Early Eocene of Schöningen - Testing effects of climate variations on coastal wetlands under greenhouse conditions**

**Olaf K. Lenz<sup>1</sup>, Volker Wilde<sup>2</sup>, Walter Riegel<sup>2</sup>**

<sup>1</sup>Senckenberg Gesellschaft für Naturforschung, Germany; <sup>2</sup>Senckenberg Forschungsinstitut und Naturmuseum Frankfurt, Germany

The Helmstedt Lignite Mining District is situated within the Paleogene Helmstedt Embayment, which represented the mouth of an estuary opening towards the Proto-North Sea between uplifts corresponding to the actual Harz Mountains in the South and the Flechtingen Rise in the North. Due to the interaction between changes in sea level, salt withdrawal in the subsurface and climate-related changes in runoff from the hinterland the area of Helmstedt and Schöningen was subject to frequent changes between marine and terrestrial conditions, repeatedly leading to peat formation. Today, a more than 200 m thick lignite-bearing Paleogene succession is limited to two marginal synclines accompanying a more than 70 km long salt wall. The position of the lignites and two major marine transgressions at Schöningen suggested a subdivision of the Paleogene strata from bottom to top in the underlying sediments of the Waseberg Formation, the Lower Eocene Schöningen Formation, the Emmerstedt Formation, the Middle Eocene Helmstedt Formation and the overlying fully marine strata of the Annenberg-, Gehlberg-, und Silberberg Formations. The conventional age model for the coal-bearing part of the Paleogene succession of the Helmstedt Mining District is mainly based on scattered radiometric ages from glauconites and biostratigraphic data from nannoplankton. More recent results from our quantitative studies of the dinoflagellate cyst *Apectodinium* and carbon isotopes from the reference section at Schöningen indicate that the lowermost part of the Schöningen Formation may still be of Paleocene age.

The marine-terrestrial transitional section at Schöningen is worldwide unique due to its completeness in time from the uppermost Paleocene into the middle Eocene. This presents a unique opportunity for studying terrestrial biodiversity and climate across more than 10 million years including the Early Eocene Climatic Optimum (EECO) and its initial decline with some of the major climatic excursions, such as, e.g., the Paleocene-Eocene Thermal Maximum (PETM). It is the aim of an ongoing project to study trends in the composition of the vegetation and in plant diversity in this paralic environment across the EECO and its gradual demise by making use of pollen and spores as proxies. However, not only the long-term climate trend, but also short-term climatic perturbations such as the PETM and the Eocene Thermal Maximum 2 (ETM-2) and its effects on the vegetation can be studied.

**9:00am - 9:15am**

### **Terrestrial archives from the Eocene greenhouse of Central Europe: Palynological studies of lacustrine sediments on the Spendlinger Horst (Southwest Germany)**

**Maryam Moshayedi<sup>1</sup>, Jürgen Mutzl<sup>1</sup>, Olaf. K Lenz<sup>1,2</sup>, Volker Wilde<sup>3</sup>, Matthias Hinderer<sup>1</sup>**

<sup>1</sup>TU Darmstadt, Germany; <sup>2</sup>Senckenberg Gesellschaft für Naturforschung, Germany; <sup>3</sup>Senckenberg Forschungsinstitut und Naturmuseum, Germany

Palynological composition of four small Eocene lakes at Messel, Prinz von Hessen (PvH), Offenthal and Groß Zimmern on the Spendlinger Horst in Southwest Germany were studied for understanding the vegetation in

Central Europe during Paleogene greenhouse conditions with respect to regional tectonic and volcanic influence. Except for PvH, which is most probably a small pull-apart basin, the other basins are maar lakes and formed as a consequence of phreatomagmatic eruptions. Based on revised  $^{40}\text{Ar}/^{39}\text{Ar}$  dates the eruptions at Offenthal ( $47.71/47.87 \pm 0.3$  Ma) and Messel ( $48.11/48.27 \pm 0.22$  Ma) are nearly of the same age around the Lower/Middle Eocene boundary. Palynostratigraphic analyses indicate a Lower Eocene age for the studied part of PvH and a Middle Eocene age for Groß Zimmern. Our quantitative palynological studies revealed different pollen and spore assemblages in each basin, but similar general trends in the evolution of the vegetation can be recognized in all of the basins. The succession in the maar lakes starts with the progressive recolonization of the area in the vicinity of the craters by pioneering elements such as ferns or Restionaceae and continues into a paratropical rainforest and, finally, a climax vegetation with a dominance of juglandaceous and fagaceous plants. Nevertheless, each basin has its unique story to tell. In Messel the following undisturbed record of about 600.000 years reveals the influence of orbital forcing on the climate and the composition as well as on the diversity of the climax vegetation during the early Middle Eocene. A climax vegetation comparable to Messel is not documented at Offenthal mainly due to a significant shorter time period reflected in the respective succession of lake sediments. At Lakes PvH and Groß Zimmern regional tectonic activity had a much higher influence on the paleoenvironment than orbitally controlled climate change.

9:15am - 9:30am

### Assessing the Late Quaternary climatic and environmental history of the Russian Arctic – keys results of the Russian-German PLOT (Paleolimnological Transect) project

**Elodie Lebas<sup>1</sup>, Martin Melles<sup>2</sup>, Andrej Andreev<sup>2</sup>, Marlene Baumer<sup>2</sup>, Dmitri Bolshiyannov<sup>3,4</sup>, Grigory Fedorov<sup>3,4</sup>, Raphael Gromig<sup>2</sup>, Svetlana Kostrova<sup>5</sup>, Sebastian Krastel<sup>1</sup>, Anna Ludikova<sup>6</sup>, Hanno Meyer<sup>5</sup>, Luidmila Pestryakova<sup>7</sup>, Larissa Savelieva<sup>4</sup>, Lyudmila Shumilovskikh<sup>8</sup>, Dmitry A. Subetto<sup>9</sup>, Bernd Wagner<sup>2</sup>, Volker Wennrich<sup>2</sup>, Martin Werner<sup>10</sup>**

<sup>1</sup>University of Kiel, Institute of Geosciences, Kiel, Germany; <sup>2</sup>University of Cologne, Institute of Geology and Mineralogy, Cologne, Germany; <sup>3</sup>Arctic and Antarctic Research Institute, St. Petersburg, Russia; <sup>4</sup>St. Petersburg State University, St. Petersburg, Russia; <sup>5</sup>Alfred Wegener Institute for Polar and Marine Research, Potsdam, Germany; <sup>6</sup>Institute of Limnology, Russian Academy of Sciences, St. Petersburg, Russia; <sup>7</sup>North-East Federal University Yakutsk, Russia; <sup>8</sup>Georg-August University Göttingen, Dept. of Palynology and Climate Dynamics, Germany; <sup>9</sup>Institute of Northern Water Problems, Russian Academy of Sciences, Petrozavodsk, Russia; <sup>10</sup>Alfred Wegener Institute for Polar and Marine Research, Bremerhaven, Germany

The joint Russian-German project 'PLOT - Paleolimnological Transect' aims at recovering lacustrine sediment sequences along a >6000 km-long longitudinal transect across the Eurasian Arctic in order to investigate the Late Quaternary climatic and environmental history. The climate history of the Arctic is of particular interest as the region is experiencing major impact of the current climate change. The project has been funded by the German and Russian Ministries of Research for a duration of three years (2015-2018) and was conducted under the umbrella of a bilateral Russian-German agreement in the field of polar and marine research. Since 2013 extensive fieldwork, including seismic surveys, coring, and hydrological investigations, has been carried out at lakes Ladoga (NW Russia), Bolshoye Shuchye (Polar Urals), Emanda (Verkhoyansk Range), Levinson-Lessing and Taymyr (both Taymyr Peninsula). Fieldwork in the Ural Mountains and on the Taymyr Peninsula was conducted in collaboration with the Russian-Norwegian CHASE (Climate History along the Arctic Seaboard of Eurasia) project. A multiproxy approach was applied to the analytical work of all cores, including (bio-)geochemical, sedimentological, geophysical, and biological analyses. First data implies the presence of preglacial sediments in the cores from all lakes, except Lake Emanda. Age-depth models, based on radiocarbon dating, OSL dating, paleomagnetic measurements, identification of cryptotephra, and varve counting (where applicable), are in progress except for Lake Ladoga (recently published). The records shall be correlated to that of Lake El'gygytgyn (NE Russia), which represents the master record for the Siberian Arctic. The outcome of the PLOT project will be a better understanding of the temporal and spatial variability and development of the Arctic climate. Here, we present and discuss the most important results available from the geophysical site surveys and core analyses, and provide an outlook on the future strategy and foci of the

project. Key results of the project have been published in spring of this year in a special issue of the journal *Boreas*, including publications about Lake Ladoga and Lake Levinson-Lessing.

**9:30am - 9:45am**

### **The Holocene lacustrine record of the Layla Lakes (central Saudi Arabia): The use of phytolith analysis for the reconstruction of paleoenvironment and paleoclimate**

**Jürgen Mutzl<sup>1</sup>, Olaf K. Lenz<sup>2</sup>, Günter Landmann<sup>1</sup>, Matthias Hinderer<sup>1</sup>**

<sup>1</sup>*Technische Universität Darmstadt, Germany;* <sup>2</sup>*Senckenberg Gesellschaft für Naturforschung, Generaldirektion, Germany*

The Layla Lakes in central Saudi Arabia are located 300 km south of Riyadh and were fed by groundwater, but dried up in the late 1980's due to intensive groundwater use, revealing a series of 21 dry hypogene karst sinkholes of different sizes in the Jurassic Hith Formation. In one of these sinkholes with a size of 400 x 100 m and a depth of 10 m several samples were taken by a field campaign in 2011. Furthermore, a sediment core was drilled at the margin of the sinkhole, revealing a lacustrine succession of 10.8 m.

First radiocarbon ages of mollusk shells and U/Th dating of carbonates indicate that the sedimentary succession covers the last 6000 years in a region, where such a complete sedimentary record is unknown so far for the Holocene. Mineralogical and geochemical studies show with sulphates (gypsum, anhydrite) and calcites (carbonates) two distinct types of sediment in the succession which regularly alternated in their dominance. The carbonates precipitated when the exchange between groundwater and lake water was too large to achieve supersaturation of gypsum, while the sulfates mark periods of strong evaporation. This may indicate cyclic climate variations between dry and more humid phases on a millennial scale.

The sediments revealed a rich assemblage of microfossils that comprise pollen, spores, diatoms, freshwater algae, testate amobae, other non-pollen palynomorphs, but above all a diverse and abundant phytolith assemblage. Therefore, for the first time we can present a qualitative and quantitative analysis of phytoliths from central Saudi Arabia. The study suggests an occurrence of grasses, but also shrubs, rice and other larger plants in the vicinity of the lake. The diversity and the changing abundances of these plant silicates indicate vegetational trends within an island vegetation in the center of the arid region of the Arabian Peninsula. In combination with geochemical and palynological results, the phytoliths show the occurrence of at least four humid phases with flooded habitats at the edge of the lake and the distribution of a dense herbaceous vegetation.

**9:45am - 10:00am**

### **A 8.5 kyr high-resolution multi-proxy paleoclimate record from lake Voëlvlei, Southern Cape, South Africa**

**Paul Strobel<sup>1</sup>, Torsten Haberzettl<sup>2</sup>, Marcel Bliedtner<sup>1,3</sup>, Thomas Kasper<sup>1</sup>, Julian Struck<sup>1</sup>, Matthias Zabel<sup>4</sup>, Roland Zech<sup>1</sup>**

<sup>1</sup>*Physical Geography, Institute of Geography, Friedrich Schiller University Jena, Jena, Germany;* <sup>2</sup>*Physical Geography, Institute of Geography and Geology, University of Greifswald, Germany;* <sup>3</sup>*Institute of Geography and Oeschger Centre for Climate Change Research, University of Bern;* <sup>4</sup>*MARUM – Center for Marine Environmental Sciences, University of Bremen, Bremen, Germany*

South Africa is a key region for paleoclimate studies reconstructing and understanding past changes in atmospheric circulation, because it is affected by both, the mid latitude Southern Westerlies and the tropical Easterlies. However, due to the scarcity of natural archives, the climatic and environmental evolution of South Africa during the late Quaternary is highly debated. Voëlvlei is a shallow lake situated at the junction of both climate systems near the southern Cape coast, and thus an ideal archive to investigate past regional environmental changes. A 13 m long sediment core was retrieved from this site and analysed using a multi-proxy approach, including granulometric and elemental analyses (ICP-OES, CNS, XRF), as well as leaf

wax *n*-alkanes and their compound-specific  $\delta^2\text{H}$  and  $\delta^{13}\text{C}$  isotopic signature. The chronology is based on 16 radiocarbon ages and reveals a basal age of 8,480  $^{+150}_{-240}$  cal BP. Elemental analyses, e.g., Ca concentrations and Rb/Zr ratios indicate marine influence between 8,480  $^{+150}_{-240}$  and 5,090  $^{+450}_{-390}$  cal BP related to sea levels higher than today. Between 8,480  $^{+150}_{-240}$  and 5,090  $^{+450}_{-390}$  cal BP depleted  $\delta^2\text{H}$  and enriched  $\delta^{13}\text{C}$  values point to dry conditions and/or high winter rainfall contribution accompanied by strong seasonality. This leads to high allochthonous input, indicated by high Al concentrations and Al/Zr ratios. Also during this time, several marine and/or terrestrial flooding events occurred at the southern Cape coast, which is indicated by grain size variations.

From 5,090  $^{+450}_{-390}$  cal BP until today, Voëlvlei is a purely lacustrine system without marine influence. Between 5,090  $^{+450}_{-390}$  cal BP and 2,000  $^{+380}_{-180}$  cal BP re-mobilization of pre-aged terrestrial organic material is indicated by high allochthonous input (Al, Al/Zr ratios), which leads to too old  $^{14}\text{C}$  ages in the age-depth model. Enriched  $\delta^2\text{H}$  and depleted  $\delta^{13}\text{C}$  values indicate wetter but variable conditions and possibly increased summer precipitation contribution and thus less seasonality during this time.

Since 2,000  $^{+380}_{-180}$  cal BP, even more enriched  $\delta^2\text{H}$  and depleted  $\delta^{13}\text{C}$  values point to even moister conditions at the southern Cape coast leading to a more stable vegetation cover resulting in lower sedimentation rates and reduced allochthonous input (Al, Al/Zr ratios). Granulometric parameters indicate two large fluvial flooding events (at 700  $^{+440}_{-480}$  and 10  $^{+50}_{-60}$  cal BP), which deposited large amounts of sediment (~15 cm and ~30 cm).

**10:00am - 10:15am**

### **Heavy metals in surface sediments of Richards Bay Harbour: anthropogenic impact on the former Mhlatuze estuary, South Africa**

**Paul Mehlhorn<sup>1</sup>, Finn Viehberg<sup>1</sup>, Jemma Finch<sup>2</sup>, Peter Frenzel<sup>3</sup>, Olga Gildeeva<sup>3</sup>, Andrew Green<sup>2</sup>, Trevor Hill<sup>2</sup>, Marc Humphries<sup>4</sup>, Torsten Haberzettl<sup>1</sup>**

<sup>1</sup>University of Greifswald, Germany; <sup>2</sup>University of KwaZulu-Natal, South Africa; <sup>3</sup>Friedrich-Schiller-University Jena, Germany; <sup>4</sup>University of the Witwatersrand, South Africa

The establishment of the port of Richards Bay in 1976 led to the formation of a vast industrial development zone based on coal export. During harbour construction, the Mhlatuze estuary was sub-divided by a 4 km long causeway into a natural sanctuary and the industrial sector (port of Richards Bay). Since then, the Mhlatuze River flows through the sanctuary, while the port is predominantly isolated from the river catchment and concomitant sediment influx. However, ship operation and coal export, two aluminium smelters and a fertilizer plant are in close proximity to the marine harbour. This combination of associated land-use change and industrial (agricultural-) pollution has resulted in contaminant accumulation and exerts stress on the ecosystem by influencing local biodiversity. During a field campaign in August/September 2018, surface sediment samples were systematically retrieved in a dense grid and short gravity cores were recovered from different characteristic harbour sites. The sedimentological and geochemical study focuses on the estuarine system as a final sink for pollutants and nutrients. Preliminary results reveal high sedimentation rates throughout the harbour interior. The occurrence of benthos, as seen via grab sampling, seems to be restricted to remote harbour areas, as they appear less in central or dredged areas. Sediment cores will enable a reconstruction of pre-industrial reference conditions. This includes potential pollutants (e.g., heavy metals, persistent organic pollutants), eutrophication indicators (total organic carbon, phosphorous) and erosion indicators (frequency dependent magnetic susceptibility or minerogenic input indicators such as Ti) together with established bioindicators, such as Cladocera, Foraminifera, Ostracoda, pollen and diatoms. This study is integrated into the project TRACES (Tracing Human and Climate impacts in South Africa) funded by the German Ministry of Education and Research (BMBF) within the SPACES II (Science Partnerships for the Assessment of Complex Earth System Processes) programme. TRACES investigates three selected ecosystems in South Africa, and aims to establish high-resolution records (including fluvial systems, reservoirs, etc.) of anthropogenic impacts for the last 250 years.

10:15am - 10:30am

### Geometals in sediment from Densu estuary, Ghana: potential proxy's for reconstructions

Lailah Gifty Akita<sup>1</sup>, Edem Mahu<sup>1</sup>, Kwesi Appeaning-Addo<sup>1</sup>, Samuel Addo<sup>1</sup>, Juergen Laudien<sup>2</sup>, Charles Biney<sup>3</sup>, Elvis Nyarko<sup>1</sup>

<sup>1</sup>University of Ghana, Ghana; <sup>2</sup>The Alfred Wegener Institute, Helmholtz Centre for Polar and Marine Handelshafen 12 27570 Bremerhaven Germany.; <sup>3</sup>Ecosystems Environmental Solutions, GD-213-5404, Accra-Ghana

Intensive industrialization coupled with rapid urbanization in coastal area results pollution of tropical coastal systems. Complexes of physical, chemical and biological components characterize estuarine environment. An estuarine is transitional system for understanding of environmental changes from fluvial to marginal seas. The application of multiple proxies in environmental reconstruction in tropical estuaries and marginal coastal areas within West Africa, Gulf of Guinea Coast is still inadequate. The study was undertaken to evaluate the degree of metal pollution and their potential ecological risk from Densu estuary, Ghana. Sediment samples were collected with Eckman grab along ten sampling stations. The surface sediments were placed into polyethylene bags, sealed and kept in ice (-4°C), carried to the laboratory for analysis. Metals (Pb, Zn, Cu, Hg, Fe and Mn) in fine-grained fraction ( $\emptyset$  63 $\mu$ m) were measured by Graphite Furnace Atomic Absorption Spectroscopy.

Metal concentrations (mean $\pm$ SD) in sediment [mg/kg]: Zn=46.93 $\pm$  45.01; Pb= 50.88  $\pm$ 24.33, Hg=0.02 $\pm$ 0.01; Fe=569 $\pm$ 176.27;Cu; 10.92 $\pm$ 8.47; Mn=90 $\pm$ 45.68. The sequences of metals concentration in sediment from Densu estuary were as follows (decreasing order): Fe>Mn>Pb>Zn>Cu>Hg. The highest mean concentration in Fe suggesting redox condition in estuary. The estuary showed low contamination factor (CF) with respect to five metals (Zn, Hg, Fe, Cu and Mn) (CF<1) and high contamination with respect to Pb (3 $\leq$ CF<6). The maximum contamination in Pb (compared to shale background levels) suggest anthropogenic source of metal pollution. Lead can be transported via sewage sludges, agricultural farms, release from leaded petrol automobiles, coal burning, mining and smelting ores into Densu estuary. There is moderate to considerable degree of contamination (DC) (3<DC $\leq$  6) in sediment of Densu estuary. The potential ecological risk index of each metal was less than 40, indicating low potential ecological risk.

The study emphasized chemical composition of surface sediments as the basis for palaeo-pollution reconstructions in estuarine system. The results show proximal and distal sources of pollutants in tropical estuarine. The use of mean metal concentration to assess the pollution does not reflects sediment contamination, combination with sediment quality standards and geochemical indices provided a broader perspective of chemical contaminations, when combined with physical and biological components of estuarine systems, will offer in depth understanding environmental changes on spatial and temporal scales.

### Poster Presentations

Tue: 7

### Ostracod fauna associated with *Cyprideis torosa* – a tool to differentiate brackish environments

Anna Pint<sup>1</sup>, Peter Frenzel<sup>2</sup>

<sup>1</sup>Institute of Geography, Universität zu Köln, Germany; <sup>2</sup>Institute of Earth Sciences, Friedrich-Schiller-Universität Jena, Germany

*Cyprideis torosa* (Jones) is a widespread, euryhaline species mainly living in brackish waters of coastal areas. It tolerates a wide range of salinity from fresh to brackish water-transition to hyperhaline values. Specimens often dominates in oligohaline lagoons but monospecific occurrences of *C. torosa* are realized mainly in hypersaline environments in semiarid and arid regions. *C. torosa* also lives in saline inland water bodies in all climatic zones, often in high numbers. Due to its broad tolerance of salinity, from 0.5 psu (practical salinity unit) to more than 100 psu, only the associated fauna allows a more precise detection of salinity variations. Salinity variability reflects climate and environmental changes in living and ancient ecosystems. Especially in coastal regions the accompanying ostracod species may help to detect salinity changes based on the con-

nection or disconnection of coastal waters to the sea. In marginal marine environments such as estuaries, lagoons and embayments the following trend is observed: the higher the marine influence, the lower the number of *C. torosa*. We present modern and fossil examples from athalassic waters, coastal lakes and lagoons, salt marshes and estuaries from northern and central Germany, UK, Portugal, Italy, Turkey, the Arabian Peninsula, the Black Sea, the Aral Sea, USA and Chile. The examples presented here show different types of ostracod faunas accompanying *C. torosa* and are related to salinity. Comparison of modern and fossil assemblages provides similarities concerning the environment independent of the geographical situation. The accompanying ostracod taxa of *C. torosa* in fossil assemblages could help to detect environmental changes especially in coastal regions. Although a taphocoenosis may reflect thanatocoenosis incompletely, a general picture of the palaeoenvironment can be revealed.

**Tue: 8**

### **The Middle Eocene maar lake “Groß Zimmern” (Hesse, Southwest Germany): Vegetation dynamics in a disturbed lacustrine record**

**Jürgen Mutzl<sup>1</sup>, Olaf K. Lenz<sup>2</sup>, Volker Wilde<sup>3</sup>**

<sup>1</sup>Technische Universität Darmstadt, Germany; <sup>2</sup>Senckenberg Gesellschaft für Naturforschung, Generaldirektion, Germany; <sup>3</sup>Senckenberg Forschungsinstitut und Naturmuseum, Sektion Paläobotanik, Germany

The maar lake of Groß Zimmern, 10 km east of Darmstadt (Hesse, SW-Germany), is one of about half a dozen isolated Paleogene deposits on and around the Sprendlinger Horst, which is the northern extension of the Hercynian Odenwald basement immediately east of the northern Upper Rhine Graben. A scientific core from 1997 which was drilled in the center of the lake basin revealed 80 m of volcanoclastic breccia and basaltic tuffs in the lower part followed by 30 m of a lacustrine succession of clastic sediments and finely laminated bituminous shale. The bituminous shales start abruptly at the top of the volcanic succession indicating meromictic conditions for the initial part of the deposits. A holomictic lake phase with clastic sediments, which fell as talus or were transported by mass flows from a collapsing crater wall into the basin as typical for the initial lake phase of maar craters, is not preserved. Furthermore, the disturbance of the complete lacustrine succession by slumping, redeposition or in-situ deformation is remarkable. The lamination of the clastic layers is discontinuous and sometimes up to 90° tilted. Possible explanations for the strong disturbance of the sediments are regional tectonic activity, a rapidly subsiding diatreme fill or a CO<sub>2</sub> burst.

A first palynostratigraphic analysis suggests that the lake sediments are of Middle Eocene age. This age is consistent with the age of other Paleogene deposits on the Sprendlinger Horst, such as the nearby maar lakes of Messel and Offenthal. Despite the disturbance of the lacustrine succession, our quantitative and qualitative palynological study revealed different pollen and spore assemblages. In the lower part of the succession aquatic plants and swamp elements, such as Hydrocharitaceae and Taxodiaceae, as well as marsh elements, such as Restionaceae, dominate. This indicates marginal swampy areas during times of a relatively high lake level. In the upper part of the record these elements decrease significantly or disappear completely and are replaced by elements of a paratropical rainforest with dominance of pollen from the juglandaceous and fagaceous alliances. This can be interpreted by a change to less humid conditions accompanied by a falling lake level. Furthermore, our study shows that the thermal alteration index of pollen and spores surprisingly increases continuously from the lower to the upper part of the core indicating that the maturity of the organic matter increases upward.

## 4d): Latest Achievements in Scientific Ocean and Continental Drilling

Monday, 23/Sep/2019: 11:15am - 1:00pm

Session Chair: Katja Lindhorsts (Christian-Albrecht-Universität zu Kiel)

Session Chair: Ulrich Harms (GFZ - German Research Centre for Geosciences)

Session Chair: Lisa Marie Egger (Bundesanstalt für Geowissenschaften und Rohstoffe)

Location: H2

### Session Abstract

National and international Earth science programs are utilizing Scientific Drilling as a critical tool to understand climate and environmental variability, natural hazards such as earthquakes and volcanic eruptions, natural resources, the deep biosphere and other topics of socio-economic relevance. The principal goal of the session is to summarize latest scientific achievements in ocean, continental and polar drilling.

### Lecture Presentations

11:15am - 11:30am

#### The ICDP Oman Drilling Project: a status report

Jürgen Koepke<sup>1</sup>, Dieter Garbe-Schönberg<sup>2</sup>, Dominik Mock<sup>1</sup>, Samuel Müller<sup>2</sup>, and The Oman Drilling Project Science Team<sup>3</sup>

<sup>1</sup>Leibniz University Hannover, Germany; <sup>2</sup>University Kiel, Germany; <sup>3</sup>Geoscience Institutions, Worldwide

The Samail Ophiolite, in Oman and the United Arab Emirates, is the largest, best-exposed section of oceanic lithosphere in the World. The Oman Drilling Project (OmanDP) within the frame of ICDP (International Continental Scientific Drilling Program) is a comprehensive drilling program aimed in understanding essential processes related to the geodynamics of mid-ocean ridges, including the magmatic formation, their aging and the cooling/alteration by seawater-derived fluids, and their past and ongoing weathering with focus on the carbonatisation of peridotites.

Over two drilling seasons (winter 2016/17 and 2017/18), the OmanDP has sampled the Samail Ophiolite sequence from crust to basal thrust in nine diamond-cored and six rotary-drilled boreholes. The total cumulative drilled length is 5458 m, with 3221 m of which was cored at more or less 100% recovery. These cores were logged to IODP standards aboard the Japanese drilling vessel Chikyu during two two-months description campaigns in summer 2017 and 2018. In addition to sampling and analysis of rock core and cuttings, the operations include ongoing geophysical logging, fluid sampling, hydrological measurements and microbiological sampling.

Here we present a summary of both phases on active drilling in Oman and core characterization aboard the DV Chikyu, as well as an overview on the ongoing research related to the OmanDP in many countries. Finally, we will summarize the last findings related to the theme accretion and cooling of the lower Oman paleocrust, based on results of investigating the crustal drill cores GT1, GT2, and GT3 drilled in the Wadi Tayin Block of the Samail ophiolite in combination with the results of our reference profile through the Oman paleocrust, which is based on conventional sampling of the Wadi Gideah located within the Wadi Tayin Block.

11:30am - 11:45am

#### Geological Research through Integrated Neoproterozoic Drilling (GRIND): The Ediacaran-Cambrian Transition

Catherine Rose<sup>1</sup>, Anthony Prave<sup>1</sup>, Kristin Bergmann<sup>2</sup>, Simone A. Kasemann<sup>3</sup>, Francis Macdonald<sup>4</sup>, Karl-Heinz Hoffmann<sup>5</sup>, Ricardo Trindade<sup>6</sup>, Maoyan Zhu<sup>7</sup>

<sup>1</sup>University of St Andrews, School of Earth & Environmental Sciences, St Andrews, United Kingdom; <sup>2</sup>Department of

*Earth, Atmospheric and Planetary Sciences, Massachusetts Institute of Technology, Cambridge, USA;* <sup>3</sup>*MARUM – Center for Marine Environmental Sciences and Faculty of Geosciences, University of Bremen, Germany;* <sup>4</sup>*Department of Earth Sciences, University of California Santa Barbara, USA;* <sup>5</sup>*Regional Geoscience Division, Geological Survey of Namibia, Windhoek, Namibia;* <sup>6</sup>*Instituto de Astronomia, Geofísica e Ciências Atmosféricas, Universidade de São Paulo, Brazil;* <sup>7</sup>*Nanjing Institute of Geology and Palaeontology, Chinese Academy of Sciences, Nanjing, China*

The Neoproterozoic Era is one of the most dramatic in Earth history: metazoans evolved, the supercontinent Rodinia formed and broke apart, the global carbon cycle underwent high-amplitude fluctuations, oxygen concentrations rose and climate experienced at least two episodes of worldwide glaciation. However, the discontinuous and fragmented nature of outcrop-based studies has hindered developing quantitative models of Earth system functioning during that Era. The Geological Research through Integrated Neoproterozoic Drilling (GRIND) project will begin to rectify this scientific shortcoming by obtaining 13 cores, each from 150 to 550 m, through the archetype successions that record the environmental and biogeochemical context during which animals evolved. The specific targets are the Ediacaran-Cambrian transition (ECT; c. 560-530 Ma) strata of west Brazil (Corumbá Group), south China (Doushantuo, Dengying and equivalent formations) and south Namibia (Nama Group). Our objective is to create a core network of correlative ECT strata that will enable constructing a highly re-solved, temporally constrained geobiological, stratigraphic and geochemical database, as well as provide a legacy archive for future research. The goal is to understand the drivers of the Neoproterozoic Earth system revolution: it began with simple eukaryotes that populated Earth during the preceding billion years of the Mesoproterozoic, underwent multiple Snowball Earth events, and emerged with the oxygenated, diverse ecosystems of the Cambrian. The three-nation drilling programme will commence in 2019. The drill sites will sample shallow-to-deeper marine rocks across shelf-to-basin transects. The work aims to 1) construct a highly resolved temporal framework that will lead to the development of age models for the ECT; 2) refine the patterns of biotic evolution of organic-walled and mineralised microfossils, metazoans and trace fossils, and identify the links between and test hypotheses about biological evolution and environmental change, and 3) determine the palaeoenvironmental and biogeochemical conditions that led to the rise of oxygen and distinguish cause-and-effect relationships and basin-specific versus global-scale secular trends in geochemical and stable isotope patterns. All cores will be split with one-half being archived in the national repositories and used for research by GRIND-ECT scientists and for education and training for national capacity building and outreach activities. The other half will be permanently archive at the Federal Institute for Geosciences and Natural Resources in Berlin-Spandau, Germany. All cores will be available for future research and education activities and will mark the first step towards creating an on-shore continental scientific drilling archive that will match in stature that of the IODP.

**11:45am - 12:00pm**

### **Permeability estimation in sedimentary sequences: a comparison between inferences from wireline resistivity logs and computations from porosity distributions in CT scans of drillcore**

**Virginia Gail Toy<sup>1,2</sup>, Hamed Amiri<sup>3</sup>, Francesco Cappuccio<sup>1</sup>, Mai-Linh Doan<sup>3</sup>, Natalia Xie<sup>1</sup>**

<sup>1</sup>*Department of Geology, University of Otago, Dunedin, New Zealand;* <sup>2</sup>*Institute of Geosciences, Johannes Gutenberg-Universität, Mainz, Germany;* <sup>3</sup>*ISTerre, Université Grenoble Alpes, Grenoble, France*

Fluids can migrate through sedimentary sequences both in typically millimetre diameter grain-scale pores, and in networks of decimetre-to-metre scale fractures. Depending on the nature of the sequence, there can be at least an order of magnitude difference in the permeability of these two types of porosity.

Resistivity measurements made using wireline tools in boreholes are very sensitive to variations in the ability of saline (formation or drilling) fluids to circulate through wall rock, thus deviations in them can reflect variations in pore space and permeability of the drilled sequence [3]. In IODP Exp. 343: JFAST LWD medium and deep resistivity datasets [1], we infer that a gradual increase with depth within one tectonic unit [2, Unit A1 from ~690 – 810 mbsf] by 0.5 ohm-m (ie. a gradient of 0.004 ohm-m/m), reflects differences in grain scale permeability related to progressive compaction. Conversely, we infer deviations of 0.8 ohm-m isolated to 1-2

m thick intervals such as around 720 mbsf (ie. local gradients of  $>0.4$  ohm/m) occur when highly permeable fractures or faults were intercepted. Calculations of the expected effect of the latter using an adaptive mesh simulation method allows estimation of the widths of the permeable zones.

In the JFAST project, core sections were scanned on recovery using a ship-board computed tomography (CT) system [1], providing images with a  $0.18 \times 0.18 \times 0.6$  mm voxel size. This provides an alternative dataset from which to determine porosity and permeability. We have used AvizoFire and Pergeos software suites to process (ie. filter/clean) CT images, and then segmented porosity across several  $<1$  m intervals. We then employed the XLAB and Petrophysical modules for these softwares to calculate/simulate both permeability using finite volume and Stokes solver-Lattice Boltzman methods, and formation factor using Ohm's law and random walk methods. We will discuss comparisons between these analyses of the CT data and the inferences we have made from the LWD data.

[1] Chester, F.M. et al., 2012. Expedition reports Japan Trench Fast Drilling Project (JFAST). Proc. IODP; Preliminary Report 343-343T; [2] Rab-inowitz, H.S., et al. 2015. Multiple major faults at the Japan Trench: Chemostratigraphy of the plate boundary at IODP Exp. 343: JFAST. Earth & Planetary Science Letters 423, 57-68; [3] Singh, N.P., 2019. Permeability prediction from wireline logging and core data: a case study from As-sam-Arakan basin. J. Petroleum Exploration & Production Technology 9, 297-305.

**12:00pm - 12:15pm**

### **CO<sub>2</sub>-induced natural deformation structures in well HJB-1 (Cheb Basin, Czech Republic)**

**Michael Pitz, Robert Bussert**

*TU Berlin, Germany*

Small-scale deformation structures are present in the cores of a borehole drilled into an active mofette in the Cheb Basin, western Eger Rift, Czech Republic. The area is characterized by swarm earthquake activity, cold CO<sub>2</sub>-degassing in the form of mofettes and microbial activity in the deep subsurface. These seismic, hydraulic, chemical and microbial processes are closely interlinked and are likely triggered by the ascent of CO<sub>2</sub>-rich fluids from the mantle. Fluid pathways are probably deep-reaching faults in the Palaeozoic metamorphic basement and diffuse pathways in Cenozoic sediments, mainly mudstones and subordinate carbonates that are overlain by sand and gravel.

The deformation structures occur in many cores and in the core interval corresponding to the semi-consolidated mudstones below 30m. Dike-like injection structures cutting through the host rock at high angles show opening widths of up to 10cm. The deformation structures show properties that are attributable to both physical-mechanical and chemical processes: The physical processes include both ductile and brittle deformation of the host deposits as well as the upward injection of sediments, which presumably originate in beds up to 10m deeper. Chemical processes are indicated amongst others by the presence of authigenic pyrites, whose amount depends on the distance to the deformation structure. In the carbonates, solution phenomena occur. Bandings in the deformation structures and in the host rock are related to changing mineral compositions and are interpreted as reaction fronts.

The features present in the core give evidence of the chemical and mechanical interaction of the ascending, CO<sub>2</sub>-rich fluids with the surrounding rocks: fluidized sediments were injected into overlying beds, probably caused by pressurized fluids. The chemical interaction of the CO<sub>2</sub>-saturated, reducing and acidic fluids might have contributed to the weakening of the surrounding rocks along the fluid pathways. However, physical processes appear to be more important than chemical reactions. The mudstones, which are usually more resistant to chemical processes than carbonates, obviously tend to physical deformation and sediment injection under the regional conditions.

Planned research will focus on quantifying the pressure conditions necessary for the formation of the deformation structures and on the presumed chemical weakening of the integrity of the mudstones. The understanding of these relationships is probably of interest for the assessment of the integrity of caprocks conventionally considered tight and for the safety of CO<sub>2</sub> storage over geological time scales.

12:15pm - 12:30pm

### Temperate rain forests at 77°S palaeolatitude during the Late Cretaceous

Johann P. Klages<sup>1</sup>, Ulrich Salzmann<sup>2</sup>, Torsten Bickert<sup>3</sup>, Claus-Dieter Hillenbrand<sup>4</sup>, Karsten Gohl<sup>1</sup>, Gerhard Kuhn<sup>1</sup>

<sup>1</sup>Alfred-Wegener-Institut Helmholtz-Zentrum für Polar- und Meeresforschung, Bremerhaven, Germany; <sup>2</sup>Northumbria University, Department of Geography, Newcastle, United Kingdom; <sup>3</sup>MARUM – Center for Marine Environmental Sciences, Bremen, Germany; <sup>4</sup>British Antarctic Survey, Cambridge, United Kingdom

The 'greenhouse climate' of the Late Cretaceous epoch was one of the Earth's warmest periods of the past 140 Ma, particularly at high latitudes. However, records allowing insights into terrestrial environmental conditions south of the Antarctic circle during that time are extremely rare. Hence, it remains highly elusive how the sensitive South Polar environment may have been impacted by such an extreme climate. Here we report a unique sedimentary sequence that was recovered with the MeBo-70 sea floor drill rig from the central Amundsen Sea Embayment shelf, West Antarctica. The record contains ~26 m of quartzitic sandstone underlain by a lithified swamp deposit that consists of a ~2 m-long complex and intact network of *in-situ* fossil plant roots embedded in a mudstone matrix. The lower ~1.5 m of this mudstone contain a highly diverse pollen and spore assemblage, documenting a temperate coastal lowland rain forest environment with mean annual temperatures of 11-15°C at a palaeolatitude of 77°S. Hence, the drill record provides the hitherto southernmost evidence of Cretaceous terrestrial environmental conditions and reveals a 'greenhouse climate' that was capable of maintaining a temperate environment much further south than previously known. The predictive capabilities of model simulations for high-latitude climate and environment characteristics for this critical period of Earth's climatic history can therefore now be evaluated more reliably.

12:30pm - 12:45pm

### Paleoclimate, Paleoenvironment, and Paleoecology of Neogene Central America: Bridging Continents and Oceans (NICA-BRIDGE)

Steffen Kutterolf<sup>1</sup>, Mark Brenner<sup>2</sup>, Armin Freundt<sup>1</sup>, Jens Kallmeyer<sup>3</sup>, Sebastian Krastel<sup>4</sup>, Sergei Katsev<sup>5</sup>, Axel Meyer<sup>6</sup>, Liseth Pérez<sup>7</sup>, Juanita Rausch<sup>8</sup>, Armando Saballos<sup>9</sup>, Antje Schwalb<sup>7</sup>, Wilfried Strauch<sup>9</sup>

<sup>1</sup>GEOMAR, Helmholtz Center for Ocean Research, Kiel, Germany; <sup>2</sup>Department of Geological Sciences and Land Use and Environmental Change Institute (LUECI), University Florida, USA; <sup>3</sup>Helmholtz Centre Potsdam-GFZ, German Research Centre for Geosciences, Germany; <sup>4</sup>Institute of Geosciences, Christian-Albrechts-Universität zu Kiel, Germany; <sup>5</sup>Large Lakes Observatory and Department of Physics and Astronomy, University of Minnesota Duluth, USA; <sup>6</sup>Institute of Zoology and Evolutionary Biology, University of Konstanz, Germany; <sup>7</sup>Institute of Geosystems and Bioindication (IGeo), Technische Universität Braunschweig, Germany; <sup>8</sup>Particle Vision, c/o FriUp, Annexe 2, Passage du Cardinal 11, Fribourg, Switzerland; <sup>9</sup>Instituto Nicaragüense de Estudios Territoriales, Nicaragua (INETER), Dirección General de Geología y Geofísica, Managua, Nicaragua

In March 2020, we will hold a workshop in Nicaragua to plan scientific drilling in Lakes Nicaragua and Managua. Both are located in a trench-parallel half graben that hosts the volcanic front and that developed during or prior to the Pliocene, as a consequence of subduction-related tectonic changes. The lakes are uniquely suited for multidisciplinary scientific investigation of long, continuous sediment profiles because of their: 1) long records (several Myrs) of terrestrial and related marine basin development at the southern Central American margin, 2) alternating lacustrine and marine environments, 3) proximity to both the older and the younger volcanic arcs, which were separated by slab rollback, 4) significance as a hot spot for endemism, 5) strategic location for study of the great American biotic interchange. They offer the opportunity to combine seismological, volcanological, paleoclimatological, paleoecological, and paleoenvironmental studies in the ocean and on land. The Sandino Basin, offshore Nicaragua, is the oceanic continuation of the depression in which the lakes are located, and a second, seagoing drilling phase of the project will complement the lake drilling, to understand the evolution of the entire complex margin.

Drilling of the Nicaraguan lakes, under the broad umbrella of Paleoclimate, Paleoenvironment, and Paleoecology will have broad scientific and socio-economic impacts and contribute to three major societal themes addressed by ICDP: Climate & Ecosystems, Deep Biosphere, and Natural Hazards. The workshop will foster

international collaborations and serve to further define and refine the scientific objectives and hypotheses outlined in the drilling workshop proposal. Seismic pre-site surveys in the lakes approve the feasibility to drill, and will be continued.

Long, continuous sediment cores from multiple sites in Lakes Managua and Nicaragua will provide the oldest lacustrine records in continental Neotropics. They will enable (a) development of a Neotropical environmental and paleoclimate record, e.g. past moisture availability/source, (b) determination of the times and rates of marine transgressions and regressions, their tectonic and climatic controls and ecological consequences, (c) investigation of recurrence rates and magnitudes of natural hazards, e.g. eruptions, landslides, earthquakes, hurricanes, (d) constraints on the timing and magmatic compositional changes during shifts of the volcanic arc, (e) linkages between long-term terrestrial and marine paleoenvironmental records, (f) long-term basin development, and the deeper structure of western Nicaragua, and (g) assessment of climatic, geologic and (Holocene) anthropogenic influences on biodiversity and limnological variables, e.g. past freshwater/saltwater phases, initiated by tectonics, and consequent effects on micro- and macrobiota.

**12:45pm - 1:00pm**

### **Paleoenvironmental indications and cyclostratigraphic studies of sediments from tropical Lake Towuti obtained from downhole logging**

**Arne Ulfers, Katja Hesse, Christian Zeeden, Thomas Wonik**

*Leibniz Institute for Applied Geophysics, Germany*

Lake Towuti is a tectonic lake on central Sulawesi, Indonesia. It is located within the Indo Pacific Warm Pool, a convection cell which has major impact on tropical climate and the ability to project its influence on a global scale (Chiang, 2009; De Deckker, 2016). Pre-site surveys using seismic methods and piston cores indicated that sediments in Lake Towuti provide best conditions to obtain a long-term paleoclimate record in this key region (Russel et al., 2014).

During an ICDP-project in 2015, downhole logging equipment of the Leibniz Institute for Applied Geophysics was used at two drill-sites to record a series of chemical and physical parameters (spectral gamma ray, magnetic susceptibility, resistivity, sonic velocity, dipmeter, ultrasonic imaging of the borehole wall). Continuous lithological logs based on downhole logging data were constructed using cluster analysis. Although the spatial resolution of constructed logs is not as detailed as core descriptions, good correlation to core descriptions and differentiation between the upper lacustrine facies and the lower pre-lacustrine facies (Russell et al., 2016) show that cluster analysis is a powerful tool in giving an instant overview of in situ sediments and determining their physical properties.

Cyclostratigraphic methods in downhole logging can help developing a better understanding of sedimentation rates and thus improving age-depth models for lacustrine sediments (Molinie and Ogg, 1990; Hinnov, 2013; Baumgarten et al., 2015). In case of Lake Towuti, a magnetic susceptibility log from the upper lacustrine facies (0-98 meters below lake floor) was analysed to calculate changes in sediment influx. A careful pre-processing of the data is crucial to secure undisturbed amplitude spectra. This includes the identification and exclusion of event-layers (tephra and turbidite-like mass movement deposits) from the log. Also side effects of those layers to surrounding sediments were diminished from the record.

Results show a dominance of eccentricity cycles, whereupon the longer, 400 ka cycle has to be handled with caution, due to its long wavelength (~37 m wavelength in the ~98 m susceptibility log). Sedimentation rates for certain parts were calculated and complement the preliminarily age model derived from <sup>14</sup>C- (Russel et al., 2014) and tephra-dating (Deino et al., in prep.). Further refining of the model and omission of an interpretation of long cyclicities results in the most detailed age-depth model for Lake Towuti, and thus is a fundamental step towards our understanding of paleoclimate processes in this region.

## Poster Presentations

Mon: 17

### Feather feature orientations in shocked granitic rocks of the Chicxulub crater: Implications for the formation of peak rings

**Matthias Ebert, Michael Poelchau, Thomas Kenkmann**

*Albert-Ludwigs-Universität Freiburg, Department of Geology, Germany*

The Chicxulub crater is the third largest impact structure on Earth, and the only known terrestrial crater with an unequivocal topographic “peak ring”. The recent drilling into Chicxulub’s peak ring (IODP-ICDP Expedition 364, 2016) addresses several questions, including the nature and formational mechanism of peak rings [1]. In order to unravel its complex formational process we need to understand the heterogeneous deformation mechanisms that have occurred during cratering. Therefore, the new drill core provides a unique view into the deformation styles of a peak ring [1]. The sampled core reveals the occurrence of quartz grains showing shock-related feather features (FFs) within ~580 m of granitic basement rocks [2,3]. The orientation of these microstructural features is suggested to be controlled by the orientation of the principal axis of stress ( $\sigma_1$ ) within the shock wave, which indicates the propagation direction of the shock front [4]. Based on this FFs-model, we determined local  $\sigma_1$  orientations at different depth of the peak ring core in order to see if there is a consistent or interrelated orientation. This approach allows us to reconstruct rotational movements of the target rocks during cratering in general and peak ring formation in particular. Our  $\sigma_1$  data indicate that the basement rocks between ~750 and ~1200 mbsf behaved as a semi-coherent block that underwent an internal rotation or folding. The rotation axis is in NNO-SSW direction, i.e., concentric to the crater center, which emphasizes the connection between shock wave propagation and FFs formation. We could not find a trend for  $\sigma_1$  in samples below ~1200 mbsf. In this region, the peak ring shows extreme deformation that is characterized by a wide range of structures, including shear faults, zones of cataclasis, striated shear planes and dm-thick zones of foliated and crenulated mineral fabrics. The combination of these deformation processes may induce to a large number of small-scale rotational movements in the peak ring units, which is reflected by the chaotic  $\sigma_1$  orientations. This lower part of the peak ring core is interpreted as the main outward thrust zone active during imbrication of the peak ring.

[1] Morgan J. V. et al. (2016) *Science*, 354:878–882; [2] Poelchau M. H. et al. (2017) *48<sup>th</sup> LPSC*, Abstract #1924; [3] Ferrière L. et al (2017) *48<sup>th</sup> LPSC*, Abstract #1600; [4] Poelchau M. H. & Kenkmann T. (2011), *JGR Solid Earth*, 116(B2).

Mon: 18

### Deep Lake Sediment Sampling on Lake Constance using Hipercorig

**Ulrich Harms<sup>1</sup>, Ulli Raschke<sup>2</sup>, Antje Schwalb<sup>2</sup>, Volker Wittig<sup>3</sup>, Thomas Wonik<sup>4</sup>, Martin Wessels<sup>5</sup>**

<sup>1</sup>GFZ - German Research Centre for Geosciences, Telegrafenberg, 14473 Potsdam, Germany; <sup>2</sup>Institute of Geosystems und Bioindication, Technische Universität Braunschweig, Langer Kamp 19c, 38106 Braunschweig, Germany;

<sup>3</sup>International Geothermal Centre, Hochschule Bochum, Lennershofstraße 140, 44801 Bochum, Germany; <sup>4</sup>Leibniz-Institut für Angewandte Geophysik, Stilleweg 2, 30655 Hannover, Germany; <sup>5</sup>Institut für Seenforschung der LUBW, Argenweg 50, 88085 Langenargen, Germany

The sediments in Lake Constance provide distinct paleo-environmental signals which so far could only be sampled down to about 11 m depth below lake bottom although more than 100 m infill is known from seismic lines. The well-defined and horizontally-bedded lacustrine sediments of the upper tenth of meters are most likely Holocene deposits that overlay deeper undisturbed late Glacial sediments. The access to such strata that often archive key information on climate and biological evolution is not only on Lake Constance but also globally in many lakes difficult and cost intensive. In order to overcome the problems in accessing deep lake layers we have developed a compact sediment coring and barge system and tested it on Lake Constance during a shake-down cruise in May and June 2019.

The Hipercorig consists of a modular barge and sediment piston coring system with a range of up to 200

m water depth for anchoring plus 100 m deep coring in 2 m sections. The key technology is i) a hydraulic power transmission that drives a down-the-hole hammer through a high-pressure pump, ii) a contamination free usage of lake water as hydraulic medium, and iii) a lightweight and complete modular design allowing for set-up and operation without heavy machinery. Hipercorig is equipped with an anchoring system, two service and safety boats and other auxiliary equipment transportable in four 20 ft standard containers. For operations on Lake Constance, an experienced coring crew of three was complemented by a science crew of two for the initial core handling.

The test on Lake Constance was performed in 204 m deep water 2 km SSW of Hagnau, Germany. The site is located close to the deepest part of this basin with best possible preservation of a continuous and undisturbed sediment record. Coring and core recovery results as well as a first assessment of the sediments recovered will be reported in this contribution. In addition, the test on Lake Constance included a first trial of geophysical downhole logging within a piston-cored borehole from Hipercorig.

Hipercorig is available for the science community at large. Costs for transport and personal have to be covered by individual project funds. The range of utilization comprises lakes and similar aquatic environments and also land sites such as bogs and alike. The Deutsche Forschungsgemeinschaft funded the acquisition and testing. The GESEP Consortium e.V. provides oversight to ensure safe operations and long-term availability.

## **4e/f) Archives of environmental changes throughout Earth history: bio- and authigenic mineralization to paleoenvironmental reconstruction**

**Tuesday, 24/Sep/2019: 12:00am - 12:30pm & 3:45pm - 5:30pm**

**Session Chair: Johann P. Klages** (Alfred-Wegener-Institut, Helmholtz-Zentrum für Polar- und Meeresforschung)

**Session Chair: Gerhard Kuhn** (Alfred-Wegener-Institut, Helmholtz-Zentrum für Polar- und Meeresforschung)

**Location: H2**

### **Session Abstract**

**4e)** Reconstruction of environmental changes and catastrophic events throughout Earth-history is of great importance for understanding climate dynamics of the Earth-system and predict possible future climate scenarios. The sedimentary record plays a key role as archive for major extinction events, perturbations of global biogeochemical cycles and prominent climate changes. In this session we address all aspects related to paleoenvironmental studies, such as formation of bio- and authigenic minerals, processes and parameters controlling geochemical signatures, preservation and diagenetic alteration as well as sedimentological, palaeontological and stratigraphical observations and modelling approaches.

**4f)** We encourage contributions from different subdisciplines studying sedimentary archives from various perspectives, including paleoenvironmental reconstructions, experimental and modelling approaches, biomineralization processes and proxy development.

## Lecture Presentations

12:00pm - 12:30pm Session Keynote

### The expression of global Oceanic Anoxic Events (OAE) in continental interiors: An example from the Early Jurassic Toarcian OAE

**Micha Ruhl<sup>1,2</sup>, Weimu Xu<sup>1,2</sup>, Hugh Jenkyns<sup>2</sup>, Stephen Hesselbo<sup>3</sup>**

<sup>1</sup>Department of Geology, Trinity College Dublin, The University of Dublin, Ireland; <sup>2</sup>Department of Earth Sciences, University of Oxford, Oxford, UK; <sup>3</sup>Camborne School of Mines, University of Exeter, Exeter, UK

The early Toarcian Oceanic Anoxic Event (T-OAE; ~182 Ma) was marked by persistent marine anoxia–euxinia and globally significant burial of organic matter, associated with a major global carbon cycle perturbation, likely linked to Karoo–Ferrar volcanism. Although the T-OAE is well studied in the marine realm, accompanying climatic and environmental change in continental interiors is poorly understood. Here, we examine the freshwater lacustrine Da’anzhai Member (Sichuan Basin, China), which consists of organic-rich laminated black shales and ostracod- and bivalve-bearing limestones that formed in a major continental lake system in the latest Early Jurassic.

The Da’anzhai Member is characterized by a stepped negative shift of ~7‰ in  $\delta^{13}\text{C}_{\text{TOC}}$  and ~4‰ in  $\delta^{13}\text{C}_{n\text{-alkanes}}$ , as is also typically observed in lower Toarcian marine records from Europe. Re-Os dating of the Da’anzhai black shale suggests a depositional age of  $180.3 \pm 3.2$  Ma, equally suggesting an early Toarcian age. These data, combined with the superabundance of the terrestrial thermophylic pollen *Classopollis classoides*, known to represent an ‘environmental-stress species’ characteristic of the early Toarcian, indicate that the lacustrine Da’anzhai Member was deposited contemporaneously with the T-OAE.

Rhythmic changes in depositional conditions observed along a depth transect in the basin occur possibly on astronomical time-scales allowing for high-resolution temporal constraints. It suggests precession-controlled changes in lake-level and organic productivity during the Early Toarcian OAE in the lacustrine Sichuan Basin. Biomarker and geochemical analyses further suggest increased lacustrine productivity, probably related to enhanced weathering and riverine nutrient supply, and a progressive change towards a stratified, anoxic lake environment, promoting burial of ~500 Gt organic carbon largely derived from atmospheric  $\text{CO}_2$ . Massive carbon sequestration in expanding major lakes represents a new, unexplored, negative feedback in the global exogenic carbon cycle that potentially impacted the nature and duration of the T-OAE.

3:45pm - 4:00pm

### Carbonates with spherulites and cone-in-cone structures from the Precambrian of Arctic Norway, and their palaeoenvironmental significance

**Guido Meinhold<sup>1,2</sup>, Sören Jensen<sup>3</sup>, Magne Høyberget<sup>4</sup>, Arzu Arslan<sup>1</sup>, Anette E. S. Högström<sup>5</sup>, Jan Ove R. Ebbestad<sup>6</sup>, Teodoro Palacios<sup>3</sup>, Heda Agić<sup>7</sup>, Wendy L. Taylor<sup>8</sup>**

<sup>1</sup>School of Geography, Geology and the Environment, Keele University, United Kingdom; <sup>2</sup>Department of Sedimentology and Environmental Geology, Göttingen University, Germany; <sup>3</sup>Área de Paleontología, Universidad de Extremadura, Spain; <sup>4</sup>Rennesveien 14, Mandal, Norway; <sup>5</sup>Arctic University Museum of Norway, UiT – The Arctic University of Norway, Norway; <sup>6</sup>Museum of Evolution, Uppsala University, Sweden; <sup>7</sup>Department of Earth Science, University of California at Santa Barbara, USA; <sup>8</sup>Department of Geological Sciences, University of Cape Town, South Africa

The Neoproterozoic-Cambrian succession in the remote Digermulen Peninsula of the Tanafjorden area in eastern Finnmark, northern Norway, has attracted renewed research interest because of new findings of Ediacaran-aged fossils (e.g. Jensen et al., 2018, Canadian Journal of Earth Sciences). Hitherto, the entire upper Ediacaran and Cambrian succession here was believed to be siliciclastic. However, during recent fieldwork, the Digermulen Early Life Research Group made the first discovery of carbonates within the 2nd cycle of the Mandrapselva Member of the Stáhpogieddi Formation of the Vestertana Group (Meinhold et al., 2019, Precambrian Research). Carbonates occur as calcareous siliciclastic beds, lenses, and concretions, some with calcite spherulites and cone-in-cone calcite, in a mudrock to fine-grained sandstone succession from ap-

proximately 3 m to 26 m above the base of the 2nd cycle of the Manndrapselva Member. They occur c. 40 m below the Ediacaran–Cambrian boundary, which is well defined by trace fossils. Thin-section petrography and scanning micro X-ray fluorescence elemental mapping reveal a layered composition of the calcareous sedimentary rocks. In some of those, well-developed nested cones of cone-in-cone calcite form the outer layer. Thin clay coatings outline individual cones. The inner layers are composed of (1) carbonate with calcite spherulites (grainstone) and (2) thinly laminated fine-grained calcareous siliciclastics (mudstone and wackestone) indicated by elevated concentrations of Al, Si, Fe, and Ti. The inner siliciclastic layers contain framboidal pyrite and probably organic matter. Formation of calcite spherulites probably took place at the sediment–water interface or a few centimetres below, either in a coastal littoral environment or in situ in the sublittoral zone under high alkaline conditions. The cone-in-cone calcite formed during burial diagenesis and clearly before low-grade metamorphism and cleavage formation. Timing of deformation and metamorphic overprint match the Caledonian orogeny (Meinhold et al., 2019, GFF). This new record of carbonates with calcite spherulites and cone-in-cone structures from the Ediacaran of Arctic Norway adds to their rare occurrences in the geological record.

#### 4:00pm - 4:30pm Session Keynote

### Coral geochemistry: a window into the biomineralisation process

**Nicola Allison**

*University of St. Andrews, United Kingdom*

Coral reef accretion rates are influenced by seawater pH and understanding the impact of changes in atmospheric CO<sub>2</sub> on coral biomineralisation is key to predicting the future of reef environments and interpreting their past development. Coral aragonite precipitates from an extracellular calcifying fluid (ECF) which is derived from seawater and enclosed in a semi-isolated space between the skeleton and the overlying coral tissue. Corals actively increase the pH of the ECF and it is likely that the [DIC] (dissolved inorganic carbon) is concentrated above that of seawater. Skeleton precipitation is also influenced by extracellular soluble and insoluble organic materials which play a key role in crystal nucleation and growth.

To investigate controls on reef accretion my research group studies the geochemistry of modern and fossil field specimens and of corals cultured over a range of seawater pCO<sub>2</sub> and temperature. We use skeletal boron geochemistry ( $\delta^{11}\text{B}$  and B/Ca) to estimate the pH and dissolved inorganic carbon chemistry of the ECF and the organic composition of the skeleton to infer the biomolecules present at the calcification site. Our findings demonstrate that the pH, DIC and biomolecules at the calcification site vary significantly in response to changes in seawater pCO<sub>2</sub> and temperature. To investigate how these factors interplay to control skeletal accretion we are now precipitating synthetic aragonites under simulated biological conditions. Our data indicate that skeletal organic materials have been paramount in controlling aragonite precipitation in past reef environments and can suppress accretion even when the calcification fluid has a high pH and [DIC]. Resolving the full roles of biomolecules in CaCO<sub>3</sub> accretion is a key step in understanding controls on biomineralisation in both the past and future.

#### 4:30pm - 4:45pm

### Understanding the Interaction between Glaciers and Volcanoes through Glacier Cave Research

**Linda Sobolewski, Andreas Pflitsch**

*Ruhr-University Bochum, Germany*

Volcanoes often reach sufficient heights which allow glaciers to form. Whereas their maximum extent could be observed during the Pleistocene, an immense retreat is documented since the beginning of the 20<sup>th</sup> century as a result of climate change and global warming. Glaciers are retreating at an alarming rate, taking with them valuable scientific information. The research field of glaciology already is well-established today.

However, information about the internal workings of a glacier, conditions inside the ice or the influence of underground heat are still missing. Cave systems, often generating under the immense snow and ice masses, first give us the chance to obtain a rare view into the interior structure.

Our research comprises extensive studies inside several glacier caves on volcanoes of the Cascade Volcanic Arc, a subduction zone ranging from Mt. Garibaldi in British Columbia to Lassen Peak in the northern part of California. We primarily focus on Mt. Hood, Mt. St. Helens, and Mt. Rainier, as these volcanoes reveal unique, and moreover, three completely different types of glaciers: retreating on Mt. Hood, growing on Mt. St. Helens, balanced on Mt. Rainier. Considering this, no glacier cave is like any other. We could observe very unstable systems on Mt. Hood, whereas continuous caves on Mt. St. Helens and Mt. Rainier could be observed.

During our expeditions we focus on surveying the glacier caves, as well as measuring climate data such as air temperature, air moisture, and air currents. The measuring program consists of short- and long term measurements. Temperature and humidity sensors stay permanent, ultrasonic anemometers and thermal cameras only stay for a few days during our field trips.

All cave systems are influenced by volcanic activity through hot springs or fumaroles. Both are significant factors affecting englacial air masses and leading to self-energizing processes.

Some cave systems can have an extent of several hundred meters. Therefore, they contribute a high ratio to the mass and energy balance of a glacier. Other important aspects comprise the investigation of volcanic hazards in terms of glacial outbursts, lahars and other water-mobilized flows, as well as to examine the effects of global warming on our glaciers.

Further expeditions are in preparation to observe the glaciers and their caves, and to intensify and expand the measurements. Future expeditions to Mt. Hood, Mt. St. Helens, and Mt. Rainier are planned.

#### **4:45pm - 5:15pm Session Keynote**

### **The geosphere and the climate system: A new dimension of Earth system interaction**

**Gregor Knorr<sup>1</sup>, Lars Rüpke<sup>2</sup>**

<sup>1</sup>Alfred Wegener Institute, Bremerhaven, Germany; <sup>2</sup>GEOMAR, Kiel, Germany

Climate change as recorded in paleoclimate archives during the last 100 Ma indicates a wide range of climate transitions that involve complex Earth system interaction including the geosphere. Feedback mechanisms of climatically induced changes of the geosphere on the climate system itself are still poorly understood. Recent research has shown that the Earth's geosphere and climate interact closely on a wide spectrum of timescales ( $10^3$ - $10^6$  years), which suggests a strong potential for such feedbacks between these sub-systems, e.g. via submarine volcanism or sedimentary processes in response to glaciation and sea level changes. Furthermore, the impact of e.g. long-term geodynamic processes on the climate system, including threshold behavior emphasizes the potential of climatically induced solid earth changes that, in turn, affect climate and how climate variations can modulate the impact of geosphere changes. This suggests a more complex level of Earth system interactions.

**5:15pm - 5:30pm**

**Preliminary data from short sediment drill cores beneath the Ekström Ice Shelf, Antarctica**

**Nikola Koglin<sup>1</sup>, Gerhard Kuhn<sup>2</sup>, Christoph Gaedicke<sup>1</sup>, Olaf Eisen<sup>2,3</sup>, Andreas Läufer<sup>1</sup>, Raphael Gromig<sup>2</sup>, Emma Smith<sup>2</sup>, Jan Tell<sup>2</sup>, Ralf Tiedemann<sup>2,3</sup>, Frank Wilhelms<sup>2,4</sup>, Xiaopeng Fan<sup>5</sup>, Boris Biskaborn<sup>6</sup>, Gong Da<sup>5</sup>**

<sup>1</sup>Bundesanstalt für Geowissenschaften und Rohstoffe (BGR), Hannover, Germany; <sup>2</sup>Alfred-Wegener-Institut Helmholtz-Zentrum für Polar- und Meeresforschung, Bremerhaven, Germany; <sup>3</sup>Department of Geosciences, University of Bremen, Bremen, Germany; <sup>4</sup>Department of Crystallography, Geoscience Centre, University of Göttingen, Göttingen, Germany; <sup>5</sup>Polar Research Center, Jilin University, Changchun, China; <sup>6</sup>Alfred-Wegener-Institut Helmholtz-Zentrum für Polar- und Meeresforschung, Potsdam, Germany

In preparation for a major drilling campaign beneath the Ekström Ice Shelf (EIS), East Antarctica, three pre-site surveys in 2016/17, 2017/18 and 2018/19 were conducted comprising seismic reflection surveying and sediment coring. The aim of these campaigns was to get information about the structure and stratigraphy of the uppermost part of the sediments beneath the EIS, in particular to track the Explora Wedge basalt as counterpart to the rift volcanism in southern Africa that has formed during the break-up of Gondwana in early Jurassic, and the Meso- to Cenozoic sediments that overly it. During coring activities in 2017/18 and 2018/19, several sediment cores and samples were obtained by different methods: Wippermann grabber, gravity corer, UWITEC percussion driller and vibro corer. While the cores collected during the most recent season are still being analysed, the cores from the season 2017/18 have been opened and images, physical properties, XRF-core-scanning, and samples were taken. Disturbed sediment (mainly surface) samples were dried and separated by their grain size and pebbles from these samples were collected and will be analysed separately.

Here, we focus on the pebbles, which potentially provide information about the Explora Wedge and the stratigraphic classification of the upstream pre-glacial sediments that are mostly covered mostly by young glacial debris. Pebbles range from 0.5 mm to several centimetres in size. Those pebbles, which originate from the drill cores show a thin Fe-Mn oxyhydroxide coating. Large pebbles additionally have a coating of biota (e.g., bryozoa and sponges). Some dense pebbles might indicate a basaltic origin. Pebbles from disturbed samples show no coating and can be grouped by their rock type, if recognisable, or macroscopic appearance. The largest group includes sedimentary rocks, which are subangular to rounded, fine grained and light beige with black fragments. Another group consists of rocks that have a dense appearance with dark grey to black colour that resemble basaltic material, all of which being mainly angular but also subangular to rounded. The remaining pebbles are mainly very dense with different colours (reddish, brownish, light grey), which might have originated from fine grained silty to clayey ocean floor sediments. Additionally, quartz and carbonatic material was found. The two main groups, basaltic and light sedimentary pebbles, might stem from the rocks of interest – the Explora Wedge volcanics and the pre-glacial sediments. Further investigations of these pebbles, e.g. geochemistry, will help to identify the stratigraphic composition of the ocean floor beneath the EIS.

**Poster Presentations**

**Mon: 19**

**The distribution of rare earth elements and yttrium (REY) between the truly dissolved, nanoparticulate/colloidal and suspended loads during high and low discharge in the Kalix and Råne Rivers, Northern Sweden**

**Nadine Elisabeth Weimar<sup>1</sup>, Katja Schmidt<sup>1,2</sup>, Erika Kurahashi<sup>1</sup>, Michael Bau<sup>1</sup>**

<sup>1</sup>Jacobs University Bremen, Germany; <sup>2</sup>BGR, Marine Resource Exploration, Hannover, Germany

Rivers play a major role for the trace element composition of the ocean. The following three different size fractions can be distinguished in river water: (i) suspended particles (>0.2 µm), (ii) nanoparticles and colloids (NPCs; 0.2 µm - 10kDa), and (iii) the truly dissolved fraction (<10kDa). Trace elements such as REY can be associated with all of these size fractions. As elements sorbed onto suspended particles and NPCs are removed

from the water column during estuarine mixing, only the truly dissolved fraction reaches the ocean. However, detailed knowledge of the REY distribution between these different fractions is so far rather limited due to sometimes challenging ultrafiltration procedures.

We investigated the distribution of REY in two northern Swedish rivers, the Kalix and the Råne, during times of low river discharge (February 2017) and high river discharge (May 2019) with the aim to determine how the seasonal variation in two boreal rivers influences the REY distribution between the different size pools. This will help to better understand the role of NPCs in the transport of these particle-reactive elements into the oceans.

The Kalix and the Råne are two pristine rivers which are not regulated and which flow into the Baltic Sea. The catchment area of both rivers consists of only recently exposed granitic tills of Archean age. The Kalix River has a catchment area of 18,130 km<sup>2</sup> and the Råne River a smaller one of 4207 km<sup>2</sup>. Boreal rivers often display flat shale-normalized REY patterns, but may also show strong seasonal changes [1]. Our REY results for the dissolved fraction (<0.2 µm) of the Kalix and the Råne rivers during low discharge also show such flat patterns together with a negative Ce anomaly. In marked contrast, the truly dissolved fraction shows a strong difference between the heavy and light REY (HREY and LREY, resp.), resulting in increasing HREY/LREY and Y/Ho ratios with decreasing filter pore size. In the dissolved fraction (<0.2 µm) of the Kalix River, 16-20% of LREY and 38-54% of HREY are bound to small organic NPCs between 1 kDa and 10 kDa, and only 2-3% of LREY and 6-12% of HREY are truly dissolved, while in the Råne River these fractions are about 3-4% and 6-9%. These results from 2017 for low river discharge will be compared to most recent data from 2019 for high river discharge.

[1] Pokrovsky et al. (2014) Ocean Sci. 10, 107-125.

Mon: 20

## Calcification, skeletal structure and composition of the cold-water coral *Desmophyllum dianthus*

**Kristina K. Beck<sup>1,2</sup>, Grit Steinhofel<sup>1</sup>, Jürgen Laudien<sup>1</sup>, Gernot Nehrke<sup>1</sup>, Marlene Wall<sup>3</sup>, Jan Fietzke<sup>3</sup>, Claudio Richter<sup>1,2</sup>, Gertraud M. Schmidt-Grieb<sup>1</sup>**

<sup>1</sup>Alfred Wegener Institute Helmholtz Centre for Polar and Marine Research, Bremerhaven, Germany; <sup>2</sup>University of Bremen, Bremen, Germany; <sup>3</sup>GEOMAR Helmholtz Centre for Ocean Research, Kiel, Germany

In the naturally acidified Comau Fjord (Chile), high densities of the cosmopolitan cold-water coral *Desmophyllum dianthus* are found at or below aragonite saturation ( $\Omega_{ar} \leq 1$ ). However, it is not known so far if seasonal changes in  $\Omega_{ar}$  lead to seasonal differences in calcification rates and the corals' ability to up-regulate the pH in the calcifying fluid ( $pH_{cf}$ ). Corals were sampled in Comau Fjord along both horizontal and vertical pH gradients ( $pH_T = 7.6-7.9$ ,  $\Omega_{ar} = 0.76-1.45$ ). The calcification rates (buoyant weighing technique) of *D. dianthus* were compared between austral summer 2016/2017 and winter 2017 and related to the respective physico-chemical conditions in the water column ( $T$ ,  $\Omega_{ar}$ ). In order to determine the biological  $pH_{cf}$  up-regulation of *D. dianthus*, the skeletal boron isotopic composition ( $\delta^{11}B$ ) was measured in the upper part of the calyx between the septa, using a UV femtosecond laser ablation system coupled to a multicollector inductively coupled plasma mass spectrometer (LA-MC-ICP-MS). Higher growth rates of *D. dianthus* were found in summer than in winter. Surprisingly, growth of *D. dianthus* was highest in near-bottom, undersaturated waters in both seasons ( $\Omega_{ar} = 0.76$  and  $0.84$ ) and cross-transplanted specimens from shallow to deep waters were able to acclimatise to  $\Omega_{ar} < 1$ . Therefore, the present study shows that  $\Omega_{ar}$  alone is a poor predictor of *D. dianthus* growth. Skeletal analyses show a complex relationship between  $\delta^{11}B$  and the structure of the coral skeletons.  $\delta^{11}B$  measurements are highly variable, which may be attributed to the high calcification rates in the upper part of the coral calyx. Therefore, high resolution analyses of the skeletal composition and micro-structure will be conducted along the entire longitudinal section of *D. dianthus* skeletons using Raman microscopy and scanning electron microscopy (SEM). In addition,  $\delta^{11}B$  will be measured in different skeletal parts and compared to skeletal structure analyses for a reliable reconstruction of seawater pH at high temporal resolution using skeletons of *D. dianthus* grown under laboratory and field conditions (Comau Fjord, Chile).

**Mon: 21****The relation between  $\Delta^{17}\text{O}$  and bodymass for bioapatite****Dingsu Feng, Andreas Pack***Georg-August-Universität Göttingen, Abteilung Isotopengeologie, Geowissenschaftliches Zentrum, Goldschmidtstraße 1, 37077 Göttingen, Germany*

The reconstruction of paleo-atmospheric  $\text{CO}_2$  levels by proxies is still one of the most important challenges of modern climate research. The  $\Delta^{17}\text{O}$  of air  $\text{O}_2$  varies with atmospheric  $\text{CO}_2$  concentrations. Bao et al. (2008) presented an approach for reconstruction of the atmospheric  $\text{CO}_2$  levels on the basis of a  $^{17}\text{O}$  anomaly in sulfates. Pack et al. (2013) proposed that bioapatite of terrestrial mammals can also be used as a proxy for the  $\Delta^{17}\text{O}$  of ambient air and hence atmospheric  $\text{CO}_2$  levels. Mammals breathe in  $\text{O}_2$  to metabolize carbohydrate, fat, and protein. The  $\Delta^{17}\text{O}$  anomaly of air  $\text{O}_2$  is transferred to the reaction products  $\text{CO}_2$  and  $\text{H}_2\text{O}$ . Both  $\text{CO}_2$  and  $\text{H}_2\text{O}$  equilibrate with body water so that the anomaly is transferred from inhaled  $\text{O}_2$  to body water of mammals. Bioapatite crystallizes in isotopic equilibrium from body water. Because body water contains a fraction of anomalous  $\text{O}_2$  from the respiration of air  $\text{O}_2$ , bioapatite should carry information on the isotope composition of air  $\text{O}_2$ . The amount of oxygen from respired air  $\text{O}_2$  can be estimated using a mass balance model (Pack et al. 2013). This mass balance model, however, has large intrinsic uncertainties and must be compared to large data. For better interpretation, we achieve to obtain more data from modern animals.

We collected modern samples of bioapatite that crystallized at temperatures between  $0^\circ\text{C}$  and  $37^\circ\text{C}$ . For the sample preparation, the modern samples were heated to  $1000^\circ\text{C}$  to remove the carbonate fraction of the bioapatite in the furnace. The triple oxygen isotope measurements of the phosphate fraction of the bioapatite were conducted by infrared laser fluorination using purified  $\text{F}_2$  in combination with gas chromatography isotope ratio monitoring gas mass spectrometry.

A new database of animals from desert to aquatic habitats will be systematically built up.

[1] Bao et al. (2008). *Nature* **54**: 349-392; [2] Pack et al. (2013) *Geochimica et Cosmochimica Acta*. **102**, 306-317.

**Mon: 22****Palynofacies as an indicator for transgressive-regressive trends in offshore marine mudstones – a critical evaluation****Hauke Thöle<sup>1,2</sup>, Ulrich Heimhofer<sup>1</sup>, Andre Bornemann<sup>2</sup>, Jochen Erbacher<sup>2,3</sup>***<sup>1</sup>Leibniz Universität Hannover, Germany; <sup>2</sup>Bundesanstalt für Geowissenschaften und Rohstoffe (BGR), Hannover, Germany; <sup>3</sup>Landesamt für Bergbau, Energie und Geologie (LBEG), Hannover, Germany*

Stratigraphic distribution patterns of particulate organic matter (POM) within sediments have been widely used for facies recognition and paleoenvironmental interpretation as well as to decipher proximal to distal trends within fine-grained sediments. The Lower Cretaceous mudstone-dominated succession in the eastern Lower Saxony Basin (LSB) offers an excellent opportunity to critically evaluate palynofacies parameters which have been commonly used to identify transgressive-regressive (T-R) cycles in marine sediments. For the seemingly monotonous succession, a robust sequence stratigraphic framework has been established by integrating high-resolution elemental intensity data from XRF-core scanning with organic carbon isotope chemostratigraphy and biostratigraphic information from four drill cores. Stratigraphic trends in Si/Al ratios are interpreted to reflect grain size variations and enable identification of six T-R cycles during the Berriasian to Aptian interval in the LSB. The composition and distribution of the POM has been assessed by analysis of 220 strew mounts using transmitted-light microscopy. POM is dominated by opaque and translucent phytoclasts ( $\phi = 49.3\%$ ) with amorphous organic matter ( $\phi = 13.2\%$ ) being mostly of subordinate importance. Marine and terrestrial palynomorphs account for roughly similar fractions with 21.1% and 16.3%, respectively. Overall, the POM composition indicates deposition in a mud-dominated distal to proximal shelf setting. The ratio of opaque versus translucent phytoclasts (OP/TR ratio) shows a distinct long-term increase from the Berriasian onwards with maximum values during the Lower Hauterivian, followed by a subsequent decrease in OP/TR

ratio. This trend broadly reflects the overall transgressive-regressive evolution of the succession interpreted from Si/Al changes. On the other hand, the ratio of terrestrial versus marine palynomorphs (T/M ratio), often applied as indicator of proximal to distal trends and distances from the coastline, shows no correlation with the T-R cycles inferred from XRF-core-scanning data. Interestingly, systematic long- and short-term trends visible in T/M ratio correspond to variations in the XRF-derived Ca/Ti stratigraphic trend, which is interpreted to reflect variations in carbonate content. This may indicate that the T/M ratio in the LSB is largely controlled by variations in marine palynomorph flux, probably related to productivity changes of the organic-walled microplankton. In summary, the comparison of the palynofacies parameters with the independently derived T-R cycle framework for the Early Cretaceous mudstone-dominated succession shows an overall good correspondence with the OP/TR ratio. In contrast, application of the T/M ratio must be used with caution since other factors (e.g. productivity) may exert a significant influence on this ratio.

## Mon: 23

### Distribution patterns of some 'rhenotypic' faunal elements related to a sea-level rise during the Emsian/Eifelian transition in the eastern Rhenish Massif (Sauerland and Bergisches Land).

**Simon Felix Zoppe**

Goethe-Universität, Institut für Geowissenschaften, Altenhöferallee 1, 60438 Frankfurt am Main, Germany

Distribution patterns of marine invertebrates were analysed with regard to a documented facies shift during the Lower/Middle Devonian (= Emsian/Eifelian) transition in the eastern Rhenish Massif (Sauerland and Bergisches Land). During this time interval, the southeastern Sauerland was part of a shelf/basin transition zone at the southern margin of Laurussia (Old Red Continent), which is characterized by this major shift from neritic ('rhenotypic') to pelagic ('hercynotypic') environments (see e.g. <sup>[1][2]</sup>). This facies shift was driven by a sea-level rise transgressed from southeast direction. So far, analysed taxa include the branching tabulate coral *Coenites vermicularis* (McCoy, 1850) and the spiriferid brachiopod *Paraspirifer* (*Paraspirifer*) *cultrijugatus* (Roemer, 1844) *sensu stricto* (including form a *sensu* Solle, 1971).

In the research area, the earliest known occurrences of *Paraspirifer cultrijugatus* are restricted to the uppermost Emsian (upper Kondel substage) of the southeastern Sauerland (e.g. <sup>[1]</sup>; own collections). In the northwestern Sauerland, *Paraspirifer cultrijugatus* persisted into the lowermost Eifelian <sup>[3]</sup>. The youngest known occurrence is from the lowermost Hobräck Formation in the Bergisches Land <sup>[4]</sup>, and could be of special interest regarding to the extinction event of the 'OCA fauna' (*sensu* Struve, 1982b<sup>[5]</sup> & add. Jansen, 2016<sup>[6]</sup>) in the lowermost Eifelian. The precise stratigraphic position of the extinction of this brachiopod assemblage was approximately determined just in parts of the research area (compare with <sup>[3]</sup>).

The tabulate coral *Coenites vermicularis* is well known from the lowermost Eifelian (upper *Cultrijugatus* Beds and Hobräck Formation) in the northwestern Sauerland <sup>[3][7][8]</sup>. *Coenites vermicularis* was quite abundant and an important 'baffler' in the first biostromal reef ecosystems of this area (e.g. "Meinerzhagener Korallenkalk") <sup>[3][8]</sup>. The oldest known occurrences of *Coenites vermicularis* are from siliciclastic strata of the *Orthocrinus* Formation (uppermost Emsian) in the southeastern Sauerland (e.g. <sup>[7]</sup>; own collections).

This preliminary overview suggests that both species show westward directed patterns of colonization across the eastern 'Rhenish shelf' (today's Sauerland and Bergisches Land), which were most likely caused by a sea-level rise during the Emsian/Eifelian transition. The resulting facies changes (e.g. in sediment flux, water energy or substrate composition) possibly limited the suitable bottom conditions for both benthic organisms in the southeastern Sauerland. However, in the northwestern Sauerland and Bergisches Land both taxa still persisted into the Lower Eifelian. Further work and comparisons with other marine invertebrates would be necessary to verify this trend.

[1] Langenstrassen, F. (1972) *Göttinger Arb. Geol. Paläont.*, **12**: 1-106; [2] Goldring, R. & Langenstrassen, F. (1979) *Spec. Pap. Palaeont.*, **23**: 81-97; [3] Avlar, H., & May, A. (1997) *Coral Res. Bull.*, **5**: 103-119; [4] Solle, G. (1971) *Abh. hess. L.-Amt Bodenforsch.*, **59**: 1-163; [5] Struve, W. (1982b) *Cour. Forsch.-Inst. Senckenberg*, **55**: 401-432; [6] Jansen, U. (2016) *Spec. Pap.*, **423**: 45-122; [7] May, A. (2003) *Geol. Paläont. Westf.*, **60**: 47-79; [8] Ernst, A., May, A., & Marks, S. (2012) *Facies*, **58**: 727-758.

## 4g): Advances in geochronology from modern to deep time

Tuesday, 24/Sep/2019: 8:30am - 10:00am

Session Chair: Jacek Raddatz (Goethe Universität Frankfurt)

Session Chair: Ulf Linnemann (Senckenberg Naturhistorische Sammlungen Dresden)

Location: H2

### Session Abstract

To fully understand the complexity of Earth History relies on precise and accurate chronologies. With recent advances in analytical geochemistry there are more and more possibilities to answer unsolved questions and target new aims, especially in geochronology. This session aims to bring together contributions from various fields in geosciences dealing with new analytical methods, new isotope systems, new archives as well as other improvements in geochronological techniques. We especially encourage contribution that combine different approaches from modern to deep time and improve existent techniques.

### Lecture Presentations

8:30am - 9:00am *Session Keynote*

#### High-resolution calibration of Earth system processes with precise and accurate U-Pb geochronology

Urs Schaltegger

*University of Geneva, Switzerland*

High-precision U-Pb geochronology went through substantial development during the last 15 years. Increased precision, accuracy, within-lab repeatability and inter-lab reproducibility enabled geoscientists to address an entirely new set of scientific questions that were inaccessible before. Assuring highest precision and accuracy requests (i) knowledge of the sample material (mostly zircon) in terms of its crystallization history and state of its crystal lattice; (ii) most precise and reproducible application of sample preparation techniques for zircon, called “chemical abrasion”, to mitigate radioactive decay damage and associated partial loss of radiogenic daughter products; (iii) reproducible procedures of element separation, isotope dilution and mass spectrometry, constantly verified through analysis of synthetic and natural reference materials; and (iv) perfect knowledge of random and systematic errors and their correct propagation into the final result. Metrology and correct statistics are foundations of precise geochronology and are very often decisive about whether we can claim absence or existence of correlation between processes.

The Earth system has undergone uncountable dramatic overturns within the geo-, hydro, atmo- and biosphere in the last ca. 3 billion years. Depending on our temporal resolution, we call them “events” (in deep time, with a duration we cannot resolve), or “transitions” (in the Phanerozoic, where we can resolve process durations through geochronology). I will present in the talk examples that show how high-precision geochronology cannot only reconstruct durations and process rates, but allows distinction between mechanisms:

(i) we may infer causal coupling of events, such as eruption of large igneous provinces producing global environmental change and causing biotic crisis, through high-precision temporal coincidence;

(ii) we can demonstrate that eccentricity-forced climate cycling is at the origin of the depositional mega-cycles of Early Proterozoic Banded Iron Formations;

(iii) we reconstruct the durations of carbon isotope excursions during the Early Triassic post-extinction biotic recovery, and demonstrate that a negative carbon isotope excursion of 100'000s of years duration points to alteration-erosion cycles of LIP flood basalts, rather than to direct triggering of climate change from volatile injection into the atmosphere, thus, in other words, distinguish between triggers and feedbacks.

I acknowledge years-long collaboration with the members of my research group at University of Geneva.

9:00am - 9:15am

### Challenges for the accuracy of U-Th systematics in marine carbonate archives of extreme environments: identifying and overcoming limitations of early diagenesis

**Volker Liebetrau<sup>1</sup>, Stefan Krause<sup>1</sup>, Anton Eisenhauer<sup>1</sup>, Tyler Jay Goepfert<sup>1</sup>, Rashid Rashid<sup>2</sup>, Jacek Raddatz<sup>3</sup>, Hana Jurikova<sup>4</sup>, Nicolaas Glock<sup>1</sup>, Sebastian Büsse<sup>5</sup>, Stanislav Gorb<sup>5</sup>**

<sup>1</sup>GEOMAR Helmholtz Centre for Ocean Research Kiel, Germany; <sup>2</sup>Geological Institute, Zanzibar University, Tanzania;

<sup>3</sup>Institute of Geosciences, Sedimentology and Georesources, Goethe University Frankfurt, Germany; <sup>4</sup>German Research Centre for Geosciences - Helmholtz Centre Potsdam, Germany; <sup>5</sup>Zoological Institute, Functional Morphology and Biomechanics, Christian-Albrechts-University Kiel, Germany

Reliable proxy records of extreme environments receive increasing attention in order to identify the full range of environmental and climate changes within different time intervals of the past. Furthermore, in case of biogenic archives they may provide realistic estimates of species dependent resilience potential and adaptability to extreme conditions.

Marine carbonates represent important paleo-proxy archives as environmental conditions are recorded geochemically during their formation. Combined with U/Th age dating climatic variability spanning geological time scales can be determined. The accuracy of U-Th based proxy approaches is largely dependent on the degree of diagenesis experienced. Due to elevated concentrations of U and Sr and other trace metals, when compared to calcitic species, especially aragonitic coral and shell structures provide sensitive and for precise U-Th geochronology suitable recorder.

Nevertheless, often they need to be considered as potential open systems with regard to high susceptibility for alterations in uranium and thorium isotope systematics by secondary precipitation, dissolution, recrystallization, uptake and exchange processes.

Although the analytical techniques developed impressively to extreme precisions and sample throughput efficiencies limitations introduced by diagenesis are still of major impact on the accuracy and robustness of geochronological records.

General improvements are reached by combining micro-CT pre-investigation with micro-sampling techniques in order to identify and subsample pristine remains of the primary skeleton.

This approach is supported by electron micro probe, scanning electron microscopy and epi-fluorescence microscopy to identify skeleton parts characterized by secondary mineral precipitation and organic components, indicating mineral alteration by the activity of endolithic organisms.

Applied on recent to subrecent coral micro atolls and fossil *Tridacna* spp. from Zanzibar (Tanzania), this study reveals small-scale heterogeneities in U-Th systematics of different time scales.

In addition the impact of potential variations of initial U-Th isotope uptake systematics in extreme environments including cold water coral habitats will be discussed with regard to natural limitations on theoretical and analytical precision.

Besides the aspect of long-term diagenesis and secondary mineralization this study investigates the impact of biologically-driven geochemical carbonate alteration during and shortly after corals live span.

9:15am - 9:30am

### Advances in rutile petrochronology

**Ellen Kooijman<sup>1</sup>, Melanie Schmitt<sup>1</sup>, Matthijs Arjen Smit<sup>2</sup>**

<sup>1</sup>Swedish Museum of Natural History, Stockholm, Sweden; <sup>2</sup>University of British Columbia, Vancouver, Canada

Rutile petrochronology has become an increasingly significant tool for deciphering the timing and conditions of petrological processes. Rutile provides a reliable single-mineral thermometer – the Zr-in-rutile thermometer – capable of retaining temperature information during ultra-high temperature metamorphism. The mineral is a main host of HFSE, including Zr, Hf, Nb and Ta, concentrations of which can be diagnostic of petrological history and sedimentary provenance. Most importantly, rutile exhibits high U/Pb and enables

U-Pb thermochronology in the intermediate temperature range through laser ablation inductively coupled plasma mass spectrometry (LA-ICPMS).

The spatial resolution of rutile U-Pb dating by LA-ICPMS has so far been limited to c. 35  $\mu\text{m}$ , owing mostly to the amount of rutile needed for analysis and the use of circular ablation spots. Modern laser ablation systems enable the analysis of rectangular spots, for example to target narrow compositional zones in samples. This approach could significantly enhance radial spatial resolution. Nevertheless, the approach has so far not yet been tested for rutile U-Pb micro-analysis. Here we used this feature as part of a new approach that integrates in situ U-Pb thermochronology by LA-multi-collector-ICPMS with diffusion zoning analysis to determine thermal histories from single rutile grains. The optimal ablation spot dimension of 11x55  $\mu\text{m}$  allowed much-improved radial spatial resolution, while maintaining the  $\sim 2\%$  (2 s.d.) uncertainty that rutile U-Pb dating by LA-ICPMS is capable of.

The new analytical approach was applied to rutile grains extracted from: 1) a slowly cooled granulite from the Saglek Block (SB), Nain Province, Labrador, Canada, and 2) a tectonically exhumed eclogite from the UHP zone of the Western Gneiss Complex (WGC), Norway. The materials revealed age gradients over 140 Ma (SB) and 30 Ma (WGC) over a distance of 40-50  $\mu\text{m}$  (SB) and 200  $\mu\text{m}$  (WGC), both of which could be resolved at a precision of 1.5-2.0 % (2 s.d.) and spatial resolution of  $\sim 14 \mu\text{m}$ . Diffusion zoning length was used with well-established Pb diffusion parameters [1] to determine the thermal histories of both terranes over a temperature range of up to  $\sim 300 \text{ }^\circ\text{C}$ .

The data demonstrate that rutile U-Pb micro-analysis yields reliable and precise temperature and age information that can be combined to resolve full thermal histories from single crystals. This novel approach to the toolbox of rutile petrochronology has great potential for research in lithosphere dynamics and tectonics.

[1] Cherniak (2000) Contrib. Mineral. Petrol. 139. 198-207.

**9:30am - 9:45am**

### **Towards in-situ U-Pb dating of sulphates**

**Aratz Beranoaguirre<sup>1,2,3</sup>, Axel Gerdes<sup>1,2</sup>, Richard Albert<sup>1,2</sup>, Leo J. Millonig<sup>1,2</sup>**

<sup>1</sup>FIERCE (Frankfurt Isotope and Element Research Centre); <sup>2</sup>Goethe-Universität Frankfurt; <sup>3</sup>University of the Basque Country UPV/EHU, Leioa, Spain

Sulphates such as anhydrite or gypsum occur in numerous environments and can provide information about, e.g., the depositional history of sedimentary basins. However, sulphates are prone to (de-) hydration reactions. Therefore it is often difficult to ascertain, if a sulphate is primary or secondary in origin. Direct dating of sulphates would provide the means to distinguish between primary crystallization and secondary fluid circulation events.

Taking advantage of the U-Pb small scale isochron (SSI) method, recently developed at Goethe-University Frankfurt for the in-situ dating of carbonates, we applied this approach to sulphates. In-situ analyses were performed using an Excimer laser coupled to an Element2-XR SF-ICPMS. This method is based on the fact that sulphates contain low but variable amounts of U and  $\mu$  ( $^{238}\text{U}/^{204}\text{Pb}$ ). Therefore, several analyses (10 to 50) will yield variable U/Pb ratios and define an isochron in the  $^{207}\text{Pb}/^{206}\text{Pb}$  vs  $^{238}\text{U}/^{206}\text{Pb}$  space. The age is given by the lower intercept of this isochrons with the Concordia curve and its intercept with the y-axis is interpreted to be the initial Pb isotope composition.

The feasibility of laser ablation based method requires reference material of known age that behaves similar to the sulphates in order to correct the laser induced fractionation and instrumental drift. Due to a lack of appropriate reference material we used carbonates as matrix-matched reference material. Preliminary results indicate that the analysed anhydrite and gypsum contain a significant proportion of common-Pb, but the dispersion of the analysis is sufficient to obtain U-Pb ages with a precision of 5-10%.

Our approach demonstrates that the SSI technique could successfully be applied to the in-situ U-Pb dating of (some) sulphates. Nevertheless, more work is needed to standardise the protocol, which will require the analysis of samples with known age among other tasks.

9:45am - 10:00am

### In-situ U-Pb garnet dating. Strengths and weaknesses

**Richard Albert, Leo J. Millonig, Aratz Beranoaguirre, Axel Gerdes**

*FIERCE, Frankfurt Isotope and Element Research Center. Goethe Universität, Germany*

Due to its stability over a wide range of pressure-temperature conditions and bulk rock compositions, garnet is the most widely used major phase for interpreting the genesis of many igneous and metamorphic rocks via geothermobarometry. For these studies time is a very important variable, which has been addressed using garnet as a geochronometer, with the Sm-Nd, Lu-Hf and, rarely, U-Pb dissolution methods.

*In-situ* dating techniques, which provide texturally constrained ages, have only recently been applied to garnet. Skarn garnet (grossular to andradite compositions, “grandite”), has high U concentrations (c. 5 to 40 ppm) and shows to be a promising target for U-Pb dating [1, 2, 3, 4]. Garnet from igneous rocks like carbonatites and alkaline complexes (calcic garnets, schorlomite-andradite) is also promising [5]. Garnet from metamorphic lithologies, such as metasedimentary or metabasic rocks, have proven to be much more challenging [6] due to high amount of inclusions and low U concentrations (< 1 ppm).

One of the main requirements for laser ablation mass spectrometry is the use of matrix matched standardization, due to the element fractionations observed when sample and reference materials are not matrix matched. This requirement is a major issue, due to the huge compositional variation within the garnet group and the scarcity of garnet reference materials available to the scientific community.

This communication will show a wide range of data on several garnet compositions and analytical setups to explore the potential, feasibility and limitations of this emerging *in-situ* U-Pb garnet dating technique.

[1] Seman *et al.* (2017) *Chem. Geol.* **460**, 106-116; [2] Wafforn *et al.* (2018) *Econ. Geol.* **113**, 769-778; [3] Fu *et al.* (2018) *Minerals* **8**, 128; [4] Burisch *et al.* (2019) *Earth and Planetary Sci. Letters.* **519**, 165-170; [5] Yang *et al.* (2018) *J. Anal. At. Spectrom.* **33**, 231; [6] Millonig *et al.* (2019) Submitted.

## Poster Presentations

Tue: 9

### Radiation damage in zircon - A Raman multi-band approach

**Birk Härtel, Raymond Jonckheere, Lothar Ratschbacher**

*TU Bergakademie Freiberg, Germany*

Raman spectroscopic investigations of zircon have received attention in geochronology concerning radiation damage. Especially the effects of radiation-damage on the closure temperatures of the fission-track and (U-Th)/He-dating methods have been investigated. The total radiation-damage density of a zircon grain reflects two competing processes: The accumulation of damage due to the radioactive decay of U and Th substituted into the zircon structure, and the annealing caused by reconstitution of the lattice at elevated temperatures. Although most studies have focussed on the broadening and shift of the  $\nu_3(\text{SiO}_4)$  internal stretching band, other Raman bands can be used equally for the estimation of the radiation-damage density. We measured the positions and widths of the external rotation band, the  $\nu_3$  band, and the  $\nu_2(\text{SiO}_4)$  internal bending band at approx. 356, 1008, and 439  $\text{cm}^{-1}$ , respectively. We measured the spectra of 300 zircon grains from igneous rocks from Saxony using a TriVista spectrometer (Princeton Instruments) with a 633 nm laser for excitation. We chose the spectral range between 150 and 1100  $\text{cm}^{-1}$  at a spectral resolution of approx. 0.8  $\text{cm}^{-1}$ . A principal component analysis of the positions and widths of these Raman bands shows that the first principal component positively correlates with the  $\nu_3$  and external peak positions, whereas it exhibits a strong negative correlation with all three peak widths. Based on our knowledge on peak broadening, it can thus be interpreted as a measure of crystallinity as opposed to radiation damage. On the other hand, the  $\nu_2$  position change is almost parallel to the second principal component and shows different trends relating the band width and position among the studied samples. The weak dependence of the  $\nu_2$  position on radiation damage makes it less susceptible to peak

asymmetry caused by a gradient of band positions. Therefore, its width can be used to check for band position gradients in samples in which the other bands are broad and difficult to fit. Furthermore, the correlation of the band widths suggests that several bands may be combined for estimating the damage density. It is therefore advantageous to calibrate the widths of the three bands against the radiation dose, calculated from the age and actinide contents in non-annealed geologic samples. This calibration can enable us to calculate damage densities in a more robust way by checking for the concordance of dose with respect to several Raman bands.

**Tue: 10**

### **Insights into Fe-duricrust evolution in French Guiana using (U-Th-Sm)/He dating of supergene iron oxides and oxyhydroxides**

**Beatrix Heller<sup>1,2</sup>, Silvana Bressan-Riffel<sup>3</sup>, Cécile Gautheron<sup>1</sup>, Thierry Allard<sup>2</sup>, Guillaume Morin<sup>2</sup>, Jean-Yves Roig<sup>4</sup>, Renaud Coueffe<sup>4</sup>**

<sup>1</sup>GEOPS, Université Paris Sud / Paris Saclay, France; <sup>2</sup>IMPMC, Sorbonne Université, France; <sup>3</sup>Institute of Geosciences, Federal University of Rio Grande do Sul, Brazil; <sup>4</sup>BRGM (French Geological Survey), France

Laterites are deep weathered soils, which form under tropical climate conditions and currently cover about 1/3 of the Earth's continental surface. Despite their widespread occurrence and their importance as continental interface, little is known about the timing of their formation and evolution, as responses to paleoclimatic cycles. This study focuses on the tectonically stable Amazon craton, where laterites could have formed during the entire Cenozoic era. Although various models exist for the landscape evolution in this area, the ages of the lateritic formation are poorly documented. Laterites often contain a duricrust, which is composed mainly of hematite and goethite. By dating these mineral phases using the (U-Th-Sm)/He method, this project aims to better understand the timing of duricrust formation and the relation with paleoclimatic events.

The samples of this study originate from Northeastern French Guiana, where lateritic Fe-duricrusts developed on Paleoproterozoic ultramafic rocks. Duricrust samples were sawed into slices and individual generations of iron (oxyhydr)oxides were separated by micro-drilling. The material was gently crushed in a steel mortar, cleaned in ultrasonic bath and individual grains were selected by handpicking. Several distinct facies in the duricrusts were examined by SEM and XRD in order to determine their structure, chemistry and the hematite/goethite ratio. The latter was calculated using the Rietveld method.

The duricrust samples show a wide range of different textures, are often heterogeneous and may contain up to 5 different generations of iron (oxyhydr)oxides. Preliminary ages indicate formation of iron (oxyhydr)oxides beginning in the late Paleogene and continuing during the entire Neogene. While the older ages correspond mainly to hematite-rich generations, the younger ones are dominantly composed of goethite. The U, Th and Sm contents are generally low and do not seem to affect the ages.

**Tue: 11**

### **U-Th-total Pb geochronology of uraninite and its secondary phases (Evje-Iveland Pegmatite Field, Norway)**

**Deniz Öz<sup>1</sup>, Frank Tomaschek<sup>1</sup>, Ronald Werner<sup>2</sup>, Thorsten Geisler<sup>1</sup>**

<sup>1</sup>Universität Bonn, Germany; <sup>2</sup>Evje og Hornnes geomuseum Fennefoss, Postboks 24, N-4748 Rysstad, Norway

The late Svenconorwegian Evje-Iveland Pegmatite Field, southern Norway, went through a complex geological evolution. This project aims to unravel the timing of different fluid interactions by U-Th-total Pb chemical dating of uraninite and its secondary phases.

The investigated sample from the former U-mine Einkerilen consists of an 1.2 mm large uraninite crystal along with albite, chlorite, muscovite, and magnetite. Petrological observations strongly indicate the dissolution and/or alteration of uraninite and the mobilization and oxidation of uranium ( $U^{4+} \rightarrow U^{6+}$ ) as a result of fluid flow along fractures and grain boundaries. The alteration/oxidation of uraninite itself is evident from BSE images and occurred along internal cracks. In addition, aggregates of uranophane,  $Ca(UO_2)_2SiO_3(OH)_2 \cdot 5H_2O$ , and veins of its polymorph uranophane- $\beta$  were identified by Raman spectroscopy and EPMA analyses.

925 quantitative EPMA analyses were collected on uraninite and uranyl silicate phases. The oldest chemical uraninite ages form a distinct age group with an error-weighted mean of  $989 \pm 19$  Ma. The main uraninite population yields a U-Th-total Pb model age of  $912 \pm 3$  Ma that is well in the range of radiometric ages reported so far for the crystallization of minerals of the Evje-lveland pegmatites. In contrast, one corner of the crystal gave significantly younger ages, which range between  $468 \pm 14$  and  $620 \pm 16$  Ma. The current interpretation of the results is that the magmatic uraninite crystallized at  $989 \pm 19$  Ma. Accordingly, the host pegmatite melt could well be a differentiation product of the 982 Ma old Høvringsvatnet granite. At  $912 \pm 3$  Ma, the pegmatite was infiltrated by U-rich solutions which caused a pseudomorphic replacement of the magmatic uraninite, but left over relic magmatic domains. Later, this new uraninite was also hydrothermally altered, causing partial oxidation.

The U-Th-Pb data of two of the three analysed uranophane- $\beta$  veins plot on a single, well defined PbO-UO<sub>2</sub>\* isochron, yielding an average initial Pb content of  $8123 \pm 223$  ppm and a chemical age of  $135 \pm 3$  Ma. In fact, an even younger fluid event is indicated by the analysed uranophane aggregate that gives a well-defined PbO-UO<sub>2</sub>\* isochron age of  $34 \pm 1$  Ma, when assuming negligible common Pb contents in uranophane. These results suggest two U mobilisation events that were caused by hydrothermal fluids of different chemistry that may have been mobilised by faulting related to tectonic activity of the North Sea rift system.

**Tue: 12**

### **Aqueous alteration events in silicified wood from Escalante, Utah, USA**

**Frank Tomaschek<sup>1</sup>, Moritz Liesegang<sup>2</sup>, Carole T. Gee<sup>2</sup>, Alicia Krick<sup>1</sup>, Markus Lagos<sup>1</sup>, Paul Guagliardo<sup>3</sup>, Thorsten Geisler<sup>1</sup>**

<sup>1</sup>Institut für Geowissenschaften, Bereich Endogene Prozesse, Universität Bonn, Poppelsdorfer Schloss, 53115 Bonn, Germany; <sup>2</sup>Institut für Geowissenschaften, Bereich Paläontologie, Universität Bonn, Nußallee 8, 53115 Bonn, Germany; <sup>3</sup>Centre for Microscopy, Characterisation and Analysis, University of Western Australia, 35 Stirling Highway, Crawley, WA 6009, Australia

The U-Pb system of hydrous silica phases potentially provides a means to constrain the timing of aqueous alteration events in the sedimentary realm. To test this proposition, we analyzed silicified wood from the Escalante Petrified Forest State Park in southern Utah, USA. Our analytical approach combines optical microscopy, cathodoluminescence and back-scattered electron imaging, electron microprobe analysis, NanoSIMS trace element mapping, structural characterization of silica phases using hyperspectral Raman imaging, and isotopic U-Pb analysis by LA-ICP-MS.

The Escalante Petrified Forest State Park features silicified wood in fluvial gravel and sandstones of the Brushy Basin Member of the Upper Jurassic Morrison Formation. On the regional scale, Lower Cretaceous beds of the Dakota Formation rest with an erosional unconformity on the Jurassic strata. The analyzed, several dm-sized chunk of permineralized conifer wood shows a patchy and fragmentary preservation of the original cellular structure. A textural sequence of discrete chalcedony generations was identified in wood domains and several generations of cross-cutting mm-sized veins.

On the  $\mu\text{m}$ -scale, chalcedony in cell walls and lumina is distinct in cathodoluminescence response, trace element content, and structure. Notably, chalcedony in cell walls is low in aluminium and moganite content, compared to chalcedony in the lumina. Detailed trace element maps on the nano-scale reveal that cell walls consist of relict islands (Al-poor, Na-rich), that are crosscut by radial dissolution channels. These channels have the same trace element signature as the adjacent lumina (Al-rich, Na-poor) and correlate chemically with chalcedony of a texturally early vein generation. U-Pb isotopic analyses of chalcedony from wood and vein domains define a uniform age group of  $139 \pm 4$  Ma. This age postdates the accepted chronostratigraphic age of the Brushy Basin Member (152-150 Ma), and may therefore be unrelated to the initial wood mineralization process. Apparently, the U-Pb system of the wood domains was reset during the formation of the texturally early veins. In addition, vein centers with a texturally later chalcedony generation yield an age of  $101 \pm 3$  Ma. In conclusion, U-Pb data of silicified wood from Escalante records a protracted sequence of chalcedony-forming episodes. Domains of silicified wood were penetratively modified in a discrete hydrologic event during the Lower Cretaceous, which correlates with the timing of the regional basin inversion.

## 5) Magmatic systems and experimental petrology

### 5a) Volatiles in the Earth's Mantle – Elemental Budgets & Cycles

Monday, 23/Sep/2019: 9:00am - 1:00pm

Session Chair: Tobias Grützner (Universität Münster)

Session Chair: Yannick Bussweiler (University of Münster)

Session Chair: Carla Tiraboschi (WWU Münster)

Location: H4

#### Session Abstract

Volatiles (e.g., H, C, N, S, halogens, noble gases) play an important role in petrological, geochemical, and geophysical processes in the Earth's mantle. Their presence can affect phase stabilities and initiate weakening and melting, with the potential to produce significant geophysical anomalies. Moreover, volatiles are involved in metasomatic processes, the products of which can be studied directly in mantle xenoliths. This session aims to attract researchers studying any aspect of the Earth's deep volatile budget and cycle. We invite experimental and theoretical geochemists, isotope geochemists, mineralogists, and geophysicists to cover this topic from different perspectives. Potential specific topics include: 1) transport and recycling of volatiles in subduction zones, 2) incorporation and storage of volatiles in (nominally anhydrous) mantle minerals, 3) distribution and budget of volatiles in the Earth's mantle, 4) effect of volatiles on petrological processes (e.g., melting), geochemical processes (e.g., element mobility, isotope fractionation, oxidation states) and geophysical properties (e.g., rheology, conductivity).

#### Lecture Presentations

9:45am - 10:00am

#### Identifying the mineralogy of a metasomatised mantle source by halogen partitioning experiments: A new approach

**Stamatis Flemetakis, Stephan Klemme, Arno Rohrbach, Andreas Stracke, Jasper Berndt**

*WWU Münster, Germany*

During the last years there is a growing interest into the behavior of halogens during magmatic processes to better constrain the global geochemical cycling and abundance of the elements in the silicate Earth [1-12].

Amphiboles and phlogopitic-mica often contain weight percent of F (and less Cl) [13-15], thus making these minerals the prime carriers of halogens inside the mantle. We conducted amphibole-melt and phlogopite-melt partitioning experiments in complex chemical systems i.e.  $\text{Na}_2\text{O-K}_2\text{O-CaO-MgO-Al}_2\text{O}_3\text{-SiO}_2$  and  $\text{Na}_2\text{O-FeO-CaO-K}_2\text{O-MgO-Al}_2\text{O}_3\text{-SiO}_2\text{-TiO}_2$ , for all four halogens (F, Cl, Br, I) at 1.4 GPa and temperatures between 1015°C and 1300°C. Halogen concentrations in the experimental products were measured by EPMA, using an analytical protocol following [16-17], and new in-house glass standards for halogens [18]. We obtained new mineral/melt halogen partition coefficients ( $D^{\text{min/melt}}$ ) for amphibole, phlogopite and clinopyroxene. These data show that with low amounts of Ti in amphibole (< 0.32 a.p.f.u.), F is becoming incompatible ( $D_F \sim 0.6$ ). [19].

The experimentally derived D values were used to calculate the F/Cl and F/Nd values of melts derived from a metasomatised mantle for different amounts of phlogopite and amphibole present in the source. We compared our calculated ratios to measured ratios of melt inclusions from settings, like arcs, that these phases are most likely present at the mantle source during melting. Our calculated range of F/Cl and F/Nd agrees with published data for such melts indicating that, under certain constraints, the F/Cl and F/Nd ratio of melt inclusions can be used as a proxy for the relative amount of amphibole and phlogopite of a metasomatised mantle source.

[1] Hauri et al., 2006; [2] Beyer et al., 2012; [3] Beyer et al., 2016; [4] Bernini et al., 2013; [5] Fabbrizio et al., 2013a; [6] Dalou et al., 2012; [7] Dalou et al., 2014; [8] Joachim et al., 2015; [9] Joachim et al., 2017; [10] Foley et al., 1986; [11] Foley, 1991; [12] Grützner et al., 2017; [13] Edgar et al., 1994; [14] Moine et al., 2000; [15] Liu et al., 2011; [16] Zhang et al., 2015; [17] Zhang et al., 2017; [18] Flietakis et al., 2019; in prep. [19] Flietakis et al., 2019; submitted.

**10:00am - 10:15am**

### **Initial CO<sub>2</sub> content in parental arc magmas estimated using micro-Raman spectroscopy and mass-balance calculations: a case study of Karymsky volcano (Kamchatka, Russia)**

**Nikita Mironov<sup>1</sup>, Maxim Portnyagin<sup>2</sup>, Daria Tobelko<sup>1</sup>, Sergey Smirnov<sup>3</sup>, Stepan Krasheninnikov<sup>1</sup>, Andrey Gurenko<sup>4</sup>**

<sup>1</sup>Vernadsky Institute (GEOKHI RAS), Russian Federation; <sup>2</sup>GEOMAR, 24148 Kiel, Germany; <sup>3</sup>IGM SB RAS, 630090, Novosibirsk, Russia; <sup>4</sup>CRPG, 54501 Vandoeuvre-lès-Nancy, France

We present new data on CO<sub>2</sub> content in melt inclusions (MIs) from Karymsky volcano estimated using micro-Raman spectroscopic data on CO<sub>2</sub> density of fluid bubbles and volume proportions of glass and fluid inside inclusions (e.g. Moore et al., AmMiner 2015; JVGR 2018). This study was focused on the ways of simple and more precise quantification of 3-D MIs size and estimation of the initial CO<sub>2</sub> content in the most primitive melts.

Sixteen MIs studied in olivine Fo77-89 were partially crystallized. Before analysis, they were reheated during 5 min at 1170 °C and quenched. After quenching they consisted of glass and bubbles. The bubbles were measured for CO<sub>2</sub> density in IGM SB RAS, Novosibirsk, using Horiba LabRam HR800 (532 nm, 1800g). The measured CO<sub>2</sub> density ranges from 0.03 to 0.21 g/cm<sup>3</sup>. Inclusion thickness, which is usually not reported in MI studies, was quantified in two ways. First, it was measured with built-in microscope micrometer and further corrected for the refractory index of olivine of 1.68 (average for Ng-Np in olivine Fo80-90). Second, the 3-D size was measured using two orthogonal sections of olivine grains. Both methods yielded comparable results for the same inclusions. The maximum difference for the estimated relative volume of fluid bubble did not exceed 0.8%. The bubbles occupy from 3 to 5.7%, not exceeding critical value of ~6-8% (e.g. Aster et al., JVGR, 2016) suggested for originally homogeneous MIs.

Minimum concentration of bulk MIs CO<sub>2</sub>, accounting only gas bubbles was calculated by mass-balance approach. These concentrations range from 0.05 to 0.45 wt.% and likely represent variably degassed melts originated from the initial primitive melts with CO<sub>2</sub> ≥ 0.45 wt.% (Mironov et al., RusGeolGeoph, 2019). Noticeably, using less precise MIs volume estimates (width=thickness) is not accurate in many cases and results in unexpected under- or overestimated initial CO<sub>2</sub> content.

SIMS analyses of CO<sub>2</sub>, H<sub>2</sub>O, D/H, S, Cl in MIs glasses are currently in progress. The data will be used to quantify the total amount of CO<sub>2</sub> in MIs and to evaluate possible H<sub>2</sub>O loss from inclusions, and they will be shown at the meeting to discuss the depth where parental arc magmas start to crystallize and the sources of CO<sub>2</sub> in arc magmas.

This work has been supported by Russian Foundation for Basic Research grant 19-05-00934 and by Europlanet 2020 RI that has received funding from the European Union's Horizon 2020 research and innovation programme under grant agreement No 654208.

**10:15am - 10:30am**

### **Dissolution of graphite in high-pressure aqueous fluids: the roles of crystallinity and of coexisting silicates and carbonates**

**Simone Tumiatì**

*University of Milan, Italy*

Organic matter, showing variable degrees of crystallinity and thus of graphitization, is an important source of carbon in subducted sediments, as demonstrated by isotopic signature of deep and ultra-deep diamonds and volcanic emissions in arc settings. Estimates of dissolved CO<sub>2</sub> in subduction-zone fluids are based mainly on

thermodynamic models, relying on a very sparse experimental data base. We present experimental data on the interaction of aqueous fluids with graphitic carbon in relatively complex systems diverging from the ideal C-O-H model. The redox state of the experiments was always constrained, using double capsules and either fayalite-magnetite-quartz (FMQ) or nickel-nickel oxide (NNO) buffers. Experiments have been performed at pressures up to 3 GPa and temperatures up to 800°C to retrieve the dissolution susceptibility of elemental carbon in aqueous fluids: 1) in the COH system, using amorphous carbon instead of crystalline carbon; 2) in silicate-bearing systems, investigating the systems  $\text{SiO}_2$ -COH (graphite + quartz/coesite) and  $\text{MgO-SiO}_2$ -COH (graphite + forsterite and enstatite); 3) in carbonate-bearing systems, investigating the  $\text{CaCO}_3$ -COH (graphite + aragonite) and the  $\text{CaCO}_3+\text{SiO}_2$ -COH (graphite + aragonite + coesite) systems.

At 1 GPa and 800°C, carbon dioxide produced by oxidation of amorphous carbon shows higher fluid concentrations (+16–19 mol%) compared to crystalline graphite, meaning that amorphous carbon is more prone to oxidation. In contrast, fluids interacting with amorphous carbon at the higher pressure of 3 GPa show only a limited increase in  $\text{CO}_2$  ( $f\text{H}_2^{\text{NNO}}$ ) or even a lower  $\text{CO}_2$  content ( $f\text{H}_2^{\text{FMQ}}$ ) with respect to fluids interacting with crystalline graphite. At the same P–T conditions, the  $\text{CO}_2$  content of fluids interacting with crystalline graphite and silicates exceeds the amounts measured in the pure COH system by up to 30 mol%, as a consequence of a decrease in water activity probably associated with the formation of organic complexes containing Si–O–C and Si–O–Mg bonds. On the other side, the dissolution susceptibility of graphite seems to be unaffected by the presence of calcite at 3 GPa, 700°C. The contemporaneous presence of calcite and quartz, however, induces an increase of the dissolved graphite, confirming the important role of silica in enhancing the solubility of graphite.

The interaction of deep aqueous fluids with silicates and with “disordered” graphite are novel mechanisms for controlling the composition of subduction COH fluids, promoting the deep  $\text{CO}_2$  transfer from the slab–mantle interface to the overlying mantle wedge.

### 11:15am - 11:45am Session Keynote

#### Redox control on nitrogen isotope fractionation during planetary core formation

Celia Dalou<sup>1</sup>, Evelyn Füri<sup>1</sup>, Cécile Deligny<sup>1</sup>, Laurette Piani<sup>1</sup>, Marie-Camille Caumon<sup>2</sup>, Mickael Laumonier<sup>3</sup>, Julien Boulliung<sup>1</sup>, Mattias Edén<sup>4</sup>

<sup>1</sup>Centre de Recherches Pétrographiques et Géochimiques, CNRS-UL, France; <sup>2</sup>GeoRessources, Université de Lorraine, CNRS, France; <sup>3</sup>Université Clermont Auvergne, CNRS, IRD, OPGC, France; <sup>4</sup>Physical Chemistry Division, Stockholm University, Sweden

The origin and evolution of Earth’s nitrogen is often discussed by comparing the large variation of N isotopic compositions among Earth’s building blocks (chondrites) to the signatures of various terrestrial reservoirs. Here, we demonstrate that planetary differentiation processes, such as core formation, may have significantly modified the N isotopic composition of the proto-Earth.

We experimentally determined N isotopic fractionation during metal-silicate partitioning (i.e., planetary core formation) over a large range of oxygen fugacities ( $\text{DIW} -3.1 < \log f\text{O}_2 < \text{DIW} -0.5$ ) at 1 GPa and 1400 °C using a piston cylinder apparatus. We developed an *in-situ* analytical method to measure the N elemental and isotopic compositions of experimental run products composed of Fe-C-N metal alloys and basaltic melts by ion probe. Our results show substantial N isotopic fractionations between metal alloys and silicate glasses, i.e., from  $-257 \pm 24\%$  to  $-49 \pm 1\%$ , over three log units of  $f\text{O}_2$ . These large fractionations under reduced conditions can be explained by the large difference between N bonding in metal alloys (Fe-N) and in silicate glasses (as molecular  $\text{N}_2$  and NH complexes). We show that the  $\text{d}^{15}\text{N}$  value of the silicate mantle could have increased by  $\sim 20\%$  during core formation due to N segregation into the core as the  $f\text{O}_2$  of the magma ocean increased. This study shows that the magnitude of N isotopic fractionation varies significantly as a function of the redox history of the early Earth. Therefore, distinct N isotopic ratios among Earth’s reservoirs or between planetary bodies may reflect different planetary evolution processes as opposed to different N sources.

11:45am - 12:00pm

## The role of C-O-H fluids on partial melting of eclogite and lherzolite under reducing conditions

Zairong Liu<sup>1,2</sup>, Arno Rohrbach<sup>1</sup>, Stephan Klemme<sup>1</sup>, Stephen Foley<sup>2</sup>, Jasper Berndt<sup>1</sup>

<sup>1</sup>Münster University, Germany; <sup>2</sup>Macquarie University, Australia

C-O-H fluids are the most reactive fluids that play a key role in mantle metasomatism, in the continuous degassing and the magmatic processes on Earth. They are well known to cause partial melting of eclogite and peridotite at much lower temperatures than in dry conditions, and thus causing heterogeneities in the Earth's mantle<sup>[1]</sup>. However, under reducing conditions, in which case the C-O-H fluids consist mostly of H<sub>2</sub>O + CH<sub>4</sub><sup>[2,3]</sup>, the effect of the C-O-H fluids on the melting process of eclogite and lherzolite is not well constrained. So far, there is no direct measurement of melt compositions with presence of C-O-H fluid under reducing condition. We performed experiments with eclogite and lherzolite at 2 GPa and 6 GPa, 900–1500 °C at different redox conditions. Under oxidizing conditions, both starting compositions contained about 5 wt.% H<sub>2</sub>O; while at reducing conditions the identical compositions contained 5 wt.% H<sub>2</sub>O and CH<sub>4</sub>. We applied double capsule techniques at reducing conditions to control oxygen fugacity.

Our experiments show that:

- (1) The difference in  $f_{O_2}$  between buffer of outer capsule and sample of inner capsule was less than one log, which means that controlling  $f_{O_2}$  at reducing conditions was successful.
- (2) Under reducing conditions, both the solidi of eclogite and lherzolite with C-O-H fluids are subparallel to the anhydrous solidi but about 200 °C lower, and 100 °C higher than those of oxidizing conditions.
- (3) The mineralogy of eclogite and lherzolite depends on  $f_{O_2}$ . A) Higher  $f_{O_2}$  and H<sub>2</sub>O activity leads to the presence of amphibole in the eclogite. B) At reducing conditions, clinopyroxene is still stable in the residue during partial melting of lherzolite and its stability field expands to higher temperatures; C) At 2 GPa, garnet only presents in the residue of partial melting of eclogite at low  $f_{O_2}$ .
- (4) For partial melting of lherzolite with C-O-H fluid under reducing condition, the melt compositions are rather quartz normative than olivine normative.

Solidus and phase relations at reducing condition may be helpful to understand magmatism on the early Earth and magmatism in deeper and perhaps more reducing realms of Earth's mantle. Compositional variations in the melts may thus be useful to identify the redox conditions of the melt sources.

[1] Litasov, K. D., et al. 2014. *EPSL*, 391: 87-99; [2] Frost, D. J. and C. A. McCammon. 2008. *Annu. Rev. Earth Planet*, 36: 389-420; [3] Foley, S. F. 2010. *JP*, 52(7-8): 1363-1391.

12:00pm - 12:15pm

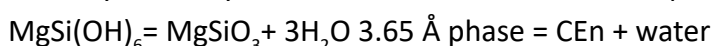
## Amorphous precursor phase observed at mantle conditions during hydration of clinoenstatite to 3.65 Å phase, MgSi(OH)<sub>6</sub>

Monika Koch-Müller, Richard Wirth, Oona Appelt, Bernd Wunder

Deutsches GeoForschungsZentrum, Potsdam, Germany

Numerous studies have shown that dehydration of serpentine causes intermediate-depth earthquakes. However, earthquakes are also observed at the bottom of the mantle transition zone, possibly caused by dehydration embrittlement. Possible carriers of water to these depths are Dense Hydrous Magnesium Silicates (DHMS) and deep seismicity might be caused by dehydration of the DHMS. An important DHMS is the 10 Å phase, Mg<sub>3</sub>Si<sub>4</sub>O<sub>10</sub>(OH)<sub>2</sub>·xH<sub>2</sub>O. At pressures above 10 GPa the 10 Å phase transforms to another important DHMS, namely the 3.65 Å phase. Wunder et al. (2011) synthesized the 3.65 Å phase and determined the chemical formula as MgSi(OH)<sub>6</sub>.

To study the dehydration mechanism of the 3.65 Å phase we investigated the reaction



Up to now we performed three reversed experiments (MA-526, -527 and -535) in a rotating Multi-Anvil Press at 10 GPa/550 °C (24 hours), 10 GPa/470 °C (96 hours) and 10 GPa/600 °C (72 hours), respectively. In MA-526 and -535 we observed the dehydration of the 3.65 Å, thus the formation of CEn and in MA-527 we observed the hydration of CEn, thus the formation of the 3.65 Å phase. The reactions were very sluggish and not complete even after 96 hours. We investigated the recovered samples by electron microprobe and transmission electron microscopy. In the hydration experiment a few large (30 - 50 µm) remnants of CEn without any cracks could be found surrounded by cracked submicron-sized CEn. In this debris-like areas an amorphous phase (0.85 Mg : 1.05 Si with about 20 wt% of water) was found which further was consumed and finally formed the 3.65 Å phase (1 Mg : 1 Si with 34% H<sub>2</sub>O). Thus, the submicron-sized broken CEn transforms via an amorphous water-bearing precursor phase to the 3.65 Å phase. From the back scattered images of the recovered sample of the dehydration experiment we can clearly see that there is a high porosity due to dehydration and that the 3.65 Å phase is being consumed. There are still some educt CEn as perfect crystals present but the product CEn form the majority as fine grained (submicron-sized) newly formed crystals. Even having a different origin, the textures of the CEn crystals in both, hydration and dehydration experiments are similar, showing perfect large crystals together with submicron-sized grains.

[1] Wunder et al. (2011) *Am Mineral*, 96, 1207 - 1214.

**12:15pm - 12:30pm**

### Experimental evidence and implications of coupled silica and water loss from melt inclusions in olivine

**Maxim Portnyagin<sup>1</sup>, Nikita Mironov<sup>2</sup>, Roman Botcharnikov<sup>3</sup>, Andrey Gurenko<sup>4</sup>, Renat Almeev<sup>5</sup>, Cornelia Luft<sup>3</sup>, Francois Holtz<sup>5</sup>**

<sup>1</sup>GEOMAR, 24148 Kiel, Germany; <sup>2</sup>Vernadsky Institute, 119991 Moscow, Russia; <sup>3</sup>Inst. Geosc., Mainz Univ., 55128 Mainz, Germany; <sup>4</sup>CRPG, 54501 Vandoeuvre-lès-Nancy, France; <sup>5</sup>Inst. Miner, Hannover Univ., 30167 Hannover, Germany

The majority of melt inclusions reported in olivine Fo>88 mol% from subduction-related rocks have SiO<sub>2</sub>-undersaturated compositions, which are distinctive from those of predominantly SiO<sub>2</sub>-saturated primitive (Mg#>0.65) island-arc rocks. A number of models has been proposed to explain the origin of these melts by melting of ultramafic lithologies under the lower crustal and mantle conditions. All these models implied that low-Si melts existed in nature and were preserved in melt inclusions, but not in rock compositions. In our recently published paper [doi:10.1016/j.epsl.2019.04.021] we propose an alternative hypothesis implying that these inclusions do not represent large volume natural magmas but originate by modification of initially SiO<sub>2</sub>-saturated melts after entrapment in olivine.

We performed experiments with natural olivine Fo85-90 from Klyuchevskoy volcano (Kamchatka, Russia), which contained SiO<sub>2</sub>-undersaturated (SiO<sub>2</sub>~48 wt%) strongly dehydrated (H<sub>2</sub>O<0.1 wt%), but initially H<sub>2</sub>O-rich melt inclusions. We show that experimental treatment of these olivines at 300 MPa H<sub>2</sub>O pressure and 1200 °C temperature causes a concomitant enrichment of melt inclusions in H<sub>2</sub>O and SiO<sub>2</sub> so that re-hydrated inclusions (4-5 wt% H<sub>2</sub>O) become as SiO<sub>2</sub>-saturated (SiO<sub>2</sub>~52 wt%) as primitive Klyuchevskoy rocks. A reverse process occurs for experimental dehydration of H<sub>2</sub>O-rich inclusions and results in coupled depletion of melt in H<sub>2</sub>O and SiO<sub>2</sub>. The estimated H<sup>+</sup> diffusion rate, FTIR spectra of de- and hydrated olivines and the stoichiometry of coupled SiO<sub>2</sub> and H<sub>2</sub>O loss/gain suggest H<sup>+</sup> diffusion in the octahedral metal (Mg, Fe) vacancies in olivine and formation of metal-deficient olivine (MgH<sub>2</sub>SiO<sub>4</sub> and/or FeHSiO<sub>4</sub>) on inclusion walls during melt dehydration. Reverse process of defect olivine dissolution on inclusion walls occurs during melt hydration.

We conclude that the previously reported SiO<sub>2</sub>-undersaturated compositions of many melt inclusions from island-arc rocks could originate by dehydration of the initially trapped primitive SiO<sub>2</sub>-saturated H<sub>2</sub>O-rich melts. Our results show that the initial H<sub>2</sub>O content of 5-6 wt% may be typical for island-arc magmas, in contrast to the results based on direct determination of H<sub>2</sub>O in potentially dehydrated melt inclusions. The higher H<sub>2</sub>O in primary arc melts implies the existence of a 'crustal filter' controlling the water content which, can be

preserved in melt inclusions, and also the lower mantle temperatures and more efficient water turnover at subduction zones.

## 12:30pm - 12:45pm

### Al, Fe and H incorporation in natural rutile

**Bastian Joachim-Mrosko<sup>1</sup>, Jürgen Konzett<sup>1</sup>, Thomas Ludwig<sup>2</sup>, Roland Stalder<sup>1</sup>**

<sup>1</sup>University of Innsbruck, Austria; <sup>2</sup>Heidelberg University, Germany

Rutile is one of the most common accessory minerals in igneous and metamorphic rocks and their high- and ultrahigh-pressure counterparts. Though nominally anhydrous, rutile may store trace amounts of water and thus has the potential to transport volatiles to depths beyond sub-arc magmatism and even down to the lower mantle.

We investigated experimentally the incorporation of Al, Fe and H in natural rutile embedded in a granitic host rock at fixed  $\mu(\text{Al}_2\text{O}_3)$ , at  $\Delta f\text{O}_2$  between QFM-1 and QFM-2, in the P-T range 2-7 GPa, and at temperatures between 1173-1373 K.

SIMS analyses shows in all experiments diffusion profiles of  $\text{H}_2\text{O}$ , which are significantly shorter compared to diffusion profiles of  $\text{Al}_2\text{O}_3$  and FeO. Microprobe analyses further reveal a complex distribution of oxygen defects at the scale of the diffusion profiles. FTIR-analyses point toward the incorporation of hydrogen dominantly as Fe-H and Ti-H related defects (Bromiley and Hilairret, 2005).

Based on these results, we suggest a complex combination of mechanisms that explains the incorporation of Al, Fe and hydrogen in rutile at the experimental high-pressure conditions. These are amongst others:

The incorporation of Al on octahedral Ti-sites and, at high pressures, on interstitial sites in combination with the formation of oxygen vacancies (Bromiley and Hilairret, 2005).

Incorporation of  $\text{Fe}^{3+}$  on a Ti-site charge balanced by the incorporation of  $\text{H}^+$  (Bromiley and Hilairret, 2005)

Formation of vacancies on Ti-sites accompanied by incorporation of oxygen (Dohmen et al., 2019) and hydrogen.

Calculated diffusion profiles further reveal a sudden increase in  $\text{Al}_2\text{O}_3$  concentrations between 3.5 and 4.0 GPa that is related to the incorporation of aluminum into (0 ½ 0) octahedral interstices resulting in a  $\text{CaCl}_2$  type  $\text{TiO}_2$  phase after quenching. A second sudden increase in maximum  $\text{H}_2\text{O}$ ,  $\text{Al}_2\text{O}_3$  and FeO-solubilities is observed between 6 and 7 GPa that may be explained by the transition from the  $\text{CaCl}_2$  type to an  $\alpha$ - $\text{TiO}_2$  type polymorph (Escudero et al., 2011).

[1] Bromiley and Hilairret (2005), *Min.Mag.* 69, 345-358; [2] Dohmen et al. (2019), *Phys. Chem. Mineral.* 46, 311-332; [3] Escudero et al. (2011), *J. Phys. Chem.* 115, 12196-12201

## 12:45pm - 1:00pm

### Electrical conductivity of forsterite aggregates containing $\text{H}_2\text{O}$ -NaCl fluids at 800 °C and 1 GPa: implications for the high electrical conductivity anomalies in subduction zones

**Yongsheng Huang<sup>1</sup>, Haihao Guo<sup>2,3</sup>, Takayuki Nakatani<sup>1,4</sup>, Michihiko Nakamura<sup>1</sup>, Hans Keppler<sup>2</sup>**

<sup>1</sup>Department of Earth Science, Tohoku University, Japan; <sup>2</sup>Bayerisches Geoinstitut, University of Bayreuth, Germany;

<sup>3</sup>Earth and Planetary Sciences, McGill University, Canada; <sup>4</sup>Geological Survey of Japan, Japan

Recently, growing numbers of magnetotelluric (MT) observations have revealed the ubiquitous presence of high electrical conductivity anomalies (0.01–1 S/m) in the lower crust and mantle wedge of subduction zones. Both silicate melts and aqueous fluids are plausible candidates to account for the high electrical conductivity anomalies, because aqueous fluids liberated from the subducting slab trigger hydrous partial melting in the overlying lithosphere in subduction zones. While partial melting is expected beneath the arc, aqueous fluid is the only conductive phase in the fore-arc regions where the temperature is too low to cause partial melting. Therefore, laboratory data on the electrical conductivity of fluid-bearing rocks are vital to interpret the MT

data especially in fore-arc regions. NaCl is now recognized to be an important constituent of subduction zone fluids. We have therefore performed in situ electrical conductivity measurement of texturally equilibrated aggregates in the system forsterite–H<sub>2</sub>O–NaCl (5 wt% NaCl) at 800 °C and 1 GPa with various fluid fractions of 0.5, 2.5, 5.0, and 10.0 wt % to investigate the origin of the high conductivity anomalies observed in subduction zones. Experimental durations were 8-9 days to assure attainment of textural equilibrium. The conductivity was measured every day during the run. The recovered samples show that the fluid was homogeneously distributed. The conductivities rapidly decreased during the first day and then gradually reached a constant value due to fluid loss. Our results show that conductivity increases with the fraction of NaCl-bearing aqueous fluids (from 0.0017 to 0.48 S/m with initial fluid fractions 0.5-10 wt%). The dependence of fluid fraction on conductivity is non-linear. The conductivity rapidly increases with increase in initial fluid fraction from 0.5 to 2.5 wt%, indicating there could present a threshold of fluid fraction for establishing interconnection. The bulk electrical conductivity in the forsterite–H<sub>2</sub>O–NaCl system is governed by the fluid connectivity and the total concentrations of dissolved ionic species in the aqueous fluids. The dominant connectivity paths depend on the geometrical distribution of aqueous fluids in a fluids-bearing rock system. For an interconnected fluid pathway, the circuit may approach the response of the grain interior and aqueous fluids in a parallel circuit. Without an interconnected fluids pathway, the circuit may be closer to the response of the grain interior and aqueous fluids in a series circuit. To understand the fluid fraction dependency in terms of microstructure, we are planning to constrain the fluid geometries using X-ray computer tomography (CT).

## Poster Presentations

Tue: 13

### NMR analysis on fluorine defects in forsterite and wadsleyite

**Tobias Grützner<sup>1</sup>, Christopher Beyer<sup>2</sup>, Svyatoslav Shcheka<sup>3</sup>, Michael Fechtelkord<sup>2</sup>, Stephan Klemme<sup>1</sup>**

<sup>1</sup>*Institut für Mineralogie, Universität Münster, Germany;* <sup>2</sup>*Institut für Geowissenschaften, Universität Bochum, Germany;* <sup>3</sup>*Bayrisches Geoinstitut, Universität Bayreuth, Germany*

Halogens, especially Fluorine, are important volatile components of the upper mantle. Whilst the role of water in the Earth's mantle has been studied in great detail, there is only scant data on the influence of F or Cl on mantle processes. However, recent experimental studies show that F is less incompatible than water in forsterite and enstatite [1], but it tends to be more incompatible than water in wadsleyite [2]. This implies that F may be fractionated from water in the upper mantle and the Earth's mantle transition zone.

To further our understanding of how F is incorporated into olivine, we synthesized F-saturated forsterite at pressures between 1 to 8 GPa and 1500-1700 °C in piston cylinder and multi anvil presses at Münster. We also synthesized F-saturated wadsleyite at 21 GPa and 1700-1900 °C using the 5000 ton multi anvil press at the BGI in Bayreuth. Additional experiments were conducted in a F- and water-saturated system to study the interaction between water and F in nominally anhydrous minerals (e.g. forsterite). The experiments were characterized with EPMA and Raman Spectroscopy in Münster and <sup>19</sup>F MAS NMR spectroscopy was performed in Bochum.

Preliminary results show that F defects coupled with Mg vacancies are the most important mechanism by which F is incorporated into forsterite. This is independent of P, T and water content. Therefore, F incorporation is different from the favoured mechanism for OH incorporation in high-pressure forsterite, i.e. Si vacancies [3]. In wadsleyite F incorporation seems to be dominated by humite-type defects.

The different incorporation mechanisms for F and OH in forsterite and wadsleyite may help to better constrain storage of both volatiles in the mantle. Further results and implications will be presented at the conference.

[1] Grützner et al., 2017, *GCA* **208**, 160-170; [2] Grützner et al., 2018, *EPSL* **482**, 236-244; [3] Xue et al., 2017, *Am. Min.* **102**, 529-536.

Tue: 14

**A preliminary density model for carbonate-rich melts based on high pressure experimental data.****Malcolm Massuyeau, Xenia Ritter, Carmen Sanchez-Valle***University of Münster, Institute for Mineralogy, Münster, Germany*

Volatiles cycles have a leading place in the evolution and fate of a planet. Depending on its nature, speciation, abundance and mobility, volatiles define the habitability conditions at the surface and greatly affect the physicochemical properties of the inner layers. Conversely, chemical and physical interactions between the inner and outer Earth's layers shape the evolution of the volatiles cycle. Among those various environments, the Earth's mantle constitutes a major actor of this cycle by hosting considerable proportions of carbon, and also hydrogen, both volatiles playing a critical role on melting properties of mantle peridotite, with the highest effects due to CO<sub>2</sub>. Understanding the exchanges and fluxes of carbon (and water) between the upper mantle and exosphere remains a primary goal in the Earth sciences community. Yet, this task is critically prevented by the lack of fundamental constraints on the mobility and migration rates of volatile-bearing melts (i.e., CO<sub>2</sub>-H<sub>2</sub>O-bearing melts) that are important conveyors for the distribution of volatiles. Although the density (and viscosity) data that control the mobility of carbon-rich melts in the mantle is becoming progressively available, density models for multi-component melts at mantle conditions are still lacking. Here we combine recent high pressure density data obtained by the synchrotron X-ray absorption technique with ambient pressure density and sound velocity data to propose a preliminary model for the density of dry and hydrous carbonate melts to 4 GPa and 2000 K. The calibration range spans the conditions for incipient melts stabilized in the upper mantle. Further, the applications of this model to quantify the migration/ascent/emplacement of melts through the mantle and the implications for volatiles mobility and recycling in the deep Earth are discussed.

## 5b) Volcanic geology

Tuesday, 24/Sep/2019: 3:45pm - 5:30pm

Session Chair: Christoph Breitzkreuz (TU Bergakademie Freiberg)

Session Chair: Thomas Walter (GFZ)

Location: Schloss: S10

### Session Abstract

Volcanism, in the past and today, represents an important interface between the lithosphere and exogenic spheres. Studies of its (paleo-) environmental influence and complex interactions are of paramount relevance for understanding the crustal structure and morphology, as well as hazards and resources. At the same time, volcanoes and related products allow to reveal rifting environments, ocean and intraplate islands, arcs, and associated magmatic plumbing systems. Herewith we cordially invite presentations on field- to lab studies, employing geologic mapping, geophysical imaging, remote sensing, chemical and monitoring studies, and also invite parametric studies, from analog to analytical to numerical modeling and experiments on ancient and active volcanic fields.

### Lecture Presentations

3:45pm - 4:00pm

#### Integration of SAR and Seismic Interferometry imaging techniques to investigate volcanism at Campi Flegrei caldera

Susi Pepe<sup>1</sup>, Luca De Siena<sup>2</sup>, Andrea Barone<sup>1,3</sup>, Raffaele Castaldo<sup>1</sup>, Luca D' Auria<sup>4</sup>, Mariarosaria Manzo<sup>1</sup>, Francesco Casu<sup>1</sup>, Maurizio Fedi<sup>1</sup>, Riccardo Lanari<sup>1</sup>, Francesca Bianco<sup>5</sup>, Pietro Tizzani<sup>1</sup>

<sup>1</sup>National Research Council (CNR) of Italy – Istituto per il Rilevamento Elettromagnetico dell'Ambiente (IREA), via Diocleziano 328, 80124 Napoli, Italy.; <sup>2</sup>Institute of Geosciences, Johannes Gutenberg Universität, Mainz, Germany.;

<sup>3</sup>Department of Earth, Environmental and Resources Science, University of Naples "Federico II". Monte Sant'Angelo (L building), Via Cinthia 21, 80126, Napoli, Italy.; <sup>4</sup>Istituto Vulcanologico de Canarias, 38320 San Cristóbal de La Laguna, S/C de Tenerife, Spain; <sup>5</sup>Istituto Nazionale di Geofisica e Vulcanologia, Sezione Osservatorio Vesuviano, Via Diocleziano 328, 80124 Napoli, Italy

Observations from satellites provide high-resolution images of ground deformation at surface allowing the use of advanced modelling to model deformation sources. Nevertheless, both satellite observations and models remain biased without precise information about the structure of the volcano: obtaining this information is difficult if not impossible to achieve given the often sparse or clustered distribution of seismicity in volcanic areas. In this study, we combined two interferometric techniques to interpret the 2011-13 unrest at Campi Flegrei caldera (CFC). The first is Synthetic Aperture Radar (SAR) applied on COSMO-SkyMed data, which provides highly-resolved spatial and temporal images of ground deformation. The second is Ambient Noise Tomography (ANT), which images the structure of the caldera using ambient noise continuously produced by the seashore. ANT is applied together with the Total Horizontal Derivative (THD) for the analysis of the vertical component of the ground deformation field, evidencing how the complexity of the caldera structures are a source of ground deformation. Both the THD maps and the ANT images are finally compared with the hypocenter distribution of the earthquakes recorded between January 2011 and December 2013, with the aim of highlighting which of these boundaries releases stress. The comparison shows that the caldera rim and the remnant of previous eruptions may act as a barrier for the horizontal propagation of the magmatic intrusion within sill-like structures. High-velocity anomalies, THD boundaries, and seismicity coincide with extinct volcanic vents in the eastern part of the caldera (Solfatara/Pisciarelli and Astroni). Such a coincidence hints at a significant role of the extinct plumbing system in constraining the eastward propagation of magmatic fluids. The ANT results show that these bounding structures are located at depths spanning from ~1 to ~1.7 km. The small secondary deformation source active throughout the last 40 years at Solfatara in this

depth range is thus likely due to structural effects, specifically deep high-velocity structures under the areas intersected by the last venting at the caldera. A comparison of the SAR and seismic imaging represents a good option to quantitatively model in space and time the characteristics and nature of the deformation source. It provides a new perspective to better understand the origin of deformation signal at volcanoes where magma propagation within sills is expected, as for the CFC case.

**4:00pm - 4:15pm**

### **Lava dome growth monitoring at Nevado del Ruiz using high-resolution TerraSAR-X amplitude imagery**

**Thomas Walter**

*GFZ, Germany*

Nevado del Ruiz volcano, Colombia, is renowned for its major 1985 disaster, which is why the volcano activity and its hazards are closely monitored. However, the details of the process occurring inside the summit crater region, such as explosive dome growth, remain hidden due to the difficult access and harsh conditions impeding direct observations. The crater region of Nevado del Ruiz is covered by clouds and degassing throughout most of the year. We therefore employ Synthetic Aperture Radar (SAR) acquisitions from the German TerraSAR-X satellite to investigate the lava dome evolution through the years 2015-2018. The data was acquired in 1-m high resolution spotlight mode and is enabling us to monitor deformation and surface characteristics of the lava dome at unprecedented details. The analysis of amplitude image stacks shows that the dome is subject to expansion and vertical growth. Dome perimeter measurements allow to identify increased growth rate at the end of the year 2016. Moreover, the development of We compare SAR measurements to satellite thermal data, retrieved by MODIS and SENTINEL-2 platforms, that highlight an increase in heat radiation during December 2015 and January 2017, and a shift of thermal anomalies location from the center of the growing dome to a ring at the dome perimeter.

**4:15pm - 4:30pm**

### **Mediterranean S1 Tephra as a Marker Horizon for the Fertile Crescent: Source Evidence and Characterization of the 9 ka Dikkartin Dome (Mt. Erciyes, Turkey) Eruption**

**Bjarne Friedrichs<sup>1</sup>, Axel K. Schmitt<sup>1</sup>, Julie C. Schindlbeck-Belo<sup>1</sup>, Martin Danisik<sup>2</sup>, Gokhan Atici<sup>3</sup>, Esra Yurteri<sup>3</sup>, Mehmet Cobankaya<sup>3</sup>, Susanna F. Jenkins<sup>4</sup>, R. Stephen J. Sparks<sup>5</sup>**

*<sup>1</sup>University of Heidelberg, Germany; <sup>2</sup>Curtin University, Perth, Australia; <sup>3</sup>General Directorate of MTA, Ankara, Turkey;*

*<sup>4</sup>Nanyang Technological University, Singapore; <sup>5</sup>University of Bristol, United Kingdom*

“Levantine ash” was first described around Cyprus 45 years ago, but it took until the last decade to be rediscovered in the Yammouneh basin (Lebanon) and a sediment core offshore Israel. It was subsequently named “S1 tephra” based on its stratigraphic position within the lower part of the eponymous sapropel layer, the youngest in the Mediterranean. More recently, S1 tephra was also reported to be preserved in sediments of the Dead Sea, Tayma paleolake (Saudi Arabia), and Sodmein cave (Egypt).

The Dikkartin dome eruption of Mt. Erciyes (Central Anatolia, Turkey) has been postulated as the source of the S1 tephra based on major element and morphological analyses of volcanic glass shards. However, this correlation remained tenuous because radiometric dating and differentiation between Dikkartin and other young dome eruptions at Mt. Erciyes as potential sources were lacking. Here, we present the first radiometric age of  $9.0 \pm 0.6$  ka ( $1 \sigma$ ,  $n = 19$ ) for the explosive Dikkartin eruption, based on internally consistent zircon double dating by (U-Th)/He and U-Th disequilibrium methods. New field observations and comprehensive major and trace element compositions determined for glass shards from proximal and distal samples confirm the explosive Dikkartin eruption as the source of S1 tephra.

Isopleths of maximum lithic clast sizes of the predominantly southeasterly-distributed fall deposit translate into eruption column heights of ca. 23 km and a VEI 4 or 5 (volcanic explosivity index;  $>0.4$  km<sup>3</sup> of tephra) cat-

egory for the Dikkartin eruption. Furthermore, our data identify the nearly coeval Karagüllü dome eruption of Mt. Erciyes (Central Anatolia, Turkey) as the source of another tephra presently only documented for the southeastern Black Sea, indicating a northeastern distribution of this fall deposit.

With its dispersion covering the western part of the Fertile Crescent and its Early Holocene age, S1 tephra is identified as a key marker horizon in the center of the Neolithic revolution, both in space and time. Identification of the Dikkartin tephra across a broad proximal area from the northeast to the south of Mt. Erciyes may reflect a long-duration eruption that dispersed into multiple wind fields and across multiple seasons. By contrast, the Karagüllü tephra to the northeast of Mt. Erciyes is consistent with a winter eruption (October to April) assuming present-day stratospheric wind patterns. Modelling of tephra dispersal is ongoing.

**4:30pm - 4:45pm**

### **Parameters controlling the cyclic activity of silicic volcanic systems: evidence from Milos (Greece)**

**Xiaolong Zhou, Pieter Vroon, Klaudia Kuiper, Jan Wijbrans**

*Vrije Universiteit Amsterdam, The Netherlands*

The cyclic activity of silicic volcanic systems has been known for a long time, and the study of this cyclicity is hampered by the lack of sufficiently good information on the time lines of many active volcanic systems. There is no clear explanation what processes are responsible for the cyclicity of volcanic eruptions. In many volcanic systems, activity is concentrated in short intervals, and longer periods of quiescence. The reason why this distribution exists is still not very well understood.

Upper crustal magma chamber processes are generally assumed to cause this cyclicity of the volcanic activity. However, over the last two decades it has become clear that this classical crustal magma chamber model is oversimplified. Many studies on the residence times of crystals and thermal models point to the existence of crystal mushes, which spend substantial time at sub-solidus temperatures but only enter partial melt phase for short periods of time. The location of these magma chambers with a crystal mush zone is still a matter of debate, many geochemical imprints indicate the storage and fractionation of magma occurring at the Moho (~30 km), and at shallower depths (10-20 km).

One of the models, the Deep Crustal Hot Zone (DCHZ) attempts to quantify this process by estimating the frequency of magma injection ( $t_i$ ) and the average flux of magma from depth for long-term ( $Q_{av}$ ). A Caricchi's Monte Carlo simulations model provides solutions to quantitatively estimate these two parameters. Based on this model, previous geochronological and volcanological work, and our new twenty-three  $^{40}\text{Ar}/^{39}\text{Ar}$  ages on Milos, the least  $t_i$  and  $Q_{av}$  correspond to two long periods of volcanic quiescence (1.55-1.04 Ma and 0.59-1.04 Ma). The higher  $Q_{av}$  during the first 1.5 Ma could produce the main volcanic complex of Milos (~90% by volume). Combined with  $t_i$  and  $Q_{av}$ , it is useful to detect the boundary time of tectonic events. For Milos, we inferred the linkage between Milos, as the junction of old western and young eastern volcanic centers in South Aegean Volcanic Arc (SAVA), and the young eastern arc.

**4:45pm - 5:00pm**

### **Physical volcanology of Quaternary ignimbrites in the Aragats Volcanic Province (Lesser Caucasus): a lithofacies-based approach**

**Hripsime Gevorgyan<sup>1,2</sup>, Christoph Breitzkreuz<sup>1</sup>, Khachatur Meliksetian<sup>2</sup>, Yura Ghukasyan<sup>2</sup>, Ruben Jrbashyan<sup>2</sup>, Arsen Israyelyan<sup>2</sup>, Jörg A. Pfänder<sup>1</sup>, Daniel Miggins<sup>3</sup>, Anthony Koppers<sup>3</sup>**

*<sup>1</sup>Institute of Geology, TU Bergakademie Freiberg, Bernhard-von-Cotta Straße 2, 09599 Freiberg, Germany; <sup>2</sup>Institute of Geological Sciences, National Academy of Sciences of Armenia, Marshal Baghramyan Avenue, 0019 Yerevan, Armenia; <sup>3</sup>College of Earth, Ocean, and Atmospheric Science, Oregon State University, Corvallis, OR, USA*

Revised Quaternary stratigraphy of ignimbrites and associated fallout deposits of the Aragats Volcanic Province (AVP; western Armenia) and new  $^{40}\text{Ar}/^{39}\text{Ar}$  data obtained for each ignimbrite unit allow correlation with

previously dated pyroclastic deposits and a reconstruction of the eruption sequence. The succession indicates that Aragats stratovolcano underwent a series of effusive and explosive eruptions. Each eruption stage started with basaltic and basalt-andesitic lava flows followed by Plinian fallout ash layers and by ignimbrites. The AVP records the 650 ka Gyumri ignimbrite eruption, which was the youngest Plinian eruption episode (estimated about 1 Ma between 1.5-0.5 Ma). Detailed field investigations show that extensive ignimbrite units (e.g. Gyumri, Qasakh, and Baghramyan) are related to initial Plinian eruptions with fallout followed by eruption column collapse events. Nevertheless, in the base of three ignimbrite units (Amberd, Artik, and Shamiram-Byurakan), fallout deposits are missing.

Predominantly trachydacitic to rhyolitic in composition, the ignimbrites of AVP display variable characteristics such as color, welding degree, eutaxitic fabric, rheomorphism, sheet and columnar jointing, and varying phenocryst population. The lower and upper parts of each unit are represented by non- to weakly welded lithic-rich ignimbrites while the central part is characterized by strongly welded ignimbrites. In places, contact zones between ignimbrite units comprise black-reddish vitrophyre. Several of the ignimbrite units are compositionally zoned and contain andesitic to rhyolitic Fiamme, and banded pumices indicative of magma mingling immediately prior to eruption. Identification of previously unrecognized lithic-rich breccias above lava-like ignimbrite unit indicates caldera-forming or vent widening processes in the history of Aragats stratovolcano.

The majority of the erupted pyroclastic material was deposited around the Aragats stratovolcano and in the volcanic ring plain, as well as along big valleys. Detailed logging and lateral tracing of these proximal and distal deposits have allowed detailed study of the lithofacies of the AVP ignimbrites and the reinterpretation of its eruptive history. Plinian eruption followed by pyroclastic fountaining fed an initial unsteady pyroclastic flow that evolved into a sustained pyroclastic density current, which spread across the entire region.

**5:00pm - 5:15pm**

### **Understanding the 1888 sector collapse of Ritter Island (Papua New Guinea) by integrating 3D seismic data and Discrete Element Models**

**Morelia Urlaub<sup>1</sup>, Julia Morgan<sup>2</sup>, Christian Berndt<sup>1</sup>, Jens Karstens<sup>1</sup>**

<sup>1</sup>GEOMAR Helmholtz Zentrum für Ozeanforschung Kiel, Germany; <sup>2</sup>Rice University, Houston

Volcanic flank collapses are common in the life cycle of volcanoes. These events can be devastating, in particular at coastal or ocean island volcanoes due to their tsunamigenic potential. Yet, reasons for catastrophic collapses are not well understood, leaving us unprepared to these events. In 1888, the western flank of Ritter Island (Papua New Guinea) collapsed and slid into the Bismarck Sea triggering a tsunami, which devastated the coasts of the neighbouring islands. In this study, we aim to identify the processes that led to collapse. We extract the geological configuration of Ritter Island, pre- and syn-collapse deformation patterns of the volcano as well as post-collapse landslide emplacement dynamics from high-resolution 3D seismic data collected in 2016 during RV Sonne cruise SO252. These information feed into 2D Discrete Element Models, with which we seek to simulate the collapse. The models successfully reproduce compressive deformation of sediments adjacent to Ritter Island as observed in the seismic data. However, catastrophic failure does not occur naturally, even when introducing zero-friction detachment surfaces. This implies that other processes, such as an eruption or uni-lateral spreading, must have decreased edifice stability.

**5:15pm - 5:30pm**

### **Rejuvenated volcanism at a Cretaceous seamount off El Hierro (Canary Islands)**

**Andreas Klügel<sup>1</sup>, Miriam Römer<sup>1</sup>, Heinrich Villinger<sup>1</sup>, Folkmar Hauff<sup>2</sup>, Sebastian Krastel<sup>3</sup>**

<sup>1</sup>Fachbereich Geowissenschaften, Universität Bremen, Germany; <sup>2</sup>GEOMAR, Helmholtz-Zentrum für Ozeanforschung, Kiel; <sup>3</sup>Institut für Geowissenschaften, Christian-Albrechts-Universität zu Kiel

Henry Seamount is located ca. 40 km southeast of El Hierro, the youngest of the Canary Islands, rising 700 m

above 3600-3800 m deep sea floor. During METEOR cruise M66/1 in 2005 a reconnaissance dredging campaign yielded barite-metasomatized trachytic rocks, barite fragments, and shells from vesicomid clams. Radiocarbon age determinations of two shells yielded 3.4 and 18.6 ka, which indicates Holocene fluid venting at the seamount [1]. In contrast, trachytes were Ar/Ar age dated to ca. 126 Ma, indicating that the volcano pre-dates Canary volcanism and probably became extinct during the Cretaceous. In order to discover and sample fluid venting sites, Henry Seamount was investigated in detail during METEOR cruise M146 in 2018. Hydroacoustic surveys and TV-sled dives revealed large areas of the summit area densely covered with clam shells; living species were neither observed nor sampled. The observations clearly indicate formerly widespread venting sites at the seamount, but local oxygen reduction potential (ORP) anomalies recorded during the TV-sled dives document that some fluid discharge is still going on. In contrast, heat flow measurements taken along profiles in the vicinity of the seamount showed no fluid flow-related anomalies.

Surprisingly, some grab samples and a gravity core recovered glassy basaltic ash and some lava fragments, which undoubtedly originated from Henry Seamount. Many basalt samples are exceptionally fresh, suggesting a young age probably contemporaneous to the subaerial activity of El Hierro island (<1.1 Ma); a Cretaceous age similar to the trachytes is unlikely. The volcanic activity probably provided the heat for local hydrothermal activity, but did not affect the thermal regime in the surrounding sediments.

The basalt samples show different lithologies and include tephritic, phonotephritic and trachybasaltic compositions, with major and trace element characteristics similar to recent El Hierro lavas. The Sr-Nd-Pb isotopic compositions overlap completely with those of recent El Hierro lavas and cover a similar range. These results suggest that recent melts erupted at Henry Seamount and El Hierro originate from the same mantle source. The rejuvenated activity at Henry Seamount may reflect sporadic lateral movement of rising El Hierro magmas within the upper mantle or lower crust, or an incipient shift of volcanic activity due to movement of the African plate over the Canary hotspot. It appears possible that the seemingly extinct seamount may continue to grow in the future.

[1] Klügel et al. (2011), *Geology* 39, 855-858.

**Wednesday, 25/Sep/2019: 8:30am - 10:30am**

**8:30am - 8:45am**

### **Facies analysis, depositional style and geochemistry of Ediacaran volcano-sedimentary successions at the NE Edge of Saghro inlier (Eastern Anti-Atlas, Morocco)**

**Zakarya Yajoui<sup>1</sup>, Christoph Breitkreuz<sup>2</sup>, Brahim Karaoui<sup>3</sup>, Abdelkader Mahmoudi<sup>1</sup>**

<sup>1</sup>*Department of Geology, Faculty of Sciences, Moulay Ismail University, Meknes, Morocco;* <sup>2</sup>*Institut für Geologie und Paläontologie, Technische Universität Bergakademie, Freiberg, Germany;* <sup>3</sup>*Department of Geology, Faculty of Sciences and Techniques, Moulay Ismail University, Errachidia, Morocco*

The NE edge of the Saghro inlier (Eastern Anti-Atlas) exposes excellent outcrops of the Ediacaran Ouarzazate Supergroup volcano-sedimentary succession. It corresponds to sequences of variable thickness and lateral extent, which were the subject of detailed geological investigation including fieldwork, facies analysis and geochemistry of major and trace elements.

Several volcano-sedimentary lithofacies have been mapped: 1) welded rhyolitic ignimbrite, crystal-rich and lithic poor; 2) non-welded rhyolitic ignimbrite, crystal- and lithic-rich; 3) basalt to andesite lava, vesicular, with top breccia; 4) SiO<sub>2</sub>-rich lava, crystal-rich; 5) laminated fallout composed of alternating silt- to gravelly sandstone; 6) surge deposit, composed of alternating silt- and sandstone, with low angle cross-bedding; 7) mafic monomict hydroclastic deposit; 8) pyroclastic dykes, lithic-rich, vertically oriented fiamme; 9) polymict lahar deposit; 10) subvolcanic systems dominated by andesitic dyke swarm and also rare SiO<sub>2</sub>-rich dykes and sills have been mapped. These diverse lithofacies are associated with various volcanic forms such as; i) Caldera complexes; ii) subaerial basalt to andesitic lava; iii) SiO<sub>2</sub>-rich lava; iv) fallout and surge deposits prob-

ably related to plinian eruption; v) phreatomagmatic eruption related to minor tephra cone; vi) debris flow deposit; viii) dyke and sill swarms.

Major and traces element geochemistry of the succession shows high-K calc-alkaline, alkali-calcic to alkaline affinities. They also show significant enrichment of LILEs and exhibit slightly negative anomalies in HFSE. REE patterns show moderate enrichment in LREE relative to flat HREE, with strong negative Eu anomaly. Geotectonic diagrams plot the succession within volcanic arc.

The succession at the NE edge of the Saghro inlier, shows lithofacies, volcanic styles and geochemistry similar with the upper part of Ouarzazate Supergroup described in other areas in the Anti-Atlas Mountains. The volcanic succession originated from continental arc magmatism related subduction of oceanic crust beneath the northern margin of the Gondwana (WACadomian subduction).

**8:45am - 9:00am**

### **Cambrian alkaline submarine to emergent volcanism near Ouinguigui (Ougnat inlier, eastern Anti-Atlas, Morocco)**

**Jacob Brauner<sup>1</sup>, Martin Arndt<sup>1</sup>, Zakarya Yajoui<sup>2</sup>, Brahim Karaoui<sup>3</sup>, Abdelkader Mahmoudi<sup>2</sup>, Christoph Breitzkreuz<sup>1</sup>**

<sup>1</sup>TU Bergakademie Freiberg, Germany; <sup>2</sup>Département de Géologie, Université Moulay Ismail, Meknès, Morocco;

<sup>3</sup>Département de Géologie, Faculté de Science et Technique, Université Moulay Ismail, Errachidia, Morocco

The Cambrian volcanosedimentary succession of Ouinguigui southeast of the Ougnat inlier in the eastern Anti-Atlas (Morocco) was characterized by a multi-disciplinary approach of field work, facies analysis and geochemical analysis. The investigation revealed a complex emplacement history including various forms of alkaline volcanism.

The sedimentary sequence reflects a development from fan-delta and shoreface deposits (Tikirt and Akerouz Member), interrupted by a transgressive phase (Micmacca Breccia Member) and upper offshore deposits, towards a post-transgressive clastic environment (Feijas Internes- and Tabanit Group). Volcanic activity comprises four main phases, accompanying SW-vergent tilting of the underlying basement block. Phase I starts with the emplacement of diatremes within the Jbel Wawrmast Formation and Jbel Afraou Formation, resulting from phreatomagmatic eruptions of basaltic magma in a coastal environment. During Phase II, large volumes of basaltic lava erupted through fissures and formed a lava delta in the eastern part while the middle and western parts of the Ouinguigui area reflect subaqueous to emergent (phreato-)magmatic eruptions. Phase III and IV are reflected by the emplacement of subvolcanic intrusions consisting of trachy andesites and trachytes.

The deposits have to be understood in the context of a rifting activity where the eastern and central Anti-Atlas is related to joint tectonic branches in a remote setting. Indicators are the regional fault patterns resembling the orientation of supra-regional lineaments. Additionally, whole rock geochemical analysis of 13 samples confirms an alkaline character for the Ouinguigui within-plate magmatism, which derived from a garnet lherzolite source.

The volcanic eruption styles are linked to water depth. This dependency can be observed on a small scale by comparing the western and eastern parts of the Ouinguigui area (Phase II). On a larger scale the Ouinguigui area is remarkable, compared to other examples from the central to eastern Anti-Atlas like the Jbel Boho and Jbel Tazoult n'Ouzina, because of the contrasting physical volcanology and chronology.

9:00am - 9:15am

### Volcanic evolution and petrology of a late- to post-Variscan volcanic system: The Carboniferous Altenberg-Teplice Caldera (Germany-Czech Republic)

**Raymundo Casas-García<sup>1</sup>, Vladislav Rapprich<sup>2</sup>, Christoph Breitkreuz<sup>1</sup>, Yulia V. Kochergina<sup>2,3</sup>, Martin Svojtka<sup>4</sup>, Bernhard Schulz<sup>5</sup>, Alexander Repstock<sup>1</sup>, Manuel Lapp<sup>6</sup>, Klaus Stanek<sup>1</sup>, Mandy Hofmann<sup>7</sup>, Ulf Linnemann<sup>7</sup>**

<sup>1</sup>Institute for Geology, TU Bergakademie Freiberg, Germany; <sup>2</sup>Czech Geological Survey, Czech Republic; <sup>3</sup>Charles University, Czech Republic; <sup>4</sup>Czech Academy of Sciences, Czech Republic; <sup>5</sup>Institute for Mineralogy, TU Bergakademie Freiberg, Germany; <sup>6</sup>Saxon State Agency for Environment, Agriculture, and Geology, Germany; <sup>7</sup>Senckenberg Naturhistorische Sammlungen Dresden, Germany

The Teplice Rhyolite (TR) intra-caldera deposits of the Altenberg-Teplice Caldera (ATC) in Central Europe were investigated by lithofacies analysis, stratigraphy, whole-rock chemistry, and laser ablation U-Pb zircon dating. The TR Formation was separated into nine members that document three eruptions. Periods of volcanic quiescence occurred between the eruptions, as suggested by presence of thin sedimentary horizons. The first two eruptions were characterized by opening and clearing of vents that produced lithic-rich ignimbrites with lateral lithofacies changes, followed by lava flows/domes. Eruption style was likely low pyroclastic fountaining coupled with effusive lava extrusion. A basal fallout deposit was identified only for the second eruption and stands for a sustained buoyant eruption column. The final third eruption registered further vent opening, a waxing phase, and lava outpour. Vent opening phase was similar to those in previous eruptions. Waxing phase generated voluminous, massive, poorly sorted, very crystal-rich (>50 vol.%) ignimbrites that exhibit an increase in crystal contents with stratigraphic height and chemical variations that point to deposition by progressive aggradation. Low pyroclastic fountaining fed these high-particle concentration currents, whose deposits were covered by a lava flow. Partially to densely welded TR ignimbrites show eutaxitic textures, deformed glass shards, spherulites, perlitic cracks, and microcrystalline to granophyric textures. Horizontal and vertical lithofacies changes in ignimbrites and the association between the interpreted feeding conduits and faulting indicate that the TR was extruded through faults or fissure vents.

A minimum ejecta volume of ~320 km<sup>3</sup> and a volcanic explosivity index of 7 were estimated for the TR. NE-SW-trending rhyolitic dykes associated with regional fault systems and ATC vents may imply that the trap-door caldera collapse was influenced by post-Variscan tensional stress regime (approx. NNW-SSE direction). Overall, the TR has a rhyolitic composition with A-type granite signature and a normal chemical zoning. More detailed whole-rock and mineral chemical data in concert with Nd-Pb isotopic compositions are being analyzed and interpreted to: (i) evaluate more accurately the normal chemical zoning throughout the TR and (ii) establish the magma source region (mantle vs. crust), a controversial topic for the Erzgebirge/Krušné hory. U-Pb zircon dating rendered an age range of 323-312 Ma that, compared to literature data, suggest caldera volcanism between ~325-317 Ma.

9:15am - 9:30am

### The Lower Permian Rochlitz caldera: A supervolcano in Central Europe

**Marcel Hübner<sup>1</sup>, Christoph Breitkreuz<sup>1</sup>, Anna Pietranik<sup>2</sup>, Ulf Linnemann<sup>3</sup>, Franziska Heuer<sup>4</sup>, Alexander Repstock<sup>1</sup>**

<sup>1</sup>TU Bergakademie Freiberg, Germany; <sup>2</sup>University of Wrocław, Poland; <sup>3</sup>Senckenberg Naturhistorische Sammlungen Dresden, Germany; <sup>4</sup>Museum für Naturkunde Berlin, Germany

Catastrophic outbursts of supervolcanoes haunted the Late Paleozoic Central Europe forming numerous large caldera systems comparable to those known from the Cenozoic Pacific ring of fire. The North Saxon Volcanic Complex (NSVC) comprises a large, two-cycle, deeply eroded, nested caldera complex, hosting the Rochlitz (RVS)- and the Wurzen Volcanic Systems (Repstock et al. 2018). Several outcrops and drill cores disclose the calderas edifice, comprising hundreds of meters of crystal-rich pyroclastics and subvolcanic bodies (Eigenfeld 1978). Combining physical volcanology, petrography, geo- and mineral chemistry and age dating, the Rochlitz Volcanic System provides information about the chronology and style of eruption and the understanding of the magmatic plumbing system beneath a supervolcano.

With a maximum thickness of at least 400 m and an aerial extent of approximately 800 km<sup>2</sup> of the caldera fill ignimbrites, the calculated minimum volume of 1160 km<sup>3</sup> for RVS corresponds to a volcanic explosivity index (VEI) of 8, and thus it qualifies as a supereruption. In the course of the climactic eruption stage two different crystal-rich (35 to 47 vol.%) ignimbrites were deposited – the voluminous rhyolitic Rochlitz- $\alpha$  ignimbrite and followed by the low-volume trachydacitic Rochlitz- $\beta$  ignimbrite, with elevated Nb- and Ti-values. These two types display a transition from *monotonous rhyolites* to *monotonous intermediates*. Changing oxygen isotopic data of zircon ( $\delta^{18}\text{O}$  from 5.7 to 8.9 ‰) support this interpretation. Pyroclastic fountaining along NW-SE oriented fissures is assumed to be the dominant eruption style during the climactic stage.

Ti-in-biotite thermo- and barometry together with zircon morphology point to an average crystallization temperature of 755 °C and a pressure of 4 kbar, resulting in a depth of the upper magma reservoir at around 15 km. New SHRIMP- and LA-ICPMS data on zircon from different stratigraphic positions of the RVS reveal an average age of 293 Ma for the climactic phase. The wide range of ages displays a long-lasting magma chamber of the RVS, typical of *monotonous intermediates*. The RVS and other Permocarboniferous large volcanic complexes in Central Europe presumably formed under a post-Variscan rift regime.

[1] Eigenfeld, F., 1978. Zur geologischen Entwicklung der vulkanischen Gesteine im Süd- und Ostteil des NW-Sächsischen Vulkanitkomplexes. Diss., Martin-Luther-Univ. Halle-Wittenberg, Halle (Saale) [unpublished]; [2] Repstock, A., Breitzkreuz, C., Lapp, M., Schulz, B., 2018. Voluminous and crystal-rich igneous rocks of the Permian Wurzen volcanic system, northern Saxony, Germany. Physical volcanology and geochemical characterization. Int. J. Earth Sci., 6 (9), 1485–1513.

**9:30am - 9:45am**

### **A competition between magma mingling and mixing: The *monotonous intermediates* of the Late Paleozoic North Saxon Volcanic Complex in Central Germany**

**Alexander Repstock<sup>1</sup>, Christoph Breitzkreuz<sup>1</sup>, Marcel Hübner<sup>1</sup>, Bernhard Schulz<sup>2</sup>, Rolf L. Romer<sup>3</sup>**

<sup>1</sup>Institute for Geology, TU Bergakademie Freiberg, Germany; <sup>2</sup>Institute for Mineralogy, TU Bergakademie Freiberg, Germany; <sup>3</sup>Deutsches GeoForschungsZentrum Potsdam, Germany

The reconstruction of *monotonous intermediate* magma systems beneath supervolcanoes is a challenging task in volcanology and igneous petrology. The deeply eroded Late Paleozoic North Saxon Volcanic Complex (NSVC) hosts intra-caldera ignimbrites that are particularly well suited for modelling crystal-rich magma bodies and their dynamics. The NSVC experienced cataclysmic supereruptions, which formed at least two large voluminous crystal-rich (<58 vol.%) pyroclastic deposits, the Rochlitz and Wurzen ignimbrites. We combine textural, chemical, and isotope analyses on juvenile rocks and crystal fragments to unravel the pre-eruptive conditions in the magma reservoir.

The NSVC ignimbrites revealed a strong mingling character by the presence of different types of fiamme, including fine-grained rhyolitic fiamme and porphyritic (trachy-)dacitic fiamme. The latter represent juvenile fragments of mixed dacitic magma, whereas fiamme of rhyolitic composition are the result of fractionation in the magma body. Erratic coarse porphyritic rhyodacitic fiamme represent rheologically deformed and partially molten fragments of the batholith. All juvenile fragments reveal inherited geochemical signatures of the Cadomian basement, most prominently initial  $\epsilon\text{Nd}$  of -7 to -6 and  $^{87}\text{Sr}/^{86}\text{Sr}$  of 0.7064 to 0.7108. Due to the longevity of these *monotonous intermediate* magma chambers, the crust-melt interaction and the basement signature is stronger than in ephemeral rhyolitic magma chambers.

In contrast to other voluminous and crystal-rich Cenozoic pyroclastic units (e.g. Fish Canyon Tuff), the Rochlitz and Wurzen ignimbrites revealed mineral phases which are rather characteristic for a crystal-poor Snake River-type ignimbrite than *monotonous intermediate*. Pyroxene is the predominant ferromagnesian silicate (up to 6.7 vol.% of crystals in bulk matrix), whereas subordinate biotite (up to 5.5 vol.%) represents the only hydrous phase in NSVC ignimbrites. Precisely, the common appearance of mineral phases of different origins indicate contemporaneously tapped cooler (ca. 720 °C for biotite) and superheated magma batches (ca. 1050 °C for pigeonite). The crystallization pressure of calcic clinopyroxene and biotite suggests depths around 25 to 15 km and 11 km for the middle and upper crustal magma bodies.

Possibly related to insufficient H<sub>2</sub>O supply in the magma system, the NSVC magmas have not been completely mixed prior to eruption. Continuous injection of mantle-derived magmas strengthens the mingling character.

## 9:45am - 10:15am Session Keynote

### Timescales and processes within transcrustal magmatic systems

**Olivier Bachmann<sup>1</sup>, O. Laurent<sup>1</sup>, C. Huber<sup>2</sup>, M. Townsend<sup>2</sup>, W. Degruyter<sup>3</sup>, O. Karakas<sup>1</sup>, J. Cornet<sup>1</sup>, J. Wotzlaw<sup>1</sup>**

<sup>1</sup>ETHZ, Inst. of Geoch. and Petr., Zürich, Switzerland; <sup>2</sup>Brown University, Providence, RI, USA; <sup>3</sup>Cardiff University, Cardiff, United Kingdom

Volcanic edifices, as large as they may be, are only the tip of gigantic magmatic icebergs; they cap plumbing systems that grow and mature over time, potentially extending from the crust-mantle boundary to the surface. What happens in these crustal-scale magmatic systems controls: (a) the volcanic record at the surface, (b) the formation of key ore deposits in and around the magma bodies, and (c) the formation rate and chemical-isotopic compositions of new continental crust. This talk will discuss new results on crustal cross-sections in a post-collisional rifting environment (Ivrea zone, Italy), a island arc (Famatian region, Argentina) and an Archean block (Barberton, South Africa). In these three end-member settings, we will discuss the minimum duration of peak magmatism at each location based on new high-precision U-Pb zircon dating and the relationships between volcanic and plutonic lithologies. Furthermore, we will review the most important magma reservoir processes that control the chemical signatures of volcanic-plutonic rocks and igneous distillation, considering the effect of three distinct phases (crystals-melt-fluid, in decreasing order of viscosity and density) on mechanical separation in a gravity field. We will also discuss the potential impacts of external factors (e.g., tectonic forces, seismic waves, magma recharge) on phase separation.

## Poster Presentations

Mon: 24

### Alkaline volcanism on Patmos (Aegean Sea) – constraints from new radiogenic isotope data and <sup>40</sup>Ar/<sup>39</sup>Ar dating

**Katharina Boehm, Klaudia Kuiper, Pieter Vroon, Jan Wijbrans**

*Department of Earth Sciences, Faculty of Science, VU University Amsterdam, De Boelelaan 1085, 1081 HV Amsterdam*

The island of Patmos, in the eastern Aegean Sea, consists almost entirely of volcanic rocks of the late Miocene to Pliocene. Magmatism on Patmos was governed by subduction of the African below the Eurasian plate, back-arc extension, slab roll back and the final propagation of the Northern Anatolian Fault into the Aegean, accommodating westward extrusion of Anatolia.

The volcanic rocks of Patmos are special in terms of their alkalinity and variety in rock types. Fractionation, assimilation and mixing were the main processes, which lead to the production of suites of ne-Trachybasalts, hy-Trachyandesites, hy-Trachybasalts, trachytes, phonotlites and rhyolites. However, the volcanics of Patmos are not the only alkaline rocks in the Aegean- Western Anatolian realm. There are several late Miocene alkaline centers e.g. in Foca, Urla, Kula, Biga and Thrace. In the present study we verify whether or not these alkaline centers can be divided into isotopically distinct groups and how their age relations are with respect to each other. Further we strive to isotopically define the source evolution of the ne-trachybasalts and the timing between the different lava series on Patmos.

We present new radiogenic isotope data, including Pb, Nd, Hf, Sr, major and trace element data and additionally new precise <sup>40</sup>Ar/<sup>39</sup>Ar age data on Patmos and Chillomodi. We sampled volcanic series, ranging from basaltic trachyandesites, to phonolites and rhyolites, with SiO<sub>2</sub> from 52.7 -78.5 wt% and K<sub>2</sub>O from 1.9 -11.7 wt%. The <sup>206</sup>Pb/<sup>204</sup>Pb ratios of 18.8-18.9 are likely to be elevated due to assimilation of arc crust and sediments. The <sup>143</sup>Nd/<sup>144</sup>Nd values also fall in proximity to the Eastern Mediterranean Sediment (0.51239-0.51254). Trace element abundances are typical for alkaline arc lavas with enrichments in LREE and depletions in Nb, rela-

tive to N-MORB. Further characteristics are a distinct negative Ba anomaly, negative Eu anomaly, elevated Hf and Zr and for some sample depletion in Y with respect to N-MORB. Trace element ratios suggest a low subduction imprint in the phonolites and some of the younger volcanic rocks. Variations between the various volcanic lava series support models of AFM. Additionally, radiogenic isotopes place constraints on the source of the primitive alkaline magmas. Our work provides new insights into the characteristics and proportions of fluids derived from subducted oceanic crust, proportions of melts of subducted sediments, and the influx of depleted (or enriched) mantle.

**Mon: 25**

### **The Pliocene pyroclastic succession of Ani, Armenian-Turkish border: geochronology, geochemistry and paleomagnetic constraints**

**Hripsime Gevorgyan<sup>1,2</sup>, Uwe Kirscher<sup>3</sup>, Christoph Breitkreuz<sup>1</sup>, Khachatur Meliksetian<sup>2</sup>, Arsen Israyelyan<sup>2</sup>, Valerian Bachtadse<sup>4</sup>, Daniel Miggins<sup>5</sup>, Anthony Koppers<sup>5</sup>**

<sup>1</sup>*Institute of Geology, TU Bergakademie Freiberg, Bernhard-von-Cotta-Straße 2, 09599 Freiberg, Germany;* <sup>2</sup>*Institute of Geological Sciences, National Academy of Sciences of Armenia, Marshal Baghramyan Avenue, Yerevan 0019, Armenia;* <sup>3</sup>*Terrestrische Paleoklimatologie, Department of Geosciences, Eberhard Karls University Tuebingen, Sigwartstr. 10, 72076 Tuebingen, Germany;* <sup>4</sup>*Department of Earth and Environmental Sciences, Geophysics, Munich University, Theresienstr. 41, 80333 Munich, Germany;* <sup>5</sup>*College of Earth, Ocean, and Atmospheric Science, Oregon State University, Corvallis, OR, USA*

Post-collisional Late Miocene to Holocene volcanic activity in Eastern Anatolia led to the formation of voluminous alkaline and high-K calc-alkaline volcanic rocks of highly variable composition ranging from basalt to rhyolite. Both the East Anatolian and the Armenian volcanoes record a large-scale regional magma generation in the lithospheric mantle usually associated with slab-breakoff processes. Nearly identical trace element patterns in these rocks provide strong evidence for a genetic relationship between the lavas and pyroclastic rocks from East Anatolia (Turkey) and those from the western border of the Aragats Volcanic Province (AVP) in Armenia.

The Ani pyroclastic succession crops out on the western periphery of Aragats volcano, near the Anipemza and Kharkov villages, situated on the Armenian-Turkish border, on both sides of Akhuryan river canyon. The Ani sequence commences with a c. 15 m thick package of Plinian pumice fall deposits that show conspicuous upward coarsening and enrichment of lithic fragments. It is covered by an 18 m thick yellow-colored pumice-rich (~ 40 vol%) dacitic to trachydacitic ignimbrite sheet. Based on i) the geochemical data obtained from selected pumice, bulk rock and fallout deposits, ii) the spatial distribution and thickness of the pyroclastic unit (~32 m), and iii) the geomagnetically reconstructed direction of the pyroclastic flows, the eruption center is presumably located in the nearby eastern periphery of the Kars Plateau in Turkey. According to available geological relationships of the Ani ignimbrites with dolerite basalts of the Akhuryan canyon, as well as new <sup>40</sup>Ar/<sup>39</sup>Ar age determinations and magnetostratigraphy, the Ani ignimbrites are referred to the late Upper Pliocene or the Gauss normal polarity chron.

## 5c) Intraplate volcanism, mantle plumes and continental breakup

Wednesday, 25/Sep/2019: 1:00pm - 3:00pm

Session Chair: Stephan Homrighausen (GEOMAR Helmholtz Centre for Ocean Research Kiel)

Session Chair: Guillaume Jacques (Bundesanstalt für Geowissenschaften und Rohstoffe)

Location: Schloss: S10

### Session Abstract

Volcanic island chains are believed to be produced by long-lived stationary thermal anomalies, where hot material rises in the form of a plume from the deep mantle to the base of the lithosphere. The classical model predicts a plume-head often associated with Large Igneous Provinces (LIPs) and continental breakup. The mantle plume theory has been recently questioned and alternative models, such as tectonic related processes (plate model) were introduced.

We welcome any contribution from geochemistry, geochronology, geophysics and tectonics. Questions to be addressed include but are not restricted to: Do mantle plumes rise from the base of the lower mantle? Do they tap ancient reservoirs of recycled materials? Is continental breakup triggered by mantle plumes or vice versa? What is the causal link between major volcanism and plate tectonics?

### Lecture Presentations

1:00pm - 1:30pm *Session Keynote*

#### Did Gondwana breakup trigger the formation of a(nother) Large Igneous Province in the southwestern Indian Ocean?

Christine Meyzen<sup>1</sup>, M. Maia<sup>2</sup>, J.P. Morgan<sup>3</sup>, T. Waight<sup>4</sup>, C. Hemond<sup>2</sup>, A. Marzoli<sup>1</sup>, A.Y. Borisova<sup>5</sup>, H. Sato<sup>6</sup>

<sup>1</sup>Università degli Studi di Padova, Italy; <sup>2</sup>CNRS-Université de Bretagne Occidentale, France; <sup>3</sup>Royal Holloway, University of London, UK; <sup>4</sup>University of Copenhagen, Denmark; <sup>5</sup>GET, Université Paul Sabatier, CNRS, France; <sup>6</sup>Senshu University, Kanagawa, Japan

Opening of the southwestern Indian Ocean during the complex break-up of the Gondwanan supercontinent may have led to the isolation of continental slivers by progressive ridge jumps and to the formation of a large igneous oceanic plateau. Poor magnetic and bathymetric data coverage and poor sampling in this region result in the chronology and spatial ridge configuration consecutive to Gondwana break-up being rather conjectural, however recent plate tectonic reconstructions point to the formation of a Large Igneous Province at ~83 Ma which includes the Crozet Bank (CB), and the Del Cano, Conrad (CR) and Aphanasy Nikitin (ANR) Rises. These reconstructions mainly rely on the identification of an extinct rift lying in the contours of anomaly C33 separating the CB, Del Cano and CR. However, there is an asymmetric distribution of both magnetic anomalies C34 (to the North of CR) and C31-32 (encompassing CB) relative to this structure. In addition, dredging of abundant continental rocks along the Ob seamount crowning the CR, coupled with its anomalous gravity signal, raises the question whether this seamount is of oceanic origin or might have captured some continental material during break-up. The extreme EM1-like isotopic signature exhibited by most lavas from the CR is consistent with the latter assumption, as is the pronounced EM1-like signature of lavas from its closest counterpart, the ANR. However, this EM1-like component appears to be an isotopically heterogeneous low <sup>206</sup>Pb/<sup>204</sup>Pb end member at the basin scale. Furthermore, none of these low <sup>206</sup>Pb/<sup>204</sup>Pb end members meet the isotopic criteria to be the same low <sup>206</sup>Pb/<sup>204</sup>Pb end-member mantle source of the oldest islands (Possession and East) of the Crozet archipelago. However, in Sr-Nd-Pb isotopic space, two samples from the Conrad Rise closely resemble those of the oldest Crozet islands, and more surprisingly those of the distant Reunion-Mauritius and St Paul-Amsterdam hotspot island chains. The isotopic similarity of these samples with the C component attests to the presence of a large fraction of this end-member in their mantle source, while the weaker signals of EM and DM components suggest that the source has not behaved as an open

mixing system during most of its evolution, suggesting a long-term isolation from convection mixing. We suggest that the C-like component might hence be sourced from the African large low-shear-velocity province, while the EM1 component might represent continental remnants inherited from the Gondwana break-up that only reside at shallow levels within the upper mantle.

**1:30pm - 1:45pm**

### **What geology tells about the role of mantle plumes in Pangea dispersal**

**A.L. Peace<sup>2</sup>, J.J.J. Phethean<sup>3</sup>, D. Franke<sup>1</sup>, G.R. Foulger<sup>3</sup>, T. Doré<sup>4</sup>, N. Kuszni<sup>5</sup>, J.G. McHone<sup>8</sup>, S. Rocchi<sup>7</sup>, C. Schiffer<sup>6</sup>, M. Schnabel<sup>1</sup>, J.K. Welford<sup>2</sup>**

<sup>1</sup>BGR, Germany; <sup>2</sup>Department of Earth Sciences, Memorial University of Newfoundland, St. John's, Canada;

<sup>3</sup>Department of Earth Sciences, Durham University, UK; <sup>4</sup>Equinor (UK) Ltd., One Kingdom Street, London W2 6BD, UK;

<sup>5</sup>University of Liverpool, School of Earth and Environmental Sciences, Liverpool, UK; <sup>6</sup>Department of Earth Sciences Uppsala University Villavägen 16, Uppsala, Sweden; <sup>7</sup>Dipartimento di Scienze della Terra, Università di Pisa, Pisa, Italy;

<sup>8</sup>Dexters Lane, Grand Manan, New Brunswick E5G3A6, Canada

The breakup of Pangaea was accompanied by extensive, episodic, magmatic activity. Several Large Igneous Provinces (LIPs) formed, such as the Central Atlantic Magmatic Province (CAMP) and the North Atlantic Igneous Province (NAIP). Notwithstanding the prevalent assumption that continental breakup is engineered by thermal anomalies that rise from the deep mantle, continental rifts often coincide with aborted rift basins, major rift-orthogonal shear zones, or triple junctions. We present the chronology of Pangaea breakup and related large-scale magmatism. We review the Triassic formation of the Central Atlantic Ocean, the breakup between East and West Gondwana in the Middle Jurassic, the Early Cretaceous opening of the South Atlantic, the Late Cretaceous separation of India from Antarctica, and finally the formation of the North Atlantic in the early Cenozoic. We demonstrate that throughout the dispersal of Pangaea, major volcanism typically occurs distal from the locus of rift initiation and initial oceanic crust accretion. There is no location where extension propagates away from a newly formed LIP. Instead, at LIPs there are major lithosphere-scale shear movements, aborted rifts and splinters of continental crust rifted far out into the oceanic domain. Thus, this review highlights significant spatial-temporal mismatches between the locations of LIPs and the axes of disintegration of Pangaea. Rifting and breakup driven primarily by far-field extensional forces, with magmatism occurring as a consequence, under strong lithospheric control, is much more consistent with observations that are common throughout the regions we review.

**1:45pm - 2:00pm**

### **New constraints on the evolution of Mesozoic rifting in the Eastern Cordillera of Colombia**

**Martin Reyes Correa, Jonas Kley**

*University of Göttingen, Geoscience Center, Göttingen, Germany*

The Eastern Cordillera of Colombia is bounded by the Middle Magdalena Valley basin in the west and by the Llanos Foothills in the east. It is an exceptional case of a Mesozoic rift basin that became inverted during the Cenozoic Andean Orogeny to form a high mountain range. Both the eastern and western margins of the Eastern Cordillera were thrust over the adjacent post-rift basins during inversion, resulting in a complex combination of thick-skinned and thin-skinned structures. The geological evolution of the rift basins in the study area is key to understanding the structural configuration of basins both in the Eastern Cordillera and the Middle Magdalena Valley. As of now, the influence of the geometry and evolution of the synrift and postrift successions has been only inferred at the depth range and level of detail covered by industry-design seismic acquisition. Nevertheless, the presence of outcropping structures and exposed Mesozoic units allow to revisit and re-evaluate the kinematics of these structures in the Eastern Cordillera, through detailed geological mapping with a focus on stratigraphic and structural data. Surface mapping can be correlated with subsurface data in order to analyze the timing and sense of fault displacements, and constrain the evolution of structures in the Middle Magdalena Valley, particularly by use of structural modeling. The timing of rifting and age ranges of

synrift units are constrained by new U/Pb zircon dating of the volcanism event(s) developed during the rifting phase. All of this new information will be combined to generate a consistent model of thrust belt evolution including the geometry and evolution of inherited structures in the Eastern Cordillera and Middle Magdalena Valley basin. Our first new geochronological data suggest that the rifting events were associated initially to the break-up of Pangea.

**2:00pm - 2:15pm**

### **The evolution of intraplate volcanoes in extensional tectonic environments: constraints from João de Castro Seamount, Azores**

**René H.W. Romer<sup>1</sup>, Christoph Beier<sup>1,2</sup>, Karsten M. Haase<sup>1</sup>**

<sup>1</sup>GeoZentrum Nordbayern, Friedrich-Alexander Universität Erlangen, Germany; <sup>2</sup>Department of Geosciences and Geography, University of Helsinki, Finland

Intraplate magmatism in tectonically influenced environments may lead to the formation of both large, central volcanoes and linear eruptive centres along narrow rift zones. In the Eastern Azores both, volcanic islands and seamounts are influenced by a combination of intraplate magmatism and extensional lithospheric stresses forming volcanic edifices oriented along the regional tectonic stress field. The volcanic rift zones are in part directly linked to the magmatic activity of the Azorean central volcanoes. However, it is unclear how the formation of central volcanoes is initiated and whether volcanism along the rift zones represents an early or a late stage of volcanic evolution.

The João de Castro seamount is an active, solitaire, submarine central volcano that is influenced by NE-SW extensional stresses along the ultraslow-spreading Terceira Rift. New bathymetric data reveal that João de Castro is similar to other Azorean central volcanoes, where rift zones adjoin the central volcano in the NW. In contrast to other Azorean volcanoes, however, structural features of João de Castro are remarkably well defined over the entire edifice, i.e. the linear eruptive centres emerge from the flanks and top area of the edifice into distal areas of the central edifice. This suggests that the magma transport system of the central volcanoes and rift zones is connected. Here, we test whether the structural connection between central volcano and rift zone can be used to reconstruct the initial formation phase of João de Castro using new bathymetric, petrographic and geochemical data of a set of volcanic glasses and whole rocks sampled during cruises M113 and M128 with R/V *Meteor*. Our new data will reveal whether João de Castro formed above an already established volcanically active rift system or if the linear eruptive centres along the rift zones are the result of shallow dikeing from the main volcanic edifice. We interpret that João de Castro seamount may represent a transitional stage in the evolution between an early volcanic rift zone and the mature voluminous central volcanoes known from most Azorean Islands and thus may be representative of the early stages of intraplate volcanic evolution.

**2:15pm - 2:30pm**

### **Geochemical and isotopic characterization of single olivine-hosted melt inclusions**

**Mischa Böhnke, Felix Genske, Andreas Stracke**

*Institut für Mineralogie, Westfälische-Wilhelms Universität Münster, Corrensstr. 24, 48149 Münster, Germany*

Whole rock MORB and OIB samples are widely used to infer the present and past composition of Earth's mantle [1]. Basalts represent mixtures of melts from different mantle reservoirs. However, the geochemical and isotopic composition of the produced basalts are variably affected by processes such as partial melting, melt mixing and contamination during ascent through the crust. All of these processes obscure the true magnitude of source heterogeneity. In contrast, olivine-hosted melt inclusions (MI) from basalts reflect individual melts, trapped during melt extraction and melt evolution in the shallow mantle and crust. Especially olivines with high Mg# (>85) are promising targets for MI analysis because they likely contain near-primary melt compositions at an earlier stage of melt aggregation than the erupted lavas. Hence studying the isotopic composition of MI can yield insights into Earth's mantle beyond what can be learned from whole rock basalts.

A number of MI studies with in-situ methods (SIMS, LA-ICP-MS) have revealed significant variation in radiogenic isotopes (Pb, Sr, Nd) within single lava flows, but the precision and accuracy of these methods are limited by low ion yields due to small sample sizes and the need to correct for isobaric interferences [2]. Conventional MC-ICP-MS on chemically purified samples provides improved precision and accuracy at the cost of additional labor, as isolating single MI for analytical work is difficult and time intensive.

In this study, we developed a new time-efficient method to isolate and extract MI from their host crystals using a miniaturized core drill. After non-destructive characterization via EMPA, samples are dissolved in acids for the separation of Sr (and Nd) by low-blank, miniaturized cation exchange chromatography with total procedural blanks of < 1 pg Sr. The

analysis of MI samples with less than 10 ng of Sr allows resolving small isotopic variations within individual lava flows. This information, when combined with trace element data, can be used to distinguish source information from more recent processes such as partial melting, mixing, and crustal contamination. To validate our method and to get further insights into the processes shaping Earth's mantle, we processed well characterized Ankaramite samples from the islands of Flores and Tristan da Cunha. First results support the notion that the mantle is isotopically more heterogeneous than suggested by the observed lavas.

[1] Stracke, A., (2012), *Chem. Geol.*, 330:274-299; [2] Jackson, M.G. and Hart, S.R., (2006), *Earth Planet. Sci. Lett.*, 245(1-2):260-277.

**2:30pm - 2:45pm**

### **Formation of Megacryst Phases by Interaction of Aillikite Melts with Lithospheric Mantle—Evidence from HP-HT Experiments and Natural Samples from the Arkhangelsk Province, Russia**

**Yannick Bussweiler<sup>1</sup>, Alexey Kargin<sup>2</sup>**

<sup>1</sup>*University of Münster, Germany;* <sup>2</sup>*Institute of Geology of Ore Deposits, Petrography, Mineralogy and Geochemistry, Moscow, Russia*

Kimberlites are rare volcanic rocks that are economically and scientifically important because they carry a diverse cargo of mantle xenoliths, xenocrysts (e.g. diamond), and megacrysts. The latter are large nodules (> 1 cm) commonly composed of the minerals garnet, orthopyroxene, clinopyroxene, and ilmenite. Megacrysts are commonly divided into a Cr-rich and a Cr-poor suite, but their respective origins are still debated. Recent studies have proposed that they may form due to varying degrees of interaction between proto-kimberlite melts and the surrounding lithospheric mantle (Bussweiler et al. 2018).

It was recently suggested that aillikite melts may act as the proto-kimberlite melt based on a comparison of the chemistry of their respective olivines (Nosova et al. 2018). Thus, aillikites can potentially pre-condition the lithospheric mantle by forming Cr- and Ti-rich megacrysts that are later sampled by subsequent kimberlite eruptions. The Arkhangelsk Province, Russia, is a good natural laboratory to test this hypothesis because both kimberlites and aillikites occur (along with related ultramafic alkaline rocks) and also contain Cr-rich megacrysts (Kargin et al. 2017).

Here, we further test this idea by simulating the interaction of aillikite melts with depleted lithospheric peridotite (harzburgite) in high-pressure and high-temperature (HP-HT) reaction experiments using a multi-anvil press. Starting mixtures were prepared from synthetic compounds to produce a typical aillikite composition (Tappe et al. 2006) and a typical cratonic harzburgite composition (McDonough & Rudnick 1998). Experiments were performed at 4 GPa and 1200°C at varying weight proportions of aillikite (0, 10, and 50%) reacting with harzburgite. The experimental results are compared with natural samples of megacrysts as well as orthopyroxene-garnet-ilmenite xenoliths from the Grib kimberlite, Arkhangelsk Province, Russia.

[1] Bussweiler, Y., Pearson, D.G., Stachel, T. and Kjarsgaard, B.A., 2018. *Mineralogy and Petrology*, 112(2), pp.583-596; [2] Kargin, A. V., Sazonova, L. V., Nosova, A. A., Lebedeva, N. M., Tretyachenko, V. V., & Abersteiner, A. (2017). *Lithos*, 292, 34-48; [3] McDonough, W.F. and Rudnick, R.L., 1998. *Reviews in mineralogy*, 37, pp.139-164; [4] Nosova, A., Sazonova, L., Kargin, A., Pervov, V., Lebedeva, N. and Shcherbakov, V., 2018. In *EGU General Assembly Conference Abstracts*, 20, p. 12352; [5] Tappe, S., Foley, S.F., Jenner, G.A., Heaman, L.M., Kjarsgaard, B.A., Romer, R.L., Stracke, A., Joyce, N. and Hoefs, J., 2006. *Journal of Petrology*, 47(7), pp.1261-1315.

2:45pm - 3:00pm

### Experimental melting of mixed lherzolite + kaersutite-rich metasome in the garnet stability field

**Tobias Grützner<sup>1</sup>, Yannick Bussweiler<sup>1</sup>, Jasper Berndt<sup>1</sup>, Stephan Klemme<sup>1</sup>, Dejan Prelević<sup>2,3</sup>**

<sup>1</sup>University of Münster – Institute for Mineralogy, Münster, Germany; <sup>2</sup>University of Mainz – Institute of Geoscience, Mainz, Germany; <sup>3</sup>University of Belgrade - Faculty of Mining and Geology, Belgrade, Serbia

It is well known that the high Na/K alkaline basalts from intraplate continental and oceanic settings demonstrate substantial geochemical similarities suggesting comparable petrogenesis. In the early seventies it was proposed that these lavas are produced by a small degree of partial melting of a peridotitic mantle source but more recent data show that the trace element and isotopic signatures of high Na/K alkaline basalts from intraplate continental and oceanic settings may be derived from a more enriched source than the fertile lherzolitic mantle. Several models are introduced for this enrichment, including recycling of oceanic lithosphere into the Earth's convecting mantle with subsequent transformation into pyroxenitic/eclogitic lithologies, "digestion" of enriched lithospheric mantle via subduction, delamination, or interaction with plumes as well as metasomatic mantle enrichment which may lead to the formation of volatile-rich veins in oceanic and continental mantle lithosphere.

In our experimental study, we simulate melting processes within the veined metasomatized mantle at 1-4 GPa. We combine synthetic lherzolite (KLB-1) with a natural kaersutite-rich metasome from Kula Volcanic Region, Western Anatolia, in which these rock types make up two halves each capsule, in order to systematically monitor the effects of the P-T change on the major and trace element compositions of the melt infiltrating the peridotite. Experimental samples were then analyzed with EPMA and LA-ICPMS.

Below 1250 °C two distinctive melt compositions are produced: the metasome-melt has similar SiO<sub>2</sub>, but much higher K<sub>2</sub>O (9 wt.%) contents compared with the infiltration-melt produced within peridotitic part by melt-mantle interaction due to the assimilation of opx and ol crystallization. The infiltration melts are silica-rich (up to 50 wt.% SiO<sub>2</sub>), with low Na<sub>2</sub>O/K<sub>2</sub>O ~1, resembling Alpine-Himalayan orogenic belt high-K calc-alkaline and shoshonitic lavas.

Infiltration melts produced at 1 GPa strongly resemble Kula intraplate lavas, not only on major elements but also in trace element pattern. With varying temperature, we were able to cover the entire range of erupted lava in Kula – from basanite to phonotephrite.

These experiments illustrate that melting of mixed source regions is not simply a question of producing and mixing two melt types; rather, the melt produced in the rock with the lower melting temperature reacts with the mantle peridotite, changing its mineralogy and taking up some of its components.

## Poster Presentations

Tue: 15

### Demenitskoy Smt. (East Atlantic) and the importance of small, isolated intraplate seamounts in the ocean basins

**Xiaojun Long<sup>1</sup>, Jörg Geldmacher<sup>1</sup>, Kaj Hoernle<sup>1,2</sup>, Folkmar Hauff<sup>1</sup>, Jo-Anne Wartho<sup>1</sup>, Dieter Garbe-Schönberg<sup>2</sup>**

<sup>1</sup>GEOMAR Helmholtz Centre for Ocean Research Kiel; <sup>2</sup>Institute of Geosciences, Christian-Albrechts-University Kiel

The world's ocean basins are dotted with thousands of solitary seamounts or small, isolated seamount clusters, which are apparently not related to mantle plumes (too short-lived, no linear hotspot track or age progression) or extensional fracture zones (no edifice alignment). Such small-volume volcanism has been largely neglected, remains poorly surveyed and is rarely sampled. In a pilot study of the Canary Basin (central East Atlantic), lavas from several isolated seamounts (< 3200 m height) were dredged and geochemically analyzed. Results indicate that seamounts even within a spatially small area (~1000 km) can apparently be created by completely different geodynamic processes: intraplate, ridge and fracture zone volcanism. Of particular

interest is the solitary guyot-shaped Demenitskoy Smt. that rises 3,200 m high on ~110 Ma old oceanic crust. The estimated subsidence model age ( $^377$  Ma) and calculated  $^{40}\text{Ar}/^{39}\text{Ar}$  recoil model age ( $87.8 \pm 2.2$  Ma;  $2\sigma$ ) indicate intraplate formation on 20-30 Ma old lithosphere, consistent with the major and trace element composition of the alkaline Demenitskoy lavas suggesting small degrees of melting and high-pressure magma fractionation. Their moderately enriched Nd, Pb (double-spike) and Hf isotopic compositions (e.g.,  $^{206}\text{Pb}/^{204}\text{Pb}_{\text{in}} = 18.87\text{-}19.01$ ,  $^{207}\text{Pb}/^{204}\text{Pb}_{\text{in}} = 15.60\text{-}15.61$ ,  $^{143}\text{Nd}/^{144}\text{Nd}_{\text{in}} = 0.51295\text{-}0.51297$ ) could be explained by a mixture of the global common mantle HIMU endmember or the “C” component (Hanan and Graham, 1996, *Science* 272) with the local upper mantle MORB source. As evident by the depletion of heavy REEs ( $(\text{Sm}/\text{Yb})_n = 1.9\text{-}3.1$ ), the Demenitskoy magma source must contain residual garnet. If formed from garnet pyroxenite (eclogite) instead of garnet peridotite, melting could have been as shallow as 1.3 GPa (~44 km) (e.g. Hirschman and Stolper, 1996, *Contr. Min. Petrol.* 124) and could therefore have occurred at the base of 20-30 Ma old (~50-60 km thick) lithosphere. Although the cause of Demenitskoy volcanism is still enigmatic, gravity measurements and elastic flexure modelling indicate that the most of the world’s seamounts are not related to deep-sourced mantle plumes but are instead formed relatively close to mid-ocean ridges (Watts et al. 2006; *JGR*, SE 111), as suggested for the Demenitskoy Seamount. Our study is therefore also a plea for the long overdue systematic investigation of small-scale, isolated seamount volcanism, which could be used to map the composition of the upper mantle beneath the ocean basins in more detail than reflected by high-degree spreading center magmatism.

**Tue: 16**

### **Double Age progressive hotspot tracks – Primary EM I-type and secondary HIMU mantle plumes in the South Atlantic**

**Stephan Homrighausen<sup>1</sup>, Kaj Hoernle<sup>1,2</sup>, Hongpu Zhou<sup>1</sup>, Jo-Anne Wartho<sup>1</sup>, Folkmar Hauff<sup>1</sup>, Reinhard Werner<sup>1</sup>, Dieter Garbe-Schönberg<sup>2</sup>**

<sup>1</sup>GEOMAR Helmholtz Centre for Ocean Research Kiel, Germany; <sup>2</sup>Christian-Albrechts-University of Kiel, Germany

The age progressive Tristan-Gough and Shona volcanic chains in the southern South Atlantic are characterized by a common EM I-type signature. The oldest portions of these submarine hotspot tracks were overprinted by HIMU-type late-stage volcanism. The superimposed HIMU-type Seamounts were emplaced ~30-50 Ma after the underlying EM I-type basement formed and point to a complex evolution with multiple source areas. We report new  $^{40}\text{Ar}/^{39}\text{Ar}$  ages and geochemical data (trace elements and Sr-Nd-Pb-Hf isotope ratios) from Late Cretaceous lavas from the continental extension of the Tristan-Gough track. The common St. Helena HIMU-type signature and the temporal and spatial proximity to the Walvis Ridge HIMU volcanism imply a genetic connection. Together with new  $^{40}\text{Ar}/^{39}\text{Ar}$  age data from three Walvis Ridge Seamounts, the HIMU volcanism displays an age progressive trend, pointing to a stationary HIMU melt anomaly. Interestingly, HIMU volcanism in the entire Southeast Atlantic and Southwest Africa is focused on the Tristan-Gough, Discovery and Shona tracks, close to their continental extensions. The Shona HIMU volcanism, for example, can be traced from the oldest portion of the Shona track to basalts and melilitites of the Western Cape Province (Janney et al., 2002, *J. Petrol.* 43, 2339-2370) and several Group I kimberlites (i.e., Monastery, Kaalvallei, Frank Smith, Thaba Putsoa, De Beers, Jagersfontain and Wesselton) in Southwest Africa (Collerson et al., 2010, *Physics of the Earth and Planetary Interiors* 181, 112-131; Janney and Bell, 2017, 11th Int. Kimberlite Conf. 11IKC-4630). The secondary and age progressive Walvis and Shona HIMU lineaments have similar plate velocities as predicted by the submarine EM I-type hotspot tracks, supporting stationary HIMU melt anomalies in the vicinity of the EM I mantle plumes. The presently active locations of the EM I-type Tristan-Gough, Discovery and Shona hotspots overlie the margin of the African Large Low Velocity Province (LLSVP), whereas the St. Helena HIMU-type melt anomalies (including St. Helena) are located above a more central portion of the LLSVP. We propose that the EM I and HIMU hotspots sample distinct portions of the African LLSVP.

Tue: 17

**Geochemical evolution of the Main Deccan Volcanic Province, NW-India****Patrick A. Hoyer<sup>1</sup>, Karsten M. Haase<sup>1</sup>, Marcel Regelous<sup>1</sup>, Frédéric Fluteau<sup>2</sup>**<sup>1</sup>*GeoZentrum Nordbayern, FAU, Erlangen, Germany;* <sup>2</sup>*Institut de Physique du Globe de Paris, Paris Diderot University, Paris, France*

Continental flood basalt provinces (CFBs) were formed during catastrophic events with the eruption of enormous volumes of mainly tholeiitic basalts within a relatively short period of time. These massive volcanic eruptions often correlated with periods of widespread environmental changes, global mass extinction and continental break-up. The Deccan Traps in northwest India are connected to the active Réunion mantle plume and volcanism was shown to migrate southwards due to northward movement of the Indian Plate across the plume. Age dating suggests that most of the lavas erupted between 66.4 and 65.4 Ma but that the eruption volume apparently increased significantly during the last stages of volcanism (Sprain et al., 2019). Thus, significant variations in mantle melting and sources are expected in the different Deccan lava formations, many of which have not been studied geochemically. Here we present the first geochemical data of samples drilled from the paleomagnetically defined 3500 m thick composite section of the Main Deccan Volcanic Province (Chenet et al., 2009). The about 150 drill cores cover almost the complete Deccan stratigraphy from the Jawhar to Mahabaleshwar formations and will be analysed for major and trace elements as well as for Sr, Nd, Hf and Pb isotope ratios. Preliminary data show that the MgO contents in the basalts range from 12 to 4 wt.% with the most primitive basalts occurring in the lower lava formations. Large variations of K/Ti ratios between 0.2 to 1.5 in basalts with 9 wt.% MgO indicate variable magma sources. Highly variable ratios of immobile incompatible trace elements between and within the different Deccan sections imply variable assimilation of crustal components and multiple mantle sources (e.g. Nb/Th = 1.0 to 18.1; Ba/Nb = 4.4 to 56.0; Zr/Nb = 9.4 to 26.4). These combined geochemical data provide more detailed information about the relations between the different lava flows and potential changes of source regions as well as melting processes and dynamics during the formation of the Deccan CFB.

[1] Chenet et al., 2009. *J. Geophys. Res.* 114; [2] Sprain et al., 2019. *Science* 363, 866-870.

Tue: 18

**Storage, transport and emplacement of low-ti dacites in the Southern Paraná-Etendika LIP: Geochemical characterization and implications for trans-atlantic correlations****Matheus Silva Simões<sup>1</sup>, Evandro Fernandes Lima<sup>2</sup>, Lucas May de Magalhães Rossetti<sup>2</sup>, Carlos Augusto Sommer<sup>2</sup>, Lucy Takehara Chemale<sup>1</sup>**<sup>1</sup>*Geological Survey of Brazil, Brazil;* <sup>2</sup>*Federal University of Rio Grande do Sul*

The Paraná-Etendeka Large Igneous Province (PELIP) was emplaced during the early stages of the Gondwana break-up at ~134 Ma. The southern portion of this province is composed of basalts and basaltic andesites, which are interleaved with silicic volcanic rocks in the top of the pile. The low-Ti metaluminous dacites from PELIP, known as Palmas type/Caxias do Sul- sub-type, have large volume (~20,000 km<sup>2</sup>), very high magmatic temperatures (1000-1100°C), low water content (<2wt.%) and viscosities comparable with those of andesitic magmas (10<sup>4-5</sup>Pa s). Geobarometry indicate their maximum depth of generation at ~15 km, in the ductile-brittle transition zone of the crust. They are the product of low-pressure fractional crystallization of contaminated basalts, with large amounts of crustal assimilation. Their storage was very short, since they erupted in less than 1Ma, and their transport was characterized by an efficient drainage system, with structurally-controlled conduits passing through a loose crust, where progressive extension was taken place. The volume of PELIP silicic volcanic rocks in Brazil is ~3/4 of the total, and they are considered to be emplaced as lava flows, domes, coulees and SR-type lavas. In Namibia, the volume of silicic units is ~1/4 and they are described as rheomorphic ignimbrites. Trans-Atlantic correlations based on geochemistry reinforce the affinity of Caxias do Sul magma-type (Brazil) with the Grootberg unit (Namibia). Although, in TiO<sub>2</sub> x Fe<sub>2</sub>O<sub>3(t)</sub> and Zr/Y

x  $\text{Fe}_2\text{O}_{3(t)}$  diagrams there are overlaps with the Wereldsend unit, and distinct Zr/Nb patterns of units from Brazil and Namibia are evident. The abundance of Pb is a distinctive feature between the two parts of PELIP. In Brazil they have Pb amounts close to those of basalts: ~2-6 ppm, while in Namibia the basalts display this same range of Pb (<6 ppm), but the silicic volcanic rocks have 10-30 ppm. Decreasing Pb assimilation from the bottom to the top of the silicic units in Namibia is demonstrated by the decrease of Pb/Cu ratios (from 2 to 0.5). In Brazil all silicic rocks have Pb/Cu inferior than 0.4. Pb contents of basaltic and silicic rocks have strong correlation with Sr-Nd-Pb isotopes, with  $r^2$  values of ~0.5 for Brazilian samples and ~0.7 for Namibian samples. We suggest that, during assimilation and fractional crystallization (AFC) processes, the Brazilian silicic rocks assimilated dominantly granites and gneisses from the basement. The AFC process for Namibian silicic units was ruled by major assimilation of basement (meta)sedimentary rocks as shale, slate and schist.

## 5d) The role of subduction zones on Earth's dynamic evolution

Tuesday, 24/Sep/2019: 3:45pm - 5:30pm

Session Chair: Stephan König (Universität Tübingen)

Location: Schlossplatz 4: SP4 201

### Session Abstract

Subduction zones are an important factor of a dynamic Earth. Subduction of material into the mantle leads to a clash of oxidized surface material with Earth's reduced interior. As such evolving atmospheric oxygenation and increased redox contrast between surface and mantle has played a crucial role in mantle-crust-atmosphere interaction through geological time. Metamorphic reactions in the forearc and short-circuit recycling of some components affects the nature of arc magmatism, while long-term subduction recycling leads to distinct signatures of deep-originated plume-derived magmas. Moreover, secular mantle evolution may occur in response to continuous billion-year long input of changing surface material. Therefore, high pressure metamorphic belts, arc- and plume-related volcanic rocks as well as direct mantle samples provide important perspectives on surface-interior interaction while encompassing different time spans. We welcome contributions across all fields of the Earth Sciences including but not limited to mineralogical, (isotope-) geochemical, petrological investigations and field studies addressing the effect of subduction recycling and an evolving surface on Earth's dynamic evolution.

### Lecture Presentations

3:45pm - 4:15pm

*Session Keynote*

#### Mantle controls on the variability of chalcophile elements in subduction-related magmas

**Frances E. Jenner**

*The Open University, United Kingdom*

The Earth's mantle is chemically and isotopically heterogeneous. This variability can be attributed to processes such as prior melt extraction, retention or enrichment and recycling of crustal components during subduction of the oceanic slab or delamination of the continental crust. Thus, variability in the mantle and the mantle wedge should have increased throughout the history of the Earth. In addition to mantle heterogeneity, global subduction related magmas show extreme variations in compositions that can be attributed to variable slab-to-mantle-wedge fluxes.

A variety of increasingly sophisticated tools (e.g., stable isotopes) and across disciplinary approaches (i.e, the merging of the fields of metamorphic and igneous petrology) have been used to place constraints on the role

of the subducting slab on controlling the variability of subduction-related magmas. Some of the chalcophile elements are extremely enriched in subduction-related magmas compared to MORB (e.g., As, Sb, Tl, Bi), which demonstrates the instability of their mineral hosts during subduction. However, the contents of other redox sensitive chalcophile elements (e.g., Se, S, Cu, Ag and Au) of subduction-related magmas are commonly lower than average primitive MORB magmas. These findings indicate that the abundances of many redox sensitive elements in arc magmas are controlled by the mantle wedge and not the subducting slab. However, studies regarding the potential for chalcophile element variability in the mantle and the relative partitioning of chalcophile elements during mantle melting versus crustal processes lags behind studies of the lithophile elements. Consequently, it is not currently possible to use of chalcophile elements abundances of subduction-related magmas to place constraints on conditions in the mantle wedge.

Here I present new data for mantle-derived melts from various global locations to demonstrate that trends in chalcophile elements that have previously been attributed exclusively to fractional crystallisation are in fact dominated by mantle heterogeneity and differences in degree of melting of the source. In addition, I demonstrate a previously undocumented difference in the relative partitioning of the chalcophile elements during mantle melting versus crustal processes that can be used to place constraints on the causes of heterogeneity in the mantle and the mantle wedge.

**4:15pm - 4:30pm**

### **Deserpentinization is not the reverse of serpentinization: implications for redox budget transfer and the oxidation of arc-magma source zones**

**Katy Evans<sup>1</sup>, Ron Frost<sup>2</sup>**

<sup>1</sup>Curtin University, Australia; <sup>2</sup>University of Wyoming, USA

Serpentinites are chemically simple but the sequence of reactions as they hydrate and dehydrate is complex. It has been proposed that redox budget released by dehydrating serpentinites is the long-sought answer to the question of the source of oxidation for the source zone for arc magmas. However, a number of aspects of deserpentinization need to be better understood to test this hypothesis. One such aspect is the possibility that the redox budget added to rocks during serpentinization is released during deserpentinization.

To assess this possibility it is necessary to consider the consequences of four major differences between serpentinization and deserpentinization: (1) serpentinization is not isochemical, but deserpentinization is likely to be isochemical, except for volatiles; (2) serpentinization is commonly externally fluid-buffered, while deserpentinization is commonly internally rock-buffered; (3) serpentinization involves interactions between fluids and rocks that are initially far-from-equilibrium and deserpentinization involves production of fluids that are close to fluid–rock equilibrium; and (4) the length scale of equilibrium during serpentinization is orders of magnitude smaller than the length scale of equilibrium during deserpentinization. The implications of these differences for redox budget transfer have not yet been explored in detail, but are discussed briefly here.

**4:30pm - 4:45pm**

### **Tracing atmospheric oxygenation with selenium isotopes in mantle melts**

**Aierken Yierpan, Stephan König, Jabrane Labidi, Johannes Redlinger, Maria Isabel Varas-Reus, Ronny Schoenberg**

*Isotope Geochemistry Group, Dept. of Geosciences, Eberhard Karls Universität Tübingen*

Selenium behaves as a chalcophile element in magmatic systems. Stable Se isotopes fractionate during redox reactions and can thus be used to trace Earth's surface redox evolution [1]. Marine sediments show significant Se isotope variation, with  $\delta^{82/76}\text{Se}$  values ranging between  $-3\%$  and  $+3\%$ , and an apparent shift towards lighter values from Precambrian ( $\sim+0.5\%$ ) to Phanerozoic ( $\sim-0.2\%$ ) times [1, 2, 3]. In contrast, Se isotope variability in mantle-derived melts, based on a limited dataset, is rather small yet still resolvable ( $\delta^{82/76}\text{Se}$  values  $\sim-0.3\%$ – $+0.3\%$ ) [4, 5, 6]. Because there is little Se isotope fractionation (within  $\pm 0.09\%$ ; 2 s.d.) caused by partial melting or magma differentiation [5], Se isotope variations in basaltic melts might track recycling

of surface materials due to the contrasting difference in both Se abundances and isotope compositions between the igneous and surface reservoirs [e.g., 1, 5].

In this work, we present new high-precision Se isotope data for a suite of well-characterized MORB glasses from the Atlantic ridge, influenced locally by the Shona and Discovery plumes. Previous studies of these basalts revealed that recycled components were incorporated in their mantle sources [e.g., 7]. The samples devoid of plume influences show similar  $\delta^{82/76}\text{Se}$  values as average MORB ( $-0.16 \pm 0.13\%$ ; 2 s.d.,  $N = 27$ ) previously reported for the Pacific-Antarctic ridge [5]. In contrast, the samples influenced by enriched components originating mainly from the Discovery plume show heavier  $\delta^{82/76}\text{Se}$  values. For the first time, we show that Se isotope ratios are correlated with sulfur isotope ratios, as well as radiogenic isotope tracers. This illustrates a binary mixing between the depleted mantle and subducted components, which must be of sedimentary origin. We constrain the Se isotope composition of the recycled component and compare it to literature data for sediments. We further address the implication of our results in the context of ancient redox conditions of the Earth's surface.

[1] Stüeken (2017) *Rev in Min & Geochem* **82**, 657-682; [2] Mitchell et al. (2016) *EPSL* **441**, 178–187; [3] Pogge Von Strandmann et al. (2015) *Nat Commun* **6**, 10157; [4] Yierpan et al. (2018) *G-cubed* **19**, 516–533; [5] Yierpan et al. (2019) *GCA* **249**, 199–224; [6] Kurzawa et al. (2019) *Chem Geol*; [7] Labidi et al. (2013) *Nature* **501**, 208–211.

**4:45pm - 5:00pm**

### **Simulating mantle metasomatism by reacting carbonate-rich sediment with peridotite at forearc mantle P-T conditions**

**Fatma Gülmez, Dejan Prelevic, Stephan Buhre, Jennifer Günther**

*JGU University of Mainz, Germany*

In the subduction zones recycling of the crustal material to the mantle wedge introduce silica-rich components and volatiles to depleted mantle lithologies, which reappear in the arc lavas commonly of andesitic compositions. The silica-undersaturated and extremely K-rich lavas typically do not appear in the active volcanic arc setting and if occur they represent more an exception. Rather than homogeneous peridotite, their source is heterogeneous with the metasomatic assemblages - metasomes - situated in the veins within peridotitic wall-rock, originated through the melt-mantle interaction at the plate boundaries during the previous subduction.

The Late Cretaceous Pontide arc is a unique subduction zone where the Si-undersaturated ultrapotassic lavas were produced within the forearc basins under the control of extensional tectonics due to a slab roll-back mechanism. The general geochemical and isotopic aspects of Pontide ultrapotassic rocks indicate the involvement of at least two different components: i) silicic melts responsible for extreme enrichment of potassium and LIL elements, and ii) carbonatitic melts that induced silica deficiency with high MgO and CaO contents.

In order to put more constraints on the origin of Pontide ultrapotassic lavas, we performed a series of 2GPa experiments in a piston-cylinder apparatus at a temperature range of 800-900°C. Our ultimate aim was to produce metasomes that would be able to produce Si-undersaturated ultrapotassic melts in a second stage melting, in relatively cold forearc mantle. We combine carbonate-rich sediment (marl) with either harzburgite or lherzolite, in which these rock types make up two halves each capsule, in the presence of water (20 wt. % of the marl volume).

In all our reaction experiments the thin reaction layer, as well as pocket-like domains within the peridotitic parts of the capsules, clinopyroxene and phlogopite were produced. In addition to that, dolomite was observed within the mantle lithologies regardless of temperature condition. We placed a layer of diamond aggregates at the bottom of the inner capsule with the aim of trapping initial melts/fluids from marl melting in which two different melt compositions, silica and calcium-rich were revealed.

**5:00pm - 5:15pm****Preliminary experimental results on phase relations in the system  $K_2O$ - $MgO$ - $Al_2O_3$ - $SiO_2$ - $H_2O$  at 7-12 GPa to understand phase relations after deep subduction of continental crust****Dennis Berkels<sup>1</sup>, Hans-Joachim Massonne<sup>1</sup>, Thomas Fockenberg<sup>2</sup>**<sup>1</sup>Universität Stuttgart, Germany; <sup>2</sup>Ruhr-Universität Bochum, Germany

Diamond-bearing felsic rocks from the German Erzgebirge in Saxony and the Kokchetav Massif in Kazakhstan indicate deep burial of continental crust material to depths of more than 150 km. The subduction of oceanic crust and lithospheric delamination with lower crust involved are possible mechanisms to form these rocks [1,2]. Previous experimental studies with metapelitic bulk compositions show the importance of dense high-pressure phases like stishovite and  $KAlSi_3O_8$  with hollandite structure forming at about 10 GPa which can result in densities of felsic continental crust material exceeding those of the surrounding mantle and further subsidence and subduction [3,4,5]. In addition, newly derived thermodynamic data in the System  $K_2O$ - $MgO$ - $Al_2O_3$ - $SiO_2$ - $H_2O$  (KMASH) indicate the stability of further potassium bearing phases like Si-wadeite, dark and white mica coexisting with kyanite or OH-topaz, garnet and orthopyroxene.

The KMASH-system represents a simplified chemical system for silicon-rich rocks which is used in this study to simulate phase relations in metapelitic rocks at conditions of 7-12 GPa and 700-1200°C on the one hand and, on the other, to optimize thermodynamic databases. For this purpose, various synthetic gels were prepared and kept in a multi-anvil Walker-type apparatus at constant P-T-conditions. Chemical analyses of the products were performed with the electron microprobe and the scanning electron microscope.

Experimental products of aluminium-rich bulk compositions obtained at pressures below 10 GPa exhibit phengitic mica, with rising silicon contents at increasing pressures, almosilicates, Si-wadeite, and coesite or stishovite. Also the magnesium-rich run products lack previously expected phlogopite, but contain unusual silica-rich micas close to the hypothetical aluminium-free end-member  $KMg_{2.5}[Si_4O_{10}](OH)_2$ . Phengite decomposes and K-hollandite forms at pressures of about 10 GPa, resulting in relatively high rock densities as expected from thermochemical calculations. In Mg-rich bulk compositions also garnet with minor marjorite components and orthopyroxene formed at these conditions. Synthesis experiments were also performed at 9 GPa to better characterize the coexistence of di- and trioctahedral silica-rich micas and the extent of their solid-solution series.

[1] Andersen, T.B., Jamtveit, B., Dewey, J.F., Swensson, E., 1991, *Terra Nova*, 3, 303-310; [2] Massonne, H.J., 2005, *International Geology Review*, 47, 792-804; [3] Irifune, T., Ringwood, A.E., Hibberson, W.O., 1994, *Earth and Planetary Science Letters*, 126, 351-368; [4] Dobrzhinetskaya, L.F. and Green, H.W., 2007, *Journal of Metamorphic Geology*, 25, 83-96; [5] Ono, S., 1998, *Journal of Geophysical Research*, 103, 18253-18267

**5:15pm - 5:30pm****Alternation of shoshonitic and calc-alkaline magmatism during subduction migration – a cross section through Aegean magmatism****Anna Schaarschmidt<sup>1</sup>, Karsten M. Haase<sup>1</sup>, Reiner Klemd<sup>1</sup>, Panagiotis C. Voudouris<sup>2</sup>, Vasilios Melfos<sup>3</sup>**<sup>1</sup>GeoZentrum Nordbayern, FAU Erlangen-Nürnberg, Germany; <sup>2</sup>Department of Mineralogy-Petrology, University of Athens, Greece; <sup>3</sup>Department of Mineralogy, Petrology and Economic Geology, Aristotle University of Thessaloniki, Greece

The Cenozoic magmatic activity in the Aegean followed the southward migration of the Hellenic subduction zone due to slab retreat from the Rhodope Massif in the north to the South Aegean Volcanic Arc (SAVA). The continuous subduction of the African Plate beneath Eurasia caused metasomatism of the mantle wedge and mixing with variable slab components. Based on new and published data, we define a succession of magmatic centers coeval with back-arc basin formation ranging in age from 32 Ma in the NE to active volcanoes in the SW at the SAVA. Partial melting of metasomatized mantle generated magmas that all show a typical arc signature with enrichment of the fluid-mobile large ion lithophile elements (LILE) and depletion of Nb and Ta relative to La, but above that, Aegean magmas show distinct chemical variations.

In NE Greece calc-alkaline magmatism alternates with shoshonitic magmatism at a short distance within a few million years. New major element, trace element and Sr, Nd, Pb isotopic data on the shoshonitic Maronia pluton and the calc-alkaline Kassiteres pluton in NE-Greece reveal a mantle source, that was enriched by different components of fluids and sedimentary melts from the subducting slab. The shoshonitic pluton has higher LILE, Pb, P and Ce/Yb than the calc-alkaline pluton, but both have similar variations in Sr, Nd, and Pb isotopes. Sr and Nd isotopic ratios show, that the magma evolution is controlled by fractional crystallization without a significant influence of crustal assimilation. Further south, on the islands of Samothraki and Limnos, the magma composition shows more crustal input, but high-K calc-alkaline and shoshonitic magmatism remains active at the same time. High P contents in the shoshonitic magmas possibly indicate the input of P-rich sediments. Thus, the amount and the composition of subducted sediments may have changed in the past 32 Ma. The trace element and isotope composition of the calc-alkaline Kassiteres pluton in NE Greece generally resembles the Pliocene to Pleistocene arc magmas from the SAVA, which indicates a similar genesis. Therefore, the variability of arc magmatism during subduction migration is revealed along this cross-section through the Aegean.

## Poster Presentations

Tue: 19

### Molybdenum isotope systematics at convergent plate margins – the effect of deep sea pelagic sediments

**Qasid Ahmad<sup>1</sup>, Martin Wille<sup>1</sup>, Carolina Rosca<sup>2</sup>, Stephan König<sup>2</sup>**

<sup>1</sup>University of Bern, Switzerland; <sup>2</sup>University of Tübingen, Germany

Subduction zone magmatism at convergent plate margins is closely associated with the formation of continental crust through geological history. These settings are also characterized by the highest mass fluxes between crust and mantle, where the slab-derived fluids (and possibly slab melts) facilitate the element transfer into the mantle wedge. Recently, Mo and its isotopes have been applied to investigate the slab-mantle wedge transport and ultimately the incorporation of this element into arc lavas. Significant stable Mo isotope fractionation is induced during Earth's surface processes leading to distinct Mo concentrations and Mo isotopic ratios in different marine sediments. One sedimentary endmember are Mn-rich deep sea pelagic clays with a high authigenic Mo concentration, which dominate the sedimentary subduction input at the Tonga Trench due to its remote location from continental shelf areas.

To better constrain if and how subducted sediment imprint the recycling of Mo at subduction zones, new Mo isotopic analyses on arc volcanic rocks (basalts and basaltic andesites) from the Tongan subduction zone are presented. Additionally, pelagic sediment and altered oceanic crust samples from IODP site 595 were analyzed. Together with major and trace element concentration data, this approach allows us to calculate the isotopic mass balance between Mo input by subducted continental material (SCM) and Mo output at arc magmatism. This is necessary to evaluate the role of sub arc processes on the Mo budget and the isotopic input on Mo to the deeper mantle. In comparison with published Mo isotopic data from other convergent margin settings with different SCM input, our new data will constrain the role of sediments on Mo recycling at arc settings.

Tue: 20

### Variations in Fe<sup>3+</sup>/Fe<sup>T</sup> ratios in igneous amphiboles as a function of oxygen fugacity in hydrous arc magmas

**Barbara C Ratschbacher<sup>1</sup>, Claire E Bucholz<sup>1</sup>, Jennifer M Jackson<sup>1</sup>, Natalia V Solomatova<sup>1,2</sup>, Emma S Sosa<sup>1</sup>**

<sup>1</sup>California Institute of Technology, United States of America; <sup>2</sup>Ecole Normale Supérieure Lyon, LGLTPE, Lyon, France

The oxygen fugacity of arc magmas potentially plays an important role in generating the calc-alkaline compositional trend that characterizes continental crust, the composition of magmatic fluids, and the transport of redox-sensitive elements during formation of ore deposits. In extrusive and intrusive igneous rocks, magmatic

oxygen fugacity is determined either through Fe-Ti oxybarometry, bulk rock/glass  $\text{Fe}_2\text{O}_3/\text{FeO}$  contents, and/or equilibrium among coexisting ferromagnesian silicates (e.g., olivine-orthopyroxene-spinel oxygen barometer). However, subsolidus re-equilibration or secondary alteration as well as the restriction of these minerals to certain rock types can make it problematic to constrain magmatic in a wide range of calc-alkaline rocks.

The mineral amphibole, through the incorporation of  $\text{Fe}^{2+}$  and  $\text{Fe}^{3+}$  into its crystal structure and its common occurrence in hydrous arc magmas, has the potential to provide quantitative constraints on variations in magmatic . However, the relationship between the  $\text{Fe}^{3+}/\text{Fe}^{\text{T}}$  ratio in amphibole and ,  $\text{Fe}^{3+}$  incorporation into the amphibole structure, and amphibole chemistry are not well understood.

To address these questions, we will present major and minor element composition (determined via EMPA), hydrogen isotopes and  $\text{H}_2\text{O}$  contents (determined via SIMS), and  $\text{Fe}^{3+}/\text{Fe}^{\text{T}}$  ratios analyzed by single crystal synchrotron-based Mössbauer spectroscopy (SMS) of natural and experimentally synthesized amphiboles, which crystallized from magmas recording a wide range of magmatic (dNNO = -1.0 to +3.0, log units below and above the Ni-NiO buffer).

We will show that a combination of  $\text{H}_2\text{O}$  contents and hydrogen isotope compositions in natural amphibole allows distinguishing between post-crystallization dehydrogenation and associated oxidation of  $\text{Fe}^{2+}$  to  $\text{Fe}^{3+}$  and magmatic  $\text{Fe}^{3+}/\text{Fe}^{\text{T}}$  ratios. Forthcoming magmatic  $\text{Fe}^{3+}/\text{Fe}^{\text{T}}$  ratios will be related to sample constrained through Fe-Ti oxide oxybarometry and used to explore (1) ferric iron accommodation in amphibole and (2) a potential change of  $\text{Fe}^{3+}/\text{Fe}^{\text{T}}$  ratios with changing magmatic in each sample.

**Tue: 21**

### **Variably depleted mantle wedge sections beneath Tonga – insights from stable Zn isotope systematics in arc lavas**

**Carolina Rosca<sup>1</sup>, Stephan König<sup>1</sup>, Martin Wille<sup>2</sup>, Marie-Laure Pons<sup>1,3</sup>, Ronny Schoenberg<sup>1</sup>**

<sup>1</sup>Department of Geosciences, University of Tübingen, Germany; <sup>2</sup>Institute of Geological Sciences, University of Bern, Switzerland; <sup>3</sup>CERGE, Aix Marseille Universite, France

Transition metal stable isotope systematics of terrestrial igneous reservoirs may help to better understand the recycling behavior of these elements through Earth's interior. However, isotopic variations of 'heavy' elements caused by magmatic processes are subtle and difficult to resolve. Within this scope we have improved our precision on MC-ICP-MS Zn isotope measurements to  $< \pm 0.02$  ‰ on  $^{66}/^{64}\text{Zn}$  for single runs (2SD, multiple digestions of reference materials) using a  $^{64}\text{Zn}$ - $^{67}\text{Zn}$  double spike. With this step forward, we investigated the systematics governing the Zn transport and isotope fractionation at subduction zones. For this study, the focus was set on volcanic rocks from the Tongan subduction zone - where the pre-subduction mantle wedge composition ( $\text{Sm}/\text{La} \gg 1$ ) is amongst the most depleted for worldwide arc settings. Additional analyses of samples from IODP site 595 provide an insight to the input to this subduction factory. Primitive lavas (basalts and basaltic andesites;  $\text{MgO} > 5$  %) display subtle, yet resolvable Zn isotopic variations between the central Tonga islands Tofua, Late, Kao and Ata, as well as differences to  $^{66}/^{64}\text{Zn}$  values of MORB and the subduction input. In addition, Zn-isotopes and Zn/La are correlated with fluid indices such as Ba/Th, suggesting potential mobilization of Zn from the subducting plate and/or overlying sediments into the mantle wedge prior to melting. Yet, striking negative correlations observed between Zn-isotopes and Sm/La of the lavas point towards a link between Zn-isotopic composition and relative mantle depletion beneath individual volcanic edifices. The presence of variably depleted mantle-wedge sections along the Tonga arc has been previously suggested on the basis of radiogenic Sr-Nd-Pb isotope systematics (e.g. Todd et al. 2017). This is the first time that such a situation is also depicted by Zn isotopes. However, concomitant occurrence of these features complicates a straightforward deconvolution of the Zn-isotope variations seen in arc lavas and fluid-induced transport cannot be simply ruled out and will be discussed in this presentation.

[1] Todd E., Gill J.B., Pearce J.A. (2012). A variably enriched mantle wedge and contrasting melt types during arc stages following subduction initiation in Fiji and Tonga, southwest Pacific. *Earth and Planet. Sci. Lett.* 335-336, 180-194.

Tue: 23

## Crustal recycling within the mantle: reaction experiments on the origin of ultrapotassic magma

**Anastasia Zemlitskaya<sup>1</sup>, Dejan Prelevic<sup>1,2</sup>, Stephan Buhre<sup>1</sup>, Michael W. Förster<sup>3</sup>**

<sup>1</sup>Institute of Geosciences, J.-J.-Becher-Weg 21, Johannes Gutenberg University, 55099 Mainz, Germany; <sup>2</sup>Faculty of Mining and Geology University, Đušina 7, 11000 Belgrade, Serbia; <sup>3</sup>Department of Earth and Planetary Sciences, 16 University Avenue, Macquarie University, NSW 2109, Sydney

Geochemical data imply that the high-K calc-alkaline, shoshonitic, and lamproitic magmas typical for Mediterranean orogenic volcanism cannot be sourced from a normal four-phase mantle (Conticelli *et al.*, 2009). Alternatively, partial melting of potassium-rich metasomes comprised of phlogopite-bearing pyroxenites within peridotitic mantle is proposed to produce high-K melts resembling lamproitic composition (Forster *et al.*, 2017). However, the genesis of metasomes is still unclear.

We simulate non-equilibrium reaction experiments that are analogue to the vein-plus-wall-rock melting model (Foley, 1992), to produce phlogopite-rich metasomes as a result of interaction between crustal-derived melt and mantle. In addition, three different capsule architectures [mantle:crust:water; 1:1:10 wt%; b)1:2:20 wt%; c) 1,1:2:10 wt%] were builded.

For this approach, we selected three crustal compositions to localize the direct precursors of the metasomes: i) sediment (ODP161-976, Mediterranean Sea); ii) allanite-bearing gneiss (Schwarzwald); iii) lawsonite blueschist (Tavşanlı zone). The experiments were carried out at 2 GPa pressure and between 850 °C and 900°C temperature with run durations of two weeks. Each material was combined with pre-synthesized synthetic mantle material (harzburgite: AVX, lherzolite: KLB-1).

The first two capsule architectures consisted of each crustal material and pre-synthesized synthetic mantle material in a two-layer arrangement without being mixed. The third capsule architecture consisted of two different mantle materials simultaneously in contact with different crustal components. To recover the melts, a diamond fluid-trap was added beneath the crustal component of the third capsule architecture.

Our observation on the experimental charges offers valuable informations concerning variation in metasome components and metasome genesis itself. The composition of the reactants is crucial for the modal composition of the produced metasomes. The modal composition varies in the appearance and amount of the key minerals: phlogopite, diopside, pargasite and enstatite.

[1] Conticelli, S., Guarnieri, L., Farinelli, A., Mattei, M., Avanzinelli, R., Bianchini, G., Boari, E., Tommasini, S., Tiepolo, M., Prelević, D. & Venturelli, G. (2009). Trace elements and Sr-Nd-Pb isotopes of K-rich, shoshonitic, and calc-alkaline magmatism of the Western Mediterranean Region: Genesis of ultrapotassic to calc-alkaline magmatic associations in a post-collisional geodynamic setting. *Lithos* **107**, 68-92; [2] Foley, S. F. (1992). Vein-plus-wall-rock melting mechanisms in the lithosphere and the origin of potassic alkaline magmas. *Lithos* **28**, 435-453; [3] Forster, M. W., Prelevic, D., Schmuck, H. R., Buhre, S., Veter, M., Mertz-Kraus, R., Foley, S. F. & Jacob, D. E. (2017). Melting and dynamic metasomatism of mixed harzburgite plus glimmerite mantle source: Implications for the genesis of orogenic potassic magmas. *Chemical Geology* **455**, 182-191.

## 5e) Stable isotope fractionation at high temperatures

### Poster Presentations

Tue: 24

#### Chromium isotope fractionation during magma differentiation

**Felix Genske, Andreas Stracke, Stephan Klemme**

*Institut für Mineralogie, Westfälische Wilhelms-Universität Münster, Corrensstrasse 24, 48149 Münster, Germany*

The stable Cr isotopic composition ( $\delta^{53}\text{Cr}$ ) of the bulk silicate earth (BSE) is defined with a relatively large uncertainty at  $-0.12 \pm 0.10\text{‰}$  (2 S.D.), owing to variability in chondrites [1, 3, 5] and terrestrial mantle rocks [2, 6]. Variability reported for mantle-derived materials ranges from  $-1.36\text{‰}$  to  $+1.22\text{‰}$  in  $\delta^{53}\text{Cr}$  [2, 6], including peridotites, basalts and alteration products thereof. The origin of this variability remains unclear, because detailed studies on the behaviour of Cr isotope fractionation during magmatic processes, such as partial melting, fractional crystallisation and degassing, remain scarce.

In addition, international rock standards are rarely reported, making it difficult to assess whether inter-laboratory bias contributes to the uncertainty of the absolute value and range of BSE's stable Cr isotopic composition. We report an extended  $\delta^{53}\text{Cr}$ -data set on USGS and GSJ-GRS materials, covering ultramafic (peridotite) to more silicic (andesite) compositions.

The proposed  $\delta^{53}\text{Cr}$  value of BSE [e.g., 1, 4, 5] is based on compiled data of mantle rocks, including primitive basalts and pristine peridotites, yet providing a range that is larger than analytical uncertainty of about 0.02 to 0.04‰. Hence, part of the variability could be introduced by magmatic processes. Moreover, small-scale stable Cr isotope fractionation in lunar rocks could be caused by fractional crystallisation [1].

Here, we present high-precision double-spike Cr isotope data (MC-ICPMS, TIMS) on well-characterised oceanic island basalt (OIB) suites from Tristan da Cunha, Gough island and the Azores islands to assess the magnitude of Cr isotope fractionation during magmatic differentiation. The different OIB suites allow inferring the Cr isotope fractionation along distinct liquid lines of descent at variable P-T-fO<sub>2</sub> conditions, and also allow estimating the  $\delta^{53}\text{Cr}$  of their mantle sources. Across the studied islands we observe isotopic fractionation with  $\delta^{53}\text{Cr}$  ranging from  $-0.35$  to  $-0.05\text{‰}$  on Corvo, from  $-0.17$  to  $+0.16\text{‰}$  on Gough and from  $-0.12$  to  $-0.01\text{‰}$  on Tristan. However, in lavas with MgO >5 wt.% and Cr >100 ppm the Cr isotopic composition is largely controlled by magmatic differentiation, whereas higher  $\delta^{53}\text{Cr}$  in more evolved lavas may be attributed to Cr volatility. After correction for these processes we estimate parental  $\delta^{53}\text{Cr}$  across the islands (Tristan:  $-0.10\text{‰}$ , Gough:  $-0.12\text{‰}$ , Corvo:  $-0.09\text{‰}$ ), all within the range of the BSE.

[1]Bonnand, P. et al. (2016). GCA175; [2]Farkaš, J. et al. (2013). GCA; [3]Moynier, F. et al. (2011). Science331, 1417–1420; [4]Schoenberg, R. et al. (2008). ChemGeol249; [5]Schoenberg, R. et al. (2016). GCA; [6]Xia, J. et al. (2017). EPSL464.

Tue: 25

#### Sulfur isotope measurements of reference materials using MC-ICP-MS

**Suzette Timmerman, Felix Genske, Andreas Stracke**

*Westfälische Wilhelms-Universität Münster, Germany*

Extreme sulfur isotope heterogeneity in surface reservoirs [1] and differences in isotopic composition between S-species allow for tracing of the global S-cycle. Due to its different valence states and volatility, sulfur can affect the oxidation state of a magma, partitioning of metals in sulfides, and is important in volcanic degassing [2]. Sulfur isotope compositions can provide insights into these processes, due to isotope fractionation of its stable isotopes <sup>32</sup>S, <sup>33</sup>S, <sup>34</sup>S, <sup>36</sup>S.

At the moment sulfur isotope measurements are limited to in-situ ion microprobe analyses of sulfides and through combustion of large quantities of rock powders (>30 µg S) in combination with gas source mass spectrometry. However, there is currently no established method to measure sulfur isotope compositions on small quantities of sulfur from silicate rocks. Therefore, we have developed a method to extract sulfur from

rock powders for measuring the sulfur isotope composition in small quantities of S (1  $\mu\text{g}$  S) with multi-collector inductively coupled plasma mass spectrometry (MC-ICP-MS).

Sulfur is leached out of rock powders (<50 mg) with 2 ml aqua regia overnight at 140°C with a yield of 80 to 100%, and separated by anion exchange chromatography (AG1-X8, 200-400 mesh) resin. Sulfur isotope measurements are conducted in high-resolution mode on a Thermo Scientific Neptune *Plus*, using an ESI APEX-Omega sample introduction system. Oxide and hydride interferences are avoided by measuring on the low mass side of the peak plateau. Sulfate solutions with different S isotope values were measured with standard-sample bracketing and yield reproducible results across analytical sessions. A Merck  $\text{SO}_4$  solution ( $\delta^{34}\text{S} = +4.4\text{‰}$  V-CDT; calibrated by gas source mass spectrometry) is used as a standard and reproduces to better than 0.2‰ for  $\delta^{34}\text{S}$ , 0.2‰ for  $\delta^{33}\text{S}$ , and 0.15‰ for  $\Delta^{33}\text{S}$  during an analytical session of  $\approx$ 16 hours. Bulk rock sulfur isotope compositions will be presented for reference materials; e.g. BHVO-2, BCR-2, and JGb-1.

[1] Canfield and Farquhar (2009) PNAS 106, 8123-8127; [2] Wallace and Edmonds (2011) RMG 73, 215-246.

Tue: 26

## An experimental approach to determine Calcium isotope fractionation between minerals and melts

**Nikolaus Gussone, Jennifer Schwenne, Andreas Stracke, Stephan Klemme**

*Institut für Mineralogie, Universität Münster, Germany*

Calcium is a major element in geological reservoirs on Earth such as the mantle, oceanic and continental crust, sediments and ocean water, and plays important roles for characterizing and quantifying mass transfer between these reservoirs. Recent experimental data, and measurements on natural silicate rocks and minerals provide increasing evidence for significant stable Ca isotope fractionation at high temperatures, between mineral and melt and between different silicate minerals (e.g. [1], [2]). Consequently, Ca isotope ratio may provide additional constraints for identifying different mantle sources, and for characterizing magmatic processes and mass fluxes.

Here, we present initial results from mineral/melt partitioning experiments that were conducted at atmospheric pressure at varying temperatures, to determine Ca isotope fractionation factors between silicate melts and minerals. The synthesized crystalline phases diopside, titanite, perovskite and wollastonite are consistently enriched in light isotopes by 0.1 to 0.2‰ relative to the melt.

Based on the experimentally determined mineral-melt fractionation factors and co-genetic inter-mineral-isotope fractionation factors obtained from lherzolites and eclogites, we modelled the Ca isotope evolution of magma during partial melting of mantle peridotites and crystallization of mantle-derived magmas. Increasing degrees of partial melting leads to an enrichment of heavy Ca in the residual mantle peridotite by up to 0.5 ‰ due to progressive exhaustion of isotopically light clinopyroxene. Generated melts are offset by  $\sim$ 0.1‰ from source, but vary little with increasing extent (and pressure) of melting. Fractional crystallization of a mantle melt, however, can cause significant Ca isotope fractionation during the course of magma crystallization, due to crystallization of isotopically light clinopyroxene and plagioclase. Most of the observed range in Ca isotope variability of Ocean Island Basalts (0.66 to 1.09‰ rel. SRM 915a) relative to the bulk earth value of  $\sim$ 1‰ can thus be explained by the combined effects of partial melting and fractional crystallization, and do not require significant Ca isotope variability in Earth's mantle, e.g., due to recycling of Ca-rich continental materials [3].

[1] Amini M. et al. (2009) Calcium Isotopes ( $\delta\text{Ca-44/40}$ ) in MPI-DING Reference Glasses, USGS Rock Powders and Various Rocks: Evidence for Ca Isotope Fractionation in Terrestrial Silicates. *Geostand. Geoanalytical Res.* 33, 231–247; [2] Huang S. et al. (2010) Calcium isotopic fractionation between clinopyroxene and orthopyroxene from mantle peridotites. *Earth Planet. Sci. Lett.* 292, 337–344; [3] Huang, S. et al. (2009) Ancient carbonate sedimentary signature in the Hawaiian plume: Evidence from Mahukona volcano, Hawaii. *Geochem. Geophys. Geosys.* 10, Doi: 10.1029/2009gc002418.

Tue: 28

## Molybdenum isotope fractionation between melt, exsolved fluid and hydrothermal minerals at the magmatic-hydrothermal transition

**Anne Kaufmann, Thomas Pettke, Edel O'Sullivan, Martin Wille**

*Institute of Geological Sciences, University of Bern, Switzerland*

Molybdenum isotopes of igneous rocks show a much larger variability (up to 0.6‰  $\delta^{98/95}\text{Mo}$ ) than has previously been assumed for the continental crust (0-0.2‰). Two processes have been put forward to account for this, (i) magmatic fractionation (Voegelin et al., 2014) and (ii) source variability delivered from the subducting slab to arc magmas. Moreover, studies focusing on magmatic-hydrothermal mineralisation have discovered a large spread in Mo isotope compositions of molybdenites, which cannot be explained by mass-dependent fractionation alone (Greber et al., 2011, 2014). Data acquired so far document increasingly heavier  $\delta^{98}\text{Mo}$  with progressive hydrothermal evolution (Greber et al., 2014), hinting at significant fractionation between an increasingly heavy aqueous fluid while lighter isotopes are bound in precipitating  $\text{MoS}_2$ . On the other hand, Shafiei et al. (2015) observed the opposite trend with heavier  $\delta^{97/95}\text{Mo}$  values (0.0 - +0.92‰) of early stage molybdenites, followed by a late stage with  $\delta^{97/95}\text{Mo}$  values restricted to -0.31 - +0.27‰. They postulated this to reflect the involvement of multiple fluid types (brine, vapour, or aqueous liquid) with different physico-chemical properties that dominated during the two mineralisation stages. All these observations indicate that significant Mo isotope fractionation can occur during high-temperature processes.

We investigate the magmatic-hydrothermal transition using miarolitic cavities of the Torres del Paine igneous complex (Patagonia, Chile). They formed during successive stages of magma emplacement at shallow crustal levels (0.75 – 1 kbar) and document the magmatic-hydrothermal history from approx. 750°C down to <300°C. Bulk rock  $\delta^{98}\text{Mo}$  ratios vary between +0.05 and +0.46 ‰  $\delta^{98}\text{Mo}_{\text{NIST}}$ , a range reported for other calc-alkaline magmas elsewhere (e.g., Wille et al., 2018; Willbold and Elliott, 2017). Cavity mineral (amphibole, biotite, titanite, and molybdenite) and aqueous fluid isotopic measurements are currently underway; preliminary data indicate that biotite has a very light isotopic signature (<-1‰  $\delta^{98}\text{Mo}_{\text{NIST}}$ ) compared to the bulk rocks, whereas molybdenite exhibits only moderately light  $\delta^{98}\text{Mo}_{\text{NIST}}$  values of -0.24 to -0.20‰. Together, this data set allows the quantification of isotopic distribution coefficients between minerals and aqueous fluid, a necessary step in better understanding the relevant processes producing isotopic variability in the continental crust.

[1] Greber et al. (2011) *GCA*, 75, 6600-6609; [2] Greber et al. (2014) *Lithos*, 190-191, 104-110; [3] Shafiei et al. (2015) *Miner Depos*, 50, 281-291; [4] Voegelin et al. (2014) *Lithos*, 190, 440-448; [5] Willbold and Elliott (2017) *Chem Geol*, 449, 253-268; [6] Wille et al. (2018) *Chem Geol*, 485, 1-13.

Tue: 29

## Lithium chemical and isotope diffusion in natural olivines and its implications on the timing of magmatic events

**Lena K. Steinmann<sup>1</sup>, Martin Oeser<sup>1</sup>, Renat R. Almeev<sup>1</sup>, Maxim Portnyagin<sup>2</sup>, Stefan Weyer<sup>1</sup>**

<sup>1</sup>*Leibniz Universität Hannover, Institut für Mineralogie, Germany;* <sup>2</sup>*Helmholtz Centre for Ocean Research Kiel (GEOMAR), Germany*

Fractional crystallization during cooling of a magma commonly results in a compositional contrast between minerals and the evolving melt causing chemical diffusion. This process frequently generates coupled chemical and isotopic zoning in magmatic minerals. Isotopic zoning can be strong at magmatic temperatures and can be utilized to identify the diffusive origin of zoning and furthermore help reconstructing complex evolution histories of magmatic systems. Recent studies have been investigating the behavior of Li diffusion in olivines, because Li is a fast-diffusing element, with <sup>6</sup>Li diffusing faster than <sup>7</sup>Li, which allows for elucidating relatively fast-paced magmatic events.<sup>1,2</sup> We apply our newly developed *in situ* femtosecond LA-MC-ICP-MS analytical technique for high precision Li isotope profile analyses in minerals with low Li concentration levels to investigate olivines from different geotectonic settings.<sup>3</sup>

## 5) Magmatic systems and experimental petrology

Two major questions are addressed here: (1) Is there a coupling of Li and Fe-Mg chemical zoning and (2) are Li chemical and isotopic composition coupled? If Li chemical zoning is generated by a similar diffusion mechanism to that of Fe-Mg inter-diffusion, Li diffusion profiles are expected to be more expanded, since it has been found that Li diffuses one order of magnitude faster than Fe and Mg.<sup>2</sup> Such expanded Li chemical profiles were observed for samples from the continental intra-plate Massif Central region and also for subduction-related Klyuchevskoy olivines, which yield a more complex growth history than Massif Central olivines. Lithium chemical and isotopic profiles in both samples reveal decreasing Li concentrations from rim to core of the mineral grains and intra-grain isotope variations. Notably, the extent of isotope variation within one profile varies in Massif Central and Klyuchevskoy olivines ( $\Delta^7\text{Li}^{\text{min-max}} = 21.5$  to  $35$  ‰ and  $\Delta^7\text{Li}^{\text{max-min}} = 3.5$  to  $6$  ‰, respectively), whereas the concentration gradient from rim to core is similar. Reasons for this decoupling need to be further clarified but could be related to a combination of diffusion and crystal growth. Consequently, the combination of Li isotopic and chemical zoning profiles might further elucidate processes which are not displayed by the Fe-Mg system and provide information on the time-series of magmatic processes.

[1] Richter et al. (2017); [2] Dohmen et al. (2010); [3] Steinmann et al. (2019)

## 5f) The distribution and influence of volatile elements in the Earth's interior and their exchange with the surface

Wednesday, 25/Sep/2019: 8:30am - 10:30am

Session Chair: Daniel Frost (University of Bayreuth)

Session Chair: Vladimir Matjuschkin (Universität Frankfurt am Main)

Location: Schloss: Aula

### Session Abstract

The Earth's interior is an important reservoir for volatile elements such as carbon, hydrogen, nitrogen and halogens which are exchanged with the surface through the processes of subduction and volcanic outgassing. The mechanisms through which volatile species migrate within the interior, their involvement in melting and metasomatic processes and their influences on transport properties are, however, poorly understood. Similarly, we have an incomplete picture of the seafloor alteration processes that lead to the subduction of volatile species, the forms in which volatile elements are stored in the interior and the processes that lead to their eventual release to the surface. It is also increasingly being recognised that the redox state of the Earth's interior influences and may also be influenced by the occurrence of volatile species. In this session, we welcome contributions from observational, computational and experimental fields that deal with our current understanding of this deep volatile cycle and its implications for the geodynamic and geochemical evolution of the Earth. This might also include geophysical studies on the detection of deep volatiles, variations in the volatile cycle in the past in addition to cosmochemical assessments of how volatiles were accreted to the Earth.

### Lecture Presentations

8:30am - 9:00am *Session Keynote*

#### Role of high pressure hydrous phase in lower mantle dynamics

Eiji Ohtani<sup>1,2</sup>, Itaru Ohira<sup>3</sup>, Jenifer Jackson<sup>4</sup>, Takayuki Ishii<sup>2</sup>, Wen-Pin Hsieh<sup>5</sup>

<sup>1</sup>Tohoku University, Japan; <sup>2</sup>Bayerisches Geoinstitut, University of Bayreuth, Germany; <sup>3</sup>HPCAT, Geophysical Laboratory, USA; <sup>4</sup>California Institute of Technology, USA; <sup>5</sup>Academia Sinica, Taiwan

Volatile cycling is an important process which can affect the structure and dynamics of the earth's mantle.  $\delta$ -phase solid solution is one of the most important candidates which carries water into the lower mantle through slab subduction [e.g.1]. The compressional behavior and spin states of  $\delta$ -(Al, Fe)OOH phases were investigated with synchrotron X-ray diffraction (XRD) and Mössbauer spectroscopy (SMS) at high pressure. We also measured the thermal conductivity under the similar pressure conditions by using time domain thermoreflectance (TDTR) technique [2].

SMS measurements revealed that there is a spin transition of Fe<sup>3+</sup> at pressures between 30 and 45 GPa at room temperature. We observed an anomaly in the compression curve, i.e., minor increase in density and large drop of the bulk modulus,  $K_T$ , resulting in large drop of the bulk sound velocity,  $V_\phi$ , at around 35-40 GPa associated with the spin transition [3]. Similar anomalies due to the spin transitions have been observed also in Fe<sup>3+</sup> bearing NAL phase [4] and siderite FeCO<sub>3</sub> [5] in the upper part of the lower mantle. Our thermal conductivity measurements of  $\delta$ -(Fe, Al)OOH revealed a rapid increase of thermal conductivity with a peak at around 30-40 GPa associated with the spin-transition.

Seismological studies have reported laterally heterogeneous  $\rho$  and  $V_\phi$  in the upper part of the lower mantle [e.g. 6]. Additionally, there are viscosity anomalies in the upper part of the lower mantle [e.g. 7]). Our experiments revealed that  $\delta$ -(Fe, Al)OOH has the elastic and thermal conductivity anomalies associated with the spin transition, i.e., it reduces the bulk sound velocity, and increases the thermal conductivity which may create thermal anomalies in this region. Therefore, the high pressure hydrous phase  $\delta$  existing in the descending slabs may be responsible for the elastic, thermal, and rheological anomalies in the upper part of the lower mantle.

[1] Ohtani et al. (2018) *Jour Asian Earth Science*, 167, 2-10; [2] Cahill, 2004. *Rev. Sci. Instrum.*, 75(12), 5119–5122; [3] Ohira et al. (2019), *Am. Mineral.* in press; [4] Wu et al. (2015) *Earth Plant. Sci. Lett.*, 434, 91-100; [5] Lobanov et al. (2015). *American Mineralogist*, Volume 100, pages 1059–1064; [6] Masters, G. et al. (2000) In Karato et al., Eds., *Geophys. Mono.* 117, p. 63–87, AGU; [7] Rudolph et al. (2015) *Science*, 350, 1349-1352.

**9:00am - 9:15am**

### Formation of diamond from methane-rich fluids

**Vladimir Matjuschkin<sup>1</sup>, Alan B. Woodland<sup>1</sup>, Daniel Frost<sup>2</sup>, Gregory Yaxley<sup>3</sup>**

<sup>1</sup>Universität Frankfurt am Main, Germany; <sup>2</sup>Universität Bayreuth; <sup>3</sup>The Australian National University

Natural diamonds can form by various geochemical reactions, including a solid phase transformation from graphite or precipitation from metasomatic fluids and melts [1]. Each mechanism requires a unique geochemical environment as well as pressure, temperature and oxygen fugacity ( $fO_2$ ) conditions. Our study is focused on the metasomatic origin of diamonds and their formation from reduced, methane-rich fluids. High-pressure experiments were performed using a novel capsule design [2] in a belt and multi-anvil apparatus. We demonstrate that methane-rich fluids are stable at magmatic conditions with log oxygen fugacities approaching IW+0.5 to IW+1 (as monitored by Ir-Fe alloys); conditions which are similar to those prevailing in the upper mantle. Spontaneous diamond crystallization is observed at pressures from 5 to 7 GPa, which marks a minimum pressure for natural diamond stability. Diamond is apparently produced under equilibrium  $fO_2$  conditions with **no** diamond seed crystals added to the experiments. The synthesized diamonds have a natural Raman spectroscopic signature with a sharp peak at 1332 $cm^{-1}$  and are produced within a matter of hours, without employing any metal, metal carbides or carbonatite melt as catalysts. We describe several mechanisms involving hydrogen and silicate melt that can contribute to diamond formation. In addition, we report on the chemical composition of coexisting silicate melt, the incorporation of H into coexisting silicate phases (as measured by FTIR), as well as the compositional characteristics of the fluids from which the diamonds formed.

[1] Smart KA, Chacko T, Stachel T, Muehlenbachs K, Stern R, Heaman LM (2011) Diamond growth from oxidized carbon sources beneath the Northern Slave Craton, Canada: A  $\delta^{13}C-N$  study of eclogite-hosted diamonds from the Jericho kimberlite. *Geochim Cosmochim Acta* 75:6027-6047; [2] Matjuschkin V, Woodland AB, Yaxley GM (2019) Methane-bearing fluids in the Upper Mantle: an experimental approach. *Contrib Mineral Petrol* 174:1

**9:15am - 9:30am**

### Formation of diamonds from reduced COH fluids and their genetic link to pyroxenite/eclogite in the Earth's upper mantle

**Niklas Ottersberg<sup>1</sup>, Jasper Berndt<sup>2</sup>, Niels Jöns<sup>1</sup>, Christopher Beyer<sup>1</sup>**

<sup>1</sup>Institut für Geologie, Mineralogie und Geophysik, Ruhr Universität Bochum, Germany; <sup>2</sup>Institut für Mineralogie, Westfälische Wilhelms-Universität Münster, Germany

The chemical signature of majoritic garnets, found in diamonds recovered from depths exceeding 250 km, suggests a genetic link between the formation of diamond and eclogite/pyroxenite in Earth's deep upper mantle [1,2]. Reduced COH fluids, composed of a mixture of  $CH_4$  and  $H_2O$ , are likely candidates for the diamond-forming fluid [3,4] that reacts with  $Fe^{3+}$ -rich majoritic garnets [5].

We conducted a series of high-pressure and high-temperature experiments from 8 to 16 GPa and 1300 to 1500 °C in the multi-anvil apparatus under Fe-saturated conditions employing the double capsule technique. Starting materials were set as a sandwich of synthetic anhydrous lherzolite on top of a glass layer with andesitic to dacitic compositions. We used stearic acid ( $C_{18}H_{36}O_2$ ), which decomposes into a mixture of methane, water and carbon, as fluid source. Run products were analysed using the electron microprobe for chemical compositions and scanning electron microscopy / Raman spectroscopy to identify graphite/diamond.

Recovered charges crystallized to a sequence of eclogitic melt, garnet websterite and peridotite. Pyroxene in the proximity to peridotite was identified as orthopyroxene, while those close to the crystallized melt are

characterized as clinopyroxene. Garnet in the reaction zone have intermediate compositions in terms of Ca-content and magnesium number ( $Mg\# = Mg/(Mg+Fe)$ ) as proposed between eclogite ( $Mg\# < 65$ ,  $CaO > 8$  wt-%) and peridotite ( $Mg\# > 86$ ,  $CaO < 5$  wt-%). In the ongoing part, we observed the presence of amorphous carbon/diamond in the crystallized melt and reaction layer but not in the peridotite layer.

Our results will contribute to grasp the modes of diamond formation in the sublithospheric mantle. Furthermore, our experiments are aimed at understanding the genesis of pyroxenite in the deep mantle and its role in relieving chemical heterogeneities.

[1] Kiseeva, E.S., Wood, B.J., Ghosh, S., Stachel, T., 2016, *Geochemical Perspective Letters*, 2, 1-9; [2] Beyer, C., Frost, D.J., 2017, *Earth and Planetary Science Letters*, 461, 30-39; [3] Stachel, T., Luth, R.W., 2015, *Lithos*, 220-223, 200-220; [4] Smit, K.V., Stachel, T., Luth, R.W., Stern, R.A., 2019, *Chemical Geology*, In press; [5] Rohrbach, A., Ballhaus, C., Golla-Schindler, U., Ulmer, P., Kamenetsky, V.S., Kuzmin, D.V., 2007, *Nature*, 449, 456-458

**9:30am - 9:45am**

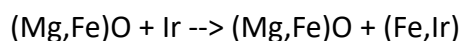
### **Understanding the redox conditions during diamond anvil cells experiments**

**Serena Dominijanni, Catherine A. McCammon, Leonid Dubrovinsky, Daniel J. Frost, Nobuyoshi Miyajima, Tiziana Boffa Ballaran**

*Bayerisches Geoinstitut, Germany*

The distribution and circulation of oxygen in the Earth's interior strongly controls the redox state of the mantle that affects the global geodynamic cycle of the volatile elements. Understanding the oxygen fugacity ( $f_{O_2}$ ) conditions of the Earth's mantle is a crucial issue since it exerts a first order control on subduction, convection, partial melting and metasomatism processes as well as on the minerals phase equilibria. Laser heated diamond anvil cell (DAC) experiments allow us to reach high pressures and temperatures conditions of the deep Earth's interior. However, so far the redox conditions during diamond anvil cell (DAC) experiments have never been constrain. Adopting the redox sensor approach, we investigated the  $f_{O_2}$  variation during DAC experiments using a mixture of synthetic ferropericlasite ( $Mg_{0.75}Fe_{0.25}O$ ) and pure Ir powder in order to crystallize an Fe-Ir alloy and use it to calculate the oxygen fugacity. Double side laser heating experiments were performed employing piston-cylinder type BX90 diamond anvil cells at ID15b, ID27 and ID18 beamlines of the European Synchrotron Radiation Facility (Grenoble, France) where powder X-ray diffraction (XRD) and Synchrotron Mössbauer Source (SMS) data have been collected. After recovering, the samples were chemically characterized using the Energy-Dispersive X-ray Spectroscopy (EDS) and the Electron Energy Loss Spectroscopy (EELS) at Bayerisches Geoinstitut (Bayreuth, Germany).

Preliminary results from powder X-ray diffraction data show that, after heating, an Fe-Ir metal alloy that can be indexed in the Fm-3m space group is formed by the reaction of pure Ir and Fe from ferropericlasite according to the reaction:



The compressibility of the Fe-Ir alloy and ferropericlasite was measured up to  $\sim 60$  GPa and SMS data were collected before and after heating. X-ray diffraction results coupled with energy-dispersive X-ray spectroscopy (EDS) measurements and a simple thermodynamic model indicate that the redox conditions during the DAC experiments were close to the iron-wüstite (IW) buffer, although some inhomogeneity was observed. Further chemical analyses and additional experiments are ongoing to understand the variation of oxygen fugacity in a DAC during laser heating.

9:45am - 10:00am

### The oxygen fugacity of sublithospheric diamond formation and the conditions encountered during their ascent to the surface

**Caterina Melai<sup>1</sup>, Daniel J. Frost<sup>1</sup>, Tiziana Boffa Ballaran<sup>1</sup>, Catherine McCammon<sup>1</sup>, Katharina Marquardt<sup>2</sup>**

<sup>1</sup>University of Bayreuth, Germany; <sup>2</sup>Imperial College, London

Although relatively rare, ferropericlasite appears to be one of the most common inclusions to be found in sub-lithospheric diamonds, which provide some of the only direct evidence for the passage of carbon bearing fluids and melts in the deep mantle. Numerous studies have examined ferropericlasite inclusions in the hope of providing information on the formation conditions of these deep diamonds, which could potentially be in the transition zone or lower mantle. TEM investigations have provided evidence for Fe<sub>2</sub>O<sub>3</sub>-rich phases, such as magnesioferrite, exsolving from the ferropericlasite matrix, which potentially can provide information on the post entrapment conditions experienced by the diamonds during their path to the surface. The ferric iron content of the entire inclusion before exsolution also provides information on the oxygen fugacity ( $fO_2$ ) at which the diamond was formed and, therefore, an indication of the medium from which it was formed. To interpret this information requires a model for the ferric iron content of ferropericlasite as a function of MgO content, P, T and  $fO_2$  conditions up to those where exsolution of Fe<sub>2</sub>O<sub>3</sub>-rich phases occurs. Recent discoveries of many new mixed valence iron oxide phases adds further complexity to this issue.

In order to model the ferric iron content of ferropericlasite multianvil experiments have been performed between 6 – 25 GPa and 1200-1800°C using a starting composition of (Mg<sub>86</sub>Fe<sub>14</sub>)O and (Mg<sub>50</sub>Fe<sub>50</sub>)O plus varying amounts of Fe<sub>2</sub>O<sub>3</sub> (20 %, 10%, 5%). Pt powder was added to the experiments to act as a redox sensor and minor amounts of Ni, Cr, Mn and Na were also added. Samples were then analysed using scanning electron microscopy, the electron microprobe, Mössbauer spectroscopy and X-ray diffraction. In the recovered experiments, ferropericlasite coexists with magnetite-magnesioferrite solid solution up to 10 GPa and Mg<sub>2</sub>Fe<sub>2</sub>O<sub>5</sub>-Fe<sub>4</sub>O<sub>5</sub> solid solution at higher pressures. In the calculation of the oxygen fugacity a ferropericlasite model in the FeO-Fe<sub>2/3</sub>O-MgO system was developed. The results show that magnetite-magnesioferrite solid solution should not be in equilibrium with ferropericlasite in the diamond stability field as the oxygen fugacity would be too high. Our results imply that the exsolution of Fe<sup>3+</sup> rich phases observed in natural samples likely occurred at pressures corresponding to the transition zone or deeper.

10:00am - 10:15am

### Mantle thermometry using sulphide inclusions in diamonds

**Sumith Abeykoon, Anna M. Rebaza, Daniel J. Frost, Vera Laurenz, Nobuyoshi Miyajima**

*Bayerisches Geoinstitut, University of Bayreuth, Germany*

Inclusions contained in diamonds provide some of the only pristine samples from Earth's deep interior. The compositions of syngenetic inclusions can in principle record information on the conditions at the time of entrapment and the nature of the rocks with which the diamond forming media were in equilibrium. If thermometers and barometers could be applied to such samples they would provide information on the deep mantle geotherm. Sulphide inclusions are the most common type of inclusion in natural diamonds and are also widely used for Re-Os dating of diamond formation. Previous studies have measured a significant amount of oxygen in natural sulphide inclusions in diamonds. A systematic parameterization of sulphide oxygen concentration could potentially be used to understand the formation conditions of diamonds. Furthermore, mantle sulphide inclusions sometimes contain additional phases such as molybdenite (MoS<sub>2</sub>) that must have exsolved from the FeS rich liquid after entrapment. Analysis of this exsolution can provide information on the post-entrapment conditions.

We have conducted an experimental study to determine the oxygen concentration in sulphide liquids at conditions of diamond formation and to examine the effects of other components such as Ni, Cu and Mo on the oxygen content and phase relations of sulphide liquids. High pressure (3 – 11 GPa) and high temperature (1573-1973 K) experiments were conducted in a multi-anvil apparatus to equilibrate a mantle peridotite as-

semblage with iron sulphide melts. Ni, Cu, Mo, CO<sub>2</sub>, H<sub>2</sub>O were also added to examine their influences and all runs were performed in graphite capsules. Recovered run products were analyzed for their chemical compositions with the electron microprobe.

We measured significant amounts of oxygen in quenched FeS dominated melts with equivalent FeO contents of up to 16 weight %. The experiments indicate that the oxygen concentration is mainly controlled by the FeO activity in coexisting silicate phases and the temperature. In order to fit the data and to account for the observed FeO dependence, we developed a thermodynamic model using an end-member equilibrium between olivine, pyroxene and FeO in the sulphide melt. Using this relationship with measurements of oxygen concentrations reported in natural sulphide inclusions in diamonds reveals temperatures for lithospheric diamond formation in the range of 1140 – 1410 °C. Pressures for some of these samples can be determined from the proportion of the majorite component in garnet inclusions in the same diamonds allowing an estimation of the geotherm.

**10:15am - 10:30am**

### **Water partitioning between upper mantle minerals and melts**

**Dmitry Bondar, Hongzhan Fei, Tony Withers, Tomoo Katsura**

*University of Bayreuth, Germany*

Water in the Earth's upper mantle is predominantly stored in nominally anhydrous minerals (NAMs) such as olivine, orthopyroxene, clinopyroxene and garnet. Since incorporated water has a strong influence on mantle properties, namely melting temperature, rheology, electrical conductivity and seismic velocity, it is important to know the distribution of water among phases. Knowledge of how water partitions between upper mantle minerals and melts is essential for estimation of water content in incipient melts at different depths, water transport by these melts, and total amount of water in the upper mantle.

There are several studies providing data on water partitioning between NAMs and melts. The most challenging part of these studies is to quench melt coexisting with mineral phases to form glass at elevated pressures (>2 GPa), which is necessary to measure water partitioning with high accuracy. It also becomes more difficult to quench melt with higher Mg/Si ratio into glass, which is necessary in order to crystallize olivine from the melt. Previous studies produced mantle minerals coexisting with quenched melt up to only 5 GPa, namely olivine at ≤3 GPa, orthopyroxene at ≤4 GPa, clinopyroxene and garnet at ≤5 GPa. As a result, there is no systematic pressure, temperature and water content dependence of water partitioning due to the data scattered over the narrow pressure range. Many authors also reported that glasses in some run products were not transparent, which implies micro-crystals may have crystallized in those studies.

The difficulty of quenching melt into glass lies in the insufficient cooling rate. The cooling rates of regular piston-cylinder and multi-anvil experiments used for these purposes are 120°/sec and 500°/sec, respectively. Quenching glass at elevated pressures and at various compositions is important not only for measuring water partitioning, but also for a number of other tasks, such as melt structure studies and partitioning of other components and elements.

The purposes of the present study are (1) to develop a multi-anvil technique allowing much faster cooling rate than conventional ones and (2) to measure water partitioning between upper mantle minerals and melts for a pressure range from 1 to 13 GPa, which covers the whole upper mantle. Our design for a fast-cooling multi-anvil technique has already produced a very high quenching rate (5200°/sec). As a result, completely transparent glass was successfully quenched coexisting with garnet at 6 GPa. We plan to improve the fast quenching technique to allow quenching melts under even wider conditions.

## Poster Presentations

Tue: 30

### The effect of F on the stability of antigorite and the transfer of halogens in the deep mantle

**Stamatis Flemetakis, Stephan Klemme, Arno Rohrbach, Jasper Berndt**

*WWU Münster, Germany*

Halogens are, along with other volatile elements, transferred via subduction of oceanic crust and lithosphere into the mantle. Subduction of serpentinized material enhances the transport of volatiles to the depths because serpentine minerals contain approximately 13 wt.% volatiles including halogens [1]. Understanding the storage of F in serpentine-group minerals can thus improve our comprehension of the deep geochemical cycle of halogens.

We examined the effect of F on the P-T stability of antigorite, i.e. we studied the breakdown reaction: antigorite = forsterite + clinoenstatite + H<sub>2</sub>O. We used natural antigorite (1.2 wt.% Al<sub>2</sub>O<sub>3</sub> and 0.86 wt.% FeO), synthetic forsterite and synthetic enstatite, as starting materials and we doped the experiments with 1.5 wt.% F and variable amounts of H<sub>2</sub>O. The experimental conditions ranged from 2.2 to 5 GPa and 560 °C to 800 °C. We measured F contents of antigorite by EPMA using analytical protocol [2] that we enhanced with new in-house glass standards for halogens [3]. The F content of the antigorite crystals ranged from 0.15 - 0.2 wt.%. Our preliminary results show that minor amounts of F have no significant effect on the P-T stability of antigorite. Additional experimental work will be conducted with higher F contents in order to examine the stability of an F-rich antigorite phase at the same conditions. Interestingly F systematically enters the structure of the mineral despite the presence of a fluid phase in the experimental product. Since our experiments were under F-undersaturated conditions it is demonstrated that F can readily enter the structure of antigorite in significant amounts i.e. 1500-2000 ppm, and thus make it a carrier of F in the deep mantle.

[1] Ulmer and Trommsdorff 1995; [2] Zhang et al., 2015; [3] Flemetakis et al., 2019; in prep.

Tue: 31

### The role of oxygen fugacity on the stability of serpentinites in subduction zones

**Lisa Eberhard, Daniel Frost, Catherine McCammon**

*University of Bayreuth, Germany*

Serpentinization leads to oxidation of the lithosphere both through the formation of magnetite and through the development of raised levels of ferric iron in the serpentine minerals themselves. Natural serpentinites display almost a complete range of possible ferric/ferrous ratios. Although experimental determinations of serpentine stability in subduction zones are in poor agreement, no one has examined whether variations in the ferric iron content might explain these discrepancies. There are also no thermodynamic data available to evaluate the stability of the serpentine ferric iron component. During subduction the partitioning of ferric iron between serpentine and other minerals particularly during dehydration could have important effects on the oxygen fugacity of the mantle, which could have implications for the speciation of fluids and the stability of carbonates, reduced carbon and sulphides.

In high pressure and temperature experiments we have examined the stability of antigorite-bearing serpentine and a carbonated serpentinite (ophicarbonate) as a function of P, T and oxygen fugacity. In these experiments the oxygen fugacity is buffered by using metal oxide assemblages such as Re-ReO<sub>2</sub> and through the equilibrium between graphite and carbonate minerals. Starting materials were natural serpentinites mainly composed of antigorite but different samples were employed with initially high and low ferric/ferrous ratios. Varying proportions of calcium carbonate were then added to some assemblages to create an ophicarbonate. Experiments were performed for approximately 3 days. Run products were examined using the electron microprobe and the ferric/ferrous ratios were determined using Mössbauer spectroscopy.

Antigorite breaks down over a small temperature interval of approximately 50 K. In the presence of carbonate the onset temperature of antigorite breakdown is lowered but the temperature of its final disappearance is unchanged. Increasing the ferric iron content of antigorite appears to be coupled to a small increase in the thermal stability. The results enable the ferric/ferrous ratio of antigorite to be determined as a function of oxygen fugacity. At a buffered oxygen fugacity the ferric iron content of antigorite decreases with temperature and this decrease is even stronger once antigorite starts to breakdown. This means that in a subducting assemblage with a constant bulk ferric/ferrous ratio the oxygen fugacity must increase as antigorite breaks down. This may lead to the oxidation and mobilisation of reduced species in the surrounding slab such as graphite, from organic sources, or sulphides.

## Tue: 32

### Pargasite stability in the upper mantle at H<sub>2</sub>O-undersaturated conditions

**Marija Putak Juricek, Hans Keppler**

*BGI, University of Bayreuth*

Pargasitic amphibole is the most commonly occurring hydrous mineral in mantle xenoliths and investigation of pargasite stability at H<sub>2</sub>O-undersaturated conditions can provide useful constraints for understanding deep water cycle.

While it has been shown that higher alkali content stabilizes pargasite to higher P and T, the effect of water on amphibole stability is not so straightforward. At H<sub>2</sub>O-saturated conditions, alkali elements partition strongly into aqueous fluid and become less available for crystallization of amphibole. As a result, amphibole seemingly becomes stable at higher P and T when less H<sub>2</sub>O is added to the starting material. This observation inspired the hypothesis that pargasite may be an ubiquitous phase in the upper mantle, which contains only a few hundred ppm of H<sub>2</sub>O. However, previous studies determined pargasite stability at H<sub>2</sub>O-saturated conditions, where solid phases coexist with an aqueous fluid during experiments. Such environments are not representative of the nearly dry ambient upper mantle.

Because of the high specific surface area of powders, adsorption of atmospheric H<sub>2</sub>O on fine grained starting materials makes attaining defined H<sub>2</sub>O activities by adding small amounts of water to the sample difficult or impossible. Instead, reduced water activities may be precisely controlled by diluting the water with another inert component. Under such conditions, solid phases are expected to coexist with a low water activity fluid throughout the experiment. As molecular nitrogen is mostly insoluble in upper mantle minerals, we used it in a series of piston cylinder experiments to buffer water activity of the fluid to a desired low value.

Our experiments demonstrate that pargasite is not stable in equilibrium with fluids diluted to  $X_{\text{H}_2\text{O}}=0.1$ , while the amphibole stability field can extend to 4 GPa and above 1100 °C at high and intermediate water activities ( $X_{\text{H}_2\text{O}}=1$  to 0.5). This suggests that the ambient upper mantle has a nominally anhydrous assemblage while regions affected by metasomatic fluids may be more abundant in pargasite, and therefore retain more water, than previously thought.

## Tue: 33

### Tracing redox evolution of arc magmas during amphibole fractionation in the deep crust: Constraints from cumulate xenoliths from Ichinomegata Maar, NE Japan

**Naoya Tsushima, Michihiko Nakamura, Yasuhiro Yanagida, Takeyoshi Yoshida**

*Division of Earth and Planetary Materials Science, Department of Earth Science, Graduate School of Science, Tohoku University*

Oxygen fugacity ( $f\text{O}_2$ ) of subduction zone magmas is higher than that of mid ocean ridge basalt (MORB) or oceanic island basalt. It is still under debate whether the oxidized nature of subduction zone magmas is derived from the mantle source or acquired through their differentiation in the crust (e.g., Lee et al., 2012

Science). Since the valence state of sulfur in the magma is sensitive to the redox state, stability and composition of sulfide and sulfate minerals can be a good tracer of  $fO_2$  of magmas. Amphibole fractionation in arc's deep crust has recently been considered as the primary mechanism for producing calc-alkaline magmas. The Ichinomegata maar, NE Japan, is known for its occurrence of wide variety of deep-crust and upper mantle xenoliths. A recent petrologic study revealed that a series of adcumulate mafic xenoliths from the Ichinomegata, which were confirmed isotopically as cognate, shows good agreement with the experimental study (Nandedkar et al., 2014 CMP) in terms of mineral assemblage evolution and solid solution compositions, and that they are fractionated counterparts of the silicic end-member of their host calc-alkaline magma (Yanagida et al., 2018 G3). Therefore, those cumulate samples may represent the differentiation condition of arc magmas. In this study, we found both pyrrhotite and anhydrite from the xenoliths samples. Almost all the pyrrhotite grains occur as small rounded inclusions mainly in hornblende, whereas some as a relatively large irregular shaped interstitial phase. Magmatic pyrrhotite shows almost constant non-stoichiometric compositions (Fe+Ni+Cu/S) and a trend from Ni-rich to Cu-rich metal composition.

Anhydrite occurs as inclusions in plagioclase of leuco-hornblendite xenoliths. The coexistence of anhydrite and pyrrhotite shows  $fO_2$  of  $\sim +1$  log unit above Ni-NiO buffer, being consistent with the  $fO_2$  calculated from the pyrrhotite non-stoichiometry. These  $fO_2$  are almost the same as the average value of arc magmas and clearly higher than that of MORB. This study shows that the Ichinomegata magma was oxidized already at the early stage of fractionation in the deep crust, suggesting oxidized nature of its source mantle.

**Tue: 34**

### Trace element partitioning between Cl- and S-bearing aqueous fluid and basaltic melt

**Anastasia Zemlitskaya<sup>1</sup>, Roman E. Botcharnikov<sup>1,2</sup>, Insa T. Derrey<sup>2</sup>, Maxim V. Portnyagin<sup>3,4</sup>, Regina Mertz-Kraus<sup>1</sup>, Stephan Buhre<sup>1</sup>, Stefan Weyer<sup>2</sup>, Francois Holtz<sup>2</sup>**

<sup>1</sup>Johannes Gutenberg University Mainz, Germany; <sup>2</sup>Leibniz University Hannover, Germany; <sup>3</sup>GEOMAR, Helmholtz Centre for Ocean Research Kiel, Germany; <sup>4</sup>Vernadsky Institute of Geochemistry and Analytical Chemistry Moscow, Russia

Entrapment of synthetic fluid inclusions in quartz is an efficient experimental approach to study trace element partitioning between magmatic phases. Quartz has a simple composition and a low level of trace elements making it an ideal fluid inclusion host for felsic magmatic/hydrothermal (quartz-saturated) systems which is not however suitable for basaltic systems. Here we present a method of synthetic fluid inclusions in olivine as a tool providing partition coefficients of trace elements between Cl- and S-bearing aqueous fluids and basaltic melts ( $D_{\text{fluid/melt}}$ ). In the experiments we used pre-cracked San Carlos olivine and a natural basaltic melt characteristic for Mutnovsky volcano. The fluid component was added as an aqueous solution with different NaCl and S concentrations.

A sequence of experimental runs was conducted in an internally heated pressure vessel at  $T = 1030$  °C,  $P = 300$  MPa,  $\log fO_2$  close to NNO+1 at fluid-saturated conditions.

The resulted basaltic glasses were analyzed by EMPA and LA-ICP-MS, whereas the synthetic fluid inclusions trapped in the olivine were analyzed by microthermometry and LA-ICP-MS using UV-femtosecond-laser and freezing cell.

Though there is a more challenging analytical approach for fluid inclusions in olivine than in quartz, the first results demonstrate an affinity for the fluid phases ( $D_{\text{fluid/melt}} > 1$ ) for a number of studied elements (e.g., B, Na, S, Cu, Zn, Rb, Cs, Hf, Au, Pb) and relatively low ( $D_{\text{fluid/melt}} < 1$ ) values for others (e.g., Al, Ca, Sr, Ba). Moreover, the data show a significant difference to the fluid-melt partitioning of elements in rhyolitic systems.

## 5g) Reconstructing the evolution (P-T-t-X) of magmatic processes

Tuesday, 24/Sep/2019: 8:30am - 10:00am

Session Chair: Lennart A. Fischer (University of Freiburg)

Session Chair: Bastian Joachim-Mrosko (University of Innsbruck)

Location: Schloss: S10

### Session Abstract

The texture and composition of igneous rocks, minerals and glasses store thermochemical information on the evolution of a magmatic environment, which makes them a time-sensitive recorder of the conditions present during their formation. This session is devoted to all studies that try to decipher and reconstruct the evolution of magmatic processes including the P-T-time path and the composition of magma reservoirs, conduits or lava flows. We welcome natural, experimental and theoretical studies from petrologists, mineralogists and geochemists to cover this topic from different perspectives.

### Presentations

8:30am - 8:45am

#### On the formation of oceanic layered gabbros: drillcore GT1 of the ICDP Oman Drilling Project

Dominik Mock<sup>1</sup>, Benoit Ildefonse<sup>2</sup>, Dieter Garbe-Schönberg<sup>3</sup>, Samuel Müller<sup>3</sup>, David Neave<sup>4</sup>, Jürgen Koepke<sup>1</sup>

<sup>1</sup>Leibniz Universität Hannover, Germany; <sup>2</sup>Université de Montpellier; <sup>3</sup>Christian-Albrechts-Universität zu Kiel;

<sup>4</sup>University of Manchester

As the largest and best-exposed analogue of fast-spreading oceanic crust on land, the Oman ophiolite provides an ideal field laboratory for investigating lower crustal accretion processes at fast-spreading mid-ocean ridges. In the Oman Drilling Project within the frame of ICDP (International Continental Scientific Drilling Program), five 300 to 400 m long cores from the mantle to the dyke/gabbro transition were drilled to sample the entire crust coherently. The core drilled at Site GT1 is located in the Wadi Gideah (Wadi Tayin Massif, Samail ophiolite) and is well embedded within a reference profile through the whole Oman paleocrust established by conventional sampling in that Wadi [1]. GT1 covers the lower part of the plutonic crust which is composed of layered gabbro. In order to understand lower crustal accretion, with a particular focus on the formation of modal layering at different scales, we have investigated this core with diverse petrographic, petrological, bulk-geochemical, and microstructural tools.

The vast majority of cored lithologies are olivine gabbro with subordinate gabbro. In addition, a few coherent, cm-thick troctolitic and ultramafic (dunitic, wehrlitic) layers have been observed. Wehrlitic layers are of particular interest because they imply that moderate water activities locally suppressed plagioclase nucleation during primary crystallization. This is in contrast with the reference profile where no wehrlitic samples were observed. Mineral analyses reveal Mg#s (where  $Mg\# = Mg / (Mg + Fe) \times 100$ ; molar basis) between 74 and 86 in clinopyroxene and Ca#s (where  $Ca\# = Ca / (Ca + Na) \times 100$ ; molar basis) in plagioclase varying between 68 and 87. Most olivines are heavily altered with primary relicts showing Mg#s between 70 and 83. These compositions are in good agreement with those from the reference profile, however, due to the higher spatial resolution by drilling, clear trends on a scale of tens of meters are observed: both Mg# and Ca# show minima at a crustal height of 1050 m above the Moho and increase progressively both up and down section. The BA index of plagioclase (quantifying the plagioclase pole figure symmetry) obtained by Electron Backscatter Diffraction correlates negatively with the petrological trends, indicating that more fractionated mineral compositions are being more strongly foliated. An explanation for this correlated variations along the core could be an influx of more evolved melt associated with a stronger crystallographic orientation due to compaction, indicating that this part of the lower crust was probably formed by in-situ crystallization in a system of multiple sill intrusions [2].

8:45am - 9:00am

### Tracing heterogeneous intercumulus processes by rutile: examples from the Bushveld Complex

Armin Zeh<sup>1</sup>, Dominik Gudelius<sup>1</sup>, Allan Wilson<sup>2</sup>

<sup>1</sup>KIT Karlsruhe, Germany; <sup>2</sup>WITS Johannesburg, South Africa

Mafic cumulus rocks of the Bushveld Complex (BC) contain rutile of highly variable composition. On hand specimen scale, rutile crystals show enormous inter-grain differences in trace element contents, e.g., Nb (3 to 54.000 ppm), but scarcely any intra-grain zoning. We suggest that these differences mainly result from primary processes during rutile nucleation and growth and can be used to unravel intercumulus processes in detail. Textural relationships, compositions, and modelling results indicate that rutile crystallized during two major magmatic stages. Early rutile (Rt1) was formed together with chromite and orthopyroxene from SiO<sub>2</sub>-undersaturated melts at T>1200°C. These grains show relatively low, but variable contents in Nb (3 - 1530 ppm), Zr (48 - 2250ppm), and Zr/Nb ratios (0.2 - 48). The variations can be explained by Rayleigh fractionation during rutile+chromite crystallization in heterogeneous melt batches, which result from incomplete mixing of resident fractionated magma with replenished primitive parental magma. Late rutile (Rt2) was formed from highly fractionated intercumulus melts as indicated by commonly much higher Nb contents (up to 54.0000 ppm) and local intergrowths with zircon and quartz. Enormous compositional variations of Rt2, up to 4 orders of magnitude (!), also suggest Rayleigh-like fractionation. Rt2 mostly yield Zr-in-rutile temperatures between 935°C and 690°C, overlapping with Ti-in-zircon temperatures obtained from co-existing zircon. Higher temperatures up to 1060 °C point to crystallization from SiO<sub>2</sub>-undersaturated melts, and must be considered as maximum temperatures.

9:00am - 9:15am Paul Ramdohr Award (2018)

### Soufflé collapse: Vesicle shrinkage in hydrous silicate melts during quench

Anja Allabar, Marcus Nowak

University of Tübingen, Germany

Vesicle formation by phase separation of hydrous silicate melt and subsequent vesicle growth and coalescence are the fundamental mechanisms that control melt degassing and thus magma dynamics prior and during volcanic eruptions. A common experimental procedure to investigate the degassing behavior is the hydration and subsequent decompression of melt at magmatic temperature ( $T$ ) and pressure ( $P$ ). Finally, the partially degassed melts are quenched to vesiculated glass for post-mortem analysis.

However, the glass porosity ( $\Phi_{\text{glass}}$ ) does not necessarily represent melt porosity prior to quench due to vesicle shrinkage during cooling. Vesicle shrinkage has been described by (1) the decrease of molar volume ( $V_m$ ) of H<sub>2</sub>O (EOS shrinkage, Marxer et al. 2015) and (2) resorption of H<sub>2</sub>O from fluid vesicles back into the melt (resorption shrinkage, McIntosh et al. 2014), driven by increasing H<sub>2</sub>O solubility with decreasing temperature at  $P < 300$  MPa (Holtz et al. 1995).

We performed decompression experiments with hydrous phonolitic melt in an internally heated argon pressure vessel. The melts were hydrated at 200-270 MPa and 1523 K for 96 h and subsequently continuously decompressed at 1323-1373 K with 0.024-1.7 MPa·s<sup>-1</sup> to final pressures ( $P_{\text{final}}$ ) between 110 MPa and 20 MPa. At  $P_{\text{final}}$  the samples were either quenched with 44 K·s<sup>-1</sup> or 16 K·s<sup>-1</sup>, isobarically or with a  $P$  drop. Vesicle number densities ( $VND$ ) and  $\Phi_{\text{glass}}$  were determined with transmitted light microscopy and quantitative BSE image analysis.

Although all melts underwent near-equilibrium degassing after phase separation,  $\Phi_{\text{glass}}$  values are significantly lower than the calculated equilibrium porosities ( $\Phi_{\text{equ}}$ ) at  $P_{\text{final}}$  (e.g. 0.5 %  $\Phi_{\text{glass}}$  instead of 27 %  $\Phi_{\text{equ}}$ ). This is attributed to significant vesicle shrinkage during quench. The experimental data show that isobaric slow quench favors vesicle shrinkage compared to fast quench accompanied by decreasing  $P$ .

Our dataset is compared with previously published data of phonolite decompression experiments that also

underwent near-equilibrium degassing but where performed at various  $P$  and  $T$ , pressure media, quench techniques and quench rates. This experimental compilation shows that the deviation of  $\Phi_{\text{glass}}$  from  $(\Phi_{\text{equ}})$  is controlled by the contributions of EOS- and resorption- shrinkage, which depend significantly on the experimental procedure. Thus, it is important to consider possible vesicle shrinkage when porosity data from post-mortem analyzed experiments are used for interpreting melt degassing.

[1] Marxer et al. (2015) *J Volc Geotherm Res* 297: 109-124; [2] McIntosh et al. (2014) *EPSL* 401: 1-11; [3] Holtz et al. (1995) *Am. Min.* 80: 84-108

**9:15am - 9:30am**

### **Advances in high-temperature rheometry methods: a silicate melt case study**

**Christopher Giehl<sup>1,2</sup>, Lennart Fischer<sup>3</sup>, Mario Kleindienst<sup>2</sup>**

<sup>1</sup>Anton Paar Germany GmbH, Ostfildern, Germany; <sup>2</sup>Anton Paar GmbH, Graz, Austria; <sup>3</sup>Institute of Earth and Environmental Sciences, University of Freiburg, Germany

Rotational rheometry is a common method to determine the flow and deformation behaviour of materials in a wide range of industries. The benefits of air-bearing rotational rheometers are their capability to provide absolute viscosity values with low torque limits at defined shear rates and the possibility to measure in oscillatory mode. The latter enables to measure the visco-elasticity of materials, with relative contributions of viscous and elastic portions determined quantitatively. Oscillatory measurements are also possible at temperatures where samples are solid and therefore not accessible with rotational measurements. Combined with a high temperature furnace, this enables to assess the rheology of crystallizing silicate melts from superliquidus conditions to solidification of the melt, as well as the glass transition temperature in non-crystallizing systems.

This study presents temperature-dependent viscosity and visco-elasticity measurements of a tephritic dyke rock from Fohberg (Schwarzwald, SW Germany). The powdered sample was first heated to 1500 °C and then cooled down with 2 K/min at a constant shear rate of 1 s<sup>-1</sup>. Viscosity increases continuously from 1.801 Pas at 1500 °C to 171.6 Pas at 1110 °C, followed by a steep increase to 6668 Pas at 1071 °C where the torque limit is reached. The same temperature ramp was performed using an oscillatory mode (deformation 1% > 1200°C, 0.1% < 1200 °C; angular frequency 10 rad s<sup>-1</sup>). The sample is nearly ideally viscous across the whole temperature range with an elastic portion smaller than 10%, which instantly increases to 50% at 1140 °C. Complex viscosities recalculated from complex shear moduli increase from 2.328 Pas at 1500 °C to 698.2 Pas at 1140 °C. The results indicate a transition of the rheological behaviour from near-newtonian at 1500 °C to shear-thinning at about 1200 °C and lower. This is in agreement with phase equilibrium modelling indicating a liquidus temperature of 1202 °C and the presence of mineral phases below that temperature. The viscosities measured in rotation are lower than viscosities measured in oscillation, thus in agreement with the increasing degree of shear-thinning towards lower temperatures due to increasing solid fraction. The difference of the solidification point between rotational (1100 °C) and oscillatory (1140 °C) tests indicates an influence of the mechanical deformation on the crystallization kinetics of the tephritic melt. The results support the presumption that continuous flow of the melt induces a continuous crystallization, e.g. shear-induced crystallization, whereas oscillatory measurements induce a single crystallization event with sudden changes in rheological properties.

**9:30am - 10:00am** *Session Keynote*

## **Rheological and Thermal Evolution of Magmatic Systems: Insights into the Volcanic Past on Earth and other Planets and Moons in our Solar System**

**Alexander Sehlke**

*NASA Ames Research Center, United States of America*

Volcanic terrains cover large areas on Earth and other planetary bodies in our solar systems. Their morphological diversity is largely governed by eruptive conditions such as effusion rate, and the fundamental thermo-physical properties of the magma and lava, including temperature ( $T$ ), composition ( $X$ ), viscosity ( $\eta$ ), the volume fractions of entrained crystals ( $\varphi_c$ ) and vesicles ( $\varphi_b$ ), as well as bulk density ( $\rho$ ) and thermal conductivity ( $\kappa$ ). All of these properties itself dependent on temperature. As such, the rheological and thermal evolution of magmatic and volcanic systems is complex, however, can be reconstructed by morphological and petrological studies in the field and laboratory. This presentation discusses these thermo-physical feedback relationships applied to lava flows on Earth and other planets, how these properties evolve during cooling and crystallization, as well as the morphological changes associated with it. For example, crystal content drastically changes the rheological behavior of magmas, promoting a change from smooth pāhoehoe to rough `ā`ā lava flow morphologies; latent heat of crystallization may buffer the temperature of the lava, causing the lava to remain hot and lower bulk viscosity for some time, enabling the lava flow further distances. Therefore, understanding the evolution of thermo-physical properties during cooling and crystallization is necessary and critical to model magmatic systems, both in terms of their past and future, on Earth and elsewhere in our solar system.

## 5h) Processes and timescales in the evolution of transcrustal magma systems: from field and geochemical observations, through experiments to modelling

Monday, 23/Sep/2019: 9:00am - 10:30am

Session Chair: Axel Karl Schmitt (Heidelberg University)

Session Chair: Francois Holtz (Leibniz Universität Hannover)

Location: Schloss: S10

### Session Abstract

This session aims at presenting new approaches to better understand transport, compositional processing, storage, and rejuvenation of magma on its move from the mantle to the surface. We invite the presentation of results from petrological, geochemical, and geochronological investigations focusing on the volcanic record of natural magma systems as well as experimental, geophysical and modelling studies that quantify rates and processes of transcrustal magma transport.

### Lecture Presentations

9:00am - 9:15am

#### Ignimbrites and silicic magmatism in the Central Andes: Sources, timing and processes of magma generation

Gerhard Wörner<sup>1</sup>, Elena Belousova<sup>2</sup>, Jelte Keeman<sup>3</sup>, Simon Turner<sup>4</sup>, Axel Schmitt<sup>5</sup>, John Hora<sup>6</sup>

<sup>1</sup>Universität Göttingen, Geowissenschaftliches Zentrum, Germany; <sup>2</sup>Earth and Planetary Sciences, Macquarie University, NSW 2109, Australia; <sup>3</sup>Earth and Planetary Sciences, Macquarie University, NSW 2109, Australia;

<sup>4</sup>Earth and Planetary Sciences, Macquarie University, NSW 2109, Australia; <sup>5</sup>Universität Heidelberg, Institut für Geowissenschaften, Heidelberg, Germany; <sup>6</sup>Czech Geological Survey, Prag, Czech Republic

Silicic magmatism in the Central Andes forms dominantly rhyolitic to dacitic volcanic deposits that range from large-volume ignimbrites (>1000 km<sup>3</sup>) to small local dome eruptions. The mass proportion between mantle-derived magmatic contributions to crustal melting ranges from 20 to 70 % based on Sr-O isotope data obtained on separated feldspar and quartz contained as crystal cargo. New O-Hf isotope data from in-situ ion-probe and laser ablation measurements of U-Pb-dated zircons further constrain the type and proportion of crustal input into silicic magmas. Systematic variations in time and space in these geochemical parameters are documented in representative samples covering the entire Central Andes over a 20 Ma history, and a 800 km distance. Variations are related to crustal thickening through time during the Andean orogenesis and increasing crustal input during ignimbrite flare-ups and as the crust becomes thermally evolved and primed for melting.

Old, relict zircon representing the metamorphic basement involved in crustal melting are exceedingly rare. This reflects the high temperatures of melting, exceeding zircon saturation temperatures in the andesitic precursors of silicic ignimbrite magmas. This observation distinguishes silicic ignimbrite magmatism from granitoid intrusions in orogenic settings that often contain abundant older zircons inherited from the crust. Zircons in young (<100 ka) and small-volume silicic domes such as those from Parinacota volcano document the residence times of small silicic magma reservoirs underneath local stratovolcanoes. Based on U-series disequilibrium dating these zircons formed over timescales of >300 ka.

Overall, the zircon record demonstrates that distinct isotopic signatures are controlled by the variable composition and the age of crustal components that make up the different crustal domains of the Central Andes.

**9:15am - 9:30am**

### **Towards 3D geodynamic modelling of the Altiplano-Puna magma system**

**Arne Spang, Tobias Baumann, Boris Kaus**

*Johannes Gutenberg-Universität Mainz, Germany*

The Altiplano-Puna Magma Body (APMB) in the central Andes is considered to be the largest active melt zone in the Earth's crust today. For the past decades, multiple research projects have looked at the uplift rates above the APMB and successfully reproduced the observations with 2D or 3D numerical models, using simplified (elastic) rheologies and/or source geometries.

Yet, rocks are not just elastic but have a temperature-dependent viscoelastic rheology. Here, we therefore develop 3D models of the system using such more realistic rheologies, while also taking observed gravity anomalies into account. By forward modelling the gravitational effect of the APMB and the thickened Andean crust, we try to unite geometries inferred from S-wave tomography with crustal density models and bouguer data.

The resulting 3D setup and the 3D thermo-mechanical finite difference code LaMEM is then used to make predictions about surface deformation which can be compared to observations made by InSAR and GPS studies. The ultimate goal is the creation of a numerical model which is consistent with a large amount of geophysical data and can be used to better constrain the geometry and geophysical properties of the APMB as well as to understand why uplift rates at the surface above it have decreased since the mid-2000s.

We find that only an APMB with a maximum thickness of 13 to 19 km and a corresponding density contrast to the surrounding host rock of 100 to 200 kg/m<sup>3</sup> satisfies both, tomography and bouguer data. Furthermore, results of early geodynamic models suggest that the observed surface deformation can be reproduced by the buoyancy effect of the APMB alone.

**9:30am - 9:45am**

### **Deep crust hot zone: the control of depth on magmatic differentiation**

**Nicolas Riel, Boris Kaus, Lisa Rummel**

*University of Johannes Gutenberg, Germany*

The primary composition of magmatic products in arc systems is thought to be refined in the lowermost crust to uppermost mantle. In this deep hot region of the arc crust, geological evidence indicate that mantle-derived magmas and *in situ* products of lower crust partial melting are reacting in a pervasive melt system and eventually extracted toward higher level of the crust (through dyke systems). Resolving the relative contribution of mantle-derived magma and partial melting products of pre-existing crust is crucial to: (1) quantify crustal growth rate, (2) better understand the compositional range of arc magmatic series and (3) constrain chemical differentiation and gravitational stability of the lower crust.

In this study, we use a thermal-two-phase flow model coupled with thermodynamic calculations to investigate how the depth of hot crust zone controls arc magmatism and lower crust differentiation. Our results are then compared to the well-exposed lower arc sections of Talkeetna (max 10 kbar) and Kohistan-Ladakh (max 16 kbar).

**9:45am - 10:00am**

### **Evolution of transcrustal magmatic systems investigated by petrological-geodynamical models**

**Lisa Rummel<sup>1</sup>, Boris J.P. Kaus<sup>1</sup>, Tobias S. Baumann<sup>1</sup>, Richard W. White<sup>2</sup>, Nicolas Riel<sup>1</sup>**

<sup>1</sup>*Johannes Gutenberg University Mainz, Germany;* <sup>2</sup>*School of Earth & Environmental Sciences, University of St Andrews, Scotland, UK*

The evolution of crustal magmatic systems is incompletely understood, as most studies are limited either by

their temporal or spatial resolution. Exposed plutonic rocks represent the final stage of a long term evolution punctuated by several magmatic events with different chemistry and generated under different mechanical conditions. Although the final state can be easily described, the nature of each magmatic pulse is hampered. This study presents a new method to investigate the compositional evolution of plutonic systems while considering thermal and mechanical processes. A thermomechanical code (MVEP2) extended by a semi-analytical dike/sill formation algorithm, is combined with a thermodynamic modelling approach (Perple\_X) to investigate the feedback between petrology and mechanics. Melt is extracted to form dikes while depleting the source region. The evolving rock compositions are tracked on markers using a different phase diagram for each petrological composition. The rock compositional evolution is thus tracked with a high precision by means of a database with more than 50,000 phase diagrams. This database is able to describe how density, melt fraction, the chemical composition of melt and solid fractions and mineralogical assemblages change over crustal to uppermost mantle  $P$ - $T$  conditions for a large range of rock compositions. Each bulk rock composition is composed of the 10 major oxides ( $\text{SiO}_2$ - $\text{TiO}_2$ - $\text{Al}_2\text{O}_3$ - $\text{Cr}_2\text{O}_3$ - $\text{MgO}$ - $\text{FeO}$ - $\text{CaO}$ - $\text{Na}_2\text{O}$ - $\text{K}_2\text{O}$ - $\text{H}_2\text{O}$ ) including an oxygen buffer. The combined modelling approach is applied to study the chemical evolution of the crust during arc magmatism and related melt extraction and magma mixing processes. Basaltic sills are periodically injected into the crust to model heat influx from the mantle. Accumulated sills turn into long-lived mush chambers by using a lower rock cohesion or due to high intrusion depths. The resulting melts can be highly evolved and are extracted to form dikes in the overlying crust. Associated partial melting of crustal host rocks is promoted by the water amount, and occurs around dense distributed dikes and sills. High silica rocks (e.g. granites) are generated by partial melting of the host rocks, melt segregation within dikes, and from fractional crystallization of basalts.

**10:00am - 10:15am**

### **First steps in linking melt-matrix-two-phase flow with fast melt transport via dykes in a continental crust scenario**

**Herbert Wallner, Harro Schmeling**

*Goethe University Frankfurt, Germany*

Magmatic systems are studied in various geoscientific disciplines, but across the particular views the different aspects are strongly coupled. Even the physical understanding is poor. Numerical modelling is a way to study and improve the knowledge of melting and melt ascent, but for now under continuous development.

Our approach is based on conservation equations of mass, momentum, and energy for melt and solid, respectively, including full compaction of the solid matrix. We apply non-linear visco-plastic rheology using power law parameters of quartzite or granite and plasticity derived from Byerlee's Law. For melting and freezing a simplified binary melting model is utilized. Meta-greywacke serves as the initial rock type for solidus and liquidus definition. Their chemical composition, i.e. the enrichment or depletion in  $\text{SiO}_2$  of the advected silicic melt and solid, is tracked. Melt mobility depends on the viscosity of the melt and the permeability of the partially molten rock; they essentially determine the Retention number.

Plutonism and additionally second phase segregation, for instance by accumulating melt beneath the solidus of the stiff upper crust, can be modelled by this physics. However, observations show additional fast melt transport mechanisms acting on a short time scale. These symptomatically cannot be handled numerically by the same approach due to the difference of timestep-length of several orders.

A widely used practice is the extraction of melt and its intrusion in a given emplacement level or extrusion to the surface. Our approach uses a parametrization of three critical parameters where vertically connected partially melted zones serve as source region of extraction. The source regions undergo compaction, inducing under-pressure attracting ambient melt. In a higher, colder crustal level the emplaced melt dilatates the matrix, and usually freezes immediately; heating and an increase of enrichment occurs. Such approaches locally violate mass and momentum equations more or less, and, more importantly, magma is redistributed at ad-hoc positions.

The most obvious fast magma transport mechanism through the subsolidus region is dyking. The process can be subdivided in the nucleation or generation, the propagation in an elastic medium exposed to regional stresses, and stagnation of dykes.

Aim of our research project is modelling the combination of two-phase flow, and consistently draining the melt from the top of the partially molten regions forming dykes, propagate their magma volume dynamically through the elastic subsolidus region, and treat stagnant dykes as intrusion. Our concept, progress, and first results will be presented.

**10:15am - 10:30am**

### **Evolution of magmatic systems at different temporal and spatial scales – what did we learn from zircon U/Pb dating?**

**Urs Schaltegger<sup>1</sup>, Blair Schoene<sup>2</sup>, Alexey Ulianov<sup>3</sup>, Richard Spikings<sup>1</sup>, Othmar Müntener<sup>3</sup>**

*<sup>1</sup>Department of Earth Sciences, University of Geneva, Switzerland; <sup>2</sup>Department of Geosciences, Princeton University, USA; <sup>3</sup>Institute of Earth Sciences, University of Lausanne, Switzerland*

Any magmatic process inside the Earth's crust can be broken down into incremental additions or episodic extraction of melt to and from a magma-rich reservoir, respectively. From these observations it has been concluded that the existence of magmatic liquid is an ephemeral phenomenon and that magma systems are mostly solid during most of their lifetime. This rather parcimonious view has some notable exceptions that demonstrate, e.g., the existence of crystal-poor high-silica melt reservoirs beneath large caldera systems.

Through chemical and isotopic analysis of the accessory mineral zircon we get insight into processes such as magma generation, mixing of crystals and liquids, sequential magma extraction, ascent and emplacement. A U-Pb zircon date is a snapshot from this complex evolution, and is overall an information of when the thermal and compositional conditions for zircon saturation were achieved.

The talk will use the well-studied Adamello intrusive complex in northern Italy, and U/Pb dates, oxygen and Hf isotopic as well as chemical composition of zircon, to address some of the following points: 1) a magmatic system starts via assembly of small magma volumes from various sources at middle crustal level during its initial stage; 2) the evidence that melts and crystals interact and exchange; 3) the assembly of composite plutons from individual magma batches happens over 1-2E6 year timescales; 4) document the buildup of a nested intrusive series over 1E7 years duration through magma batches that are small enough to crystallize and cool individually to 300°C; and 5) point out the buildup of a hot zone in the lower crust over time, traced by increasing bulk assimilation of crust.

## 5h) Processes and timescales in the evolution of transcrustal magma systems: from field and geochemical observations, through experiments to modelling

Monday, 23/Sep/2019: 11:15am - 1:00pm

Session Chair: Axel Karl Schmitt (Heidelberg University)

Session Chair: Francois Holtz (Leibniz Universität Hannover)

Location: Schloss: S10

### Lecture Presentations

11:15am - 11:45am *Session Keynote*

#### Quantitative magma plumbing studies: Accessing the dynamic evolution of transcrustal magmatic systems in space and time

Maren Kahl<sup>1</sup>, Enikő Bali<sup>1,2</sup>, Guðmundur H. Guðfinnsson<sup>1</sup>, David A. Neave<sup>3</sup>

<sup>1</sup>Institute of Earth Sciences, University of Iceland, Iceland; <sup>2</sup>Faculty of Earth Sciences, University of Iceland, Iceland;

<sup>3</sup>School of Earth and Environmental Sciences, The University of Manchester, UK

Tracking the crustal storage and transfer of magmas on their way to eruption is an important goal in volcanology. Most information about magma migration within volcanic plumbing systems is typically obtained with geodetic and seismic methods. As magma ascends towards the surface, its physico-chemical properties change to the extent it may affect style, intensity and duration of future eruptions. Tracking how, where and over what timescales magma chemistry changes as magma moves is crucial for anticipating future volcanic hazards and risks.

We apply an integrated method, linking Systems Analysis, diffusion chronometry, melt inclusion geochemistry and thermobarometry to constrain pressure-temperature-composition-time (P-T-X-t) paths of sub-surface magma processing within two contrasting volcanic settings in Iceland: off- vs. on-rift. We investigated eruption products from two postglacial events from the *Snæfellsnes volcanic belt (SVB)*, a typical flank zone setting in W-Iceland: *Búðahraun (Búð)* ~5.0-8.0 ka and *Berserkjahraun (Bers)* ~4.0 ka. And from *peistareykir*, an on-rift system, in the Northern Volcanic Zone (NVZ): *Bóndhólshraun (Bón)* <10ka. We analysed olivine, plagioclase and clinopyroxene macrocrysts, matrix glass and olivine-hosted melt inclusion compositions.

Olivine macrocrysts from *SVB* are characterized by normal and complex reverse zonation with core and rim compositions within the range  $Fo_{66-91}$ . Olivine macro and phenocrysts from *Bón* (NVZ) are predominantly normally zoned with core and rim compositions in the range  $Fo_{80-90}$ . Clinopyroxene and plagioclase compositions are within the range  $Mg\#71-89$  and  $An_{53-88}$ , respectively. Mineral-liquid equilibria calculations reveal that macrocryst rims from the studied on-and off-rift settings are in chemical equilibrium with the erupted melts, whereas the macrocryst cores are too primitive, indicating a possible mush origin of these cores.

Clinopyroxene-liquid thermobarometry applied to eruption products from *SVB* returns pressures and temperatures within the range 5.4-8.7kbar and 1178-1270°C for clinopyroxene cores ( $Mg\#77-84$ ), and 1.0-5.4kbar and 1123-1192°C for clinopyroxene rims ( $Mg\#72-76$ ). OPAM barometry, applied to matrix glass and melt inclusion analyses from *Bón* (NVZ), return a mean equilibration pressure of  $4.6\pm 0.6$ kbar. Temperatures obtained from olivine-liquid thermometry return ~1220°C for ~ $Fo_{86}$  (macrocryst rims) in equilibrium with the average matrix glass ( $Mg\#_{liq}$  60.5) and ~1247°C for ~ $Fo_{89.3}$  (macrocryst cores) in equilibrium with primitive melt inclusions (~ $Mg\#_{liq}$  67.80).

Fe-Mg diffusion chronometry applied to olivine crystals from *Bón* (NVZ) return timescales within the range of 17 days up to 2.6 years (79% shorter than 4 months). Olivines from *SVB* return slightly shorter timescales ranging from a few days up to 7 months, with the majority (61%) being shorter than 60 days.

11:45am - 12:00pm

### Constraining pre-eruptive history by diffusion chronometry: Laacher See (Germany) and Taapaca volcano (Chile)

**Smruti Sourav Rout, Gerhard Wörner**

*Georg-August-Universität, Göttingen, Germany*

Time-scales extracted from chemically zoned minerals provide insights into crystal residence time, magma storage and compositional evolution of magmas and allow better constraints on pre-eruptive history of large and potentially dangerous magma chambers. We applied diffusion chronometry to different eruption products from Laacher See volcano (Germany) and Taapaca volcano (Chile).

(a) Laacher See volcano: (1) Sanidine phenocrysts from phonolite-basanite hybrid rocks show thin late-stage resorption-overgrowth interfaces related to the most recent basanite recharge event. Diffusion modelling of Ba-diffusion across these interfaces constrain the time between magma mixing and eruption to be 4-7 years. Diffusion time-scales obtained from interior resorption and regrowth zones suggest a recharge frequency of every 1.5-3 ky in the past history of the magma reservoir. (2) Carbonatitic syenites are interpreted to represent a crystallizing carapace around the phonolite magma. The pre-eruptive, core-rim Na-K diffusion in sanidines constrains the effective storage temperature at 630-670 °C. These values along with a conduction model constrain the radial inward growth rate of the syenite carapace at ~8 cm/year. Uphill diffusion modeling across exsolution boundaries in sanidine gave a maximum time between the destabilisation of the carapace and eruption of only 40-50 days. (3) Crystal mushes that form accumulation of phenocrysts are generally devoid of zoned crystals. Only crystals with resorbed boundaries or very thin overgrowths (a few microns) with very sharp compositional changes imply the activation of cumulates only months before eruption.

(b) Taapaca volcano: Sanidine megacrysts in dacites show repetitive, sharp jumps in Ba concentration at resorption interfaces that reflect frequent heating events during their growth. These distinct growth bands formed at temperatures of ~700 to 850 °C pressures of 1-3 kbar based on amphibole-thermometry and Al-in-Hornblende barometry for each growth zone separately. A non-isothermal diffusion modeling of Ba-profiles across individual diffusive boundaries gave diffusion times ranging from 1 to 50 ky and total residence times of 30 to 470 ky for different crystals from different stages of eruption. All crystals show late oscillatory overgrowths that indicate multiple heating events in the magmatic system at increased frequency only ~1 to 3 ky before eruption.

Based on these diffusion times and storage temperatures, genetic models for the process and timing of storage and activation are presented for both the magma systems with respect to the current discussions regarding cold- versus hot-storage models.

12:00pm - 12:15pm

### Timescales of magmatic processes during the eruptive cycle 2014-2015 at Piton de la Fournaise, La Réunion, obtained by Mg-Fe diffusion modelling in olivine

**Caren Sundermeyer<sup>1</sup>, Andrea Di Muro<sup>2</sup>, Boris Gordeychik<sup>1,3</sup>, Gerhard Wörner<sup>1</sup>**

<sup>1</sup>*Geowissenschaftliches Zentrum, Georg-August-Universität, Göttingen, Germany;* <sup>2</sup>*Observatoire Volcanologique du Piton de la Fournaise, Institut de Physique du Globe de Paris, Bourg Murat, La Réunion, France;* <sup>3</sup>*Institute of Experimental Mineralogy RAS, Chernogolovka, Russia*

Diffusion modelling of zoned crystals is an important tool to estimate crystal residence times in magma reservoirs, between magma mixing, ascent, and eruption. At Piton de la Fournaise (La Réunion, Indian Ocean) eruptions are frequently fed from a shallow magma reservoir and a complex sill and dyke system that is periodically refilled with mafic magmas from depth. A new eruptive cycle initiated in June 2014 after 41 months of quiescence. Four small eruptions in June 2014, February 2015, May, and July lasted only few days and produced mostly evolved basalts, whereas during the large August-November 2015 eruption magmas became increasingly more mafic.

Diffusion profiles were analyzed in olivines from ten quenched lava and tephra samples covering the eruptive sequence in 2014-2015 to constrain the residence times of crystal populations in the plumbing system. The timescales obtained by Mg-Fe diffusion modelling were linked to monitored geophysical data such as seismicity, ground deformation, and soil CO<sub>2</sub> flux. Olivines show three types of zoning (normal, reverse, and complex) and various core compositions (Fo<sub>73-85</sub>). Olivine crystals were periodically reactivated from different, resident magma batches (in calculated equilibrium with Fo<sub>77.7-84.6</sub>) during three main episodes of days to seven months prior to the eruptions in (1) June 2014 and (2) February 2015 and during the eruptions in (3) July and August-November 2015.

Short residence times of olivines erupted in more evolved magmas of June 2014 and May 2015 eruptions (in equilibrium with Fo<sub>77-80</sub>) correlate with shallow seismicity and ground deformation at that time. This indicates that the small eruptions were fed from magmas residing directly at the top of the shallow reservoir. Other olivines started to equilibrate to more mafic compositions (Fo<sub>81-84.6</sub>) at the same time, but these crystals remained unerupted until later in July and August-November 2015. The absence of deep seismicity prior to May 2015 suggests that these olivines were reactivated probably from crystal mush in the central reservoir (~6-8 km depth) during basaltic recharge and magma mixing. These hybrids remained in the plumbing system for > 237 days until their eruption in September-November 2015. However, residence time of olivines erupted during July 2015 show strong similarities to those of the large August-November eruption, which marks the transition between earlier shallow fed eruptions and the large, deeply fed August-November eruption.

**12:15pm - 12:30pm**

### Halogen diffusion in dry rhyodacitic melt

**Yves Feisel<sup>1</sup>, Jonathan M. Castro<sup>1</sup>, Donald B. Dingwell<sup>2,3</sup>**

<sup>1</sup>Johannes Gutenberg-Universität, Mainz, Germany; <sup>2</sup>Ludwig Maximilians Universität, München, Germany; <sup>3</sup>Gutenberg Research Center, JGU Mainz, Germany

Chemical diffusion of the halogens (F, Cl, Br, I) in halogen-enriched dry rhyodacitic melt synthesized from natural Hekla pumice (Iceland) and Cordón Caulle lava (Chile) was studied experimentally using the diffusion couple technique. Experiments were conducted in vertical tube furnaces over the temperature range 750 - 950 °C at 1 bar for durations from 1 to 35 days. Concentration profiles of F and Cl in the experimental samples were measured with an Electron Microprobe, while some additional measurements of all four halogens including Br and I were undertaken using a Secondary Ion Mass Spectrometer.

All investigated halogens exhibit Arrhenian behaviour during diffusion. Fluorine diffusivity is almost identical in both compositions while chlorine diffuses slightly faster in the Cordón Caulle melt than in Hekla. In the temperature range investigated, fluorine has diffusion coefficients on the order of 10<sup>-15</sup> to 10<sup>-13</sup> m<sup>2</sup>/s while chlorine diffusivity on average is almost 2 orders of magnitude slower. Preliminary data on bromine and iodine diffusivities indicate even slower diffusion, with coefficients in the range of 2x10<sup>-17</sup> to 1.3x10<sup>-15</sup> m<sup>2</sup>/s and 1.7x10<sup>-17</sup> to 3.9x10<sup>-16</sup> m<sup>2</sup>/s, respectively. The activation energies for fluorine and chlorine were calculated to be equal within error at 223 ± 31 and 229 ± 52 kJ/mol.

These results are the first halogen diffusion data in natural anhydrous rhyodacitic melts obtained by the diffusion couple technique and, to our knowledge, the very first to investigate iodine diffusion in volcanic melts. Further diffusion couple experiments are underway to investigate halogen mobilities in hydrous silicic melts and at pressurised conditions. We nevertheless suggest that the pronounced differences in diffusivity amongst the halogens indicate that a strong diffusive fractionation may be possible, especially under conditions of rapid magma ascent and bubble growth, as this would favour partitioning of the relatively fast-diffusing halogens into growing bubbles. Halogen species ratios monitored in actively degassing vents could in turn be used as a measurable probe of volcanic unrest. The correlation between atomic radius and diffusivity compared to more primitive melts suggests that the halogen diffusion mechanism is dependent on the melt structure and that pronounced fractionation is therefore likely expected in evolved systems only.

12:30pm - 12:45pm

**Antecrysts – angels or devils in  $^{40}\text{Ar}/^{39}\text{Ar}$  geochronology? Examples from Cape Verde seamounts.****Jo-Anne Wartho, Lisa Samrock, Thor Hansteen***GEOMAR Helmholtz Centre for Ocean Research Kiel, Germany*

The traditional concept of magmatic systems has changed from high-melt fraction “magma chambers” to low-melt-fraction “mush reservoirs” [e.g., 1]. This new hypothesis now more easily explains the presence of older antecrysts/xenocrysts found within younger magmas. These older crystals can offer important information on the formation, crystallisation, mixing, and storage of minerals in magmatic systems, but they can also greatly complicate  $^{40}\text{Ar}/^{39}\text{Ar}$  geochronological analyses. We present an extensive laser  $^{40}\text{Ar}/^{39}\text{Ar}$  single-crystal total-fusion and single-/multiple-grain step-heating dating study of individual K-bearing crystals (K-feldspar, biotite and nepheline) from two Cape Verde seamounts, in the central Atlantic Ocean, to explain these complications.

The Cape Verde Archipelago (10 volcanic islands and several seamounts) originates from igneous activity related to a mantle plume over a period of 26 Ma to present. A sample from the Senghor Seamount yields a single population of  $^{40}\text{Ar}/^{39}\text{Ar}$  ages from biotites and K-feldspars, indicating a simple co-magmatic age of  $14.622 \pm 0.027$  Ma (all errors are  $2\sigma$ ;  $n = 70$ ). Alternatively, 5 samples from the active Cadamosto Seamount, located  $\sim 425$  km SW of Senghor Seamount, yield a much more complicated range of K-feldspar and nepheline single-crystal  $^{40}\text{Ar}/^{39}\text{Ar}$  ages. The K-feldspars record ages ranging from  $11.5 \pm 6.5$  to  $611.9 \pm 8.8$  ka ( $n = 140$ ), whereas the nephelines yield ages from  $169.5 \pm 16.5$  ka to  $1.522 \pm 0.008$  Ma ( $n = 27$ ). K-feldspars in the 5 samples yielded 3 different eruption ages ( $21.14 \pm 0.62$ ,  $51.8 \pm 2.4$ , and  $97 \pm 14$  ka), but some petrologically-identified K-feldspar and nepheline antecrysts yield orders of magnitude older ages [2]. Step-heating of one multi-crystal K-feldspar sample gives plateau ages of  $126.5 \pm 3.3$  and  $131.9 \pm 3.7$  ka,  $\sim 30$ -35 ka older than the 97 ka eruption age, thus highlighting the danger of multi-grain step-heating  $^{40}\text{Ar}/^{39}\text{Ar}$  dating in antecryst-bearing samples.

A better awareness of the possibility of the presence of antecrysts in geological material can be coupled with careful petrological examination of samples to determine the most appropriate  $^{40}\text{Ar}/^{39}\text{Ar}$  dating technique. In addition, advances in high-sensitivity multi-collector noble gas mass spectrometers now allow higher resolution  $^{40}\text{Ar}/^{39}\text{Ar}$  dating on much smaller samples (e.g., laser step-heating of  $\sim 765$  ka single K-feldspars [e.g., 3]). This should help to resolve the complications of antecrysts in samples, and turn them from potential foes to friends.

[1] Jackson et al. 2018. *Nature* 564:405-409; [2] Samrock et al. 2019. *Lithos* in review; [3] Anderson et al. 2017. *PNAS* 114:12407-12412.

12:45pm - 1:00pm

**Millennial to decadal magma evolution in an arc volcano from zircon and tephra of the 2016 Santiaguito eruption (Guatemala)****Alejandro Cisneros de León<sup>1</sup>, Axel K. Schmitt<sup>1</sup>, Sonja Storm<sup>1</sup>, Bodo Weber<sup>2</sup>, Julie C. Schindlbeck-Belo<sup>1</sup>, Robert B. Trumbull<sup>3</sup>, Francisco Juárez<sup>4</sup>**

<sup>1</sup>*Universität Heidelberg, Germany*; <sup>2</sup>*Departamento de Geología, Centro de Investigación Científica y de Educación Superior de Ensenada (CICESE)*; <sup>3</sup>*GFZ German Research Centre for Geosciences, Potsdam, Germany*; <sup>4</sup>*Instituto Nacional de Sismología, Vulcanología, Meteorología, e hidrología (INSIVUMEH)*

The Santa María-Santiaguito volcanic complex collectively is one of the most active and dangerous volcanoes in the entire Central American volcanic arc. Within 20 years of the destructive Plinian eruption of the Santa María stratocone (Guatemala) in 1902, the Santiaguito volcanic dome complex started to form by parasitic vent eruptions which have lasted over nearly a century. Because of the frequent eruptions of Santiaguito, it offers unique opportunities to study secular changes in its subvolcanic magma reservoir at high temporal resolution. Ash collected days and hours after eruptions of Santiaguito during an unusually explosive

interval in August 2016 represents some of the least evolved compositions (60-62 % SiO<sub>2</sub>) with the lowest <sup>87</sup>Sr/<sup>86</sup>Sr isotope ratios ever reported for the system. This extends the multi-decadal trend of Santiaguito to progressively less evolved magma compositions with time, relative to the 1902 event which erupted overwhelmingly dacitic pumice. Santiaguito's geochemical changes are indicative of increasingly larger contributions of fresh basaltic andesite magma recharge mixing with dacitic magma that remained after the 1902 eruption. High-resolution secondary ion mass spectrometry (SIMS) <sup>238</sup>U-<sup>230</sup>Th disequilibrium dating and geochemistry of zircon from Santiaguito ash and Santa María 1902 pumice reveal the presence of evolved and zircon-saturated melts over the entire ca. 100 kyr interval of basaltic andesite eruptions that constructed the Santa María central cone. Quartz diorite basement xenoliths (~55 % SiO<sub>2</sub>) with Eocene zircons are common in the Santa María 1902 deposits, and a few equally old zircon xenocrysts within Santiaguito ash suggest that vestiges of assimilated Eocene crustal rocks are present in the modern magma system. Zircon crystals in andesitic Santiaguito tephra are identical in age and trace element signature to those in the 1902 pumice. This is direct evidence for the persistence of residual evolved magma with crystals dating back to the Santiaguito cone-forming stage between ca. 100 and 25 ka and the pre-1902 eruptive quiescence which lasted for ca. 25 kyr. It also indicates that residual dacite still contributes to Santiaguito andesitic magmas. Zircon survival in Santiaguito andesite requires comparatively brief timescales of magma mixing between basaltic andesite and resident dacite magmas because otherwise zircon would become resorbed.

## Poster Presentations

Mon: 26

### Geodynamic constraints on the initiation of mélange diapirs from subducting slabs

**Nicolas Berlie<sup>1</sup>, Boris Kaus<sup>1</sup>, Horst R. Marschall<sup>2</sup>**

<sup>1</sup>Johannes Gutenberg University Mainz, Germany; <sup>2</sup>Goethe University, Frankfurt am Main, Germany

Subduction zones represent an important part of the general volcanic activity and magma production on our planet. Numerous geochemical analyses have been performed over time on those magmas and the results suggest a mixing between the crustal components of the subducting slab and the mantle. The mixing process likely takes place at the interface between the slab and the mantle wedge, where mélange rocks form comprising of crustal and mantle rocks and hydrous fluids extracted from the slab. This mélange layer would then evolve into diapirs and rise in the asthenosphere until it reaches melting conditions suitable for the creation of magmas. Here, we study the geodynamic feasibility of this process and the conditions that determine the ability of the mélange to peel off from the slab and to form diapirs as well as the size of those diapirs. We perform 2D finite element calculations focusing on two different setups to observe the initiation and later the evolution of the diapirs with time. Results confirm that this mechanism is feasible under a specific range of condition and we show how the lateral extents of those diapirs along the slab depends on the geometry of the slab, the rheological and density parameters of the mélange layer and the overlying mantle. We also investigate the P-T paths followed by the diapirs and the implications on their mineralogical compositions.

Mon: 27

### Times of magma ascent and residence reflected in Mg/Fe and Ni diffusion in olivine from arc lavas in Kamchatka

**Tatiana Churikova<sup>1,2</sup>, Boris Gordeychik<sup>1,3</sup>, Gerhard Wörner<sup>1</sup>, Andreas Kronz<sup>1</sup>, Maria Pevzner<sup>4</sup>, Yaroslav Muravyev<sup>2</sup>, Alexander Belousov<sup>2</sup>, Oleg Dirksen<sup>2</sup>**

<sup>1</sup>Geowissenschaftliches Zentrum Göttingen, Abteilung Geochemie, Georg-August-Universität Göttingen, Göttingen, Germany; <sup>2</sup>Institute of Volcanology and Seismology FEB RAS, Petropavlovsk-Kamchatsky, Russia; <sup>3</sup>Institute of Experimental Mineralogy RAS, Chernogolovka, Russia; <sup>4</sup>Geological Institute RAS, Moscow, Russia

Time scales of residence and ascent for Kamchatka magmas are presented based on zoned olivines from basalts of distinct volcanic modes: maars, monogenic cones, dikes and stratovolcanoes.

The time scales were estimated by Ni-Mg/Fe diffusion modeling of zoning in olivine crystal cores and outer rims by quantitative geochemical profiles. Modeling is based on the analytical solution of diffusion equation to approximate measured geochemical profiles and estimates for P and T from Al-in-olivine thermometry and cpx-melt barometry.

Olivine crystals in basalts erupted from of maars preserved the most diverse types of compositional zonation – normal, inverse, and even oscillatory in Fo<sub>78</sub> to Fo<sub>92</sub> olivines. The size of olivine crystals in maar eruptions is small (<0.3 mm) compared to olivines from other eruptive regimes, which indicates short crystal growth times. Crystal residence times and time of magma ascent are estimated at 100-2000 and 1-10 days, respectively. Magmas erupted in maars thus move most rapidly to the surface.

In lavas erupted at monogenic cones, oscillatory zonation in olivine is absent, but normal and inverse zoning are found in all samples, with sharp gradients between the cores and outer parts of crystals. The size of the crystals in monogenic cones is larger than for maar lavas (<0.5 mm). The time of magma ascent varies from 10 to 60 days. Residence time, estimated for few crystals lasted up to 300 days.

The size of olivine crystals in dikes and stratovolcanoes are larger (0.8-1 mm), which indicates a relatively longer time of crystal growth in their feeding systems. The majority of crystals show normal zoning. Compositional gradients in Fo and Ni between the olivine cores and outer parts are smoother, indicating longer diffusion times. Also, olivine with reverse zoning and compositional gradients in their cores are rare in samples from stratovolcanoes. Diffusion therefore probably erased earlier zonation gradients. The diffusion times for dikes and stratovolcano lavas were estimated up to 200 and 1500 days, respectively.

The implication of these results is as follows: Maar eruptions are fed from rapidly ascending magmas that do not reside, cool and fractionate during ascent fast from their mantle reservoirs. Monogenetic cones are similarly sourced from magmas that ascended relatively fast. By contrast, lavas erupted in stratovolcanoes and those that ascended through their feeder dikes have longer residence times in crustal magma systems, where crystallization, mixing and magma processing occurs.

Research was supported by grants GSF Wo 362/51-1 and RFBR 16-55-12040.

**Mon: 28**

### **Variations of Fo and Ni in the centres of olivine cores reflect processes of crystallization and diffusion**

**Boris Gordeychik<sup>1,2</sup>, Tatiana Churikova<sup>1,3</sup>, Alexander Simakin<sup>2,4</sup>, Thomas Shea<sup>5</sup>, Gerhard Wörner<sup>1</sup>**

<sup>1</sup>Geowissenschaftliches Zentrum Göttingen, Abteilung Geochemie, Georg-August-Universität Göttingen, Göttingen, Germany; <sup>2</sup>Institute of Experimental Mineralogy RAS, Chernogolovka, Russia; <sup>3</sup>Institute of Volcanology and Seismology FEB RAS, Petropavlovsk-Kamchatsky, Russia; <sup>4</sup>Institute of Earth Physics RAS, Moscow, Russia; <sup>5</sup>Department of Geology and Geophysics, University of Hawai'i, Honolulu, USA

Mg and Ni are both compatible elements in olivine. Fractional crystallization of olivine typically results in a concave up trend on a Fo-Ni diagram. “Ni-enriched” olivine phenocrysts that fall off and above the crystallization trend of are commonly observed in subduction and intraplate settings. To explain such “Ni-enriched” olivine crystals, we develop a set of theoretical and computational models to describe how primitive (high-Fo, high-Ni) olivine phenocrysts from a parent basalt re-equilibrate with an evolved (low-Fo, low-Ni) melt through diffusion. These models describe Fo and Ni decreasing in olivine cores during protracted diffusion for different crystal shapes and variable relative diffusivities for Ni ( $D_{Ni}$ ) and Mg-Fe exchange ( $D_{Fo}$ ). Such dependence is considered as a diffusion trend responsible for the formation of Ni-enriched olivine phenocrysts. Theoretical models show if the diffusivity of Ni is lower than the diffusivity of Fo, then affected by diffusion the olivine phenocrysts form a concave down trend that contrasts with the concave up crystallization trend. These models with different geometries allow showing the diffusion trend does not depend on the size of the crystal and weakly depends on its shape. In addition, it is shown that the anisotropy of the diffusion coefficient affects the diffusion trend in the same way as a change in the crystal shape and both features, anisotropy and shape, do not significantly change the concave down diffusion trend. Three-dimensional numerical

diffusion models using a range of realistic olivine morphologies with anisotropy corroborate this conclusion. Thus, the curvature of the concave down diffusion trend is mainly determined by the ratio of the diffusion coefficients  $D_{\text{Ni}}/D_{\text{Fo}}$ . The initial and final points of the diffusion trend are determined by the compositional contrast between mafic and more evolved melts that have mixed to cause disequilibrium between olivine cores and surrounding melt. These endmember compositions may also vary in nature. We present several examples of measurements on olivine from arc basalts from Kamchatka, and several published olivine datasets from mafic magmas from non-subduction settings (lamproites and kimberlites) that are consistent with diffusion-controlled Fo-Ni behavior. In each case the ratio of the Ni and Fo diffusion coefficients is indicated to be  $<1$ . These examples show that crystallization and diffusion can be distinguished by concave up and concave down trends in Fo-Ni diagrams.

Research was supported by grants GSF Wo 362/51-1 and RFBR 16-55-12040.

**Mon: 29**

### **Divergent compositional domains in the shallow plume mantle beneath the West Eifel volcanic field, W Germany**

**Andreas B. Kaufmann<sup>1</sup>, Stephen J. G. Galer<sup>2</sup>, Dieter F. Mertz<sup>1</sup>**

<sup>1</sup>*Institute for Geosciences, University of Mainz, Germany;* <sup>2</sup>*Max Planck Institute for Chemistry Mainz, Germany*

Low-SiO<sub>2</sub> volcanic activity in the Pleistocene West Eifel volcanic field (WEVF) is related to a seismological low-velocity anomaly in the upper mantle ("Eifel Plume" [1]). In the WEVF, two geographical groups can be distinguished by their characteristic elemental and isotope compositions combined with their geochronological evolution [2]. Lava flows  $>480$  ka exclusively occur in the NW,  $<80$  ka flows extruded in the SE. However, there are two specific flows, from Sarresdorf and Emmelberg, that do not fit into this general time-space-composition pattern within the WEVF.

Lava flow Sarresdorf is located in the NW, i.e. within the  $>480$  ka group, but is characterized by an  $^{40}\text{Ar}/^{39}\text{Ar}$  plateau age of  $32 \pm 13$  ka ( $1\sigma$ ), along with the highest Nb/Ta (22.7), Lu/Hf (0.07) and Sr concentration of  $1810 \mu\text{g g}^{-1}$  (other flows average ca.  $1000 \mu\text{g g}^{-1}$ ) as well as the lowest  $(\text{Ti}/\text{Eu})_{\text{N}}$  (0.56) among the West Eifel flows ( $n = 27$ ) investigated. This specific composition is interpreted as resulting from the influence of carbonatitic melts, which is supported by elemental evidence from other volcanic fields [3, 4].

Lava flow Emmelberg has an  $^{40}\text{Ar}/^{39}\text{Ar}$  plateau age of  $49 \pm 2$  ka ( $1\sigma$ ) and extruded at the geographical boundary between the  $<80$  ka and  $>480$  ka compositional groups. With respect to the  $<80$  ka-old group, it has elevated  $(\text{Zr}/\text{Sm})_{\text{N}}$  of 1.07 and  $\text{K}_2\text{O}/\text{TiO}_2$  of 0.95 as well as more radiogenic  $^{208}\text{Pb}/^{204}\text{Pb}$  of ca. 39.45 at a given  $^{206}\text{Pb}/^{204}\text{Pb}$  of 19.36-19.51 and more radiogenic Sr. This composition is consistent with the occurrence of zircon megacrysts in the Emmelberg lava originating from mantle melts which differentiated into syenite intrusions [5]. Since lavas of the  $>480$  ka group to a large extent show higher  $(\text{Zr}/\text{Sm})_{\text{N}}$  (0.82-1.22) and  $\text{K}_2\text{O}/\text{TiO}_2$  (0.81-1.25) compared to that of the Emmelberg lava, it appears that sub-surface syenite intrusions are common within the region comprising the  $>480$  ka-old lavas, i.e. in the NW of the West Eifel.

Since the surface-projected seismological *P*-wave anomaly corresponds geographically to the  $<80$  ka-lava region in the SE, but not to that of the  $>480$  ka volcanism in the NW, the younger plume activity appears to lack syenitic products at depth.

[1] Ritter et al. (2001), *Earth Planet. Sci. Lett.* 186, 7-14; [2] Mertz et al. (2015), *J. Geodyn.* 88, 59-79; [3] Pfänder et al. (2012), *Geochim. Cosmochim. Acta* 77, 232-251; [4] Brandl et al. (2015), *J. Petrol.* 56, 1743-1774; [5] Schmitt et al. (2017), *J. Petrol.* 58, 1841-1870.

**Mon: 30****U/Th disequilibrium dating of Late Quaternary perovskite****Yi Sun, Axel Karl Schmitt***Heidelberg University, Germany*

Perovskite occurs as an accessory phase in late Quaternary alkali basalts of the West Eifel Volcanic Field (WEVF). It is often present as euhedral to skeletal-arborescent crystals in clefts or vesicles of lava flows, which indicates late-stage formation during or briefly after eruptive emplacement. Selected perovskite crystals from four different volcanoes (Rother Kopf, Grauley, Loehley, Emmelberg) were dated by a novel method of  $^{238}\text{U}/^{230}\text{Th}$  perovskite geochronology using secondary ion mass spectrometry (SIMS). In addition, trace element abundances in perovskite were determined with SIMS to provide insight into the conditions and processes related to its formation.

Perovskite crystals from the WEVF contain Fe, Nb, LREE and in some cases Sr as minor elements in concentrations up to several wt%. Traces of Ta, U and Th are present in concentrations of a few  $1000 \mu\text{g g}^{-1}$ . Comparatively high Pb with common isotopic composition renders U-Pb perovskite dating of such young crystals impossible. Perovskite crystals from the older activity period of the WEVF (Rother Kopf, Grauley, Loehley) are enriched in Th relative to U, with observed  $(^{238}\text{U})/(^{232}\text{Th})$  activity ratios ranging from 0.114 to 0.824. By contrast, Emmelberg perovskite from the younger WEVF eruptive pulse are generally highly enriched in U with  $(^{238}\text{U})/(^{232}\text{Th})$  activity ratios up to 14. Perovskite from Rother Kopf, Grauley and Loehley have reached secular equilibrium, consistent with known or inferred eruption ages  $>480$  ka from the literature. Emmelberg perovskite analyses, by contrast, plot along a well-defined isochron in the  $(^{230}\text{Th})/(^{232}\text{Th})$  versus  $(^{238}\text{U})/(^{232}\text{Th})$  diagram yielding an isochron age of  $48.4 \pm 2.4$  ka ( $2\sigma$ ). The  $^{238}\text{U}/^{230}\text{Th}$  perovskite age for Emmelberg volcano closely agrees with published  $^{40}\text{Ar}/^{39}\text{Ar}$  leucite ages averaging  $49 \pm 4$  ka, albeit with smaller uncertainties. This underscores that  $^{238}\text{U}/^{232}\text{Th}$  perovskite ages represent eruption ages due to their rapid crystallization in a late-magmatic, pneumatolytic stage shortly after lava flow formation. The results demonstrate the potential of perovskite for  $^{238}\text{U}/^{230}\text{Th}$  disequilibrium geochronology for late Pleistocene samples where analytical precision at the millennial timescale can be achieved. Perovskite present in deposits from late Pleistocene-Holocene alkaline volcanism such as in Southern Italy or the East African Rift are possible targets for this method.

## 6) Metamorphic systems

### 6a) Metamorphic processes

Wednesday, 25/Sep/2019: 1:00pm - 3:00pm

Session Chair: Michael Bröcker (WWU Münster)

Session Chair: Reiner Klemd (Universität Erlangen)

Location: H4

#### Session Abstract

Understanding and quantifying the processes that modify and shape the surface of the Earth requires the determination of accurate dates and rates. Thus, the improvement and development of existing and new dating methods is essential for a better understanding of Earth's surface processes and their relation to climate and tectonics. Currently employed geochronological methods include, for example, exposure and burial dating with cosmogenic nuclides, luminescence, radiocarbon, and paleomagnetic dating. This session invites contributions on developments and applications of all dating methods relevant to decipher Late Cenozoic landscape evolution, climate change, and active tectonics. The keynote speakers Georgina King (Lausanne) and Vincent Godard (Aix-Marseille) will give talks on luminescence thermochronometry and the use of  $^{36}\text{Cl}$  in carbonate landscapes. Interested participants are invited to visit the cosmogenic nuclide laboratory in Münster and discuss all aspects of  $^{10}\text{Be}$  separation and target preparation with R. Hetzel and T. Dunai.

#### Lecture Presentations

1:00pm - 1:30pm *Session Keynote*

#### Early Paleozoic blueschists from the Scandinavian and Svalbard Caledonides – what can they tell us?

Jarosław M. Majka<sup>1,2</sup>, Karolina Kościńska<sup>2</sup>, Christopher J. Barnes<sup>2</sup>, Michał Bukala<sup>2</sup>

<sup>1</sup>Uppsala University, Sweden; <sup>2</sup>AGH University of Science and Technology, Kraków, Poland

Blueschists are tracers of fossil subduction zones that provide valuable information on the early evolutionary stages of cold subduction systems. Although the global number of discoveries of blueschists is continuously increasing, early Paleozoic blueschists remain real rarities. Thus, they provide unique insight into relatively old, cold subduction systems, perhaps some of the earliest that operated on Earth. There are several localities of blueschists identified within the North Atlantic Caledonides, including those from the Appalachians as well as the British, Scandinavian and Svalbard Caledonides. The latter two occurrences are especially spectacular and preserve mildly retrogressed garnet-bearing and garnet-absent blueschist facies rocks that formed along quite cold c. 7-9°C/km geothermal gradients. This cold thermal regime allowed for stabilization of such low temperature-high pressure (LT-HP) phases such as carpholite and lawsonite, among the others. Thus, these rocks indeed serve as unique messengers from early Paleozoic subduction systems.

Here, we are focusing on blueschists (and associated eclogites) from the Vestgötabreen Complex of the Svalbard Caledonides and the Tsäkkok Lens of the Seve Nappe Complex in the Scandinavian Caledonides. Both LT-HP units are late Cambrian to early Ordovician and comprise metabasalts (including pillow lavas) hosted in metasediments. Both units are thought to have formed as a result of subduction of continent-ocean transition zone lithosphere beneath an island arc. Indeed, island arc lithologies that are broadly coeval with age of the blueschist formation were identified either in close proximity to the blueschist occurrence (i.e. the Virisen Arc of the Köli Nappe Complex that directly overthrusts the Tsäkkok Lens) or in a distal position (the M'Clintock Arc of the Pearya Terrane, Ellesmere Island, that may be correlated with the Vestgötabreen blueschists). Interestingly, both of these blueschist facies complexes share many similarities, for instance the

aforementioned presence of lawsonite (or pseudomorphs thereof), broadly similar age of metamorphism, comparable lithological assemblages, corresponding pressure-temperature histories, and a record of probable, seismically induced fabrics. Hence, the immediate question arises, where these two LT-HP complexes connected in both space and time? Notwithstanding the answer, it is apparent that one or more cold subduction systems, remarkably similar to Mesozoic and Cenozoic equivalents, were already active during the earliest stages of closure of the Iapetus Ocean. This observation, in turn, allows for investigation of the global evolution of mechanisms governing large-scale tectonic processes, of mass transfer at the slab mantle interface, and of possible triggers of intermediate depth earthquakes, since the early Paleozoic until recent.

**1:30pm - 1:45pm**

### **Evolution of a suture zone (Baie Verte Line; W Newfoundland, Canada) during a “hard” continent-arc collision: evidence from conditions and timing of metamorphism**

**Arne P. Willner<sup>1</sup>, Johannes Glodny<sup>2</sup>, Masafumi Sudo<sup>3</sup>, Cees R. Van Staal<sup>4</sup>, Alexandre Zagorevski<sup>5</sup>**

<sup>1</sup>Ruhr-Universität Bochum, Germany; <sup>2</sup>Geoforschungszentrum Potsdam, Germany; <sup>3</sup>Universität Potsdam, Germany;

<sup>4</sup>Geological Survey of Canada Vancouver, Canada; <sup>5</sup>Geological Survey of Canada Ottawa, Canada

The Baie Verte Line (BVL) in western Newfoundland marks a suture between an upper plate of obducted suprasubduction zone oceanic crust (Baie Verte Oceanic tract BVOT) and Ordovician volcanosedimentary rocks overlying the Dashwoods microcontinent and a lower plate of Laurentian margin metasediments and adjoining oceanic lithosphere. The uppermost unit of the underthrust Laurentian margin preserves the ocean-continent transition zone represented by the Birchy Complex (BC; 554-564 Ma protoliths; van Staal et al. 2014). The structurally overlying BVOT (487-491 Ma protoliths; Castonguay et al. 2014) formed in the Taconic seaway and was obducted at ~481-470 Ma. Laurentian margin was subducted under the BVOT to maximum depths by ~465 Ma in the BC (Castonguay et al. 2014). Lower and upper plate were deformed and intruded by voluminous plutons during the Salinic orogeny (426-445 Ma) followed by formation of a metamorphic core complex in the upper plate at 405-362 Ma (Anderson et al. 2001).

We derived first pressure-temperature (PT) data of the low grade rocks on both sides of the BVL by pseudo-section techniques as well as related metamorphic ages. Peak PT conditions in the BC vary within the range 7-10.5 kbar, 380-545°C (metamorphic gradient ~15°C/km) exceeding those of the BVOT (3-7 kbar, 270-400°C; metamorphic gradients between 15°C/km and 30°C/km).

Our new white mica Ar/Ar-spot ages and Rb/Sr mineral isochron ages invariably record events following the closure of the Taconic seaway. BC yielded ages ranging from 453±1 to 421±9 Ma which are interpreted as (re) crystallisation ages related to latest Taconic and Salinic deformation events. The BC was buried to maximal depth and concomitantly was extruded and exhumed within the upper part of a wedge during continued Taconic convergence and deformation. Younger out-of-sequence stacking and reburial during Salinic deformation was related to a subduction polarity reversal.

BVOT yielded younger ages (439±4 to 356±5 Ma) which are also interpreted as (re)crystallisation. The metamorphic gradient increased with time related to thermal relaxation. Only few Salinic ages are preserved, when W-vergent thrusting buried the upper plate rocks to depths of 10-25 km for the first time. Younger recrystallization ages (356±5 - 396±9 Ma) are related to extensional deformation during formation of the metamorphic core complex at the initial stages of formation of intracontinental Late Paleozoic Pangaeian basins.

[1] Anderson, S.D. et al. 2001, *The Journal of Geology* **109**, 191–211; [2] Castonguay, S. et al. 2014, *Geoscience Canada* **41**, 459-482; [3] van Staal, C.R. et al. 2013, *Geoscience Canada* **40**, 94–117

1:45pm - 2:00pm

### Subduction Initiation & metamorphic sole formation from the Lycian ophiolites, SW Turkey: Evidence for timing of plate boundary magmatism and metamorphism

**Osman Parlak<sup>1,2</sup>, Istvan Dunkl<sup>3</sup>, Albrecht von Quadt<sup>4</sup>, Fatih Karaoglan<sup>1</sup>, Timothy M Kusky<sup>2</sup>, Chao Zhang<sup>5</sup>, Lu Wang<sup>2</sup>, Jürgen Koepke<sup>5</sup>, Zeki Billor<sup>6</sup>, Willis A. Hames<sup>6</sup>, Emrah Simsek<sup>1</sup>, Gökçe Simsek<sup>1</sup>, Tugce Simsek<sup>1</sup>**

<sup>1</sup>Cukurova University, Geological Engineering Department, Adana, Turkey; <sup>2</sup>State Key Laboratory of Geol. Processes and Min. Resources, Center for Global Tectonics, School of Earth Sci., China University of Geosciences, Wuhan 430074; <sup>3</sup>Geoscience Center, University of Göttingen, Goldschmidtstr 3, 37077 Göttingen, Germany; <sup>4</sup>Institute of Geochemistry and Petrology, ETH Zurich, 8092 Zurich, Switzerland; <sup>5</sup>Institut für Mineralogie, University of Hannover, Callinstrasse 3, 30167 Hannover, Germany; <sup>6</sup>Auburn University, Department of Geology and Geography, Auburn, Alabama 36849, USA

The ophiolite-related units in the Lycian nappes are characterized by peridotites, metamorphic sole and ophiolitic mélangé in SW Turkey. The Lycian mélangé has been interpreted as an accretionary complex emplaced in the Late Cretaceous. The Lycian peridotites are represented by variously depleted mantle. The metamorphic sole, displaying approximately 350 m structural thickness, is tectonically sandwiched between the ophiolitic mélangé at the bottom and the peridotites at the top. The peridotite and metamorphic sole were intruded by numerous post-metamorphic and undeformed isolated dykes. The tectonic contact between metamorphic sole and the peridotite was also intruded by a 3 m thick undeformed isolated dyke which postdates intraoceanic metamorphism and high-temperature ductile deformation. Protolith of the amphibolites from the metamorphic sole was derived from alkali and tholeiitic magma sources. The isolated dykes are exclusively basaltic in composition and were derived from an island arc tholeiitic magma source. The post-metamorphic isolated dyke cutting the tectonic boundary between the metamorphic sole and the mantle tectonites yielded  $94.0 \pm 1.9$  Ma zircon U-Pb age, suggesting the timing for termination of deformation along the oceanic decoupling surface. The isolated dyke cutting the metamorphic sole yielded  $95.2 \pm 4.6$  Ma titanite U-Pb age. The isolated dyke cutting the peridotites yielded  $88.7 \pm 1.5$  Ma zircon U-Pb age. Metamorphic sole amphibolites from Köyceğiz area yielded U-Pb as well as Ar-Ar ages such as:  $202.7 \pm 5.4$  to  $89.6 \pm 1.8$  Ma (zircon);  $90.6 \pm 8.3$  Ma (titanite) and  $98.44 \pm 0.42$  to  $96.96 \pm 0.24$  Ma (amphibole). Metamorphic sole amphibolites from Yeşilova area yielded U-Pb as well as Ar-Ar ages such as:  $118.0 \pm 8.0$  to  $117.1 \pm 2.1$  Ma (zircon);  $84.2 \pm 2.5$  Ma (rutile) and  $94.37 \pm 0.28$  to  $93.49 \pm 0.17$  Ma (amphibole). In general, U-Pb and Ar-Ar ages from the metamorphic sole and the isolated dykes overlap within  $1\sigma$  error. This may suggest that subduction initiation and metamorphic sole formation were contemporaneous within the Neotethyan oceanic basin in late Cretaceous. However, U-Pb isotopic age on zircon ( $202.7 \pm 5.4$  Ma) and Ar-Ar isotopic age on amphibole ( $96.96 \pm 0.24$  Ma) from the metamorphic sole (K14-8) suggest that the metamorphism along the intra-oceanic decoupling surface during subduction initiation were not able to reset U-Pb clock. The late Triassic age (202 My) may also suggest the existence of mafic crust within the Neotethyan oceanic basin. This work was funded by TÜBİTAK (Project No 113Y412).

2:00pm - 2:15pm

### Low pressure-high temperature metamorphism and migmatization in the Proterozoic Epupa Complex, NW Namibia.

**Patrick Bobek<sup>1</sup>, Soenke Brandt<sup>1</sup>, Reiner Klemd<sup>1</sup>, Ewereth Muvangua<sup>2</sup>**

<sup>1</sup>GeoZentrum Nordbayern, Erlangen, Germany; <sup>2</sup>Ministry of Mines and Energy, Windhoek, Namibia

The Epupa Complex (EC) represents the largest pre-Pan-African basement complex of northern Namibia (Brandt et al., 2003) and constitutes the southwestern margin of the Archean to Paleoproterozoic Congo Craton. The complex consists of high-grade metamorphic, widely migmatized ortho- and paragneisses and was intruded by the 1385-1319 Ma Kunene Intrusive Complex (Drüppel et al., 2007). Anorthosite emplacement caused regional-scaled upper-amphibolite facies contact metamorphism (1340-1320 Ma) in the southern part (Orue Unit) of the EC (Brandt et al., 2008). The rocks of the Orue Unit are associated by granulite facies

rocks that were affected by Mesoproterozoic UHT metamorphism ( $1450\pm 50$  Ma; Brandt et al., 2003, Seth et al., 2003). In the northern part of the EC a sequence of migmatitic ortho- and paragneisses (Eyao Unit) is exposed along the Kunene River that has not been studied in detail so far. The sequence was intruded by granites with emplacement ages of ca. 1835 Ma (Kröner et al., 2015). Field relationships suggest that the rocks of the Eyao Unit were affected by a  $> 1835$  Ma high-grade metamorphic event that was presumably completely erased in the EC rocks of the southern part during the high-grade metamorphic Mesoproterozoic overprints. To characterize the geodynamic significance of this so far poorly known Paleoproterozoic event at the southern margin of the Congo Craton we have reconstructed the P-T evolution of the Eyao Unit rocks. Conventional geothermobarometry and P-T pseudosection modelling in the MnNCKFMASHTO system for metapelites with strongly variable bulk rock XMg revealed simple heating-cooling P-T paths without significant pressure variation that culminate at upper-amphibolite to granulite facies peak-conditions of ca.  $720^{\circ}\text{C}$  and ca. 4 kbar. Grt-Crd peak-assemblages are restricted to relatively Fe-rich migmatitic metapelites (XMg: 0.27-0.41). Migmatitic Grt-free Crd and non-migmatitic Opx-Crd assemblages occur in magnesian metapelites (XMg: 0.71 and 0.74). The geochronological study of the rocks that is currently in progress will help to resolve whether the P-T paths and the very high geothermal gradient (ca.  $60^{\circ}\text{C}/\text{km}$ ) recorded by the low-pressure-high temperature rocks record a contact-metamorphic overprint related to the emplacement of a large gabbro complex into the Eyao rocks or to regional-scale lithospheric delamination at the southern margin of the Congo craton.

[1] Brandt et al., (2003) *Journal of Petrology*, 44(6), 1121-1144; [2] Brandt et al., (2008) *Journal of metamorphic Geology*, 26(9), 871-893; [3] Drüppel et al., (2007) *Precambrian Research*, 156(1-2), 1-31; [4] Kröner et al., (2015) *Tectonophysics*, 662, 125-139; [5] Seth et al., (2003) *Precambrian Research*, 126(1-2), 147-168.

**2:15pm - 2:30pm**

### **Reconstitution of mineral compositions reflecting peak-metamorphic conditions: Ti-in-quartz thermobarometry applied to ultrahigh-temperature granulites**

**Jürgen Reinhardt, Dirk Frei**

*Department of Earth Sciences, University of the Western Cape, South Africa*

Thermobarometry and P-T path reconstruction in granulites can be problematic for a variety of reasons. While typical mid-amphibolite-facies rocks tend to reveal at least part of their prograde history through host-inclusion relationships, growth zoning of minerals, prograde reaction textures and widespread preservation of peak mineral equilibria, granulites tend to have lost most of their pre-peak “memory”, including microstructural features and the record of their prograde reaction history. While the high temperatures are conducive to thorough chemical equilibration between minerals, they almost inevitably cause post-peak modifications of mineral assemblages and mineral compositions, particularly if cooling rates are low. Thermobarometry that is based on solid solutions (solvus thermometry, major- or trace-element saturation of minerals) will be affected by such cooling-induced modifications.

A common cooling-related feature in high-grade rocks is exsolution. Where it can be argued that the mineral grains behaved as closed systems, the compositional re-integration of the exsolved phase and its host phase should provide an original mineral composition that reflects peak metamorphic conditions. The observation of widespread rutile unmixing in quartz from UHT granulites present as xenoliths in South African kimberlites has led us to test the viability of reconstitution of original Ti-rich quartz compositions and the compatibility of the Ti-in-quartz thermometer (“TitaniQ”; Wark & Watson, 2006, *Contrib. Mineral. Petrol.* 152; Thomas et al., 2010, *Contrib. Mineral. Petrol.* 160) with the UHT mineral assemblages observed in these rocks.

The samples considered here contain the assemblage garnet-sillimanite-mesoperthite-quartz-rutile, with sapphirine and spinel as inclusions in garnet. In quartz grains, evenly distributed rutile forms a regular distribution pattern of three sets of thin needles, evidently related to the crystal structure of the host quartz. The crystallographic relationship between the two minerals confirms the unmixing of  $\text{TiO}_2$  from high-temperature quartz. Similar rutile textures are also observed in the coexisting garnets. There is abundant, coarser-grained rutile in the matrix, providing conditions of  $\text{TiO}_2$  saturation during metamorphism.

We analysed quartz + rutile domains in large enough quartz host grains with Laser-Ablation ICP-MS, maximising the analysed volume by using a large-radius laser beam. The measured Ti trace element levels at about 700 ppm of the “reconstituted” quartz are indeed in line with the UHT conditions recorded by the mineral assemblages. Hence, this method allows to apply the TitaniQ thermometer where granulites have experienced significant retrograde overprinting, provided that the unmixing is regular on a small enough length scale and quartz did not recrystallize under post-peak conditions.

**2:30pm - 2:45pm**

### **Grain and phase boundaries in rocks of the upper crust and at the earth's surface**

**Jörn H. Kruhl<sup>1</sup>, Richard Wirth<sup>2</sup>, Luiz F.G. Morales<sup>3</sup>, Elnaz Raghimi<sup>1</sup>, Christoph Schrank<sup>4</sup>, Wolfgang Schmahl<sup>1</sup>, Anja Schreiber<sup>2</sup>**

<sup>1</sup>Dept. of Earth and Environmental Sciences, Ludwig-Maximilians-Universität München, Germany; <sup>2</sup>Helmholtz Centre Potsdam, GFZ German Research Centre for Geosciences, Germany; <sup>3</sup>Scientific Center for Optical and Electron Microscopy (ScopeM), ETH Zürich, Switzerland; <sup>4</sup>School of Earth, Environmental and Biological Sciences, Queensland University of Technology, Brisbane, Australia

Transmission electron microscopy (TEM) and 3D FIB/SEM nanotomography are applied to grain and phase boundaries between quartz, plagioclase, K-feldspar, clinopyroxene, amphibole and calcite. The samples come from a variety of metamorphic, plutonic, and volcanic rocks, which experienced cooling and decompression after highly variable P-T peak conditions. Most of the boundaries are partially open in the range of up to several hundred nanometers and partly to totally filled with secondary minerals, such as actinolite, biotite, sheet silicates, ilmenite, and crystalline as well as amorphous quartz. Up to few square micrometer large cavities develop due to dissolution during fluid flow.

The open grain and phase boundaries, together with cavities, form porosities of up to ~2 Vol-% and a connected network that provides permeability. Consequently, the open and partly filled pore space increases the reactivity of rocks as well as weathering and disaggregation, and affects the physical properties, such as strength, conductivity, elasticity and seismic wave velocity. In addition, it forms a potential reservoir for fluids and for fluid transport to deeper parts of the continental crust or, in case of ocean floor basalt, to the upper mantle.

The filling with secondary minerals and correlations between grain sizes and widths of the open and/or filled grain and phase boundaries suggest that opening is probably induced by exhumation when cooling at temperatures below the diffusion threshold of the various minerals and decompression leads to grain-scale thermal-elastic internal stresses that overcome the strength of grain and phase boundaries. Due to the anisotropy of thermal and elastic material properties, boundaries are kept open even at confining pressures of several hundred MPa.

The cracking of boundaries during exhumation along geologically relevant P-T paths are simulated at the grain scale with 3D numerical forward modelling. In addition, numerical studies are performed if and how mean grain size affects grain-boundary fracturing. Empirical scaling relations for finite grain-boundary crack width and the proportion of cracked grain boundaries as a function of mean grain size, and temperature as well as pressure interval will be derived.

## Poster Presentations

Tue: 36

**A Barrovian-type overprint of high pressure rocks: PTt-evolution in the Ordovician Corner Brook Complex (W-Newfoundland, Canada)**

**Thilo Bißbort<sup>1</sup>, Arne P. Willner<sup>1</sup>, Johannes Glodny<sup>2</sup>, Cees R. van Staal<sup>3</sup>, Hans-Peter Schertl<sup>1</sup>, Alexandre Zagorevski<sup>4</sup>**  
<sup>1</sup>Ruhr-Universität Bochum, Germany; <sup>2</sup>Deutsches Geoforschungszentrum Potsdam, Germany; <sup>3</sup>Geological Survey of Canada Vancouver, Canada; <sup>4</sup>Geological Survey of Canada Ottawa, Canada

The Corner Brook and Fleur de Lys metamorphic complexes in western Newfoundland, comprise metasedimentary rocks of the partially subducted Humber margin of Laurentia metamorphosed at medium grade and intermediate to high pressure conditions during the collision with outboard arcs. Both complexes are interpreted as parts of an extruded wedge. The Corner Brook Complex (CBC) consists of metapelitic and metapsammitic rocks showing a pronounced Barrovian zonation in the field. PT paths derived by PT pseudosection calculation indicate an evolution of the complex at four stages: (I) Burial of Peri-Laurentian continental crust after closure of the intervening oceanic seaway initiated prograde garnet growth at 500-550°C, 6.2-9.3 kbar. (II) Maximum submergence of the CBC at 520-610 °C, 8.2-11.7 kbar was followed by extrusion and exhumation with simultaneous thermal relaxation. (III) Out-of-sequence imbrication within the complex was accompanied by extensive fluid flow and a final stage of thermal relaxation (560-650 °C, 6.9-9.2 kbar) forming the Barrovian zonation. As a result the observed peak T mineral assemblages formed and only relics of the former high-pressure stage remained. Interrelated PT paths of opposing direction can be related to stacking in midcrustal levels. (IV) Late emplacement of the complex involved upper crustal folding and large-scale brittle thrusting.

We dated two samples with a predominating stage III assemblage by Rb-Sr mineral isochrones at 429±6 and 440±6 Ma. These ages confirm previous ages (U/Pb zircon 434 Ma, monazite 430 Ma, rutile 437 Ma; Ar/Ar white mica 413-430 Ma; Cawood et al. 1994) and are related to the Salinic orogenic overprint (~440-420 Ma). Extensive fluid influx had a notable impact on the evolution of various segments of the complex with strongly variable extent. Features produced by fluid-rock interaction are the partial resorption of garnet formed at high pressure and formation of megablasts where fluid flow was intense. By contrast in the Fleur de Lys Complex west of the town of Baie Verte the age of the maximum burial is known (e.g. in eclogite U/Pb metamorphic zircon 465 Ma, Castonguay et al. 2014; Rb-Sr mineral isochron 461 Ma, Willner et al. 2015). Nevertheless this complex was also overprinted by Salinic deformation during exhumation, but to minor extent compared to the CBC.

[1] Castonguay, S., van Staal, C.R., et al. (2014) *Geoscience Canada* **41**, 459-482; [2] Cawood, P.A., Dunning, G.R., et al. (1994) *Geology* **22**, 399-402; [3] Willner, A.P., Glodny, J., et al. (2015) *International Eclogite Conference Rio San Juan 2015, Program with Abstracts*, 104.

Tue: 37

**Investigation of U-Pb ages from the Bantimala Complex, SW Sulawesi, Indonesia: Protolith ages and an unusual zircon population**

**Mischa Böhnke<sup>1</sup>, Michael Bröcker<sup>1</sup>, Adi Maulana<sup>2</sup>, Reiner Klemd<sup>3</sup>, Jasper Berndt<sup>1</sup>**  
<sup>1</sup>Institut für Mineralogie, Westfälische-Wilhelms Universität Münster, Corrensstr. 24, 48149 Münster, Germany;  
<sup>2</sup>Department of Geology Engineering, Hasanuddin University, 90245 Makassar, Indonesia; <sup>3</sup>GeoZentrum Nordbayern, Universität Erlangen, Schlossgarten 5a, 91054 Erlangen, Germany

Indonesia is a tectonically active region with a complex geodynamic history. Beginning in the Mesozoic Gondwana derived continental fragments collided and amalgamated along various subduction zones and formed a difficult to decipher tectonic mosaic. To unravel the temporal evolution of the Central Indonesia Accretionary Collision Complex (CIACC) accurate and precise geochronological data is needed. Rb-Sr and K-Ar isotopic ages of the rare occurrences of high-pressure/low-temperature metamorphic rocks offer information about the Cretaceous subduction and collision history in the CIACC (Parkinson et al. 1998). U-Pb zircon dating however,

offers the possibility to date pre-metamorphic events to improve our understanding of the large-scale geodynamic processes in the Indonesian region.

In this study, we present U-Pb ages of two HP/LT rocks from the Bantimala Complex located on the island of Sulawesi. Our data provide first constraints for previously unknown protolith ages, indicating a Late Triassic-Early Jurassic time of formation (205-185 Ma). Furthermore, the zircon population of a retrogressed eclogite records a more complex history including evidence for igneous crystallization, metamorphic recrystallization or growth, inheritance and variable degrees of Pb-loss. Metamorphic rims yielded a U-Pb age of ca. 133 Ma, that is at least 3 Myr older than the corresponding Rb-Sr white mica age for this rock. Interestingly we found numerous Palaeozoic and Proterozoic zircons (400-260 Ma and 2.55-1.4 Ga) significantly older than the assumed protolith age. Petrographic observations point to a basaltic or gabbroic origin of this rock and are not consistent with a continental crustal origin of the zircon population. We favor the interpretation that zircons older than the protolith age represent detrital grains from subducted sediments that had been incorporated in mafic melts directly derived from a contaminated mantle source. The presence of continentally-derived detrital zircons that have presumably been included during melt formation in the mantle has not yet been described for any eclogite- and/or blueschist-facies rock of basaltic or gabbroic parentage.

[

1] Parkinson et al. (1998), *Island Arc* 7, 184-200.

## Tue: 38

### Structural and petrographic description of an ultramafic complex in the north of the Fjällfjäll-window (North Sweden)

**Laura Meyer**

*Martin-Luther-University Halle-Wittenberg, Germany*

In context of a bachelor thesis a serpentinite conglomerate was mapped in North Sweden, north of the Gottern lake in July 2018. The investigated ultramafic complex appears for more than 20 km on the surface of the central Caledonians Northwest of the Fjällfjäll-window. In the working area there were three different units found, which are components of a nappe complex (Köli-Nappe, upper allochthon). During the Caledonian orogeny this complex was piled up along with other nappe complexes as a result of the formation of an orogenic wedge.

In addition to the ultramafic complex, the units of a meta-granite (in the west of the mapping area) and a quartz phyllite (west- and eastwards of the ultramafic complex) were found. The outcrop of these units stretches from northwest to southeast.

The conglomerate consists mainly of mafic components that have been formed in the serpentinization of olivine: serpentine (chrysotile), muscovite, magnetite and chlorite. Its matrix is often very rich in carbonate. Actinolite, biotite as well as hematite and other ore phases are available.

The components of the conglomerate have a diameter of 1 mm to 20 cm. They are well preserved in the center. Outcrops in the center of the complex have a massive appearance, whereas at its edge a strong foliation is formed. The meta-granite has a mylonitic structure consisting mainly of quartz, plagioclase, muscovite, garnet and amphibole. The quartz phyllite is characterized by its foliation of quartz and muscovites, which are folded. Internally, crenulation folds were observed in this unit. They arose during a mylonitization of the material, which was accompanied by the thrusting of the three units to the east-southeast.

Also the periphery area of the serpentinite conglomerate was sheared in a ductile state. This was followed by a boudinage of the complex, which is clearly visible in the outcrop. The main S<sub>n</sub>-foliation adapts to the boudinage, but shows predominantly a southwest-northeast strike direction and a dip of the layers to the southeast. The first rock-forming process was the collision of the continents Baltica and Laurentia and the associated closure of the Iapetus ocean. As a result, dunite was displaced from the oceanic crust to continental crust. There was a short transport of the material from the hinterland to the beach area in which boulders were formed. Subsequently, the material was formed retrograde metamorphically at about 550 °C and 5

kbar and belongs to greenschist to amphibolite facies.

**Tue: 39**

### Contradictory in-situ U-Pb ages from major and accessory metamorphic phases

**Leo J. Millonig<sup>1</sup>, Richard Albert<sup>1</sup>, Dov Avigad<sup>2</sup>, Axel Gerdes<sup>1</sup>**

<sup>1</sup>Department of Geosciences, Goethe University Frankfurt, Germany; <sup>2</sup>Institute of Earth Sciences, Hebrew University of Jerusalem, Israel

A common credo in metamorphic petrology is that inclusions are as old, or older than, the surrounding host phase. This holds true in most cases. However, in other cases, *e.g.*, monazite in garnet yields younger ages than the surrounding garnet (Hagen-Peter et al., 2016). Since metamorphic ages are commonly obtained from the accessory phases, this may lead to erroneous conclusions with respect to the timing of metamorphism. Furthermore, studies that investigate the geochronology of accessory and major metamorphic phases are still sparse, although the metamorphic history of a rock can be best unraveled, if in-situ U-Pb ages of both, major and accessory phases, are tied to the pressure-temperature evolution of that rock.

In our study area, the Arabian-Nubian Shield (ANS), which forms the northern branch of the East African Orogen, evolved from intra-oceanic island arcs into a mature continental crust in the course of ~300 m.y. of Neoproterozoic Pan-African orogeny. The metapelitic Elat Schist in southern Israel records two metamorphic events that affected the northern part of the ANS, but the significance, extent and the exact timing of these events is controversially discussed.

Previous geochronological studies on metamorphic monazite, in conjunction with field evidence, indicate that the main period of regional amphibolite-facies metamorphism occurred at ~620 Ma, just prior to and coeval with regional-scale intrusions of late-orogenic granitoids. However, other field observations from the Elat area provide evidence that regional metamorphism also occurred prior to ~705 Ma. This older age is inferred from an EW trending, vertically-foliated, ~705 Ma greenschist-facies dike swarm, which cross-cuts the shallow-dipping foliation of the garnet-bearing Elat Schist, thus indicating a more prolonged metamorphic evolution.

In order to gain a more comprehensive understanding of the metamorphic history of this area, we applied in-situ U-Pb dating of monazite, garnet and staurolite to metapelitic samples from the Elat area. Our preliminary results suggest that garnet and staurolite grew at  $\geq 700$  Ma, whereas monazite grew at ~600-620 Ma and preserves no evidence for the  $>700$  Ma metamorphic event. Although the interpretation of U-Pb garnet and staurolite data is complicated due to monazite and/or zircon inclusions, staurolite from this study yields well-defined isochrones and seems to be particularly well-suited for giving meaningful metamorphic ages.

[1] Hagen-Peter, G., Cottle, J.M., Smit, M., Cooper, A.F., 2016. Coupled garnet Lu-Hf and monazite U-Pb geochronology constrain early convergent margin dynamics in the Ross orogen, Antarctica. *Journal of Metamorphic Geology* 34, 293–319. <https://doi.org/10.1111/jmg.12182>

**Tue: 40**

### Petrological and Lu-Hf age constraints for eclogitic rocks from the Pam Peninsula, New Caledonia

**Stephan Taetz<sup>1</sup>, Erik Scherer<sup>1</sup>, Michael Bröcker<sup>1</sup>, Timm John<sup>2</sup>, Carl Spandler<sup>3</sup>**

<sup>1</sup>Institut für Mineralogie, Westfälische Wilhelms-Universität Münster, Corrensstraße 24, 48149 Münster, Germany;

<sup>2</sup>Institut für Geologische Wissenschaften, Freie Universität Berlin, Malteserstr. 74-100, 12449 Berlin, Germany;

<sup>3</sup>Economic Geology Research Centre, James Cook University, Townsville, 4811, Australia

We report new petrological and geochronological data for eclogitic rocks of the Pouébo Eclogite Mélange in the New Caledonian high-pressure/low-temperature (HP/LT) belt. Pseudosections were calculated to link newly determined Lu-Hf dates with P-T conditions corresponding to garnet growth. This modeling indicates that garnet crystallization started in the blueschist facies and continued into the eclogite facies to approximately 560 °C and

2.05 GPa, coinciding with early stages of omphacite formation. We interpret the Lu-Hf garnet-omphacite dates of  $38.27 \pm 0.14$ ,  $36.5 \pm 0.7$ , and  $38.42 \pm 0.15$  Ma to mark the highest-grade metamorphic stage of our samples. These dates are indistinguishable from those reported earlier from K-Ar and Ar-Ar in mica<sup>1,2</sup>, which had been interpreted as cooling ages, and about 6 Myr younger than those from U-Pb in zircon<sup>3</sup>, which had been considered to date peak metamorphism. The new dates are within error of those from Rb-Sr in white mica in a nearby metasomatic vein system that is considered to represent the blueschist-to-eclogite transition<sup>4</sup>. This implies that eclogite facies metamorphism in parts of the PEM lasted at least until ca. 38 Ma and is thus younger than previously thought. The Lu-Hf garnet and Rb-Sr white mica dates cannot be reconciled with a simple cooling history of a coherent tectonic block, as assumed earlier on the basis of Ar-Ar dates within the same range (41-36 Ma). We conclude that the younger Lu-Hf and Rb-Sr dates either record different P-T-t histories of individual blocks, or that the K-Ar and Ar-Ar data are compromised to variable extents by excess Ar. The HP stage is followed by rapid exhumation and cooling with exhumation rates of  $\sim 1.5\text{-}2$  cm/yr.

[1] Baldwin, S. L., Rawling, T. & Fitzgerald, P. G. (2007). *Geol. Soc. Am. Spec. Pap.* 419, 117–134; [2] Vitale Brovarone, A., Agard, P., Monié, P., Chauvet, A. & Rabaute, A. (2018). *Earth-Sci. Rev.* 178, 48–67; [3] Spandler, C., Rubatto, D. & Hermann, J. (2005). *Tectonics* 24. <sup>4</sup>Taetz, S., John, T., Bröcker, M. & Spandler, C. (2016). *Contrib. Mineral. Petrol.* 171, 90.

## 6b) Reaction and deformation

Tuesday, 24/Sep/2019: 8:30am - 10:00am

Session Chair: Claudia A. Trepmann (Ludwig-Maximilians University Munich)

Session Chair: Sumit Chakraborty (Ruhr Universität Bochum)

Location: Vom Stein Haus, Aula / VSH 219

### Session Abstract

The session focusses on the interplay between metamorphic/metasomatic reactions and deformation as well as the influence of such interplay on the rates of the various processes. All contributions that address the pressure, temperature, stress and time evolution in deforming and reacting rocks using observations on natural systems as well as theoretical, experimental and analytical approaches are welcome.

### Lecture Presentations

8:30am - 9:00am Session Keynote

#### Deformation facilitated by transformative processes: mineral reactions and diffusion creep in the mafic system

Holger Stunitz<sup>1,2</sup>, Nicolas Mansarde<sup>2</sup>, Sina Marti<sup>3</sup>, Hugues Raimbourg<sup>2</sup>, Jacques Precigout<sup>2</sup>, Renee Heilbronner<sup>4</sup>, Jiri Konopasek<sup>1</sup>, Oliver Pluemper<sup>5</sup>, Ane Finstad<sup>1</sup>, Kai Neufeld<sup>1</sup>, James McKenzie<sup>4</sup>

<sup>1</sup>University of Tromsø, Norway; <sup>2</sup>University of Orléans, France; <sup>3</sup>Edinburgh University; <sup>4</sup>Basel University, Switzerland;

<sup>5</sup>Utrecht University, Netherlands

Mafic rocks with their main constituents pyroxene, plagioclase, and amphiboles are mechanically very strong, even at high pressures and temperatures, because intracrystalline plasticity is difficult to activate. As large parts of the oceanic lithosphere and lower continental crust consist of mafic rocks, their rheology may control large parts of the earth's crust.

Experiments in solid medium apparatus in the temperature range between 750 and 900°C show that mechanical weakening is always associated with zones of mineral reactions. Deformation is strongly partitioned into these zones. The dominant deformation mechanism is always dissolution precipitation creep, a form of diffusion creep. Reaction products nucleate and produce fine grained aggregates. The resulting phase mixing

effectively inhibits grain growth, leading to a stable microstructure. Localization of deformation in this way depends, among other factors, on the metastability of reaction products. Fast nucleation from large overstepping facilitates efficient switch to diffusion creep deformation.

Deformation at high stresses at lower temperatures (300 to 600°C) can produce amorphous material by high defect densities, i.e. mechanical wear, without melting. These zones localize strain as they appear to have low viscosity. The amorphous material is metastable and may later be favored sites of nucleation of stable minerals. Stress concentrations can arise in all polycrystalline materials without applying very high bulk stresses, so that the observed processes may constitute viable mechanism of deformation in natural rocks.

In natural rocks the same transformation processes in deformation zones as in experiments can be observed. Reactants dissolve and the precipitating stable phases show anisotropic growth and strong mineral fabrics, constituting a transformation processes that leads to pronounced weakening of the rock. The strong fabrics produced are commonly not expected during deformation by diffusion creep. However, anisotropic growth of new phases can produce such fabrics, and dislocation creep deformation as a process can clearly be excluded in some cases.

**9:00am - 9:15am**

### **Growth related defect microstructures in replacement reactions**

**Kilian Pollok, Falko Langenhorst**

*Institute of Geosciences, Friedrich Schiller University Jena, Germany*

Fluid-mediated replacement reactions have been recognised as an important driver of geodynamical processes. Deformation microstructures are often used to document metamorphic events, whereas local stresses are typically released during fluid- or melt-mediated mineral reactions. However, the microstructural inventory of growth induced defects of mineral reactions is largely unknown. For example, strong localisation of shear stresses can lead to seismic failure even at eclogite facies conditions, producing frictional melting and fast crystallisation that leaves a rich defect microstructure behind (Pollok et al., 2014). Furthermore, fluid-mediated interface coupled dissolution-precipitation reactions in a salt model system revealed microstructures that resemble those created by deformation (Spruzeniece et al. 2017).

Here, we show using transmission electron microscopy that growth-related defects must be considered to be common in fluid-mediated replacement processes at crustal conditions. Examples include chlorapatite to hydroxylapatite replacement experiments (100 MPa, 500 °C) and a naturally regressed rock (eclogite to amphibolite, ~500 °C, 1 wt% H<sub>2</sub>O).

Hydrothermal replacement of chlorapatite by hydroxylapatite is topotactic and associated with a negative relative volume change which results in a significant porosity in replaced part. The interface is sharp at atomic scale and the crystallographic information completely transferred producing a single crystal as replacement. The pore sizes vary from tens of nm to the µm scale. Small pores are usually strongly elongated parallel to the c axis and only a few lattice planes wide. They produce a strain field and were probably filled by trapped fluid. Weak-beam dark field imaging reveals numerous dislocations in various configurations for the replaced part, whereas the parent crystal is free of defects.

In the regressed rock, omphacite is replaced by amphibole, plagioclase and quartz leaving a streaky replacement texture with rhythmic quartz trails that still indicate the fluid flow direction. Surprisingly, the pervasive fluid flow at grain scale seems not impose any stress gradients due to volume changes of mineral reactions. Plagioclase shows well equilibrated exsolution textures and straight grain boundaries towards amphibole. However, amphibole displays stacking faults starting at pores now filled with sheet silicates. Quartz shows numerous dislocations which cannot be the result of deviatoric stresses. Both examples indicate that the defect microstructures are growth-induced and that a detailed and comprehensive microstructural analysis is necessary to distinguish them from deformation.

[1] Pollok, K., Heidelbach, F., John, T., Langenhorst, F. (2014), DOI: 10.1016/j.chemer.2014.04.001; [2] Spruzeniece, L., Piazzolo, S., Maynard-Casely, H.E. (2017), DOI: 10.1038/ncomms14032

9:15am - 9:30am

## Wall-rock damage and alteration in orthogneisses from Lofoten as revealed by CL imaging, EBSD, and TEM analyses

**Kristina G. Dunkel<sup>1</sup>, Luiz. F. G. Morales<sup>2</sup>, Bjørn Jamtveit<sup>1</sup>**

<sup>1</sup>PGP, The Njord Centre, University of Oslo, Norway; <sup>2</sup>ScopeM, ETH Zürich, Switzerland

Although earthquakes themselves are short events, the damage they produce can have long-lasting effects on the further tectonic and metamorphic developments of the rocks they affected (Jamtveit et al., 2018). For example, faults can serve as fluid pathways or work as precursors for ductile shear zones. A common feature of seismic damage is the wall rock damage caused by the propagation of the dynamic rupture front.

Pulverization of wall rock is commonly described in shallow seismic faults (e.g., Dor et al., 2006), and comparable crystal-plastic fragmentation has been observed from deep crustal earthquakes as well (Austrheim et al., 2017). However, the wall rocks to many deep pseudotachylytes appear undamaged in optical and backscatter electron microscopy. This is also the case in monzonitic to gabbroic orthogneisses from Moskenesøya, in the southern part of the Lofoten Vesterålen Archipelago in Norway. These orthogneisses are cut by pseudotachylytes, which generally have the same mineralogy as the wall rock. The pseudotachylytes range from pristine (with preserved spherulites) to sheared. Although the wall rock appeared undamaged in optical and backscatter observation, cathodoluminescence (CL) imaging of the feldspar minerals (and minor quartz) revealed a multitude of healed fractures and alteration rims.

This shows that a) wall rock damage during deep crustal earthquakes may be more common than assumed, despite the high confining pressure, and b) CL imaging can be a very helpful tool to document (pre-existing) microstructures.

The CL spectra of the wall rock feldspars show several peaks that are not trivial to interpret; hence we investigate these feldspars further with electron backscatter diffraction and transmission electron microscopy to get a better understanding of the crystallographical and chemical changes that took place during and after the seismic event.

[1] Austrheim, H., Dunkel, K.G., Plümper, O., Ildefonse, B., Liu, Y. & B. Jamtveit (2017): Fragmentation of wall rock garnets during deep crustal earthquakes. *Science Advances* 3, e1602067; [2] Dor, O., Ben-Zion, Y., Rockwell, T.K. & J. Brune (2006): Pulverized rocks in the Mojave section of the San Andreas Fault Zone. *Nature* 434, 749-525; [3] Jamtveit, B., Ben-Zion, Y., Renard, F. & H. Austrheim (2018): Earthquake-induced transformation of the lower crust. *Nature* 556, 487-491.

9:30am - 10:00am Session Keynote (Goldschmidt-Prize 2018)

## Quantifying non-hydrostatic, reaction-induced stresses during metamorphic hydration reactions

**Oliver Plümper<sup>1</sup>, Floris Teuling<sup>1</sup>, David Wallis<sup>1</sup>, Thomas Müller<sup>2</sup>**

<sup>1</sup>Utrecht University, Department of Earth Sciences, Utrecht, The Netherlands; <sup>2</sup>University of Leeds, School of Earth and Environment, Leeds, United Kingdom

Hydration reactions are a fundamental metamorphic process and play a critical role in Earth's tectonics and water budget. Petrological observations emphasized that volume expansion during hydration was accommodated by pressure solution or tectonic extension. However, these reactions can also generate significant non-hydrostatic stresses. Resultant dilatant fracturing can increase permeability, driving reaction fronts forward, but constraints on magnitude and distribution of reaction-induced stresses as well as the contribution of thermal contraction to this stress are largely unknown. Here we apply high-angular resolution electron backscatter diffraction (HR-EBSD) to the simple case of deformed calcite surrounding brucite after periclase. By cross-correlating regions of interest within diffraction patterns, HR-EBSD provides a precise determination of lattice strains and residual stresses. Using finite element modelling coupled to HR-EBSD we estimate the stresses induced by thermal contraction, indicating that the minimum reaction-induced residual stresses are about one gigapascal. The stress fields extend tens of micrometres away from hydration sites. High twin,

fracture, and dislocation densities in calcite near brucite likely formed by relaxation of these stresses. In summary, these non-hydrostatic stresses are large enough to lead to inelastic and elastic deformation, likely influencing far-field stress states and affecting local reaction thermodynamics.

**Tuesday, 24/Sep/2019: 10:45am - 12:30pm**

**10:45am - 11:00am**

### **Magnetic signatures of rock deformation**

**Agnes Kontny, Boris Reznik, Mario Walter, Helena Fuchs, Frank Schilling**

*KIT, Germany*

Magnetic properties of rocks are pressure-sensitive and frequently used for revealing the dynamics of tectonic-related deformation phenomena within the Earth's crust [1]. Among different magnetic methods, the anisotropy of magnetic susceptibility (AMS) is a well-established method in petrofabric analyses. In metamorphic rocks, AMS can be pronounced and magnetic lineations and foliations are the result of plastic deformation under directional static stress [2]. A serious modification of magnetic properties occurs during hypervelocity impacts. Magnetic and microstructural studies have shown that e.g. a decrease in magnetic susceptibility is mainly related to a shock-induced refinement of magnetic domains in a cooperative process of brittle and ductile deformation mechanisms [3]. Up to now, modification of magnetic properties are mainly reported from static or dynamic shock-related deformation experiments. However, it is generally accepted that tectonic stress accumulates non-uniformly, but remains quite low until a rapid stress variation occurs shortly before and after earthquake propagation or volcano eruption. Rapid stress increase may be especially favorable if tectonic loading exhibits a cyclic or fatigue character. Knowledge on the effect of cyclic, frequency-dependent loading on the magnetic behavior (magnetic fatigue) of rocks is poor up to now. Therefore, we carried out cyclic uniaxial compression experiments using an universal testing Instron machine and a GABO Eplexor Dynamic Mechanical Analysis (DMA) system. Modifications in magnetic properties were studied by measuring the low-field magnetic susceptibility and the Verwey transition temperature of magnetite. Again, a cooperative interplay of brittle and ductile deformation mechanisms can be observed explaining the observed magnetic fatigue effect. We expect from this project basic knowledge on the piezomagnetic stress sensitivity of crustal rocks, which is currently poorly constrained. The outcome might be applied in geosciences to understand the influence of deformation on magnetic signals in tectonically active areas and help to interpret their temporal variations.

[1] Nagata, T., and H. Kinoshita (1964), *Nature*, 204, 1183–1184; [2] Kontny et al. (2012), *Int. J. Earth Sci.*, 101(3), 671–692, doi:10.1007/s00531-011-0713-8; [3] Reznik et al. (2016), *Geochemistry, Geophysics, Geosystems*, 17, 2374–2393, doi: 10.1002/2016GC006338.

**11:00am - 11:15am**

### **Variations of magnetic Verwey transition: New insights through magnetic susceptibility of magnetite-rich rocks deformed under laboratory seismic-related fatigue loadings**

**Helena Fuchs, Boris Reznik, Frank Schilling, Agnes Kontny**

*Karlsruher Institut für Technologie, Germany*

At about 120 K magnetite undergoes a sharp Verwey transition ( $T_V$ ) caused by atom coordination changes through a monoclinic to cubic phase transition (e.g. Dunlop and Özdemir 1997).  $T_V$  is sensitive to composition, oxidation and pressure and can be determined by temperature-dependent magnetic susceptibility measurements (k-T curves, see e.g. Reznik et al., 2016 and references therein). The shape across the transition is rather complex in magnetite-bearing rocks compared to single crystal experiments, consisting of at least a sigmoidal increase followed by exponential decay.

In the present work a new approximation procedure is developed which considers the complete shape of

the transition region for modelling, using superposition of infinitesimally small magnetite volumes similar to magnetic domains whereby different transition temperatures for different domains are assumed. Such temperature variations may be caused e.g. by internal stresses. The procedure allows a precise fitting even in the range of peak susceptibility where both, sigmoidal increase and exponential decay, have a strong influence on the measured susceptibility, leading to a quantitative determination of shape parameters correlating with deformation conditions of the examined rocks.

As a first approximation some simple assumptions on magnetic behavior are made. Verwey transition of a single volume element is modelled as an instantaneous increase of susceptibility at  $T_v$  with rising temperature. Above  $T_v$  susceptibility is modelled assuming an inverse temperature dependence based on Curie's law, similar to Hrouda et al. (1997). We suggest that the paramagnetic contributions can be caused by surface defect structures in magnetite indicating strain. Gaussian distributions of transition temperatures over the magnetite volume allow modelling of the observed sigmoidal increase and identification of populations showing distinct magnetic behavior.

To clarify whether k-T curves across the Verwey transition are sensitive to strain, we subjected metamorphic quartz-magnetite ore to cyclic uniaxial loading at different frequencies and applied the approximation procedure to k-T curves. Defects in magnetite for these seismic-related fatigued samples are presented by Reznik et al. (this vol.).

[1] Dunlop and Özdemir (1997), *Rock magnetism, fundamentals and frontiers*, Cambridge University Press, 573 p; [2] Hrouda, F. et al. (1997), Refined technique for susceptibility resolution into ferromagnetic and paramagnetic components base on susceptibility temperature-variation measurement, *Geophys. J. Int.* 129, 715-719; [3] Reznik, B. et al. (2016), Shock-induced deformation phenomena in magnetite and their consequences on magnetic properties, *Geochem. Geophys. Geosyst.* 17, 2374-2393; [4] Reznik et al. (2019), Magnetic and microstructural fatigue of a magnetite-quartz rock, *Geo Münster* 2019.

## 11:15am - 11:45am Session Keynote

### Chemical effects in stressed systems: think global, act local

**John Wheeler**

*University of Liverpool, United Kingdom*

The Earth is under stress on all scales from mineral grains to mantle. Stresses result from buoyancy forces on the largest scales, plate boundary forces on an intermediate scale, but are heterogeneous right down to grain scale. Since chemical effects such as solid state reaction are influenced by pressure, they must be influenced by stress – but how? It is remarkable that there is no consensus on such a fundamental question, even when reaching beyond geoscience. I explain my view, based on theory in and beyond geoscience linked to experiments. I assert the requirement that a coherent view must incorporate diffusion creep and pressure solution, since these are chemical effects driven by stress (Wheeler, 1987). Some current approaches are not viable because the mathematics is in contradiction to the operation of such processes.

We are used to using Gibbs free energy as a fundamental quantity in thermodynamics, a global quantity related to a whole set of minerals. We read in dozens of texts that G is minimised at chemical equilibrium if pressure (P) and temperature (T) are externally controlled. This is correct, but the assumption that G remains a fundamental description of thermodynamics in stressed systems – commonly made – is not true. There is no law of thermodynamics that says that G exists, and can be useful in calculations. Instead it is a derived quantity based on a more fundamental assertion that the entropy of a system will be maximised at chemical equilibrium. The mathematical proof that G is minimised at equilibrium is valid for a system under (isotropic) pressure P, but falls apart under stress.

Instead we must deal with local equilibria and accept there is no global chemical equilibrium in a stressed system (except under very special circumstances). Diffusion creep is an illustration of this statement. So long as stress is applied, material diffuses, entropy is generated and there is no prospect of chemical equilibrium. How can equilibrium exist, then, if other minerals are present? Instead, chemical potentials can be defined and as local quantities form the foundation for quantifying the effects of stress. As in hydrostatic thermody-

namics, if there is global disequilibrium, we can still use *local* equilibria to quantify evolution and kinetics (the growth of reaction rims is an example). In crystalline materials under stress, interfaces play a key role in defining local equilibria. The fundamental equation is for chemical potential for phase A at an interface across which the normal stress is  $s_n$  is

$$\mu^A = F^A + \sigma_n V^A \quad (1)$$

where  $V$  is molar volume and  $F$  is Helmholtz free energy. This equation successfully describes diffusion creep and pressure solution (where chemicals diffuse from high to low  $s_n$ ) and forceful crystallization, where diffusion leads to increase in  $s_n$  at particular interfaces. It explains instabilities at stressed interfaces, and has been verified in electrochemical experiments. It is used to explain reaction rate and morphology in the germanate olivine  $\rightarrow$  spinel reaction and in olivine  $\rightarrow$  wadsleyite. The same equation is implicit in the interpretation of quartz  $\rightarrow$  coesite experiments in which stresses were quantified. There are some other expressions for chemical potential which involve all three principal stresses (Wheeler, 2018), but equation (1) remains key to understanding. Wheeler (2014) used equation (1) to show how, in a model rock with multiple minerals, the effects could be major, though the reaction mechanism needs to be taken into account before making specific predictions. Thus, constructing a coherent theory for nonhydrostatic thermodynamics is important because there are major effects to be modelled and investigated. Such theory must be founded on descriptions of local processes before being upscaled to think globally.

[1] Wheeler, J., 1987. The significance of grain-scale stresses in the kinetics of metamorphism. *Contributions to Mineralogy and Petrology*, **97**, 397-404; [2] Wheeler, J., 2014. Dramatic effects of stress on metamorphic reactions. *Geology*, **42**(8), 647-650; [3] Wheeler, J., 2018. The effects of stress on reactions in the Earth: sometimes rather mean, usually normal, always important. *Journal Of Metamorphic Geology*, **36**, 439-461.

11:45am - 12:00pm

## Metamorphic Pressures from Elastic Geobarometry: A novel formalism with application to the Rhodope Metamorphic Province, Greece

**Evangelos Moulas<sup>1</sup>, Dimitrios Kostopoulos<sup>2</sup>, Elias Chatzitheodoridis<sup>3</sup>**

<sup>1</sup>Institute of Geosciences, Johannes Gutenberg University Mainz, Germany; <sup>2</sup>Faculty of Geology and Geoenvironment, Department of Mineralogy and Petrology, National and Kapodistrian University of Athens, Greece; <sup>3</sup>Department of Geological Sciences, School of Mining and Metallurgical Engineering, National Technical University of Athens, Greece

Mineral inclusions will unavoidably tend to develop stress and pressure variances with respect to their hosts during the metamorphic evolution of rocks. The reason for these variances is the difference in the elastic properties of the minerals themselves. In this work, we present a novel formulation for the calculation of the entrapment (i.e. initial) pressure of host-inclusion systems based on analytical solutions of linear elasticity. We discuss the discrepant results obtained by different authors employing different analytical solutions and explore the assumptions lying behind each method. Our new formulation is tested against recently published experiments on quartz inclusions in garnet (QuiG) at pressures up to 3GPa, and we find a very good agreement between calculated and experimental pressure values (within 10% relative error). We subsequently apply our new elastic geobarometer to a calc-silicate gneiss from the Rhodope Metamorphic Province (N. Greece). The conditions of metamorphic recrystallization, calculated by phase equilibria modeling ( $730 \pm 40^\circ\text{C}$ ,  $\sim 1.2 \pm 0.1\text{GPa}$ ), are reproduced to within 0.15GPa ( $\sim 710 \pm 40^\circ\text{C}$ ,  $\sim 1.34 \pm 0.05\text{GPa}$ ). Our findings clearly show that estimated entrapment pressures may be relaxed during metamorphic rock evolution and that the pressure of a host-inclusion system may be reset close to that of the metamorphic peak. Elastic geobarometry can thus provide excellent independent estimates of the pressure conditions of metamorphic recrystallization.

**12:00pm - 12:30pm Session Keynote**

## **What's Next? Exploring the future of metamorphic geology**

**Lucie Tajcmanova**

*Heidelberg University, Germany*

Metamorphism imposes first order control on geodynamic processes. In fact, mineral reactions within the lithosphere, involving deformation, and fluid/melt flow, are responsible for mountain building, volcanic eruptions and triggering earthquakes. Petrologists and structural geologists are driven by the same essential curiosity about metamorphic processes affecting the Earth's crust and lithosphere and use different tools to understand these processes.

In the last 100 years, the work on mineral reactions and microstructures in metamorphic rocks has focused on inverse and forward chemical modelling of phase equilibria and on their description through chemical potential relationships which are believed to control the mass transfer in rocks.

Significant advances have also been made in the analytical techniques developments. Currently, high resolution analytical devices have become more available to the Earth sciences, and reveal the three-dimensional size, shape and distribution of microstructural features down to the nanometre-scale. Interestingly, the smaller the scale considered, the more heterogeneous an apparently uniform rock sample is. This heterogeneity is not only characterized by variation in chemical composition but also in mechanical properties. This needs to be accounted for.

These new, and I would say sometimes very "fresh" (last 5 years), observations led to re-evaluating the appropriateness of our quantification tools for processes in metamorphic rocks. During mineral reaction, the overall mechanical state of the rock is very important. The mechanical effects may influence element transport and mineral assemblage in rocks which can, in turn, significantly control the mechanical-chemical coupling rates and mechanisms of various processes in the Earth's interior. At present, we can even directly measure stress/pressure variations in rock microstructures using state-of-the-art analytical methods such as HR-EBSD, Raman spectroscopy or X-ray micro-diffraction.

Considering the interplay of metamorphic reaction and mechanical properties in our quantification approaches is critical for correct interpretation of observations in metamorphic rocks. The recent development of the new quantification approaches taking into account mechanics has thus opened new horizons in understanding the phase transformations in the Earth's lithosphere.

In this contribution, the classical tools, developed in the last 100 years, will be discussed taking into account the new analytical and quantification advances in order to underpin the key research directions that metamorphic geology field may explore in next 100 years.

**12:30pm - 12:45pm**

## **Chemically induced recrystallization: Implications for grain recycling and diffusion chronometry**

**Sumit Chakraborty, Christopher Beyer**

*Ruhr Universität Bochum, Germany*

It is known that recrystallization is often induced by strain. On the other hand, the response to chemical gradients is thought to be chemical diffusion of elements. We use experimental studies using single crystals of CaTiO<sub>3</sub> (perovskite) to show that in response to imposed concentration gradients of Pb, the response may be diffusion or recrystallization, depending on the magnitude of the chemical gradient. For low gradients, Pb diffuses into the CaTiO<sub>3</sub> crystals by normal mechanisms of lattice diffusion. However, the entry of the much larger Pb cation in the lattice causes strain, and ultimately produces defects and dislocations in the crystal. These dislocations act as preferred sites where Pb gets trapped, thereby reducing the overall flux of Pb in spite of the presence of dislocations which may act as fast transport pathways. This aspect of segregation of atoms to dislocations (analogous to grain boundary segregation) has been ignored in discussions of

enhanced diffusion in deformed / deforming media. A consequence of such trapping is that local regions of increased concentrations of Pb as well as dislocations are formed. When the imposed Pb gradient is large, it appears that such segregation dominates over diffusion resulting in the formation of new, Pb-rich crystals [(Pb,Ca)TiO<sub>3</sub>]. In time series experiments, such a recrystallization front propagates systematically into the single crystal. The process occurs in parallel with lattice diffusion. This mode of transport, with an enhanced flux of Pb, can result in faster transport rates and more rapid resetting of chemical signatures in natural systems. Similar segregations of REE in zircons have been observed and may have implications for the resetting of chemical signatures in zircons and other minerals. Implications of these results for grain recycling and diffusion chronometry will be discussed.

## Poster Presentations

Mon: 31

### The role of chemically induced stresses in the mechanisms of element exchange between minerals – an experimental study based on pyroxenes

Jennifer Primocerio<sup>1</sup>, Sumit Chakraborty<sup>1</sup>, Katharina Marquardt<sup>2</sup>, Thomas Fockenberg<sup>1</sup>

<sup>1</sup>Ruhr-Universität Bochum, Germany; <sup>2</sup>Imperial College London, UK

The mechanism by which element transfer processes occur in minerals remains unclear. Recent technological developments now make it possible to observe the different steps by which compositional changes occur in mineral pairs. Pyroxenes, very common terrestrial and extraterrestrial minerals, have been studied for decades now. So, in this study we built on the available information to analyze the element transfer processes using orthopyroxene-clinopyroxene pairs.

For this purpose, we synthesized crystals of ortho- and clinopyroxene of different Fe/Mg ratios from appropriate oxide mixes. The synthesis experiments were carried out at high temperatures (1000 – 1250 °C) at atmospheric pressures as well as at high pressures (15 kbar) in a piston cylinder apparatus. We performed three kinds of element exchange experiments: (A) polished sample cubes of natural crystals with deposited thin films (produced using pulsed laser deposition, PLD) at 1 bar and 1000-1200 °C in a gas mixing furnace. (B) Anneals of powder mixes of pre-synthesized pyroxenes at 1 bar, 1000-1200 °C in a gas-mixing furnace. (C) Anneals of the same mixes in the piston cylinder apparatus at 15 kbar and 900-1200 °C. The starting materials and run products were further characterized using BSE (back-scattered electron) imaging, chemical analysis in the electron microprobe at different analytical conditions, and structural and chemical characterization in the TEM (transmission electron microscopy) of lamellae produced by focused ion beam (FIB) thinning.

It is generally assumed that the compositions at the interface of two grains attain equilibrium instantaneously, whereas the rest of the crystals equilibrate by diffusion. We observed that the samples equilibrate by a different, multi-step process.

Experiments of type (A) demonstrate that recrystallization and element exchange (e.g. the incorporation of the larger Ca ion in the lattice) of two pyroxenes in a direct interface cause distortion of the lattice and produce mismatch dislocations which can then act as fast diffusion pathways. In experiments of type (B) and (C) compositions equilibrate step wise along two different paths, depending on whether the T-X combination is above or below the pyroxene miscibility gap. Grains recording different stages of compositional evolution may be seen in a single sample. Newly recrystallized grains have a low density of dislocations, compared to grains with the starting composition which have a high density of defects of different kinds.

Thus, the process of equilibration involves both, recrystallization and diffusion in tandem, rather than exclusively the one or the other.

**Mon: 33****Episodic deformation and metamorphic reactions at decreasing distances to the tip of a seismic active fault zone – the record of mylonites from the DAV, Eastern Alps****Claudia A. Trepmann<sup>1</sup>, Felix Hentschel<sup>1</sup>, Emilie Janots<sup>2</sup>**<sup>1</sup>Ludwig-Maximilians University Munich, Germany; <sup>2</sup>University Grenoble, ISTERre, France

Microfabrics in quartz-rich mylonites from the Deferregen-Antholz-Vals (DAV) shear zone in the Eastern Alps that underwent Alpine episodic stages of deformation and metamorphism (450-300°C) are presented. During an initial stage, dislocation glide of quartz was the dominant deformation mechanism, as indicated by quartz grains with long axes of several hundreds of  $\mu\text{m}$  and width of a few tens of  $\mu\text{m}$  that are preferentially oriented with the c-axis at low angle to the y-axis of the finite strain ellipsoid. Monazite grains are surrounded by apatite, allanite and epidote forming elongate corona microstructures that are aligned in the foliation and deflecting it. These corona microstructures indicate coeval metamorphic breakdown reactions of monazite. At a later stage of greenschist facies conditions at which biotite was still stable, shear bands formed associated with fracturing of all rock-forming minerals. Distributed fracturing at these conditions indicates high differential stresses and strain rates. Mainly quartz and minor biotite precipitated from the pore fluid along the shear band boundaries and in the interspace between fragments, indicating that fluid availability increased transiently, probably related to increased connectivity of the pore space due to fracturing. Quartz grains within shear bands show c-axis being preferentially perpendicular to the shear band boundary. At a final stage but at still metamorphic conditions, cataclasis of the mylonites occurred locally, as indicated by breccias with cm-scaled rounded mylonitic components in a mica-rich matrix. The fault rocks from the DAV record systematically changing rheological behaviour during various stages of deformation at greenschist facies conditions from dislocation glide-controlled deformation of quartz to cataclasis. The time-dependent rheological behaviour is suggested to be dominantly governed by the changing stress and strain rate conditions, as opposed to changing temperature conditions. We interpret the record to represent episodic deformation and metamorphic reactions at decreasing distances to the tip of a seismic active fault zone.

**6c) Fluid-rock interaction: from mechanisms to rates – from atoms to plates****Monday, 23/Sep/2019: 11:15am - 1:00pm****Session Chair: Oliver Plümper** (Utrecht University)**Session Chair: Helen E King** (Utrecht University)**Session Chair: Esther Martin Schwarzenbach** (Freie Universität Berlin)**Location: Schloss: S8****Session Abstract**

Reactions between fluids and rocks have a fundamental impact on the geodynamics and geochemistry of the Earth at all scales. Fluid-rock interactions strongly affect the petrophysical properties and chemical and isotopic composition of reacted rocks. Therefore, they play an important role in processes such as plate tectonics, economic deposit formation, and global geochemical cycles. The fact that fluid has migrated through rocks is evident from the presence of geological structures including veins, metasomatic alteration zones, (de)hydration reaction fronts and porosity observed from the micron down to nanometre scale. Metasomatic alteration zones, but also ore deposits, point to the chemical effect of fluid flow that facilitates element mobilisation. Mechanical effects of fluid flow are expressed in phenomena such as zones of localised deformation.

The underlying mechanisms as well as the rates of fluidrock reactions are still poorly understood, despite the current field, experimental, and theoretical arguments for the importance of fluidrock interaction for geodynamic and geochemical processes. This is mainly because rocks only provide a snapshot in time, while processes like deformation, reaction, and fluid flow are complex coupled processes, which provide a challenge for numerical modelling as well as for interpreting and controlling experiments. Numerical modelling, experiments, and comprehensive field and laboratory studies that focus on the mechanisms, rates, interplay between fluid flow, reaction, deformation and mass transport processes, or the connection between small to large scales, will help to improve our understanding of fluidrock interactions.

Thus, we invite observational, analytical, experimental and numerical contributions that shed light on the coupled processes of fluid flow, reaction, deformation and fluidmediated mass transport at all scales, both from a fundamental and applied point of view.

## Lecture Presentations

11:15am - 11:30am

### Dissolution rate variability of the four different etch pit steps of the 104 calcite crystal face

**Elisabete Trindade Pedrosa<sup>1</sup>, Ricarda D. Rohlf<sup>1</sup>, Cornelius Fischer<sup>4</sup>, Andreas Luttge<sup>1,2,3</sup>**

<sup>1</sup>Faculty of Geosciences, University of Bremen, 28359 Bremen, Germany; <sup>2</sup>Marum - Center for Marine Environmental Sciences, University of Bremen, Leobener Strasse, 28359 Bremen, Germany; <sup>3</sup>MAPEX - Center for Materials and Processes, University of Bremen, Bibliothekstraße 1, 28359 Bremen, Germany; <sup>4</sup>Institute of Resource Ecology, Department of Reactive Transport, Helmholtz-Zentrum Dresden-Rossendorf, 04318 Leipzig, Germany

When a mineral surface gets in contact with a fluid phase it will start dissolving. Given specific undersaturated and transport fluid conditions, the process of dissolution will win against its backward reaction of precipitation. Calcite has been studied extensively because it has proven very useful in unraveling the mechanisms of mineral (carbonate) dissolution. Nanoscopic techniques have shown that the overall dissolution process is driven by the propagation of atomic steps originated at crystal defects (e.g., point, line, and/or impurities) and edges. Over time, the surface morphology of the dissolving crystal gives origin to features such as crystallographically oriented etch pits that can develop into similar microscale features. Nanoscale measurements have shown that the dissolution rate of these steps is faster for obtuse ( $[481]^+$  and  $[441]^+$ ) than acute ( $[441]^-$  and  $[481]^-$ ) steps<sup>1</sup>. The contribution of the different crystal defects and their nanoscopic features to macroscale dissolution rates is still largely unknown. To capture the evolution of these nanoscopic features we exposed a single crystal of calcite (104) to a rapidly flowing aqueous fluid (pH = 8.6) for reaction time intervals of 24 hours for a total of 156 hours. The full surface topography and surface dissolution rates of the sample (2.0 × 2.6 mm) were measured by vertical scanning interferometry (VSI). The recorded topography maps show crystallographically oriented etch pits that coalesce and form larger pits as large as 100 μm. Other features, such as macrosteps (≈ 50 μm) are formed by the interaction of etch pits organized in rows. The reaction rate maps showed that the four calcite (104) steps have different dissolution rates over time. This is unexpected because the two acute steps and the two obtuse steps are crystallographically mirrors of each other. Moreover, given sufficient reaction time, acute step etch pit walls were highly reactive and collided. This type of dissolution mechanisms has not been reported in previous work and suggests that micron scale mechanisms are not a replica of nanoscale mechanisms. A statistical analysis of the prevalence of such features and its rates will contribute for a holistic understanding of mineral dissolution through time and space.

[1] Liang, Y. and Baer, D.R., 1997. Anisotropic dissolution at the CaCO<sub>3</sub>(1014)-water interface. *Surf. Sci.*, 373, 275–287.

11:30am - 11:45am

**Mesoscale Calcite Dissolution Modelling – Parametrization and Data Analysis****Ricarda D. Rohlfs<sup>1</sup>, Inna Kurganskaya<sup>1</sup>, Cornelius Fischer<sup>4</sup>, Andreas Luttge<sup>1,2,3</sup>***<sup>1</sup>Faculty of Geosciences, University of Bremen, 28359 Bremen, Germany; <sup>2</sup>Marum - Center for Marine Environmental Sciences, University of Bremen, Leobener Strasse, 28359 Bremen, Germany; <sup>3</sup>MAPEX - Center for Materials and Processes, University of Bremen, Bibliothekstraße 1, 28359 Bremen, Germany; <sup>4</sup>Institute of Resource Ecology, Department of Reactive Transport, Helmholtz-Zentrum Dresden-Rossendorf, 04318 Leipzig, Germany*

We considered a calcite cemented Rotliegend sandstone and its interaction with water, assuming the dissolution would be driven mainly by the fastest-dissolving mineral, calcite. In this study, we discuss the evolution of a dissolving calcite cleavage surface modelled with kinetic Monte Carlo (kMC) methods, varying key parameters like defect density and defect distribution. Our focus is on upscaling the data generated by kMC simulations to larger scales.

To understand the complex processes governing reactive transport in reservoir rocks, the interaction of fluids with mineral surfaces has to be examined at different scales. Macroscopically, the movement of the fluid through the pore network has to be considered. At the mesoscale, the heterogeneity of dissolution (or precipitation) rates promotes the evolution of rough surface topographies. These affect the fluid transport, and thus local concentrations and activities in turn influencing the reaction rates. At the atomistic scale, an understanding of elementary chemical reactions is needed to be able to predict how the overall surface will evolve in any future bottom-up model.

When modelling a complex system like this, it is necessary to connect several simulation types spanning vastly different length scales. The scope of available modelling approaches ranges from Density Functional Theory (DFT) and Molecular Dynamics (MD) calculations at the atomistic scale over kMC simulations and methods of computational geometry at the mesoscale up to continuum scale techniques, e.g., Lattice Boltzmann/Navier-Stokes reactive transport simulations. Since small-scale approaches are computationally expensive, it is not possible to model a whole rock using atomistic or even mesoscale techniques. However, data gained from these types of simulations can be used to parametrize larger-scale models if processed in a suitable fashion.

The direct output parameters of kMC simulations are the surface topography of a reacted surface, the time, and local reaction rates at different surface positions. From these data we generate rate maps and rate spectra reflecting the heterogeneity of dissolution rates. Our results show how parameter variation in the kMC simulation input can influence the statistics of reaction rates at the mesoscale. We demonstrate the dependence of reaction rates on defect distributions rather than just defect densities on the dissolution rate spectra, and the physical meaning of changed kMC output parameters in terms of processes at the calcite surface. We show different ways of processing and analyzing rate spectra statistically. We also discuss strategies of data reduction to make kMC-generated rates accessible for implementation into other models.

11:45am - 12:00pm

**Experimental Constraints on Hydrothermal Indium Transport****Anselm Loges<sup>1</sup>, Thomas Wagner<sup>2</sup>***<sup>1</sup>Freie Universität Berlin, Institut für Geologische Wissenschaften, Malteserstr. 74-100, 12249 Berlin, Germany; <sup>2</sup>Applied Mineralogy and Economic Geology, RWTH Aachen, Wüllnerstr. 2, 52062 Aachen, Germany*

Indium (In) is an element that has recently gained great economic importance due to its application in strategic energy and information technologies. Future In shortages projected by the European Commission Joint Research Council are due to insufficient exploration for In resources, reflecting the poor understanding of the hydrothermal ore-forming processes that result in economic enrichment of In. Key questions are the relative importance of different geologically relevant ligands for hydrothermal In complexation and the efficiency of different ore-deposition mechanisms for formation of economic deposits. Quantitative understanding of the solubility and transport of In would be critical for geochemically modeling the formation of hydrothermal In

mineralization, but no experimental high-temperature data have been available. Therefore, new experimental hydrothermal solubility and spectroscopic data on fluoride and chloride complexes of indium have been generated by this project. These provide the relevant input thermodynamic data that make it possible to predictively model In transport and deposition in hydrothermal ore-forming systems. The strong differences in complexation behavior across the hydrothermal temperature range of 200-400 °C relevant for such systems explains the large variability of different In deposit styles.

We have performed batch equilibration experiments to determine the solubility of In solids in F- and Cl-bearing solutions (150-250 °C) and EXAFS studies to assess F- and Cl-complexation of In (30-400 °C). The effects of pH and mixed-ligand complexation were also investigated. The data show that the  $\text{In}^{3+}$  cation exhibits an unusual behavior in aqueous solutions because it predominantly forms complexes with F at ambient temperatures but prefers Cl above 200 °C. Because the transition temperature is crossed in the typical temperature range of hydrothermal ore-forming systems, this has far-reaching consequences for hydrothermal transport and precipitation of In in natural environments. Depending on the fluid composition (concentrations of F<sup>-</sup> and Cl<sup>-</sup>) and pH, the solubility of indium will either decrease or increase during cooling upon ascent of a fluid. We conclude that this unusual complexation behavior of In is the key reason why indium is heterogeneously distributed in hydrothermal ore deposits.

**12:00pm - 12:15pm**

### **Extreme W enrichment in highly serpentinised abyssal peridotites from IODP Leg 209**

**Ramon Reifenröther, Carsten Münker, Birgit Scheibner**

*Universität zu Köln, Germany*

An in-depth knowledge of the geochemical cycle of W is crucial for the understanding of, e.g., core-mantle interactions and subduction zone dynamics. As W, Th, Ta, and U are all characterized by similar melt incompatibility, their respective element ratios are not affected by magmatic processes and were taken as constant to mass balance the global W geochemical cycle (e.g. [1]). Compared to intensive studies on continental crust and arc settings, the oceanic crust remains largely unexplored for such elemental mass balances. Nevertheless, the understanding of W behaviour within various portions of the oceanic crust is critical to infer potential W redistributions during alteration processes.

In previous work we demonstrated selective W enrichment relative to Th, U, and Ta within altered upper oceanic crust originating from IODP hole 1256D. Elemental ratios of W/Th, Ta/W and W/U show only little overlap with pristine MORB ratios and indicate even larger W enrichment than reported for arc lavas worldwide that were analysed in previous studies [2]. As the crust drilled in hole 1256D formed at the Cocos-Pacific plate boundary during periods of superfast spreading rates it was possible to sample material from most major alteration types of the lava section down to the gabbros.

The samples recovered during Leg 209 from the Mid-Atlantic Ridge are highly serpentinised abyssal peridotites and associated gabbroic rocks from the lower oceanic crust formed at slow spreading rates. A total of 6 different sites, each with a distinctive alteration style, was examined in this study. We present high-precision W-Th-U-Ta data obtained by isotope dilution measurements using mixed U-Th, W-Ta-Zr-Hf-Lu tracers and W double spike with a Thermo Neptune MC-ICP-MS at the University of Cologne. The overall W concentrations are markedly elevated close to the seafloor (c.200 ppb) and decrease downwards to 20–70 ppb. Compared to Ta, Th, and U, W is locally enriched by a factor of more than 5. Additionally, U is enriched compared to Th by a factor of more than 20. Most elements like Lu, Hf, Zr, Ta, and Nb are strongly depleted compared to their abundances in altered oceanic crust from hole 1256D, reflecting pristine igneous signatures. Our results underline the widespread fractionation of W from U-Th-Ta in altered oceanic crust, indicating even stronger enrichment of W in strongly serpentinised portions of the lower oceanic crust.

[1] König et al. (2008) *Earth and Planetary Science Letters*, 274(1-2), 82–92; [2] König et al. (2011) *Geochimica et Cosmochimica Acta*, 75 2119–2136

12:15pm - 12:30pm

**The influence of a nanophase on mineral equilibration in the system  $\text{Al}_2\text{O}_3\text{-SiO}_2\text{-H}_2\text{O}$** **Dina Simona Schultze<sup>1</sup>, Richard Wirth<sup>2</sup>, Bernd Wunder<sup>2</sup>, Gerhard Franz<sup>1</sup>**<sup>1</sup>Technische Universität Berlin, Germany; <sup>2</sup>Deutsches GeoForschungs Zentrum Potsdam, Germany

The metastable association of corundum and quartz is rare in nature but occurs frequently in experiments where according to thermodynamic predictions aluminium silicate polymorphs should form instead. The cause for this obstruction of the reaction  $\text{Al}_2\text{O}_3 + \text{SiO}_2 \rightarrow \text{Al}_2\text{SiO}_5$  is so far unknown but is often attributed to kinetic inhibitions. In order to overcome slow reaction rates we conducted a series of experiments in which reaction promoting conditions were tested. Since mineral reactions typically tend to proceed faster in wet than in dry systems, all experiments included substantial amounts of fluid ( $\text{H}_2\text{O} \pm$  additional solutes). The reaction towards  $\text{Al}_2\text{SiO}_5$  was, however, not observed; on the contrary, the presence of aqueous fluid seems to promote the metastability of corundum and quartz.

Cold seal hydrothermal autoclave experiments and piston cylinder experiments were conducted in a range of 500–800°C and 5–18 kbar, in runs of 7–20 days. Investigating the metastable products from several experiments in detail showed that an Al-Si-H-bearing nanometer-sized phase formed inside and on the corundum crystals during shorter experimental runs. This phase resembles an incomplete dioctahedral phyllosilicate structure, consisting of at least one silica tetrahedral plane that developed along the basal plane of corundum (as observed by TEM). The nanophase controls the growth behavior of its host, which appears in thin plate like crystals, consisting almost exclusively of faces in {0001}. At the same time, the nanophase isolates corundum and quartz along their interface. This isolation of the bulk phases likely prevents the reaction towards the stable aluminium silicate.

Prolonged experimental duration leads to recrystallization or annealing of the corundum including the nanophase and to the formation of quartz inclusions inside the host crystal, a process that increases the bulk phases volume and simultaneously reduces the phase boundary area between them, thereby providing further opportunity to expand their coexistence.

Apart from its size, the transient nature of the nano phase makes it difficult to be detected both in experiments and even more in natural samples. Our findings, however, emphasize how vastly the formation and modification of nanophases influence and even control geochemical reactions and kinetics under metamorphic conditions in one of the most important chemical systems of the earth's crust. We demonstrate that localized phase assemblages with an Al-Si-H-bearing nanometer-sized phase on the corundum surface can explain the metastability plaguing experimental studies in this system without invoking further unknown kinetic factors.

12:30pm - 1:00pm *Session Keynote***Coupling 2D numerical modelling of microscale dehydration to fully quantitative automated mineralogy mapping****Johannes Christiaan Vrijmoed<sup>1</sup>, Yury Podladchikov<sup>2</sup>**<sup>1</sup>Freie Universität Berlin, Germany; <sup>2</sup>University of Lausanne, Switzerland

Understanding the physical-chemical processes in subduction zones is of primary importance to build more predictive models for geohazards such as volcanism above the slab, or earthquakes at depth. One of the fundamental processes in subduction zone systems is the release of fluids from dehydration reactions at depth. Crustal rocks at the ocean floor bound water in minerals by alteration processes and mantle rocks below may also be strongly hydrated for example in bending faults of the slab. These hydrated oceanic crust and mantle rocks release fluids once they enter the subduction zone as they are heated up in the Earth. They are then potentially linked to earthquakes, or trigger melting which ultimately results in volcanism at the surface above a subduction zone.

The mechanism of fluid expulsion, porosity generation and formation of fluid pathways that are formed from

the microscale up to the meso-scale is poorly understood. Previous work in this direction has shown that at the sub-micron to micron scale hydration starts in isolated pockets. It is dominated by local chemical heterogeneities which control spatial variations in the dehydration reactions. Afterwards fluids get channelized at the mm-, cm- and m- scale, but how this process operates is unclear. As first step, quantitative information from calibrated microprobe X-ray maps was used in a numerical model which simulated the process of dehydration and fluid flow on a 1x1 mm domain [1]. One limitation has been that the size of the domain where high resolution quantitative information could be obtained was restricted to the mm-scale.

Here we use Zeiss Mineralogic mapping to enlarge the modelling domain from the mm- to the cm- scale and expand the domain at which numerical modelling can be done. The results show that using the newest EDX mapping techniques the compositional information is sufficiently quantitative to be used in the numerical modelling. This opens the possibility to understand how sub-micron pockets of fluids can connect into larger pathways. Hence, it will be an important step in understanding how fluid can travel up from the subducting slab where they can ultimately trigger melting or may be responsible for earthquakes.

[1] Plümper, O., et al., *Fluid escape from subduction zones controlled by channel-forming reactive porosity*. Nature Geoscience, 2017. **10**(2): p. 150-156.

## Poster Presentations

Mon: 34

### Chemical controls of the aqueous environment on mineral growth and dissolution

**Helen E King**

*Utrecht University, The Netherlands*

Interfacial processes of mineral growth and dissolution are dictated by the local chemical environment. Even the distance from equilibrium, called the solution saturation, is dependent on the aqueous environment. If we look at organic molecules that do not interact directly with dissolved ions we can see that solubility changes with ionic strength [1]. This is known as salting out and is caused by the change in the network and hydration properties of water molecules, altering enthalpy and entropy contributions within the solution. When dissolved ions can interact with each other, as is common for mineral constituents, the story becomes more complicated. In this case, ion-pair formation can alter the saturation of the aqueous solution with respect to the mineral [2]. Furthermore, ions in the solution may also interact directly with the mineral surface [3], enhancing or inhibiting the addition or removal of ions and molecules to/from the surface. In this presentation I will review our knowledge of how aqueous solutions affect the growth and dissolution of carbonate minerals, which have been studied in detail at the interfacial level. Through this I will show that one of our major challenges to predict and understand fluid-rock interaction is modelling and characterizing the aqueous environment and its transitory nature.

[1] Whitehouse, B. G. The effects of temperature and salinity on the aqueous solubility of polynuclear aromatic hydrocarbons. *Mar. Chem.* 1984, **14**, 319–332; [2] King, H. E.; Satoh, H.; Tsukamoto, K.; Putnis, A. Nanoscale observations of magnesite growth in chloride- and sulfate-rich solutions. *Environ. Sci. Technol.* 2013, **47**, 8684–8691; [3] King, H. E.; Putnis, C. V. Direct observations of the influence of solution composition on magnesite dissolution. *Geochim. Cosmochim. Acta* 2013, **109**, 113–126.

Mon: 35

### Tectonometamorphic and hydraulic processes along a fossil subduction plate interface in the northern Mirdita Ophiolites (Bajram Curri, Albania)

**Madeline Richter<sup>1</sup>, Georg Löwe<sup>1</sup>, Kujtim Onuzi<sup>2</sup>, Kamil Ustaszewski<sup>1</sup>**

<sup>1</sup>University Jena, Germany; <sup>2</sup>Polytechnic University of Tirana, Institute of GeoSciences, Tiranë, Albania

The obduction of ophiolites onto passive margins is preceded by intraoceanic subduction. During incipient subduction, metamorphic soles with HT-assemblages form along the plate interface by overthrusting flu-

id-rich lower-plate material with hot, dry ultramafics of the upper plate. As lower plate material undergoes prograde metamorphism and dewatering, fluids are transferred along the plate interface and into the upper plate, assisting serpentinisation of upper plate mantle. To better understand interrelated tectonometamorphic and hydraulic processes associated with incipient intraoceanic subduction, we mapped ~35 km<sup>2</sup> along the northern Mirdita Ophiolite near Bajram Curri, Albania. The Mirdita massif forms part of the Western Vardar Ophiolite Unit, cropping out along the entire length of the Balkan Peninsula. Oceanic lithosphere formed in the Triassic to Jurassic and was obducted onto the Adriatic passive margin by Late Jurassic. Lower plate material was progressively incorporated into a several km thick tectonic mélange at the base of the obducting ophiolite. Within the tectonic mélange, we distinguished several isoclinally folded units with mostly NE-plunging fold axes. Successions of sub-greenschist-facies turbiditic slates, arenites and olistoliths dominate structurally lower parts. Strata are coherent and exhibit a scaly or block-in matrix fabric, typical of broken formations. Structurally higher parts of the mélange contain intercalations of quartz-sericite schist, calc-schist, meta-chert, chlorite schist and Tlc-bearing serpentinite, indicating greenschist- to amphibolite-facies conditions. Structurally highest parts of the mélange consist of amphibolite and Grt-bearing paragneis. We hence observe an inverted metamorphic field gradient, typical of metamorphic soles worldwide. The base of coherent upper plate ultramafics, forming the actual plate interface, dips SE and truncates the folded, underlying tectonic mélange. Harzburgites show protomylonitic fabrics defined by finegrained matrix Ol and porphyroclasts of Opx. Arrays of abundant, systematically oriented, mm- to cm-thick veins crosscut basal harzburgites. Thin sections show three Srp vein generations in harzburgites. The first generation produces mesh-textures around Ol. Second generation veins are largest with up to 1.5 mm width consisting of fibrous Srp and opaque phases. They partly follow the metamorphic foliation formed by polymineralic layers of Ol+Opx. Third generation of yellow Srp dissects all other vein types. Bastitisation of Opx evolves at higher degrees of serpentinisation. Vein density substantially decreases upsection. There, massive harzburgites include Cr-Spl-rich dunite lenses. Our observations hence suggest that serpentinisation of peridotites by hydraulic fracturing is strongly localized along and immediately above the subduction interface and that this process is linked to dewatering of subducting material, which itself undergoes prograde metamorphism.

**Mon: 36**

### **Sulfide mineralogy as a tracer for fluid-rock interaction in serpentinites**

**Esther Martin Schwarzenbach<sup>1</sup>, Roxana Rohne<sup>1</sup>, Oliver Plümper<sup>2</sup>**

<sup>1</sup>Freie Universität Berlin, Germany; <sup>2</sup>Utrecht University, Utrecht, The Netherlands

Fluid-rock interaction in ultramafic rocks leads to highly reducing conditions due the oxidation of ferrous iron in primary mineral phases. In both oceanic and continental sites of peridotite alteration (serpentinization) this results in fluids highly enriched in H<sub>2</sub> and/or CH<sub>4</sub> gas. In this regard, serpentinization systems are some of the most reducing environments found on Earth allowing for the stabilization of native metals and metal alloys and thus affecting the petrophysical properties of the oceanic lithosphere. At the Chimaera hydrothermal field in Turkey highly CH<sub>4</sub>-enriched fluids issue from an ultramafic basement that is undergoing serpentinization by circulation of meteoric water, though partial serpentinization already took place during mantle exposure along an oceanic spreading center. Here, we study the sulfur geochemistry and mineralogy of highly serpentinized peridotites to track sulfur sources, mobilization mechanisms of sulfur and the evolution of the redox conditions during hydrothermal alteration of these rocks.

Our results show that exposure of mantle rock to seawater along an oceanic spreading center in the Cretaceous resulted in the incorporation of seawater-derived sulfate as reflected in  $\delta^{34}\text{S}_{\text{sulfate}}$  values between 10.7 and 20.4‰. Simultaneously, water-rock interaction resulted in the modification of the primary mantle sulfide assemblages. In particular, the presence of awaruite and native Cu reflect highly reducing fluid conditions whereas hematite and magnetite record oxidizing conditions suggesting considerable changes in the redox conditions during fluid-rock interaction. These changes in redox conditions and the resulting disequilibrium conditions are also reflected in distinct decomposition features in sulfides with formation of e.g., native Cu as thin exsolutions. Furthermore, we infer that strong redox gradients on the micrometer scale are the result

of late stage fluid infiltration – most likely during continental serpentinization and associated with highly reducing fluids – which overprinted earlier sulfide and metal mineral assemblages from oceanic serpentinization. These observations provide evidence that redox conditions strongly vary during the evolution of peridotite-hosted hydrothermal systems.

## Mon: 37

### Solubility of forsterite, enstatite and magnesite in redox-buffered high-pressure COH fluids

**Carla Tiraboschi<sup>1</sup>, Simone Tumiati<sup>2</sup>, Dimitri Sverjensky<sup>3</sup>, Thomas Pettke<sup>4</sup>, Peter Ulmer<sup>5</sup>, Stefano Poli<sup>2</sup>**

<sup>1</sup>WWU Münster, Germany; <sup>2</sup>University of Milan, Italy; <sup>3</sup>Johns Hopkins University, USA; <sup>4</sup>University of Bern, Switzerland;

<sup>5</sup>ETH Zürich, Switzerland

High-pressure fluids are able to mobilize and transport significant amounts of dissolved species resulting from fluid-rock interaction. Experimental constraints on the extent of mineral dissolution are therefore crucial to understand metasomatic processes closely related to the mass transport of elements by high-pressure fluids.

We experimentally investigated the dissolution of forsterite, enstatite and magnesite in graphite-saturated COH fluids synthesized employing a rocking piston cylinder apparatus at pressures from 1 to 2 GPa and temperatures from 700 to 1100 °C. Synthetic forsterite, enstatite, and nearly pure natural magnesite were used as starting materials. Redox conditions were buffered by Ni–NiO–H<sub>2</sub>O ( $\Delta\text{FMQ} = -0.21$  to  $-1.01$ ), employing a double-capsule setting. Fluids, binary H<sub>2</sub>O–CO<sub>2</sub> mixtures at the  $P$ ,  $T$ , and  $f\text{O}_2$  conditions investigated, were generated from graphite, oxalic acid anhydrous (H<sub>2</sub>C<sub>2</sub>O<sub>4</sub>) and water. Their dissolved solute loads were analyzed through an improved version of the cryogenic technique, which takes into account the complexities associated with the presence of CO<sub>2</sub>-bearing fluids. The experimental data show that forsterite + enstatite solubility in H<sub>2</sub>O–CO<sub>2</sub> fluids is higher compared to pure water, both in terms of dissolved silica ( $m\text{SiO}_2 = 1.24$  mol/kg<sub>H<sub>2</sub>O</sub> vs.  $m\text{SiO}_2 = 0.22$  mol/kg<sub>H<sub>2</sub>O</sub> at  $P = 1$  GPa,  $T = 800$  °C) and magnesia ( $m\text{MgO} = 1.08$  mol/kg<sub>H<sub>2</sub>O</sub> vs.  $m\text{MgO} = 0.28$  mol/kg<sub>H<sub>2</sub>O</sub>) probably due to the formation of organic C–Mg–Si complexes.

Our experimental results show that at low temperature conditions a graphite saturated COH fluid interacting with a simplified model mantle composition, characterized by low MgO/SiO<sub>2</sub> ratios, would lead to the formation of significant amounts of enstatite if solute concentrations are equal. On the other hand, at high temperatures these fluid, characterized by MgO/SiO<sub>2</sub> ratios comparable with that of olivine, would be less effective in metasomatizing the surrounding rocks. However, the molality of COH fluids increases with pressure and temperature, and quintuplicates with respect to carbon-free aqueous fluids. Therefore, in the mantle wedge, the amount of fluid required to metasomatize the surrounding peridotite decreases in the presence of carbon with increasing temperatures, leading to the formation of orthopyroxene-rich levels. COH fluids are thus effective carriers of C, Mg and Si in the mantle wedge up to shallowest level of the upper mantle.

## 7) Earth Surface Processes and Basin Analysis

### 7a) Quaternary Geochronology

Monday, 23/Sep/2019: 9:00am - 10:30am

Session Chair: Ralf Hetzel (Institut für Geologie und Paläontologie)

Session Chair: Tibor János Dunai (Univ. Köln)

Location: H3

#### Session Abstract

Understanding and quantifying the processes that modify and shape the surface of the Earth requires the determination of accurate dates and rates. Thus, the improvement and development of existing and new dating methods is essential for a better understanding of Earth's surface processes and their relation to climate and tectonics. Currently employed geochronological methods include, for example, exposure and burial dating with cosmogenic nuclides, luminescence, radiocarbon, and paleomagnetic dating. This session invites contributions on developments and applications of all dating methods relevant to decipher Late Cenozoic landscape evolution, climate change, and active tectonics. The keynote speakers Georgina King (Lausanne) and Vincent Godard (Aix-Marseille) will give talks on luminescence thermochronometry and the use of  $^{36}\text{Cl}$  in carbonate landscapes. Interested participants are invited to visit the cosmogenic nuclide laboratory in Münster and discuss all aspects of  $^{10}\text{Be}$  separation and target preparation with R. Hetzel and T. Dunai.

#### Lecture Presentations

9:00am - 9:30am Session Keynote

#### OSL and ESR thermochronometry of the Japanese Alps

Georgina E King<sup>1</sup>, Shigeru Sueoka<sup>2</sup>, Sumiko Tsukamoto<sup>3</sup>, Frederic Herman<sup>1</sup>, Floriane Ahadi<sup>4</sup>, Cecile Gautheron<sup>4</sup>, Guillaume Delpech<sup>4</sup>, Takahiro Tagami<sup>5</sup>

<sup>1</sup>University of Lausanne, Switzerland; <sup>2</sup>Japan Atomic Energy Agency, Japan; <sup>3</sup>Leibniz Institute for Applied Geophysics, Hannover, Germany; <sup>4</sup>UMR Interactions et Dynamique des Environnements de Surface, Université de Paris, Sud, France; <sup>5</sup>Department of Geology and Mineralogy, Kyoto University, Japan

Optically stimulated luminescence (OSL) and electron spin resonance (ESR) thermochronometry are recently developed techniques that can constrain exhumation histories at sub-Quaternary timescales. Both techniques are based on constraining the dynamic equilibrium between electron charge trapping and de-trapping in minerals, in response to in-situ radiation and rock cooling. Numerical models have recently been developed that allow exhumation histories to be inferred by translating rock cooling rates into an exhumation rate using knowledge of the Earth's thermal field. In contrast to OSL which can only be applied over timescales of up to ~400 ka, ESR signals saturate later, and may be applicable over the whole Quaternary period. This potentially extends the applicability of trapped-charge dating based thermochronometric methods, beyond regions that experience extremely high rates of exhumation (e.g. eastern Himalayan syntaxis). This presentation will introduce the foundation of ESR and OSL thermochronometry, before discussing application of these methods to the Japanese Alps.

Japan is one of the most tectonically active locations on Earth. The Japanese Alps bisect the island of Honshu and are thought to have been uplifted within the late Pleistocene. OSL and ESR thermochronometry were applied to a suite of bedrock samples collected from the Hida and Kiso ranges to constrain their evolution. Whereas initial results from the Hida range show that the ESR and OSL data yield similar cooling histories, indicating rapid exhumation of ~10 mm/a over the past 100 ka, the Kiso range experienced lower rates of exhumation. Potential causes of this difference in exhumation rates will be discussed.

9:30am - 9:45am

**Reconstructing production, mixing and erosion of soils using single-grain OSL methods****Tony Reimann***Wageningen University, Soil Geography and Landscape group, The Netherlands*

The *soil mantle* is the Earth's living skin; it provides vital ecosystem services regarding food production, clean water or climate change mitigation making it a key zone for our future wellbeing. Despite its importance it is surprising how little is known about many fundamental processes of soil formation (e.g. soil production or bioturbation) or soil-landscape interactions (e.g. soil erosion by creep). In this contribution I outline how single-grain Optically Stimulated Luminescence (OSL) methods can be utilised to capture soil geomorphological processes on a time resolution of decades to millennia potentially bridging between short scale high resolution instrumental inventories and highly averaged large scale geological reconstructions ( $>10^{3-4}$  years) using inventories of terrestrial cosmogenic nuclides (TCN).

After briefly reviewing the current state-of-research regarding OSL and soil process reconstructions I would like to focus on our proof-of-concept case at the Santa Clotilde Critical Zone Observatory (SC-CZO) in SE Spain. For this proof-of-concept case we (i) develop a new tailor-made OSL single-grain methodology (Reimann et al., 2017); (ii) conceptualise expected trends in our OSL inventories for four soil profiles along a hillslope catena and tested the conceptual model with our single-grain OSL data (Román-Sánchez et al., 2019a) and finally (iii) propose an analytical solution to the diffusion-advection equation to quantitatively model soil particle motion along the hillslope catena (Román-Sánchez et al., 2019b).

Our studies demonstrate that single-grain OSL-based inventories have the potential to simultaneously inform on production, mixing and erosion of soil material at the SC-CZO. Furthermore they provide unique insights into soil landscape co-evolution through meaningful rates of bioturbation and soil creep.

[1] Reimann, T., Román-Sánchez, A., Vanwallegem, T., Wallinga, J. (2017): Getting a grip on soil reworking – single-grain feldspar luminescence as novel tool to quantify soil reworking rates. *QG* 42, 1-14; [2] Román-Sánchez, A., Reimann, T., Wallinga, J., Vanwallegem, T. (2019a): Bioturbation and erosion rates along the soil-hillslope conveyor belt, part 1: insights from single-grain feldspar luminescence. *ESPL*, doi:10.1002/esp.4628; [3] Román-Sánchez, A., Laguna, A., Reimann, T., Giráldez, J.V. Peña, A., Vanwallegem, T. (2019b). Bioturbation and erosion rates along the soil-hillslope conveyor belt, part 2: quantification using analytical solution of the diffusion-advection equation. *ESPL*, doi: 10.1002/esp.4626

9:45am - 10:00am

**Mass movements: can they be dated using luminescence from rock surfaces?****Reza Sohbaty<sup>1</sup>, Andrew Murray<sup>2</sup>, Larry Smith<sup>3</sup>, Martin Stange<sup>4</sup>, Mayank Jain<sup>1</sup>**

<sup>1</sup>Center for Nuclear Technologies, Technical University of Denmark, Risø Campus, DK-4000, Roskilde, Denmark; <sup>2</sup>Nordic Laboratory for Luminescence Dating, Department of Geoscience, Aarhus University, Risø Campus, DK-4000, Roskilde, Denmark; <sup>3</sup>Department of Geological Engineering, Montana Tech of the University of Montana, 1300 W. Park St., Butte, MT 59701, United States; <sup>4</sup>Faculty of Geosciences, University of Bremen, 28359 Bremen, Germany

Mass movements such as rockfalls, landslides and debris flows pose a serious hazard to human population and infrastructure in mountainous areas [1]. Moreover, mass movements are one of the major processes of slope erosion and thus a significant component of landscape evolution; as a result, they have become one of the most studied processes in engineering geology and geomorphology. Knowledge of the return frequency of mass movements lies at the heart of these studies and is a key to understanding their forcing mechanisms. However, the measurement of this return frequency on a scale longer than the historical record has been greatly hampered by a lack of reliable geochronological tools to date past mass movements. Recently, rock surface luminescence dating has been successfully used to determine the age of a rockfall event in Utah, USA [2], as well as the burial of colluvial and fluvial cobbles elsewhere [e.g. 3,4]. The great advantage of this new technique over the established methods such as radiocarbon dating and cosmogenic nuclide is that i) it is directly applied to rock surfaces and ii) it is equipped with an internal record of the degree of pre-burial inheritance (if any) in the chronometric signal; this is preserved in the luminescence-depth profile in the target surface.

Here we present the application of rock surface burial dating to cobbles collected from two illustrative mass-movement sites: i) abandoned floodplain deposits, southern Pyrenees, NE Iberia, ii) megaflood deposited gravel bar, Montana, USA. The luminescence signal characteristics and depth profiles are measured in several cobbles from each site. The observed luminescence-depth profiles show that despite the unsuitable bleaching conditions in these depositional settings, finding cobbles whose surfaces were sufficiently bleached prior to burial is likely. The bleaching of the cobble surfaces most likely takes place on the hillslopes and before entrainment in the mass movement.

[1] Dilley *et al.* (2005). Natural disaster hotspots: a global risk analysis. The World Bank; [2] Chapot *et al.* (2012). Constraining the age of rock art by dating a rockfall event using sediment and rock-surface luminescence dating techniques. *Quaternary Geochronology*, 13, 18-25; [3] Sohbati *et al.* (2012). Optically stimulated luminescence (OSL) dating of quartzite cobbles from the Tapada do Montinho archaeological site (east-central Portugal). *Boreas* 41, 452–462; [4] Jenkins *et al.* (2018). A new approach for luminescence dating glaciofluvial deposits - High precision optical dating of cobbles. *Quaternary Science Reviews*, 192, 263–273.

**10:00am - 10:15am**

### **Direct dating of faulting in the absence of overlying sediments**

**Sumiko Tsukamoto<sup>1</sup>, Benny Guralnik<sup>2</sup>, Kiyokazu Oohashi<sup>3</sup>, Makoto Otsubo<sup>4</sup>**

<sup>1</sup>Leibniz Institute for Applied Geophysics, Germany; <sup>2</sup>Technical University of Denmark; <sup>3</sup>Yamaguchi University;

<sup>4</sup>Geological Survey of Japan, National Institute of Advanced Industrial Science and Technology

Past activity of active faults is typically estimated from deformed Quaternary sediments, containing both measurable displacement markers and dateable material. In crystalline bedrock areas, faults can be recognised geologically- or geomorphologically without overlaying dateable Quaternary units. For such faults, there is currently a lack of broadly applicable methodology to evaluate their activity indices. In this study, we introduce a novel concept to evaluate the fault activity by optically stimulated luminescence (OSL) dating of fault rocks. The level of the OSL signal saturation ( $n/N$ ) has the potential to quantify the activity of faults where slip rates are presently poorly constrained or unknown.

We show the preliminary results for an outcrop of the Atotsugawa Fault (central Japan), where the past activity is well known. The fault core consists of fault gouge and breccia including granite clasts. Four test samples were taken, including a location previously dated by quartz OSL (Ganzawa *et al.*, 2013) to  $200 \pm 200$  years, which is broadly consistent with the last large earthquake at 1858. The equivalent dose ( $D_e$ ) and dose response curves were obtained using pulsed OSL to minimise signal contamination by feldspar OSL. Relatively uniform  $D_e$  values and  $n/N$  were calculated for all samples from the fine grain quartz (4-11 mm), and the ages ranged between  $42 \pm 11$  ka and  $56 \pm 19$  ka, except for one younger sample with a higher environmental dose ( $19 \pm 5$  ka). Although all the apparent ages appear ca. two orders of magnitude older than those of Ganzawa *et al.* (2013), the relatively uniform values (mean age:  $47 \pm 4$  ka; mean fraction of saturation:  $0.33 \pm 0.02$ ) can be considered as representative of the activity of the Atotsugawa Fault during a similar timescale. These apparent ages, together with a trap depth of  $1.66 \pm 0.03$  eV and a frequency factor of  $1 \times 10^{13} \text{ s}^{-1}$  (Murray and Wintle, 1999), and an estimated recurrence interval of the Atotsugawa Fault of 2.5 ka (Research Group of Atotsugawa Fault, 1989), were used to predict the fault shear heating that has repeatedly occurred during past large earthquakes. Our modelling suggests that flash heating of the fault gouge during each large earthquake is broadly equivalent to  $250 \text{ }^\circ\text{C}$  for 10 s. Inverting our exercise, we suggest that if one can estimate the degree of recurrent flash heating independently (e.g. via shearing experiments), it is in turn possible to calculate a recurrence interval for a given fault.

**10:15am - 10:30am****The cosmogenic  $^{10}\text{Be}$ (meteoric)/ $^9\text{Be}$  ratio as a tracer of weathering and erosion in lithologies with and without quartz****Friedhelm von Blanckenburg, Hella Wittmann, Dannhaus Nadine**

GFZ Potsdam, Germany

A perfect clock of the stability of the Earth surface is one that combines a first isotope the flux of which depends on the release rate during erosion, and a second isotope produced at constant rate. The ratio of the meteoric cosmogenic nuclide  $^{10}\text{Be}$  to stable  $^9\text{Be}$  is such a system. We provide a quantitative framework of its use in terrigenous weathering systems [1].

In a weathering zone some of the  $^9\text{Be}$ , present typically in 2.5ppm concentrations in felsic rock, is released and partitioned between a reactive phase (adsorbed to clay and hydroxide surfaces), and into the dissolved phase. The combined mass flux of both phases is defined by the soil formation rate and a mineral dissolution rate – and is hence proportional to the chemical weathering rate and the denudation rate. At the same time, the surface of the weathering zone is continuously exposed to fallout of meteoric  $^{10}\text{Be}$ . This  $^{10}\text{Be}$  percolates into the weathering zone where it mixes with dissolved  $^9\text{Be}$ . Both isotopes may exchange with the adsorbed Be, given that equilibration rate of Be is fast relative to soil residence times. Hence a  $^{10}\text{Be}/^9\text{Be}$ (reactive) ratio results from which the total denudation rate can be calculated provided that the flux of meteoric  $^{10}\text{Be}$  is known. In rivers, when reactive Be and dissolved Be equilibrate, a catchment-wide denudation rate can be determined from a sample of filtered river water.

We have tested this approach in sediment-bound Be and dissolved Be in water of the Amazon and Orinoco basin [2]. In the Amazon trunk stream and tributaries  $^{10}\text{Be}/^9\text{Be}$ (reactive) these two phases equilibrate.  $^{10}\text{Be}/^9\text{Be}$  ratios range from  $5 \times 10^{-9}$  for the Brazilian shield rivers to  $2 \times 10^{-10}$  for the Beni river draining the Andes, corresponding to denudation rates of 0.01mm/yr for the shields and 0.5mm/yr for the Andes, compatible with denudation rates from in situ-produced cosmogenic  $^{10}\text{Be}$ .

Further we have for the first time applied  $^{10}\text{Be}/^9\text{Be}$  to mafic lithologies [3] in three small (<1 km<sup>2</sup>) Czech catchments. Denudation rates from ( $^{10}\text{Be}/^9\text{Be}$ ) agree with D (*in situ*  $^{10}\text{Be}$  from quartz eroded from felsic layers) within a factor of 2 or better.

The new  $^{10}\text{Be}/^9\text{Be}$  denudation rate meter is now becoming applicable to granitoid, mafic, ultramafic rocks, and, potentially, also shales and carbonate.

[1] von Blanckenburg et al. Earth and Planetary Science Letters 351, 2012; [2] Wittmann, H., et al. JGR Earth Surface, 2015; [3] Dannhaus et al. Geochim Cosmochim Acta 222, 2018

**Monday, 23/Sep/2019: 11:15am - 1:00pm****11:15am - 11:30am****Geomagnetic field reconstructions as late Quaternary dating tools****Monika Korte<sup>1</sup>, Sanja Panovska<sup>1</sup>, Maxwell C. Brown<sup>2</sup>, Andreas Nilsson<sup>3</sup>**<sup>1</sup>GFZ German Research Center for Geosciences, Germany; <sup>2</sup>Institute of Earth Sciences, University of Iceland, Iceland;<sup>3</sup>Lund University, Sweden

Records of past geomagnetic field variations, both in intensity and directions, can aid in dating sediment records, volcanic rocks, archaeological artefacts or any other material carrying a remanent magnetization acquired from the paleomagnetic field. However, a prerequisite is reference curves that give reliable representations of magnetic paleosecular variation (PSV) for the locations of interest. These rely on a sufficient number of archeo- or paleomagnetic data, obtained by state-of-the-art laboratory practices, and with good independent age control. We provide an overview over late Quaternary regional reference curves and global

magnetic field models and their application to aid in dating time series and individual spot values. We discuss caveats and limitations of paleomagnetic dating. Although the geomagnetic field is mostly dominated by a global dipole geometry, smaller scale field contributions lead to regional differences in field variations, which cannot be neglected for dating purposes at least on a sub-millennial scale. The smoothed representation of geomagnetic variations in sediments and magnetic field reconstructions also has to be taken into account.

### 11:30am - 12:00pm Session Keynote

#### Dynamics and evolution of carbonate landscapes inferred from cosmogenic nuclides

Vincent Godard<sup>1</sup>, Franck Thomas<sup>1</sup>, Lucilla Benedetti<sup>1</sup>, Olivier Bellier<sup>1</sup>, Vincent Ollivier<sup>2</sup>, Esmail Shabani<sup>3</sup>, Jules Fleury<sup>1</sup>, ASTER Team<sup>1</sup>

<sup>1</sup>Aix-Marseille Univ, CNRS, IRD, INRA, Coll France, CEREGE, Aix-en-Provence, France; <sup>2</sup>Aix-Marseille Univ, CNRS, MC, LAMPEA, Aix-en-Provence, France; <sup>3</sup>Institute for Advanced Studies in Basic Sciences, Gava Zang - Zanjan, Iran

Topographic evolution integrates elementary processes acting at the hillslope scale into the long-wavelength framework of landscape dynamics. Understanding this evolution requires the quantification of denudation rates of eroding landscapes and the assessment of their links with the morphological properties of the topographic surface. The study of Earth surface processes has strongly benefited over the last two decades of advances in geochronological techniques such as cosmogenic nuclides, which allows to constrain the pace of denudation processes. However, most studies have relied on the determination of <sup>10</sup>Be in various types of materials, and, as such, have been restricted to quartz rich lithologies. In comparison, available data are still sparse in carbonate terrains, which cover a significant part of the Earth's surface. In addition to these methodological considerations, the geomorphological evolution of carbonate landscapes poses major questions, such as the relative importance of chemical and mechanical weathering, or the nature of the interaction between hillslope and fluvial processes.

We measured long-term denudation rates using in situ-produced <sup>36</sup>Cl concentrations in bedrock, regolith clasts and stream sediments in various sites of the Luberon carbonate range in Provence, Southeastern France. At the scale of the range, we observe a clear contrast between the local denudation rates from the flat summit surface, clustered around 30 mm/ka, and the basin-averaged denudation rates across the flanks, ranging from 100 to 200 mm/ka. This difference highlights the transient evolution of the range, whose topography is still adjusting to previous uplift events, as well as an important control of slope-dependent processes. At shorter wavelength, we focus on the influence of high-resolution hillslope morphology on surface processes. We observe a linear relationship between denudation rate and hilltop curvature until a major transition where denudation becomes constant and decoupled from morphology. We interpret this transition as a shift from transport to weathering-limited regime for hillslope dynamics, and toward a situation where hillslope denudation can not match the base level lowering rate. This persistent disequilibrium in the channel/hillslope coupling could potentially explain the development of high local relief in many Mediterranean carbonate landscapes.

### 12:00pm - 12:15pm

#### Reconstruction of the Landscape Evolution of South Central Africa: A Case Study on Waterfalls of Northern Zambia and South-Eastern D.R. Congo

Spiros Olivotos<sup>1</sup>, Samuel Niedermann<sup>1</sup>, Vasiliki Mouslopoulou<sup>1</sup>, Silke Merchel<sup>2</sup>, Fenton Cotterill<sup>3</sup>, Tyrel Flugel<sup>4</sup>, Andreas Gärtner<sup>2</sup>, Georg Ruge<sup>2</sup>, Andreas Scharf<sup>2</sup>, Bodo Bookhagen<sup>5</sup>, Marie-Josée Nadeau<sup>6</sup>, Regis Braucher<sup>7</sup>

<sup>1</sup>GFZ Potsdam, Germany; <sup>2</sup>Helmholtz-Zentrum Dresden-Rossendorf (HZDR), Germany; <sup>3</sup>Stellenbosch University, South Africa; <sup>4</sup>Umvoto Africa (Pty) Ltd, South Africa; <sup>5</sup>University of Potsdam, Germany; <sup>6</sup>NTNU, Trondheim, Norway; <sup>7</sup>CEREGE CNRS Aix Marseille Univ., IRD, INRA, Collège de France, Aix-en-Provence, France

Northern Zambia and the south-eastern Katanga Province of D.R. Congo lie within the southwest extension of the East African Rift System, which is one of the most significant present-day examples of active tecton-

ics. Seismotectonic research in the area has been scarce, despite the fundamental impacts of neotectonics, which controls landscape evolution southwest of the Tanganyika graben. Nevertheless, the formation of the Congo-Zambezi watershed has been constrained from the combination of geological and biological evidence at ~2 Ma (Cotterill & de Wit 2011).

A preliminary Google Earth mapping has revealed two major sets of fault systems (Mweru and Upemba). Analysis of the seismicity patterns recorded within the two fault systems during the last 35 years provides indications for fault interactions over earthquake timescales, highlighting the fact that they are currently active.

This study is part of an interdisciplinary project combining DNA sequencing of selected fish groups to define molecular clocks together with surface exposure dating of key landforms using in-situ produced cosmogenic nuclides. This technique can be applied to quantify how long rocks have been exposed at “knickpoints” since they were first formed (Burbank & Anderson 2012). For that purpose, quartz-rich samples were collected from selected waterfalls with the aim of quantifying exposure ages and erosion/retreat rates. Expecting complex exposure scenarios both radionuclides  $^{10}\text{Be}$  and  $^{26}\text{Al}$  and the stable noble gas  $^{21}\text{Ne}$  were combined in all samples.

Preliminary results from Northern Zambia indicate burial for at least several hundred thousand years. This specific burial may confirm the existence of a significantly deeper and larger Paleo-Lake Mweru before the modern drainage evolved (Dixey, 1944). More results are expected soon to confirm or dismiss this hypothesis. Furthermore, samples taken at different distances below the Kiubo and Luvilombo Waterfalls (D.R.C.) yield preliminary ages between ~7 and 40 ka, increasing with distance from the falls and thus reflecting waterfall retreat. Extrapolating to the original knickpoint location should enable us to estimate the time of its formation.

[1] Burbank D.W. & Anderson R.S. 2012. *Tectonic Geomorphology. Second Edition. Wiley-Blackwell, Chichester*; [2] Cotterill F.P.D. & de Wit M.J. 2011. *South African Geographical Journal* 114: 489-514; [3] Dixey F. 1944. *South African Geographical Journal* 47, 01: 9-45.

**12:15pm - 12:30pm**

## **Can cosmogenic nuclide exposure dating help to solve the existing controversy about the evolution of hyperaridity in the Atacama Desert?**

**Benedikt Ritter<sup>1</sup>, Steven A. Binnie<sup>1</sup>, Finlay M. Stuart<sup>2</sup>, Joel Mohren<sup>1</sup>, Tibor Dunai<sup>1</sup>**

<sup>1</sup>University of Cologne, Germany; <sup>2</sup>Scottish Universities Environmental Research Centre, UK

The Atacama Desert of northern Chile and Peru is one of the driest places on Earth, with a modern hyperarid core, receiving less than 2 mm/yr of precipitation. Although the main factors forcing aridity have been identified, their timing and succession is still being debated. Most paleoclimate studies in the Atacama Desert have been carried out on the fringes of the extreme hyperarid zone (here, hyperarid regions are considered to be those displaying <2 mm/yr modern precipitation), in regions that still receive noticeable amounts of precipitation and/or runoff from the high Andes. From the different study areas and archives used, contradictory views have emerged regarding the onset, duration, and intensity of hyperaridity and interspersed ‘wetter’ (still arid) periods. With the help of cosmogenic nuclide exposure dating ( $^{21}\text{Ne}$ ,  $^{10}\text{Be}$ ), in combination with diverse paleoclimate archives and age data of various dating techniques, a progress towards a better understanding of the evolution of hyperaridity in the Atacama Desert can be achieved.

**12:30pm - 12:45pm****Using TCN to decipher a steep erosional gradient in the hyperarid core of northern Chile over multiple time scales****Joel Mohren, Steven A. Binnie, Benedikt Ritter, Tibor J. Dunai***University of Cologne, Germany*

Despite persisting and long-term hyperarid conditions, numerous small-scale drainage systems have formed in Coastal Cordillera of northern Chile, which are mostly isolated from river networks and associated processes originating in the Precordillera or the High Andes to the east. Thus, these catchments provide valuable natural laboratories to investigate the interplay between erosion, atmospheric deposition, tectonics and local (micro-) climatic conditions. In this study, we present a set of cosmogenic  $^{10}\text{Be}$ ,  $^{26}\text{Al}$  and  $^{14}\text{C}$  derived, catchment-wide erosion rates along a short (2.5 km) E-W transect located on the northern rim of the Río Loa canyon in the hyperarid core of the Atacama Desert (latitude  $21.4^\circ\text{S}$ ). The inferred process rates reflect localized tectonic movements, geologically recent base level lowering, time-integrated (micro) climatic gradients and the presence/absence of gypcrete. Taken together with the analysis of catchment-averaged geomorphologic parameters, these findings point towards the presence of two fundamentally different erosional regimes in this small study area, which are sharply delineated along a topographically modest tectonic ridge. To the west, a detachment-limited erosion regime prevails, while in the east a transport-limited regime is dominant. The presence of gypcrete, whose prevalence is governed by (micro-) climatic conditions, appears to be a crucial factor determining the erosional regime. Assuming constant erosion rates beyond the nominal erosional time scales of the methodology used, the volume of material removed would point to an onset of this differential evolution near to the Pliocene/Pleistocene boundary. However, present-day crust abundance and distribution as mapped in the field and by using an unmanned aerial vehicle (UAV) indicate a polyphase (at least two-phase) incision of the channels. To test whether the development of the observed geomorphic gradient has been accelerated or decelerated during the Holocene, we measure in-situ cosmogenic  $^{14}\text{C}$  to distinguish between long-term Quaternary ( $^{10}\text{Be}$ ) and Holocene ( $^{14}\text{C}$ ) erosion patterns.

**Poster Presentations****Mon: 38****A constant slip rate for the western Qilian Shan frontal thrust during the last 200 ka consistent with GPS-derived and geological shortening rates****Ralf Hetzel<sup>1</sup>, Andrea Hampel<sup>2</sup>, Pia Gebbeken<sup>1</sup>, Qiang Xu<sup>3</sup>, Ryan D. Gold<sup>4</sup>***<sup>1</sup>Institut für Geologie und Paläontologie, WWU Münster, Germany; <sup>2</sup>Institut für Geologie, Leibniz Universität Hannover, Germany; <sup>3</sup>Institute of Tibetan Plateau Research, Beijing, China; <sup>4</sup>Geologic Hazards Science Center, U.S. Geological Survey, Golden, Colorado, USA*

Active thrust faulting at the front of the Qilian Shan accommodates the northeastward growth of the Tibetan Plateau, however, the lifespan of individual faults and their slip history on different timescales remain largely unknown. Here, we show that the main range-bounding thrust fault of the western Qilian Shan has accrued tectonic slip at an almost constant rate during the last  $\sim 200$  ka, and possibly since fault initiation in the mid-Miocene. Our finding is based on  $^{10}\text{Be}$  exposure ages from a flight of five deformed fluvial terraces along the Hongshuibai river, which constrain the vertical slip rate of the Qilian Shan frontal thrust to be  $1.2 \pm 0.1$  m/ka during the last 200 ka. With a fault dip of  $30 \pm 5^\circ$  constrained by seismic reflection data, we obtain a horizontal shortening rate of  $2.0 \pm 0.3$  m/ka. This value is consistent with both the short-term shortening rate of  $1.7 \pm 0.3$  mm/a derived from GPS data and the long-term shortening rate of  $2.1 \pm 0.4$  m/ka, which is based on a balanced geological cross-section. The latter provides a total shortening estimate of  $25 \pm 3$  km since the thrust fault initiated  $12 \pm 2$  Ma ago. The agreement between the shortening rates on the range of timescales between  $10^0$  and  $10^7$  years suggests that the western Qilian Shan frontal thrust has slipped at a steady rate since its initiation and implies that this fault is the main structure responsible for the growth of the western Qilian Shan.

Mon: 39

### Spatial patterns of erosion and landscape evolution in a bivergent metamorphic core complex revealed by cosmogenic $^{10}\text{Be}$ : The central Menderes Massif (Western Turkey)

Caroline Heineke<sup>1</sup>, Ralf Hetzel<sup>1</sup>, Nils-Peter Nilius<sup>2</sup>, Christoph Glotzbach<sup>3</sup>, Cüneyt Akal<sup>4</sup>, Marcus Christl<sup>5</sup>, Andrea Hampel<sup>2</sup>

<sup>1</sup>WWU Münster, Germany; <sup>2</sup>Leibniz Universität Hannover, Germany; <sup>3</sup>Universität Tübingen, Germany; <sup>4</sup>Dokuz Eylül University Izmir, Turkey; <sup>5</sup>ETH Zürich, Switzerland

In extensional provinces with low-angle normal faulting – such as the Aegean region – both tectonic processes and erosion induce landscape change, but their interaction during the evolution of topography and relief accompanying continental extension has rarely been addressed. Here we present local and catchment-wide  $^{10}\text{Be}$  erosion rates that document the spatial pattern of erosion in the central Menderes Massif, a metamorphic core complex consisting of two asymmetric mountain ranges (Bozdağ and Aydın) bound by detachment faults and active grabens. Catchment-wide erosion rates on the northern flank of the Bozdağ Range are rather low (40–110 mm/kyr), but reach values of >300 mm/kyr on the steep southern escarpment; a pattern that reflects both topography and bedrock lithology. In the Aydın Range, erosion rates are generally higher – with mean erosion rates of ~190 and ~260 mm/kyr on the northern and southern flank, respectively – and more variable along-strike. In both ranges, the erosion of ridge crests, which we determined using amalgamated bedrock clasts, proceeds at rates of 30–90 mm/kyr. The difference between local and catchment-wide erosion rates indicates that topographic relief increases in most parts of the massif in response to ongoing fault-related uplift and concomitant river incision. The analysis of river profiles, drainage divide position and mobility suggests that rock uplift is strongest in the eastern Bozdağ Range and declines along-strike. Our findings document that tectonic processes exert a significant control on landscape evolution during active continental extension and are reflected in both the topographic signature and the spatial pattern of erosion.

Mon: 40

### A global geomagnetic field reconstruction of the past 100 ka

Sanja Panovska<sup>1</sup>, Monika Korte<sup>1</sup>, Catherine Constable<sup>2</sup>

<sup>1</sup>GFZ German Research Centre for Geosciences Potsdam, Germany; <sup>2</sup>University of California San Diego, Scripps Institution of Oceanography, USA

The geomagnetic core field varies on time scales from months, years, centuries, to millennia. These variations are best studied using empirical spherical harmonic global models of Earth's magnetic field. Ground-based geomagnetic observatories and satellite missions provide a detailed view of the short-term variations. Paleo- and archeomagnetic data can be used to model the long-term variations. However, global field reconstructions become increasingly challenging with age, not least due to uncertainties in dating of the input data. We recently derived the first global geomagnetic field reconstruction spanning the past 100 kyr, named GGF100k. One characteristic of the long-term variations are geomagnetic excursions - events when field directions deviate strongly from an axial-dipole dominated field, associated with globally low field intensities. The Laschamp excursion, is the globally best documented event and happened 41 ka ago. Some other, probably only regionally manifested excursions, have been described in the 0-100 ka time interval. Here we discuss the potential and limitations of using GGF100k as a paleomagnetic dating tool. Global field reconstructions show that care should be taken when using geomagnetic excursions as stratigraphic markers, as the field direction signature might only be regional or offset in time in different regions. We also point out the importance of good independent chronologies for paleomagnetic sediment records and volcanic data to improve global paleomagnetic field reconstructions like GGF100k for their broad applications in studying the geomagnetic field evolution, for estimating the past geomagnetic shielding effect, and for dating purposes.

**Mon: 41****An engineering geomorphologic characterization of the Kaju River near Qasr-e-qand city****Mahdiyeh Sotoudeh<sup>1</sup>, Jafar Rahnamarad<sup>1</sup>, Amir Hamzeh Keykha<sup>2</sup>, Kazem Shabanigoraji<sup>1</sup>**<sup>1</sup>*Department of Geology, Zahedan Branch, Islamic Azad University, Zahedan, Iran,;* <sup>2</sup>*Department of Civil Engineering, Zahedan Branch, Islamic Azad University, Zahedan, Iran,*

Kaju River is one of the main streams of the Bahukalat River in the southern province of Sistan and Baluchistan, in Iran. The river extends approximately 200 km from the mountains of Qasr-e-qand and flows southward to Oman Sea. In this paper, we investigate the morphology, the spatiotemporal evolution and the engineering geomorphological characterization of the Kaju River. The data we use to analyze the geomorphology stems from library studies, field visits, geospatial map surveys, and aerial imagery. In recent years, the route of this river has changed significantly due to environmental and human factors. Environmental factors include frequent destructive floods, and increasing and decreasing sediment yield, whereas human factors include building and bridge constructions and side erosions due to the drainage of agricultural wastewater and urban sewage. We used the oldest available images which were scale 1:40000 aerial photographs from 1955. Based on the data analyzed in this paper, we determined the river's characteristics such as central angle, type, longitudinal profile, and radius of curvature to width ratio. We also estimated the trend of changes and parameters such as slope and bending components, leading to the conclusion that the Kaju river as an adult river. The general shape of the Kaju River follows the geological conditions of the area. The river, with its many irregular branches, is flowing in a plain area with high hillsides. Tectonic factors have caused multiple bends along the river. The river bed's width and large sediment yield indicate that the river is mostly arterial. Towards the river's end, expected the river bed's hard lithology, its route has rotated more than 90 degrees. This seasonal river, with its unexpected destructive floods, has a very wide mainstream bed during its typical flow, but during high water moments, the floodplain goes underwater. Finally, we show that agricultural land developments in the riverside's proximity along the river's route and the lack of awareness about efficient and eco-conscious ploughing and agricultural waste disposal methods have led to significant environmental degradation and changes in river morphology.

**Mon: 42****Glacial evolution using <sup>36</sup>Cl moraine dating in the Krnica Valley, Julian Alps, Slovenia****Ron Steven<sup>1</sup>, Silke Mechernich<sup>1,2</sup>, Ariane Binnie<sup>1</sup>, Manja Zebre<sup>3</sup>, Roberto R. Colucci<sup>4</sup>, Jerney Jez<sup>5</sup>, Petra Jamsek Rupnik<sup>5</sup>**<sup>1</sup>*Institute of Geology and Mineralogy, University of Cologne, Germany;* <sup>2</sup>*Federal Institute of Hydrology, Germany;* <sup>3</sup>*Department of Geography and Earth Sciences, Aberysthwyth University, UK;* <sup>4</sup>*Department of Earth System Sciences and Environmental Technology, ISMAR Trieste – CNR, Italy;* <sup>5</sup>*Geological Survey of Slovenia, Ljubljana, Slovenia*

The impact of past climate change in the eastern Alps is rather unknown in relation to other parts of the Alps and central Europe. To fill this gap, the reconstruction of the age and size of glaciers can provide a better understanding of the glacier fluctuations and climate variability in the Alps since the Last Glacial Maximum (LGM).

Here we focus on the Krnica Valley, which is a 9 km long valley in the Julian Alps (Slovenia), located in an area characterized by very high mean annual precipitation that locally exceeds 3300 mm water equivalent. The valley is orientated to the north and indicates at least four moraine stages. The stratigraphically youngest moraine, associated with the Little Ice Age cooling, occupies the cirque threshold at 1910 m a.s.l. (stage I moraine after Kozamernik et al., 2017). Further down valley at 1830 m a.s.l. occurs the frontal moraine of stage II. Moraine stages III and IV are preserved as lateral moraines, the latter reaching down to 1100 m a.s.l. Stage III moraine is significantly less vegetated and higher in its average altitude with respect to stage IV. The equilibrium line altitudes (ELAs) for the glacial advances associated with moraine stages I, II and III were estimated at 1973 m, 1923 m and 1812 m, respectively (Kozamernik et al., 2017).

The bedrock and the blocks on the moraines are composed of upper Triassic limestone and dolostone, which

is suitable for Chlorine-36 ( $^{36}\text{Cl}$ ) dating. At well-preserved and stable boulders of moraines II-IV, hand sized samples were taken, their orientation and topographic shielding was documented. While the sampled boulders of stage III and IV are still under preparation, first results of five boulders from stage II indicate agreeing  $^{36}\text{Cl}$  concentrations, which will be calculated to exposure ages as soon as all required chemical data is available.

Further field investigations, glacier-climate modelling and final age calculation of the sampled boulders are aimed to clarify the local glacier fluctuations along with regional paleoclimatic interpretation.

**Mon: 43**

### **The evolution of low relief landscapes in the Eastern Alps constrained by a multi-system approach**

**Andreas Wölfler<sup>1</sup>, Christoph Glotzbach<sup>2</sup>, Andrea Hampel<sup>1</sup>, István Dunkl<sup>3</sup>**

<sup>1</sup>*Institute for Geology, Leibniz Universität Hannover, Callinstraße 30, 30167 Hannover, Germany;* <sup>2</sup>*Department for Geology and Geodynamics, Universität Tübingen, Wilhelmstraße 56, 72074 Tübingen, Germany;* <sup>3</sup>*Geoscience Center, Sedimentology and Environment Geology, Universität Göttingen, Goldschmidstraße 3, 37077 Göttingen, Germany*

The Eastern Alps comprise several domains, which are characterized by distinct geomorphologic features. The western footwall of the Katschberg normal fault in the Eastern Alps display high and rugged topography and high relief that is the result of the exhumation processes since the Miocene. In contrast, smooth topography and distinctly gentler dipping slopes occur to the east of the Katschberg normal fault, which are interpreted as remnants of paleosurfaces. These relict surfaces are preserved at elevations between 1.800 and 2.500 m a.s.l. Although these low relief landscapes have since long been recognized, little is known about their age and temporal evolution. To unravel their temporal and geomorphological history we use new low-temperature thermochronological data as well as  $^{10}\text{Be}$ -derived denudation rates of river catchments and exposure ages of glacially polished quartz veins. The new low-temperature thermochronological data display a zircon (U-Th)/He age of  $77.8 \pm 7.8$  Ma that is interpreted to reflect late Cretaceous cooling after Eo-Alpine metamorphism. Apatite fission track and (U-Th)/He ages are significantly younger and range from 36.8 to 31.3 Ma. Time-temperature history modelling of the cooling ages suggests enhanced cooling in the Eocene followed by thermal stagnation. Thus, the rocks of the study area have been in upper crustal sections (2-3 km) since the Eocene-Oligocene boundary (roughly between  $\sim 40$  and  $\sim 35$  Ma). The enhanced cooling in the Eocene is probably related to an increasing relief due to shortening, folding and thrusting in the Eastern Alps triggered by the onset of collision between the European margin and the Adriatic microplate. Catchment-wide erosion rates derived from cosmogenic  $^{10}\text{Be}$  analysis range from  $98 \pm 9$  to  $180 \pm 20$  mm/kyr. Under the assumption that rock exhumation occurred solely by erosion, the long-term average erosion rate derived from the thermochronological data range between  $\sim 50$ - $90$  mm/kyr. These long-term rates are remarkably similar to the  $^{10}\text{Be}$ -derived catchment-wide erosion rates, despite the different timescales over which the two methods integrate. Together, these data suggest that erosion rates did not change significantly over the last  $\sim 40$  Ma. Four  $^{10}\text{Be}$  exposure ages from glacially polished quartz veins cluster between  $14.5 \pm 1.4$  and  $16.8 \pm 1.6$  ka. We interpret these ages as the record of the melting of glaciers in the study area shortly after the Oldest Stadial.

**Mon: 44****Quantifying river incision into low-relief surfaces using local and catchment-wide  $^{10}\text{Be}$  denudation rates****Reinhard Wolff<sup>1</sup>, Ralf Hetzel<sup>1</sup>, Marcus Strobl<sup>2</sup>**<sup>1</sup>*Institut für Geologie und Paläontologie, Westfälische Wilhelms-Universität Münster, Corrensstr. 24, D-48149 Münster, Germany;* <sup>2</sup>*Steinbuch Centre for Computing, Karlsruhe Institute of Technology, Hermann-von-Helmholtz-Platz 1, D-76344 Eggenstein-Leopoldshafen, Germany*

Relief generation in non-glaciated regions is largely controlled by river incision into bedrock but datable fluvial terraces that allow quantifying incision rates are not always present (e.g. Ahnert, 1970; Whipple et al., 1999; Burbank and Anderson, 2012). Here we suggest a new method to determine river incision rates in regions where low-relief surfaces are dissected by streams. The approach consists of three steps and requires the  $^{10}\text{Be}$  concentrations of a stream sediment sample and a regolith sample from the low-relief surface. In the first step, the spatial distribution of  $^{10}\text{Be}$  surface concentrations in the given catchment is modelled by assuming that denudation rates are controlled by the local hillslope angles. The slope-denudation rate relation for this catchment is then quantified by adjusting the relation between slope angle and denudation rate until the average  $^{10}\text{Be}$  concentration in the model is equal to the one measured in the stream sediment sample. In the second step, curved swath profiles are used to measure hillslope angles adjacent to the main river channel. Thirdly, the mean slope angle derived from these swath profiles and the slope-denudation relation are used to quantify the river incision rate (assuming that the incision rate equals the denudation rate on adjacent hillslopes). We apply our approach to two study areas in southern Tibet and central Europe (Black Forest). In both regions, local  $^{10}\text{Be}$  denudation rates on flat parts of the incised low-relief surface are lower than catchment-wide denudation rates. As the latter integrate across the entire landscape, river incision rates must exceed these spatially averaged denudation rates. Our approach yields river incision rates between  $\sim 15$  and  $\sim 30$  m/Ma for the Tibetan study area and incision rates of  $\sim 70$  to  $\sim 100$  m/Ma in the Black Forest (Wolff et al., 2018). Taking the lowering of the low-relief surfaces into account suggests that relief in the two study areas increases at rates of 10–20 and 40–70 m/Ma, respectively.

[1] Ahnert F. 1970. Functional relationships between denudation, relief, and uplift in large, mid-latitude drainage basins. *American Journal of Science* 268: 243–263; [2] Burbank DW, Anderson RS. 2012. *Tectonic Geomorphology*, Second Edition. Wiley-Blackwell Chichester, West Sussex. 472 pp; [3] Whipple KX, Kirby E, Brocklehurst SH. 1999. Geomorphic limits to climate-induced increases in topographic relief. *Nature* 401: 39–43; [4] Wolff R, Hetzel R, Strobl M. 2018. Quantifying river incision into low-relief surfaces using local and catchment-wide  $^{10}\text{Be}$  denudation rates. *Earth Surface Processes and Landforms* 43: 2327–2341.

**7b) Sediment generation and quantitative provenance analysis****Wednesday, 25/Sep/2019: 8:30am - 10:30am****Session Chair: Paula Castillo (Westfälische Wilhelms-Universität Münster)****Location: H3****Session Abstract**

The provenance signal stored in detrital sediments is intricately linked to diverse processes of sediment generation, and to modification during transport and storage. Thus source-sink relationships may be complicated to decipher or even obscured by climatic, geomorphic, tectonic and diagenetic factors.

This session welcomes contributions quantitatively analysing sediment generation and provenance by considering petrographical, geochemical, geochronological and textural properties of detrital sediments. Considerations of novel methods and approaches, case studies combining ancient and modern examples, and modeling studies are particularly welcome.

## Lecture Presentations

8:30am - 8:45am

### Studies on the Marinoan tillite of the Port Nolloth Zone in southern Namibia: zircon analyses on matrix and pebbles and their significance for provenance studies of glacial deposits

**Mandy Hofmann<sup>1</sup>, Johannes Zieger<sup>2</sup>, Andreas Gärtner<sup>1</sup>, Rita Krause<sup>1</sup>, Ulf Linnemann<sup>1</sup>**

<sup>1</sup>Senckenberg Naturhistorische Sammlungen Dresden, Germany; <sup>2</sup>Senckenberg Museum für Naturkunde Görlitz

Southern Namibia comprises the western part of the Kalahari Craton as well as its sedimentary cover and the orogenic Gariep Belt in the west.

The Port Nolloth Group, as part of the Gariep Belt, comprises metasediments and volcanic rocks of Neoproterozoic age. Within these successions the Marinoan Snowball-Earth tillite crops out. Stratigraphic correlations are difficult due to orogenic metamorphic overprint and the strongly folded and sheered rocks in this region. But, the direct contact to a Marinoan-type cap carbonate allows the differentiation from younger and older diamictites of this region and their correlation.

We present and discuss new data on the Marinoan tillites and their cap carbonates from the Witpuetz Farm, the Namuskluft, and the Dreigratberg in southernmost Namibia. Previous works were based on U-Pb ages of detrital zircons from the matrix of the Snowball Earth tillites. Our new data shows why the analyses of diamictite matrix samples are so important and why they need to be distinguished from the information hold by the pebbles within the tillite matrix.

8:45am - 9:00am

### The evolution of the southern Namibian Karoo aged basins – Implications from detrital zircon data

**Johannes Zieger<sup>1</sup>, Marika Stutzriemer<sup>2</sup>, Mandy Hofmann<sup>3</sup>, Andreas Gärtner<sup>3</sup>, Axel Gerdes<sup>4</sup>, Linda Marko<sup>4</sup>, Ulf Linnemann<sup>3</sup>**

<sup>1</sup>Senckenberg Museum für Naturkunde Görlitz; <sup>2</sup>TU Dresden; <sup>3</sup>Senckenberg Naturhistorische Sammlungen Dresden;

<sup>4</sup>Institut für Geowissenschaften, Mineralogie, Goethe Universität Frankfurt

Detrital U-Pb zircon age dating and grain morphometrics were used for provenance determination and for obtaining maximum age of deposition for the Lower Permian Dwyka Group and for the Middle to Upper Permian Ecca Group of Namibia's Aranos and Karasburg Basins. Thirteen sedimentary samples and one ash fall sample were analysed using laser ablation - single collector - inductively coupled plasma – mass spectrometry (LA-ICP-MS). The results reveal a prominent Cambrian to Neoproterozoic (500-750 Ma) population, a second Lower Neoproterozoic to Mesoproterozoic (950-1300 Ma) population, and a third Upper Palaeoproterozoic (1775-1950 Ma) population. Multiple evidences (e.g. roundness of investigated zircon grains,  $\epsilon_{\text{Hf}}$  values, and previous works) suggest the zircon populations are part of a Gondwana wide recycling system where basins act as intermediate reservoirs and disperser. Classic source to sink dynamics do not apply. A fourth Permian age population (255-296 Ma) consisting of euhedral zircon grains is assumed to be derived directly from their protolith. Since no felsic Permian rocks occur in the southern African region these findings suggest a significant input by ash fall, which may be linked to the Choiyoi Group volcanism in southwestern Gondwana. The results reveal a c. 42 Ma lasting evolution of the Karasburg Basin and a shorter c. 30 Ma lasting evolution of the Aranos Basin. The lowermost datable unit is an ash bed of the Ganigobis Shale Member of the Zwartbas Fm (Dwyka Group) which gave an age of c. 296 Ma, whereas the Aussenkjer Fm represents the uppermost Namibian Karoo aged strata with a maximum age of deposition of c. 254 Ma.

9:00am - 9:30am *Session Keynote***OH defects in quartz as monitor for igneous, metamorphic, and sedimentary processes****Roland Stalder***Universität Innsbruck, Austria*

Quartz is able to incorporate trace amounts of protons by coupled substitutions that are charge balanced by metal cations. Depending on the charge balancing cation, the structurally incorporated protons form different types of OH-dipoles, which physically behave similar to OH-groups in nominally hydrous minerals and commonly are referred as OH-defects or “defect water”. The OH-defect inventory in a quartz crystal can be characterized by type and abundance and generally reflects the formation conditions. Initially formed under water pressure in igneous systems, OH-defects may (or may not) later be modified by metamorphic processes and reveal parts of their geological history. OH-defects in quartz from unmetamorphosed granite bodies reveal interesting differentiation trends, but are successively destroyed during metamorphic overprint, where their concentration is decreased, the defect structure changed and a trend towards a homogeneous defect partitioning from grain to grain is observed. However, below 300°C OH-defects are retained over geological time scales and thus make sediments and sedimentary rocks valuable archives to preserve the pre-sedimentary OH-defect chemistry.

The major impediment to use OH-defects as discrimination tool is the fact the OH-defect signal is overshadowed by the much more abundant molecular water present in most quartz crystals as fluid (and or melt) inclusions. A distinction between molecular water and OH-defects can be achieved by polarised FTIR spectroscopy measurements on oriented crystals, where the unwanted isotropic signal can be eliminated by subtraction of the two polarized measurements. In order to do so, appropriate crystal sections either are selected from a petrographic thick section or are prepared by manually alignment parallel to the crystallographic c-axis.

In this contribution OH-defects of detrital quartz from river (Elbe, Rhine) and beach (Baltic and North Sea) sediments, sandstones (subarkose to qtz-arenite) of different ages (Proterozoic to Mesozoic) are compared to potential source rocks (Hercynian and Proterozoic granites). Important findings, reflected by both recent granite outcrops and siliciclastic sediments, suggest that detrital quartz derived from the Proterozoic Scandinavian Shield is in average nearly an order of magnitude less rich in OH-defects than detrital quartz derived from the Hercynian orogeny. Furthermore, individual signatures can be traced back to potential source rocks (and/or source areas) and may be used as tool for to estimate mixing proportions of different sources. The benefit of the new method is also discussed in the context of findings from studies using other methods such as the evolution of heavy minerals and/or zircon age spectra.

9:30am - 9:45am

**OH defects in quartz as a provenance tool: Application to fluvial and deep marine sediments from SW Japan****Dominik Jaeger<sup>1,2</sup>, Roland Stalder<sup>1</sup>, Hideki Masago<sup>3</sup>, Michael Strasser<sup>2</sup>***<sup>1</sup>Institute of Mineralogy and Petrography, University of Innsbruck, Austria; <sup>2</sup>Department of Geology, University of Innsbruck, Austria; <sup>3</sup>Japan Agency for Marine-Earth Science and Technology*

Hydrogen-related point defects (OH defects) in the crystal lattice of detrital, monocrystalline quartz have been proposed as an indicator to distinguish different sediment sources, making it a potential tool for provenance analysis. This study tests this novel technique on samples from SW Japan by comparing the results of OH defect analyses with those of “classical” provenance studies. OH defects of 188 detrital, monocrystalline quartz grains from five rivers (Fuji, Tenryu, Nagara, Yoshino, and Shimanto) and four offshore wells drilled in the Nankai Trough area (ODP site 1177; IODP sites C0002, C0007, C0012) are characterized using Fourier-transform infrared (FTIR) spectroscopy. Considerable differences in OH defect concentrations are identified between individual river samples. A general increase of values from east to west is observed. Possible links to the respective source geology are established. Very low OH defect contents (< 1 wt. ppm

water) of sediment from the Fuji and Tenryu rivers may be a result of high deformation and exhumation in the Izu-Honshu collision zone. Moderate to high OH defect contents of Nagara and Yoshino river samples (up to 50 wt. ppm water) are similar to the values of the global average in continental crust, possibly due to a mixing of various source lithologies. High and very diverse OH defect contents of Shimanto River sediments (up to 211 wt. ppm water) are likely an effect of extensive sediment reworking and mixing in the Nankai accretionary wedge. The OH defect signal is shown to be traceable through the offshore sedimentary record. In the western Shikoku Basin (ODP site 1177), turbidite deposits at 15 Ma and 7 Ma show a very similar signal as recent Shimanto river sediment, whereas eastern Shikoku Basin sediments (IODP Site C0012), at 15 Ma and 6 Ma strongly resemble present day Nagara and Yoshino river sediments. Sediments deposited in the Nankai trench wedge at 1 Ma (IODP Site C0007) indicate a shift towards lower OH defect concentrations. This may be due to increased, trench parallel sediment flux from the low-OH defect Fuji and Tenryu river sources, as proposed by previous studies. This study presents the first OH defect dataset in detrital quartz from rivers and offshore drill sites in a subduction zone environment, introducing OH defects as a new useful tool for sediment provenance analysis in active convergent margin settings.

**9:45am - 10:00am**

### **Dispersed occurrence of mafic and felsic ultrahigh-pressure rocks in the central Saxonian Erzgebirge (Germany) revealed by diamond and coesite inclusions in detrital garnet**

**Jan Schönig<sup>1</sup>, Hilmar von Eynatten<sup>1</sup>, Guido Meinhold<sup>1,2</sup>, Keno Lünsdorf<sup>1</sup>**

<sup>1</sup>Geoscience Center Göttingen, Georg-August-University Göttingen, Germany; <sup>2</sup>School of Geography, Geology and the Environment, Keele University, Keele, Staffordshire, ST5 5BG, UK

Ultrahigh-pressure (*UHP*) metamorphism of continental crust is intimately connected to deep subduction processes, which are characteristic of modern-style plate tectonics (Stern, 2005, *Geology*). Until recently, the search for *UHP* rocks was restricted to targeted field mapping and subsequent investigation of potential *UHP* rocks. Although sedimentary provenance tools like the chemical composition of white mica or garnet are useful to identify high-pressure (*HP*) sources, it is not possible to confidently discriminate *HP* and *UHP*. Schönig et al. (2018, *Scientific Reports*) presented coesite inclusions in detrital garnets of a modern sand sample from a small catchment in the Western Gneiss Region of Norway, demonstrating that mineralogical evidence for *UHP* metamorphism is recorded in the detritus. However, it is questionable if the preservation of coesite in detrital garnets is a local or general phenomenon and if the introduced technique is able to trace *UHP* metamorphism in larger catchments.

To test this approach, we investigated the inclusion assemblage of detrital garnets from modern sand samples of tributaries draining the area around the Saldenbach reservoir in the central Saxonian Erzgebirge. Mineralogical evidence for *UHP* metamorphism in this area is scarce and restricted to diamond-bearing paragneiss lenses at the eastern shore of the reservoir (e.g., Nasdala and Massonne, 2000, *European Journal of Mineralogy*), a coesite-bearing eclogite at the northern shore (Massonne, 2001, *European Journal of Mineralogy*), and coesite-bearing granulite blocks ~4.5 km further east (Marschall et al., 2009, *Journal of the Geological Society*). However, based on geothermobarometry and inclusions interpreted as pseudomorphs after coesite and K-cymrite (e.g., Massonne 2011, *GeoLines*), *UHP* metamorphism supposedly affected a wider area. Thus, the study area is not only suitable to test the reproducibility of detecting *UHP* metamorphism in the detritus of larger catchments but also to give further insights into the distribution and characteristics of *UHP* rocks.

Frequent findings of coesite and diamond inclusions combined with geochemical composition of the detrital host garnets show that (1) coesite-bearing rocks in the central Erzgebirge are common, distributed over the investigated area, and include mafic and felsic lithologies; (2) diamond-bearing rocks effectively transfer *UHP* signatures to the sedimentary record, representing the first report of metamorphic diamond inclusions in detrital mineral grains; (3) analyzing small inclusions is crucial to identify *UHP* metamorphic rocks; and (4) the applied method is appropriate to detect *UHP* rocks in large catchments based on the two most prominent indicator minerals coesite and diamond (Schönig et al., accepted, *Geology*).

**10:00am - 10:30am** *Leopold-von-Buch-Plakette 2019*

## **Pangea and the Lower Mantle**

**Xavier Le Pichon<sup>1</sup>, A.M. Celâl Şengör<sup>2</sup>, Caner Imren<sup>2</sup>**

<sup>1</sup>*Collège de France, France;* <sup>2</sup>*Istanbul Teknik Üniversitesi, Turkey*

The peripheral Pangea subduction zone closely followed a polar great circle that we relate to the band of faster-than-average velocities in lowermost mantle. Both structures have an axis of symmetry in the equatorial plane. Assuming geologically long term stationarity stability of the deep mantle structure, we use the axis of symmetry of Pangea to define an absolute reference frame. This reference frame is close to the slab remnants and NNR frames of reference but disagrees with hot spot-based frames. We apply this model to the last 400Myr. We show that a hemispheric supercontinent appeared began forming as early as 400 Ma. However, at 400 Ma, the axis of symmetry was situated quite far south and progressively migrated within the equatorial plane that it reached at 300Ma. From 300 to 110-100Ma, it maintained its position within the equatorial plane. Thus, Pangea was already in a hemispheric configuration with a peripheric subduction zone during the Devonian formation stage. Its southern position at this stage and its progressive northward migration toward an equilibrium equatorial position may then be interpreted as due to a recently established convection of order 2 that led to true polar wandering. This would indicate further that the African Large Low Shear Velocity Province (Burke's 'Tuzo') above the Core Mantle Boundary already existed although it has been significantly modified since. The stationarity of Pangea within a single hemisphere surrounded by subduction zones led to thermal isolation of the underlying asthenosphere and consequent heating as well as a large accumulation of hot plume material. The change in sea level from a high stand before 380Ma to a low stand between 260 and 180Ma may be understood as resulting from the change from well mixed mantle to isolated mantle below each hemisphere that would be expected in such a geodynamic situation.

## **7b) Sediment generation and quantitative provenance analysis**

**Wednesday, 25/Sep/2019: 1:00pm - 3:00pm**

**Session Chair: Guido Meinhold** (Keele University)

**Location: H3**

### **Lecture Presentations**

**1:00pm - 1:30pm** *Session Keynote*

## **Relative importance of palaeogeography versus solid Earth degassing rate in the Phanerozoic climatic evolution**

**Yves Godderis<sup>1</sup>, Yannick Donnadieu<sup>2</sup>, Pierre Maffre<sup>1</sup>**

<sup>1</sup>*Geosciences Environnement Toulouse;* <sup>2</sup>*CEREGE*

Over the last 800 million years of the Earth history, the atmospheric CO<sub>2</sub> content has widely fluctuated, resulting in ample climatic changes. Potential causes of those CO<sub>2</sub> changes are well-known. CO<sub>2</sub> is released into the ocean-atmosphere system by the volcanic activity, by the oxidation of fossil organic carbon exposed at the continental surface, and by the dissolution of continental carbonate minerals under the corrosive action of sulphuric acid (itself generated by the oxidation of pyrite in tectonically active area). Atmospheric CO<sub>2</sub> is consumed by the chemical weathering of silicate rock, and by the burial of organic carbon into sediments.

The efficiency of those processes is dependent on their spatial distribution at the Earth surface. CO<sub>2</sub> can be released by magmatic activity directly into the atmosphere or into the ocean. Oxidation of fossil organic carbon and release of sulphuric acids occur in tectonically active mountain ranges. Silicate weathering is a function of the spatial distribution of the continents, of the lithology, of the vegetation, of the physical erosion. Organic carbon burial depends on the sedimentation rate driven by physical erosion.

Accounting for the role of the spatial distribution of carbon fluxes on the long term climate evolution is a main challenge. New numerical models, which couples 3D-climatic models to model describing the biogeochemical cycles open the door to the integration of the spatial factor into our description of what drives the long term climate of our planet.

In the first part of the talk, we will focus on the modulation of continental silicate weathering by continental drift. Up to know, the boosting of silicate weathering by the dislocation of the Rodinia supercontinent within the warm and humid tropical belt remains the sole explanation for the onset of the snowball glaciations in the Neoproterozoic. Conversely, the assembly of Pangea promoted the development of continental scale aridity, leading to the collapse of the CO<sub>2</sub> consumption by silicate weathering, and dramatically warming the Earth surface.

The second part of the talk will be devoted to an exploration of the role of large mountain ranges on the climatic long term evolution. We will show that the incorporation of a mechanistic description of physical erosion in deep time climate-carbon model open the door to the quantification of the role of silicate weathering versus organic carbon in modulating the Earth climate.

**1:30pm - 1:45pm**

### **Meanders Displacement Due to Implementation of Organizing Plans in the Bahokalat River, South East of Iran**

**Kazem Shabanigoraji, Jafar Rahnamarad**

*Azad university of Iran, Iran, Islamic Republic of*

Bahuklat River is one of the most important rivers in Sistan and Balouchestan province, which passes through the Bahuklat area into the Oman Sea. In order to evaluate the displacement of the meanders and the effect of river regeneration plans on its morphology from the Shirgoaz dam to the Oman Sea, geometric characteristics of the meanders and the textural properties of the river channel sediments have been studied. The effect of human interference on river morphology during field surveys based on aerial photos (1957) and satellite imagery (2003-2015) has been investigated. The river sediments are remarkably fine grained, with poorly sorted and positive skewness. The average curvature coefficient of the Bauchalkat River in the studied area is 1.38, indicating a twisting and roughness of the river route. The highest frequency of the central angle of the meander arc is in the range of 85 to 158 degrees, which is related to the pattern of the developed meander. The curvature radius of the arches studied in the Bahukalat River varies from 100 to 810 meters. Between the radius of curvature and Meander Valley length, the experimental relation ( $R_c = 17.4L_v^{0.73}$ ) is established. The  $R_c/\lambda$  curve versus curvature coefficient in the Bauchalkat river shows that the  $R_c/\lambda$  value is minimized in a 1/3 curvature. The existing facilities along the Baqulakat River route and the margin of the river include Baqulakat diversion dam, Jor village levees, Rimdan bridge, Bahtokalat fountain, flood strap walls, levees and cultivation in the riverside, which during the change in the channel duct and the velocity of the flow of water leads Changes in the morphology of the Bauchalkat channel have been made. In order to protect the agricultural land, the villagers have built up levees in the riverside area. During flood events, due to the erodability of the soils of the area, flood deviations sometimes occur and cause damage. Following this, the morphology of the river has also been changed so that the displacement of the Meander rings occurs, and sometimes crevasse splays are formed after the broken up of the embankments. It seems that the presence of suitable vegetation and shrubs on the overbank of the Bauchalkat River has increased the marginal resistance of the river to erosion, so that the lateral erosion, followed by the migration and lateral displacement of the Meander rings, has decreased.

**1:45pm - 2:00pm****Provenance analysis of carbonate and radiolarite pebbles of Jurassic sedimentary mélanges in the Circum Pannonian orogens (Western Tethys)****Hans-Jürgen Gawlick, Sigrid Missoni***Montanuniversität Leoben, Austria*

Component analyses of ancient Neo-Tethys mélanges along the Eastern Mediterranean mountain ranges allow both, a facies reconstruction of the Middle Triassic to Middle Jurassic outer passive margin of the Neo-Tethys and conclusions on the processes and timing of the Jurassic orogenesis. This Middle-Late Jurassic mountain building process in the Western Tethyan realm was triggered by west- to northwestward-directed ophiolite obduction onto the former passive continental margin of the Neo-Tethys.

Ophiolite obduction onto the former passive continental margin started in the Bajocian and trench-like deep-water basins formed in sequence within the northwest-/westward propagating nappe fronts in the footwall of the obducting ophiolites. Deposition in these basins was characterized by coarsening-upward cycles, i.e. forming sedimentary mélanges as synorogenic sediments, in cases tectonically overprinted. In the Middle Jurassic, the oceanic realm and the most distal parts of the former passive margin were incorporated into the nappe stacking. Bajocian-Callovian ophiolitic and Meliata mélanges were formed as most oceanward preserved relics of trench-like basins in front of the propagating ophiolitic nappe stack, often with incorporated components from the continental slope. In the course of ongoing ophiolite obduction, thrusting progressed to the outer shelf region (Hallstatt Limestone facies zone). In Bathonian/Callovian to Early Oxfordian times the Hallstatt nappes with the Hallstatt mélanges were established, expressed by the formation of the up to 900 m thick basin fills comprising its material mainly from the outer shelf region. In Callovian to Middle Oxfordian times the nappe stack reached the former carbonate platform influenced outer shelf region. Newly formed basins received material from this shelf region, occasionally mixed with material from the approaching ophiolite nappes. Ongoing shortening led to the formation of the proximal Hallstatt nappes with concomitant mobilisation of Hallstatt Mélanges. Persistent tectonic convergence caused the partial detachment and northwest- to west-directed transport of the older basin groups and nappes originally formed in a more oceanward position onto the foreland.

Comparison of mélanges identical in age and component spectrum in different mountain belts (Eastern Alps/Western Carpathians/Dinarides/Albanides/Pelso) figured out one Neo-Tethys Ocean in the Western Tethyan realm, instead of multi-ocean and multi-continent scenarios. The evolution of several independent Triassic-Jurassic oceans is unlikely considering the fact that re-sedimentation into newly formed trench-like basins in front of a west- to northwestward propagating nappe stack including ophiolite obduction is nearly contemporaneous along the Neotethyan Belt. The Middle to Late Jurassic basin evolutions with their sedimentary cycles and component spectra are comparable everywhere.

**2:00pm - 2:15pm****Provenance of central Arctic Ocean ice-rafted debris: the first U-Pb zircon ages for Lomonosov Ridge during the late Quaternary****Maximilian Dröllner<sup>1,2</sup>, Rüdiger Stein<sup>2</sup>, Heinrich Bahlburg<sup>1</sup>, Jasper Berndt<sup>3</sup>, PS115/2 Science Party<sup>2</sup>**

<sup>1</sup>*Institut für Geologie und Paläontologie, Universität Münster, Corrensstraße 24, 48149 Münster, Germany;* <sup>2</sup>*Alfred Wegener Institute, Helmholtz Centre for Polar and Marine Research, Am Handelshafen 12, 27570 Bremerhaven, Germany;* <sup>3</sup>*Institut für Mineralogie, Universität Münster, Corrensstraße 24, 48149 Münster, Germany*

Accurate reconstruction of sea ice history in the Arctic Ocean is crucial to decipher variations in a system known for its sensitivity to climate change. Analysis of purely terrigenous ice-rafted debris allows for relating detritus in marine sediments to specific source areas in the Circum-Arctic region. Key areas to be distinguished are Canadian Arctic Archipelago, Mackenzie river, East-Siberian Sea, Laptev Sea, Kara Sea, and Barents Sea. Identification of the source area(s) can be used to rate input of the Beaufort Gyre and/or the Transpolar Drift as these currents sample source areas of ice-rafted debris to a different extent. We present first U-Pb ages

on detrital zircons from late Quaternary strata in the Arctic Ocean. Marine sediment core PS115/2\_14-3, obtained in Expedition PS115/2 in 2018, is located on the Lomonosov Ridge in the central Arctic Ocean. We reconstruct ice-rafted debris trajectories during the late Quaternary, as references we choose modern river compositions. This dataset yields  $n > 1100$  zircon ages for sediments representing glacial-interglacial cycles. Zircon ages range from the late Mesozoic to the Mesoarchean. Major age peaks are 230-300 Ma, 1.8-2 Ga, and 2.6-2.8 Ga. These peaks contain approximately 55 % of the combined zircon population. A gap of ages between  $\sim 1$  to 1.5 Ga is present. Kernel density estimates and Multidimensional scaling analysis show only small intersample variations. However, signatures can be correlated to specific source areas. Preliminary results indicate a predominantly Eurasian provenance (i.e. Barents Sea, Kara Sea, Laptev Sea, and East-Siberian Sea with varying contributions). This study highlights the benefits of U-Pb detrital zircon geochronology in ice-rafted debris provenance analysis for realistic sea ice transport reconstructions.

**2:15pm - 2:30pm**

### **Provenance, facies, geochronology and tectonic evolution of continental extensional basins: a case study of the Permian-Triassic Mitu Group (Central Andes, Peru)**

**Fernando Panca<sup>1</sup>, Heinrich Bahlburg<sup>1</sup>, Jasper Berndt<sup>1</sup>, Axel Gerdes<sup>2</sup>**

<sup>1</sup>Universität Münster, Germany; <sup>2</sup>Goethe-Universität Frankfurt, Germany

The Permian-Triassic transition from the Late Paleozoic arc regime of southwestern margin of Gondwana to the Andean accretionary orogen initiated in the Early Jurassic is marked in the Central Andes by the development of extensional basins, presumably formed in back-arc or rift-related settings.

In the Peruvian Andes, the basin fills consist of stratigraphically poorly controlled red beds and volcanosedimentary successions commonly known as the Mitu Group and equivalents. The Mitu succession is characterized by bi-modal alkaline to calc-alkaline lavas, ignimbrites and tuffs that are interbedded with thick continental successions deposited in fluvial, floodplain and alluvial environments.

We present results of our analysis of the facies evolution and provenance of twelve Permian-Triassic stratigraphic sections along the Eastern Cordillera of Peru encompassing  $\sim 1200$  km of the Mitu basin. Our study aims at constraining the sedimentology, chronology, spatial development and tectonic setting of evolving depocenters by single-grain studies of heavy minerals, LA-ICP-MS dating and Lu-Hf isotope analysis of detrital zircons.

Previous studies indicate that the Upper Permian part of the Mitu Group overlies the limestones and subordinate sandstones of the Lower Permian Copacabana Group above a hiatus, and that the timespan of the extensional tectonics and the depositional evolution of the basin fill is still unclear.

However, our new results using facies analysis and U-Pb dating of detrital zircons indicate the absence of a significant hiatus in the Cusco region, exhibiting a mixed carbonate-siliciclastic transition from marine (Copacabana Group, maximum depositional age of  $262.6 \pm 1.5$  Ma) to continental conditions (Mitu Group, maximum depositional age of  $260.3 \pm 3.7$  Ma) during the Upper Guadalupian. A sandstone at the top of Mitu section in Cusco with a maximum depositional age of  $197.3 \pm 2.7$  Ma indicates that the Mitu sedimentation and extensional tectonics may have persisted until the Early Jurassic. Concordia ages on volcanic zircons from crystal-rich ignimbrites exhibit consistent ages, establishing, at least, four volcanic episodes during the basin filling:  $260.2 \pm 1.9$  Ma (Guadalupian to Lopingian, Upper Permian),  $252.9 \pm 1.3$  Ma (Transition Upper Permian-Lower Triassic),  $236.0 \pm 0.94$  Ma (Carnian, Upper Triassic) and  $223.0 \pm 2.0$  Ma (Norian, Upper Triassic). Upper Permian-Early Jurassic detrital and volcanic zircons extracted from sandstones and ignimbrites, respectively, yield a large  $\epsilon_{\text{Hf}}(t)$  variation between  $+5.54$  and  $-12.00$ , suggesting variable degrees of contamination of mantle-derived magmas with crustal components. The relative abundance of inherited zircons and the distribution of  $\epsilon_{\text{Hf}}(t)$  values indicates that older crustal rocks significantly contributed to the development of magmatism and volcanism in the Mitu basin.

2:30pm - 2:45pm

### The missing link of Rodinia break up in western South America: A zircon U-Pb and Hf isotope study of the volcanosedimentary Chilla beds (Altiplano, Bolivia)

Heinrich Bahlburg<sup>1</sup>, Udo Zimmermann<sup>2</sup>, Jasper Berndt<sup>4</sup>, Axel Gerdes<sup>3</sup>

<sup>1</sup>Institut für Geologie und Paläontologie, WWU Münster, Germany; <sup>2</sup>Department of Petroleum Engineering, University of Stavanger, Norway; <sup>3</sup>Institut für Geowissenschaften, Goethe Universität Frankfurt, Germany; <sup>4</sup>Institut für Mineralogie, WWU Münster, Germany

Quantitative provenance analysis allows for gauging the relative contributions from different source regions to a sediment. This is particularly helpful in the analysis of syn- and postorogenic detritus from collision zones involving markedly different terranes.

The assembly of Rodinia involved the collision of eastern Laurentia with SW Amazonia during Grenville time. The tectonostratigraphic record of the central Andes registers a gap of ca. 300 Myr between 1000 Ma and 700 Ma, i.e. from the base of the Neoproterozoic to the youngest part of the Cryogenian. This gap encompasses the time of final assembly and break-up of the Rodinia supercontinent in this region.

We present new petrographic and whole rock geochemical data, and U-Pb ages combined with Hf isotope data of detrital zircons from the volcanosedimentary Chilla beds exposed on the Altiplano west of La Paz, Bolivia. The presence of basalt to andesite lavas and tuffs of continental tholeiitic affinity provides evidence of a rift setting for the volcanics, and, by implication, the associated sedimentary rocks. U-Pb ages of detrital zircons (n=124) from immature, quartz-intermediate sandstones range between 1750 and 925 Ma. A youngest age cluster (n=3) defines the maximum depositional age of 925±12 Ma. This is considered to coincide with the age of deposition as the Ediacaran and younger ages so typical of Phanerozoic units of this region are absent from the data.

The zircon age distribution shows major maxima between 1300 and 1200 Ma (37% of all ages), the time of the Rondonia-San Ignacio and Sunsás (Grenville) orogenies in SW Amazonia. A provenance mixing model considering the Chilla beds, Paleozoic Andean units and data from eastern Laurentia Grenville sources shows that over 90% of the clastic input was derived from Amazonia. This is also borne out by classical multidimensional scaling analysis (MDS) of the age data.

We also applied MDS to combinations of U-Pb age and Hf isotope data, namely eHf(T) and <sup>176</sup>Hf/<sup>177</sup>Hf values, and demonstrate again a very close affinity of the Chilla beds detritus to Amazonian sources. We conclude that the Chilla beds represent the first and hitherto only evidence of Rodinia break-up in Tonian time in Andean South America.

## Poster Presentations

Tue: 41

### Late Palaeozoic and Early Mesozoic evolution of the Palaeotethys: new insights from sandstone provenance (Karaburun Peninsula and Konya Complex, Turkey)

Kersten Löwen<sup>1</sup>, Guido Meinhold<sup>1,2</sup>, Arzu Arslan<sup>2</sup>, Talip Güngör<sup>3</sup>, Jasper Berndt<sup>4</sup>

<sup>1</sup>Department of Sedimentology and Environmental Geology, Göttingen University, Germany; <sup>2</sup>School of Geography, Geology and the Environment, Keele University, United Kingdom; <sup>3</sup>Department of Geological Engineering, Dokuz Eylül University, Buca-İzmir, Turkey; <sup>4</sup>Institute of Mineralogy, Westfälische Wilhelms-University Münster, Germany

The Eastern Mediterranean region experienced intense geodynamic reorganization during the Palaeozoic and Mesozoic era due to the opening and closure of the Palaeo- and Neotethyan oceans (e.g. Şengör et al., 1984, Geological Society, London, Special Publications). As a result, the geology of Turkey was shaped by the accretion of several oceanic and continental fragments. Different palaeotectonic models and implications for the evolution of the Palaeotethys are strongly debated in the literature. In this regard, the investigation of Upper Palaeozoic and Lower Mesozoic ocean-related sedimentary successions is of special importance. Such

occurrences are sparse in the Eastern Mediterranean since they are either overlain by younger Mesozoic units or primary structures and information are obscured by metamorphism and/or deformation due to Alpine overprint. However, Upper Palaeozoic and Lower Mesozoic Palaeotethys-related successions have been identified at a number of locations from the eastern Aegean region to south-central Turkey. Even though these areas have been the subject of several studies, their role within the Palaeotethyan realm is controversial. We studied Upper Palaeozoic and Lower Mesozoic siliciclastic sedimentary rocks from these areas by a multi-method approach combining, for example, thin-section petrography, bulk-rock geochemistry, and U–Pb geochronology of detrital zircons. Provenance sensitive data of samples from the Upper Palaeozoic Halıcı Formation of the Konya Complex in south-central Turkey indicate sediment supply from mainly low- to medium-grade metamorphosed sedimentary rocks of felsic character. The detrital zircon record documents sediment supply from different sources. Some samples show great similarities with the Palaeozoic sandstones from the cover sequence of the Saharan Metacraton and the Arabian–Nubian Shield, whereas the other samples indicate a provenance that must be sought in units with a southern Eurasian affinity. The upper limit for sediment deposition in the Halıcı Formation is mostly constrained by Early Palaeozoic zircon populations, however, sediment accumulation in Pennsylvanian–Cisuralian time is more likely, contemporaneously with the Upper Palaeozoic succession on the Karaburun Peninsula in western Turkey. Overall, our new provenance data reveal great similarities between the Konya Complex and comparable units from the eastern Aegean region (e.g. Löwen et al., 2017, *International Journal of Earth Sciences*; Löwen et al., 2018, *Sedimentary Geology*) but also highlight distinct differences in terms of sediment composition and provenance (Löwen et al., 2019, *International Geology Review*).

**Tue: 42**

### **Crustal growth history of the Iberian Peninsula constrained by detrital zircon in modern rivers**

**Paula Castillo, Heinrich Bahlburg, Jasper Berndt**

*WWU Münster, Germany*

The Iberian Peninsula is located in the southwest corner of Europe and represents the bridge between the European, African and Atlantic tectonic plates. Five large river systems in the peninsula drain their main geological domains. From north to south: the Douro, Tagus, Guadiana, and Guadalquivir Rivers; and to the east, the Ebro River. All together, these rivers drain approximately 383300 Km<sup>2</sup>, which represent more than 64% of the total area of the Iberian Peninsula. Considering sorting and transport effects, sediments from these rivers reflect the composition of the respective continental crust, and therefore allow for the analysis of its evolution. The analysis rests mainly on detrital minerals that permit the reconstruction of the isotopic and temporal evolution of the crust.

We present U-Pb ages of detrital zircon from medium- to coarse-grained sands collected from the mouths of the five major rivers draining the Iberian Peninsula. Detrital zircons from all samples display a major age group at 370–290 Ma, consistent with sources formed during the Variscan Orogeny, a major zircon-forming event in the Iberian Peninsula. This age group is particularly important in sediments from the Douro, Tagus, and Guadiana Rivers, representing 45%, 52%, and 46% of the total detrital zircons, respectively. Rocks of this age crop out widely in the western part of the Iberian Peninsula, in what is called the Iberian Massif. Detrital zircons of 700–540 Ma age are also an important age cluster, especially in rivers draining the south and southwest of the Iberian Peninsula. Detrital zircons of these ages represent more than 20% of the total in the Tagus, Guadiana, and Guadalquivir Rivers. Sources of 700–540 Ma were formed during the Cadomian Orogeny and are mainly located in the southern part of the Iberian Massif. Youngest detrital zircons are in the range of 250–230 Ma for all rivers, but the Guadiana River, which contains 6 detrital zircons of c. 70 Ma. Oldest detrital zircons are in the range of c. 2700–1800 Ma and are particularly important in the Guadalquivir River, representing about 20% of the total. The sample collected from this river also contains 3 detrital zircons of c. 3000 Ma.

**Tue: 43****OH defects in detrital quartz: a proxy for reconstructing the tectonic environment of sedimentary deposits?****Dominik Jaeger<sup>1,2</sup>, Roland Stalder<sup>1</sup>, Michael Strasser<sup>2</sup>**<sup>1</sup>*Institute of Mineralogy and Petrography, University of Innsbruck, Austria;* <sup>2</sup>*Department of Geology, University of Innsbruck, Austria*

OH defects (hydrogen-related point defects) in the quartz crystal lattice have been recognized to be a function of temperature, pressure, and chemical environment during crystallization and/or metamorphic overprint. This information is preserved in detrital quartz grains throughout the sedimentary cycle, allowing for discrimination between different source lithologies. Thus, the OH defect inventory of quartz is a novel and highly promising tool for provenance analysis.

Generally, young magmatic sources tend to produce more defect-rich grains than old metamorphosed ones (likely due to annealing of defects during thermal overprint and/or deformation), as observed in Proterozoic versus Phanerozoic basement throughout northern and central Europe. Further, heavily deformed and rapidly uplifted regions were found to produce grains of very low defect content. The distribution of OH defect concentrations within a given sample appears to be largely controlled by the diversity of the source rocks themselves. This means that sediments from geologically diverse areas are expected to produce a broader distribution of defect contents than those that are geologically monotonous.

We hypothesize that the range and frequency distributions of OH defects in detrital quartz grains can, on a continental scale, be used to infer the tectonic environment of their formation (e.g., passive vs. active margin provenance). This is based on the consideration that passive continental margins tend to have extensive watersheds, integrating source lithologies ranging from ancient cratonic material to young orogenic sediments. In contrast, active margins tend to have more segmented watersheds (due to more prominent topography) and, in the case of subduction zones, young igneous rocks are common. Therefore, passive margin deposits should be generally more diverse in their OH defect concentrations, whereas active margins are expected to produce a narrower range of values with a higher proportion of defect-rich grains if quartz bearing igneous rocks are present.

This concept is currently being tested on samples from rivers and marine drill cores collected at representative continental margins worldwide. The study areas include the Nankai Trough (subduction zone), Bengal Fan (active orogen), Amazon Fan and samples from/offshore Namibia (both passive margins). Here, we present and discuss the conceptual approach and evaluate first results of this study.

**Tue: 44****Preliminary study on stratigraphy, facies analysis and petrography of Neoproterozoic meta-sediments, magmatic bodies and volcanoclastic deposits in Skoura inlier (Central High Atlas, Morocco).****Amar Karaoui<sup>1</sup>, Abdelkader Mahmoudi<sup>1</sup>, Brahim Karaoui<sup>2</sup>, Zakarya Yajoui<sup>1</sup>, Christoph Breitzkreuz<sup>3</sup>**<sup>1</sup>*Faculty of Sciences, Moulay Ismail University, Meknes, Morocco;* <sup>2</sup>*Faculty of Sciences and Techniques, Moulay Ismail University, Errachidia, Morocco;* <sup>3</sup>*Technische Universität Bergakademie Freiberg, Germany*

The Precambrian rocks of Skoura inlier outcrop on the southern flank of the Central High-Atlas of Morocco that lies between the Anti-Atlas belt and the Meseta domain. By its pivotal position, our investigations allow to highlight the geodynamic evolution of the Anti-Atlas-Skoura-Meseta domain during the Ediacaran period at the NW Gondwana margin and their relation to the other peri-Gondwana terrains.

The Skoura inlier exposes meta-sedimentary rocks attributed to the Lower Ediacaran. The sediments comprise mainly turbiditic sequences, up to 5 km thick, constituted of meta-pelites alternating with sandstones, greywackes, siltstones and subordinate conglomeratic layers. Different sedimentary structures (flute cast, ripple mark, rip up) are observed, indicating turbiditic current mechanism and point to shallowing of the ba-

sin from the west to the east of the study area. They were deformed under lower green-schist metamorphic conditions and are intruded by magmatic bodies consisting mainly of ultramafic to intermediate compositions and also by felsic bodies. This sequence is unconformably overlain by an Upper Ediacaran succession, up to 400 m thick, of lava and volcanoclastic rocks (pyroclastic flow- and fall deposits) with interbedded fluvial sediments. These deposits are grouped into four associations of different environments of deposition (pyroclastic deposits; coherent lava body; alluvial fan facies; fluvial facies).

Our preliminary investigations in the Precambrian rocks of the Skoura inlier show several similarities with neighbouring Anti-Atlas Mountains. The meta-sedimentary sequences display very similar facies characteristics and can be comparable with the Saghro Group dated to the Lower Ediacaran, described in the Siroua, Saghro and Ougnat inliers. However, the volcano-sedimentary formations are comparable with the described upper Ediacaran Ouarzazate Supergroup. These imply probably that the evolution of the Precambrian rocks in the Skoura inlier has undergone a similar geodynamic evolution as the Anti-Atlas belt.

**Tue: 45**

### **Mineralogy, geochemistry and U-Pb zircon ages of diverse Tonian orthogneisses of the Pearya Terrane, northern Ellesmere Island, Canada**

**Nikola Koglin<sup>1</sup>, Vanessa Schmelz<sup>2</sup>, Solveig Estrada<sup>1</sup>, Karsten Piepjohn<sup>1</sup>, Ulf Linnemann<sup>3</sup>**

<sup>1</sup>Bundesanstalt für Geowissenschaften und Rohstoffe (BGR), Hannover, Germany; <sup>2</sup>Lehrstuhl für Geodynamik und Geomaterialforschung, Universität Würzburg, Germany; <sup>3</sup>Senckenberg Naturhistorische Sammlungen Dresden, Germany

The exotic composite terrane Pearya (northern Ellesmere Island, Canadian Arctic) consists of five tectono-stratigraphic successions with ages from Neoproterozoic to Silurian. Orthogneisses of the Neoproterozoic Succession I show a huge mineralogical and textural diversity. Such rocks were already analysed by several authors (Trettin et al., 1992, 1987; Malone et al., 2017; Estrada et al., 2018) for their geochemical and isotopic composition and U-Pb ages. During the BGR-expedition “CASE 19” in 2017, 29 orthogneisses from the area around Yelverton Inlet were collected and analysed for their trace element content and seven of them were dated using the U-Pb isotopic system to find possible correlations between macroscopic diversity, with geochemistry and/or age. Additionally, data from the afore mentioned previous studies were used for comparison.

The gneisses can be grouped by their biotite content, grain size and texture. Gneisses with high biotite content are enriched in Ti, Al, Mg, Ca, Fe, V, Nb, Ta, Zr and Hf and depleted in SiO<sub>2</sub> and K<sub>2</sub>O compared to low-biotite gneisses. The high-biotite and low-biotite gneisses show granodioritic and granitic composition, respectively, and plot in all relevant diagrams for geotectonic settings in the field of active continental margins. Concordia ages of the gneisses range from 958–1004 Ma, This is similar to ages obtained by Trettin et al. (1992, 1987), Malone et al. (2017) and Estrada et al. (2018). Correlations between mineralogy, geochemistry or U-Pb ages are not visible. However, data from previous studies show a spatial correlation of ages. Concordia ages of gneisses in the Deuchars Glacier Belt (DGB) cluster around 1000 Ma and are systematically higher than those of the Mitchell Point Belt (MPB), which show ages between 958 and 980 Ma (Trettin et al., 1992, 1987; Estrada et al., 2018, this study). One gneiss of this study from a new outcrop due to glacier melting at Cape Evans yielded a similar age as for the DGB. Additionally, all ~1000 Ma gneisses (DGB and Cape Evans) have in common to show a lack of foliation (Estrada et al., 2018; this study). Further investigations, e.g. Hf isotopes on zircon, could help to understand the possible geodynamic connection of Cape Evans and the DGB.

[1] Estrada et al. 2018. *J Geodyn.* 120, 45–76; [2] Malone et al. 2017. *Precambrian Res.* 292, 323–349.

Trettin et al. 1987. *Can J Earth Sci.* 24, 246–256; [3] Trettin et al. 1992. In: *Radiogenic Age and Isotopic Studies: Report 6.* Geol. Survey Canada, 3–30.

Tue: 46

## Genesis and petrography of the “Mammendorfer Sandstone”

**Lisa Laslo**

*Martin-Luther-University Halle-Wittenberg, Germany*

In the quarry of the Cronenberger Steinindustrie Franz Triches GmbH & Co KG in Mammendorf (Saxony-Anhalt) the sediments of the Oberrotliegend II were investigated. These sediments had a thickness of about 14 m and could be mainly addressed as reddish and brown colored conglomerates, sandstones and siltstones. There were seven laterally offset and detailed sub-profiles recorded which were summarized in an entire profile. As a result, the individual types of lithofacies could be determined and the sedimentary cycles were clarified. Thus, representative rock samples were taken from suitable layers, which were sawn, ground and further processed into thin-sections. Subsequent investigations of the thin-sections revealed interesting and sometimes unexpected results with regard to the composition of the rocks and their delivery areas. In order, to obtain a qualitative and quantitative insight, a grain count was performed on all thin-sections.

During the field surveys a lot of information was collected, allowing conclusions to be drawn regarding the educational area and the depositional environment. There could be three major cycles distinguished, which, due to the sedimentary facies, speaks for a deposition during or as a result of heavy precipitation events. This suggests that the sediments were deposited in the facies of an alluvial floodplain, which, however, was ephemeral superimposed by a fluvial and lacustrine facies.

Furthermore it was determined that the grain composition in the sampled layers remained almost identical and only the percentage parts changed. From this it can be concluded that the delivery areas did not change during the sedimentation and the already deposited sediments were not overlaid by any sediment beds with a different grain composition.

Tue: 47

## The ‘life cycle’ of coesite-bearing garnet: From inclusion entrapment over exhumation, surface weathering, erosion and sedimentary transport, to its deposition

**Jan Schönig<sup>1</sup>, Hilmar von Eynatten<sup>1</sup>, Guido Meinhold<sup>1,2</sup>, Keno Lünsdorf<sup>1</sup>**

<sup>1</sup>*Geoscience Center Göttingen, Georg-August-University Göttingen, Germany;* <sup>2</sup>*School of Geography, Geology and the Environment, Keele University, Keele, Staffordshire, ST5 5BG, UK*

Schönig et al. (2018, Scientific Reports) introduced an approach of capturing the distribution and characteristics of ultrahigh-pressure (UHP) metamorphic rocks by identifying coesite inclusions in detrital garnet using Raman spectroscopy. This approach was first successfully applied in the Western Gneiss Region of Norway and proof of concept has been demonstrated by application to the Saxonian Erzgebirge of Germany (Schönig et al., accepted, Geology). Although this approach seems very efficient, it is still time consuming and analytical time may be saved by focusing on a specific grain-size fraction. In general, high-grade metamorphic garnets are often enriched in the coarse sand fraction compared to fine sands due to grain-size inheritance from source to sink (Krippner et al., 2015, Sedimentary Geology). Contra-intuitively, Schönig et al. (2018, Scientific Reports) observed an opposite trend for the Norwegian coesite-bearing garnets.

Here we extend the UHP mineral inclusion data of Schönig et al. (accepted, Geology) from the 125–250 µm garnet fraction of the Erzgebirge by analyzing the 63–125 and 250–500 µm fractions. Although data collection is not complete yet, preliminary results indicate that eclogitic garnets are more frequent in the coarse fraction, while coesite-bearing garnets do not always follow the same trend and are sometimes enriched in the finest fraction, in particular if transport distances are longer. Coesite inclusions show a trend regarding size with inclusions <12 µm being always monomineralic and intact, whereas inclusions >20 µm are always bimineralic (coesite + quartz), having fractures which originate from the inclusion/host boundary and spread out into the host, and these fractures often form the detrital garnet surface. 12–20 µm sized inclusions are occasionally monomineralic but mainly bimineralic with a tiny quartz rim and fractures which do not reach the garnet surface.

Based on these preliminary observations, we propose that usually different sized coesite inclusions are entrapped at *UHP* conditions. During exhumation the inclusion pressure in all coesite inclusions uniformly increases but large inclusions fracture the garnet host earlier (at higher temperature) and transform more coesite to quartz than medium-sized inclusions due to their higher initial fracture length facilitating fracture propagation, while small inclusions <12  $\mu\text{m}$  seem to stay intact. Upon exposure to surface weathering, erosion and sedimentary transport, the usually large coesite-bearing garnets will progressively disintegrate along fractures originating from the large bimineralic inclusions leading to fine sand garnet fragments containing small monomineralic coesite inclusions, whereas bimineralic inclusions are rarely preserved in the detritus.

**Tue: 48**

### **Paleozoic accretionary orogens along the Western Gondwana margin**

**Sebastián Oriolo<sup>1</sup>, Bernhard Schulz<sup>2</sup>, Siegfried Siegesmund<sup>3</sup>**

<sup>1</sup>CONICET-Universidad de Buenos Aires. Instituto de Geociencias Básicas, Aplicadas y Ambientales de Buenos Aires (IGEBA); <sup>2</sup>TU Bergakademie Freiberg/Sachsen, Germany; <sup>3</sup>Geoscience Centre, Georg-August-Universität Göttingen

Accretionary orogens have been largely recognized along the Western Gondwana (i.e., Africa and South America) margin during the entire Paleozoic. In the case of southwestern Gondwana, Paleozoic subduction along the proto-Pacific margin gave rise to the Terra Australis Orogen, which is well-recorded in southwestern South America and southernmost Africa [1, 2]. On the other hand, subduction and oceanic basin opening controlled the northwestern Gondwana margin dynamics, as evidenced in northern Africa and Avalonian-Cadomian terranes of Europe [3]. However, no clear relationships between northwestern and southwestern Gondwanan regions were so far established.

In both regions, the onset of subduction and subsequent continental arc development is recorded by the late Ediacaran-Cambrian. In South America, the Early Cambrian Pampean Orogeny was succeeded by Late Cambrian-Ordovician continental arc magmatism and back-arc extension. Similarly, contemporaneous subduction with associated back-arc extension is recorded along northwestern Gondwana, triggered by the northward drift of Avalonian-Cadomian terranes and the consequent opening of the Rheic ocean. In this sense, Late Cambrian-Ordovician retreating orogens characterized both northwestern and southwestern Gondwanan margins.

In contrast to the Early Paleozoic, the Late Paleozoic evolution of Gondwana is intimately related to advancing orogens, which culminated with the final assembly of Pangea. In South America, the Gondwanide Orogeny is ubiquitously recorded in the Andean basement, Patagonia and Sierras Australes, and can be tracked further east in the Cape Fold and Thrust Belt of South Africa. The onset of Gondwanide tectonometamorphic processes, which were essentially related to subduction, is recorded in the Late Carboniferous [4]. In a similar way, Avalonian-Cadomian basement inliers of Europe and northern Africa record the Carboniferous-Permian Variscan Orogeny, associated with subduction and subsequent continental collision [5].

Though still unclear, the coeval development of Paleozoic advancing and retreating orogens along the Western Gondwana margin suggests a common evolution, possibly related to secular variations in global tectonic processes. In the case of the Late Paleozoic evolution, the massive development of advancing external orogens might be linked with the supercontinent cycle, particularly with introversion processes during the assembly of Pangea.

[1] Cawood, P.A. 2005. *Earth-Science Reviews* 69, 249-279; [2] Siegesmund, S., et al. 2018. *Geology of Southwest Gondwana*. Springer; [3] Nance, R.D., et al. 2010. *Gondwana Research* 17, 194-222

[4] Oriolo, S., et al. 2019. *Tectonics*, (in review); [5] Stampfli, G.M., et al. 2013. *Tectonophysics* 593, 1-19.

Tue: 49

## High-n sample comparison of detrital age spectra from pre-orogenic units of the Variscan-Appalachian belt

**Tobias Stephan**

*TU Bergakademie Freiberg, Institut für Geologie, Freiberg, Germany*

The possibility to date detrital heavy minerals and, therefore, to constrain the age of igneous and/or high-grade metamorphic protoliths of sedimentary rocks gains growing significance. The increasing datasets demand statistical and quantitative evaluation tools that allow a fast comparison of data. However, the objective extraction of provenance information requires thoughtful selection of parts of the dataset that actually carry provenance information and the omission of parts that are shared by all objects. Here, we present an approach of semi-automatic provenance end-member identification.

The age distributions of sedimentary rocks should not be compared with the one of magmatic rocks because of different preservation. Furthermore, comparison also will fail when age spectra contain grains that do not provide any source information, e.g. discordant grains and ages that reflect the youngest and shared orogenic event exclusively producing juvenile grains. The similarity of the rocks can be determined by using Multi-dimensional Scaling (MDS) that transfers the Kolmogorov-Smirnov distances between the age distributions into Euclidean distances. The shape of the resultant MDS configuration depends on the number of sources and sedimentary mixing and recycling process during the source-to-sink transport. A simple two-source scenario results in an elongate MDS configuration with the provenance end-members at the ends of the configuration. Because the distance between the end-members is proportional to the mixing between the sources, MDS provides a semi-quantitative measure for the fraction of sedimentary source mixing. In a multi-source scenario, provenance end-members can be objectively identified by unsupervised density-based clustering algorithms.

The approach is exemplified for the Variscan-Appalachian belt, which provides a wide range of tectonic fragments of potentially contrasting provenance that have been juxtaposed during the Late Paleozoic orogeny. We compiled ca. 70000 detrital zircon U–Pb ages from 780 Precambrian to Lower Paleozoic sedimentary rocks of the orogenic belt. Our results reveal four provenance end-members contributing to the sedimentary rocks in the Gondwana-Laurussia plate boundary zone, that provide crucial paleogeographic constraints.

Tue: 50

## Trace element inventory of detrital garnet: a case study from the Central Alps

**Laura Stutenbecker<sup>1</sup>, Peter M.E. Tollan<sup>2</sup>**

*<sup>1</sup>TU Darmstadt, Germany; <sup>2</sup>University of Bern, Switzerland*

Garnet is a popular provenance tracer of orogenic sediments, due to its common occurrence as a detrital phase, and significant major element compositional diversity that reflects variations in the bulk chemistry and equilibration conditions of the source rock. If the source rocks are similar in nature, however, then the major element concentrations of garnet may not differ enough to distinguish detrital contributions from different geological units. Trace elements in garnet, on the other hand, are far more sensitive to small changes in equilibration conditions of both magmatic and metamorphic rocks, and hence offer greater potential for provenance tracing.

This contribution develops the use of major and trace elements in detrital garnet as a provenance proxy in the Central Alps and its adjacent northern foreland basin, the Swiss Molasse basin. A compilation of published and own garnet compositions from the Alps ( $n \approx 1600$ ) shows that, except for a few exceptions, most alpine garnets are almandine-rich with variable contents of grossular, pyrope and spessartine. Based on this major element data, four partially overlapping clusters of source rocks can be identified: Eclogite-facies garnets with high pyrope and grossular contents, granulite-facies garnets with high pyrope contents, greenschist-facies garnets with high grossular and spessartine contents and finally amphibolite-facies garnets with

high almandine contents and a wide spread in grossular and spessartine contents. Within the large cluster of amphibolite-facies garnets, major element concentrations do not seem to show systematical variations amongst different type of source rocks (e.g. between meta-sedimentary or meta-igneous amphibolite-facies rocks), which is inconsistent with the significant petrological diversity of this group.

To provide greater resolution on the source rock characteristics, we performed laser ablation ICP-MS analyses on garnets separated from four different amphibolite-facies source rocks from the Central Alps and on detrital garnets from three sedimentary rocks from the Molasse basin. Statistical analysis of the trace element data set focused on the fractionation of high field strength, large ion lithophile, and rare Earth elements. Significantly greater compositional diversity can be identified based on these geochemical discriminators between garnets with otherwise indistinguishable major element characteristics. Our preliminary results show that the combination of major and trace element chemistry can improve the source rock discrimination by up to 40%.

## 7c) Rock and fluid dynamics in deep sedimentary systems

Tuesday, 24/Sep/2019: 3:45pm - 5:30pm

Session Chair: Rüdiger Lutz (BGR)

Location: H3

### Session Abstract

Sedimentary basins contain the vast majority of all energy resources, including coal, petroleum, natural gas and are also the most important storage site for anthropogenic solids and fluids. During basin evolution organic matter-rich sediments and sedimentary rocks are exposed to changing pressure and temperature conditions, which lead to mineralogical and geochemical reactions. Systematic and innovative studies on rock properties, laboratory experiments under well-defined physical and chemical conditions as well as numerical modelling are required to determine rates of transformation, but also fluid flow at different scales.

We invite contributions to this session dealing with sedimentary systems and their constituent elements. We welcome basin modeling studies from crustal to reservoir scale, studies on various aspects of the petroleum system, e.g. source rock deposition, maturation, petroleum generation, expulsion and biodegradation, studies on temperature and heat flow evolution in sedimentary systems based on petrological, mineralogical, and geochemical data as well as studies on porosity and permeability evolution, transport and storage of fluids.

### Lecture Presentations

3:45pm - 4:00pm

#### Geochemical and petrographical analysis of the Mesozoic Birkhead and Murta source rock formations, Eromanga Basin, Central Australia

**Joschka Röth, Ralf Littke**

*RWTH Aachen University, Germany*

Since the 1950's, the Jurassic to Cretaceous Eromanga Basin, in conjunction with the underlying Late Carboniferous to Middle Triassic Cooper Basin, comprise Australia's most significant onshore petroleum province. While most generating source rocks have been identified in the Permian formations of the underlying Cooper Basin, burial depth and thermal maturity levels of the source rock formations from the Eromanga sequence were mainly considered too low. However, more recent studies suggest sweet spots with locally increased organic matter content and elevated thermal maturity which could have contributed to oil accumulations in the Eromanga Basin. In this study we are examining the source rock potential of the Middle Jurassic Birkhead and Early Cretaceous Murta formations to verify this hypothesis.

A set of 55 rock cores from eight petroleum exploration wells (Bookabourdie-5, Jackson-2, Limestone Creek-7, Limestone Creek-8, Moorari-4, Poonarunna-1, Thungo-1, and Winna-1) were sampled in 2018 from the core repositories of South Australia and Queensland state governments.

Geochemical and petrographical analysis of this sample set, such as organic richness (total organic carbon (TOC)), hydrocarbon potential (Rock-Eval S1 and S2), sulfur content, maceral composition, thermal maturity ( $T_{\max}$  vitrinite reflectance ( $VR_r$  %)), and saturated and aromatic biomarker composition (gas chromatography-mass spectrometry) have been conducted to evaluate the respective source rock properties.

Combined preliminary results from the Murta and the Birkhead formations suggest mixed kerogen types II and III from fresh water / lacustrine paleodepositional environments (sulfur content 0.05 - 0.33 %; average = 0.12 %) with low to excellent organic richness (0.50 - 16.83 %; average = 2.74 %). All samples indicate comparably low thermal maturity levels of 0.5 - 0.7  $VR_r$  % (with corresponding  $T_{\max}$  425 - 440 °C) and can be characterized as fair to good oil source rocks which are currently in the transition to the early oil window (or located within). Generally higher S1 values and corresponding higher production indices of the Murta fm suggest either more intense generation by this particular source rock or a certain degree of contamination from underlying source rocks.

Together with the outcomes of further geochemical, petrographical and burial history analyses the observed results will serve as inputs to an integrated 3D basin modelling study from which we expect new insights into the tectono-thermal evolution, petroleum generation history (kerogen maturation, hydrocarbon generation), and prediction of migration and accumulation locally within the Eromanga Basin, calibrated against present-day Eromanga oil accumulations.

**4:00pm - 4:15pm**

### **Bound gas in near-surface sediment from the Barents Sea and North East Greenland Shelf**

**Philipp Weniger, Martin Blumenberg, Kai Berglar, Martin Krüger, Rüdiger Lutz**

*Bundesanstalt für Geowissenschaften und Rohstoffe (BGR), Germany*

On the Barents Sea Shelf numerous observations of hydro acoustic anomalies or seafloor depressions were reported in the past decade, which are characteristic for active or past fluid seepage from the seafloor. While the exact origin of gas from seeps is still unknown, most studies propose either an origin from destabilization of methane hydrate or leakage of petroleum reservoirs in the deeper subsurface.

When hydrocarbons migrate to the seafloor by micro- or macroseepage, traces of the seeping gas are bound to the near-surface sediment. If the geochemical and stable isotope signature remains unaltered, analysis of this bound gas can provide information on the genetic gas origin and thus help understand the source of seeping hydrocarbons.

BGR conducted several marine seismic expeditions to the northern Norwegian Barents Sea and the East Greenland Shelf to study the structural evolution of the Arctic North Atlantic. During three of these expeditions near-surface sediments were collected by gravity coring. The geochemical and stable carbon isotope composition of bound gas from these near-surface sediments was analyzed to find evidence of gas seepage and investigate the genetic origin of bound gas.

Bound gas from locations near the Western Barents Sea Margin and the margins of the Olga Basin are characterized by concentrations significantly above background and stable carbon isotope compositions typical for thermogenic gas, suggesting an origin from petroleum systems in the deeper subsurface. Some areas of the Barents Sea with low bound gas concentration show contribution of microbial gas, which may be of autochthonous origin.

Bound gas concentration anomalies were also observed in sediments from the Danmarkshavn Basin and north of the Wandel Sea Basin on the NE Greenland Shelf. While some of these gases show thermogenic geochemical and stable isotope signatures similar to bound gas from the Barents Sea, many bound gases with anomalous high concentration have unusual stable carbon isotope signatures (e.g.  $\delta^{13}C_{CH_4} > \delta^{13}C_{C_2H_6}$ ), which could result from microbial methane oxidation.

These observations reveal different regional geochemical patterns of bound gases, which indicate differences in their genetic origin but also reflect different degrees of microbial alteration.

#### 4:15pm - 4:30pm

### Kinetic modeling of Westphalian coals: Insights from artificial heating experiments on a maturity sequence

**Felix Froidl, Alireza Baniasad, Ralf Littke**

*RWTH Aachen, Germany*

The Ruhr area has been the major coal-mining district in Western Europe. The coal-bearing Pennsylvanian (Westphalian) strata crop out in the south and are situated much deeper further north, where they are source rocks for many gas field such as Groningen (Littke et al., 1995).

The samples represent a broad maturity range (0.55 – 2.86 %VR<sub>l</sub>), but are composed of the same vitrinite-rich primary organo-facies (evaluated based on petrography, elemental analysis and geochemical data).

In this study, two open system pyrolysis devices, i.e. Rock-Eval 6 and Source Rock Analyser (SRA) were used. Reservoir method (200 - 650 °C, non-isothermal heating) and various heating rates from (0.7 – 40 K/min) were applied. Obtained kinetics with Rock-Eval constantly show lower activation energies than kinetics obtained by SRA. This observation is related to different positioning of the thermocouples of both pyrolysis devices and reveal temperature control issues. Therefore, a correction function was developed to shift  $T_{peak}$  of Rock-Eval to the already temperature corrected SRA results.

Different kinetic optimizations were conducted i.e. i) multi run kinetics with variable- and ii) fixed frequency factor as well as iii) single ramp kinetics with a fixed frequency factor of  $2 \times 10^{14} \text{ s}^{-1}$ . The results were tested in simple conceptual 1-D basin models (20 depositional events, each 300 m thick, constant heat flow of  $60 \text{ mW/m}^2$ ) with two different geological heating rates of 3.78 and  $10.99 \text{ °C/Ma}$ .

The sample sets reveal that with increasing maturity of coals, the obtained activation energy distributions shift to higher values, resulting in lower TR for the given model. Furthermore, signal yields (S2-Peaks) decrease,  $T_{max}$  increase and HI drops except for the most immature sample. Single-ramp kinetics reveal kerogen conversion at lower temperatures ( $\sim 10 \text{ °C}$  earlier generation) than multi-run kinetics. Kinetic optimizations only based on best mathematical fit do not provide meaningful natural kerogen conversion. Multi-run kinetics with a meaningful frequency factor of  $2 \times 10^{14} \text{ s}^{-1}$  well reflect the expected kinetic trends of coal conversion. However, high amount of retained, not expelled generated bitumen makes the application of kinetic parameters based on open system kinetics difficult for coals.

#### 4:30pm - 4:45pm

### Thermal effects of magmatism on surrounding sediments and petroleum systems in the northern offshore Taranaki Basin, New Zealand: a numerical basin modelling study

**Anna Kutovaya<sup>1</sup>, Karsten Kroeger<sup>2</sup>, Hannu Seebeck<sup>2</sup>, Stefan Back<sup>3</sup>, Sebastian Grohmann<sup>1</sup>, Ralf Littke<sup>1</sup>**

<sup>1</sup>Institute of Geology and Geochemistry of Petroleum and Coal, RWTH Aachen University, Aachen, Germany; <sup>2</sup>Institute of Geological and Nuclear Sciences, Lower Hutt, New Zealand; <sup>3</sup>Geological Institute, RWTH Aachen University, Aachen, Germany

Petroleum systems modelling is a useful tool for assessment of the burial history providing valuable information about the timing of petroleum generation and migration. Hydrocarbon generation associated with strata rapidly heated by magmatic intrusion has been studied numerically for several regions (Galushkin, 1997; Jones et al., 2007; Senger et al., 2017). In the past two decades numerical forward modelling of petroleum systems has been extensively used in exploration geology. However, modelling of petroleum systems influenced by magmatic activity has not been a common practice, because it is often associated with additional uncertainties and thus is a high risk for exploration. Subsurface processes associated with volcanic activity

extensively influence all the elements of petroleum systems and may have positive and negative effects on hydrocarbon formation and accumulation. We integrated 3D seismic data, geochemical and well data to build detailed 1D and 3D models of the Kora Volcano – a buried Miocene arc volcano in the northern Taranaki Basin, New Zealand (Stagpool and Funnell, 2001) and examined the impact of magmatism on the source rock maturation and burial history in the northern Taranaki Basin. The Kora field contains a sub-commercial oil accumulation in volcanoclastic rocks that has been encountered by a well drilled on the flank of the volcano. By comparing the results of distinct models of magmatic activity we concluded that it had a local effect on the thermal regime in the study area and resulted in rapid maturation of the surrounding organic matter-rich sediments. Distinct scenarios of the magmatic activity age (18, 11 and 8 Ma) show that the re-equilibration of the temperature after intrusion takes longer (up to 5 Ma) in the scenarios with younger emplacement age (8 Ma) due to an added insulation effect of the thicker overburden. Results of the modelling also suggest that most hydrocarbons expelled from the source rock during this magmatic event escaped to the surface due to the absence of a proper seal rock at that time.

**4:45pm - 5:00pm**

### **3D basin and petroleum system modelling in the North Sea Central Graben: a cross-border Dutch, German and Danish pilot study**

**Jashar Arfai<sup>1</sup>, Rüdiger Lutz<sup>1</sup>, Maryke den Dulk<sup>2</sup>, Finn-Christian Jakobsen<sup>3</sup>, Susanne Nelskamp<sup>2</sup>, Stefan Ladage<sup>1</sup>, Peter Britze<sup>3</sup>**

<sup>1</sup>Bundesanstalt für Geowissenschaften und Rohstoffe (BGR), Stilleweg 2, 30655 Hannover; <sup>2</sup>Geological Survey of the Netherlands (TNO), Princetonlaan 6, 3584CB Utrecht, The Netherlands; <sup>3</sup>Geological Survey of Denmark and Greenland (GEUS), Øster Voldgade 10, DK-1350 Copenhagen K, Denmark

In Europe's major petroleum province – the North Sea – a Geological Analysis and Resource Assessment of Hydrocarbon Systems (GARA) is being carried out as part of the overarching GeoERA framework. Here, we report first results of a 3D basin and petroleum system model developed in a cross-border area of the Dutch, Danish and German North Sea Central Graben area. This pilot study reconstructs the cross-border thermal history, maturity and petroleum generation of potential Lower and Upper Jurassic source rock units. This 3D pilot study incorporates new aggregated and combined layers from all three countries.

Eight key horizons covering the offshore realms of the Dutch, German and Danish North Sea are selected for building the stratigraphic and geological framework of the 3D basin and petroleum system model. The latter, includes the North Sea Central Graben region and its surrounding platforms and structural highs, depth and thickness maps of important stratigraphic units as well as the main fault and salt structures. Petrophysical parameters and generalized facies information from well reports are assigned to the different key geological layers. The model is further calibrated with temperature and maturity data from wells and publications. The time span from the Late Permian to the Present is represented by the model including two erosional phases related to large-scale tectonic events during the Late Jurassic and Late Cretaceous. Additionally, salt movement through time expressed as diapirs and pillows is considered within the 3D basin and petroleum system model.

**5:00pm - 5:15pm**

### **Petroleum Systems Modeling in the Northwestern Part of the Persian Gulf, Iranian sector: 3D Basin Modeling**

**Alireza Baniasad, Ralf Littke**

*RWTH Aachen University, Germany*

A 3D conceptual model of the northwestern part of the Persian Gulf is developed based on seismic interpretation tied to several well data to address the burial and thermal history of the basin from the Cretaceous up to present-day and to investigate the location of hydrocarbon generation kitchens and migration pathways.

The study area covers 20000 km<sup>2</sup> of the Iranian sector of the Persian Gulf incorporating the intra-shelf Gotnia Basin in the north and Arabian carbonate platform to the south. The model consists of 24 events including four erosional events / hiatuses and is calibrated applying bottom hole temperature and vitrinite reflectance data in several locations taking into account variable heat flows. Suitable calibration is achieved applying present-day basal heat flow values of 48-63 mW/m<sup>2</sup> increasing from NE to SW of the study area following the general crustal thickness variations across the Arabian-Eurasia Plate boundary. Palaeo heat flows were assumed to be around 50±10 mW/m<sup>2</sup> in the Late Jurassic decayed to the Middle Miocene prior to the Zagros orogeny. The compressional regime between the Eurasia and Arabo-African Plates which led to the Zagros folding and coinciding with increasing in basal heat flows has significantly influenced the burial and thermal evolution of the region. The sedimentation rates in the region reaches to more than 500m/Ma during the main phase of the Zagros orogeny caused by massive influx of eroded materials into the basin. The highest rate of sedimentations were calculated at the location of main depocenters, i.e. the Binak Trough and Northern Depression separated from each other by the Khafji-Norooz Arch. The model results indicate that the organic-rich successions of the Neocomian and Albian have been buried deep enough in these depressions to be rendered thermally mature at present-day. Binak Trough has been the main depocenter area for sediments after the Zagros folding, where most hydrocarbons are derived from. Early oil window maturity has been reached between the late Cretaceous (Neocomian source rock) and early Miocene (Albian source rock). Due to continuous sedimentation and low heating rate, hydrocarbon generation until present-day is plausible. Applying different kinetic models as well as implementing fault systems, the presented conceptual model is intended to study the hydrocarbon migration and accumulation in the study area assisting in better understanding of petroleum systems and developing future exploration strategies.

**5:15pm - 5:30pm**

### **Reservoir quality controls in deeply buried Rotliegend sandstones and their outcrop analogs**

**Alexander Monsees<sup>1</sup>, Benjamin Busch<sup>1</sup>, Nadine Schöner<sup>2</sup>, Christoph Hilgers<sup>1</sup>**

<sup>1</sup>*Department of Structural Geology and Tectonics, Institute of Applied Geosciences, Karlsruhe Institute of Technology (KIT);* <sup>2</sup>*Winterhall Dea Deutschland AG*

As fluid flow primarily occurs in the matrix of siliciclastic sandstone reservoirs, diagenetic processes, such as authigenic mineral precipitation as well as chemical and mechanical compaction have a major impact on the reservoir quality and need to be understood for reservoir quality assessment (Taylor et al., 2010; Busch et al., 2017). Petrographic analyses in concert with porosity and permeability measurements were employed to characterize the reservoir quality of two natural gas wells in northern Germany. Three outcrops of Rotliegend fluvio-eolian sandstones in Bebertal, Cornberg, and the Vale of Eden (Cumbria, UK) were assessed as possible reservoir analogs.

Point-counting and cathodoluminescence analyses were applied to derive the detrital and authigenic compositions. Porosity and permeability measurements on reservoir samples at temperatures up to 140° C and 50 MPa confining pressure were performed to additionally visualize reservoir quality changes at depth.

Cornberg was identified as a feasible analog to the less porous sections (<7 %) of the studied reservoirs in terms of the amount of intense quartz-, kaolinite- and carbonate cementation. The samples from the Vale of Eden represent the most porous reservoir sections (>10%) due to inhibited quartz cementation by continuous illite coatings in some samples (>75% coating coverage). The samples from Bebertal are characterized by intermediate illite coating coverages and resulting intermediate amounts of quartz cementation similar to some reservoir sections.

Results also highlight the significance of illitic clay mineral coatings in regards to their capability to inhibit syntaxial overgrowth cementation as well as their influence on chemical compaction (pressure dissolution, Kristiansen et al., 2011). The larger the grain coating coverage in contact with the intergranular volume (IGV), the fewer quartz cement is present in the samples. Conversely, the more illite is present at grain contacts, the higher the potential for chemical compaction, reducing the IGV. Permeabilities measurements of 0.007-293.9

mD at 1.2 MPa confining pressure are reduced by different orders of magnitude for differently cemented and compacted sandstones. Permeabilities for less cemented samples are reduced by below one order of magnitude, permeabilities for highly cemented samples are reduced by one-two orders of magnitude, permeabilities for less cemented and thus well coated samples but highly compacted sandstones are reduced by up to three orders of magnitude.

These results indicate that reservoir quality of deeply buried sandstones is governed by grain coatings which impact cementation. Such microscale processes are essential for further upscaling of rock properties and flow modeling to reservoir scale.

## Poster Presentations

Tue: 51

### Abiotic oxidation of H<sub>2</sub> by the redox-active minerals hematite and pyrite at dry and wet underground storage conditions (120°C, 100 bar H<sub>2</sub>)

**Theodor Alpermann, Christian Ostertag-Henning**

*Bundesanstalt für Geowissenschaften und Rohstoffe, Germany*

The underground storage of hydrogen is an important option for buffering seasonal electricity production from intermittent renewable energy sources. Suitable storage sites are salt caverns and porous sandstone formations. The assessment of potential storage sites requires sufficient knowledge about the fluid flow and reactive transport properties of H<sub>2</sub> in the subsurface. But up to now there is a lack of data about the properties of H<sub>2</sub> in the deep subsurface, for instance about kinetics of H<sub>2</sub>-consuming processes like microbial consumption or abiotic oxidation reactions. To improve the data basis for future modelling, experimental investigations within the project *H<sub>2</sub>\_React* will provide data on e.g. fluid flow properties, solubility and redox reactions of H<sub>2</sub>. Our contribution focuses on the investigation of abiotic reactions of H<sub>2</sub> with redox-active minerals occurring as accessory minerals in sandstone reservoir rocks or shale cap rocks under dry and wet conditions. We aim to (1) identify the most reactive minerals towards H<sub>2</sub> at in situ-conditions and (2) to determine the kinetic parameters of their reaction with H<sub>2</sub>.

Our experiments were conducted in sealed gold capsules in PARR autoclave vessels at 120°C and 200 bar pressure with 100 bar H<sub>2</sub> partial pressure for up to 14 d. The consumption of H<sub>2</sub> in the experiments was quantified by subsequent analyses by mass spectrometry. An additional headspace-GC analysis provided data on the amount of generated volatile reaction products like H<sub>2</sub>O and H<sub>2</sub>S.

Hematite and pyrite are by far the most reactive minerals at dry reaction conditions. While the conversion of hematite to magnetite was accompanied by an almost complete consumption of the applied amount of H<sub>2</sub>, pyrite appears to react with a limited amount of H<sub>2</sub> in an equilibrium reaction. The amount of generated H<sub>2</sub>S corresponds to the amount of H<sub>2</sub> consumed by pyrite reduction. Furthermore, smectite and goethite oxidized small amounts of H<sub>2</sub> at the dry reaction conditions. Ongoing experiments focus on the kinetic parameter of the hematite and pyrite reduction by H<sub>2</sub> and the reactivity of several redox-active minerals towards H<sub>2</sub> in the wet system. The obtained kinetic data will improve the assessment of potential sites for underground hydrogen storage concerning the impact of abiotic redox reactions as sink for stored H<sub>2</sub> and source for detrimental gases as H<sub>2</sub>S.

Tue: 52

## Carnian outer continental shelf successions in the Western Tethys realm

**Sigrid Missoni, Hans-Jürgen Gawlick**

*Montanuniversität Leoben, Austria*

The deposition of open-marine sediments in the Western Tethys realm started in the Middle Anisian (Late Pelsonian), time equivalent with the opening of the Neo-Tethys. Due to the continental-break-up a horst-and-graben morphology was formed. Shallow-water carbonates, open-marine limestones, radiolarites, bentonite horizons, volcanic resediments, and silicified mudstones to hemipelagic carbonate sequences in upsection position characterize in general the Middle Triassic sedimentation on the outer continental shelf (Hallstatt succession). The paleoenvironmental evolution in the depositional setting was controlled by stratified volcanic activities and a related ocean-acidification. Shallow-water carbonate production on the mid continental shelf lasted from the latest Ladinian onwards. Hinterland influence and thickness of sediment deposition varies with the palaeogeographic position on the shelf.

In the Carnian the studied open-marine succession in Montenegro (Dinarides, Budva unit) consists of grey-red-dish hemipelagic carbonates with stratified accumulations of halobiids. In this temporary very low-energetic environment shed mass transport deposits, whose clasts derived from the former horst complexes. A long lasting sub-marine gap of the entire Julian to Tuvallian 1 is related to a very long lasting emergence of the Wetterstein Carbonate Platform, and no siliciclastic influence from the hinterland as known in more northern areas (Alps, Carpathians). From the Tuvallian 2 onwards the continuing hemipelagic carbonatic sequence is characterized by an increasing energy level in the depositional environment that is reflected in unsorted accumulations of echinoids and halobiids, but also in a gradual oxygenating sediment colour. The shedding of the mass transport deposits lasted until the earliest Tuvallian 3, which corresponds with the time contemporaneous volcanic activity known in the eastern Mediterranean orogen. The clast spectra consist predominantly of recycled Carnian sequences. An order of dissolution and recrystallization reactions in the lithifying breccia caused to a fermentative decomposition of the organic matter, metal sorption onto suspended particles, and to the formation of authigenic minerals. The latest Tuvallian 3 to earliest Lacinian 1 is nicely documented by conodonts and associated macrofossils as *Halobia* sp., *H. beyrichi* (Mojsisovics) and *H. styriaca* (Mojsisovics). From the Late Carnian onwards lasted on the shelf a normal-marine depositional environment with high sedimentation rates of grey hemipelagic carbonates.

This Carnian trend in the open-marine Hallstatt limestone succession can be directly correlated with other high resolution Hallstatt limestone successions, dated by means of conodonts in the e.g. Eastern Alps, Western Carpathians, Dinarides and Turkey. A deposition in an independent deep-water basin (Mirdita-Pindos) is not mirrored in the depositional characteristics or tectonostratigraphic events.

## 7d) The stable isotope toolbox in sedimentary systems: From water-rock-biosphere interactions to (palaeo-) environmental reconstructions

Tuesday, 24/Sep/2019: 09:00 am - 10:00am

Session Chair: Dorothee Hippler (Graz University of Technology)

Session Chair: Michael E. Boettcher (Leibniz Institute for Baltic Sea Research)

Location: H3

### Session Abstract

Light and heavy stable isotope signatures in sediments and ambient waters (e.g. seawater, rivers, lakes, springs) act as highly useful proxies storing crucial information for the reconstruction of (palaeo-) environments on regional and global scales, as well as water-rock-biosphere interactions in a variety of sedimentary systems. The development of isotope signals is thereby related to element sources (e.g. weathering) or to the processes and pathways of mineral formation as part of the biogeochemical element cycles. For a proper application of these proxies, careful calibrations are required from natural and experiment samples and the mechanisms impacting fractionation and thus signal formation must be understood. Biogenic and abiogenic sedimentary archives span the whole time range from the Precambrian until today. Post-depositional alteration (e.g., mineral recrystallization; sulfurization of organic matter; selective mineralization of organic compounds) may further modify primary signals thereby (partly) destroying the original information, but providing new evidence for (e.g.) water-solid interactions during (microbially-catalyzed) diagenetic processes.

The significance of some of these sedimentary archives, as proxy for their ambient fluids and vice versa of these fluids for the reconstruction of water-rock-biosphere interactions shaping the archives, is often obtained from time-resolved records. Whereas mass-dependent effects in the systems of light stable isotopes (e.g. H, C, O, N, S) have received much attention since the pioneering studies in 1947 (although still not fully understood), more recently also metal isotope signatures, non-mass dependent effects and isotope clumping are expanding the stable isotope tool box.

Here we invite contributions involving field, experimental and theoretical studies that contribute to a better understanding of mechanisms responsible for the (trans-) formation of solid and aqueous stable isotope signatures from different marine and terrestrial sedimentary systems.

### Lecture Presentations

9:00am - 9:15am

#### Early microbial impact on carbonate diagenesis in lagoon sediments on Aldabra, Western Indian Ocean

Dario Fussmann<sup>1</sup>, Avril von Hoyningen-Huene<sup>2</sup>, Dominik Schneider<sup>2</sup>, Andreas Reimer<sup>1</sup>, Rolf Daniel<sup>2</sup>, Gernot Arp<sup>1</sup>

<sup>1</sup>Geoscience Centre, Georg-August-University, Germany; <sup>2</sup>Department of Genomic and Applied Microbiology, Georg-August-University, Germany

An expedition to the Aldabra Atoll, conducted in November 2017, at the end of dry season, revealed new insights regarding the sedimentation, pore water chemistry and the microbial impact on early diagenesis of fine grained carbonate sediments. Aldabra, located in the western Indian Ocean, northwest of Madagascar, is an elevated atoll consisting of karstified, Pleistocene reef limestones surrounding an approximately 30 kilometres long and 10 kilometres wide, flat lagoon. Sedimentation strongly varies within the inshore waters, due to tidal currents, organic input and the relief of the submerged limestones. 40 to 70 cm long, soft sediment cores were taken at four different sites:

(i) One at the northern lagoon margin, which was strongly affected by tidal currents and organic input of

seabirds. (ii) One site at the southern lagoon margin, surrounded by mangrove shrubs and (iii) a site in the southwest, where vast flats of carbonate silt and sand were observable. Furthermore, sediment cores were gathered in the south eastern part of Aldabra, a region called Cinq Cases (iv), which comprises a lacustrine, landlocked setting.

The water chemistry at the lagoon margins shows elevated values with respect to alkalinity and nutrients compared to open marine conditions, due to influx from mangrove swamps during low tide. The northern cores show a thin layer of brownish carbonate mud above gastropod shell accumulations and exhibit anoxic conditions throughout the section. Similar redox values are found in cores from the southern site, which contain a homogeneous section of white-grey carbonate mud. In contrast, the sediments in the southwestern lagoon consist of an oxic section of white-grey carbonate silt to sand, whereas Cinq Cases pools deposits show oxic to anoxic, grey carbonate mud.

With respect to pore water chemistry, all cores except the one from the southwestern site, show elevated nutrient and lower pH values. Furthermore, nutrient peaks at the top of anoxic zones are rather distinct in lower permeability levels, which can be provided by microbial mats.

Metagenomic and metatranscriptomic analysis, in combination with pore water analysis, stable isotope measurements, and SEM investigations will be used to test potential alteration effects by the microbial communities on the carbonate components.

**9:15am - 9:30am**

### **Impact of ambient conditions on the Si isotope fractionation in marine pore fluids during early diagenesis**

**Sonja Geilert<sup>1</sup>, Patricia Grasse<sup>1</sup>, Kristin Doering<sup>2</sup>, Klaus Wallmann<sup>1</sup>, Claudia Ehlert<sup>3</sup>, Martin Frank<sup>1</sup>, Florian Scholz<sup>1</sup>, Mark Schmidt<sup>1</sup>, Christian Hensen<sup>1</sup>**

<sup>1</sup>GEOMAR Helmholtz Centre for Ocean Research Kiel, Germany; <sup>2</sup>Department of Oceanography, Dalhousie University, Halifax, Canada; <sup>3</sup>Max Planck Research Group for Marine Isotope Geochemistry, ICBM, University of Oldenburg, Germany

Marine reverse silicate weathering is controlled by biogenic silica (bSiO<sub>2</sub>) dissolution and silicon (Si) re-precipitation as authigenic aluminosilicates, and is thus an important control on the marine Si cycling and the interlinked carbon cycle. However, the exact processes controlling bSiO<sub>2</sub> dissolution and authigenic aluminosilicate precipitation are still poorly constrained. In this study, reverse silicate weathering is investigated applying stable Si isotopes ( $\delta^{30}\text{Si}$ ) in the Guaymas Basin, Gulf of California, which is characterized by high biological productivity, bSiO<sub>2</sub>-rich sediments, and hydrothermal activity. Three fundamentally different environmental settings are investigated including the oxic deep basin, a hydrothermal site, and a site within the Oxygen Minimum Zone (OMZ) on the slope of the Guaymas Basin. The average pore fluid  $\delta^{30}\text{Si}_{\text{pf}}$  signatures differ significantly between the three settings, with  $-0.14 \pm 0.29\%$  (1SD, n=5) in the OMZ,  $+1.20 \pm 0.14\%$  (1SD, n=17) in the deep oxic basin, and  $+1.99 \pm 0.18\%$  (1SD, n=3) close to a hydrothermal vent field. The pore fluid  $\delta^{30}\text{Si}_{\text{pf}}$  signatures are not only influenced by bSiO<sub>2</sub> dissolution, but also by clay dissolution and different degrees of authigenic aluminosilicate precipitation. While authigenic aluminosilicate precipitation dominates within the deep oxic basin and in the vicinity of a hydrothermal vent, dissolution processes dominate in the OMZ. This is most likely due to high mass accumulation rates (MAR) of lithogenic material and interlinked enhanced clay dissolution rates. Additionally, coupling of Si to the Fe redox-cycle, which preferentially transfers the light Si isotope from the water column to the sediment, shifts the OMZ pore fluid  $\delta^{30}\text{Si}_{\text{pf}}$  signatures to lower values. Further, light  $\delta^{30}\text{Si}$  values in pore fluids and bottom waters confirm earlier studies suggesting an isotopically light benthic Si flux in upwelling regions. Ambient environmental conditions, in particular the redox state and lithogenic MARs, significantly influence reverse silicate weathering and thereby the Si isotopic composition of the benthic Si flux and consequently affect the entire marine Si (isotope) cycle.

**9:30am - 10:00am** *Gustav-Steinmann-Medal*

### **Alexander von Humboldt, Paleoaltimetry and Geobiodiversity**

**Page Chamberlain**

*Stanford University, United States of America*

Today, Alexander von Humboldt would be known as an Earth System scientist. He was the first to recognize the deep connections between the Earth's envelopes – the atmosphere, biosphere, hydrosphere, and lithosphere. If armed today with our modern models and instruments one wonders what his ascent of Chimborazo would have revealed.

Indeed, after twenty years of stable isotope paleoaltimetry we now are well versed in the topographic history of the Earth's major Cenozoic mountain belts. We are poised with this information to address key questions on the links and feedbacks between climate and tectonics, and their relationship to geobiodiversity. But, where do we start? In this presentation, I will use our, and others, studies of the Cenozoic North American Cordillera to highlight how paleoaltimetry and geobiodiversity might be integrated. In my view, there are several ways to proceed. First, we need spatially large and temporally deep isotopic data sets. This is not straightforward as the cores of mountain ranges often consist of crystalline rocks with no clear precipitation proxy and the flanks of these ranges have basins have proxies that have often been modified by intense evaporation. Here, I show how recent advances in triple oxygen isotope measurements allow us to use hydrothermally altered granites and chert from closed-basin lake systems to determine the oxygen isotope composition of precipitation, thereby extending our isotope records spatially and temporally. Second, we need models that accurately predict the isotopic composition of precipitation that can be applied to length scales that are relevant to our studies. To this end, we have developed one-dimensional vapor transport models that account for the hydrologic balance of the land surface and atmosphere. These models can be used to interpret isotopic data sets along vapor transport pathways over continents and supplant simple Rayleigh-based approaches. Third, we need to integrate these isotopic studies with paleontological records. This includes analysis of how changes in landscape hypsometry and climate influenced the biodiversity of mammals and the rise of grasslands in continental interiors during the late Cenozoic.

## **7d) The stable isotope toolbox in sedimentary systems: From water-rock-biosphere interactions to (palaeo-) environmental reconstructions**

**Tuesday, 24/Sep/2019: 10:45am - 12:30pm**

**Session Chair: Dorothee Hippler** (Graz University of Technology)

**Session Chair: Michael E. Boettcher** (Leibniz Institute for Baltic Sea Research)

**Location: H3**

**10:45am - 11:00am**

### **Radiogenic and stable Strontium isotopic fingerprints of ecosystem nutrition**

**Ralf Andreas Oeser<sup>1</sup>, Friedhelm von Blanckenburg<sup>1,2</sup>**

<sup>1</sup>GFZ German Research Centre for Geosciences, Germany; <sup>2</sup>Freie Universität Berlin, Institute of Geological Science, Germany

The conversion and transfer of rock-derived elements like calcium (Ca) and strontium (Sr) through regolith to plants can be traced and quantified using radiogenic ( $^{87}\text{Sr}/^{86}\text{Sr}$ ) and stable ( $\delta^{88}\text{Sr}$ ) Sr isotope ratios. Radiogenic strontium isotope ratios are widely used to trace sources in environmental studies from the soil to catchment scale. Although Sr is not a plant-essential nutrient itself,  $^{87}\text{Sr}/^{86}\text{Sr}$  ratio is applied as ecological tracer to detect

the source and uptake depth of the nutrient Ca in different ecosystems. Opposite to the  $^{87}\text{Sr}/^{86}\text{Sr}$  ratio of single minerals and plants which is not being altered during dissolution or plant uptake,  $^{88}\text{Sr}$  and  $^{86}\text{Sr}$  fractionate upon phase transformation and plant uptake. Alike other stable isotope systems, changes in  $\delta^{88}\text{Sr}$  from reactant to product are used to observe and quantify processes in the Critical Zone.

The Chilean Coastal Cordillera with its steep climate and vegetation gradient accommodates a natural laboratory to determine potentially occurring variations in ecosystem-nutrition strategies based on changes in the degree of weathering. In three study sites located in semi-desert, Mediterranean, and temperate climate zones, we determined the radiogenic and stable Sr isotope composition in bulk bedrock, regolith, and plant samples. From regolith samples the bioavailable fraction, that is assumed to be representative for soil water, has been extracted using a sequential extraction method and analyzed in terms of element concentration and Sr isotope composition.

Results indicate that the bioavailable fraction of soil and saprolite amounts up to 40%. Differences in the pattern of the bioavailable fractions' radiogenic Sr isotope composition of regolith samples implicate that at each site, different minerals are being weathered and contribute to the soil waters' Sr isotope ratio. Stable Sr isotope composition of bulk bedrock and regolith vary between 0.25 and 0.3‰, not deviating from bulk silicate Earth's  $\delta^{88}\text{Sr}$  value. However,  $\delta^{88}\text{Sr}$  values of the bioavailable fraction deviate up to 0.6‰ from that of bulk material. A pattern applies to the study sites: the higher the degree of chemical weathering, the higher the absolute difference between bulk regolith and the corresponding bioavailable fraction.

In the semi-arid site, most plant samples'  $^{87}\text{Sr}/^{86}\text{Sr}$  ratio is alike the bioavailable fraction in regolith, testimony for element uptake from soil waters into plants. However, this observation does not hold true for the Mediterranean and humid study site. Stable Sr isotopes do fractionate whilst uptake into plants and upon translocation within plants. However, the magnitude and direction of this fractionation is species dependent.

**11:00am - 11:15am**

### High-precision triple oxygen isotopes of Archean carbonates

**Oliver Jäger<sup>1</sup>, Jakub Surma<sup>1</sup>, Nina Albrecht<sup>2,1</sup>, Christian Marien<sup>3</sup>, Wanli Xiang<sup>1</sup>, Konstantin Kontekakis<sup>1</sup>, Joachim Reitner<sup>1</sup>, Andreas Pack<sup>1</sup>**

<sup>1</sup>Georg-August-Universität Göttingen, Germany; <sup>2</sup>Thermo Fisher Scientific (Bremen) GmbH; <sup>3</sup>University of Cologne, Germany

The isotopic composition of oxygen in chemical sediments systematically increase over Earth's history. Carbonates from the Archean show a systematic shift in  $\delta^{18}\text{O}$  by about 10 to 15‰ towards lower values compared to their Phanerozoic counterparts [1]. Three different scenarios are suggested to explain this observation: (I) hot Archean oceans (II) depletion of  $^{18}\text{O}$  in Archean oceans compared to present day and (III) diagenetic alteration of the primary isotopic signature. Recent advances in high-resolution gas source isotope ratio mass spectrometry provide a new tool that may allow to decipher the origin of this isotopic shift observed in the early rock record. High-precision measurements of  $^{18}\text{O}/^{16}\text{O}$  and  $^{17}\text{O}/^{16}\text{O}$  were performed on oxygen ion fragments ( $^{16}\text{O}^+$ ,  $^{17}\text{O}^+$ ,  $^{18}\text{O}^+$ ) generated in the ion source from  $\text{CO}_2$  gas [2]. Isobaric interferences on  $m/z=17$  ( $^{16}\text{OH}^+$ ) are separated by means of high mass resolution. The  $\text{CO}_2$  was liberated from carbonate samples by orthophosphoric acid digestion and subsequently analyzed on a *Thermo Scientific 253 Ultra* dual-inlet gas source isotope ratio mass spectrometer [3]. This novel approach extends the oxygen isotope space by another dimension and permits to assign the discussed isotopic shift to a certain scenario. Here we present first triple oxygen isotope data for Archean and Phanerozoic carbonates. Taking the temperature dependent variations of the fractionation factor ( $\alpha^{18/16}$ ) and the triple oxygen isotope fractionation exponent ( $\theta$ ) into account, carbonates that deviate from the predicted equilibrium with ambient formation waters can be identified. Minerals that were altered by or formed in meteoric water can be distinguished from minerals that precipitated in equilibrium with ambient sea water. Therefore, triple oxygen isotope analysis of carbonates cannot only be used as a new single-phase paleothermometer but also holds the potential to trace the origin of carbonates.

[1] Shields and Veizer, 2002, *Geochem., Geophys., Geosyst.*, 10.1029/2001GC000266; [2] Getachew et al., 2019, *Rapid Commun. Mass. Spectrom.*, 10.1002/rcm.8478; [3] Eiler et al., 2013, *Int. J. Mass. Spectrom.*, 335, 45-56

**11:15am - 11:30am****Characterization and differentiation of two different marbles as possible reservoir rocks in geothermal systems by stable isotope investigations – An example from Western Anatolia, Turkey****Dorothee Siefert<sup>1,3</sup>, Markus Wolfgramm<sup>2</sup>, Thomas Kölbl<sup>3</sup>, Elisabeth Eiche<sup>1</sup>, Jochen Kolb<sup>1</sup>**<sup>1</sup>Karlsruhe Institute of Technology; <sup>2</sup>Geothermie Neubrandenburg; <sup>3</sup>EnBW Energie Baden-Württemberg AG

The Buyuk Menderes Graben, Western Turkey, has experienced a fast development of geothermal power generation capacity in recent years. With so far 1,347 MW installed power, Turkey aims to achieve 2,000 MW until 2020 (Richter, 2019). The complexity of the structural setting regarding the configuration of tectonic plates and their movement (Reilinger et al., 2006), amongst other factors, are reasons for the development of different rift structures in Western Anatolia. Crustal thinning resulting from the north-south directed extension (Bozkurt and Oberhänsli, 2001) leads to an increased geothermal gradient and thus, promising conditions for geothermal energy.

In the context of a geothermal exploration project in Western Turkey, an approximately 3800 m deep well was drilled. For further exploration and with respect to future drillings in that area, a closer look on possible reservoir rocks is essential. The reservoir rocks consist mainly of marble and marble schist intercalations (Şimşek, 2003). It is aimed to get a better understanding of the local geology by geochemical correlation of the carbonate-bearing cuttings with surface analogue samples from the surrounding.

Cramer (2004) describes a detailed set of petrographic and geochemical methodological approaches to distinguish carbonate rocks, marble in particular, which we followed in our study. Different marble sections at the northern and southern rim of the Buyuk Menderes Graben have been sampled systematically. Surface samples (n=7) and eight cutting samples from different depth intervals were analysed by thin-section microscopy, X-ray fluorescence, ICP-MS and by stable isotope geochemistry.

Two different kinds of marbles are distinguished, based on combined geochemical analyses and stable isotopic signatures ( $\delta^{18}\text{O}$  and  $\delta^{13}\text{C}$ ) of surface analogues and cuttings. Both, cutting and surface samples of the first group show  $\delta^{13}\text{C}_{\text{VPDB}}$  values between + 1.5 ‰ and + 4.2 ‰ and  $\delta^{18}\text{O}_{\text{VPDB}}$  from - 6.9 ‰ to - 12.5 ‰, where the cuttings show generally lower values in that range. The isotope values of the second group show a wider scatter, with  $\delta^{13}\text{C}_{\text{VPDB}}$  values between - 5.5 ‰ and + 1.8 ‰ and  $\delta^{18}\text{O}_{\text{VPDB}}$  from - 23.9 ‰ to - 15 ‰. Based on this, the two groups are correlated to two of the four known geological nappes in the area. While the marble sections are indistinguishable regarding their mineralogical composition as the marbles of both nappes consist of mainly calcite, stable isotope analysis is a powerful tool for stratigraphic correlation in the field and for cuttings or drill cores.

**11:30am - 11:45am****Hydrochemistry and isotope hydrology of thermal springs in the Alps****Theis Winter<sup>1</sup>, Elco Luijendijk<sup>1</sup>, Christoph von Hagke<sup>2</sup>, Grant Ferguson<sup>3</sup>**<sup>1</sup>Georg-August-University Göttingen, Germany; <sup>2</sup>RWTH Aachen University, Germany; <sup>3</sup>University of Saskatchewan, Canada

Thermal springs in orogenic belts are the most visible signs of heat transfer from the crust to the surface and provide a significant amount of heat transport in orogenic belts. However, because of the complex geological structure in mountain belts hydrothermal systems in orogenic belts are not entirely understood. In this study we try to address this problem by collecting and analysing information on hydrochemistry and isotopic data for around 150 springs in the Alps. We calculated (i) the mean elevation of the recharge area of the springs by comparing stable isotopes  $\delta^2\text{H}$  and  $\delta^{18}\text{O}$  of springs to isotopic data in precipitation from the Global Network of Isotopes in Precipitation (GNIP) and (ii) the maximum temperature of spring water by using the silica geothermometer. This information will provide a better understanding of the dynamics of thermal springs and the pathways of fluid flow. We found out that the lowest isotopic values are usually in higher elevations

corresponding to the elevation effect. Existing geographical deviations are caused by rain shadow and different origin of rain masses. The stable isotopes  $\delta^2\text{H}$  and  $\delta^{18}\text{O}$  can help us locate the recharge area of springs and identify mixing between different groundwater types. The silica geothermometer provide information on the maximum temperature of spring water, which is complicated by mixing between deep and shallow groundwater sources.

## Poster Presentations

Mon: 45

### Biological and lithological controls on Mg isotope fractionation in a forested watershed (the Black Forest, Germany)

**Di Cai<sup>1</sup>, David Uhlig<sup>2</sup>, Michael J. Henehan<sup>1</sup>, Daniel A. Frick<sup>1</sup>, Friedhelm von Blanckenburg<sup>1</sup>**

<sup>1</sup>GFZ German Research Centre for Geosciences; Section 3.3 Earth Surface Geochemistry; Telegrafenberg, D-14473 Potsdam, Germany; <sup>2</sup>Institute of Bio- and Geosciences (IBG-3) Agrosphere, Forschungszentrum Jülich, Wilhelm Johnen Str., 52425 Jülich, Germany

We investigated variations in the stable isotope composition of magnesium (Mg) at a long-term experimental field site (Conventwald) from the Black Forest, Germany. From a 20 m drill core through the regolith, we analysed unweathered paragneiss bedrock, saprolite and soil, considering bulk geochemistry and the chemistry of differentiated clay-sized and exchangeable fractions. Additionally, plant tissues and time-series of groundwater, interflow and stream water were analysed. We investigated Mg isotope fractionation at different timescales: the geological timescale (how rock is converted into soil), the ecological timescale (how plants recycle nutritive elements) and the hydrological timescale (how biotic and abiotic processes affect water chemistry).

We observed the  $^{26}\text{Mg}/^{24}\text{Mg}$  ratio in both bulk regolith and the clay-sized fraction ( $\delta^{26}\text{Mg} = +0.01$  to  $+0.13\text{‰}$ ) to be isotopically heavier than bedrock ( $\delta^{26}\text{Mg}_{\text{regolithbedrock}} = 0.19\text{‰}$ ). In situ analyses of bedrock minerals by femtosecond laser ablation revealed that of the two main Mg-containing minerals, chlorite is isotopically 0.2‰ heavier than amphibole. Therefore, we propose that preferential dissolution of amphibole leads to enrichment of Mg with high  $\delta^{26}\text{Mg}$  in regolith. This is supported by mineralogical observations that amphibole is strongly depleted in the regolith.

Within the ecosystem, different plant species and compartments of plants show a larger range of isotopic compositions. Roots of both beech and spruce are isotopically similar at 0.18‰, while their foliage are around 0.35‰ (beech) and 0.74‰ (spruce), indicating fractionation during translocation within plants. Exchangeable Mg of soil, which should be the nutritive source for plants, has  $\delta^{26}\text{Mg}$  of 0.72 to 0.41‰ consistent with preferential uptake of isotopically heavy Mg by plants.

Hydrologically speaking, stream water shows little  $\delta^{26}\text{Mg}$  variability throughout a hydrological year. It has isotopically lighter Mg than bedrock ( $\delta^{26}\text{Mg}_{\text{water}} = 0.58$  to  $0.72\text{‰}$ ) and is isotopically similar to the exchangeable fraction. Since it appears secondary mineral formation plays little role in regulating Mg isotope fractionation, the isotopic composition of stream water is likely controlled by biological processes. We hypothesize that release of light Mg isotopes from leaf litter decomposition, and uptake of heavy Mg isotopes by plants, set the composition of exchangeable Mg, which in turn buffers the composition of Mg in stream water.

Why plants, the exchangeable fraction, and stream water are all isotopically lighter than bedrock, and where the correspondingly heavy Mg isotopes are sequestered, remains enigmatic. Nevertheless, our study demonstrates that Mg isotopes reflect geological and ecological processes in forested watersheds.

Mon: 46

## Reconstruction of multimillennial changes in Eastern Tropical Pacific oxygen-minimum zones

Sümeyya Eroglu<sup>1</sup>, Renato Salvatelli<sup>2</sup>, Florian Scholz<sup>1</sup>, Christopher Siebert<sup>1</sup>, Ralph Schneider<sup>2</sup>, Martin Frank<sup>1</sup>

<sup>1</sup>GEOMAR Helmholtz Centre for Ocean Research Kiel, Wischhofstraße 1-3, 24148 Kiel, Germany; <sup>2</sup>Institute of Geosciences, University of Kiel, Ludewig-Meyn-Straße 10, 24118 Kiel, Germany

The spatial extent and intensity of oxygen minimum zones (OMZ) in the Eastern Tropical North and South Pacific are controlled by ventilation, atmospheric dynamics, and biological productivity. Here, we present data of redox-sensitive trace metals (e.g. molybdenum, vanadium, uranium) of sediments and paleorecords from the Gulf of California OMZ, the center of the Peruvian shelf OMZ and its southern margin. The bottom waters of all these sites are presently anoxic, yet differ in water depth, primary productivity and particle rain in the water column. These different depositional conditions affect the metal influx, e.g. the mode of Mo supply and its isotopic composition (reported as  $\delta^{98}\text{Mo}$ ).

The paleorecords cover almost the complete Holocene (~10,000 years), which was characterized by warm climate but interrupted by large multidecadal to millennial changes in ocean circulation, upwelling intensity and productivity that likely affected the spatial extent and intensity of the OMZs along the Eastern Tropical North and Pacific. By choosing different core locations along the OMZs we aim to interpret differences in elemental behavior of redox sensitive trace metals in terms of dynamic changes in the depositional conditions linked to climatic variations. The record from the Gulf of California shows low metal concentrations and no significant variations over time (Mo: 4-9  $\mu\text{g/g}$ , V: 58-107  $\mu\text{g/g}$ , U: 4-8  $\mu\text{g/g}$ ). The Peruvian records, in contrast, show overall higher concentrations and a larger variability, which are interpreted to reflect changes in the dynamics of the OMZ ("center" Mo: 19-98  $\mu\text{g/g}$ , V: 61-307  $\mu\text{g/g}$ , U: 5-24  $\mu\text{g/g}$ ; "margin" Mo: 3-36  $\mu\text{g/g}$ , V: 98-280  $\mu\text{g/g}$ , U: 2-16  $\mu\text{g/g}$ ). The  $\delta^{98}\text{Mo}$  signatures of the Gulf of California record are relatively uniform at  $+1.76 \pm 0.15 \text{‰}$  (2SD) and close to isotopically heavy seawater. In this given environment, we interpret these results to indicate diffusive Mo supply to the sediment. In contrast, the Peruvian OMZ "center" record shows overall lighter Mo isotope compositions and larger variability at  $+1.46 \pm 0.27 \text{‰}$  (2SD), which indicates supply of isotopically light Mo via particles [1]. These observations allow us to interpret Mo isotope variations in paleorecords regarding changes in the depositional conditions of permanent anoxic settings, e.g. upwelling intensity, ocean ventilation, and Fe cycling at the sediment-water interface along the shelf. We discuss the implications of these variations for the reconstruction of the paleoceanographic conditions at the Eastern Tropical North and South Pacific during the Holocene.

[1] Scholz et al. (2017) GCA 213, 400-417

Mon: 47

## Boron isotopes by femtosecond LA-ICP-MS with application to pH reconstruction in biogenic carbonates

Grit Steinhoefel, Kristina Beck, Albert Benthien, Klaus-Uwe Richter, Gertraud M. Schmidt-Grieb, Jelle Bijma

AWI Bremerhaven, Germany

In this study, we explore the capability of our customized UV femtosecond laser ablation system coupled to a Nu Plasma II MC-ICP-MS to determine B isotope composition by investigating standard materials of various matrices and foraminifera and coral samples. Boron isotope ratios were determined on ion counters using NIST SRM 610 as reference material. Multiple analysis of silicate and carbonate standard materials including NIST SRM 612, the MPI-DING series (komatiite to rhyolite glasses), IAEA-B-8 (clay) and JcP-1 (coral) reveal average  $d^{11}\text{B}$  values, which agree well with published data. The reproducibility is better than 0.8‰ (2 SD). Investigations of the benthic foraminifera species (*C. wuellerstorfi*) from the ODP core 1092 show little inter- and intra-shell variability in  $d^{11}\text{B}$ . Average  $d^{11}\text{B}$  values reveal small variations around 14‰ at the time of cooling of Antarctica ~14 Myr ago, which indicate a change in deep water pH of ca. 0.1 pH units. Furthermore,

we studied recent cold-water corals (*D. dianthus*) from the Comau Fjord (Chile), a field site showing spatial and seasonal variation in seawater pH (7.59 to 7.86).  $\delta^{11}\text{B}$  values ranges between 23.5 and 27.0‰, which is controlled by ambient seawater pH but likely also by nutrient availability and precipitation rates. Our results demonstrate that fs-LA-ICP-MS provides a unique *in situ* technique to determine B isotope ratios at high spatial resolution for pH reconstruction.

**Mon: 48**

### **Sediments of the supposed Ries impact ejecta-dammed “Rezat-Altmühl-Lake” (Miocene, Southern Germany)**

**Lingqi Zeng<sup>1</sup>, Dag Ruge<sup>1</sup>, Günther Berger<sup>2</sup>, Karin Heck<sup>3</sup>, Stefan Hölzl<sup>3</sup>, Andreas Reimer<sup>1</sup>, Dietmar Jung<sup>4</sup>, Gernot Arp<sup>1</sup>**

<sup>1</sup>Geoscience Center, Universität Göttingen, Germany; <sup>2</sup>Sudetenstraße 6, Pleinfeld, Germany; <sup>3</sup>RiesKraterMuseum, Nördlingen, Germany; <sup>4</sup>Geological Survey, Bavarian Environment Agency, Hof/Saale, Germany

Lacustrine and fluvial sediments are sensitive for climatic and other past environmental changes. The sediments of the Miocene Rezat-Altmühl-Formation have been previously considered as deposits of a lake dammed by Ries impact ejecta: a succession from redbrown clay to whitegrey marls and limestones. At first glance, they reflect increasing humid climatic conditions within the Miocene. However, recent biostratigraphic dating suggests a pre-impact age for the Rezat-Altmühl-Formation, thereby questioning the model of an ejecta-dammed lake.

In the investigated Pleinfeld drill core of the Rezat-Altmühl-Formation, the succession is characterized by floodplain fines, with paleosols and intercalated thin fluvial sandstone beds; to the top, the succession changes to carbonate-rich palustrine marls and limestones. No pebbles from the Ries ejecta material have been detected, only local clasts of the Mesozoic Keuper, Schwarzjura, and Braunjura Group, in addition to rare lydites. Likewise, fossils of the formation are dominated by terrestrial gastropods and only rare aquatic organisms (charophytes). Stable carbon and oxygen isotope results also do not favour a lacustrine origin. Samples from the entire drill section have a low, invariant  $\delta^{18}\text{O}$  and a highly variable  $\delta^{13}\text{C}$ , which reflects a short water residence time and a variable degree of pedogenesis, respectively. Carbonate  $^{87}\text{Sr}/^{86}\text{Sr}$  ratios of entire drill section show a nearly unidirectional increasing trend, indicating a change of source of solutes from Triassic Keuper to Jurassic Schwarzjura-Braunjura rocks.

Our results suggest that the Rezat-Altmühl-Formation formed by a meandering, low-gradient river system with a narrow stream bed and dominant floodplains, rather than by the reportedly ejecta-dammed lake. The increasing trend of carbonate content in the succession reflects base-level changes from Upper Triassic Keuper to Lower/Middle Jurassic bedrocks, most likely related to an epirogenetic base-level change. This study invokes that similar successions changing from redbrown paleosol to carbonate may be unrelated to climate change but could reflect base-level and provenance controls.

## 8) Applied and Environmental Geosciences

### 8a) Geological and hydrogeological characterisation of reservoir rocks

Wednesday, 25/Sep/2019: 1:00pm - 3:00pm

**Session Chair: Patricia Göbel** (Westfälische Wilhelms-Universität Münster)

**Session Chair: Matthias Hinderer** (Technische Universität Darmstadt)

**Session Chair: Maria-Theresia Schafmeister** (University of Greifswald)

**Location: Schlossplatz 7 Hof: SP 7**

#### Session Abstract

In this session we want to initiate an interdisciplinary discussion about different and innovative methods and concepts to characterize reservoir rocks at various scales. The primary focus is on porosity and permeability, their quantification, heterogeneity and genesis and involves all rock types either suitable as reservoir rocks or as seals. Welcome are a priori geological concepts, outcrop-analogue studies, experimental lab set-ups in the laboratory, statistic concepts, modelling approaches and management systems. We are looking forward to interesting insights of research work as well as case studies, and in particular aim to bridge geology and hydrogeology.

#### Lecture Presentations

**1:00pm - 1:30pm** *Rolf & Marlies-Teichmüller-Award*

#### **Coal as a Natural Archive: New Implications from the Miocene Lignites of the Lower Rhine Basin**

**Henny Gerschel**

*TU Bergakademie Freiberg, Germany*

Natural archives such as ice cores, dripstones or ocean / lake sediments are intensively used for the reconstruction of climatic conditions. Also, peat soundings of recent moors found their way into the environmental research of the youngest geological past. The potential of lignite as an environmental and climate archive, on the other hand, is largely underestimated (apart from pollen analysis). Yet it is precisely lignite - as fossil testimony to former large-scale moorlands - that has a high significance with regard to earlier ecological and climatic developments. The moor facies analysis goes far beyond palaeobotanical and/or petrographical typing of lignite and inevitably leads to the reconstruction of phytocenoses, biochemical degradation processes in the paleo-moor and their ecological conditions.

New studies on Neogene lignites of the Lower Rhine Basin show this in an exemplary manner. They prove the development of moors during the Miocene by petrographic investigations of samples from several mapping campaigns. The basis for this is the causal relationship between petrography and genesis of coal: Thus, the macro- and microscopic habitus of lignite results directly from the ecological and climatic conditions at the time of peat formation. This in turn can be used to subdivide different moor facies.

As shown in the studies, the sampled seams can be clearly divided internally into moor sequences. These reflect the local development of bogs during a certain period of time depending on predominantly environmental factors. Furthermore, the individual cycles can be traced over large parts of the basin. However, their facial structure changes in a horizontal direction. The respective position and the resulting sedimentation conditions within the former bay (rather on land or sea side) play an important role. In addition, facial changes in the vertical direction of the investigated profile from the Lower Miocene to the Upper Miocene were determined. These can be traced back to climatic changes and the associated ecological changes.

Researching lignite as a petrographic rock in its entirety using the methods of organic petrology has great potential regarding environmental reconstruction and climate change in the geological past. It contributes significantly to a better understanding of the natural development of moorlands. Thus, it could also contribute to current issues in dealing with such ecosystems. Therefore, organic petrology and moor facies analysis should receive broader scientific attention in the future.

**1:30pm - 1:45pm**

### **Deep Geothermal Energy Potential at Weisweiler, Germany: 3D-Modelling of Subsurface Mid-Palaeozoic Carbonate Reservoirs**

**Tobias Fritschle<sup>1</sup>, Martin Salamon<sup>1</sup>, Martin Arndt<sup>1</sup>, Thomas Oswald<sup>2</sup>**

<sup>1</sup>Geological Survey of North Rhine-Westphalia, De-Greif-Strasse 195, 47803 Krefeld, Germany; <sup>2</sup>RWE Power AG, Cologne site, Stüttgenweg 2, 50935 Köln, Germany

Devonian and Carboniferous carbonate rocks are present in the subsurface of the Weisweiler lignite-fired power plant near Aachen, Germany. The utilisation of these carbonate rocks for the purpose of deep geothermal energy extraction from both the Devonian and Carboniferous reservoirs is currently being investigated within the scope of the transnational EU-INTERREG-funded “Roll-out of Deep Geothermal Energy in North-West Europe (DGE-ROLLOUT)” project.

Marine transgressive-regressive cycles during mid-Palaeozoic times enabled the formation of extensive reef complexes at the southerly continental shelf of the Laurussian palaeocontinent. Supported by favourable climatic conditions including warm, clear and shallow waters, the Givetian to Frasnian Massenkalk facies and the Dinantian Kohlenkalk Group, each comprising a thickness of several hundreds of meters, were deposited in North-West Europe.

In the Weisweiler area, these Palaeozoic carbonate rocks were covered by voluminous paralic sediments, subsequent to their deposition, and were deformed to large-scale, generally southwest-northeast-trending, syncline-anticline structures during the Variscan Orogeny. Alpine (post-)orogenic processes further induced faulting, resulting in fault-block tectonics in an area of tectonic subsidence, i.e., the Lower Rhine Embayment. 3D-modelling of the depths and dimensions of the Weisweiler subsurface carbonate reservoirs is carried out using the commercial software *Move* [v2018.2.0; Midland Valley Exploration Ltd]. The model in progress is fed by lithostratigraphic data obtained from drilling operations, constraints of mapping projects, and interpretations of seismic profiles.

Preliminary results show a complex geotectonic environment including steeply folded lithological units and possibly several overthrust faults. The minimum depth of the top of the carbonate rocks is estimated to c. 1.000 m, taking into account a thickness of the nearby exposed Namurian strata of 500 m. In addition, the significant multiphase karstification of the Palaeozoic carbonates, which can be observed in nearby exposed counterparts, further supports their enhanced geothermal exploitation potential.

3D-modelling will aid to constrain a target area for exploration drillings, which will then enable geochemical and petrophysical investigations on the Palaeozoic rocks. The possibility of deep geothermal energy extraction from the Weisweiler subsurface, and hence, the evaluation of the probability for the transition of a conventional lignite-fired power plant towards its utilisation of renewable “green” energy, is carried out in close collaboration with the RWE Power AG, GZB, and DMT GmbH & Co. KG, all partners within the DGE-ROLLOUT project. The successful realisation of this project may serve as a pilot for similar projects considering the forthcoming fossil fuel phase-out.

**1:45pm - 2:00pm****Geothermal potential of Dinantian carbonates in the subsurface of North Rhine-Westphalia, Germany****Martin Salamon<sup>1</sup>, Martin Arndt<sup>1</sup>, Tobias Fritschle<sup>1</sup>, thomas Oswald<sup>2</sup>**<sup>1</sup>*Geological Survey of North Rhine Westphalia, Germany;* <sup>2</sup>*RWE Power AG*

In course of the fossil fuel phase-out, the demand for renewable energy is growing progressively. Despite the continuous increase in the exploitation of renewable energy resources, only a minor proportion is contributed by geothermal energy, in NW-Europe (NWE). However, as currently 53 % of the energy consumption of NWE corresponds to heat demand, the expansion of geothermal energy supply is highly desirable. Therefore, the Deep Geothermal Energy (DGE) Rollout Project within the EU Interreg-Programme focusses on geological units, which can be used for geothermal energy extraction. Promising layers are represented by the Dinantian (Lower Carboniferous) carbonates, which are already exploited successfully, for example, at the Californië site in the Netherlands.

The Dinantian in NWE is characterised by three main depositional areas: (1) the shallow-marine ramp and platform carbonates around the Brabant Massif and on intrabasinal highs, (2) a calciturbiditic facies, which was shed from these carbonate ramps and platforms, and (3) the deep-marine Kulm basin, dominated by the sedimentation of siliciclastic flysch that derived from the uprising Variscides in the south. Additionally, eustatic sea-level changes caused lateral and vertical facies shifts within the basin in the course of time and space, which caused various facies intercalations. Ramp and platform carbonates are broadly developed in Belgium and the Netherlands. They consist of Tournaisian dolomites and Viséan limestones, which contain porous reef structures likely including significant karstification, caverns and fissures, which represent an ideal aquifer for the use of geothermal energy, assuming their occurrence in a suitable depth. Due to many siliciclastic intercalations, particularly the pelitic units, the Kulm facies is rather unsuitable for geothermal exploitation.

In the Lower Rhine Graben, the Kohlenkalk-Group is situated in greater depths due to the ongoing tectonic subsidence since the Tertiary. The well Schwalmtal 1001 in the Lower Rhine Graben shows the most promising lithological profile for the purpose of geothermal exploitation. It lies within a halfgraben structure west of the Viersen Fault and reaches the Dinantian carbonates at a depth between 1,625 m and 1,770.7 m. The well Winterswijk-01, which lies close to the Dutch/German border, reaches the Dinantian platform carbonates in even greater depths between 4,275 and 4,461 m.

The successful geothermal projects in the Netherlands prove that the Dinantian carbonates are a promising geological unit for heat production. Thus, depending on the geotectonic setting in Germany, the platform carbonates of the “Kohlenkalk” Group may be utilised for the extraction of geothermal energy.

**2:00pm - 2:15pm****Thermo-Hydraulic Heterogeneity Assessment Across First-Order Hiatal Surfaces – A Case Study from the Post-Variscan Nonconformity****Adrian Linsel, Sebastian Weinert, Kristian Bär, Matthias Hinderer***Technische Universität Darmstadt, Germany*

The Post-Variscan Nonconformity (PVNC) is a first-order hiatal surface that spreads across central Europe and constitutes a major diachronous lithological and petrophysical contrast within the Paleozoic to Mesozoic strata. Recently, deep geothermal heat and power projects target resources at the PVNC. This requires quantitative information of the lithological architecture and physical heterogeneity across this surface as they govern the reservoir quality during exploitation.

In this study, the lithological architecture and thermo-hydraulic heterogeneity across the PVNC are characterized for two cored scientific wells of 68 and 80 m length in a proximal outcrop analogue area of the Upper Rhine Graben, where Rotliegend volcano-sedimentary cover rocks are nonconformably overlying igneous Paleozoic basement rock. Thermophysical (thermal conductivity, thermal diffusivity, specific heat capacity)

and hydraulic (porosity, matrix permeability) laboratory measurements and geological logging, including the rock quality designation index, form the datasets of this study. Multivariate geostatistical methods are used for spatial heterogeneity analysis.

The cover rocks, comprising breccias, conglomerates, wackes, arenites and mudstones from an alluvial fan depositional environment interfingering with effusive basalts, display low to very low hydraulic matrix permeability and intermediate thermal conductivity. Debris flows and sheet floods represent the most abundant sedimentary elements. Rock quality designation index of the basement rocks that comprise altered, weathered and deformed diorite, granite and quartz-monzodiorite, is reduced in the palaeo weathering zone and in local dykes forming potential pathways for fluid flow.

Thermal properties clearly group into the observed lithological and depositional classes, however, the palaeo weathering zone levels off the physical contrast in the topmost part of the basement due to alteration and grain framework disaggregation. Significant linear and non-linear positive correlations between the hydraulic parameters were discovered. Thermal and hydraulic parameters correlate negatively. Semivariance of each reservoir parameter is strongly increasing across the PVNC, hence statistical interpolations including this horizon should be based on robust semivariance models.

## 2:15pm - 2:30pm

### **Towards a better understanding of the central German Buntsandstein aquifer system: Combined study of petrological, facial and petrophysical observations**

**Michaela Aehnelt<sup>1</sup>, Cindy Kunkel<sup>2</sup>, Dieter Pudlo<sup>1</sup>, Reinhard Gaupp<sup>1</sup>, Kai Uwe Totsche<sup>1</sup>**

<sup>1</sup>Friedrich Schiller-Universität Jena, Germany; <sup>2</sup>Leibniz-Institut für Angewandte Geophysik (LIAG), Hannover, Germany

The Lower Triassic Buntsandstein is an economically important clastic underground reservoir and aquifer unit in the Central European Basin (e.g. for hydrocarbon reservoirs, gas storage, geothermal energy use, drinking water supply). Its quality mainly controls its prospectivity, storage capacity and exploitability. Thus, predictions for the realization of economic intentions depend most notably on a substantial understanding of the parameters that control reservoir quality, such as rock composition, facies and diagenetic evolution. Therefore, research of even small-scale heterogeneities is necessary.

The study area is the Thuringian Syncline, which is a small sub-basin of the North German Basin located at its southern margin. One of its major aquifers are built from siliciclastic sediments of the Buntsandstein, which are characterized by rapide changes of depositional environments from channel to sandflat to lacustrine depositions resulting in large heterogeneities at a relatively small scale (few to some hundred meters). Furthermore, burial history and subsequent basin inversion and uplift led to only minor depths of 700 to 1000 m in the center of the syncline and an exposure at the surface at syncline margins, which allows for the exploration of the recent impact of meteoric water infiltration vs. former burial evolution on aquifer quality. We combined a petrographic study focusing on mineral composition and diagenetic evolution with a facies study (including lithofacies type and depositional environment characterization) and linked the results with petrophysical data like permeability and porosity. The corresponding dataset consists of measurements on more than 300 plug samples from 12 wells and 7 outcrops.

All in all, the Buntsandstein exhibits a very complex relationship of hydraulic parameters with diagenetic evolution in relation to depositional preconditions. The more southern the sampled deposits occur, the better is their aquifer quality, due to an increase in grain size towards the basin margin and a decrease in mud content. High amounts of channel deposits in the sandstones result in an increase in aquifer quality. Finally, there is a major influence of telodiagenetic processes and meteoric water infiltrations on aquifer quality. This is related most likely to present-day cement dissolution and mineral alteration, especially in the vadose zone.

**2:30pm - 2:45pm****Log derived permeability estimation of Valanginian (Lower Cretaceous) sandstone units of the Lower Saxony Basin****Roberto Pierau<sup>1</sup>, Sandra Schumacher<sup>2</sup>, Robert Schöner<sup>1</sup>**<sup>1</sup>LBEg, Germany; <sup>2</sup>BGR, Germany

Several sandstone units with a potential for geothermal applications are expected in the North German Basin. The distribution of sandstone units of Valanginian age (Lower Cretaceous) in the Lower Saxony Basin has been mapped at the Landesamt für Bergbau, Energie und Geologie to identify potential geothermal aquifers and to determine their sedimentological and hydraulic properties. Facies changes were analyzed on well sections using Gamma ray and Spontaneous potential logs, core description and thin section analysis. A lithostratigraphic correlation was established to map the major sandstone units. Three regionally relevant sandstone units could be verified: the Bentheim Sandstein, the Dichotomiten-Sandstein and the Hauptsandstein. In a first step, hydraulic properties of each sandstone complex were determined using porosity and permeability data of core plug measurements. The majority of these data available at the Landesamt für Bergbau, Energie und Geologie derives from wells of hydrocarbon fields. In a second step, porosity and permeability were determined from well sections. Porosity was calculated from Sonic, Density or Neutron logs using established evaluation methods (Wyllie et al 1956). Permeability was estimated using the porosity/permeability function of Pape et al. (1999)

$$k = A\phi + B(\phi)^2 + C(10\phi)^{10}$$

where the permeability (k) is calculated from log derived total porosity ( $\phi$ ) and empirical parameters (A, B and C). In this study, the empirical parameters were determined for individual sandstone unit, for individual hydrocarbon fields, or even for single wells separately by calculating a distinct correlation function for the available plug measurement data.

Assuming that porosity and permeability data from plug measurements are statistically representative for a specific sandstone unit, this approach allows to determine continuous porosity and permeability logs for each well, as long as suitable geophysical well log data is available. As a result, porosities and permeabilities of Valanginian sandstones in the Lower Saxony Basin could also be determined for many wells outside of known hydrocarbon fields. This approach helps characterizing the hydraulic properties of potential geothermal aquifers on a regional scale.

**2:45pm - 3:00pm****Thickness distribution and sequence stratigraphy of the late Jurassic Malm reservoir in Bavaria: implications for geothermal exploration****Martin Elsner, Achim Schubert***Erdwerk GmbH, Germany*

Carbonates of the late Jurassic Malm aquifer in the North Alpine Foreland Basin (Molasse Basin) host the most important hydrogeothermal resources in Germany. So far, more than 50 geothermal wells have been drilled successfully, and a geothermal power of approximately 700 MW<sub>th</sub> and 25 MW<sub>el</sub> is installed. Data for this study are derived from outcrop analogues in the Swabian and Franconian Alb, from several seismic lines and cubes, and from wells. The focus is on the area of greater Munich and Eastern Bavaria, where geothermal gradients and reservoir permeability are most favourable.

Two hyper-facies are distinguished within the Malm: the 'bedded facies' (Bankfazies), comprising of well bedded limestones with interbedded marls and representing deeper, quiet water sedimentation, and the 'massive facies' (Massenfazies), consisting of sponge-microbial-bioherms and bioclast-peloid-(oid)-sand bodies, deposited at higher water energy. East of a line Donauwörth-Fürstenfeldbruck-Starnberg, the massive facies is frequently dolomitized, thus gained some secondary porosity, and shows the highest matrix permeability. Stratigraphically, the massive facies ranges mainly from the Kimmeridgean to the Tithonian and is less devel-

oped in the lowermost Malm of Oxfordian age. Its widest occurrence is during the Kimmeridgean. Reservoir quality depends mainly on the proportion of dolomitization, on shape and size of dolomite crystals, and on the intensity of palaeokarst development. Average permeabilities of successful geothermal projects vary over several orders of magnitude from 1 mD to 10 D. Where dolomitization is absent, pack- and grainstones show the highest permeability, and karstification is crucial for sufficient flow rates.

Analysis of the thickness distribution shows a maximum of 600-650 m around Munich, declining to less than 500 m towards Northwest and Southeast. The decline to Northwest can be attributed to later erosion, reducing the effective reservoir thickness. As dolomitization is largely missing here, permeability relies on primary porosity and karstification, for which prediction is difficult. Multilateral wells may be useful to improve the reservoir development and increase production rates to economic viability.

A sequence stratigraphic approach indicates that the decline of thickness towards Eastern Bavaria is likely due to a later onset of sedimentation, probably during the late Oxfordian or even the Kimmeridgean. Therefore, the lowermost Malm may be absent here, but as this part is largely unproductive, the effective reservoir thickness is not affected, and exploration in Eastern Bavaria can follow the same approach as in the area of greater Munich.

## Poster Presentations

Tue: 54

### **Buntsandstein (Lower Triassic) reservoirs in Northeast Germany: perspectives for geothermal use**

**Owen Dunkerley, Martin Sattelberger, Gregor Barth, Karsten Obst**

*Geological Survey of Mecklenburg - Western Pomerania, LUNG M-V, Germany*

Sandstones deposited in large basin environments often have good reservoir quality, e.g. for hydrothermal use or to store energy. The Mesozoic successions of the North German Basin (NGB) have a high geothermal potential and will contribute to the sustainable energy transition.

During the Middle Buntsandstein of the Lower Triassic, up to 50 m thick, well sorted sandstone units of fluvial origin intercalated with alternating clay-silt intervals were deposited at the northeastern margin of the North German Basin. These sandstones are characterised by high porosity up to 30 % and permeability values ranging between 250-1100 mD. These geothermal reservoirs are currently used for spa purposes in Binz on Rügen Island (1020 m, 28.5°C).

Geothermal projects are planned for the three imperial baths (Kaiserbäder Ahlbeck, Herigsdorf, Bansin) on Usedom Island. There the potential reservoirs of the Detfurth and Hardegsen Fm occur at depths between 1,600 m and 1,900 m, containing saline water with temperatures of 60°C to 70°C.

To support future exploitation of geothermal resources in this area, a high resolution 3D model of the Middle Buntsandstein will be developed within the framework of the GeoFaces project. The model is based on data from 17 wells and nearly 40 2D seismic profiles and will minimise the risk of poor investment.

Tue: 55

### **4D Geo-Positron-Emission-Tomography (GeoPET) in situ fluid flow channel visualization in an unaltered granite fracture from Soultz-sous-Forêts (France)**

**Janis Leon Pingel<sup>1</sup>, Johannes Kulenkampff<sup>2</sup>, Madeleine Stoll<sup>3</sup>, Thorsten Schäfer<sup>1</sup>, Cornelius Fischer<sup>2</sup>**

*<sup>1</sup>Friedrich-Schiller-Universität Jena, Germany; <sup>2</sup>Helmholtz-Zentrum Dresden-Rossendorf, Germany; <sup>3</sup>Karlsruhe Institute of Technology, Germany*

In this study, we investigate experimentally the fluid flow field in a granite core sample (diameter = 78 mm, length = 93 mm), containing an unaltered natural fracture <sup>[1]</sup>, by using the Positron Emission Tomography (PET). The PET method allows for the direct analysis of flow streamlines, thus providing unique insight into the fluid dynamics of complex porous materials <sup>[2,3]</sup>.

The fractured granitic drill core originates from 1957 m depth (well EPS-1) of the Enhanced Geothermal System (EGS) reference site at Soultz-sous-Forêts, France. Pulse migration experiments using different inlet-outlet positions at each side of the fracture were performed under constant flow rates of 6 or 12 mL/h, respectively, using  $^{18}\text{F}$  as PET tracer.

Revealing different flow path behaviors and dipole configurations for the flow rates applied, this study clearly shows the influence of the fracture aperture as well as its topographic features on the flow field. Observed for all experiments, under the hydrodynamic conditions applied, a flow channeling and preferential flow pattern could be observed. While the higher flow rate experiments show wider and higher dispersion of the radiotracer, especially the low velocity results show more distinctive flow paths and channeling behavior.

Furthermore, the results of this study were compared, within the timeframe possible due to the short half-life of the  $^{18}\text{F}$  tracer used ( $t_{1/2} = 109.8$  min), to the experimental and numerical 2.5D transport models (COMSOL) published by Stoll et al. (2019) [1]. While having differences in the numerical and experimental approaches, mainly affecting the fracture aperture and its geometry, the simplifications applied to the numerical models reveal a major influence on the hydrodynamic flow and channeling behavior in comparison to the PET experiments.

Providing valid results in terms of flow path propagation and hydrodynamic behavior for different experimental approaches, this study demonstrates the opportunities of experimental investigations and visualizations in comparison to numerical fluid dynamics approaches. As the 4D Geo-Positron-Emission-Tomography provides in-situ laboratory observations under a variety of fluid flow conditions, we discuss the potential influence of certain fracture characteristics on the observed flow pattern. Furthermore, future ideas of experimental and numerical optimization will be discussed.

[1] M. Stoll et al. (2019), *Journal of Contaminant Hydrology* 221, 82.; [2] J. Kulenkampff et al. (2018), *Scientific Reports* 8, 7091; [3] J. Kulenkampff et al. (2008), *Physics and Chemistry of the Earth, Parts A/B/C* 33, 937.

## 8b) Deep subsurface groundwater systems

Monday, 23/Sep/2019: 9:00am - 10:30am

**Session Chair: Sebastian Fischer** (Bundesanstalt für Geowissenschaften und Rohstoffe)

**Location: Schloss: S8**

### Session Abstract

Understanding and quantifying the processes that modify and shape the surface of the Earth requires the determination of accurate dates and rates. Thus, the improvement and development of existing and new dating methods is essential for a better understanding of Earth's surface processes and their relation to climate and tectonics. Currently employed geochronological methods include, for example, exposure and burial dating with cosmogenic nuclides, luminescence, radiocarbon, and paleomagnetic dating. This session invites contributions on developments and applications of all dating methods relevant to decipher Late Cenozoic landscape evolution, climate change, and active tectonics. The keynote speakers Georgina King (Lausanne) and Vincent Godard (Aix-Marseille) will give talks on luminescence thermochronometry and the use of  $^{36}\text{Cl}$  in carbonate landscapes. Interested participants are invited to visit the cosmogenic nuclide laboratory in Münster and discuss all aspects of  $^{10}\text{Be}$  separation and target preparation with R. Hetzel and T. Dunai.

## Lecture Presentations

9:00am - 9:30am *Session Keynote*

### The thermal provinces of Hesse, Germany

**Rafael Schäffer, Ingo Sass**

*TU Darmstadt, Germany*

The federal government of Germany has committed itself to ambitious climate protection goals in international treaties. Achieving these goals is only possible with the inclusion of all renewable energies. So far, geothermal energy plays hardly any role in the expansion of renewable energies, whereas some regions of Germany and Hesse are well suited for geothermal energy. The state of Hesse is rich in thermal springs, some of which have been used for various purposes for centuries. But little effort is made to exploit these hydrothermal systems geothermal. One reason might be that the exploration of geothermal reservoirs and the assessment of underground properties is still a major challenge.

The establishment of a hydrochemical database on reservoir fluids provides parameters for the evaluation of hydrothermal systems. The data are derived from a comprehensive literature research in cooperation with the HLNUG and the BGR.

Hydrochemical data sets from the Hessian territory that meet one of the following criteria and are not older than 1910 have been added to the database:

- water temperature at least 20 °C (definition thermal water)
- solution content at least 1 g/l (definition mineral water)
- depth at least 100 m (definition of the future formation water database of the BGR)

The database contains thousands of data sets with metadata (coordinates, altitude, tapping type, etc.), references (analysis date, citation, etc.), physical parameters (like temperature, electrical conductivity, pH), chemical parameters (concentrations of ions and elements), sum parameters, dissolved and free gas contents, as well as isotope data.

In a first evaluation step, the database is used to assess the distribution and composition of mineral and thermal waters. The most important criteria for this are the water type (e. g. Ca-HCO<sub>3</sub> or Na-Cl waters), the water temperature, the salinity, the CO<sub>2</sub> concentration and the depth of the tapping. In a second step, hydrothermal provinces are defined for Hesse and adjacent regions. Within a province, the water quality is similar, so it can be assumed that the genesis of the fluid is also similar. In a third step, hydrothermal potentials can be identified.

9:30am - 9:45am

### Reservoir rocks for geothermal applications in the North German Basin: Hydraulic characterization of Dogger sediments

**Cindy Kunkel, Thorsten Agemar**

*Leibniz Institute for Applied Geophysics (LIAG), Germany*

This study investigates the subsurface distribution of permeability and hydraulic conductivity in the western part of the North German Basin with the aim to assess the geothermal potential of sandstone formations that could play a key role in Germany's turn-around in heat production and supply ("Wärmewende"). Currently, there only exist two sites in the eastern part of the North German Basin, at Neustadt-Glewe and Waren, where geothermal energy is used for district heating.

The focus is on the Dogger sandstone formations, which are widely distributed with a mean thickness of more than 10 m and in depth greater than 800 m below ground level. The sediments were deposited in a fluvial dominated deltaic system into a shallow coastal sea, where sandstones formed in distributary channels and on sandsheets on the delta plain. The most important sandstone aquifers are the Dogger beta sandstones of the Aalenian, the Bajocian Garantianen sandstone as well as the Cornbrash-facies and the Wuerttembergica sandstones of the Bathonian.

Besides permeability and hydraulic conductivity of the reservoir rocks, especially the subsurface temperature is of importance for geothermal purposes. A combined investigation of hydraulic measurements of porosity and permeability of plugs together with data derived from geophysical borehole measurements as well as the temperature of the Dogger is carried out to assess the distribution of hydraulic conductivity. The hydraulic conductivity is then derived from the permeability data and the geothermal potential is estimated. Altogether, the Dogger data set consists of about 225 plug measurements from 200 locations and of about 150 additional data from log interpretation in 72 locations.

Preliminary results show that Bathonian and Bajocian sediments have the highest permeability and porosity values in the center of Lower Saxony, whereas the Aalenian sediments are most suitable for geothermal applications in the eastern part. Temperature anomalies of up to 30 °C higher than expected exist, but the depth of the aquifer is still the main controlling factor for the temperature. Higher permeability values (>50 mD) do not coincide with high temperatures.

Finally, these maps will be integrated into the Geothermal Information System (GeotIS). GeotIS is a digital geothermal atlas, which offers a compilation of data and information about deep aquifers. The additional data will help project planners to estimate the low enthalpy geothermal resources in the western part of the North German Basin.

**9:45am - 10:00am**

### **3D numerical modeling of cross-boundary flow in the subsurface of Berlin (Germany)**

**Maximilian Frick<sup>1</sup>, Magdalena Scheck-Wenderoth<sup>1,2</sup>, Mauro Cacace<sup>1</sup>, Michael Schneider<sup>3</sup>**

<sup>1</sup>Section 4.5 Basin Modelling, GFZ German Research Centre for Geosciences, Telegrafenberg, 14473 Potsdam, Germany;

<sup>2</sup>RWTH Aachen University, Institute of Geology and Geochemistry of Petroleum and Coal, Lochnerstrasse 4 - 20, 52056 Aachen; <sup>3</sup>Free University Berlin, Institute of Geological Sciences, Malteserstr. 74-100, 12249 Berlin, Germany

The goal of this study is to investigate the influence of cross-boundary flow on the hydraulic configuration of the shallow and deep subsurface also in respect to inter-aquifer flow and groundwater safety beneath the urban center of Berlin. To achieve this goal we built 3D hydrothermal models, which differ in the set-up of their surface and lateral forcing (boundary) conditions, to systematically investigate their impact on fresh groundwater production.

The area we investigate is part of the Northeast German Basin featuring a thick sequence (up to 5km) of differently consolidated sedimentary deposits. Of major interest in this sedimentary succession, a sequence of alternating aquifers and aquitards (geofluid reservoirs) is connected to different degrees, wherein a specific composition of its mineralized pore water has been observed. Their interconnection and the right representation becomes even more important considering the fact that the uppermost reservoir is used for drinking water production and may be incompletely sealed to the brackish and saline reservoirs below due to glacial erosional discontinuities in the separating aquitard. An understanding of the risk of saline groundwater up-coming has been targeted in this study, both naturally occurring and possibly anthropogenically triggered.

We present results for the fluid flow regimes at different depths which were correlated with available isotopic data, demonstrating that cross boundary flow is needed in order to reproduce observed groundwater compositions. We also show that hydraulic connections between the different reservoirs are likely to occur thus supporting the possibility of a contaminant rise from the saline aquifers below through either natural or anthropogenic (pumping) forcing.

## Poster Presentations

Mon: 49

### Krypton-81 feasibility study on deep thermal groundwaters in the karstified Upper Jurassic limestone of the Molasse basin (Germany-Austria)

**Michael Heidinger<sup>1</sup>, Peter Mueller<sup>2</sup>, Jake Zappala<sup>2</sup>, Roland Purtschert<sup>3</sup>, Florian Eichinger<sup>1</sup>, Gunther Wirsing<sup>4</sup>, Tobias Geyer<sup>4</sup>, Thomas Fritzer<sup>5</sup>, Doris Groß<sup>6</sup>**

<sup>1</sup>Hydroisotop GmbH, D; <sup>2</sup>Physics Division, Argonne National Laboratory, USA; <sup>3</sup>Physics Institute, University Bern, CH;

<sup>4</sup>State Authority for Geology, Mineral Resources and Mining Baden-Württemberg, D; <sup>5</sup>State Authority for Environment Bayern, D; <sup>6</sup>Department of Applied Geological Sciences and Geophysics Montanuniversity Leoben, A

The karstified Upper Jurassic limestone buried deep under tertiary sediments in the Molasse basin of south Germany and Austria is of special interest for its outstanding geothermal groundwater reservoir (up to 140 °C). Exploitation started in the 1930's (mineralwaters, therapeutic baths) and developed to the actual status of more than 80 active wells (more than 30 geothermal wells/duplets for heating and green power production). Comprehensive studies (hydrogeology, hydrochemistry, stable and radioactive isotopes, gas and rare gas composition etc.) were done on local and regional scale. But little is known about the recharge and flow mechanism of the low mineralised Na-HCO<sub>3</sub>-Cl type thermal waters with glacial melt water characteristics predominant in the central basin close to the Alps. Especially radioisotope dating information (<sup>14</sup>C-DIC, He-isotopes, etc.) lacked to answer the open transregional/transnational topics, due to the complex evolution (ion exchange, isotope exchange, gas flux, etc.) of the deep thermal groundwater system.

Because of the achievement in the ATTA-technique for <sup>81</sup>Kr-dating a feasibility study was proposed to regional/national water authorities and private geothermal plants. The results gained in 2017/18 reveal groundwater recharge during the last glacial period (Würm/Weichsel for central Europe) for the western and central part of the Molasse basin and seem to fit very well to the subglacial recharge hypotheses. For the mayor part of the karstified Upper Jurassic limestone in Molasse basin a transient groundwater flow system with very high turnover times during glacial periods is therefore plausible. In the eastern part of the Molasse basin the results show up a much slower flow system with less influence from alpine induced recharge during the latest glacial periods.

Mon: 50

### Geothermal potential and thermal energy storage of Buntsandstein and Keuper aquifers in NE Bavaria

**Cindy Kunkel<sup>1</sup>, Thorsten Agemar<sup>1</sup>, Ingrid Stober<sup>2</sup>**

<sup>1</sup>Leibniz Institute for Applied Geophysics (LIAG), Stilleweg 2, 30655 Hannover; <sup>2</sup>University Freiburg, Albertstr. 23b, 79104 Freiburg

This study investigates the hydraulic and thermic properties of siliciclastic aquifers in northern Bavaria with the aim to assess the geothermal potential of sandstone formations that could play a key role in Germany's turn-around in heat production and supply ("Wärmewende"). Due to their wide spatial distribution, their depth and temperatures, especially the Buntsandstein und Keuper aquifers hold the highest potential for geothermal applications. Up to now, both aquifers are predominantly used for balneological purposes, but they can also be suitable for thermal energy storage (ATES).

Alluvial fan deposition under arid to semiarid conditions with periodical sheetfloods from the hinterland are dominant throughout the Buntsandstein. Especially the alluvial fans at the basin margin and the tectonically stressed regions are highly permeable, whereas the fine grained deposits in the basin center show rather unfavorable hydraulic properties. Deposition during the Keuper ranges from marine to brackish to fluvial environments under variable climate conditions resulting in vertical and lateral facies changes. Especially along the basin margin hydraulic properties are favorable due to an increase in the sand fraction.

Data from pumping tests and production data are interpreted to map the hydraulic conductivity of the Ke-

uper and Buntsandstein aquifers for geothermal resources deeper than 100 m. Furthermore, temperature estimations and the depth levels of the two aquifers (Keuper 100 to 650 m, Buntsandstein 100 to 1,400 m) are incorporated. The results are visualized in form of spatial distribution maps of the hydraulic conductivity as well as temperature and will be integrated into the Geothermal Information System GeotIS (<https://www.geotis.de>).

The majority of the conductivity values of both aquifers are at depths of up to 300 m, occasionally up to 650 m. With increasing depth, the potential for geothermal utilisation decreases. In total, 76% of all values at temperatures between 10°C and 45°C are suitable for geothermal use. The Buntsandstein aquifer in the northwest and in the northeast of Bavaria as well as around Nürnberg is particularly well suited for aquifer storage due to the increased hydraulic conductivity together with temperatures around 20°C. Somewhat further north near Erlangen the temperature reaches even up to 27°C. However, in the northeastern and northwestern parts of the basin margins the temperature is only about 10°C. Keuper aquifers are suitable for energy storage in the regions north and south of Nürnberg at shallow depths, where they reach temperatures of about 15°C. However, the temperature decreases to about 10°C in the southwest.

## Mon: 51

### Developing a three-dimensional hydrogeological model based on the Konrad-site as an example to calculate the density-driven flow in deep groundwater systems

**Torben Weyand, Jürgen Larue**

Gesellschaft für Anlagen- und Reaktorsicherheit (GRS) gGmbH, Germany

In early long-term safety analyses for repositories for radioactive waste, the transport behavior of contaminants was examined based on the assumption of a freshwater groundwater system. Due to limitations in computer speed and capacity, the calculation of density-driven flow considering variations in salinity was not possible for large model domains over long simulation times. To date this still represents a geoscientific challenge.

This study contributes a three-dimensional hydrogeological model, considering several multi-aquifer-formations. The Konrad-site is used as an example to set up the model and is characterized by deep aquifers with high salinities, and a site-specific linear salinity gradient with increasing depth. The hydrogeological model takes up to 23 different geological layers into account, with several confined aquifers as potential migration paths for contaminants. The three-dimensional model is mainly based on subsurface contour maps of 15 different geological layers. Additionally, 30 two-dimensional vertical cross sections are used to validate the model. Hydraulically dominated fault zones and important geotectonic structures (salt domes) are considered to refine the model grid at specific locations.

To establish the model and further simulate the groundwater flow, the “Simulation of Processes in Groundwater” (SPRING) code is used. SPRING is suited for multidimensional hydrogeological modeling of density-driven groundwater flow through porous media considering variations in salinity. In previous studies, the density-driven flow was calculated based on representative two-dimensional cross sections also using data of the Konrad-site as an example.

In previous studies, the development of the salinity gradient over time was depicted by calculating the density driven two-dimensional flow in deep groundwater systems over long simulation times. These calculations showed that the salinity gradient measured at the site at present, can be described by long-term hydrogeological and geochemical processes of dilution and transport of saline solutions forced by the recharge of freshwater from the surface. Furthermore, the present salinity gradient at the site describes a snap-shot of a transient salt distribution in the long term, which is also interesting for the long-term stability of engineered barriers of a deep geological disposal.

Future work of this study intends to extend the numerical simulations by using the described three-dimensional model and analyze the groundwater flow in deep groundwater systems in more detail. The challenge is to develop a complex model grid with the ability to perform long-term safety analyses for large model domains over long simulation times within an adequate simulation time frame.

**Mon: 52****Reactive Reservoir Systems - Crystal Nucleation and Filter Processes in Geothermal Systems****Philipp Zuber<sup>1</sup>, Sascha Frank<sup>2</sup>, Jürgen Schreuer<sup>1</sup>, Stefan Wohnlich<sup>2</sup>**<sup>1</sup>*Crystallography, Ruhr-University Bochum, Germany;* <sup>2</sup>*Hydrogeology, Ruhr-University Bochum, Germany*

During geothermal energy generation, the change of temperature and pressure conditions can lead to supersaturation of the extracted fluids and thus to precipitation of minerals. Well-documented crystalline deposits on the inner walls of pipes are the consequences. In addition, turbulence-induced inhomogeneities and mechanical disturbances also lead to the formation of spontaneous free-floating crystal nuclei. A significant part of them are carried along and reinjected into the reservoir. There, the crystal nuclei are possible centers for crystallization and cementations processes or can accumulate by filter effects. Both processes contribute to scaling effects which limit the use of the geothermal reservoir. So far, such effects have not been considered in hydrogeochemical modelling programs, which are mainly based on the temperature and pressure dependence of solution and reaction equilibria in the reservoir.

Our investigations focus on a better understanding of the formation and growth of crystal nuclei in saturated geothermal solutions during thermal and pressure relaxation, and the development of approaches to control crystal nucleation and to minimize filter processes in the reservoir. For this purpose, a high-pressure high-temperature apparatus is used which is based on the working principle of a natural geothermal system. Two separate heating thermostats allow different temperatures to be used in the storage tank of the system and in the pressure vessel in which the rock sample is placed. Furthermore, we have the possibility to inject specific crystal seeds to study the influence of various minerals and their morphologies. Our setup allows pressures of up to 200 bar and temperatures of up to 100 °C. In addition to the determination of hydrochemical parameters, the crystallites and cements produced are characterized by optical methods, scanning electron microscopy and electron microprobe.

**8c) Geosciences and safe nuclear waste disposal – current status and future directions****Wednesday, 25/Sep/2019: 8:30am - 10:30am****Session Chair: Axel Liebscher** (Fed. Office for the Safety of Nuclear Waste Management (BfE))**Session Chair: Fabien Magri** (BfE Berlin)**Location: Schlossplatz 4: SP4 201****Session Abstract**

The Site Selection Act (StandAG) re-started the German siting process for high-level radioactive waste disposal in 2017. Disposal is foreseen in deep geological formations and considers claystone, crystalline rock and rock salt as potential host rocks. Within the stepwise siting process, geological exclusion and assessment criteria and minimum requirements are applied, surface and subsurface exploration programs are executed and preliminary safety assessments are performed.

This session welcomes contributions on current status and future directions of the different geoscientific disciplines, like geophysics, geochemistry, mineralogy, geomechanics, geomicrobiology as well as geological, relevant for safe nuclear waste disposal. Topics may include, but are not limited to, advances in exploration, monitoring and modelling tools and approaches, fundamental and applied process understanding, THMC(B) coupled modelling, experimental and field studies, safety assessment strategies or disposal concepts.

## Lecture Presentations

8:30am - 9:00am *Session Keynote*

### Geosciences and safe nuclear waste disposal – current status and future directions

**Thorsten Schäfer**

*Friedrich-Schiller-Universität Jena, Germany*

The concept of deep geological disposal of high-level heat generating nuclear waste with the option of retrievability foresees a multi-barrier system to isolate or retain the radioactive inventory for the safety assessment period. The site geology and the use of geo-materials are key components of the disposal concept. The focus of this talk is on crystalline rocks or sedimentary formations (claystone or plastic clay) discussed in Germany as potential repository host rocks.

Research in crystalline formations has focused in the last couple of years on the integrity of the geotechnical barrier (bentonite) endangered by potential erosion through future glacial melt water conditions due to climate change [1]. The influence of nanoparticulate clay phases released during this erosion process and their impact on radionuclide (RNs) mobility is another aspect tackled *inter alia* in international research activities as the Colloid Formation and Migration (CFM) project at the Grimsel Test Site (GTS, Switzerland) [2]. Here, development of new analytical protocols based on accelerator mass spectrometry (AMS) have allowed us to follow radioactive tracers over decades [3] and the combination of techniques as  $\mu$ CT, C-14-PMMA and autoradiography enabled us to precisely determine the rock matrix porosity and mineral distribution being a key to long-term retention [4]. Furthermore, fracture filling mineralogy and its reactivity are mobility decisive, as solid-solution formation might be a very efficient process to capture “irreversibly” RNs [5].

Research in sedimentary formations include a wide spectrum of argillaceous media (indurated clay-rich bedrock formations) considered in several countries for the purpose of the passive long-term management of radioactive wastes. Selected examples of (a) transport phenomena in these nano-porous systems, (b) the role of Molecular-Dynamic (MD) simulations to elucidated, at an atomic scale, the mechanisms of cation and anion interaction with clay surfaces, (c) the interfacial water structuring through compaction, and (d) the migration behavior of solutes will be presented [6]. Beside the current status on selected projects future research directions and underground research laboratory activities will be highlighted.

[1] Shelton et al. (2018) SKB Technical report TR-17-17; [2] [www.grimsel.com](http://www.grimsel.com); [3] Quinto et al. (2019) Anal. Chem. 91(7), 4585-4591; [4] Voutilainen et al. (2019) Appl. Geochem. 101, 50-61; [5] Drake et al. (2017) Environ. Sci. Technol. 17, 841-844; [6] Schäfer, Dohrmann & Greenwell (2016) CMS workshop lectures: Filling the gaps - From microscopic pore structures to transport properties in shales. The Clay Minerals Society: Vol. 21.

9:00am - 9:15am

### The Mont Terri Project: Research in a generic underground research rock laboratory

**Martin Herfort<sup>1</sup>, David Jaeggi<sup>2</sup>**

<sup>1</sup>Swiss Federal Nuclear Safety Inspectorate ENSI, Switzerland; <sup>2</sup>Federal Office of Topography swisstopo, Switzerland

The Mont Terri Project is an international research project for the hydrogeological, geochemical and geotechnical characterisation of a clay formation (Opalinus Clay) in Switzerland. Clay formations are being considered in various countries for the deep geological disposal of radioactive waste, but are also important as host rocks for carbon dioxide storage or chemical waste, or as cap rocks for oil and gas reservoirs.

The presentation briefly illustrates the history, the structure and the funding of the project. Chances and challenges of the international cooperation of currently 21 partner organisations from Belgium, Germany, France, Japan, Canada, Spain, Switzerland, United Kingdom and the USA are mentioned. Experiments cover different temporal and spacial scales, targeting methods, processes and rock properties. Key results and experiences are shown.

**9:15am - 9:30am**

### **VerSi - A method for comparing repositories for radioactive waste in different host rocks**

**Ingo Kock, Klaus Fischer-Appelt, Martin Navarro**

*GRS gGmbH, Germany*

In Germany, a site selection process for a radioactive waste repository has now started based on the new law for site selection (“Standortauswahlgesetz”). Based on this law, possible host rocks in Germany are rock salt, clay and crystalline rocks. Concepts of repositories for all these host rocks have been developed internationally. Some of these concepts already have been judged as potentially “safe”.

In order to select a site, an unknown number of repository systems in different host rocks will have to be compared. Yet, safety concepts for rock salt, clay or crystalline rocks differ greatly. How will it be possible to compare the safety of repository sites if the underlying safety concepts are so different as between clay stone and rock salt? Is it possible to consider one site or concept as “safer” or “the safest” if all candidate sites have already been identified as safe in terms of the safety requirements?

We have developed a transparent, safety-oriented approach for comparing sites with differing safety concepts in different host rocks. The underlying assumption of the approach is that all sites under consideration have already been identified as potentially safe with regard to the safety requirements. The central idea of the approach is that safety concepts which seem to be fundamentally different remain comparable regarding a very general aspect: All safety concepts rely on the assumption that important safety functions persist during the assessment time frame (e.g. prevention of brine inflow, geomechanical integrity of barriers, sorption, etc.). Thus, safety concepts can be compared with regard to the robustness of their major safety functions.

Main steps of the approach are the identification of component-specific safety functions and their evaluation in terms of relevance and robustness. The robustness of safety functions is evaluated by means of process-level considerations. For this, all kinds of geoscientific aspects (laboratory investigations, modelling, etc.) for various components (geosphere, geotechnical barriers) in a repository have to be considered. Relevance and robustness are linked and correlated in order to show deficiencies and strengths of each repository system with regard to the robustness of its major safety functions.

In principle, this method can be used by scientists and other stakeholders alike. It has already been tested for salt and clay host rocks and in principle also works for crystalline rocks. Currently under development is the implementation of enhancements including the incorporation of components and safety-functions for crystalline host rocks.

**9:30am - 9:45am**

### **Finding a suitable site for a high-level nuclear waste repository - insights into the work of the site selection team at the BGE**

**Julia Onneken, Steffen Jahn, Jennifer Klimke, Sönke Reiche, Paul Richter, Julia Rienäcker-Burschil, Eike Völkner, Wolfram Rühaak**

*BGE mbH, Germany*

The Federal Company for Radioactive Waste Disposal mbH (Bundesgesellschaft für Endlagerung mbH, BGE) is a state-owned company established in September 2016 following the ‘Act on the Organisational Restructuring in the Field of Radioactive Waste Storage’. The Repository Site Selection Act (StandAG) defines the site selection procedure, aiming to ensure the best possible safety for storing high-level radioactive waste in Germany for the duration of one million years.

The selection procedure is a participatory, transparent, learning and self-questioning process and based on scientific evidence. Initially, the whole country is taken into account, without exclusion or predetermination of any possible storage site. The procedure consists of three phases. After each phase the legislator decides about the regions considered in the next step of the site selection process.

The first phase, which is based on a number of exclusion criteria, minimum requirements and geoscientific

weighing criteria, aims to identify a set of suitable regions that will form the basis for further geoscientific exploration. For this purpose, the responsible federal and state authorities provide the necessary data. Until now, we received 340 gigabytes of data, in around a hundred different file types. The BGE reviews, homogenizes, and stores the data into databases. Based on the received data, we now apply – if feasible – six legally defined exclusion criteria, e.g. related to seismicity, volcanic activity or strong vertical uplift. After that, we use the data for identifying regions that fulfil a number of legally defined minimum requirements, e.g. associated with host rock thickness and hydraulic conductivity. As possible host rocks rock salt, claystone and crystalline rock are considered. Based on geoscientific weighing criteria, we finally evaluate the remaining regions with respect to their overall geological eligibility. This selection procedure will lead to a set of regions to be published in the third quarter of 2020 both as a report and, for fulfilling the aim of transparency, as an interactive web portal, where 3D-underground models will show the selected subsurface volumes.

**9:45am - 10:00am**

### **How does burial history influence the petrophysical properties of Jurassic shales? – Implications for radioactive waste storage in the Lower Saxony Basin**

**Eva Maria Hoyer, Reinhard Fink, Björn Kröger, Ralf Littke**

*RWTH Aachen, Germany*

In the scope of the search for an underground nuclear waste storage facility for high-level radioactive waste organic-lean Dogger  $\alpha$  and Lias  $\delta$  mudstones of the Lower Saxony Basin (LSB) in Northern Germany are considered promising targets. These formations experienced vastly different subsidence and uplift as well as temperature and pressure histories, potentially taking influence on petrophysical and geomechanical properties.

This study aims at determining the influence of maturation as a proxy for maximum burial on physical rock properties (elastic moduli, rock strength, porosity, pore structure, thermal conductivity, hydraulic conductivity) of Jurassic mudstones by conducting an analogue study on five cores (0.53 to 1.45%  $VR_r$ ).

Mineralogical and geochemical characterization reveals homogeneity within the formations over the maturity sequence allowing to relate trends observed in petrophysical and geomechanical properties to the influence of thermal maturation. With maturity effective porosity ranges between 5.2 and 11.3% exhibiting a minimum corresponding to oil-window maturity (0.88%  $VR_r$ ). This pore space evolution is found to be related to transformation of organic material and hydrocarbon generation with increasing thermal maturation as a function of organic matter content. A reversed trend is observed in rock strength and elastic moduli with UCS ranging between 26.2 and 40.88 MPa and Young's modulus between 2.14 and 7.09 GPa, indicating that the maturity controlled porosity change influences in turn the rock mechanical behavior.

Areas fulfilling exclusion criteria exist for both Dogger  $\alpha$  and Lias  $\delta$  mudstones within a extremely large maturity range of 0.55 to more than 4%  $VR_r$ . The analogue study demonstrates that thermal maturation influences the petrophysical and rock mechanical properties and hence this effect must clearly be considered in the search for an underground repository in the LSB.

**10:00am - 10:15am**

### **Investigation of porewater in bedrocks – important tools for the geohydrological characterisation and safety assessment of potential deep radioactive waste deposits**

**Florian Eichinger<sup>1</sup>, H. Niklaus Waber<sup>2</sup>**

*<sup>1</sup>Hydroisotop GmbH, Germany; <sup>2</sup>Rock-Water Interaction, Institute of Geological Sciences, University of Bern, Switzerland*

Matrix porewater in the connected inter- and intragranular pore space of low-permeable bedrock interacts with flowing fracture groundwater predominately by diffusion and thus acts as an archive of past changes in fracture groundwater compositions. The amount and composition of porewater in the rock matrix and the

volume of gas dissolved in there is significant and needs to be understood for the long-term safety of future deep repositories for radioactive waste. Based on the slow exchange between matrix porewater and fracture groundwater, matrix porewater acts as an archive of past changes in fracture groundwater compositions and thus of the palaeohydrological history of a site. In context with the assessment of a radioactive waste repository, which should be safe for hundreds of thousands of years, this allows a view back in the past and thus information for the future. Matrix porewater of crystalline and sedimentary bedrock of multiple sites is characterized using the stable water isotopes ( $\delta^{18}\text{O}$ ,  $\delta^2\text{H}$ ), stable chlorine isotopes ( $\delta^{37}\text{Cl}$ ) combined with the concentrations of dissolved chloride, bromide and diverse gas species and their isotope signatures as natural tracers. The comparison of porewater and present-day fracture groundwater tracer compositions gives information about the origin of preserved water components and the climatic conditions during infiltration. An approach of the interaction of porewater and groundwater can be done by taking the water composition and isotope, the bedrock transport properties and the distance between the two reservoirs into account. The results can further be brought into a palaeohydrological context.

**10:15am - 10:30am**

### **Fluid propagation, swelling pressure and cation exchange in sandwich sealing system**

**Katja Emmerich<sup>1</sup>, Klaus Wieczorek<sup>2</sup>, Jürgen Hesser<sup>3</sup>, Matthias Gruner<sup>4</sup>, Christopher Rölke<sup>5</sup>, Ralf Diedel<sup>6</sup>, Thomas Wilsnack<sup>7</sup>, David Jäggi<sup>8</sup>, Franz Königler<sup>1</sup>, Peter Bohac<sup>1</sup>, Rainer Schuhmann<sup>1</sup>**

<sup>1</sup>Karlsruhe Institute of Technology, Germany; <sup>2</sup>GRS Braunschweig; <sup>3</sup>BGR Hannover; <sup>4</sup>TUBAF; <sup>5</sup>IfG Leipzig; <sup>6</sup>SSG Dornburg; <sup>7</sup>IBeWa Freiberg; <sup>8</sup>Swisstopo, Switzerland

As a complement of the geological barrier, geotechnical barriers such as shaft or drift seals are of particular importance in a nuclear waste repository. Concepts of modular shaft sealing systems for German repository models NORTH and SOUTH for claystone formations contain the hydraulic sandwich sealing system as a component of the lower seal in the host rock. The sandwich sealing system consists of alternating layers of bentonite for sealing (DS) and equipotential layers (ES) with higher hydraulic conductivity.

In contrast to monolithic bentonite sealings, ES in sandwich sealing system prevent inhomogeneous liquid transport. Fingering or bypassing water will be evenly distributed within the ES and will build up a new homogeneous potential surface for the following DS. Furthermore, the sandwich sealing system offers the advantage of being perfectly adaptable to the surrounding host rock.

Functionality of the sandwich sealing system has been proved at laboratory and semi-technical scale (HTV) experiments. The next step to implementation is a large-scale in-situ experiment in a natural claystone formation at the Mont Terri rock laboratory.

Various MiniSandwich and HTV experiments were performed with NaCl brine and artificial pore water of Opalinus clay (Pearson water). HMC properties of the bentonite in DS and of ES materials have been monitored during the experiments and determined after dismantling. National Ca-bentonites from Bavaria and Westerwald were compared. Our results show that swelling pressure is not only determined by dry density (or effective montmorillonite dry density (EMDD)) and mineralogical composition, but also by initial hydration state (1W or 2W) of the smectite and cation exchange during hydration. Our results provide high quality database for numerical modelling of processes during saturation of a sandwich sealing system.

The research was supported by German Federal Ministry for Economic Affairs and Energy (02E11587A).

**Wednesday, 25/Sep/2019: 1:00pm - 3:00pm**

**1:00pm - 1:15pm**

### **Numerical modelling of fracture stability of a proposed site for a spent nuclear fuel repository in Forsmark, Sweden**

**Jeoung Seok Yoon<sup>1</sup>, Arno Zang<sup>2</sup>, Ove Stephansson<sup>2</sup>, Carl-Henrik Pettersson<sup>3</sup>, Flavio Lanaro<sup>4</sup>**

<sup>1</sup>DynaFrax UG; <sup>2</sup>Helmholtz Centre Potsdam GFZ German Research Centre for Geosciences; <sup>3</sup>Swedish Radiation Safety Authority; <sup>4</sup>Bergab

In this study, we present a 3D numerical modelling approach applied to the long-term safety assessment of an underground repository for final disposal of spent nuclear fuel. The proposed site is located in a Proterozoic, crystalline basement. The investigation is conducted for the proposed geological repository for spent nuclear fuel in Forsmark, Sweden.

The numerical modelling code used for the analyses is Particle Flow Code 3D (PFC3D), a commercial software developed by Itasca. Based on the site characterization work performed by SKB, a 3D geological model with the major faults and deformations zones was created, as well as the fracture network model of the rock mass generated from site-specific discrete fracture network data.

Using the 3D geological model of the Forsmark site, we investigated fracture stabilities of the proposed repository site under the influence of the: i) thermal load due to the heat generated from the spent nuclear fuel; ii) earthquake events occurring at the faults near to the repository; iii) earthquake events coinciding with the thermal load.

The focus of our analyses is to: i) understand in which conditions fracture slip can occur; ii) estimate the thermally induced fracture slip due to the heat generated from the spent nuclear fuel; iii) estimate the seismically induced fracture slip. We also perform analyses considering the effect of a future glaciation, which influences the stress field at the repository site and results in fault instability.

In our presentation we also discuss how this modelling approach can be applied to a long-term safety assessment for deep geological disposal of high-level radioactive waste in sedimentary formations.

**1:15pm - 1:30pm**

### **First in situ and real time observation of the alteration behaviour of Chernobyl “lava” studied by fluid-cell Raman spectroscopy**

**Mara Iris Lönart<sup>1,2</sup>, Jean-Yves Colle<sup>2</sup>, Philipp Pöml<sup>2</sup>, Jérôme Himbert<sup>2</sup>, Dario Manara<sup>3</sup>, Thorsten Geisler<sup>2</sup>, Boris Burakov<sup>4</sup>**

<sup>1</sup>European Commission, Joint Research Centre, Directorate G – Nuclear Safety and Security, P.O. Box 2340, 76125, Karlsruhe Germany; <sup>2</sup>Institut für Geowissenschaften und Meteorologie, Universität Bonn; <sup>3</sup>European Commission, Joint Research Centre, Via Enrico Fermi, 2749 I - 21027 Ispra (VA) Italy; <sup>4</sup>V.G. Khlopin Radium Institute, 28, 2nd Murinsky ave., 194021, St.Petersburg, Russia

On April 26, 1986, a severe nuclear accident occurred at the 4<sup>th</sup> Unit of the Chernobyl Nuclear Power Plant (ChNPP) accompanied by the full destruction of the reactor core. The initial explosion and fire led to interactions between molten fuel, cladding, and construction materials of the reactor (steel, concrete, sand, serpentinite) forming a highly radioactive silicate-rich corium, so-called Chernobyl “lava” which penetrated into different buildings below the reactor and solidified. In 1990, scientists of the V.G. Khlopin Radium Institute (KRI) in St. Petersburg, Russia, collected samples and discovered secondary phases on the surface of the solidified “lava”, indicating an ongoing chemical alteration. Within an KRI-JRC collaboration agreement several samples were provided to the JRC for further investigation. The laboratory characterization by EPMA and complementary Raman spectroscopic measurements provided significant information about the chemical composition and structure of the “lava” matrix and the various inclusions. In attempts to understand the degradation processes inside the shelter this study focuses on the alteration behaviour of the black “lava” in contact with an alkaline sodium carbonate solution ( $\text{Na}_2\text{CO}_3$ ; pH  $\approx$  11.8; T = 25°C), simulating water inside the ChNPP shelter. For this,

we designed a fluid-cell that enables *in situ* and time resolved Raman imaging without the need of interruption or disturbing the chemical reaction. Already within the first 28 days, the data revealed the formation of a yet unidentified secondary phase, indicating the dissolution of the glass, and/or fuel relics. This unique setup opens up new possibilities to study the kinetics of reaction and transport phenomena involved in the alteration of such complex radioactive material. A single experiment thereby delivers the information of numerous quench experiments with different samples so that complicated samples synthesis and preparation, to be performed in a radiation-protected environment, are minimized and thus also radiation dose of workers and costs. In future research we see a great potential for optimizing the development and application of the experimental method, i.e. for the performance of alteration experiments with fuel debris formed during the accident at Fukushima.

## Poster Presentations

Tue: 56

### SpannEnD – Modelling the 3D stress state of Germany

**Steffen Ahlers<sup>1</sup>, Luisa Röckel<sup>2</sup>, Andreas Henk<sup>1</sup>, Karsten Reiter<sup>1</sup>, Tobias Hergert<sup>1</sup>, Birgit Müller<sup>2</sup>, Frank Schilling<sup>2</sup>, Oliver Heidbach<sup>3</sup>, Sophia Morawietz<sup>3</sup>, Magdalena Scheck-Wenderoth<sup>3</sup>, Denis Anikiev<sup>3</sup>**

<sup>1</sup>Institut für Angewandte Geowissenschaften, TU Darmstadt, Germany; <sup>2</sup>Institut für Angewandte Geowissenschaften, KIT, Karlsruhe, Germany; <sup>3</sup>Deutsches GeoForschungszentrum (GFZ), Potsdam, Germany

One important criterion for the characterization of a potential deep geological repository for nuclear waste is the crustal stress field. However, stress data are sparse and usually incomplete regarding the six independent components of the stress tensor. The World Stress Map (WSM) is a valuable compilation of stress data, but it does not include information about stress magnitudes as only the orientation of the maximum horizontal stress ( $S_{Hmax}$ ) is provided. To receive a comprehensive and continuous 3D description of the stress field in a particular area, geomechanical-numerical modelling is required. Key objectives of the SpannEnD project (Spannungsmodell Endlagerung Deutschland) is to provide such a model for Germany and to develop methods for robust stress predictions at the local scale.

The SpannEnD model is based on finite element techniques and comprises a 3D lithosphere-scale structural model of Germany. The lateral extent of the model covers a pentagon-shaped area of Central Europe with dimensions of 1000 x 1250 km<sup>2</sup>. The model has been chosen significantly larger than Germany to reduce boundary effects in the study area. Furthermore, on the base of the observed stress orientation pattern, the boundaries have been defined parallel or perpendicular to the known orientation of  $S_{Hmax}$  to simplify the definition of the boundary conditions. The vertical extent of the model is from the surface to a depth of 100 km, incorporating several sedimentary layers, several basement units and the Mohorovičić discontinuity. The mesh is laterally homogenous with a resolution of about 2 km and vertically inhomogeneous with a decreasing resolution with increasing depth, to provide the finest mesh in the layers of the greatest interest, near the surface. These units also provide the most stress data measurements to calibrate the model. Furthermore, a selected number of important faults is implemented in the model. This structural model is discretized into about 7 million elements. For the calibration of the model we use a new compilation of stress magnitude data (see poster of Morawietz et al.). We present the workflow, the model geometry, and some first results.

Tue: 57

### Application of High Performance Computing to evaluate effects of system heterogeneity in coupled reactive transport simulations at various scales

**Guido Deissmann<sup>1</sup>, Paolo Trincherò<sup>2</sup>, Jorge Molinero<sup>2</sup>, Aitor Iraola<sup>2</sup>, Ignasi Puigdomenech<sup>3</sup>, Björn Gylling<sup>4</sup>, Dirk Bosbach<sup>1</sup>**

<sup>1</sup>Forschungszentrum Jülich GmbH, Jülich, Germany; <sup>2</sup>Amphos21 Consulting, Barcelona, Spain; <sup>3</sup>Svensk Kärnbränslehantering AB (SKB), Stockholm, Sweden; <sup>4</sup>Gylling GeoSolutions, Evanston, USA

Deep geological disposal facilities (GDF) for high-level nuclear waste are based on multi-barrier concepts, combining an engineered barrier system with a suitable repository host rock. The potential migration of

radionuclides from a GDF into the geo-/biosphere occurs mainly via water pathways, after the waste comes into contact with groundwater, subsequent to failure of the waste canisters. The long-term evolution of the geochemical conditions in a geological repository system, the release of radionuclides from the emplaced waste, and the radionuclide migration behaviour in the repository near- and far-field are governed by various strongly coupled thermo-hydraulic-mechanical-chemical-biological (THMCB) processes. The radionuclide and solute transport driven either by diffusion and/or advection involves multi-phase flow phenomena under spatially- and time-variable hydraulic and geochemical gradients. The transport phenomena are affected by various complex reactions including dissolution, (co)precipitation and adsorption, and redox processes, which may be partly induced and catalysed by microbial activity. For rigorous comparative analyses of geological repository systems, a thorough understanding and close to reality description of the coupled THMCB processes that affect the radionuclide transport on different time and length scales is required, including an understanding of the effects introduced by process couplings and system heterogeneity.

In-situ and laboratory investigations provided manifold evidence of the highly heterogeneous nature of crystalline rocks on various scales, for example, with respect to microstructure, distribution of available (reactive) mineral surfaces, or fracture networks. In this presentation, we discuss the application of reactive transport simulations using (micro-)continuum models to analyse the effects of heterogeneities in crystalline rocks on processes affecting subsurface radionuclide migration, from the (sub-millimetre) grain scale to the repository scale. Radionuclide retardation by sorption processes or solid solution formation, and redox buffering by Fe(II)-bearing minerals against the ingress of oxygenated glacial meltwaters are used as examples. Due to the high computational demands, these simulations were performed on the supercomputers JUQUEEN and JURECA at the Jülich Supercomputing Centre, using the massively parallel reactive transport code PFLOTRAN. The results of these simulations contribute to a refined understanding of the effects of system heterogeneities on key processes controlling the geochemical evolution and radionuclide migration in the subsurface. Moreover, they may serve as a starting point for the development of approaches to represent system heterogeneity on multiple scales and for upscaling strategies for larger-scale reactive transport models, thus providing a more realistic view on the evolution of repository systems.

**Tue: 58**

### **Method development for pore water extraction from consolidated clays: optimization for dissolved short-chain organic acids**

**Oliver Helten, Sandra Schumacher, Christian Ostertag-Henning**

*Federal Institute for Geosciences and Natural Resources, Hannover, Germany*

Pore water from clayrich sediments and claystones is subject of ongoing research in diverse fields of modern geosciences, covering topics such as biogeochemical processes in the Deep Biosphere, or radioactive waste management. For the latter, claystones are among the investigated host rocks for radioactive waste disposal strategies. In this context, dissolved polar organic molecules in the pore water of claystones or shales are considered as potential complexing agents for radionuclides. As such, they may have an influence on radionuclide solubility and, thereby, their mobility in pore water and the host rock formation. One subclass of the dissolved organic compounds are the short-chain organic acids in the range of  $C_1$  to  $C_5$ , which are ubiquitous organic components in the natural environment. They are products of microbial organic matter degradation, represent a microbial carbon source, and can also be formed abiotically through organic matter oxidation. When subjected to increasing thermal stress, short-chain organic acids can decompose to gases such as  $CO_2$ . Here, we present a new approach to access the short-chain organic acid pool in pore water from consolidated claystone, employing a triaxial cell for pore water squeezing. A preconditioned 200 mm long wholeround core ( $d = 97$  mm, 3.6 kg) of Opalinus Clay from the Swiss Underground research facility in Mont Terri was subjected to increasing confining pressure of up to 60 MPa, as well as additional axial load. Inorganic geochemists have successfully used similar approaches in order to obtain pore water samples from consolidated claystone (Fernandez et al., 2014)<sup>[1]</sup>.

Within the first six weeks of the ongoing squeezing experiment, the pressure in the receiving reservoir in-

creased by more than 0.2 MPa by expulsion of pore water and gases. In the long run, the application of this pore water squeezing technique shows great potential for further experiments. For instance, *in-situ* heated Opalinus Clay from a heater test (experiment HE-F) in the Mont Terri underground rock laboratory is planned to be tested to quantify changes in composition of pore water, e.g. short-chain organic acids. The here described approach will give us new insights regarding (bio-) geochemical processes in subsurface environments relevant for radioactive waste disposal and, potentially, other geoscientific fields of application.

[1] Fernández, A., et al. (2014). "Applying the squeezing technique to highly Consolidated clayrocks for pore water characterisation: Lessons learned from experiments at the Mont Terri Rock Laboratory." *Applied Geochemistry* 49: 2-21.

**Tue: 59**

### Transmission X-ray microscopy as a novel tool to study corroded silicate waste glasses

**Martin Kutzschbach<sup>1</sup>, Max Wilke<sup>2</sup>, Peter Guttman<sup>3</sup>, Katharina Marquardt<sup>4</sup>**

<sup>1</sup>*Technische Universität Berlin, Institut für Angewandte Geowissenschaften, Fachgebiet Angewandte Geochemie, Germany;* <sup>2</sup>*Universität Potsdam, Institut für Geowissenschaften, Germany;* <sup>3</sup>*Helmholtz-Zentrum Berlin, Research Group X-ray Microscopy, Germany;* <sup>4</sup>*Imperial College London, Faculty of Engineering, Department of Materials, United Kingdom*

Vitrification is a common approach for a safe long-term disposal of nuclear waste. However, once exposed to aqueous solutions, waste glasses corrode and radioactive elements are eventually re-mobilized. The dynamics of this process is largely controlled by the (much-debated) formation of surface altered layers (SAL) between pristine glasses and the weathering agent. Hence, knowledge of the morphology, chemistry and molecular structure of the SAL is an integral part of a reliable risk assessment.

X-ray microscopy (TXM) is tested as a novel analytical tool to access these parameters. For this purpose two different silicate glasses with the atomic proportions  $\text{Na}_{0.14}\text{Ca}_{0.74}\text{Mg}_{0.38}\text{Al}_{2.10}\text{Si}_{1.83}\text{O}_8$  (Ab15) and  $\text{Na}_{1.35}\text{K}_{0.02}\text{Ca}_{0.28}\text{Mg}_{0.32}\text{Al}_{0.06}\text{Si}_{3.31}\text{O}_8$  (TG) were altered in static corrosion experiments for 1h (Ab15) and 192h (TG) at temperatures of 85°C (Ab15) and 60°C (TG). Thin foils were cut perpendicular to the surface of the corroded glasses with a focused ion beam mill.

It is shown that TXM enables nanometer spatial resolution while circumventing irradiation damage, which commonly occurs during conventional transmission electron microscopy.

The thickness of the SAL is determined from optical density profiles at photon energies around the Na and O K-edges and varies between 130nm (TG) and 350nm (Ab15), while the contrast transition from the SAL to the pristine is significantly broader in the TG compared to the Ab15 glass. Based on O K-edge X-ray absorption near-edge spectra (XANES) it is shown that the Ab15 SAL is marked by an increase in siloxane bonds compared to the pristine glass, a feature which has not been detected in the corroded TG glass.

These observations point to an inter-diffusion process for the generation of the SAL in the TG glass, whereas the formation of the SAL in the Ab15 glass is best explained by a dissolution/precipitation mechanism. This suggests the coexistence of the two yet competing conceptual models for the SAL formation.

**Tue: 60**

### A unifying mechanistic model for borosilicate glass corrosion

**Christoph Lenting<sup>1,3</sup>, Moritz Bernd Karl Fritzsche<sup>2,3</sup>, Lars Dohmen<sup>2,3</sup>, Christine V. Putnis<sup>4</sup>, Matt Kirlburn<sup>5</sup>, Paul Guagliardo<sup>5</sup>, Oliver Plümper<sup>6</sup>, Martina Klinkenberg<sup>7</sup>, Thorsten Geisler<sup>2</sup>**

<sup>1</sup>*Institut für Geologie und Mineralogie, Uni Köln, Germany;* <sup>2</sup>*Schott AG, Germany;* <sup>3</sup>*Institut für Geowissenschaften, Uni Bonn, Germany;* <sup>4</sup>*Institut für Mineralogie, Uni Münster, Germany;* <sup>5</sup>*CMCA, UWA, Perth, Australia;* <sup>6</sup>*Department of Earth Sciences, Utrecht University, The Netherlands;* <sup>7</sup>*IEK-6, Forschungszentrum Jülich, Germany*

Borosilicate glasses are currently used for the immobilization of highly radioactive waste and are materials of choice for many biomedical and research industries. Nevertheless, glass is metastable and alters in contact with aqueous solutions, resulting in the formation of a complex surface alteration layer (SAL).

Until now, there is no consensus in the scientific community about the reaction and transport mechanism(s) and the rate-limiting steps involved in the corrosion of silicate glasses. Most models have the basic assumption in common that ion release from the glass network is occurring via interdiffusion and that the glass network itself is not being disrupted, only modified. On the contrary stands the interface-coupled dissolution-precipitation (ICDP) model, which first was developed for mineral replacement reactions and was recently adapted to glass corrosion. It is based on the congruent dissolution of the glass network that is spatially and temporally coupled to the precipitation and polymerization of silica, forming the amorphous corrosion rim.

Here, we present a unifying model considering surface charge effects and pH gradients within the solution boundary layer, interdiffusion, and the formation of amorphous silica based on principles of sol-gel chemistry. The focus is on the detailed description of the different reactions, transport processes and their interdependence to identify the rate-limiting reaction steps and feedback effects.

We show that most phenomena observed in experiments and nature can be well explained by an ICDP model. However, a pure ICDP mechanism is not able to explain all phenomena of glass corrosion. When the dissolution and precipitation reactions are slowed down, interdiffusion processes within the pristine glass ahead the ICDP front may start, which is also considered in the unifying model.

The corrosion of a radionuclide-binding glass matrix is naturally a sensitive issue for the safe disposal of vitrified high-level nuclear waste. A sound description of the reaction mechanisms and the identification of the rate-limiting steps is essential to predict the long-term corrosion of silicate glasses, particularly when time scales must reach several thousand to millions of years as required by safety regulations for a nuclear repository.

**Tue: 61**

### Would you like stress?

**Sophia Morawietz<sup>1</sup>, Oliver Heidebach<sup>1</sup>, Karsten Reiter<sup>2</sup>, Moritz Ziegler<sup>1</sup>, Team SpannEnD<sup>1,2,3</sup>**

<sup>1</sup>Helmholtz-Zentrum Potsdam Deutsches GeoForschungsZentrum GFZ, Germany; <sup>2</sup>TU Darmstadt, Institut für Angewandte Geowissenschaften; <sup>3</sup>KIT - Karlsruher Institut für Technologie, Institut für Angewandte Geowissenschaften

The crustal stress field plays a central role in the characterization of a deep geological repository (DGR) for nuclear waste. During the site selection, construction and storage as well as in view of the long-term stability of such a repository, factors which are influenced by the stress state must be considered. Those include the excavation damage zone, hydraulic permeability of the host rock, the self-sealing ability, the impact of seismic events, or the potential reactivation of faults as migration paths for fluids and radionuclides. Therefore, the estimation of the current stress distribution in the upper 1000 m of the subsurface is indispensable in the comparative assessment of potential DGR sites. However, the available point-wise stress data information is usually incomplete, since most of the stress indicators do not allow to derive the complete 3D stress tensor. Thus a continuous and complete description of the 3D stress state can only be estimated with a 3D geomechanical-numerical model that is calibrated using existing stress information. Yet, due to the general low stress data density, a model calibration on the scale of a DGR model is not feasible. On this account, the main goal of the project “SpannEnD” (*Spannungsmodell Endlagerung Deutschland*, Stress Model Final Deposition Germany) is the development of a 3D geomechanical-numerical model for Germany. This will provide initial stress conditions for regional and local models in a later stage of the DGR site selection process. With the World Stress Map (WSM), there is already a database of stress orientations, but since the difference between the minimum and maximum principal stress magnitude is of central importance to assess the underground stability, stress magnitude data are essential. As a basis for the calibration of geomechanical-numerical models, it is therefore crucial to compile stress magnitude data and weight them according to their reliability and informative value. A successfully calibrated model enables a prognosis for areas without any stress information. However, such a model requires reliable input data for the calibration of stress magnitudes. Here, we present the first comprehensive and publicly available stress magnitude database for Germany including a data quality ranking. The compilation strategy and data quality assessment scheme is intended to be a template for an implementation within the framework of the World Stress Map project ([www.world-stress-map.org](http://www.world-stress-map.org)) at a global scale.

## 9) The geological signatures of natural hazards and extrem events

### 9a) Natural Hazards like earthquakes, landslides, floods and sea-level changes

Monday, 23/Sep/2019: 9:00am - 10:30am

Session Chair: Silke Mechernich (Bundesanstalt für Gewässerkunde)

Session Chair: Heinrich Bahlburg (WWU Münster)

Session Chair: Anna Pint (Institute of Geography, Universität zu Köln)

Location: Schlossplatz 7 Hof: SP 7

#### Session Abstract

Natural hazards have always occurred in the Earth system and need to be evaluated cautiously in space (local, regional, global), time (duration, date), intensity and recurrence interval. All hazards require wide process knowledge to evaluate future impacts, and include global sea-level rise, marine and subaerial mass-movements, storms, tsunamis, earthquakes, and pyroclastic processes. To fully evaluate these processes, the considered time scales range from seconds to millennia.

We ask for contributions of natural hazard studies that recognize, evaluate and eventually manage past and future hazards affecting Earth and society. Interdisciplinary case studies as well as theoretical, analogue and numerical methods are explicitly invited.

#### Lecture Presentations

9:00am - 9:30am *Hermann-Credner-Award 2019*

#### **Paleoseismology in continental interiors and seismic hazard assessments - what have we learned?**

**Christoph Grützner**

*Friedrich Schiller University Jena, Institute of Geological Sciences, Germany*

In continental interiors, the recurrence intervals of earthquakes on any given fault are usually much longer than the time span covered by instrumental and historical earthquake records. This is a problem not only for studying the tectonics of these areas, but also for hazard analyses. Paleoseismology helps to extend the record for strong, surface-rupturing earthquakes, and has thus contributed significantly to our understanding of seismic activity in slowly-deforming regions. In this talk I discuss examples from three different regions and what we have learned from paleoseismological research. The Lower Rhine Embayment in Germany is an example for a continental rift with very low extension rates; the Tien Shan in Central Asia is a natural laboratory for studying shortening far away from the India-Eurasia collision; and Western Slovenia hosts a set of parallel strike-slip faults that accommodate the relative motion of the Adriatic Plate with respect to Europe. In all these regions, recent paleoseismological studies have revealed geological evidence for strong earthquakes that happened up to tens of thousands of years ago. Each site, however, comes with its own limitations and problems, which I highlight in this presentation.

**9:30am - 10:00am Session Keynote****Recent advances in qualitative and quantitative lacustrine paleoseismology****Maarten Van Daele<sup>1</sup>, Jasper Moernaut<sup>2</sup>, Marc De Batist<sup>1</sup>**<sup>1</sup>*Ghent University, Belgium;* <sup>2</sup>*Innsbruck University, Austria*

During the last decade considerable progress has been made in the field of lacustrine paleoseismology. On several locations it is now possible to not only recognize earthquake-triggered deposits (mostly turbidites), but also get a sense of the macroseismic intensity and even type of earthquake. Here, we present a summary of our recent advances in lakes on subduction zones, where due to the large depth of the earthquakes, lacustrine paleoseismic records are key to obtain a complete and accurate paleoseismic history. In Eklutna Lake (south-central Alaska), we compare turbidites triggered by a recent (2018) intraslab earthquake causing macroseismic intensities of V-V½ at the lake, with those triggered by the 1964 megathrust earthquake (VI½). While the latter triggered turbidity currents on both deltaic slopes and slopes covered with hemipelagic sediments, the V-V½ shaking only triggered failures on deltaic slopes. These results confirm earlier observations in south-central Chilean piedmont lakes that deltaic slopes have lower intensity thresholds at which turbidites can be triggered (~V½) compared to hemipelagic slopes (~VI½) (Moernaut et al., 2014). Moreover, detailed analysis of ‘hemipelagic’ turbidites in these Chilean lakes revealed that most of them are formed by remobilization of only a thin veneer (~5 cm) of slope sediments and do not result from disintegration of shaking-induced subaquatic landslides (Moernaut et al., 2017). As a (indirect) result, the turbidites’ spatial extent and thickness are related to local macroseismic intensities, and a multilake transect of such records – over distances of tens to hundreds of kilometers – allows to estimate magnitudes, rupture locations and extent of past subduction earthquakes in south-central Chile (Moernaut et al., 2014). Furthermore, also for other types of lakes a positive relationship between turbidite occurrence and macroseismic intensity exists, as a compilation from 17 Chilean lakes shows a linear relationship between macroseismic intensity and number of turbidites (Van Daele et al., 2015). However, when comparing earthquakes from different source fault systems, such as megathrust, intraslab and crustal earthquakes, turbidite-shaking relationships may become more complex. In Laguna Lo Encañado (central Chilean Andes) the prolonged shaking of megathrust earthquakes results in more voluminous co-seismic turbidites than those triggered by intraplate earthquakes, even though macroseismic intensities are not significantly different (Van Daele et al., 2019). On the other hand, the higher source frequency spectrum of intraplate earthquakes causes preferential failure of onshore rocky slopes, as the high frequency waves are less attenuated in rock than in soft sediment. Hence, – in this setting – contrarily to megathrust earthquakes, intraplate earthquakes also trigger rock slides in the lake’s catchment, which result in post-seismic turbidites that cover the co-seismic turbidite in the lake’s sedimentary record. The detailed sedimentological analysis of turbidites triggered by historical earthquakes allows to calibrate the lake records, which can now be exploited as accurate paleoseismic records.

[1] Moernaut, J., Van Daele, M., Heirman, K., Fontijn, K., Strasser, M., Pino, M., Urrutia, R., De Batist, M., 2014. Lacustrine turbidites as a tool for quantitative earthquake reconstruction: New evidence for a variable rupture mode in south central Chile. *Journal of Geophysical Research: Solid Earth* 119, 1607-1633. doi: 10.1002/2013JB010738; [2] Moernaut, J., Van Daele, M., Strasser, M., Clare, M.A., Heirman, K., Viel, M., Cardenas, J., Kilian, R., Ladrón de Guevara, B., Pino, M., Urrutia, R., De Batist, M., 2017. Lacustrine turbidites produced by surficial slope sediment remobilization: A mechanism for continuous and sensitive turbidite paleoseismic records. *Marine Geology* 384, 159-176; [3] Van Daele, M., Moernaut, J., Doom, L., Boes, E., Fontijn, K., Heirman, K., Vandoorne, W., Hebbeln, D., Pino, M., Urrutia, R., Brümmer, R., De Batist, M., 2015. A comparison of the sedimentary records of the 1960 and 2010 great Chilean earthquakes in 17 lakes: Implications for quantitative lacustrine palaeoseismology. *Sedimentology* 62, 1466-1496; [4] Van Daele, M., Araya-Cornejo, C., Pille, T., Vanneste, K., Moernaut, J., Schmidt, S., Kempf, P., Meyer, I., Cisternas, M., 2019. Distinguishing intraplate from megathrust earthquakes using lacustrine turbidites. *Geology* 47, 127-130. doi: 10.1016/G45662.1; [5] Van Daele, M., Haeussler, P., Witter, R., Praet, N., De Batist, M. (in prep). The 2018-Anchorage-earthquake turbidite in Eklutna Lake (south-central Alaska): a new calibration point for the lacustrine natural seismograph. *Seismological Research Letters*.

10:00am - 10:15am

**Palaeoseismic structures in Quaternary sediments of Hamburg (NW Germany)****Alf Grube***Geologisches Landesamt Hamburg, Germany*

North Germany is generally regarded as a low seismic area (Leydecker 2011). Magnitudes of documented earthquakes are predominantly smaller  $M=4$ ; there is generally a lack of evidence for moderate to strong earthquakes. Earthquakes are recorded back to 800 AD, Information about prehistoric earthquakes in Quaternary sediments is but scarce. Investigations at several construction sites in Hamburg-Wandsbek (NW Germany) exposed assumed palaeoseismic structures from moderate to strong earthquakes. Soft-sediment deformation structures are mainly found in the glaciolacustrine fine-grained sediments, neighbouring glaci-tectonically-deformed till areas. The documentation includes large clastic dykes, blowout-related infill-structures, special forms of diapirs, a wide range of seismites (seismically induced soft-sediment deformation structures) and special forms of flame structures. The observed structures show certain characteristics that allows differentiating them from non-seismic structures. Based on the large size of large blowout clastic dykes being up to 3.5 m wide and 3.5 m high, erratics/rafts of up to 9 kg in weight, seismites and decimetre-scale seismoslumps, the magnitude of the earthquakes could be in the order of up to  $M \geq 6$ .  $^{14}\text{C}$  ages from organic material from blowout-related infill bowls reveal ages between 31,500 and 1,200  $^{14}\text{C}$  cal a BP.

[1] Grube, A. (2019): Palaeoseismic structures in Quaternary sediments of Hamburg (NW Germany), earthquake evidence during the younger Weichselian and Holocene. – *International Journal of Earth Sciences* 108 (3): 845–861. <https://doi.org/10.1007/s00531-019-01681-2>; [2] Leydecker G (2011) Erdbebenkatalog für Deutschland mit Randgebieten für die Jahre 800 bis 2008. - *Geologisches Jahrbuch* E59:1-198.

10:15am - 10:30am

**Modeling the Holocene slip history of the Wasatch fault (Utah): Coseismic and postseismic Coulomb stress changes and implications for paleoseismicity and seismic hazard****Meike Bagge<sup>1,2</sup>, Andrea Hampel<sup>1</sup>, Ryan D. Gold<sup>3</sup>**<sup>1</sup>*Leibniz Universität Hannover, Germany;* <sup>2</sup>*Helmholtz-Zentrum Deutsches GeoForschungsZentrum (GFZ), Germany;*<sup>3</sup>*U.S. Geological Survey, 1711 Illinois Street, Golden, Colorado 80401, USA*

The Wasatch fault zone defines the eastern boundary of the actively extending Basin and Range Province (Utah, western United States) and poses a significant seismic hazard to the metropolitan areas along the Wasatch Range. A wealth of paleoseismological data documents  $\sim 24$  surface-rupturing  $M_w \geq 7$  earthquakes along the Wasatch fault during the past 6400 yr. Here, we simulated the Holocene earthquake sequence on the Wasatch, Oquirrh–Great Salt Lake, and West Valley faults using three-dimensional finite-element forward modeling with the goal to calculate coseismic and postseismic Coulomb stress changes and to evaluate the slip and magnitude of hypothetical present-day and future earthquakes (Bagge et al., *GSA Bull.*, 2019). Our results show that a good fit between modeled and observed paleoevents and time-integrated slip rates can be achieved within the uncertainties of the paleoseismological record and model parameters like the fault geometry. The Coulomb stress change analysis for selected paleoearthquakes showed that maximum positive stress changes are induced on faults located along strike of the source fault, while faults parallel to the source fault are generally located in stress shadow zones. Postseismic viscoelastic relaxation considerably modifies the coseismic stress changes; the resulting transient stress changes are recognizable for more than 100 yr after an earthquake. The modeled present-day state of Coulomb stress changes shows that the Brigham City, Salt Lake City, and Provo segments of the Wasatch fault are prone to failure in a  $M_w \geq 6.8$  earthquake. Our study shows that simulation of an entire earthquake sequence based on a paleoseismological record is feasible and facilitates identification of possible gaps and inconsistencies in the paleoseismological record. Therefore, forward modeling of earthquake sequences may ultimately contribute to improved seismic hazard estimates.

**Monday, 23/Sep/2019: 11:15am - 1:00pm**

**11:15am - 11:45am Session Keynote**

### **The geological legacy of typhoons in the Philippines**

**Max Engel**

*Royal Belgian Institute of Natural Sciences, Belgium*

The Philippines are exposed to some of the most violent tropical cyclones on Earth and future projections anticipate an increase in the frequency of the most intense typhoons in the NW Pacific basin. On 8 November 2013, Typhoon Haiyan made landfall on the Philippines reaching sustained velocities of up to 315 km h<sup>-1</sup> and gusts of up to 380 km h<sup>-1</sup>, creating a massive storm surge of up to 9 m above tide level. Across the Central Visayas archipelago, Haiyan caused more than 6000 casualties, affected more than 16 million people, and damaged more than 1 million houses. This paper presents the sedimentary and geomorphic impacts of this supertyphoon on a range of different coastal environments along a W–E transect from the island of Samar to Panay. Typical geomorphic patterns comprise horizontally and cross-bedded washover fans very close to the shore as well as intertidal coral-rubble ridges where the storm surge was simply accompanied by gravity waves. Onshore sand sheets reaching much further inland for c. 100–250 m or the transport of massive boulders of up to 170 t occurred only where the impact was amplified through seiche effects in shallow embayments, as near Tacloban on Leyte, or localized infragravity waves, as on SW Samar. The findings in general confirm facies models aiming at differentiating between storm wave and tsunami deposition along coasts worldwide but also show that localized non-linear hydraulic processes during strong storms may create patterns usually associated with tsunami deposition. Outside the tracks of the recent supertyphoons, boulder fields with clasts significantly larger as those transported by Haiyan dated to the late Holocene and indicating a stepwise formation testify to high-magnitude predecessors of Haiyan and a prevailing hazard of massive coastal inundation for the communities of Eastern Samar.

**11:45am - 12:00pm**

### **The varved sediment package of the Great Blue Hole, Lighthouse Reef, Belize (Central America), a high-resolution archive of Atlantic hurricane activity throughout the entire Common Era**

**Dominik Schmitt<sup>1</sup>, Eberhard Gischler<sup>1</sup>, Flavio Anselmetti<sup>2</sup>, Hendrik Vogel<sup>2</sup>, Jörn Peckmann<sup>3</sup>, Daniel Birgel<sup>3</sup>**

*<sup>1</sup>Institut für Geowissenschaften, J.W. Goethe-Universität, Altenhöferallee 1, 60438 Frankfurt am Main, Germany;*

*<sup>2</sup>Institut für Geologie & Oeschger Centre for Climate Change Research, Universität Bern, Baltzerstraße 1+3, 3012 Bern, Switzerland; <sup>3</sup>Institut für Geologie, Universität Hamburg, Bundesstraße 55, 20146 Hamburg, Germany*

Based on instrumental climate data of the Atlantic Ocean, the strength and destructiveness of tropical cyclones seem to be increasing dramatically in the 20<sup>th</sup> century. Tropical cyclones (TC) represent a substantial threat to life and property, especially for the population of Caribbean developing countries. Therefore, it is imperative to gain a better understanding about the origin and nature of long-term patterns of hurricane activity. In addition to socio-economical, there are also obvious scientific reasons to extend the tropical storm database far beyond available instrumental time-series. High-resolution storm archives in the Caribbean realm are generally rare, incomplete and, in parts, controversial. We report on a detailed sedimentary marine proxy record from the western Caribbean Basin that possesses annual resolution of individual TC-strikes over the entire Common Era (2000 years). The undisturbed sediment succession at the floor of the Great Blue Hole of Lighthouse Reef offshore Belize comprises fine-grained, varved sediments and intercalated coarser sandy event beds represented by a combination of fair-weather background sedimentation and TC-strike event layers. This new 8.5 m long sediment record offers the opportunity to analyze annually resolved Caribbean cyclone activity and climate back to CE 0. Our data suggest that rising and falling sea-surface temperatures (SST) play a major role for long-term cyclic shifts in hurricane activity. In particular, there is a general

increasing trend of hurricane frequency and intensity from CE 0 to modern times, which is consistent with changes in Late Holocene climate (e.g. Medieval Climate Optimum, Little Ice Age, Modern Global Warming). It is striking that anthropogenically triggered industrial climate change is -in terms of long-time hurricane activity- characterized by an amplification of the natural long-term trend. With our multi-proxy approach we are able to show a strong connection between changing hurricane activity and absolute sea-surface water temperature by means of  $\text{TEX}_{86}$  SST reconstruction. Wavelet analysis of our proxy data ( $\delta^{18}\text{O}$ ,  $\text{TEX}_{86}$ , event layer thickness and event layer frequency), indicate a multidecadal (56 year) pattern of hurricane activity during the Common Era. This prominent cycle is detectable as far back as CE 200 and may be correlated with natural multidecadal variations of ocean circulation (e.g. Atlantic Multidecadal Oscillation AMO).

**12:00pm - 12:15pm**

## **Tsunami hazard under rising sea levels and other climate change impacts**

**Robert Weiss**

*Virginia Tech, United States of America*

Assessing the future tsunami hazard is important for the socio-economic wellbeing of coastal communities. Planning of mitigation measures requires quantitative analysis of future states. This is a complex task because sea levels are rising as an effect of climate change, but also other climate-change impacts can have significant impact on the coastal systems. Given that tsunami in any given region can have a low occurrence or exceedence probability, a meaningful temporal scope for assessing the future tsunami hazard spans several decades to centuries. However, such long time intervals suffer from large uncertainties of the quantitative understanding of future climate-change impacts, such as sea-level rise.

If at all included, sea-level rise usually is included in form of the bathtub approach, which simply changes the position of the shoreline as the sea level rising or falling. However, coastal system systems can undergo significant changes on decade to century-long time scales. In this contribution, I investigate the difference in the tsunami hazard from 2000 to 2100 given projected sea-level changes and assumed temporal evolution of other climate-change impacts. I chose the barrier-island/marsh/lagoon/marsh (BLM) system because there is evidence that the BLM system may exhibit significant changes with the time scales of a century.

I consider different sea-level rise scenarios based on the Representative Concentration Pathways (RCP) scenarios 2.6 and 8.5. It should be noted that RCP 2.6 is the target of the Paris Accord, but it seems that climate change is more likely to track along the RCP 8.5 scenario. For both RCP scenario, I employ the bathtub approach to change the water level in the BLM system (hereafter referred to as static conditions), but also employ a model that allows for dynamic responses of the BLM system to sea-level change and other climate impacts (hereafter referred to as dynamic conditions).

The main result is that the bathtub approach consistently underestimates the future tsunami hazard in all percentiles, but especially in the extremes. Further, it seems that the sea level itself is not major factor that creates the stark difference in tsunami hazard between the dynamic and static condition. Other climate change impact have a more significant impact, and those climate change impacts are much less well understood and studied.

**12:15pm - 12:30pm**

### **Precursors and processes culminating in the Anak Krakatau December 2018 sector collapse and tsunami**

**Thomas Walter**

GFZ, Germany

It is 135 years after the 1883 volcano-triggered tsunami disaster, when Krakatau volcano became once more the source of a deadly tsunami striking without warning. We use data recorded on the ground and by satellite, to show that the volcano was in an elevated stage of activity throughout the year 2018, producing thermal anomalies associated with volcanic deposits, an increase of the island area and ground movement of the southwestern sector of the island towards the sea, increasing in June 2018. Following further intense activity on 22 December 2018, seismic data reveal the timing and duration when this sector collapsed. The landslide removed 102 million m<sup>3</sup> of material subaerially, which was followed by ~15 minutes of phreatic explosions. This study allows better understanding of the complex hazard cascades, including precursory thermal anomalies, island growth and deformation, followed by sector collapse, tsunami waves, and finally explosive volcanic eruptions, and has important implications for designing early warning systems.

**12:30pm - 12:45pm**

### **Project “Mass Movements in Germany (MBiD)”: A methodical approach for surveying areas prone to shallow translational landslides at regional scale.**

**Michael Fuchs<sup>1</sup>, Stefan Glaser<sup>2</sup>**

<sup>1</sup>Bundesanstalt für Geowissenschaften und Rohstoffe, Hannover; <sup>2</sup>Bayerisches Landesamt für Umwelt, Augsburg

Concerned State Geological Surveys of the Federal States (SGD) and the Federal Institute for Geosciences and Natural Resources (BGR) are currently collaborating in a joint engineering-geological hazard related project. This project, called “Mass Movements in Germany (MBiD)” is aimed to verify internationally acknowledged procedures to assess the regional landslide susceptibility and their applicability in Germany. Taking into account statistical, empirical and deterministic approaches the project illuminates necessary information requirements and constraints exemplified in pilot areas. Based on the project findings it is intended to provide practical recommendations for future landslide “hazard” studies in Germany.

Due to the lack of necessary physical input parameters, the deterministic susceptibility modeling at a smaller scale represents a special challenge. The essential point of the presented approach is the calculation of the factor of safety ( $f_s$ ) to be used to determine the failure probability. This probability featured by  $f_s$  less or equal one is more valid to recognize areas susceptible to shallow translational slides indicated by so-called “Hanganbrüche”.

The physical input parameters like *bulk density*, *angle of internal friction*, and *effective cohesion* can be gained by applying pedotransfer functions. In addition to any delineated soil legend element, soil maps at different scales provide respective soil unit profiles consisting of stacked soil horizons. The description of the soil horizons contains standardized information about the soil texture performing a link for the physical parameterization. However, the input parametrization refers not only to the parameters but also to their standard deviation depending on the scale and aggregation level of the respective soil map. Quasi-homogenous condition units serve as model input parameterized by slope angle, physical properties and their deviations.

In a pilot area situated in southern Bavaria the performance of this procedure was tested. In the year 2016, torrential rainfall affected the hilly terrain around the city of Simbach causing riverine flood accompanied by numeral shallow “Hanganbrüche” in the Molasse deposits. For testing purposes, two officially accessible soil maps at a scale of 1:50k and 1:250k were introduced for model parameterization.

The calculated failure probabilities was validated using the inventory of “Hanganbrüche” occurred during the meteorological event. The *success rate* calculated with the *area under curve* is ranging between 0.8 – 0.9. To mark soil map units with high parameterization uncertainties the F-test was applied.

12:45pm - 1:00pm

### Landslide Hazard Assessment at Sorkhab Basin Using Fuzzy Logic and GIS

**Siamak Baharvand<sup>1</sup>, Jafar Rahnamarad<sup>2</sup>, Salman Soori<sup>1</sup>, Nader Saadatkhah<sup>3</sup>**

<sup>1</sup>Department of Geology, Khorramabad Branch, Islamic Azad University, Khorramabad, Iran, Islamic Republic of; <sup>2</sup>Department of Geology, Zahedan Branch, Islamic Azad University, Zahedan, Iran, Islamic Republic of; <sup>3</sup>Civil Engineering (Geotechnical Engineering) Universiti Teknologi Malaysia (UTM)

The target of the current study is to investigate the landslide hazard assessment in the Sorkhab drainage basin using the fuzzy logic method and GIS tools. The study area is located at the 20 km of the south of the Khorramabad city (west of Iran), as the landslide-prone area due to the type of geological formations, climatic conditions and topographic conditions. This study began with data from past landslides that identified and recorded using satellite imageries and field observations. Four types of landslides were considered in this study, i.e. Complex, Debris Slide, Earth Slide and Rock Fall. In the first step, eight landslide influencing factors were considered in the analyses. These factors included slope inclination, slope aspect, land use land cover (LULC), elevation, lithology, precipitation, distance from the fault, and distance from stream and river. In the next step, the landslide inventory database was divided into two groups. The modelling group, which represented approximately 70% of the total landslides (2/3), was used as a training set to construct the susceptibility maps. The remaining 30% of landslides were used for prediction testing (1/3). The susceptibility to landslides was carried out using GIS tools and standardized using fuzzy membership functions. In this regards, the 0.1, 0.5, and 0.9 fuzzy gamma- operators have been employed to overlap the information layers and mapping of the landslide hazard zonation at the Sorkhab basin. The results show that the 0.9 fuzzy gamma-operator has relatively a high accuracy in the landslide hazard zonation in the study area. Moreover, the results obtained from using the current method show that 21.39 %, 31.86 %, 25.65 %, 16.23 % and 4.86 % of the basin area are in the risk classes with very low, low, moderate, high and very high, respectively

### Poster Presentations

Mon: 53

### Quaternary Tectonics of the Kalabagh fault, Sub Himalayas- insights from field studies, GPR and topographic analysis.

**Wahid Abbas<sup>1,2</sup>, Sajid Ali<sup>1,2</sup>, Klaus Reicherter<sup>1</sup>**

<sup>1</sup>Neotectonics and Natural Hazards, RWTH Aachen University, Lochnerstr.4-20, 52056 Aachen, Germany.;

<sup>2</sup>Department of Earth Sciences, COMSATS University Islamabad, 22060 Abbottabad, Pakistan.

The Salt Range and the Potwar Plateau marks the southern margin of Himalayas in Pakistan. Lateral extension of the Potwar plateau is controlled by strike slip faults. The Kalabagh fault marks the western margin of the Potwar plateau. It is 120 kilometers long dextral strike slip fault (McDougall and Khan 1990). In this study tectonics and morphology along the central segment of the fault, from Khairabad to Ghundi, have been investigated. Change in topography from Mianwali reentrant in the west to ramp in the east, marks Kalabagh fault zone. Friable Permian sandstone and sheared limestone mark the frontal face. Due to industrial excavations and erosive nature of the rocks, it is a bit challenging to find some classic movements or fault kinematics. Surface expressions of faulted quaternary alluvial deposits and pressure ridges have been observed. Near Khairabad and Ghundi, movements in quaternary strata have been found. Remote sensing data analysis shows deflection in streams that justify the right lateral movement. However, clear alluvial fan offsets have not been observed. But antithetic alignment of the pebbles in incised channels show back tilting due to compression. GPR data show subsurface structures striking parallel to the fault near Khairabad. Fractured pebbles in the trenches and road cuts in quaternary sediments indicate strain developed in recent deposits. Morphological evidences, GPR data, trench and excavation analysis concludes the Kalabagh fault as an active fault. Stress direction is inferred to be SW-NE. That splays out the structures N40°W to N50°W to the western side of the fault near Khairabad.

Mon: 54

## AD 1755 tsunami backwash deposits offshore – the biomarker perspective (METEOR cruise M152)

**Piero Bellanova<sup>1,2</sup>, Mike Frenken<sup>1,2</sup>, Jan Schwarzbauer<sup>1</sup>, Björn Deutschmann<sup>3</sup>, Pedro Costa<sup>4</sup>, Helmut Brückner<sup>5</sup>, Juan Ignacio Santisteban<sup>6</sup>, Jannis Kuhlmann<sup>7</sup>, Andreas Vött<sup>8</sup>, Klaus Reicherter<sup>2</sup>**

<sup>1</sup>Institute of Geology and Geochemistry of Petroleum and Coal, RWTH Aachen University, Germany; <sup>2</sup>Neotectonics and Natural Hazards Group, RWTH Aachen University, Germany; <sup>3</sup>Institute for Environmental Research, RWTH Aachen University, Germany; <sup>4</sup>Instituto Dom Luiz, Departamento de Geologia, Faculdade de Ciências, Universidade de Lisboa, Portugal; <sup>5</sup>Institute of Geography, University of Cologne, Germany; <sup>6</sup>Department of Geodynamics, Stratigraphy and Palaeontology, Fac. Geological Sciences, Complutense University of Madrid, Spain; <sup>7</sup>MARUM – Center for Marine Environmental Sciences, University of Bremen, Germany; <sup>8</sup>Institute of Geography, Natural Hazard Research and Geoarchaeology Group, Johannes Gutenberg-Universität Mainz, Germany

The deposition mechanics of tsunamis and the preservation potential of their residues in offshore areas are as yet virtually unknown. This is mainly due to the limited access to offshore archives as well as the negligible societal effect of tsunamis offshore. Therefore, tsunami research has focused on accessible, mainly sandy onshore, accumulations. However, the focus is shifting since new high-resolution methods have been developed, and the mere identification of sand sheets has reached its limits in answering today's tsunami-related research questions.

The RV METEOR cruise M152 solely focused on the investigation of offshore sedimentary archives for the identification of tsunami deposits. The Algarve coast served as a perfect study area, since it had been affected by the AD 1755 Lisbon tsunami, and numerous onshore studies had detected its geologic footprint. During the M152 cruise, a total of 19 vibracores had been recovered from the shelf up to a water depth of 100 m. Within the offshore Holocene lithostratigraphic record, up to four tsunami candidates were identified based on their sedimentological and micropaleontological properties, which differed significantly from the normal shelf sediments. Additional geochemical sampling took place for inorganic (XRF) and organic analyzes. From the latter, source-specific and indicative organic compounds were extracted using Ultra-Turrax<sup>®</sup> extraction and alkaline hydrolysis, and then analyzed via GC-MS. First results from biomarkers, such as *n*-alkanes, fatty acids and ketones, indicate that event layers contain more terrestrial input than the background sediments, which leads to the assumption that run-off and backwash of a respective paleo-tsunami transports terrestrial material far offshore onto the shelf and possibly even deeper.

Mon: 55

## Calculation for the transport of dust by the wind: from what particle size is this not possible, any longer?

**Ludwig Biermanns**

Universitaet Tuebingen, Germany

The speed, from where loose soil material begins to be transported by the wind, through deflation from a smooth ground, is the critical drag velocity (eq.1).

Dust is classified in *heavy* (1.0 to 0.1mm); *settling*, (0.1 to 0.001mm), *suspended* (< 0.001mm), and in *fine* dust (< 0.003mm).

At 0.25mm in particle-size diameter, the fluid threshold-wind velocity for transport (deflation by saltation) of particles makes 0.23m/s, as calculated example. When particle size increases, higher wind speeds are necessary for transport of dust or sand, of which the critical drag velocity for the fluid threshold is calculated:

$$v_{crit}^* = A \times [g \times d \times ((\rho_{part} - \rho_a) / \rho_a)]^{0.5} . \text{ (Bagnold, 1941: 86; 88; 101) (1)}$$

$v_{crit}^*$  = critical drag velocity [m/s];

A = 0.1 (reference value for fluid threshold (air, from where deflation of particles by saltation begins));

$g = 9.8062\text{m/s}^2$  (gravitational acceleration);

$d$  = particle-size diameter [m], (e.g.:  $0.002\text{ mm} = 2 \times 10^{-6}\text{m}$ );

$\rho_{part}$  = density of particle [ $\text{kg/m}^3$ ] (quartz grain:  $2650\text{kg/m}^3$ ; standard value);

$\rho_a = 1.204041\text{kg/m}^3$  for  $20^\circ\text{C}$  (density of dry atmospheric air, standard value).

From a diameter of  $0.25\text{mm}$  and less, wind speed for the transport of particles does not decrease as calculated, any more; from  $0.06\text{ mm}$  and less, critical drag velocity, even, rises for transport of dust, again.

Wind velocities for dust transport rise, when particles get smaller, because cohesive effects among particles increase, which hamper their uptake and transport from the ground by the wind. Reason for it is a rising ratio of clay, compared to the quartz minerals. Moreover, at decreasing particle size, fluid viscosity of the air is dominated by inertial effects of dust, because the density of the particles reach ca. 2000 times of that one from the air (cf.  $\rho_{part}$ ,  $\rho_a$ ). Sand, with speed, acts like bullets on dust. Significantly finer-grained particles, in their turn, first, are struck, dislocated from their place, distributed in the air by the bigger particles, and finally, finer dust is blown away by the wind. Displacement of particles by wind itself, however, is less possible, when they get smaller (Bagnold, 1960: 360 – 362).

[1] Bagnold, R.A. (1941): The ... – 265 p., Chapman & Hall Publ., London; [2] Bagnold, R.A. (1960): The ... – International Journal of Air Pollution, 2: 357 – 363.

## Mon: 56

### Organic geochemical signatures of the 2011 Tohoku-oki tsunami deposits (Northern Japan)

Mike Frenken<sup>1,2</sup>, Piero Bellanova<sup>1,2</sup>, Madeleine Wörner<sup>2</sup>, Verena Bischoff<sup>2</sup>, Jan Schwarzbauer<sup>2</sup>, Klaus Reicherter<sup>1</sup>

<sup>1</sup>Neotectonics and Natural Hazards Group, RWTH Aachen University, Germany; <sup>2</sup>Institute of Geology and Geochemistry of Petroleum and Coal, RWTH Aachen University, Germany

Misawa, located in the Aomori Prefecture in Northern Japan, was heavily damaged by the Tohoku-oki tsunami induced by the 2011 earthquake off the Pacific coast of Tohoku ( $9.1 M_w$ ). The tsunami, with wave heights of  $6 - 10\text{ m}$ , inundated wide areas of the coastal lowland, causing massive damages to Misawa harbor and the associated infrastructure, releasing pollutants into the nearfield environment. Furthermore, field observation showed that trash and potentially hazardous objects (such as with paint and chemical-filled barrels) were transported into the coastal defense forest, deposited in backwash direction and serve as long-term sources of pollutants released in the environment.

The geochemical signature in the obtained sediment cores indicates a distinct identification of the tsunami layer. Both, anthropogenic marker (e.g. polycyclic aromatic hydrocarbons, pesticides and halogenated compounds) and biomarker (e.g. ketones) are significantly enriched in the visible sand deposits indicating the tsunami layer. Concentration increases of anthropogenic markers are detectable as well in deposits appearing as organic-rich layers first emerging on top of the sandy tsunami deposit and increasing in thickness further inland. This layer deposited during the tsunami inundation due to eroding of increasing amounts of organic material the further inland (e.g. loose plant material and wood), can be interpreted as an “invisible” tsunami layer. Biomarkers (in this case  $n$ -alkanes) indicate higher marine input in the tsunami layer.

Organic geochemical markers also correlate with this observation concluding that the 2011 Tohoku-oki tsunami serves as a blueprint for the development of high-resolution geochemical applications in order to gain more information than standard techniques, as most of them only rely on sand deposits as marker for inundation distances from the beach.

Mon: 57

## Earthquake damage recorded along the Roman Eifel Aqueduct (Lower Rhine Embayment, Germany)

**Sabine Kummer<sup>1</sup>, Gösta Hoffmann<sup>1,2</sup>, Rosa Enrique Martinez<sup>1</sup>, Mario Valdivia Manchego<sup>1</sup>**

<sup>1</sup>University of Bonn, Germany; <sup>2</sup>RWTH Aachen University, Germany

The Lower Rhine Embayment and adjacent areas are characterised by neotectonic deformation resulting in differential crustal movement. Slip rates along the fault systems are very low ( $< 0.1\text{mm/a}$ ). Significant earthquakes are known to have occurred in the past but the faulting behaviour is not adequately known which hampers the risks assessment. We analysed the archaeological record of the largest Roman aqueduct north of the Alps. This so called aqueduct is 95.4 km long, has its source in the Eifel mountains and supplied the ancient city of Cologne with calcareous fresh water. The aqueduct crosses major faults of the Lower Rhine Embayment perpendicular.

Analyses of the aqueduct's gradient gives weak evidence for creep along the Kirspenich Fault resulting in differential movement of hanging and foot wall in the order of a few centimetres. Vertical offsets of 15 and 35 cm are documented exactly where the aqueduct crosses the Holzheim Fault system close to the city of Mechernich. Here, also structural damage of the aqueduct is recorded and archaeological evidence exists for repair works on the aqueduct. We interpret these observations as well as the construction of a 4 km long deviation as necessary measures to keep the aqueduct operational after earthquake damage. The timing of the event falls within the period of aqueduct operation which is reconstructed to be between  $80\pm 10$  CE to  $270\pm 10$  CE. Supporting evidence for earthquake activity within this period is seen in the roof collapse of the nearby Kakus cave.

## 10) Mineral Physics and Mineral Chemistry

### 10a) Minerals in the depths: an experimental approach

Tuesday, 24/Sep/2019: 9:30am - 10:00am

Session Chair: Anna Pakhomova (Deutsches Elektronen-Synchrotron)

Location: Schlossplatz 4: SP4 201

#### Session Abstract

Information on the physical and chemical properties of the constituents of the deep Earth and other planetary bodies is crucial for interpreting geophysical observations and understanding the structure and dynamics of the planets. Modern experimental techniques allow generating pressures and temperatures relevant to deep planetary interiors and, thus, bring new insights into dynamic processes and allow refinement of current structural models.

In this session, we welcome contributions further elaborating on the physical and chemical properties of materials at conditions of the deep interiors of the planets. The contributions may include for instance investigations of the elastic and plastic properties, transport properties, deep melting processes, equations of state and phase equilibria of mantle and core materials.

#### Lecture Presentations

9:30am - 9:45am

#### Ferropericlase and diamond crystallization at upper mantle conditions: implications for the origin of ferropericlase inclusions in diamond

Alan B. Woodland<sup>1</sup>, Vadim K. Bulatov<sup>1,2</sup>, Andrei V. Giris<sup>1,3</sup>, Gerhard P. Brey<sup>1</sup>, Heidi E. Höfer<sup>1</sup>

<sup>1</sup>Goethe Universität Frankfurt, Germany; <sup>2</sup>Vernadsky Institute of Geochemistry and Analytical Chemistry, Russian Academy of Sciences; <sup>3</sup>Institute of Geology of Ore Deposits, Petrography, Mineralogy and Geochemistry, Russian Academy of Sciences

The occurrence of ferropericlase inclusions in diamond is often considered to indicate an origin in the lower mantle or transition zone, (e.g. Kaminsky, 2012). This interpretation is based mostly upon the fact that ferropericlase is unstable together with low-Ca pyroxene in peridotite. However, ferropericlase inclusions exhibit a large range in  $X_{\text{Fe}}$  that is incompatible with equilibrium partitioning with peridotitic bridgmanite (Nakajima et al. 2012). Unlike bridgmanite or ringwoodite, the stability of ferropericlase is not limited to high pressures and the entire MgO-Fe<sub>x</sub>O join can be synthesized at 1 bar. Thus, it may be possible to stabilize ferropericlase under upper mantle conditions in environments with low SiO<sub>2</sub> activity (i.e. pyroxene-free). One scenario involves a redox reaction between slab-derived carbonate melt and reduced peridotite (Thomson et al. 2016). To test this hypothesis, we have performed two types of experiments at 5–12 GPa and 1500–1700°C: (i) equilibrium experiments with Ca–Mg–Fe carbonate+MgO+olivine mixtures and (ii) “sandwich” experiments with a layer of olivine placed in between layers of metallic iron and carbonate. In this way, the Fe is not in direct contact with the carbonate melt so that it functions as an “external reducer” and oxygen sink.

The equilibrium experiments produced carbonate-silicate melts saturated in olivine and ferropericlase. Melts contain 2–12 wt % SiO<sub>2</sub>, which correlates negatively with CaO and CO<sub>2</sub> and positively with T and (MgO+FeO) content. Melt compositions are similar to those reported for olivine+low-Ca pyroxene-saturated melts. However, detailed analysis indicates that ferropericlase-saturated melts cannot be produced by melting carbonate-peridotite at upper mantle conditions and crystallization of the derived melt.

In contrast, the sandwich experiments the reduction of carbonate-silicate melt follows the reaction:  $\text{MgCO}_3(\text{melt}) = \text{MgO}(\text{periclase}) + \text{C}(\text{graphite/diamond}) + \text{O}_2$ , and leads to the simultaneous crystallization of ferropericlase and diamond (or metastable graphite). This mechanism would be viable for dunitic bulk compositions, which are commonly observed in ophiolite complexes. Since no direct reaction occurs with the metallic Fe, our results can be generalized to any reducing conditions, even those that are not metal-saturated. Important is that ferropericlase crystallizing with olivine can be richer in Fe compared with ferropericlase in equilibrium with bridgmanite or ringwoodite. Thus, the large variation in mg# observed for some suites of ferropericlase inclusions in diamond (Kaminsky 2012) could in part be attributable to ferropericlase (and diamond) formation in the upper mantle.

[1] Kaminsky F (2012) *Earth-Sci Rev*, 110:127-147; [2] Nakijima et al. (2012) *J Geophys Res*, 117, B08201; [3] Thomson et al. (2016) *Nature*, 529:76-79

**9:45am - 10:00am**

### **Microstructures across phase transitions in $\text{SiO}_2$ and the origin of seismic scatterers in the mantle**

**Matthias Krug<sup>1</sup>, Estelle Ledoux<sup>2</sup>, Jeffrey Phillip Gay<sup>2</sup>, Julien Chantel<sup>2</sup>, Sergio Speziale<sup>3</sup>, Sébastien Merkel<sup>2</sup>, Carmen Sanchez-Valle<sup>1</sup>**

<sup>1</sup>*Institute for Mineralogy, WWU Münster, Germany;* <sup>2</sup>*Unité Matériaux et Transformations, CNRS, University of Lille, France;* <sup>3</sup>*GFZ Potsdam, Germany*

Geophysical observations reveal seismic scatterers in the mid-lower mantle (800 – 1800 km depth), which are characterized by a reduced shear-wave velocity of 2 – 6 % compared to average mantle (Ballmer et al. 2015, Kaneshima 2016). Most of these scatterers have been found in the vicinity of recent or ancient subduction zones (Ballmer et al. 2015). Their plate-like shape of < 10 km thickness suggests that they may be remnants of former subducted basaltic crust (Kaneshima & Hellfrich 1999, Niu et al. 2003, Niu 2014). Stishovite, a high-pressure  $\text{SiO}_2$  polymorph in subducted basaltic crust, undergoes a ferroelastic phase transition that involves elastic softening (i.e. reduction of shear-wave velocities) in the depth range of interest (Nomura et al. 2010), and thus is a potential candidate for causing the seismic anomalies. Nevertheless, the effect of such a transition on microstructures and textures is poorly understood yet might affect the seismic anisotropy and the reflectivity of seismic signals arising from the mantle. In this study, we investigate microstructural changes induced by phase transitions in high-pressure  $\text{SiO}_2$  polymorphs to discuss the mineralogical origin of seismic scatterers in the mantle. Specifically, we conducted multigrain crystallography (MGC) synchrotron XRD (e. g. Sørensen et al. 2012) experiments in  $\text{SiO}_2$  along the pressure-temperature path of a slab subducting into the lower mantle using laser heated diamond-anvil cells (LHDAC). This path involves the transitions from  $\alpha$ -quartz to coesite, from coesite to stishovite and from stishovite to post-stishovite. The orientations of individual grains inside the polycrystalline samples were measured before and after the transformations, providing constraints on the changes and inheritances of textures during the transitions.

**Tuesday, 24/Sep/2019: 10:45am - 12:30pm**

**10:45am - 11:15am Session Keynote**

### **When history is written in sample heterogeneity**

**Catherine McCammon**

*Universität Bayreuth, Germany*

Mineral physics is founded on the concept that studies of the physical and chemical properties of minerals at relevant conditions can be combined with bulk geophysical data to decipher the structure and dynamics of Earth's interior [1]. Traditionally experiments aim for homogeneous single phase run products, but in the

real world of experimentation such goals are not always realised. Deviations that are large enough to be perceived can provide a wealth of information about sample history with potential relevance to Earth processes, while deviations that are missed can lead to decades of controversy, for example the phase diagram of iron, e.g., [2]. This presentation will focus on advantages that sample heterogeneity brings, specifically in tracking the history of oxygen fugacity during experiments at high pressure and high temperature. Recent results will be highlighted, including how geographic information system software can be applied to mapping on a microscale [3].

[1] Birch F (1952) Elasticity and constitution of the Earth's interior. *J Geophys Res* 57: 227-286; [2] Morard G et al (2018) Solving controversies on the iron phase diagram under high pressure. *Geophys Res Lett* 45: 11,074–11,082, doi: 10.1029/2018GL079950; [3] Linzmeier BJ, Kitajima K, Denny AC, Cammack JN (2018) Making maps on a micrometer scale. *Eos* 99, doi: 10.1029/2018EO099269.

**11:15am - 11:30am**

### **The kinetics of the glass transition of silicate glass measured by fast scanning calorimetry**

Jürgen Schawe<sup>1</sup>, Kai-Uwe Hess<sup>2</sup>, Donald B. Dingwell<sup>2</sup>

<sup>1</sup>Mettler-Toledo GmbH, Schweiz; <sup>2</sup>Ludwig-Maximilians-Universität, Germany

Fast scanning calorimetry allows the determination of the heat capacity of small samples retrieved from high pressure, high temperature experiments (e.g. multi-anvil press or diamond anvil cell). Here, we present as a test case the cooling rate dependent vitrification process of a silicate glass (analogue basaltic melt) of approx. 50 nanograms in the cooling rate range between 0.05 and 30,000 K/s. These results are compared with the temperature dependence of the shear viscosity. The results indicate that rule of the proportionality between shear viscosity and cooling rate holds for the silicate glass. It is also indicated that the thermal retardation time is significantly larger than the shear stress relaxation time derived from viscosity measurements.

**11:30am - 11:45am**

### **Grain Size Dependency of Ge-Olivine/Spinel on Phase Transformational Faulting Mechanism for Deep-focus Earthquakes**

Sando Sawa<sup>1</sup>, Jun Muto<sup>1</sup>, Nobuyoshi Miyajima<sup>2</sup>, Hiroyuki Nagahama<sup>1</sup>

<sup>1</sup>Tohoku University, Japan; <sup>2</sup>University of Bayreuth, Germany

By the geophysical observations (e.g., Zhan et al., 2014) and deformation experiments (e.g., Green and Burnley, 1989), the phase transformational faulting mechanism is presumed as the precursor of deep-focus earthquakes which occur at the depth from 440 km to 660 km in the slab. This mechanism is that metastable olivine in the slab undergoes the phase transformation to fine-grained spinel and shear instability (faulting) occurs at fine-grained spinel. This shear instability depends on grain size. However, previous studies haven't investigated the grain size dependency of the metastable olivine (e.g., Burnley et al., 1991). In this study, to reveal the grain size dependency on the phase transformational faulting, we conducted deformation experiments of fine-grained germanate olivine as an analogue material of silicate olivine (grain size <10 μm). Depending on heat treatment on the sintered aggregates, we prepared the following two types of samples: (1) as is sample with absorbed water (AW sample), (2) sample with air dried at 900 °C (dried sample). We used a Griggs-type solid-confining media deformation apparatus. The confining pressure, temperature and strain rate are 1.2 GPa, 400~900 °C and  $2.0 \times 10^{-4} \text{ s}^{-1}$ , respectively. Although the experimental condition covers the condition where Burnley et al. (1991) reported shear instability, we didn't observe any shear instability event in experiments using AW samples. Also, Raman spectroscopy clarified that the germanate olivine in AW samples underwent the transformation to spinel at 500 °C, but the germanate olivine in dried sample did not transform to spinel at 500 °C. This indicates that the transformation temperature in AW samples lower than those in previous study (1000 °C at the experiment by Burnley et al., 1991). Microstructural analysis clarified that difference in grain sizes between olivine and nucleated spinel in AW samples was smaller than those in previous studies accompanying shear instability. Considering the result of Raman spectroscopy and the rate

equation of the transformation (Chan, 1956), both small initial grain sizes and absorbed water promote the transformation even at lower temperature. These results indicate that the phase transformational faulting mechanism has strong dependency of grain size and amount of water. In the presentation, we also report the results on larger grain sizes.

This work was supported by the JSPS Japanese-German Graduate Externship.

[1] Burnley et al. (1991), *JGR*, vol 96, 425-443; [2] Chan (1956), *Acta Metallurgica*, vol 4, 449-459; [3] Green and Burnley (1989), *Nature*, vol 341, 733-737; [4] Zhan et al. (2014), *EPSL*, vol 385, 89-96.

**11:45am - 12:00pm**

## **Petedunnite, a high-pressure indicator: Influence of Fe & $f_{O_2}$ on the stability of zinc bearing clinopyroxenes**

**Alexandra L. Huber, Soraya Heuss-Aßbichler, K. Thomas Fehr (+)**

*Ludwig-Maximilians-Universität München, Germany*

Natural clinopyroxenes are often members of the hedenbergite-diopside-johannsenite  $[Ca(Fe,Mg,Mn)Si_2O_6]$  solid solution series. They can also contain up to 12.6 wt.-% zinc (Essene & Peacor 1987). Based on our experiments it turned out that Zn in clinopyroxene is a sensitive indicator for high pressure conditions and oxygen fugacity.

Pure endmember petedunnite  $[CaZnSi_2O_6]$  (pd) shows a large stability field at high pressures ( $P > 0.8$  GPa) (Huber et al. 2012). Experiments in the system CaO-ZnO-SiO<sub>2</sub> up to 2.5 GPa and 1100 °C showed that four reactions occur with the participation of the phases petedunnite, zinc-feldspar  $[CaZnSi_3O_8]$  (zfsp), willemite  $[Zn_2SiO_4]$  (wil), hardystonite  $[Ca_2ZnSi_2O_7]$  (har) and quartz  $[SiO_2]$  (qtz): (1)  $4pd = wil + 2har + 3qtz$ ; (2)  $pd + qtz = zfsp$ ; (3)  $3pd = har + wil + zfsp$ ; (4)  $4zfsp = wil + 2har + 7qtz$ . These reactions intersect at 650(1) °C/0.78(0.01) GPa at the invariant point  $I_{pd}$ . While all petedunnite-breakdown reactions (1)-(3) show shallow positive slopes, reaction (4) displays a steep negative slope.

Remarkable similarities are between reaction (2) and reaction jadeite+quartz=albite. Analogous to a jadeitic component, an increase of zinc in clinopyroxene indicates high-pressure conditions during metamorphism. Disregarding the phase transition of quartz, reaction (1)  $[P(\text{GPa}) = -0.093(0.029) + 0.0014(0.0003) T(^{\circ}\text{C})]$  is barely temperature dependent and therefore the reaction can be used for experimental calibrations of high-pressure apparatus at  $T > 650^{\circ}\text{C}$ .

Thermodynamic mixing properties of multi-component solid solutions are controlled by the properties of their end-members. By means of emf-methods (electromotive force), it is possible to determine both, activity and stability of the hedenbergite-petedunnite solid solution series within the P-T- $\log f_{O_2}$ -field. At higher oxygen fugacity ( $f_{O_2}$ ), hedenbergite  $[CaFeSi_2O_6]$  (hed) decomposes to andradite  $[Ca_3Fe_2Si_3O_{12}]$  (and), magnetite  $[Fe_3O_4]$  (mgt) and quartz, according to the reaction  $9hed + 2O_2 = 3and + mgt + 9qtz$ . The equilibrium constant of this reaction is determined by  $f_{O_2}$ . By substituting pure hedenbergite with  $Ca(Zn_{1-x}Fe_x)Si_2O_6$ , the reaction equilibrium reflects the contribution of the chemical potential of hedenbergite in this solid solution. The emf-measurements demonstrate with decreasing  $Fe^{2+}$ - and hence increasing zinc-content in hedenbergite-petedunnite solid solutions a shift of the stability field towards higher  $\log f_{O_2}$ . According to our results,  $Ca(Zn_{1-x}Fe_x)Si_2O_6$  shows asymmetric mixing properties, which can be described by a 3-parameters-Redlich-Kister model. This indicates short-range order phenomena, which is remarkably, since no evidence of short-range order in hedenbergite-petedunnite crystals were observed at room temperature Mössbauer spectroscopy (Huber et al. 2004).

[1] Essene EJ & Peacor DR (1987) *American Mineralogist*, **72**, 157-166; [2] Huber AL et al. (2012) *American Mineralogist*, **97**, 739-749; [3] Huber AL et al. (2004) *Phys Chem Minerals*, **31**, 67-79.

**12:00pm - 12:15pm****Earth's lower mantle elasticity from mineral-physics constraints****Alexander Kurnosov<sup>1</sup>, Giacomo Criniti<sup>1</sup>, Tiziana Boffa Ballaran<sup>1</sup>, Hauke Marquardt<sup>2</sup>, Daniel J. Frost<sup>1</sup>**<sup>1</sup>*Bayerisches Geoinstitut, Universität Bayreuth, Germany;* <sup>2</sup>*Department of Earth Sciences, University of Oxford, U.K*

Recent progress in seismic tomography studies resulted in increased resolution and provided better constraints for seismic heterogeneities in the Earth's lower mantle. Temperature, chemical perturbations and crystallographic preferred orientation (CPO) of crystallites composing the Earth's interior are likely the main reasons of these heterogeneities. Therefore, several studies reported in literature, both theoretical and experimental, were aimed at constraining the effect of these parameters on the elasticity of major lower mantle forming minerals. In this way mineral-physics-based acoustic velocity models calculated from the elasticity measurements can be compared to seismic wave velocity models to constrain the chemical composition of the Earth's interior. To date, however, due to the challenge of measuring high quality elasticity data at the suitable conditions and to the complex cation substitution mechanism occurring in bridgmanite and ferropericlase, there is still not a definite consensus on whether the composition of the upper and lower mantle is the same, or whether the 660 km discontinuity also represent a chemical boundary.

Recent efforts of different research groups aimed at the investigation of the elastic properties of bridgmanite which is the most abundant mineral in the lower mantle, provided single crystal elasticity data for a range of bridgmanite compositions. In this study we will present a systematic framework describing the elasticity of bridgmanite as a function of pressure, temperature, Fe and Al substitution and oxygen vacancies, based on comparison and combination of our study and available literature data.

**12:15pm - 12:30pm****Towards studying kinetics of structural and electronic phase transitions at variable strain rates using diamond anvil cells****Christian Plücker<sup>1</sup>, Rachel Husband<sup>2</sup>, Hanns-Peter Liermann<sup>2</sup>, Guillaume Morard<sup>3</sup>, Zuzana Konopkova<sup>1</sup>**<sup>1</sup>*European XFEL, Germany;* <sup>2</sup>*DESY, Germany;* <sup>3</sup>*IMPMC CNRS, France*

The diamond anvil cell technique enables studying matter across the whole pressure range of the Earth's interior generating pressures over 300 GPa and reaching 400 GPa at its maximum [1]. Recent developments of the double stage DAC [2,3] and the toroidal diamond anvils [4] show encouraging results to reach higher pressure, while dynamically driven DACs, such as membrane-driven (mDAC) or piezo-driven (dDAC) [5], enable higher compression rates (strain rates) and in combination with fast detectors, fine sampling of data along the pressure ramp.

Thereby, Dynamic DAC techniques offer the possibilities to study conditions of large scale collisions of planetesimals and planets [6], mineral properties affected by seismic frequencies [7] and to perform time resolved studies on the effect of various compression rates on the kinetics of structural and electronic phase transitions.

We performed benchmark experiments using membrane and piezo-driven DACs on standard samples (Au, Pt, Re) while varying compression rates, gasket materials, peak pressures and hydrostatic conditions to quantify effects of the variables on deformation of the sample and sample assemble. We used the microstrain analysis based on diffraction peak broadening [8] on runs spanning 4 order of magnitude in compression rates (order of 1 GPa/s up to 10s of TPa/s). The experiments were performed at ambient temperature at the Extreme Conditions Beamline P02.2, Petra III, at Deutsches Elektronen-Synchrotron DESY, Hamburg.

Here we present our results on microstrain evolution at various compression rates from mDAC and dDAC experiments. Building on these experiments we will further focus on studying the kinetics of phase transitions in the FeO (wüstite) and (Mg,Fe)O (ferropericlase) systems, which will give us a tool to compare between existing static and shock compression results.

[1] O'Bannon et al. (2018). *Review of Scientific Instruments* 89, 111501; [2] Dubrovinsky et al. (2012). *Nature Communications* 3, 1163; [3] Sakai et al. (2018). *High Pressure Research* 38, 107-119; [4] Jenei et al. (2017). *Nature Communications* 9, 3563; [5] Evans et al., (2007). *Review of Scientific Instruments*, 78, 073904; [6] Sims et al., (2019). *Earth and Planetary Science Letters* 507, 166-174; [7] Marquardt et al., (2018). *Geophysical Research Letters* 45, 6862-6868; [8] Singh A.K., (2004). *Journal of Physics and Chemistry of Solids* 65, 1589-1596.

## Poster Presentations

Mon: 58

### Atomic structure and theoretical IR spectra of amorphous SiO<sub>2</sub> at high pressures from first-principles molecular dynamics simulations

Johannes Stefanski<sup>1</sup>, Clemens Prescher<sup>1,2</sup>, Sandro Jahn<sup>1</sup>

<sup>1</sup>Universität zu Köln, Germany; <sup>2</sup>DESY Hamburg, Germany

SiO<sub>2</sub> is the most abundant and fundamental oxide component in the Earth. Further, it is a useful and essential material in industrial processes and in daily life. Recently, several studies have been carried out to investigate changes in the atomic structure of amorphous SiO<sub>2</sub> and its structural analog GeO<sub>2</sub> as a function of pressure up to 200 GPa using state-of-the-art experimental and computational methods.<sup>1,2,3,4</sup> Some of those studies arrive at different conclusions regarding the changes of silicon and germanium coordination numbers with respect to oxygen beyond six-fold coordination with increasing pressure.

In this study, we use first-principles molecular dynamics simulations to model the atomic structure of amorphous SiO<sub>2</sub> at room temperature and four different pressure conditions (4, 40, 200 and 576 GPa). The simulation boxes contain 264 atoms (88 SiO<sub>2</sub> units). We find a good agreement between the structure factors  $S(Q)$  from x-ray diffraction experiments<sup>2</sup> and our simulations. Additionally, we used the Voronoi dipole moments<sup>5</sup> to compute IR spectra. The shape of the theoretical spectra is similar to experimental results from Williams and Jeanloz<sup>6</sup> up to 40 GPa. Further, the frequency shifts of the main bands with pressure follow the Si-O bond length change related to the coordination changes in the glass. Specifically, we observe a frequency shift of the main band to >1100 cm<sup>-1</sup> at 200 GPa with increasing proportion of sevenfold coordinated Si. We expect that we can use the computed spectra as fingerprint for future high-pressure experiments to investigate structural transformations in amorphous SiO<sub>2</sub>.

[1] Murakami, M. & Bass, J. D., *Phys. Rev. Lett.* **104**, 025504 (2010); [2] Prescher, C. et al., *Proc. Natl. Acad. Sci.* **114**, 10041-10046 (2017); [3] Pettigirard, S. *High Press. Res.* **37**, 200–213 (2017); [4] Spiekermann, G. et al., *Phys. Rev. X* **9**, 011025 (2019); [5] Thomas, M., Brehm, M. & Kirchner, B. *Phys. Chem. Chem. Phys.* **17**, 3207–3213 (2015); [6] Williams, Q. & Jeanloz, R., *Science* **239**, 902–905 (1988)

Mon: 59

### Goethite decomposition at the lower mantle conditions

Egor Koemets<sup>1</sup>, Maxim Bykov<sup>1,3</sup>, Georgios Aprilis<sup>2,3</sup>, Timofey Fedotenko<sup>2</sup>, Stella Chariton<sup>1</sup>, Elena Bykova<sup>1</sup>, Saiana Khandarkhaeva<sup>1</sup>, Iuliia Koemets<sup>1</sup>, Marcel Thielmann<sup>1</sup>, Catherine McCammon<sup>1</sup>, Natalia Dubrovinskaia<sup>2</sup>, Leonid Dubrovinsky<sup>1</sup>

<sup>1</sup>Bayerisches Geoinstitut (BGI), Universität Bayreuth, Germany; <sup>2</sup>Material Physics and Technology at Extreme Conditions, Laboratory of Crystallography, Universität Bayreuth, Germany; <sup>3</sup>Photon Science, Deutsches Elektronen-Synchrotron, Hamburg, Germany

Starting from approximately 3 billion years ago (Gy) until the Great Oxidation Event (GOE, about 2.5 Gy ago) the Earth was inhabited with anoxygenic prokaryotes that oxidized iron as a result of their vital functions (1, 2). Oxidized iron species, or rust, contained as a major component FeOOH, and were buried on the ocean floor (1, 2). As the plate tectonics started approx. 2.8 Gy ago (3), rust-bearing sediments began immersion into the Earth mantle with subducting slabs, and eventually experienced high pressures and temperatures. We studied the behavior of goethite, FeOOH, by means of in situ single crystal X-ray diffraction at pressures up to 82(2) GPa and temperatures 2300(100) K. At conditions corresponding to even coldest slabs, at the depth of about 1000 km, FeOOH decomposes forming various iron oxide phases (Fe<sub>2</sub>O<sub>3</sub>, Fe<sub>5</sub>O<sub>7</sub>, Fe<sub>7</sub>O<sub>10</sub>, Fe<sub>6.31</sub>O<sub>9</sub>) and

producing oxygen-rich fluid. Thus, our results suggest that recycling the rust in Earth mantle could contribute to oxygen release in the atmosphere, and explain the sporadic increase of oxygen level before GOE linked to the formation of Large Igneous Provinces(4).

[1] D. E. Canfield, M. T. Rosing, C. Bjerrum, Early anaerobic metabolisms. *Philos. Trans. R. Soc. B Biol. Sci.* **361**, 1819–1834 (2006); [2] S. A. Crowe *et al.*, Atmospheric oxygenation three billion years ago. *Nature*. **501**, 535–538 (2013); [3] O. Nebel *et al.*, Geological archive of the onset of plate tectonics. *Philos. Trans. R. Soc. A Math. Phys. Eng. Sci.* **376**, 20170405 (2018); [4] U. Söderlund *et al.*, Timing and tempo of the Great Oxidation Event. *Proc. Natl. Acad. Sci.* **114**, 1811–1816 (2017).

**Mon: 60**

### **The effect of carbon and silicon on the strength of iron alloys: Implications for anisotropy in the Earth's inner core**

**Ilya Kupenko<sup>1</sup>, C. Sanchez-Valle<sup>1</sup>, M. Achorner<sup>1</sup>, M. Krug<sup>1</sup>, J. Chantel<sup>2</sup>, E. Ledoux<sup>2</sup>, X. Ritter<sup>1</sup>, A. Rigoni<sup>3</sup>, H.-P. Liermann<sup>4</sup>, S. Merkel<sup>2</sup>**

<sup>1</sup>University of Münster, Germany; <sup>2</sup>Unité Matériaux et Transformations, CNRS, Université de Lille, France;

<sup>3</sup>Materialphysik, University of Münster, Germany; <sup>4</sup>Photon Science, DESY, Hamburg, Germany

The cores of terrestrial planets are comprised of Fe-Ni alloys, with around 4-7 wt% of the light element(s) that account for the observed core density deficiency and reduced seismic velocity compared to pure Fe-Ni. Carbon and silicon are both considered as major light elements of the core: both have high cosmic abundance and can be efficiently incorporated into iron-nickel metal during core formation. Moreover, the (Mg/Si) ratios of the mantle are inconsistent with those of the chondrites and the 'missing' silicon could be hosted in the core as Fe(Ni)-Si alloys.

Additionally to the average velocities mismatch, there is evidence for prominent anisotropy in the inner core, with the compressional waves traveling through the core faster in the equatorial plane than along the polar axis. The anisotropic structures in the inner core are likely formed by dynamic processes that induce the plastic deformation and development of textures of inner core materials under pressure. Yet, the effect of light elements on the plasticity of iron is poorly known, although this information is crucial for understanding how planetary cores deform.

Here we investigate the plastic deformation of hcp-Fe-Si and Fe-Si-C alloys up to 280 GPa and 180 GPa respectively at room temperature employing a technique of radial x-ray diffraction in diamond anvil cells. We utilize the radial diffraction patterns in order to map the development of texture in the sample and the dominant deformation mechanisms of the alloys. We will present the analysis of measured data and discuss their potential application to constrain plastic deformation in the cores of the Earth and other terrestrial planets.

**Mon: 61**

### **Phase stabilities and elemental redistribution processes between magnesite and mantle silicate at conditions of the lower mantle**

**Lélia Libon<sup>1</sup>, Max Wilke<sup>1</sup>, Georg Spiekermann<sup>1</sup>, Karen Appel<sup>2</sup>, Bernd Wunder<sup>3</sup>**

<sup>1</sup>Universität Potsdam, Germany; <sup>2</sup>European XFEL; <sup>3</sup>Deutsches GeoForschungsZentrum (GFZ)

Diamonds from the lower mantle are carrying, in their inclusions, important information from the deep interior to the Earth's surface. Next to the expected minerals of lower mantle conditions (Mg-Fe-Al silicates and Mg-Fe oxides), these ultra-deep diamonds contain inclusions of carbonates and give proof of the presence of carbonates in the Earth's lower mantle. In addition, these carbonate-bearing inclusions show high REE enrichment (e.g. Brenker *et al.* 2007) and thus raise questions about the role of carbonates as possible trace-element carriers in the Earth's mantle.

Carbonate stabilities at high pressure and temperature have been intensively studied the last two decades. However, the stability of carbonates in presence of mantle silicates at deep mantle conditions remains unclear. Experimental studies support that magnesite (MgCO<sub>3</sub>) in absence of other minerals is stable at P-T

conditions corresponding to the lowermost mantle (>110GPa). A reaction between magnesite and silica at lower mantle conditions may lead to formation of bridgmanite and CO<sub>2</sub>. By increasing P-T conditions along the isotherm further in diamond anvil cell experiments, CO<sub>2</sub> breaks down to form diamond and oxygen. This decomposition could indicate that the reaction of magnesite with silicate could be related to diamond formation in the lower mantle. To better constrain the stability of magnesite in the deep Earth, reactions must be studied in a chemical system which includes selected silicate phases of close-to-natural compositions. To achieve this aim, we will perform multianvil press and laser-heated diamond anvil cell (LH-DAC) experiments to investigate the reaction between magnesite and the silicate phases. In these experiments, magnesite will be reacted with two silicate glasses, enstatite-ferrosilite and haplobasaltic composition, respectively, at conditions relevant to the upper lower mantle (20-40GPa and 1500-2500K).

Additionally, the same reaction will be investigated with Sr/La/Eu-doped materials to show the trace element re-distribution between silicate phases and magnesite. One of this series is planned to be done with Sr/La doped-magnesite as starting materials. Consequently, the first step was to investigate the solubility of these trace element in magnesite. Reaction between strontianite (SrCO<sub>3</sub>) and magnesite leads to formation of Sr-dolomite (Sr<sub>0.5</sub>Mg<sub>0.5</sub>CO<sub>3</sub>) + MgCO<sub>3</sub> with a Sr content in magnesite below the detection. Whereas, reaction of La<sub>2</sub>(CO<sub>3</sub>)<sub>3</sub> \* nH<sub>2</sub>O with magnesite leads to the formation of La-bearing magnesite with La content of 1.5wt% in average + a lanthanum carbonate phase (LaCO<sub>3</sub>OH).

[1] Brenker, et al (2007). Carbonates from the lower part of transition zone or even the lower mantle. *EPSL*, 260(1-2), 1-9.

## Mon: 62

### Towards a systematic interpretation of Mg L-edge X-ray Raman scattering spectra of compressed amorphous magnesiosilicates

**Georg Spiekermann<sup>1</sup>, Sylvain Petitgirard<sup>2</sup>, Christian Albers<sup>3</sup>, Keith Gilmore<sup>4</sup>, Christoph J. Sahle<sup>5</sup>, Christopher Weis<sup>3</sup>, Manuel Harder<sup>6</sup>, Christian Sternemann<sup>3</sup>, Max Wilke<sup>1</sup>**

<sup>1</sup>Universität Potsdam, Germany; <sup>2</sup>ETH Zürich, Switzerland; <sup>3</sup>TU Dortmund, Germany; <sup>4</sup>Brookhaven National Lab, USA; <sup>5</sup>ESRF Grenoble, France; <sup>6</sup>DESY Hamburg, Germany

MgSiO<sub>3</sub> glass at high pressure is investigated as a proxy to ultramafic silicate melts originating from the Earth's mantle. Its atomic structure is intimately linked to macroscopic properties such as density and viscosity [1].

The structural complexity of this glass at high pressure and the similarity of the Si-O and Mg-O partial radial distribution functions make it desirable to apply additional, element-specific measurement techniques in addition to X-ray diffraction [2]. The method of choice is X-ray Raman scattering (XRS) spectroscopy [3,4], which is the only spectroscopic technique to access the electronic structure of light elements like O, Si and Mg in a confined environment like a diamond anvil cell [5].

We present measured and computed Mg L-edge XRS spectra of magnesiosilicate minerals and MgSiO<sub>3</sub> glass up to 60 GPa. Spectra are computed via Bethe-Salpeter calculations with the OCEAN code [6].

A systematics of Mg L-edge X-ray spectra will allow us to yield unprecedentedly direct insight into the structural changes in MgSiO<sub>3</sub> glass at high pressure.

[1] - Y. Kono and C. Sanloup (eds.): "Magmas under Pressure – Advances in High-Pressure Experiments on Structure and Properties of Melts", Elsevier Amsterdam (2018); [2] - Y. Kono, Y. Shibazaki, C. Kenney-Benson, Y. Wang and G. Shen: "Pressure-induced structural change in MgSiO<sub>3</sub> glass at pressures near the Earth's core-mantle boundary", *Proceedings of the National Academy of Sciences*, 115(8), pp. 1742-1747 (2018); [3] – H. Fukui and N. Hirakoa: "Electronic and local atomistic structure of MgSiO<sub>3</sub> glass under pressure: A study of X-ray Raman scattering at the silicon and magnesium L-edges", *Physics and Chemistry of Minerals* (2017); [4] S. K. Lee et al.: "X-ray Raman scattering study of MgSiO<sub>3</sub> glass at high pressure: Implication for triclustered MgSiO<sub>3</sub> melt in Earth's mantle", *Proceedings of the National Academy of Sciences*, 105(23), pp. 7925-7929 (2008); [5] C. Sternemann and M. Wilke: "Spectroscopy of low and intermediate Z elements at extreme conditions: in situ studies of Earth materials at pressure and temperature via X-ray Raman scattering", *High Pressure Research*, 36:3, pp. 275-292 (2016); [6] Gilmore et al.: "Efficient implementation of core-excitation Bethe-Salpeter equation calculations", *Computer Physics Communications*, 197, pp. 109 (2015)

**Mon: 63****Phase relations of Al-bearing MgFe<sub>2</sub>O<sub>4</sub>: Implications for natural occurrences in diamond****Laura Uenver-Thiele<sup>1</sup>, Alan Woodland<sup>1</sup>, Tiziana Boffa Ballaran<sup>2</sup>, Nobuyoshi Miyajima<sup>2</sup>**<sup>1</sup>*Institut für Geowissenschaften, Universität Frankfurt*; <sup>2</sup>*Bayerisches Geoinstitut, Bayreuth*

Spinel-structured phases commonly occur as inclusions in diamond [e.g.1,2,3]. Depending on their composition (e.g. MgAl<sub>2</sub>O<sub>4</sub> [4], MgFe<sub>2</sub>O<sub>4</sub> [5], FeFe<sub>2</sub>O<sub>4</sub> [6]) their phase relations at high-P and T can differ significantly from each other. MgFe<sub>2</sub>O<sub>4</sub>-FeFe<sub>2</sub>O<sub>4</sub> spinels are of special interest because of their ability to store Fe<sup>2+</sup> and Fe<sup>3+</sup>, making them redox-sensitive. Thus, they can act as indicators for P, T and redox conditions during entrapment. For example, magnesioferrite can occur in (Mg,Fe)O inclusions in diamond and has been interpreted to have either directly exsolved from (Fe,Mg)O in the upper mantle or formed from a precursor phase (e.g. (Mg,Fe)<sub>2</sub>Fe<sub>2</sub>O<sub>5</sub>, hp-(Mg,Fe)Fe<sub>2</sub>O<sub>4</sub>, (Mg,Fe)<sub>3</sub>Fe<sub>4</sub>O<sub>9</sub> at higher P [5,7]). However, natural magnesioferrite can also contain small amounts of Al and its effect on phase stabilities is currently unknown.

This study is aimed to investigate the post-spinel phase relations in multi-component spinels approaching natural compositions [i.e. (Mg,Fe<sup>2+</sup>)(Fe<sup>3+</sup>,Al)<sub>2</sub>O<sub>4</sub>] and to place constraints on the origin of such phases, as they are associated with diamond formation. Multi-anvil experiments are conducted between 8-22GPa and 1000-1600°C with several bulk compositions. Run products were analysed by EPMA, XRD and TEM. Preliminary results show that the “spinel” phase can be stabilized to higher pressure (with increasing T) depending on the amount of Al, but is limited to max. ~16 GPa (at 1600°C). Importantly, Mg<sub>2</sub>(Al,Fe)<sub>2</sub>O<sub>5</sub> becomes stable between 16-21GPa over a wide temperature range, making this post-spinel phase more relevant for mantle conditions compared to the Mg-Al endmember Mg<sub>2</sub>Al<sub>2</sub>O<sub>5</sub> [>2100°C at 20 GPa (4)]. At even higher P and T ≥ 1300°C, a hp-polymorph with M<sub>3</sub>O<sub>4</sub> stoichiometry becomes stable. Phase relations of Fe<sup>2+</sup>-rich compositions seem to differ from those containing significant amounts of Mg and involve other hp-phases such as those with an M<sub>7</sub>O<sub>9</sub> stoichiometry.

[1] Kaminsky et al. (2009) *Min Mag*, 73, 5, 797-816; [2] Kaminsky (2013) *Can Mineral*, 51, 669-688; [3] Palot et al. (2016) *Lithos*, 265, 237-243; [4] Enomoto et al. (2009) *J Solid State Chem* 182, 389-395; [5] Uenver-Thiele et al. (2017a) *Am Min* 102, 632-642; [6] Woodland et al. (2012) *Am Min* 97, 1808-1811; [7] Uenver-Thiele et al. (2017b) *Am Min* 102, 2054-2064.

**10b) Detailed insights into geodynamic processes and geotechnical applications through neutron and synchrotron X-ray diffraction****Monday, 23/Sep/2019: 11:15am - 1:00pm****Session Chair: Christian Scheffzük (Karlsruhe Institute of Technology)****Session Chair: Nikolaus Froitzheim (Universität Bonn)****Location: Schlossplatz 4: SP4 201****Session Abstract**

Detailed studies of crystallographic preferred orientations, micro and macro strain can be used to improve our understanding of geodynamical process such as mountain building, subduction and deep mantle processes. Furthermore, the characterization of geomaterials in underground infrastructures, like base tunnels, mining operations, waste disposal sites, allows us a better understanding of the underlying processes and mechanisms of static and dynamic elasticity and failure of polycrystalline composite materials, such as rocks. The complementary methods neutron and synchrotron X-ray diffraction allows imaging and in situ investigations of rock samples and artificial materials. For this session, we encourage submissions of fundamental and applied science working groups to present their research in order promote a cross border discussion of new approaches for more detailed insights into geodynamical processes and geotechnical applications.

## Lecture Presentations

**11:15am - 11:45am** *Session Keynote*

### Progress in texture analysis of rocks and sediments using synchrotron, neutron and electron beams

**Michael Stipp<sup>1</sup>, Rebecca Kühn<sup>1</sup>, Ruth Keppeler<sup>2</sup>, Rüdiger Kilian<sup>1</sup>**

<sup>1</sup>*Martin-Luther-Universität Halle-Wittenberg, Germany;* <sup>2</sup>*Rheinische Friedrich-Wilhelms Universität, Bonn, Germany*

Textures, i.e. crystallographic preferred orientations (CPOs), of polymineralic rocks and sediments containing low-symmetric minerals and significant amounts of pore and crystal water are difficult or impossible to analyze. In the last decade, however, significant advances in measurement techniques and processing routines have been made so that it is now possible to deconvolute polymineralic diffraction patterns with several different sheet silicates or clay minerals. Even weak CPOs of mineral phases can be determined that account for only 5 % of the rock volume. This allows to better constrain deformation mechanisms and partitioning or other texture-forming processes like growth fabrics. To quantify textures, i.e. pole figure maximas, it is important to apply reliable statistical procedures. Based on those, different techniques like neutron and synchrotron diffraction and also electron backscatter diffraction (EBSD) measurements can be combined to further improve CPO analysis and interpretation.

Textures of crystalline basement rocks can best be investigated using combined neutron diffraction and EBSD – both are well-established techniques. If grain size is too large, starting already at a few hundred micrometers in diameter, EBSD does not enable to determine statistically significant bulk textures. For that, neutron diffraction is the ideal tool with which large sample volumes of up to approximately 50 mm in diameter can be measured. In combination, both methods are very powerful to fully constrain bulk textures as well as details of local fabric domains. However, the analysis of samples with large amounts of water cannot be carried out with these methods. Textures of soft sediments and serpentinites, which have so far been difficult to measure due to their water contents and the artifacts caused by sample surface preparation, have recently been analyzed as complete sample cylinders of up to 20 mm in diameter using hard X-ray synchrotron diffraction. Similar to neutron diffraction results, public domain software facilitates measurement of the different mineral textures as well as their contents in volume percentages. Resulting textures of clay-rich sediments allow for the first time to investigate soft sediment deformation, compaction and diagenesis and cleavage formation on a (semi-)quantitative basis. The same is true for serpentinites from mid-ocean ridges which can be investigated with respect to ocean floor metamorphism and deformation.

Apart from detailed deformation analysis texture data can be used to quantify anisotropies of petrophysical properties that are crucial for geophysical imaging. Elastic wave anisotropies calculated from CPO data amount, for example, up to 8% for serpentinites from the Atlantis Massif oceanic core complex in the Atlantic ocean and up to 20% for micaschists from the Adula nappe in the Central Alps. Such high anisotropies need to be incorporated in any seismic interpretation and may considerably change our picture of the deeper crust and upper mantle.

11:45am - 12:00pm

### Non-invasive investigation of concrete deterioration in aggressive aqueous environments by means of neutron diffraction

**Matthias Schwotzer<sup>1</sup>, Andreas Bogner<sup>2</sup>, Jonas Kaltenbach<sup>1</sup>, Christian Scheffzük<sup>3,4</sup>**

<sup>1</sup>Karlsruhe Institute of Technology (KIT), Institute of Functional Interfaces (IFG), Germany; <sup>2</sup>Karlsruhe Institute of Technology (KIT), Materials Testing and Research Institute (MPA Karlsruhe), Germany; <sup>3</sup>Karlsruhe Institute of Technology (KIT), Institute of Applied Geosciences, Germany; <sup>4</sup>Frank Laboratory of Neutron Physics, JINR Dubna, Russia

Maximizing the service life of concrete structures is an important challenge in the context of a sustainable development in the construction sector. However, an improvement of the durability of cement-based materials requires a detailed knowledge of the mechanisms of relevant deterioration reactions. In particular, the related mechanisms due to an impact of aqueous solutions are still debatable. Here, an interplay of transport processes and reactions disturb the equilibria between solid phases and the solutions in the pore structure of the materials resulting in significant changes in the mineralogical composition. In the medium and long term, these processes lead to serious damages to construction materials. Investigations of the damaging reactions are, however, usually “invasive” and therefore only suitable to a limited extent to characterize the relevant *in situ* processes. In this context, neutron diffraction appears to be a promising tool for time-resolved monitoring of the reactions of crystalline compounds in mineral-bound materials. So, non-destructive measurements can be performed on defined volume elements. In this study, investigation concepts were developed for different scenarios of chemical attacks relevant to practice. For example, the corrosion of the steel in reinforced concrete induced by chlorides, which penetrate into the materials due to permanent contact with chloride-containing solutions (e.g. sea water and de-icing salt), represents a serious problem. Here, however, the influencing variables that regulate the reaction are not sufficiently well understood to perform reliable assessments as a basis for prevention concepts. For example, the literature contains a wide range of values for a “critical” chloride content, which is necessary to initiate corrosion. Nevertheless, non-destructive analysis could make a valuable contribution to a more detailed understanding of these mechanisms. The aim of this study was to investigate whether neutron diffraction can be used to monitor the reaction progress by time-resolved measurements on samples contaminated with chloride. Over a period of several months, it should be investigated whether the formation of corrosion products or a degradation of metallic components can be monitored. Another example is the sulphate attack on cementitious materials. In this case, sulphate uptake into the microstructure of the material leads to the crystallization of ettringite. The associated crystallization pressure causes mechanical stress and thus substantial damage. The study tried to follow the mineral reactions directly. In this contribution, first results of the research activity are presented and neutron diffraction is evaluated regarding its potential for the detailed study of material damaging reactions.

12:00pm - 12:15pm

### In situ – strain investigations for reservoir conditions using neutron time-of-flight diffraction

**Birgit I.R. Müller<sup>1</sup>, Christian Scheffzük<sup>1,2</sup>, Frank R. Schilling<sup>1</sup>**

<sup>1</sup>KIT Karlsruhe, Germany; <sup>2</sup>FLNP, JINR Dubna, Russia

The mechanical deformation of rocks is coupled to pore fluid pressure. In the poro-elastic theory, a change of pore pressure causes a deformation of the porous rock mass and *vice versa* changes of stress and volume reduction can cause changes in pore pressure if the rocks are undrained.

The understanding of the coupling of stress to changes of pore pressure in porous rocks is important for numerous fields in geosciences:

- 1) circulation of geothermal fluids,
- 2) stimulation of reservoir sections with low permeability,
- 3) injection of waste water into aquifers,

4) impoundment of hydropower reservoirs. This is because pressure induced changes of stress can lead to critically stressed faults and thus to fault reactivation. In the case of injection induced pore pressure changes, earthquakes of magnitudes  $> 5$  had been induced.

The neutron time-of-flight strain diffractometer EPSILON, which is equipped with the triaxial pressure cell TRIXI allows to determine the *in situ* - intracrystalline deformation for various pressure and stress conditions, with the focus on reservoir stress states. The new pressure cell for cylindrical saturated porous rock samples has been developed for axial loading up to 150 MPa, mantle pressure and pore pressure up to 70 MPa. The cell was designed (mostly 2015/2016), manufactured (2017) and tested (November 2017, January 2018). Due to the long neutron flight path and hence the relative low neutron flux at sample position, the measurement of strain on the rock sample of 60 mm length and 30 mm diameters require a long exposition time. Thus, a deformation experiment with a systematic change of the stress state requires beam time of 8-12 days. Here we present the very first measurement results.

**12:15pm - 12:30pm**

### **Transport of electrolyte solutions and interfacial layer in silica nanoconfinement – case of plane and parallel surfaces (nanochannels)**

**Markus Baum<sup>1</sup>, Diane Rebiscoul<sup>2</sup>, Samuel Tardif<sup>3</sup>, Francois Rieutord<sup>3</sup>, Michael Haist<sup>1</sup>**

<sup>1</sup>Leibniz University Hannover, Institute for Building Materials, Appelstraße 9a, 30167 Hannover; <sup>2</sup>CEA, ICSM – UMR 5257 CEA-CNRS-UM-ENSCM, 30207 Bagnols-sur-Cèze Cedex, France; <sup>3</sup>CEA, INAC, Minatec Campus, 38000 Grenoble, France

The understanding and the prediction of materials' behavior regarding their interactions with aqueous solutions is of great interest in various fields, such as geochemistry, catalysis and nuclear wastes. Most of these materials are completely or partially nanoporous such as cementitious materials, clay materials, and amorphous alteration layers of glasses. A strong interest exists to use model systems such as nanochannels defined as two planar and parallel plane surfaces spaced at a few nm. Indeed, the planar model systems can provide an attractive configuration for fundamental studies like filling kinetics (wetting dynamics), diffusion, and for molecular separation processes.<sup>[1]</sup> Channels with heights in the range of 2-100 nm usually still contain several hundreds of molecules in the height dimension, and typical surface effects are related to the interfacial layer or the extreme surface to volume ratio. As the channel dimension is scaled down to the nanometer range, fluids inside the channels exhibit properties which can be significantly different from the bulk properties, for instance the reduced dynamics of confined solutions, the corresponding water structure and the ion distribution at the interface.<sup>[2-4]</sup>

In this study, we propose an innovative approach to determine the filling kinetics of electrolyte solutions  $XCl_2$  ( $X = Ba^{2+}$ ,  $Ca^{2+}$  and  $Mg^{2+}$ ) in silica nanochannels by means of X-Ray Reflectivity (see Figure). This technique allows the determination of the electron density profiles perpendicular to the surface, leading to the determination of the density evolution in the nanochannels and to the characterization of the interfacial layer in confined media.<sup>[5]</sup> Furthermore, the effect of confinement size and the nature of ions on the interfacial layer were studied.

[1] Tas, N. R.; et al., A Capillary Filling Speed of Water in Nanochannels. *Appl. Phys. Lett.* **2004**, 85, 3274–3276; [2] Le Caër, S.; et al., A Trapped Water Network in Nanoporous Material: The Role of Interfaces. *Phys. Chem. Chem. Phys.* **2011**, 13, 17658; [3] Ishai, P. B. et al., Influence of Ions on Water Diffusion - A Neutron Scattering Study, *The Journal of Physical Chemistry C.* **2013**, 117, 7724-7728; [4] Mamontov, E. et al., Dynamics of Water in LiCl and CaCl<sub>2</sub> Aqueous Solutions confined in Silica Matrices: A Backscattering Neutron Spectroscopy Study. *Chemical Physics*, **2008**, 352, 117-124; [5] Bedzyk, M. J. et al., Diffuse-Double Layer at a Membrane-Aqueous Interface Measured with x-Ray Standing Waves. *Science*. **1990**, 52–56.

**12:30pm - 12:45pm****Quartz texture development in exhumation channel related shear zones of the Erzgebirge: The interplay of Grain Boundary Migration and Sub Grain Rotation****Peter Hallas, Uwe Kroner***TU Bergakademie Freiberg, Germany*

Mid-crustal exhumation channels of former intracontinental subduction zones can be observed in collisional orogens as exemplified by a well exposed shear zone suite in the Erzgebirge (N-Bohemian Massif). Here, the extrusion of deeply subducted continental material into a pre-existing medium to high grade metamorphic nappe pile can be observed. Isothermal decompression of the channel rocks caused advective heat transfer into the wall rocks characterized by heating-decompression. Available data indicates that the pervasive ductile strain accumulated at similar p-T-t conditions, i.e., at 10-14 kbar; 600-650 °C between 340 and 335 Ma. Hence, contrasting fabrics should be caused by different deformation parameter.

Kinematic indicators reveal a top to WNW overthrusting of the channel rocks onto the medium pressure gneiss complex in the foot wall and a top to ESE underthrusting in the roof shear zone indicating a general WNW exhumation direction. Progressive grain size reduction towards the shear zones indicates strain concentration towards the channel boundaries.

Here we present results from detailed studies of quartz texture analyses by time-of-flight neutron diffraction (ToF) and electron backscatter diffraction (EBSD) measurements. The combination of both methods allows the characterization of the global quartz textures as well as the investigation of contrasting texture forming processes inside the shear zone suite.

Quartz crystallographic preferred orientation (CPO) can be distinguished into two characteristic endmembers. In central parts of the upper and lower shear zone suite [0001] pole figures exhibit small girdle distributions around z or x (strain coordinates of the shear zone) and point to a {10-11}, i.e. the positive rhombs maxima in z (group 1). In contrast, the channel center as well as the foot and hanging wall of the channel, i.e. the peripheral parts of the shear zone suites are characterized by a pronounced point [0001] maxima in y (group 2) and a higher texture strength. Moreover, microstructural observations and EBSD analyses point to a higher SGR than GBM recrystallization with the dominant misorientation axes <0-110> and <11-21> in group 1. Additionally, a low intragranular misorientation density, calculated over the grain kernel average misorientation (gKAM) is recognized in this group. In contrast, group 2 is dominated by GBM recrystallization, a high gKAM and the misorientation axes <0001>. In conclusion, the textural differences of group I and II can be explained by the various interplay of GBM and SGR recrystallization and the involved crystallographic misorientation axes.

**12:45pm - 1:00pm****Determining elastic properties of rocks for a representative cross section through the Western Alps****Michael Jared Schmidtke<sup>1</sup>, Ruth Keppler<sup>1</sup>, Michael Stipp<sup>2</sup>, Nikolaus Froitzheim<sup>1</sup>***<sup>1</sup>Rheinische Friedrich-Wilhelms Universität, Bonn, Germany; <sup>2</sup>Martin-Luther-Universität Halle-Wittenberg, Halle, Germany*

Seismic imaging methods provide an increasingly higher resolution towards greater depth. However the geotectonic interpretation of these images is only possible with precise data on petrophysical properties (e.g. elastic anisotropies) of the rocks involved. In the olivine dominated mantle, the anisotropies mainly result from the strain-induced crystallographic preferred orientation (CPO) of olivine. In the polymineralic crust the situation is more complicated. CPOs of all constituent mineral phases largely contribute to the overall seismic anisotropy of the rocks.

In the context of the international AlpArray/4D-MB-project, this study focuses on collecting anisotropy data of different lithologies involved in a representative cross section through the Western Alps. The Western Alps

display a wide variety of metamorphic and unmetamorphic rocks from diverse structural levels of the earth's crust and upper mantle as well as of different paleogeographic origins. In order to obtain representative elastic anisotropies from oceanic crust, continental lower crust and upper mantle, samples were collected from three different locations in the Italian Western Alps. In the Lago di Cignana area, eclogites and blueschists of oceanic origin (Zermatt-Saas-Zone) are exposed next to metasediments of the Combin-Zone. Near Finero we sampled lower crustal rocks and mantle peridotites of the Ivrea Zone and in the Val Strona, a variety of felsic lower crustal strombolites and a marble sample were collected.

The CPOs of the constituent mineral phases of these samples were measured at the Joint Institute for Neutron Research in Dubna (Russia) using time-of-flight neutron diffraction, to gain representative bulk textures. Using these CPOs, the volume percentage of the respective mineral phases in the sample, and single crystal elastic anisotropies, the petrophysical properties of the samples were modelled. The samples can be divided into felsic and mafic samples, with felsic samples displaying P-wave anisotropies between 4.1% and 5.9%, while mafic samples show anisotropies between 1.1% and 3.8%. The P-wave velocities in the felsic samples range from 6.5 km/s to 7.2 km/s, those in mafic samples from 6.8 km/s to 7.8 km/s. Highest P-wave velocities in mica-rich felsic samples are distributed in the foliation plane, while highest velocities in mafic samples concentrate in lamination direction. Furthermore experimental P- and S-wave velocity-measurements were conducted at the CAU in Kiel (Germany). These experimental velocities were measured under confining pressures of up to 600 MPa. Calculated and experimentally measured mean velocities are similar, but anisotropies are significantly higher in the experiments, probably due to incompletely closed microcracks.

## Poster Presentations

Mon: 87

### Dynamic compression of baddeleyite in membran-driven diamond anvil cells as an analogue experiments for impact events

Falko Langenhorst<sup>1</sup>, Eric Adelhardt<sup>1</sup>, Ulrich Mansfeld<sup>1</sup>, Hanns-Peter Liermann<sup>2</sup>

<sup>1</sup>University of Jena, Germany; <sup>2</sup>Deutsches Elektronen-Synchrotron (DESY)

Fast membrane-driven diamond anvil cell (mDAC) experiments were used to simulate the effects of shock compression in rock-forming minerals [1-3]. These experiments were carried out at synchrotrons allowing to obtain time-resolved *in-situ* X-ray diffraction data of minerals during rapid compression and decompression. Despite the absence of shock waves in DAC experiments and their distinctly smaller compression rates compared to shock experiments, the mDAC technique yields known shock effects such as amorphization of quartz and feldspars [1,3] and dislocation glide in olivine [2]. Here, we performed dynamic mDAC experiments on baddeleyite (monoclinic ZrO<sub>2</sub>), an accessory mineral in planetary basalts, which is known to undergo various phase transformations. We focus on the nature and kinetics of pressure-induced phase transformations, which are much less constrained than the temperature-induced martensitic and displacive transitions.

Polycrystalline, 1 μm sized ZrO<sub>2</sub> powder served as starting material in two mDAC experiments run up to 37 GPa and 64 GPa. This powder was dynamically compressed under non-hydrostatic conditions at a rate of 1 GPa/s. X-ray diffraction patterns were acquired at beamline P02.2 of PETRAIII, DESY Hamburg at 25.6 keV using a Perkin-Elmer fast flat panel detector. Powdered gold was used as an internal pressure standard. Recovered samples were investigated by transmission electron microscopy (TEM) to detect persistent structural modifications in baddeleyite.

In agreement with previous slow compression experiments [4,5], our synchrotron X-ray diffraction experiments reveal the immediate transformation of monoclinic baddeleyite to the orthorhombic phases I, II, and III at 6, 22, and 40 GPa, respectively. On decompression these phases even persist without reversion to the baddeleyite structure. The lattice constants *a*, *b*, and *c* of the orthorhombic phases abruptly change at the transformation pressures, while the overall cell volume almost linearly increases with increasing pressure.

TEM inspection of recovered samples confirms the occurrence of nanocrystalline aggregates of the orthorhombic phases at ambient pressure. Individual nanocrystals are strongly strained but otherwise defect-free.

These observations indicate the displacive nature of the pressure-induced phase transformations. The persistence of the orthorhombic phases at ambient pressure is attributed to internal strain in nanocrystalline aggregates.

[1] Carl E.-R. et al. (2017) *Meteoritics & Planetary Science* 52:1465-1474; [2] Langenhorst F. et al. (2017) 80<sup>th</sup> Annual Meeting of MetSoc: #1987; [3] Sims M. et al. (2019) *Earth and Planetary Science Letters* 507:166-174; [4] Leger J.M. et al. (1993) *Phys. Rev. B* 47:14075; [5] Bouvier et al. P. (2000) *Phys. Rev. B* 62: 8731.

## Mon: 88

### EPSILON - the neutron time-of-flight strain/stress diffractometer and its sample environment for strain investigations in rocks

**Christian Scheffzük<sup>1,2</sup>, Birgit I.R. Müller<sup>1</sup>, Roland Tremmel<sup>1</sup>, Badmaarag Altangerel<sup>2</sup>, Frank R. Schilling<sup>1</sup>**

<sup>1</sup>Karlsruhe Institute of Technology, Institute of Applied Geosciences, Germany; <sup>2</sup>Frank Laboratory of Neutron Physics, JINR Dubna, Russia

The investigation of uniaxial and triaxial stress states in mono- and polyphase geological samples is a key to a better understanding of the deformation behaviour of rocks. The neutron time-of-flight strain/stress diffractometer EPSILON at the pulsed neutron source IBR-2M is equipped with various sample environment techniques to enable *in situ* - deformation experiments as well as at axial and triaxial deformation conditions.

The neutron diffractometer is equipped with a detector system consisting of 9 detector units at a diffraction angle of  $2\theta=90^\circ$ , so that 9 different sample directions can be investigated. Lattice spacings up to  $d=5.3 \text{ \AA}$  are achievable, so that lower symmetrical crystal structures with large elementary cells can be investigated.

An axial pressure device enables  $\sigma_{\max} = 150 \text{ MPa}$  using sample dimensions of  $\varnothing = 30 \text{ mm}$ ,  $l = 60 \text{ mm}$ ; the axial  $[\sigma_1]$  and radial  $[\sigma_3]$ -directions can be detected, simultaneously. The sample environment has been extended by a triaxial pressure device to generate the axial pressure  $\sigma_{1,\max} = 150 \text{ MPa}$ , the confining pressure  $\sigma_{3,\max} = 70 \text{ MPa}$ , and the pore pressure  $p_p = 70 \text{ MPa}$ , independently. This sample environment allows *in situ* determination of intracrystalline strain of porous polycrystalline materials.

We have developed and used this pressure device for the investigation of porous sandstone in order to generate the conditions in geological samples as they occur in upper crust reservoirs, namely in depth intervals of 3,000 to 5,000 m.

## Mon: 89

### Pressure-induced crystallographic changes of dynamically compressed quartz by X-ray diffraction and electron microscopy

**Christoph Otzen<sup>1</sup>, Hanns-Peter Liermann<sup>1</sup>, Falko Langenhorst<sup>2</sup>**

<sup>1</sup>Deutsches Elektronen-Synchrotron DESY, Germany; <sup>2</sup>Friedrich-Schiller-Universität Jena

Large asteroid impacts play a crucial role in the history of the Earth, traces of which can still be found in minerals today and provide important information about past impact events. Being robust evidence and barometers for impacts, the amorphization of tectosilicates is the most significant impact indicator. To constrain the pressure conditions for the occurrence of amorphization and observe the crystallographic changes *in-situ*, diamond anvil cell experiments are typically performed on powder samples for X-ray diffraction. Powders, having typical grain sizes in the micron to submicron range, however, are inadequate to analyze how amorphization is affected by the orientation of the crystal with respect to the direction of load. Furthermore, the small particle sizes are unrepresentative of natural target material which consists of grain sizes in the millimeter range.

In the present work, we have carried out dynamic compression experiments on various orientations of quartz single crystals at the Extreme Conditions Beamline at PETRA III, DESY, Hamburg, Germany. Aiming at creating the dynamic pressure conditions that can be found in natural impacts, we use membrane-driven dia-

mond-anvil cells to compress the samples uniaxially and rapidly to high pressures. Using transmission electron microscopy, we analyze the pressure-induced crystallographic changes of the recovered single crystals in detail. Our research provides insights into the mechanisms of pressure-induced amorphization in quartz.

**Mon: 90**

### **Synchrotron diffraction as a tool for the texture analysis of mid-ocean ridge serpentinites**

**Rebecca Kuehn<sup>1</sup>, Michael Stipp<sup>1</sup>, Bernd Leiss<sup>2</sup>, Jan Behrmann<sup>3</sup>**

<sup>1</sup>*Martin-Luther-University Halle, Department of Geodynamics, Halle (Saale), Germany;* <sup>2</sup>*Geoscience Center of the Georg-August-Universität Göttingen, Department of Structural Geology and Geodynamics, Göttingen, Germany;*

<sup>3</sup>*GEOMAR Helmholtz Centre for Ocean Research Kiel, Marine Geodynamics, Kiel, Germany*

Oceanic serpentinites comprise to a great extent the serpentine polymorphs lizardite and chrysotile. Analysis of their crystallographic preferred orientation (texture) is challenging due to the fibrous crystal habit of chrysotile. More conventional methods such as electron backscatter or neutron diffraction are inapplicable, as the first requires polished surfaces that cannot be produced, while for the second neutrons are absorbed by the hydrogen within the serpentine crystal lattice, respectively. We therefore used hard X-ray synchrotron diffraction for unpolished sample cylinders with a diameter of up to 20 mm, which is also suitable for samples containing hydrous minerals.

Measurements were conducted at the European Synchrotron Radiation Facility in Grenoble, France at beamline ID22. As beam size was limited to 1 mm, we measured several slices of the full sample cylinder to improve grain statistics. A suite of serpentinite samples from the Atlantis Massif oceanic core complex, located on the mid-Atlantic ridge at 30° N, was studied. They were cored during International Ocean Discovery Program Expedition 357.

Samples are highly altered ultramafics, containing lizardite and chrysotile, as well as magnetite and further minor minerals. The textures and microstructures vary from weakly foliated bastite-rich to strongly foliated bastite-free mesh structures. Samples with less or no bastite clasts have intense foliations defined by the orientation of the serpentizing microfractures. Serpentine texture in bastite-rich samples is dominated by the bastites, while in bastite-poor samples the texture seems to be controlled by the serpentizing microfractures. The variations could depict differences in strain, in primary composition or fabrics inherited from the peridotite.

We show that synchrotron diffraction can be successfully used to determine the textures of oceanic serpentinites. This overcomes the severe limitations posed by more conventional methods, and opens the possibility of quantitative assessment of physical properties of hydrated oceanic Earth's mantle. Even though the texture in the samples originates from different microfabrics, it may lead to enhanced anisotropic physical properties.

## 11) Crystallography

### 11a) Structural properties of minerals and materials

Wednesday, 25/Sep/2019: 8:30am - 10:30am

Session Chair: Michael Fischer (University of Bremen)

Session Chair: Thomas Malcherek (Universität Hamburg)

Location: Schlossplatz 7 Hof: SP 7

#### Session Abstract

The characterization of structure, from the atomic level to the micrometer scale, is an important area of overlap between the fields of mineralogy and materials science. This session is intended to bring together researchers from both disciplines. On the one hand, we invite “method-oriented” contributions that focus on the sophisticated application of characterization methods (e.g. X-ray, synchrotron, or neutron diffraction; vibrational spectroscopy; NMR spectroscopy; HRTEM) or of computations (e.g. density functional theory; molecular dynamics) to minerals or synthetic materials. On the other hand, more “materials-oriented” contributions are also very welcome, especially if they aim to enhance the fundamental understanding of material properties (e.g. structure-property relationships), or if they provide new insights that are relevant for technological applications of minerals or materials.

#### Lecture Presentations

8:30am - 9:00am *Session Keynote*

#### **In situ synchrotron studies of open-framework silicates at non-ambient temperature and pressure**

**Paolo Lotti**

*Earth Science Dept., University of Milano, Italy*

The combined use of synchrotron X-ray diffraction (XRD) techniques and devices for *in situ* studies at non-ambient temperature and/or pressure allowed a deep investigation of the behavior of open-framework silicates at these conditions. Displacive phase transitions are common mechanisms adopted by framework compounds to accommodate the bulk expansion or contraction, whenever structural distortion is no more possible or energetically efficient.

The zeolite mordenite, for example, crystallizes, at ambient condition, in the  $Cmc2_1$  space group and undergoes a  $P$ -induced transition to a primitive polymorph. *In situ* single-crystal synchrotron XRD allowed to identify the space group symmetry ( $Pbn2_1$ ) of the high- $P$  phase and solve its framework structure, allowing to describe the deformation mechanisms triggered by the phase transition at the atomic scale.

In the case of minerals, the fundamental thermo-elastic parameters and their relationship with the crystal structure can be accurately determined. Scapolites are common metamorphic minerals able to accommodate volatiles down to the lower crust, which members represent a complex non-binary solid solution. Modelling the role played by the crystal chemistry on the scapolites behavior is possible by investigating the response of the solid-solution members to  $T$  and  $P$  variations. Our group recently investigated the behavior of an intermediate scapolite (with anomalous  $I4/m$  symmetry) by *in situ* XRD studies at high- $P$  (ambient- $T$ ), high- $T$  (ambient- $P$ ) and combined high- $T$  and  $P$ , at synchrotron facilities, providing a comprehensive characterization of the elastic and structural response, as well as of a pressure-controlled phase transition to a triclinic polymorph (at  $\sim 9$ -10 GPa) observed at 25 and 650 °C.

*In situ* synchrotron studies on framework silicates at variable  $P/T$  also allows a better understanding of phe-

nomena, which may be exploited in materials science and technological applications, in particular promoting crystal-fluid interactions at extreme conditions. MFI-zeolites, for example, can be adopted as catalysts in the methanol-to-olefin conversion and pressure may be adopted as a tool to improve the process efficiency, by promoting a larger loading of methanol molecules into the zeolites structural pores. In situ high- $P$  powder XRD experiments on all-silica (silicalite) and slightly cation-exchanged MFI zeolites, using non-penetrating silicone oil and penetrating methanol as  $P$ -fluids, showed a higher efficiency in methanol adsorption by pure silicalite in the lower pressure regime and, conversely, a higher methanol intrusion in cation-exchanged zeolites at  $P > 0.5$  GPa.

**9:00am - 9:15am**

### Crystal Chemistry of the Ion Conducting Li-Oxide Garnet doped with Al, Ga, and Fe

**Georg Amthauer<sup>1</sup>, Daniel Rettenwander<sup>2</sup>, Reinhard Wagner<sup>1</sup>, Günther Redhammer<sup>1</sup>**

<sup>1</sup>University of Salzburg, Department of Chemistry and Physics of Materials, Austria; <sup>2</sup>Institute for Chemistry and Technology of Materials, Graz University of Technology, Austria

#### Crystal chemistry of “Li<sub>7</sub>La<sub>3</sub>Zr<sub>2</sub>O<sub>12</sub>” garnet doped with Al, Ga, and Fe: a review

Recent research has shown that certain Li-oxide garnets with more than 3 Li atoms per formula unit, such as Li<sub>7</sub>La<sub>3</sub>Zr<sub>2</sub>O<sub>12</sub> (LLZO), have high ionic conductivities, as well as good chemical and physical properties for use in solid-state batteries (Murugan et al., 2007).

“Garnet” is the common name for a large number of natural and synthetic metal-oxide phases. Conventional oxide garnets have the general formula A<sub>3</sub>B<sub>2</sub>C<sub>3</sub>O<sub>12</sub> and crystallize in the cubic space group  $la-3d$ . In LLZO the A-positions are occupied by La<sup>3+</sup>, the B-positions by Zr<sup>4+</sup>, and the C-positions by Li<sup>+</sup>. In addition to these cation sites, there are other interstices within the garnet oxygen framework, which are empty in the conventional garnet structure and which are in LLZO filled by “excess” Li<sup>+</sup> ions giving rise to the excellent ionic conductivity.

There is a low temperature tetragonal modification of pure LLZO (SG:  $I4_1/acd$ ) and a high temperature non quenchable cubic phase of LLZO (SG: ). The tetragonal phase has distinctly lower ion conductivity than the cubic phase. Fortunately, the cubic phase can be stabilized at low temperatures by doping with low amounts of Al, Ga, and Fe (Buschmann et al., 2011; Rettenwander et al. 2016). In our contribution the results of single crystal X-ray diffraction studies will be presented. While Al-doped LLZO garnets always crystallize within the space group  $Ga$  and Fe-doped LLZO garnets crystallize within the space group  $I43d$  (Wagner et al., 2016). This symmetry change is combined with an increase in ionic conductivity up to  $10^{-3}$  S cm<sup>-1</sup> which is very high for those kind of solid state electrolytes used in Li-ion batteries. These results will be discussed on the basis of the slightly different topologies of both space groups, respectively.

[1] Buschmann H., Dölle J., Berendts S., Kuhn A., Bottke P., Wilkening M., Heitjans P., Senyshyn A., Ehrenberg H. Lotnyk, A. (2011) *Physical Chemistry and Chemical Physics*, 13, 19378-19392; [2] Murugan R., Thangadurai V., Weppner W. (2007). *Angewandte Chemie, International Edition*, 46, 7778-7781; [3] Wagner, R.; Redhammer, G. J.; Rettenwander, D.; Senyshyn, A.; Schmidt, W.; Wilkening, M.; Amthauer, G. (2016). *Chem Mater* 28, 1861-1871; [4] Rettenwander, D.; Redhammer, G.; Preishuber-Pflügl, F.; Cheng, L.; Miara, L.; Wagner, R.; Welzl, A.; Suard, E.; Doeff, M. M.; Wilkening, M.; Fleig, J.; Amthauer G. (2016). *Chem Mater* 28, 2384-2392.

**9:15am - 9:30am**

### Composition dependency of the temperature-driven structural changes in (1-x)PbTiO<sub>3</sub>-xBiNi<sub>0.5</sub>Ti<sub>0.5</sub>O<sub>3</sub>

**Irina Margaritescu<sup>1</sup>, Kaustuv Datta<sup>1</sup>, Jun Chen<sup>2</sup>, Boriana Mihailova<sup>1</sup>**

<sup>1</sup>University of Hamburg, Germany; <sup>2</sup>University of Science and Technology Beijing, China

The (1-x)PbTiO<sub>3</sub>-xBiNi<sub>0.5</sub>Ti<sub>0.5</sub>O<sub>3</sub> (PT-xBNT) perovskite ABO<sub>3</sub> solid solution is a novel ferroelectric material with remarkable piezoelectric properties around the morphotropic phase boundary (MPB) and a high Curie temperature ( $T_C \sim 680$  K at  $x_{MPB} = 0.55$ ). Moreover, PT-xBNT contains a reduced amount of Pb, which makes it an attractive alternative for the current material of choice PbZr<sub>x</sub>Ti<sub>1-x</sub>O<sub>3</sub>. However, the effect of A- and B-site

co-doping on the mechanism of the temperature- and composition-induced phase transitions is not yet entirely clear. The aim of this study is to understand how the atomic structure and dynamics, which are strongly related to the properties of the material, are influenced by variations in the chemistry. In a ferroelectric solid solution, the macroscopic polarization is highly influenced by the degree of local distortion. Therefore, our focus lies on the structural changes that take place on a short- and medium-range scale. In this contribution we used temperature-dependent Raman spectroscopy (100 K to 1040 K) and neutron pair-distribution-function (PDF) analysis (300 K, 500 K, 700 K and 900 K) to investigate a series of compounds with different compositions across the morphotropic phase boundary ( $x = 0, 0.20, 0.50, 0.55$  and  $0.70$ ).

The results reveal anomalous Raman scattering related to off-centered A-site and B-site cations above the Curie temperature in all compounds (including pure PT [1,2]), indicating the presence of short-range ferroelectric order in the paraelectric phase. A gradual change in the character of the temperature-driven paraelectric-to-ferroelectric phase transition - from mainly displacive to mainly order-disorder - takes place upon doping. The analysis of the Raman scattering and the PDF reveals a competition between the polar and the antiferrodistortive order at  $x = x_{MPB}$ . Moreover, the formation of polar clusters is independent of temperature as a thermodynamic variable at the morphotropic phase boundary.

[1] Margaritescu et al. (2018) *J. Phys.: Condens. Matter* **30**; [2] Datta et al. (2018) *Phys. Rev. Lett.* **121**

9:30am - 9:45am

### Comparison of polarizability approach with Gladstone-Dale concept in mineral optics

Reinhard X. Fischer<sup>1</sup>, Robert D. Shannon<sup>2</sup>

<sup>1</sup>Universität Bremen, Germany; <sup>2</sup>University of Colorado, Boulder, USA

The Gladstone-Dale (GD) concept has been established for more than forty years since Mandarino has derived Gladstone-Dale constants for most of the common cations in oxide notation [1]. This set of constants  $k_i$  can be used to predict the mean refractive index of a mineral or inorganic compound by defining a specific chemical refractivity ( $\text{cm}^3/\text{g}$ )  $K_c = \sum_i(k_i p_i)/100$  where  $p_i$  = weight percentages of the oxide contents in the respective compounds. This quantity,  $K_c$ , is then compared to a physically derived value  $K_p = (\langle n \rangle - 1)/D$  with the density  $D$  [1,2] and the mean observed refractive index  $\langle n \rangle$ . Replacing  $K_p$  by  $K_c$  allows the calculation of the mean refractive index according to  $\langle n \rangle = \sum_i(k_i p_i)/100 \cdot D + 1$ . Mandarino [3] defined a compatibility index measuring the agreement between the two sides of  $(n-1)/D = \sum k_i p_i/100$ . This 'quality index' can be used to verify chemical compositions and refractive index determinations, and it is required, e.g., for proposals of new minerals submitted to the IMA for approval.

As an alternative to the Gladstone-Dale concept, we [4] have derived electronic polarizabilities  $\alpha_e$  for 76 cations in various coordinations,  $\text{H}_2\text{O}$ ,  $5 \text{H}_x\text{O}_y$  species, and 4 anions ( $\text{F}^-$ ,  $\text{Cl}^-$ ,  $\text{OH}^-$ ,  $\text{O}^{2-}$ ) which can be used to calculate the total polarizability  $\alpha_t$  of a mineral or synthetic compound by summing up the  $\alpha_e$  values of cations (linear term) and anions (exponential term) according to their molar fractions.  $\langle n \rangle$  can then be calculated from  $\alpha_t$  using the relationship  $\langle n \rangle = (4\pi\alpha_t / ((2.26 - 4\pi/3)\alpha_t + V_m) + 1)^{1/2}$  with the molar volume  $V_m$  [4]. This results in a higher accuracy as compared with the GD concept, especially because the polarizabilities derived from more than 2500 measurements are determined for cations with various coordination numbers. The polarizability approach can be used to predict refractive indices from chemical compositions [5], to identify possible ion conductors [6], and to determine the water content in minerals [7].

Total polarizabilities and chemical refractivities can be calculated using the program POLARIO [8].

We thank the DFG for funding (grant FI442/21-2)

[1] Mandarino, J.A. *Canadian Mineralogist* **14** (1976) 498-502; [2] **19** (1981) 441-450; [3] **17** (1979) 71-76; [4] Shannon, R.D., Fischer, R.X.: *American Mineralogist* **101** (2016) 2288-2300; [5] Shannon, R.C., Lafuente, B., Shannon, R.D., Downs, R.T., Fischer, R.X.: *American Mineralogist* **109** (2017) 1906-1914; [6] Shannon, R.D., Kabanova, N., Fischer, R.X.: *Crystal Research and Technology* (2019) in press; [7] Fischer, R.X., Burianek, M., Shannon, R.D.: *DGK* (2019) Leipzig; [8] Fischer, R.X., Burianek, M., Shannon, R.D., *American Mineralogist*, **103** (2018) 1345-1348.

9:45am - 10:00am

### High-pressure phases of feldspars with five- and six-fold coordinated aluminium

**Anna Pakhomova<sup>1</sup>, Dariia Simonova<sup>2</sup>, Egor Koemets<sup>2</sup>, Iuliia Koemets<sup>2</sup>, Georgios Aprilis<sup>3</sup>, Maxim Bykov<sup>2</sup>, Liudmila Gorelova<sup>4</sup>, Vitali Prakapenka<sup>5</sup>, Leonid Dubrovinsky<sup>2</sup>**

<sup>1</sup>Deutsches Elektronen-Synchrotron, Germany; <sup>2</sup>Bayerisches Geoinstitut, University of Bayreuth; <sup>3</sup>Materials Physics and Technology at Extreme Conditions Laboratory of Crystallography, University of Bayreuth; <sup>4</sup>Institute of Earth Sciences, Saint-Petersburg State University; <sup>5</sup>GSECARS, University of Chicago

Feldspars with a general formula  $MT_4O_8$  ( $M = Na^+, K^+, Ca^{2+}, Sr^{2+}$  and  $Ba^{2+}$ ;  $T = Si^{4+}$  and  $Al^{3+}$ ) are rock-forming minerals that make up over 50% of Earth's crust. A knowledge of the high-pressure and high-temperature behavior of feldspars is crucially important for the understanding of the chemical and thermodynamic processes within the lithosphere. A series of high-pressure single-crystal X-Ray diffraction (SCXRD) studies have been conducted up to  $\sim 10$  GPa on selected feldspar minerals with the aims of determining the variation of equation-of-state parameters with compositions and state of order [1]. Recent advances at third-generation synchrotron facilities allow to extend the pressure range of previous experiments and to get a new insight into the variation of feldspar crystal structures upon compression. Here we report on high-pressure SCXRD diffraction studies of three feldspars of high geological relevance, anortite (An),  $Ca(Al_2Si_2O_8)$ , albite (Ab),  $NaAlSi_3O_8$ , and microcline (Mc),  $(KAlSi_3O_8)$ .

Diffraction experiments were performed at the Extreme Conditions Beamline at synchrotron Petra III (Hamburg, Germany) and 13-IDD beamline at Advanced Photon Source (Argonne, United States) up to 21, 27 and 20 GPa for An, Mc and Ab, respectively. At ambient conditions the crystal structures of feldspars consist of a three-dimensional framework of strongly-bonded  $TO_4$  tetrahedra formed by the sharing of oxygen atoms between tetrahedra.  $Ca^{2+}$ ,  $Na^+$  and  $K^+$  atoms occupy the larger voids in the tetrahedral framework to provide charge balance. According to the previous observations, the compression of An and Mc at pressures up to  $\sim 10$  GPa is controlled by changes in T-O-T angles whereas  $TO_4$  units do not undergo significant distortion. We have discovered that at elevated pressures  $AlO_4$  units start to undergo pressure-induced geometrical distortion resulting in increase of Al coordination number. Thus, above 10 GPa studied feldspars transform into new high-pressure polymorphs featuring pentacoordinated (trigonal bipyramidal geometry) and/or octahedrally coordinated Al sites. In addition, high-pressure phase of Ab features [5+1] coordination of a Si site. In order to investigate HP-HT stability of the discovered polymorphs, multi anvil experiments on An and Ab have been performed in the pressure and temperature range of 13-15 GPa and 300-800 °C, respectively. The results of the multi anvil and SCXRD experiments will be discussed in detail along with application of the results to the current geological models.

[1] Angel R.J. In: Parsons I. (eds) Feldspars and their Reactions. NATO ASI Series (Series C: Mathematical and Physical Sciences). 1994, **421**. Springer, Dordrecht.

10:00am - 10:15am

### Dauphiné twin in a naturally deformed quartz: Characterization by electron channelling contrast imaging and large-angle convergent-beam diffraction

**Nobuyoshi Miyajima, Danielle Silva Souza, Florian Heidelbach**  
Bayerisches Geoinstitut, Universität Bayreuth, Germany

Dauphiné twinning occurs when high temperature quartz (h-Qtz) transforms back to low temperature quartz (l-Qtz) or l-Qtz is subjected to high shear stress. Dauphiné twins (DTs) are related to each other by a 2-fold symmetry operation about the [001] direction, this being the very symmetry lost when [001] transformed from a 6-fold to a 3-fold axis. The intergrowth of the transformation twins appears to have a symmetry equal to that of the high-temperature form. The origin and role of DTs in a naturally deformed Qtz affect the fabric development in plastic deformation. For the interpretation of quartz deformation mechanisms, it is important to identify DTs and slip systems with transmission electron microscopy (TEM). DTs are not visible in polarized light optical microscopy and conventional SEM. Dark-field (DF) TEM imaging is the best to investigate

DTs at the nanoscale. However, DTs in deformed Qtz have not yet been unequivocally characterized in TEM due to the interference with high density of dislocations and misoriented subgrain boundaries in DTs.

In the current project we successfully identified DTs in a deformed Qtz by electron channelling contrast imaging (ECCI) in a field emission scanning electron microscopy (FESEM) assisted with electron backscattering diffraction (EBSD). The DTs were then examined by using precession electron diffraction (PED) and large-angle convergent-beam diffraction (LACBED) in TEM.

TEM foils were prepared from Dauphiné twin boundaries (DTBs) characterized by ECCI, by using the site-specific focused ion beam (FIB) sampling. The DF-TEM images with diffraction vectors of rhombohedral planes, e.g.,  $g = 301$  revealed that the twin domains have different patterns of the thickness contour fringes reflected with the differences of the structure factors of negative and positive rhombohedral planes in the electron diffraction at 200 kV acceleration voltage. The LACBED pattern from the boundary indicates no mis-orientation between the twin domains. Also, PED intensities from the twin domains are consistent with those of the twin law. These results support that the different ECCI contrasts from the twin domains do not originate from the mis-orientation across the DTBs but the differences of the structure factors of positive and negative rhombohedral planes in electron diffraction at 20 kV in FESEM. The visualization mechanisms of DTs in Qtz with ECCI, for the first time, are clarified by electron diffraction analysis in TEM. Combining ECCI and FIB milling techniques to prepare site-specific TEM foils provide a robust approach to investigate DTs in Qtz at the nanoscale.

**10:15am - 10:30am**

### **First-principles calculations elucidate the dynamics of extra-framework species in zeolites**

**Michael Fischer**

*Crystallography group, Department of Geosciences, University of Bremen, Germany*

Extra-framework species play a pivotal role in determining the structure and properties of zeolites. While extra-framework metal cations act as charge-balancing species in natural zeolites and most synthetic aluminosilicate zeolites, organic cations, also termed organic structure-directing agents (OSDAs), are used in the synthesis of neutral-framework zeotypes, such as all-silica zeolites, silicogermanates, and aluminophosphates. To compensate the charge of the OSDA, inorganic anions may be added to the reaction mixture. In particular, the presence of fluoride anions during the synthesis (“fluoride route”) often affords highly crystalline, defect-free zeolites.<sup>1</sup> Moreover, some zeolite frameworks are synthetically accessible only in the presence of fluoride. Diffraction studies have delivered information regarding the equilibrium positions of OSDAs (which occupy larger cavities) and fluoride anions (which are found in small cages) for many as-synthesised neutral-framework zeotypes. The dynamic behaviour of extra-framework species is more difficult to investigate experimentally, although solid-state NMR experiments can provide useful insights, e.g. by distinguishing static and dynamic disorder of fluoride anions.<sup>2</sup>

In this contribution, ab-initio molecular dynamics calculations based on dispersion-corrected density functional theory are employed to study the fluoride anion dynamics in neutral-framework zeotypes. For the case of silicogermanates having AST topology, it is found that the local environment of fluoride, especially the distribution of Si and Ge on the surrounding tetrahedral sites, determines the bonding situation and, in turn, the dynamic behaviour.<sup>3</sup> By comparing AST-type systems containing OSDA cations of different symmetry, it is assessed to what extent the OSDA charge distribution affects the fluoride anion dynamics. The interplay between the OSDA and fluoride dynamics is then studied in considerable depth for MFI-type Silicalite-1. Here, an NMR investigation has shown that a change of the OSDA can lead to a suppression of the dynamic disorder of fluoride at room temperature.<sup>4</sup> Besides corroborating these experimental results, calculations for systems containing a number of different organic cations provide insights into more general relationships between OSDA size/symmetry and the dynamic behaviour of fluoride anions.

Funding by the Deutsche Forschungsgemeinschaft, project no. 389577027, is gratefully acknowledged.

[1] P. Caullet, J. Paillaud, A. Simon-Masseron, M. Soulard, J. Patarin, *Comptes Rendus Chim.*, 2005, **8**, 245–266; [2] H. Koller, A. Wölker, L. A. Vilaescusa, M. J. Diaz-Cabañas, S. Valencia, M. A. Cambor, *J. Am. Chem. Soc.*, 1999, **121**, 3368–3376; [3] M. Fischer, *J. Phys. Chem. C*, 2019, **123**, 1852–1865; [4] S. L. Brace, P. Wormald, R. J. Darton, *Phys. Chem. Chem. Phys.*, 2015, **17**, 11950–11953.

## Poster Presentations

Tue: 62

**Crack-enhanced weathering in engraved marble: a possible application in epigraphy****Stylianos Aspiotis<sup>1</sup>, Jochen Schlüter<sup>2</sup>, Kaja Harter-Uibopuu<sup>3</sup>, Boriana Mihailova<sup>1</sup>**<sup>1</sup>Fachbereich Geowissenschaften, Universität Hamburg, Germany; <sup>2</sup>CeNaK, Mineralogisches Museum, Universität Hamburg; <sup>3</sup>Fachbereich Geschichte, Universität Hamburg

Interpreting written artefacts provides key information about the roots of the human civilizations. However, even stone inscriptions can disappear due to surface weathering over time. Much effort has been recently put in unravelling vanished or hardly readable written artefacts on marble headstones and sculptures, through the application of non-destructive methods such as X-ray fluorescence (XRF) [1] [2]. The results could not satisfactorily detect the lost text on the basis of trace elements introduced onto the marble surface during the inscription [1]. Therefore, alternative non-invasive methods are required. Cracks and structural defects around the inscribed areas of the marble written artefacts facilitate the development of weathering products, which can be among others various oxalates, carbonate hydrates, calcium sulphates and organisms like lichen, which all can be detected via Raman spectroscopy. That means that the density of the weathering products beneath the engraved areas is higher than beneath plain marble. This lateral distribution of the weathering products can be used to map, visualize and recover lost text on intensely weathered stone inscriptions. However, the weathering rate and products depend on the local climate, urban environment and age of the written artefacts as well as the actual position and attitude of the inscriptions, which regulates the extent of exposure to wind, rain and sun. To probe the potential of Raman spectroscopy for visualization of texts on rock-base epigraphic objects, we have analyzed ancient engraved marble from Greece as well as marble gravestones from the Ohlsdorf cemetery, Hamburg, inscribed ~70 years ago. The latter were subjected to intensive bio-degradation due to the local climate. The results from line profiling on cross-section cuts indeed show larger abundance of lichen beneath the engraved letters than beneath the virgin surface of the headstone. Such evidence is provided by the intensity ratio of the peaks near 1522 cm<sup>-1</sup> (typical of lichen) and near 1087 cm<sup>-1</sup> (symmetrical CO<sub>3</sub> stretching of calcite). The results from mapping marble, after mechanically removing the surface layer to the stage that the text is not readable anymore, will be also presented.

[1] J. Powers et al., *Z. Papyr. Epigr.* (2005) 152, 221-227; [2] D. Pinna et al., *Heritage Science* (2015) 3, 1-13.

Tue: 63

**Characterization of heat-treated ceramics consisting of zoned acicular crystals with two mullite phases of different compositions****Johannes Birkenstock, Reinhard X. Fischer, Hartmut Schneider***Universität Bremen, FB5-Geowissenschaften, Germany*

We investigated acicular mullite ceramics described in [1] consisting of two distinct mullite phases, one with ~63.5 mol% Al<sub>2</sub>O<sub>3</sub> and one with ~58.9 mol% Al<sub>2</sub>O<sub>3</sub> (average composition ~62 mol% Al<sub>2</sub>O<sub>3</sub>, phase fractions ~68 and ~32 mass%, respectively) as derived from powder XRD (pXRD) data [2]. The average is close to 61.2(3) mol% as determined in single-crystal XRD (scXRD) analyses [2].

In the general compositional series <sup>VI</sup>Al<sub>2</sub><sup>IV</sup>[Al<sub>2+2x</sub>Si<sub>2-2x</sub>]O<sub>10-x</sub>, synthetic 3/2-mullites in ceramics usually have x= 0.25 (60 mol% Al<sub>2</sub>O<sub>3</sub>) whereas melt-grown synthetic 2/1-mullites possess x= 0.4 (66.7 mol%) [3]. Interestingly, none of the above compositions falls into these categories. In [1] cross sections on the acicular crystals revealed Si-rich cores (~56 % Al<sub>2</sub>O<sub>3</sub>) and Al-rich rims (~63 % Al<sub>2</sub>O<sub>3</sub>), roughly matching the XRD-derived values for the two phases.

Powdered (S1) and as-received (S2) samples were heat-treated (1550°C, 24h) and then analyzed by pXRD, and by pXRD and scXRD, respectively. Unfortunately, abrasion of the milling beads (α-Al<sub>2</sub>O<sub>3</sub>) contributed to S1 which transformed on heating to single-phase mullite with increased Al<sub>2</sub>O<sub>3</sub>-content, 62.53(9) mol% as derived from compositional refinement and 63.8(10) mol% from lattice parameter refinement.

Sample S2 still showed two mullite phases in pXRD, yet with ~14 mass% of a phase with lower Si-content, reflecting a beginning homogenization. However, the small fraction, strong peak overlap and strong parameter-correlations impeded a reliable determination of compositions from refined parameters. In scXRD, similar to [2], no distinction between the two mullite phases was possible. However, the quality of the scXRD data was sufficient to determine the average composition to 60.9(2) mol%, virtually unchanged compared to the untreated crystal (61.2(3) mol%) in [2].

As a result, it seems that heat treatment did not change the gross composition of the acicular crystals, yet we found a trend for homogenization via solid-state diffusion at high temperature. Further studies are on their way to trace down the details of this homogenization.

We thank Prof. K.T. Faber (NW University, Evanston, IL/USA) for providing the samples, and the DFG for funding (Grant FI442/24-1).

[1] A.J. Pyzik, C.S. Todd & C. Han (2008), *J. Eur. Cer. Soc.* 28, 383-391; [2] A.L. Todor, J. Birkenstock, R.X. Fischer & H. Schneider (2018), Abstract GeoBonn 2018; [3] R.X. Fischer & H. Schneider (2005), in *Mullite* (eds. H. Schneider, S. Komarneni), Weinheim: Wiley-VCH 1-46

## Tue: 64

### Polarized mapping Raman spectroscopy: Identification of particle orientation in biominerals

Jianhan He, Ulrich Bismayer

*Universität Hamburg / Mineralogy, Germany*

The identification of the texture of biominerals and particle orientations in bivalve shells of *Anodonta cygnea* was performed using polarized Raman spectroscopy mapping measurements. A single crystal of aragonite served as a reference for orientational information on the corresponding length scale. The relative intensities of different Raman modes combined with the depolarization ratio of the  $A_g$  Raman mode at  $1087\text{ cm}^{-1}$  of an aragonite single crystal was used to indicate the angular variation of the aragonite crystallites in biominerals. The imaging technique reveals that the a- and b-axis of aragonite crystallites in both, nacreous and prismatic layers do not only have one orientation, furthermore they are organized in a domain-type arrangement. The angular divergence in the prismatic layer of the shells is larger and hence, the crystallites in the nacreous layer have a higher degree of co-orientation. Results show relevant textural information about aragonitic shells and in general provide a sensitive technique to evaluate the crystal orientation in biominerals.

## Tue: 65

### Thermoelastic properties of rare-earth scandates $\text{SmScO}_3$ , $\text{TbScO}_3$ and $\text{DyScO}_3$

Christian Hirsche<sup>1</sup>, Jürgen Schreuer<sup>1</sup>, Steffen Ganschow<sup>2</sup>, Isabelle-Mercedes Schulze-Jonack<sup>2</sup>

<sup>1</sup>*Ruhr-Universität Bochum, Institut für Geologie, Mineralogie und Geophysik, Universitätsstr. 150, 44801 Bochum, Germany;* <sup>2</sup>*Leibniz-Institut für Kristallzüchtung, Max-Born-Str. 2, 12489 Berlin, Germany*

Thin-films with perovskite-type structure can exhibit a broad gamut of properties, such as ferroelectricity, ferromagnetism and colossal magnetoresistance<sup>[1]</sup>. Growing such thin-films requires substrates with similar structure and lattice parameters to minimize interfacial strain. Orthorhombic rare-earth scandate perovskites ( $\text{REScO}_3$ , space group  $Pnma$ ) can be used as substrate materials, as their lattice parameters can be precisely tuned by (partly) exchanging the RE<sup>[2]</sup>. Furthermore, they can be grown as large single crystals and have outstanding physico-chemical stability with melting temperatures above  $2000\text{ °C}$ <sup>[3]</sup>.

Knowledge of the elastic properties of a substrate and their temperature-dependence allows to estimate the interfacial stress that emerges when the substrate and thin-film are subjected to temperature changes. Therefore, we investigated thermal expansion and linear elasticity of  $\text{SmScO}_3$ ,  $\text{TbScO}_3$  and  $\text{DyScO}_3$  from 103 K to 1673 K using inductive gauge dilatometry and resonant ultrasound spectroscopy.

The crystals are elastically softest along the direction of the dominant zigzag chains of corner-connected

octahedra, [010], because longitudinal stress likely translates to increased tilt of the octahedra, rather than bond compression. With increasing charge density caused by decreasing *RE*-radius, the crystal species become stiffer and have higher elastic Debye temperatures. The anisotropy of the elastic behavior approaches tetragonal symmetry with rising temperature, which is probably caused by decreasing structural tilt as the orthorhombic structures become more and more similar to a hypothetical tetragonal high-temperature phase. Positive temperature coefficients of the shear resistance  $c_{44}$  of all three  $REScO_3$  below about 270 K (for  $SmScO_3$ ) and 470 K (for  $DyScO_3$ ) resemble the characteristic behavior of the critical parameter of the orthorhombic to monoclinic phase transitions observed in other perovskites involving shear of the (100)-plane. However, in the case of  $REScO_3$ , such phase transitions could not be activated and may require increasing pressure. The positive temperature coefficients further imply that crystal cuts can be manufactured where specific eigenfrequencies have zero temperature dependence. The acoustic wave attenuation is low in the entire temperature range.

[1] Schlom, D. G., Chen, L.-Q., Pan, X., Schmehl, A. and Zurbuchen, M. A. (2008). *J. Am. Chem. Soc.* **91**, 2429; [2] Uecker, R., Klimm, D., Bertram, R., Bernhagen, M., Schulze-Jonack, I., Brützam, M., Kwasniewski, A., Gesing, T. M. and Schlom, D. G. (2013). *Acta Phys. Pol. A* **124**, 295; [3] Christen, H. M., Jellison, G. E., Ohkubo, I., Huang, S., Reeves, M. E., Cicerella, E., Freeouf, J. L., Jia, X. and Schlom, D. G. (2006). *Appl. Phys. Lett.* **88**, 262906.

Tue: 66

### Studies on Labradorescence

**Nikolas Kraft, Gert Kloess, Hieronymus Hoelzig, Johannes Scheffler**

*Leipzig University, Faculty of Chemistry and Mineralogy, IMKM, Germany*

Labradorization is a commonly known optical effect of plagioclases with a composition of  $An_{46}$  to  $An_{60}$ . Over the last century many scientists helped to determine the crystal structure and its role in producing the labradorescence. It is the result of a spinodal decomposition. The submicroscopical lamellae, which are oriented parallel to the (010) planes, cause a diffraction of light in a similar manner as X-rays are diffracted by lattice planes in any crystal. This leads to the red, blue or yellow schiller.

The focus of this study was a large single crystal of spectrolite (6 cm x 3 cm) from Finland. Using the combination of X-ray diffraction and optical techniques, the angular dependence of the effect of labradorescence could be studied more in detail. The effect was analyzed using a universal stage combined with an optical microscope and a UV-Vis spectral photometer to measure remission spectra. The orientation of the single crystal was determined using an X-ray diffractometer with a 2D-detector. The optical effect was correlated to the orientation of the spectrolite crystal. Cabochon-like specimens from Madagascar were investigated in the same manner.

Tue: 67

### The diagenetic loop of the opal-A to opal-CT transformation

**Moritz Liesegang, Frank Tomaschek**

*Institute of Geological Sciences - University Bonn, Germany*

The diagenetic maturation of amorphous biogenic silica (opal-A) in marine sediments is the idealized model for the gradual phase transformation and structural ordering sequence from opal-A (opal-A/CT, opal-CT/A) to opal-CT, opal-C, and eventually quartz, via dissolution-precipitation processes at increasing temperature and age. This XRD-based phase maturation concept is universally applied to a variety of geological environments, for example, siliceous hot-spring deposits, alteration products of deep-weathering environments, desert varnish, and potentially biosignature-preserving silica deposits on Mars.

Here we use X-ray powder diffraction to identify peak parameters that characterize the early-stage silica maturation from opal-A to opal-CT. We analyzed several million-year-old opal-CT samples from a variety of continental deposits, and the products of opal mixing and heating experiments. XRD analysis reveals that the

calculated domain size of opal-CT from continental deposits is decoupled from the low-tridymite/cristobalite ratio inferred from the main peak position  $\sim 4.1$  Å. While the FWHM vs. peak position plot of opals forms a diagenetic loop, peak parameters for a previously suggested quantitative classification as opal-A/CT or opal-CT/A are absent. Our results suggest that the traditional diagenetic maturation indicators (main peak position and FWHM) do not record the structural order expressed by the calculated size of coherently scattering domains of opal-CT. Mixing experiments with opal-A and -CT show that the disordered component significantly modifies key parameters of the main peak at  $\sim 4.1$  Å of more mature opaline silica, especially its width. Conversely, systematic changes of the width and position of the subsidiary peak at  $\sim 2.5$  Å accurately reflect the low-tridymite/cristobalite ratio and degree of order. This information is essential for genetic reconstructions, especially of open systems with internal re-distribution and external input of dissolved silica.

Our analyses imply that the widely accepted XRD-based concept of synchronous domain growth at decreasing low-tridymite/cristobalite ratio, established for biogenic silica maturation in marine sediments, is not directly transferable to open systems. For future studies on opaline silica diagenesis, it is crucial to define if the degree of structural order refers to the range of order, low-tridymite/cristobalite ratio, existence of a specific silica phase, or a combination of these properties, to distinguish between the initially deposited opal and later diagenetic overprints.

Tue: 68

### Structural modulations in malayaite, $\text{CaSnOSiO}_4$

**Thomas Malcherek<sup>1</sup>, Bianca Paulenz<sup>1</sup>, Michael Fischer<sup>2</sup>, Boriana Mihailova<sup>1</sup>, Carsten Paulmann<sup>1</sup>**

<sup>1</sup>Mineralogisch-Petrographisches Institut, Universität Hamburg, Germany; <sup>2</sup>Fachgebiet Kristallographie, Fachbereich Geowissenschaften, Universität Bremen, Germany

Malayaite is the Sn-analogue of the common accessory mineral titanite,  $\text{CaTiOSiO}_4$ . Substitution of Sn for Ti suppresses the well known transition from  $C2/c$  to  $P2_1/c$  symmetry, as Sn does not tend to statically displace from the center of its oxygen coordination polyhedron and contrary to titanite, phonon modes associated with such displacements are stable in malayaite [1]. However, calculation of the phonon dispersion in malayaite by means of density functional perturbation theory (DFPT), indicates that a Raman active mode dominated by motion of the Ca atoms is unstable in the monoclinic crystal structure at zero temperature. Softening of this mode has been confirmed by Raman spectroscopy of a natural malayaite single crystal over a temperature range of 400 to 90 K. While single crystal X-ray diffraction indicates no deviation of the malayaite crystal structure from space group symmetry  $C2/c$  at temperatures above 90K, synchrotron X-ray diffraction at 20K does show first order satellite reflections with a modulation vector of  $\mathbf{q} = 0.27 \mathbf{b}^*$ . The structural modulations indicated by the satellite reflections are compared with the results of the DFPT calculations and discussed within the context of known instabilities of the titanite crystal structure under variable chemistry conditions.

[1] Malcherek T. & Fischer M. (2018) Phys. Rev. Mater. 2, 023602

Tue: 69

### Structural control of thermomechanical properties of monoclinic rare-earth calcium oxoborates

**Marie Münchhalfen<sup>1</sup>, Jürgen Schreuer<sup>1</sup>, Christoph Reuther<sup>2</sup>, Erik Mehner<sup>3</sup>, Hartmut Stöcker<sup>3</sup>**

<sup>1</sup>Institute of Geology, Mineralogy and Geophysics, Ruhr University Bochum, Germany; <sup>2</sup>Institut of Mineralogy, Freiberg University of Mining and Technology; <sup>3</sup>Institute of Experimental Physics, Freiberg University of Mining and Technology

Monoclinic (space group  $Cm$ ) rare-earth calcium oxoborates ( $RCOB$ ),  $RCa_4O(BO_3)_3$  ( $R$  = rare earth element), initially were studied because of their promising non-linear optical properties, but recently gathered interest as potential candidates for high-temperature piezoelectric sensing applications since they combine favorable properties like high melting point at around 1770 K, no reported structural phase transitions, high piezoelec-

tric sensitivity and high electric resistivity [1]. Since the *RCOB* structure offers different possibilities for cation substitution, a tuning of physical properties is principally possible.

Large single crystals of  $RCa_4O(BO_3)_3$  (R = Er, Y, Dy, Gd, Sm, Nd, La) were grown from melt using the Czochralski method and their electromechanical properties were studied between 100 K and 1473 K using dilatometry and resonant ultrasound spectroscopy.

Contrary to the reported lack of phase transitions, all investigated physical properties undergo reproducible discontinuities between 900 and 1300 K. Ex-situ quenching experiments were conducted and analyzed with single crystal X-ray diffraction to draw a correlation between the structure and the observed properties and discontinuities.

[1] Yu, F., Hou, S., Zhao, X., Zhang, S. (2014): IEEE Trans. Ultrason., Ferroelect., Freq. Control, **61**, 1344-1356.

Acknowledgments: The authors gratefully acknowledge financial support of the DFG (PAK921/1, SCHR 761/4: Structure/property relationships and structural instabilities of high-temperature piezoelectrics of the oxoborate family.

**Tue: 70**

## Ceramic transformations during firing of ancient Japanese stone ware (Sueki): insights from firing experiments

**Michael M. Raith, Harald Euler, Beate Spiering, Radegund Hoffbauer**

*Universität Bonn, Germany*

Sueki is high-fired Japanese stone ware (4-10<sup>th</sup> century AD) that was manufactured in wood-fired single-chamber tunnel kilns. Peak-firing temperatures around 1150 °C and a reducing atmosphere are inferred from firing experiments in re-built kilns [1] and the archaeometric study of sherds and kiln wall samples [2, 3].

To constrain the temperature regime of sequential ceramic transformations in Sueki, firing experiments along well-controlled temperature-time paths and reducing conditions were performed on a clay sample from the Nakadake archaeological kiln site (southern Japan), which closely matches the bulk chemistry and particulate mineralogy of low-fired sherds recovered from the site [2].

The essential ceramic transformations commence at firing temperatures exceeding 900 °C: (1) initiation of matrix vitrification through breakdown and melting of kaolinite and illite (900-950°C), roughly coinciding with the appearance of (Fe,Mg)-spinel, mullite and cristobalite; (2) Na↔K exchange of K-feldspar and albite clasts with the matrix, shifting feldspar compositions towards the thermal minimum (Or<sub>40</sub>Ab<sub>60</sub>) in the Ab-Or-An ternary system (900-1050°C); (3) onset of alkali feldspar melting [Afs → Liq; 1050-1100°C] with elimination of the matrix grain fraction, followed by progressive melting and elimination of large alkali feldspar clasts [Afs → Liq + Mul; ~1150°C]; (4) dissolution of plagioclase [Pl<sub>An35-65</sub> → Liq + Pl<sub>2</sub> + Mul; onset: 1150°C, completion: ~1250°C]; (5) dissolution of titanomagnetite [Mag → Liq + (Fe,Mg)-Spl ± Crd; onset: ~950°C, completion: ~1150°C]; (6) dissolution of orthopyroxene [Opx → Liq + Crd + Crn ± Spr; onset: 1150°C, completion: ~1250°C]; (7) dissolution of quartz clasts, beginning with the appearance of matrix melt (~1000°C), and progressing to complete elimination of the matrix grain fraction concomitant with advanced alkali feldspar melting (~1150°C).

Microtextural and compositional heterogeneities of vitreous domains in the highly vitrified ceramics mimic the sites of precursor particulate inclusions and clayey matrix domains. This indicates vitrification through grain boundary-controlled dissolution/melting reactions that largely retained the bulk Al/Si ratios of the precursor phases/domains, but involved efficient diffusive transfer of alkali and alkaline earth elements through the wide-meshed alumina-silicate framework of the steadily increasing melt phase.

[1] Yogo, T. & Sasaki, M. (2004). Color of Sueki - study on the experimental and technical simulation and scientific analysis. (In Japanese). *Kodai*, **112**, 122-150; [2] Raith, M. M., Hoffbauer, R., Spiering, B., Shinoto, M., Nakamura, N. (2016). *Journal of European Mineralogy*, **28**, 385-407; [3] Raith, M. M., Euler, H., Spiering, B., Hoffbauer, R., Shinoto, M., Nakamura, N. (2017). Abstract Volume, Session 9.1, A-178; [www.dmg-home.org/fileadmin/Konferenzen/Abstracts\\_GeoBremen17.pdf](http://www.dmg-home.org/fileadmin/Konferenzen/Abstracts_GeoBremen17.pdf)

Tue: 71

### Thermal stability and oxidation processes in actinolite studied by Raman spectroscopy

**Constanze Rösche, Naemi Waeselmann, Jochen Schlüter, Boriana Mihailova**

*Department Earth Sciences, University of Hamburg, Grindelallee 48, Hamburg, 20146, Germany*

Amphiboles ( $AB_2C_5T_8O_{22}W_2$ ,  $C=M1_2M2_2M3$ ) are hydrous double-chain silicates that may occur in different geological environments. Understanding the thermodynamic behavior of amphiboles at atomic-scale may have implications in several fields such as petrology or material and environmental science. In addition, the study of oxidation processes in iron-containing amphiboles is expected to be of great significance for geophysics and medical science. Amphiboles on the tremolite – ferro-actinolite join are calcium amphiboles with varying content of magnesium and divalent iron as C cations. In this work the intermediate member of the series, actinolite (ideally  $\square Ca_2(Mg_{5-x}Fe_x)Si_8O_{22}(OH)_2$ ,  $x \in (0.5, 2.5)$ ), was studied regarding its thermal stability and oxidation processes by conducting in situ Raman spectroscopic experiments in the temperature range from 300 K to 1400 K in air as well as from 100 K to 870 K in  $N_2$  atmosphere [1]. The thermal behavior of actinolite was followed by analyzing the temperature trends of the phonon wavenumbers, widths and intensities. Especially the evolution of the phonon modes associated with the O-H bond stretching,  $SiO_4$ -ring vibrations, and  $MO_6$  octahedral vibrations are of great interest for observing the ongoing dehydroxylation reaction with increasing temperatures.

The results reveal that the dehydroxylation reaction starts at 1100 K, where  $H^+$  cations begin to delocalize but stay inside the crystal bulk and under subsequent cooling reversibly localize back to oxygen at the W site. This  ${}^W OH \leftrightarrow {}^W O^{2-}$  exchange is accompanied by reversible electron delocalization leading to reversible oxidation of  ${}^{M1,M3} Fe^{2+}$  to  ${}^{M1,M3} Fe^{3+}$ . Only at higher temperatures, when their kinetic energy is high enough,  $H^+$  cations can be ejected from the crystal. At 1300 K the delocalization is completed but not all  $H^+$  cations have been ejected. The ejection of  $H^+$  cations is compensated by irreversible oxidation of divalent iron to trivalent iron. This change from ferrous to ferric amphibole is allowed because at this temperature the  $SiO_4$ -ring geometry changes in order to adapt to the smaller size of the trivalent C cation. By heating up to 1400 K all  $H^+$  cations are ejected from the crystal, which leads to a collapse of the amphibole structure and the actinolite turns into a defect-rich pyroxene. Our studies on other amphibole species showed that tremolite ( $\square Ca_2(Mg_{5-x}Fe_x)Si_8O_{22}(OH)_2$ ,  $x = 0$ ) transforms exactly at the same temperature into a defect-rich Fe-free pyroxene.

[1] Rösche, C. (2018), BSc thesis University of Hamburg,

<https://www.geo.uni-hamburg.de/mineralogie/bachelorarbeiten/roesche-bachelorarbeit.pdf>

Tue: 72

### Radiation induced lattice disordering in monazite and xenotime from Namibia

**Johannes Scheffler, Gert Kloess, Hieronymus Hoelzig, Nikolas Kraft**

*Leipzig University, Faculty of Chemistry and Mineralogy, IMKM. Germany, Germany*

Monazite and xenotime are phosphate minerals of rare earth elements, where the latter occur in the +III oxidation state. These minerals incorporate amongst others the radioactive elements Th and U. High energy radiation which is emitted during to radioactive decay is in principle capable of perturbing the crystalline lattice to the extent where it is obscured to complete vitrification.

The effect of radiation damage was studied on samples of radioactive monazite and xenotime sand from Namibia using X-ray powder diffraction. To evaluate the degree of metamictisation we performed peak profile analysis to determine micro-strain and domain size before and after annealing. For this Williamson-Hall and Warren-Averbach methods were employed. In this context it is to be pointed out, that the process of recrystallization is exothermic and releases the energy stored by the perturbation of the crystalline order.

## Tue: 73

**Comparison of the thermal expansivity of transition metal olivines**

**Peter Schmid-Beurmann<sup>1</sup>, Herbert Kroll<sup>1</sup>, Alexander Sell<sup>1</sup>, Robin Dohr<sup>1</sup>, Armin Kirfel<sup>2</sup>, Hannes Krüger<sup>3</sup>, Volker Kahlenberg<sup>3</sup>**

<sup>1</sup>Institut für Mineralogie, WWU Münster, Germany; <sup>2</sup>Steinmann Institut, RFW Bonn, Germany; <sup>3</sup>Institut für Mineralogie und Petrographie, Universität Innsbruck, Austria

To compare the thermal behaviour of end-member olivines containing cations of the transition element series Mn, Fe, Co and Ni we studied the thermal expansivity of Co and Ni olivine by X-ray powder and single crystal diffraction at ambient pressure and temperatures between 25°C and 1000°C. The anisotropy of the thermal expansion was analyzed using the Kumar equation-of-state (EoS) coupled with the thermal Mie-Grüneisen EoS. Axial compressibilities  $\beta_{T,i}$  and axial expansivities  $\alpha_i$  are related *via* thermal pressures  $(\partial P/\partial T)_i$  according to  $\alpha_i = \beta_{T,i} (\partial P/\partial T)_i$ . For olivines, the isothermal compressibilities  $\beta_{T,i}$  can be related to structural properties and suggest a sequence with  $\beta_{T,b} > \beta_{T,c} > \beta_{T,a}$  (SG *Pbnm*). According to White et al. (1985) “thermal expansion is a response to thermal pressure  $(\delta P/\delta T)$  and is the greater the more compressible the material or direction”. Thus, in the case of isotropic thermal pressures,  $\alpha_i$  and  $\beta_{T,i}$  are expected to be proportional, with  $\alpha_i$  showing the same ranking as  $\beta_{T,i}$  so that in olivines  $\alpha_b > \alpha_c > \alpha_a$ . Such expectation is fulfilled for Mg and Mn olivine but not for Fe olivine and to a lesser extent for Co and Ni olivine. In the case of Fe olivine,  $\alpha_b$  is smallest whereas in Ni and Co olivine it lies in between  $\alpha_a$  and  $\alpha_c$ .

This unusual behaviour of the thermal expansivities  $\alpha_i$  can be related to the anisotropy of the axial thermal pressures  $(\partial P/\partial T)_i$  as this quantities are part of the thermodynamic identities  $\alpha_i = \beta_{T,i} (\partial P/\partial T)_i$ . In the case of Mg and Mn olivine the axial pressures  $(\partial P/\partial T)_i$  behave rather isotropic whereas for Fe and Co olivine a strong anisotropy results in a large gap between the thermal pressures in the *b* and in the *a* and *c* directions, respectively. The thermal expansion behaviour of Fe and Co olivine compared to Mg olivine is largely related to the variation in the orientations and lengths of M1 and M2 octahedral axes. Their projections onto the *a* and *b* directions dominate the lengths of the cell edges.

When Mg is substituted by Fe or Co, the average of the angles between the two octahedral axes and the *b* direction becomes smaller, the one to the *a* direction gets larger. This effect is supposed to reduce the thermal pressure in the *b* direction explaining the small values of  $\alpha_b$  with temperature.

[1] White et al. (1985) High Temp - High Press 17: 61-65.

## Tue: 74

**Insights into the stability of 5-fold coordinated Si in MgSiO<sub>3</sub>-melts at pressures of the Earth's upper mantle**

**Maximilian Schulze<sup>1</sup>, Georg Spiekermann<sup>2</sup>, Max Wilke<sup>2</sup>, Gerhard Heide<sup>1</sup>**

<sup>1</sup>TU Bergakademie Freiberg, Germany; <sup>2</sup>Universität Potsdam, Germany

For a better understanding of the physical properties of silicate melts in the Earth's interior, like viscosity and density, structural investigations of glasses or melts under high pressures, aiming to reveal the mechanism behind pressure-driven densification, are indispensable. Therefore, various experimental investigations as well as ab-initio molecular dynamics simulations (AIMD) of MgSiO<sub>3</sub>-glasses have been performed in the past [1, 2, 3]. This chemical composition represents a simple approximation of the Earth's mantle. It is well known that the primary Si coordination number changes from 4 under ambient conditions to 6 towards higher pressures, whereas the exact transition process and thus the role of <sup>IV</sup>Si is still uncertain. Since the interpretation of spectroscopic data concerning the formation of <sup>IV</sup>Si is highly speculative, suggestions relating to this cover a broad range of pressures reaching from 3 GPa up to 20 GPa [1, 2]. Previous results from AIMD provide either insights into the mean coordination number of Si or information is limited to the presence of <sup>IV</sup>Si for single time steps. On the basis of these approaches it is impossible to determine, whether <sup>IV</sup>Si is energetically stable in MgSiO<sub>3</sub>-melts.

Our aim is to characterize fivefold coordinated Si as a species. For this purpose we carry out AIMD simulations of  $\text{MgSiO}_3$  -melts between 0 and 25 GPa. Evaluation tools that are novel to the evaluation of MD-trajectories of silicate melts will allow for insight into the stability of  $^{\text{IV}}\text{Si}$  in time. Among those are bond and cage correlation functions [4]. These tools discriminate between accidental short-lived fivefold coordination and those  $^{\text{IV}}\text{Si}$  that exist longer than just a few AIMD time steps.

[1] Moulton et al. (2016) In situ structural changes of amorphous diopside ( $\text{CaMgSi}_2\text{O}_6$ ) up to 20 GPa: A Raman and O K-edge X-ray Raman spectroscopic study. *Geochimica et Cosmochimica Acta* 178, 4161; [2] Shim, Sang-Heon; Catalli, Krystle (2009) Compositional dependence of structural transition pressures in amorphous phases with mantle-related compositions. *Earth and Planetary Science Letters* 283, 174180; [3] Ghosh et al. (2014) First-principles molecular dynamics simulations of  $\text{MgSiO}_3$  glass: Structure, density, and elasticity at high pressure. *American Mineralogist* 99, 1304 - 1314; [4] Luzar, Alenka; Chandler, David (1993) Structure and hydrogen bond dynamics of water-dimethyl sulfoxide mixtures by computer simulations. *J. Chem. Phys.* 98.

**Tue: 75**

### **Nanoindentation to evaluate the mechanical properties of geopolymers: first steps.**

**Nadja Werling<sup>1</sup>, Ruth Schwaiger<sup>2</sup>, Frank Dehn<sup>3</sup>, Rainer Schuhmann<sup>1</sup>, Katja Emmerich<sup>1</sup>**

<sup>1</sup>Competence Center for Material Moisture (CMM), Karlsruhe Institute of Technology (KIT), Karlsruhe, Germany;

<sup>2</sup>Institute for Applied Materials (IAM), Karlsruhe Institute of Technology (KIT), Karlsruhe, Germany; <sup>3</sup>Institute for Concrete Structures and Building Materials (IMB), Karlsruhe Institute of Technology (KIT), Karlsruhe, Germany

Geopolymers and supplementary cementitious materials (SCM) are potential substitutes for ordinary Portland cement (OPC). While SCM replace only a part of OPC and show either hydraulic or pozzolanic activity, geopolymer binders do not contain any OPC. In contrast to OPC, which is a hydraulic binder, geopolymers are alkaline activated binders. High Ca and low Ca/Ca-free types of alkaline activated binder are distinguished (Dehn, Koenig & Herrmann, 2017). Thereby, geopolymers contain low or even no amounts of Ca. Calcined common clays appear to be well suited as raw materials for the production of geopolymers. Due to the multiphase composition of common clays, it is necessary to study geopolymers, which are prepared of model clay minerals first. As some pure clay minerals are only available in small quantities after separation from clays, it is essential to use measurement techniques, which require only small sample sizes. Nanoindentation can be used to investigate the mechanical properties of geopolymers and to study the impact of different factors during preparation, such as solid/liquid ratio (s/l) on workability, Si/Al ratio and the concentration of the alkaline activator solution (e.g. NaOH) on the hardness and elastic modulus of geopolymers. The compressive strength is not determined directly from the nanoindentation data, though. Conversion factors allowing for estimating the strength based on the hardness values have been determined for metallic materials (Tabor, 1951). For geopolymers such conversion factors are not yet available and should be determined as part of this research project. The strength of geopolymers is a necessary variable for the comparison with OPC. Furthermore, because of the small material volume typically tested by nanoindentation, it is essential to pay attention to the mechanical size effects. There are specifications for the measurement of compressive strength of OPC and the scale effects resulting from different sample sizes (DIN EN 12390-1, DIN 1045-2). The relevant scale factors for geopolymers still have to be determined.

First nanoindentation measurements were performed with metakaolinite prepared by calcination of a Bavarian kaolin (kaolinite content > 95%) at 700 °C and different Si/Al ratios, s/l ratios and NaOH concentrations. The Si/Al ratio was varied by addition of fumed silica. Suitable workability was obtained for s/l ratios between 0.8 and 2. Our preliminary results indicate an increase of hardness and elastic modulus by the addition of  $\text{SiO}_2$ .

The project is funded by Deutsche Forschungsgemeinschaft under EM79/8-1.

Tue: 76

**Characterization of a badly crystalline phylломanganate,  $\text{Ca}_{2x}\text{Mn}_{1-x}\text{O}_2 \cdot 1.5\text{-}2\text{H}_2\text{O}$  (Lagalyite)****Thomas Witzke<sup>1</sup>, Herbert Pöllmann<sup>2</sup>, José Eduardo Gardolinski<sup>1</sup>, Marco Sommariva<sup>1</sup>**<sup>1</sup>Malvern Panalytical, The Netherlands; <sup>2</sup>Martin-Luther-University Halle-Wittenberg, Institute for Geosciences and Geography, Germany

A new phylломanganate mineral was found in the Christbescherung mine (Christbescherung Erbstolln), Großvoigtsberg near Freiberg, Saxony, and Aufgeklärt Glück mine, Hasserode, Harz, Saxony-Anhalt, Germany. The mineral gives a powder diffraction diagram with only a few, broad peaks, resembling turbostratic disordered clay minerals, and dehydrates in air to ranciéite.

Chemical analyses were carried out by XRF spectrometry and thermal analysis. The sample used for the analyses was split in two aliquots. Because of the instability and the high water content the part used for XRF was air-dried over a long time. The second aliquot was stored under wet conditions, then carefully air-dried for a short time. The hydration status was checked by XRD. Thermal analysis of the dry, but fully hydrated material was then used to recalculate the XRF analyses. For the fully hydrated material the composition  $(\text{Ca}_{0.10}\text{Mg}_{0.02})\text{Mn}^{4+}_{0.94}\text{O}_2 \cdot 2.06\text{H}_2\text{O}$  was found. Analyses of additional samples show a slight variation of the Ca-Mn<sup>4+</sup> ratio.

The fully hydrated material shows 10 Å basal spacing, the dehydrated 7 Å (ranciéite). Several dehydration and rehydration experiments showed no intermediate stage. For the structure model the octahedral MnO<sub>2</sub>-layer arrangement of hexagonal ranciéite [1] was used. A few of the Mn positions are not occupied. Ca is placed above and below these vacancies. The basal spacing indicate two water layers. Ca cations are coordinated to three water molecules. The water must be regarded as very mobile and the ideal positions just as a rough approximation. The powder diffraction data can be fitted with a monoclinic cell (C2 in the model),  $a$  5.146,  $b$  2.81,  $c$  9.98 Å,  $\beta$  94.2°,  $V$  143.9 Å<sup>3</sup> ( $Z = 2$ ), similar to synthetic material [2].

To obtain structural information, measurements for a PDF analysis (Pair Distribution Function) was performed using an Empyrean diffractometer, Mo tube, focusing X-ray multilayer mirror and the solid state GaliPIX<sup>3D</sup> detector, with a variable counting time strategy in the angular range 1.5°–145°  $2\theta$  ( $Q_{\text{max}} 16.9 \text{ \AA}^{-1}$ ). The fit of the PDF using the structure model shows a good agreement between measured and calculate data.

The mineral was named lagalyite for Gerhard Lagaly (born 1938), chemist and clay mineralogist, and is accepted by the CNMNC of the IMA. Lagalyite is closely related to the badly characterized mineral buserite (probably  $\text{Na}_{0.3}(\text{Mn}^{4+}_{0.7}\text{Mn}^{3+}_{0.3})\text{O}_2 \cdot n\text{H}_2\text{O}$ ), but not exactly the Ca analogue.

[1] Post et al. (2008) *Powder Diffraction*, **23**, 10-14; [2] Kuma et al. (1994) *Mineralogical Magazine*, **58**, 425-447

Tue: 77

**Mineralogical study of a pair of Bronze Age plaques from the Erlitou culture, China****Thomas Witzke, Nicholas Norberg, Marco Sommariva**

Malvern Panalytical, The Netherlands

A pair of plaques from a private collection showing stylized faces, probably representing mythological animals originating from the Chinese Bronze Age Erlitou culture (2000 – 1500 BC), Henan Province, were studied. They consist of bronze plates (14.1 x 9.5 and 13.8 x 9 cm) with white, light blue to darker blue inlay material. A small number of similar plaques from this culture are known and they were made by inlaying prepared pieces of turquoise into open cells to form the animal mask [1]. Characteristic elements of all these masks are the symmetry and the raised eyes.

Microscopic investigation revealed that two different materials were used. By microspot X-ray diffraction experiments (Malvern Panalytical Empyrean Diffractometer, Cu radiation), both types were identified as calcite, sometimes with traces of quartz. The material used as the main inlay component is white to light or darker blue or greenish, of irregular shape, mostly elongated and corresponds to a natural rock (marble). The

second material has a light to darker blue color and is composed of very small, white crystals (< 0.05 mm) in a fine-grained matrix. Common are small, round cavities (max. 0.5 mm in diameter) like air bubbles. This material was artificially prepared by grinding marble to a powder, and then a binder was added to create a paste. The plaques were created by fixing an openwork bronze frame outlining the contours of the face of the animal to a solid bronze plate resulting in open cells at the front. These cells were filled with the calcite-containing paste. The prepared strips of marble were then pressed into the cells. After drying, the surface was sanded and polished and finally the raise, globular eyes were glued into place. The use of calcite could indicate that the studied pair pre-dates the turquoise plaques, also a paste made of calcite was not observed in the other plaques. Microspot XRD showed that the bronze had undergone intense corrosion, mainly to rouaite ( $\text{Cu}_2(\text{NO}_3)(\text{OH})_3$ ), cuprite, malachite, anglesite, nantokite, romarchite and others. As the original color of the calcite was white, the discoloration to green/blue is a result of copper migration from the bronze over time. To our knowledge, this is the first time rouaite has been identified as a corrosion product of an antique bronze, indicating that the plaques stayed in an environment rich in nitrate.

[1] Shelach-Lavi, G. (2015): The Archeology of Early China. Cambridge University Press, 392 p.

## Tue: 78

### Hand-coloured maps – An interdisciplinary study of cartographers' historical pigments

**Peter Zietlow**

*Universität Hamburg*

So far, in cartography there is little knowledge about the historical use of colouring pigments and dyes. From the 17<sup>th</sup> up to the 19<sup>th</sup> century, printed maps acquired a unique character by colouring, which was exclusively done by hand. In our interdisciplinary project, we analyse maps from Europe and Asia with historians and area study approaches as well as methods of material science.

The project is part of the programme "The language of objects" by Bundesministerium für Bildung und Forschung. It is performed as a cooperation of Stiftung Hanseatisches Wirtschaftsarchiv, Museum am Rothenbaum and Universität Hamburg (Centrum für Naturkunde – CeNak and Centre for the Study of Manuscript Cultures – CSMC) and covers several collections of historical European and Asian maps as well as an extensive collection of minerals (CeNak) which can serve as reference for the unknown pigments. The CSMC provides the mobile laboratory for on-site measurements of the sensitive artefacts.

We use non- and minimal invasive methods such as VIS photospectrometry, X-ray fluorescence and vibrational spectroscopy in order to identify pigments applied on the maps. If the results are not sufficient, a tiny amount of extracted material can be studied by X-ray diffraction and mass spectroscopy.

The main aim of our project is to figure out, how the use of Modern Age colorants changed until the onset of the 20<sup>th</sup> century. Were certain colors significant for certain periods? Where did colorants come from and were they part of global trade? A second field of our study is the effect of environmental influences like storage conditions or water damage that alter pigments.

## 12) Mineral deposits and mining

### 12a) New Models for Old Deposits

Tuesday, 24/Sep/2019: 10:45am - 12:30pm

Session Chair: Max Frenzel (Helmholtz-Zentrum Dresden-Rossendorf)

Session Chair: Torsten Graupner (BGR)

Location: Schloss: S8

#### Session Abstract

Despite its current reliance on imports for most metal and mineral raw materials, Europe is by no means poor in mineral resources. In fact, a wealth of historic mining districts, containing a number of world-class deposits (e.g. Rammelsberg, Freiberg), indicates significant potential for future production. However, little systematic work has been done on many of the relevant districts since mining ceased between 20 to 50 years ago. As a result, there is a distinct lack of modern geological understanding, and many districts are now largely under-explored.

This session is dedicated to research that improves the understanding of historic mining districts in Europe, but particularly work conducted within the conceptual framework of mineral systems analysis. Mineral systems analysis is an approach in which ore deposits are not considered in isolation, but in a broader geo-tectonic context. It allows for the development of comprehensive exploration models, and therefore represents a key element in revitalizing exploration and mining activities in the EU.

In addition to contributions on historic mineral deposits, we also welcome contributions on active mines and recent discoveries in the region, as well as relevant sub-economic mineralizations.

#### Lecture Presentations

10:45am - 11:15am *Session Keynote*

#### New models for old districts - The Erzgebirge Metallogenic Province

**Mathias Burisch**

*TU Bergakademie Freiberg, Germany*

For close to a millennium the Variscan Erzgebirge has been one of the most important mining districts in Europe. Despite prolific exploitation through the ages, significant resources (e.g. Sn, Ag, Zn, Pb, In, Cu, Co, Ni, Li) remain unexploited/unexplored, rendering the Erzgebirge one of the most promising regions in central Europe for mineral exploration. A large variety of hydrothermal ore deposit-types are known to occur, including greisen-, skarn-, epithermal-, five-element vein and fluorite-barite-vein deposits. Some of them e.g. Altenberg, Zinnwald-Cinovec, Hämmerlein, Freiberg and Schlema are rightfully considered as world-class deposits.

Despite the apparent resource potential, the scientific knowledge of these deposits is mostly outdated, with a prevalence of outdated metallogenic paradigms and a distinct lack of modern geochemical data. Furthermore, previous research did consider the ore formation in isolation, rather than embedding local processes into the existing regional geodynamic framework. As a consequence, convincing metallogenic models are not available for most of the ore deposits of the Erzgebirge. Yet, several recent studies dedicated to examples of greisen-, skarn and epithermal mineralization have demonstrated that modern, integrative approaches and state-of-the-art analytical methods – together with a critical review of historic data provide fundamentally new insights into the genesis of ore deposits in the Erzgebirge. Yet, these new findings also highlight how much we still do not know and how much further work is needed for a comprehensive understanding of the mineral system as a whole. This understanding is essential for the development of new exploration models, which are detailed enough to explain systematic regional-, district- and deposit-scale variations. The ultimate

goal is to translate this scientific knowledge into mappable exploration criteria – that will guide future generations within this outstanding metallogenic province.

**11:15am - 11:30am**

### **Mineralogy of the polymetallic Waschleithe Zn-Pb-(W) skarn – implications for skarn genesis in the Schwarzenberg district, western Erzgebirge, Germany**

**Nils Reinhardt<sup>1</sup>, Max Frenzel<sup>2</sup>, Jens Gutzmer<sup>2</sup>, Lawrence D. Meinert<sup>3</sup>, Axel Gerdes<sup>4</sup>, Mathias Burisch<sup>1</sup>**

<sup>1</sup>TU Bergakademie Freiberg, Germany; <sup>2</sup>Helmholtz Zentrum Dresden-Rossendorf, Helmholtz Institute Freiberg for Resource Technology, Germany; <sup>3</sup>Colorado School of Mines, USA; <sup>4</sup>Goethe-Universität Frankfurt, Germany

The Schwarzenberg district (SD) in the western Erzgebirge comprises a series of polymetallic skarn bodies with significant resource potential for Sn, W, Zn, and In. Skarn mineralisation in the SD is hosted by low- to medium-grade metasedimentary units forming the so-called Schwarzenberg Gneiss Dome (SGD). Recent exploration, mainly for Sn, W, and In, targeted the large Globenstein, Hämmerlein and Tellerhäuser skarn bodies (several km strike length). Fertile skarn mineralisation in these skarns is related to the late- to post-col-lisional phase of the Variscan Orogeny (325-295 Ma). Economically important large skarn bodies as well as smaller satellites of the SGD have thus far only been investigated individually, rather than being considered part of a potentially district-wide mineralizing system (~ 12 x 15 km).

The Waschleithe skarn in the far north of the SGD is a typical example for a smaller skarn body. Considering its distal position within the SGD it provides valuable insight into district-scale mineral zoning. Mineralisa-tion occurs within two skarn horizons hosted by marble interlayered with mica schists. The sharp contact between skarn and marble is well exposed in historical mine workings. Coarse-grained pyroxene (hedenber-gite-diopside), finer-grained subordinate yellowish-green andraditic garnet and Mn-rich pyroxenoids are the dominant constituents of the prograde skarn mineral assemblage. All of them overprint the metamorphic microfabric of the marble. A retrograde skarn assemblage is only weakly developed and consists mainly of ilvaite, epidote, vesuvianite, amphibole, chlorite, quartz, fluorite and hydrothermal calcite. Ore minerals associated with the retrograde mineral assemblage may be grouped into three different assemblages: 1) magnetite, 2) sphalerite, galena, pyrite, and chalcocopyrite and 3) scheelite. The retrograde ore mineral assemblages show no association with paragenetically late chlorite, indicating that they formed relatively early during retrograde skarn formation.

The marble front, dark pyroxenes, relatively low garnet/pyroxene ratios and the presence of Mn-bearing pyroxenoids indicate that the Waschleithe skarn formed distal to its fluid source relative to skarns with a more proximal mineralogy, such as Hämmerlein. Thus, Waschleithe represents a distal equivalent to the larger skarns of the SGD situated farther to the south. A genetic link between the skarns of the SGD requires a substantial re-evaluation of the size and exploration potential of this mineral system. To test this hypothesis a comprehensive set of mineralogical, geochemical and geochronological data from several skarn bodies of the SGD is currently being acquired.

**11:30am - 11:45am**

### **Unravelling the geological structure and mineralizing vectors using detailed petrographic investigations – a case study from the Delitzsch tungsten skarn occurrence, Central Germany.**

**Tim Rödel<sup>1</sup>, Bodo-Carlo Ehling<sup>2</sup>**

<sup>1</sup>Martin Luther University Halle-Wittenberg, Germany; <sup>2</sup>Geological Survey (LAGB) Sachsen-Anhalt, Germany

The Delitzsch tungsten skarn in Central Germany is a good example for a well-documented but insufficiently researched and understood metal occurrence. Due to poor exposure and complex geological structure the project was discontinued 1990 after 20 years of exploration. Nonetheless a substantial resource of 11.46 Mio tonnes of ore grading at 0.45% WO<sub>3</sub> was estimated in 1980. Improving the model for structure and ori-

gin of the metal occurrence could provide society with a potential source for strategic metals in the future. Determining the structure and mineralogical zonation of intrusion related skarns is important for vectoring the mineralization and any genetic considerations. Although the concept of large scale mineral zonation as indicators for the skarn forming process is known for several decades they have been rarely practised. Core of the current study is detailed relogging of eight drill core profiles with a skarn intersect of more than 300 m, delineating an area of more than 10 ha. Special emphasis is put on mapping mineral paragenesis, textures, abundance, and related mineral ratios. Additionally, more than 200 petrographic thin sections have been investigated up to date aiding in verification and correction of macroscopic investigations. SEM-EDX analysis and automated mineralogy using Advanced Mineral Identification and Characterization System (AMICS) as well as element mappings by  $\mu$ XRF with Bruker M4Tornado have been carried out. The Delitzsch tungsten skarn is located 10 km NNW of Leipzig city in the state of Saxony. Neoproterozoic to Cambrian sediments outcrop beneath a cover of 90-120 m of Cenozoic sediments. Intensive contact-metasomatism of lower Cambrian carbonates and siliceous carbonates developed in consequence to the intrusion of late Carboniferous, post Variscan granodioritic melts. Results from combined relogging and detailed petrography show a systematic lateral and vertical zonation of the skarn system. Lateral zonation is controlled by fluid rock interaction between magmatic-hydrothermal fluids proximal and distal to the contact between a continuous reactive marble layer and the granodioritic intrusion. Vertical zonation is apparent due to the interaction between fluids and different host rock lithologies (hornfels, marbles, intrusive rocks). Five main skarn types can be distinguished based on mineral paragenesis, texture and spatial position with regard to the intrusive contact. Vectors for the tungsten mineralization are currently being established based on paragenetic considerations.

**11:45am - 12:00pm**

### **Epithermal Ag-(Au)-Zn-Pb mineralisation in the northern part of the Freiberg District, Germany**

**Laura Swinkels<sup>1</sup>, Constantin Rossberg<sup>1</sup>, Jan Schulz-Isenbeck<sup>1</sup>, Max Frenzel<sup>2</sup>, Jens Gutzmer<sup>2</sup>, Mathias Burisch<sup>1</sup>**

<sup>1</sup>*Institut für Mineralogie, Technische Universität Bergakademie Freiberg, Germany;* <sup>2</sup>*Helmholtz-Zentrum Dresden-Rossendorf, Helmholtz Institute Freiberg for Resource Technology, Germany*

The polymetallic veins in the Freiberg district form one of the largest epithermal systems in Europe. It produced over 5600 t of Ag during active mining between 1168 and 1969. Historically, exploration focused on the centre of the district, with peripheral sub-districts exploited only to shallow depth. Recent exploration activity focuses on these peripheral regions, yet only a limited amount of modern geochemical data is available and the underlying ore-forming processes are insufficiently understood. Here, we present preliminary geochemical, fluid inclusion, and petrographic data for 55 samples from the historical mine camps of Reinsberg and Kleinvoigtsberg (northern peripheral sub-district). Samples were selected from the scientific collections of the TU Bergakademie Freiberg and collected from outcrops in the field. They include vertical profiles of two major veins extending from 18 to 532 meters below ground level. The data is combined with previous literature descriptions to develop a genetic model for the northern sector of the Freiberg district.

Mineralisation in the Reinsberg and Kleinvoigtsberg mine camps is hosted by polystadial Ag-(Au)-Zn-Pb veins. The paragenetically oldest mineralisation, Stage I, is dominated by base metal sulphides and quartz; it has been encountered most prominently in the deepest levels of the historic mines. The occurrence of carbonates and the introduction of Ag-Sb sulphides and sulfosalts mark the transition to Stage IIa. At shallower mining levels, carbonate recedes and quartz returns as the major gangue mineral, indicating the transition to Stage IIb. Stage IIb vein infill is often breccia-textured and carry the highest silver grades (1000 to 16000 g/t). At the present day surface, veins consist of quartz and host rock fragments, forming a cockade breccia texture (stage III). Although no visible sulphides are present, such quartz breccias contain up to 2.5 g/t Au.

Recent studies show that the main ore-forming process in the northern district seems to be cooling - causing distinct district and vein-scale zoning. Effervescence of CO<sub>2</sub> is most likely the underlying process behind the transition from quartz to carbonate gangue. An understanding of mineral zonation and its underlying ore-forming processes can be translated into mappable exploration criteria. In this case, the highest ore

grades (Ag and Au) are associated with Stage IIb (Ag-Sb-sulfosalts-quartz assemblage). This assemblage occurs always wedged between the carbonate-rich assemblage of Stage IIa (below) and the sulphide-poor quartz Stage III (above). This systematic relation may well constitute an important exploration vector for the Freiberg district.

**12:00pm - 12:15pm**

### **Mineralogical and geochemical zonation in five-element (Ag-Bi-Co-Ni-As±U) veins of the Annaberg district, Erzgebirge (Germany)**

**Marie Guilcher<sup>1</sup>, Anna Schmaucks<sup>1</sup>, Jens Gutzmer<sup>2</sup>, Gregor Markl<sup>3</sup>, Mathias Burisch<sup>1</sup>**

<sup>1</sup>*Institute of Mineralogy, Technische Universität Bergakademie Freiberg, Germany;* <sup>2</sup>*Helmholtz-Zentrum Dresden-Rossendorf, Helmholtz Institute Freiberg for Resource Technology, Germany;* <sup>3</sup>*Faculty of Science, University of Tübingen, Germany*

Hydrothermal Ag-Bi-Co-Ni-As±U (five-element) veins constitute a promising source for Co and Ni for renewable energy technologies and they are widespread in the Erzgebirge metallogenic province. The Annaberg district is a particular example of a historic mining district where five-element veins abound. Between the 15<sup>th</sup> and the 20<sup>th</sup> century, 8700 t of Co, 496 t of U, and 350 t of Ag were produced in the district. Ag-Bi-Co-Ni-As±U veins and ore-shoots often occur in the vicinity of carbon-rich horizons in graphitic gneiss. U and the other metals both occur abundantly in the Annaberg district and within the same vein structures, but typically at different depths and/or local sites. U is typically enriched at shallow depth (from the surface to >200 m depth); Ag-Bi-Co-Ni-As mineralisation occurs between 50 and 200m depth; both are followed towards greater depth by fluorite-barite assemblages associated with base metal sulphides.

Preliminary petrographic observations of samples from five-element veins in the district reveal four distinct mineralisation stages. Native metals (Ag and Bi; Stage 1), are typically encapsulated by arsenides (Stage 2). The oldest arsenide minerals are nickeline, rammelsbergite, and skutterudite, followed by safflorite and loellingite. In Stage 3, safflorite and loellingite are precipitating in association with sulphide-rich assemblage (sphalerite, chalcopyrite, pyrite, and galena). Minor U-bearing minerals (coffinite and uraninite) seem to be coeval with loellingite and sulphides of Stage 3. Stage 4 consists of Ag-bearing minerals namely proustite, pearceite, acanthite associated with other sulphides. They commonly replace native metals (Stage 1) selectively and encapsulate the arsenides of Stage 2. Coeval gangue minerals are quartz, dolomite-ankerite, and calcite. Fluorite is also present, although its position in the paragenetic sequence is unclear.

The close spatial link between the carbon-rich horizons, U, and Ag-Bi-Co-Ni-As mineralisation suggests that carbon-rich horizons act as redox barriers and control deposition of redox-sensitive elements such as U, As, and associated metals. Although this spatial relationship is well documented, the underlying processes that cause this zoning are still insufficiently understood. It remains unclear if the zoning is a result of increasing/decreasing  $fO_2$  or reflects a temperature gradient; alternatively, mineral zoning may reflect multiple mineralisation events. Fluid inclusion analyses and thermodynamic computations will be carried out in order to achieve a better understanding of the hydrothermal processes that result in ore deposition. This knowledge may be used to target zones within a five-element vein district enriched in Co and/or Ni but relatively depleted in U.

**12:15pm - 12:30pm****The Niederschlag fluorite-barite deposit, Erzgebirge, Germany – a fluid inclusion study****Sebastian Haschke<sup>1</sup>, Jens Gutzmer<sup>2</sup>, Dennis Krämer<sup>3</sup>, Mathias Burisch<sup>1</sup>***<sup>1</sup>TU Bergakademie Freiberg, Germany; <sup>2</sup>Helmholtz-Zentrum Dresden-Rossendorf, Helmholtz-Institute Freiberg for Resource Technology, Freiberg, Germany; <sup>3</sup>Center for Resource and Environmental Studies, Department of Physics and Earth Sciences, Jacobs University Bremen, Germany*

The Niederschlag deposit, situated in the western part of the Erzgebirge, is actively mined for fluorite and barite since 2013 with an annual production of 100,000 t of raw fluorite and 12,000 t of barite. Hydrothermal mineralisation is bound to NE-SW trending fault structures, which are hosted by mica schists and paragneisses of the Variscan basement. With an average thickness of 3 to 4 m, the Magistralnaja vein represents the major ore body and extends in pinch and swell structures to depth of at least 800 m below sea level. Although the Niederschlag deposit is the first and only mine that (re)-opened during the last ~40 years in the Erzgebirge, the mineralisation has never been investigated with modern geoscientific methods. Consequently, only little is known about the ore-forming processes and the mineral system.

Here, we present new petrographic, fluid inclusion as well as geochemical data and a preliminary genetic model for the fluorite-barite mineralisation of the Niederschlag deposit. Mineralisation is polystadial and comprises two main stages of fluorite mineralisation. Stage I fluorite is purple to green in colour, mostly anhedral and associated with abundant quartz/chalcedony. Fluorite I and quartz are irregularly banded and form complex breccias. Sulphides are conspicuously absent from Stage I. Fluorite - and closely associated barite – of Stage II occur as coarse crystalline, massively-textured or banded vein-infill that clearly postdates Stage I. Base metal sulphides occur in minor amounts. Unfortunately, Stage I fluorite and quartz do not contain fluid inclusions suitable for microthermometry; therefore, the ore forming mechanism remains poorly constrained at present. Microthermometric analyses of primary and pseudo-secondary inclusions of fluorite II, however, reveal a high variability with moderate to high salinities (19 and 27 % eq. w(NaCl+CaCl<sub>2</sub>)) and homogenisation temperatures between 80 °C and 140 °C. Na/(Na+Ca) ratios of fluid inclusions range between 0.8 and 0.4. High variability of salinity and Na/(Na+Ca) suggests fluid mixing of at least two chemically contrasting fluids as the main ore-forming process for Stage II mineralisation. Due to striking similarities to many other fluorite-barite-Pb-Zn-Cu vein deposits in Central and Western Europe (e.g. Schwarzwald/Germany or Massif Central/ France), it is most likely that Stage II mineralisation is related to rifting associated with the Mesozoic opening of the northern Atlantic.

**12a) New Models for Old Deposits****Tuesday, 24/Sep/2019: 3:45pm - 5:30pm****Session Chair: Dennis Krämer (Jacobs University Bremen gGmbH)****Location: Schloss: S8****3:45pm - 4:00pm****New vents and extensive sulfide fields off-axis the Southeast Indian Ridge, Indian Ocean: Results from seafloor sulfide exploration****Ulrich Schwarz-Schampera<sup>1</sup>, Harold Gibson<sup>2</sup>, Dieter Garbe-Schönberg<sup>3</sup>, Meike Klischies<sup>4</sup>, Ralf Freitag<sup>1</sup>***<sup>1</sup>BGR, Germany; <sup>2</sup>Laurentian University, Sudbury, Canada; <sup>3</sup>C.-A. University Kiel, Germany; <sup>4</sup>GEOMAR, Germany*

BGR holds an 15-years exploration license for polymetallic seafloor massive sulfides in the regulatory framework of the International Seabed Authority (ISA). The claim represents an area of 10,000 skm within a 960km long and 65km wide section along the southern Central (CIR) and northern Southeast Indian Ridge (SEIR) system. Four prospecting cruises between 2011 and 2014 defined the license area; annual exploration cruises

are carried out since 2015. The 15-years program aims at the identification and outline of potential polymetallic seafloor massive sulfide deposits and includes extensive and detailed environmental base line studies of the marine environment in the claim area.

Cruise INDEX2018 defined new and extraordinary sulfide occurrences. The further improvement of the exploration concept and the prime focus on bathymetrically, volcanically and structurally prospective areas at greater distances to the axial spreading zone led to the findings of a number of new sulfide areas along the SEIR and CIR. The sulfide areas occur at shallower depths well above 3,000m water depth and three of them are venting phase separated fluids, suggesting the effective precipitation of metals in the sub-seafloor. The PENUMBRA sulfide area extends over 2,630m length, and is composed of twelve mounds, with diameters of more than 200m and up to 60m in height. Four sites show vent fluid temperatures between 320 and 352°C. The new sulfide area is located 14 km off the SEIR active spreading axis – the actually greatest known distance of a vent or sulfide field to any mid-ocean ridge and back-arc spreading zone, respectively. HUNA sulfide occurrences extend over 1.5 km with mounds up to 200x100x30m in size. HUNA is situated 12 km off the active SEIR spreading graben axis. The KAIMANA field is hosted by exhumed intrusives (gabbros, pyroxenites) of the deeper oceanic crust and occurs at 10 km distance from the axial CIR. Size and location extend the prospective area of sulfide deposition to greater distances from spreading zones and proof the distal spreading regions to represent prime exploration targets for extensive sulfide mineralization.

**4:00pm - 4:15pm**

### **The Historic Copper Mines of Southwest Ireland – A New Chronological Evaluation on Vein-hosted Mineral Deposits**

**Jürgen Lang, Patrick Meere, Richard Unitt, Sean Johnson**

*iCRAG (Irish Centre for Research in Applied Geosciences), Ireland*

Copper has been exploited in SW Ireland for thousands of years. The demand for copper world-wide has led to renewed interest in these occurrences and their overall implication for copper metallogenesis in Ireland.

The study presented here focuses on historically mined vein-hosted copper deposits in southwest Ireland, hosted in an Upper Devonian continental clastic basin sequence. The aim is to identify the dominant fluid conditions that governed mineralisation in these veins. This includes a 3dimensional model of the vein system and its structural relationship to mineralisation.

Detailed mapping in the Allihies Cu mining district (Beara Peninsula, West Cork), including macro- and micro-structural investigation, has resulted in a brand new interpretation of the temporal development of deformed and faulted ore-bearing, E-W striking, early extensional (pre-Variscan) quartz veins. These appear to occur along large scale (km-scale) E-W extensional basin faults. Minor, syn-Variscan quartz veining occurs along SW-NE trending faults and folds, matching the dominant Variscan compression. These structural observations are compared with those from vein-hosted Cu deposits on Mizen Head and Sheep's Head peninsulas, which are associated with sediment hosted Cu mineralisation. Interpretation of GIS-supported satellite imagery and drone mapping served as key tools for the visualization of large and small scale structures.

Fluid inclusion studies of mineralised, pre-Variscan quartz veins reveal fluids with homogenisation temperatures (Th LV-L) ranging from 74 °C to 314 °C. Salinities have a span from 3.2 to 28.5 wt.% (NaCl equiv.). These values show a trend from high salinities with lower homogenisation temperatures to low salinities with higher homogenisation temperatures. The pre-Variscan faults and mineralised quartz veins show Variscan deformation, including cleavage development, sinistral SW-NE strike slip faults, and semi-brittle recrystallization.

Syn-Variscan quartz-chlorite veins occur as saddle reef veins along fold axes and en echelon veins. Fluid inclusions from these veins yield Th values of about 200 °C and a salinity range between 8.2 and 19.1 wt.% (NaCl equiv.).

Re-Os geochronology measurements on historic molybdenite samples, associated with mineralisation, revealed an age of  $366.4 \pm 1.9$  Ma (Upper Devonian) for the Allihies deposit (Beara Peninsula), and  $315.5 \pm 1.6$  Ma (Late Carboniferous) for the historic Ballycummisk copper mine on the southern coast of Mizen Head.

These findings of an extensional, mineralising event, followed by the compressional Variscan regime add a geochronological control to field and fluid inclusion data, resulting in a new interpretation of copper mineralization in SW Ireland and its implications for Irish metallogenesis.

**4:15pm - 4:30pm**

### **Explaining metal zonation at the Lisheen Zn-Pb deposit, Ireland**

**Max Frenzel<sup>1,2,3</sup>, Mathias Burisch<sup>2</sup>, Markus Röhner<sup>1</sup>, Nigel J. Cook<sup>3</sup>, Sarah Gilbert<sup>3</sup>, Cristiana L. Ciobanu<sup>3</sup>, John Güven<sup>4</sup>, Jens Gutzmer<sup>1</sup>**

<sup>1</sup>*Helmholtz-Zentrum Dresden-Rossendorf, Germany;* <sup>2</sup>*Technische Universität Bergakademie Freiberg, Germany;*

<sup>3</sup>*University of Adelaide, Australia;* <sup>4</sup>*Irish Centre for Research in Applied Geoscience, University College Dublin, Ireland*

Metal zonation is an important feature of low-temperature carbonate-hosted Zn-Pb deposits. Its origin, however, remains poorly understood. In this article, we use the Lisheen deposit in Ireland as a case study to show how thermodynamic modeling can explain these zonation patterns.

Based on input data derived from fluid inclusion studies, bulk ore geochemistry and accepted models of ore formation in the Irish Orefield we construct a reaction path model that successfully accounts for the major features of the mineralization, most importantly the presence of Cu-Ni-As-rich core zones around hydrothermal feeder structures, surrounded by more distal Fe-Zn-Pb-rich mineralization. We also predict that the sulfide mineralization should be surrounded by a halo of elevated Ba, a result that may have important implications for mineral exploration in the district and analogous environments elsewhere.

The outcomes of this study support current metallogenic models for Irish-type deposits in which a deep, hot, sulfur-poor but metal-rich brine mixes with a shallow, cold, reduced and sulfur-rich reservoir. Metal zonation is a direct consequence of systematically changing fluid mixing ratios away from feeder zones.

**4:30pm - 4:45pm**

### **Genetic processes and source components in submarine iron ores: Insights from the Lahn-Dill-type iron ores, Rhenish Massif, Germany**

**Leanne Schmitt<sup>1,4</sup>, Thomas Angerer<sup>2</sup>, Thomas Kirnbauer<sup>1</sup>, Sabine Klein<sup>3,4</sup>**

<sup>1</sup>*Technische Hochschule Georg Agricola, Bochum, Germany;* <sup>2</sup>*University of Innsbruck, Austria;* <sup>3</sup>*German Mining Museum, Bochum, Germany;* <sup>4</sup>*Ruhr-Universität Bochum, Germany*

Stratiform ores associated with volcanism in submarine settings represent an important source for iron and are widely used as proxies for local to global marine depositional environments. However, the interplay of marine, microbial, volcanic, hydrothermal and diagenetic processes in these mineralizing systems are often not well understood.

Lahn-Dill-type iron ores are associated with Middle Devonian to Lower Carboniferous basaltic volcanism. Mineralization took place in two different submarine settings: (I) syndepositional in basins, with hematite and locally magnetite ores being siliceous or carbonatic. Shrinking structures indicate a formation from a gel that formed from a Fe-Si-Ca-rich hydrothermal fluid mixed with ambient seawater; (II) postdepositional, where volcanic rises reached sea level and reef development was facilitated. Here, carbonates were replaced metasomatically by hematite (or its precursor).

Whole rock geochemistry with REE of iron ores from these two settings was conducted using ICP-MS in order to understand the contribution of different source components. Ores from a syndepositional setting were sampled at the Fortuna mine (Lahn Syncline, Germany), ores from a postdepositional setting at the Briloner Eisenberg mine (Sauerland, Germany). Variable Fe grades of Fortuna (20-57 wt.%) and Briloner Eisenberg ores (10-65 wt.%) are related to heterogeneous mineralization. Average values of Al<sub>2</sub>O<sub>3</sub> (0.9 wt.%) and TiO<sub>2</sub> (0.05 wt.%) in ores from both mines imply a minor clastic contribution. Elevated V (up to 293 ppm) and Ni (up to 115 ppm) as well as Cu/Zn ratios that show a similar range compared to alkali basaltic volcanoclastic footwall rocks, indicate a volcanogenic contribution.

In both settings, ores depict similar REE fractionation suggesting variable contributions of possibly four sources. The LREE fractionation resembles ocean island basalt (OIB) compatible with a contribution from footwall rocks, whereas HREE fractionation resembles Post-Archean Australian average shale (PAAS), interpreted as a contribution from weathered continental crust. Positive anomalies for La, Gd and Y in ore and hanging wall carbonates, in conjunction with lacking negative Ce anomalies, are compatible with anoxic conditions in the Devonian sea water. The absence of a positive Eu anomaly may be evidence for low temperature (<200 °C) hydrothermal fluids being involved in metal scavenging from source rocks.

**4:45pm - 5:00pm**

### **Rare metal partitioning in a metamorphosed SHMS system: the Austroalpine polymetallic ore district**

**Thomas Angerer<sup>1</sup>, Franz Vavtar<sup>1</sup>, Albin Volgger<sup>1</sup>, Peter Tropper<sup>1</sup>, Peter Onuk<sup>2</sup>, Christoph Spötl<sup>3</sup>, Christoph Hauzenberger<sup>4</sup>, Marcel Regelous<sup>5</sup>, Gerhard Hobiger<sup>6</sup>**

<sup>1</sup>*Institute of Mineralogy and Petrography, Innsbruck University;* <sup>2</sup>*Department of Applied Geological Sciences and Geophysics, Montan-University Leoben;* <sup>3</sup>*Institute of Geology, Innsbruck University;* <sup>4</sup>*NAWI Graz Geozentrum, Graz University;* <sup>5</sup>*Geozentrum Erlangen University;* <sup>6</sup>*Geologische Bundesanstalt Wien*

Despite recent advances in the understanding of the distribution of rare metals in base metal sulphide deposits, there is still a lack of robust models defining the controlling factors for primary and secondary partitioning and mobility of minor and trace metals in whole mineral systems. A good understanding of such controlling factors strongly impacts mineral exploration and geometallurgy. To investigate the multitude of causes for rare metal (re-)distribution within a given system, we studied the metamorphosed, polymetallic, sedimentary hosted massive sulphide (SHMS) ore district of the Austroalpine Ötztal-Stubai crystalline (ÖSC) complex (Vavtar F., 1988: Die Erzanreicherungen im Nordtiroler Stubai-, Ötztal- und Silvrettakristallin. In: Arch f Lagerstforsch Geol B.-A., 9, pp 103-153). Numerous small and uneconomic deposits of sphalerite-bearing mineralisation (including the formerly significant mines of Schneeberg and Tösens) show a range of trace metal abundances, including locally significant enrichments of the rare metals In, Co, Ga, Ge, (Sn, Ag) in sphalerite. The metalliferous system of the ÖSC is an ideal study region, because the individual deposits represent a diverse range of stratiform metal/sulphide assemblages, host-rock association, gangue-material, hydrothermal remobilisation, as well as metamorphic and deformation overprint. In order to develop a model for the rare-metal distribution within this metamorphosed mineral system, we employed petrography, whole-rock geochemistry, sulphide and gangue phase chemistry (sphalerite, chalcopyrite, gahnite, garnet, amphiboles, mica), element maps at the rock and mineral scale, as well as C, O, and Sr isotope analyses of gangue carbonates.

The following parameters (from early to late and from large to small) play a significant role in the formation of base+rare metal deposits within the ÖSC mineral system: (1) Basinal setting (tectonics, magmatism, and lithostratigraphy), causing a division in two regionally distinct metal associations: the northern Cu-Fe dominated (sphalerite-poor, chalcopyrite-rich) and the southern Pb-Zn dominated (sphalerite-rich, chalcopyrite-poor) parageneses. (2) Sources and pathways of mineralising fluids (by isotopic proxies) showing variable crustal, seawater, and organic components. (3) The local depositional setting with variable lithostratigraphy, vent-proximity, mineralisation type and ore grade. (4) Secondary remobilisation in vein- and breccia-type mineralisation. (5) Prograde metamorphism. (6) Retrograde metamorphism with static annealing and/or dynamic recrystallisation by shear deformation, as well as exsolution. Parameters (1) to (3) control the rare metal abundance in the various deposits, while (4) to (6) impact on metal partitioning in sphalerite generations and competing phases. Data will be presented that illustrate the relative impact of each of these factors.

**5:00pm - 5:15pm****Regional scale geochemical investigation of precious and base metal-rich deposits in the Cyclades, Greece****Sandra C. Wind<sup>1</sup>, Mark D. Hannington<sup>1,2</sup>, David A. Schneider<sup>1</sup>**<sup>1</sup>University of Ottawa, Canada; <sup>2</sup>GEOMAR Helmholtz Centre for Ocean Research Kiel, Germany

The Aegean Sea, Greece, hosts polymetallic ore deposits, which range from mid-Miocene to modern seafloor hydrothermal systems. Subduction of the African plate beneath continental Europe created an extensional back-arc setting, wherein metamorphic core complexes are exhumed along low-angle, crustal-scale detachments. A variety of mineral deposits (e.g., carbonate replacement, skarn, vein-type, and low- to high-sulfidation epithermal) formed during different stages of back-arc evolution and are found in the metamorphic basement, unmetamorphosed hanging wall and Quaternary volcanic units along the active volcanic arc. These deposits are temporally and spatially associated with the emplacement of Miocene granitoids and the major fault systems. Many deposits contributed to the wealth of the ancient Greeks and have been mined throughout the 19<sup>th</sup> and 20<sup>th</sup> century. Despite the long mining history and detailed studies of the individual deposits, genetic models remain controversial. Fifteen deposits across ~200 km of the arc-backarc system have been sampled to track metal and fluid sources. Galena and barite mineral separates have been analyzed for their isotopic and trace element composition. A common low-temperature mineral paragenesis is found in the carbonate, skarn and epithermal deposits in the western Cyclades with sphalerite, pyrite, galena and minor chalcopyrite and sulfosalts. In contrast, precious metal-rich vein-type deposits in the northeastern Cyclades are characterized by a galena-rich, chalcopyrite, pyrite and sulfosalt paragenesis with minor sphalerite and tellurides. Large-scale regional variations in the Pb-isotope signatures of galena suggest that the basement is the main source of base metals in the Cyclades. Distinct Pb-isotope signatures indicate that base metal-rich deposits in the western Cyclades have a common lead source, with a more radiogenic lead signature, whereas lead in deposits in the northeast has a less radiogenic source. Trace element concentrations in galena indicate contributions from different fluid-rock interactions and magmatic fluid components that led to diverse precious metal enrichment. Ore-associated barite occurs in all deposit types and exhibits a very narrow range of Sr-concentrations, suggesting similar physicochemical conditions of mineralization. Barite from deposits occurring in submarine volcanosedimentary units, have a large range of Sr-concentration, indicating variable contributions from seawater. Trace element studies of barite are complemented by Sr- and S-isotope analyses. Combining the isotopic and geochemical signature of galena and barite allows for insight into the complex interplay of multiple fluid and metal sources, as well as magmatic and hydrothermal influences that led to the formation of various mineral deposit types in the Cyclades Mineral District.

**Poster Presentation****Mon: 65****Exploration, deposit evaluation and first economic information about a spodumene pegmatite in Canada Ontario****Stephan Peters, Florian Lowicki, Florian Beier, Jana Rechner, Torsten Gorka***DMT GmbH & Co. KG, Germany, Essen*

The since 1952 known Spodumene Pegmatites [1] were since that time explored three times. In the years 1955 until 1957 the first drill holes were drilled and a first shaft were sunken. In the years 2008 until 2011 a second exploration phase with more drill holes were undertaken. The last exploration phase starts in 2017. Actual a new deposit evaluation is on the way. Additional drill holes, channel samples and sample analyses are currently under investigation. A new 3D Model is under construction and first mining options are under investigation. The strike length of the pegmatites at the surface is in between 50 m up to 1.8 km. The thickness varies in between 1 to 10 m.

The majority of the pegmatites are hosted by metasediments or biotite granite. Spodumene is the domi-

nant Li-bearing mineral in all of these pegmatites. The pegmatite dyke internal zonation is in general a granitic or aplitic border zone and a spondumene, albit and quartz center zone. In some cases there are more or less aplite layer and sometimes quartz tourmaline veins occur.

The mineralisation consists of coarse-grained fresh pale green spondumene crystals oriented perpendicular to the strike of the pegmatite dyke. In the field the spondumene minerals were often in the size of fingers. In some areas the length of these crystals is up to 1 m and a thickness of up to 12 cm.

A bulk samples has been taken and first processing investigations have been done.

Today the investigation is focused in the northern areas where several spondumene pegmatites occur at the surface relatively near to each other. There are 5 pegmatites which were now new modelled in 3D. The drill holes hit the pegmatites in the maximum depth of 350 m below the surface. The distances of the drill holes is below 50 m. More than 200 drillholes were drilled in the area. The lithium oxide content of the core samples varies from low up to 2,7% (Li<sub>2</sub>O). The actual 43 101 NI resource statement and the PEA is uploaded to the SEDAR website of the Toronto stock exchange.

The next steps are the pit optimisation and more in detail geotechnical investigations about the stability of the rock mass. In general the environment and the water situation was also under investigation.

The project will be shown in the actual situation and the newest exploration results will be displayed.

## **12b): Mineral deposits of societal relevance for Europe**

**Monday, 23/Sep/2019: 9:00am - 10:30am**

**Session Chair: Antje Wittenberg (BGR)**

**Session Chair: Henrike Sievers (BGR)**

**Location: Schlossplatz 4: SP4 201**

### **Session Abstract**

Raw Materials are crucial components of a vital and wealthy society regardless a society is affected by mining, manufacturing and agriculture or it reached a de-industrialised status. Sustainable supply of raw materials always calls for accessibility to mineral deposits and productive mines. It is getting more and more challenging to meet these needs not only due to the competing land-use issues. The realisation of a low-carbon society and a self-concept of reliable sourcing increasingly require short feed strokes and local sourcing. Although Europe has a long history in mining, it is still widely underexplored in particular with modern exploration methods. A good understanding of mineral systems, mining sites and remaining resources of historical sites will stay of utmost importance.

This session thus invites contributions focussing on mineral deposits and mining activities that indicate a socio-economic importance to the German / European society in particular.

### **Lecture Presentations**

**9:00am - 9:30am Session Keynote**

#### **Decarbonisation, circular economy and deindustrialisation – a Vision for the European minerals industry?**

**Corina Hebestreit**

*Euromines, Belgium*

The European minerals is increasingly exposed to a number of international and European policies such as decarbonisation, circular economy and a general tendency to deindustrialisation due to a series of European

policies and legal measures. At first sight these seem to threaten the raw materials sector. The presentation will explore the various pressure points and the vision for the raw materials sector in light of these policies till 2050 and various strategies that could be followed at EU and national level.

**9:30am - 9:45am**

### **Historical mine sites revisited**

**Henrike Sievers<sup>1</sup>, Antje Wittenberg<sup>1</sup>, Daniel de Oliveira<sup>2</sup>**

<sup>1</sup>BGR, Germany; <sup>2</sup>LNEG, Portugal

Europe is largely dependent on raw materials imports and thus relies on global markets and supply from international sources. Nevertheless, Europe has a long lasting mining history and some deposits have been mined continuously even for hundreds of years.

Within the GeoERA the project FRAME will identify traditional mining regions or sites, which have the potential to feed in to Europe's demand of raw materials in the future. On top of the main commodities of the deposits, examined it focuses on strategic raw materials (SRM) such as (e.g. high-tech metals extracted as by-products and critical raw materials of the EU actual list). These raw materials might be contained in the ore, residues from the mining and beneficiation process.

The project aims at improving knowledge regarding the future potential of historic mine sites and will contribute to improving pan-European geological information on SRM by providing an overview and case studies on SRM contained in former mining regions. Data on deposits that are historic mine sites or part of a historic mining region and have considerable potential for SRM will be collected.

Different sources of data like national databases, literature, previous projects and expert information by the project partners were used to review and collect site-specific data on historic mine sites and their potential for SRM. Currently, national databases are the main source of information. These databases usually contain far more deposits, than those related to historic mining. In some cases they have been set up for non-geological purposes, e.g. waste management, but contain information on mine waste as one category among others. Most of the historic mine sites considered in this project so far are former base metal mines, with the largest group being deposits are Pb/Zn-deposits.

The project will feed site-specific data of ore deposits and mine wastes with CRM potential into the pan-European knowledge base on raw materials: the GeoERA Information Platform.

This project is part of FRAME, with is part of the GeoERA project ([www.geoera.eu](http://www.geoera.eu)) co-funded through the European Union's Horizon 2020 research and innovation program under grant agreement No 731166.

**9:45am - 10:00am**

### **The Path to European Rare Earth Element Security**

**Mark Stephen Saxon, Robert Pell**

*Leading Edge Materials Corp, Canada*

Situated in southern Sweden, the Norra Kärr heavy rare earth element deposit presents the opportunity for long term resource security for the European Union.

The deposit is unique in mainland Europe, being a large nepheline rich peralkaline intrusion, where REEs are hosted within the zircono-silicate mineral eudialyte. Norra Kärr is enriched in the magnetic metals dysprosium, terbium and neodymium, along with zirconium and hafnium, which are critical for emerging technologies.

Through ongoing geometallurgy and processing research, the project has the opportunity for very high resource efficiency. A marketable nepheline/feldspar industrial minerals product has been developed to substantially reduce waste materials remaining on site.

Norra Kärr presents the opportunity to showcase a new generation of European mining. By intergrating pro-

duction of multiple high value products to maximise resource efficiency, with the lowest impact mine design the project will fit comfortably within a populated area with multiple land use pressures. Through collaborative design, the mine site will incorporate tourism and sporting opportunities, and will become a positive feature of the region.

Furthermore, through integration of Life Cycle Analysis data in site planning Norra Kärr, will demonstrate the lowest impact production of rare earth elements, and offset production in sites with higher environmental and social impacts.

**10:00am - 10:15am**

### **Extraction of lithium from geothermal brines of the Upper Rhine Graben using manganese oxide adsorbents – A first approach**

**Klemens Slunitschek, Dr. Jochen Kolb, Dr. Elisabeth Eiche**

*Karlsruhe Institute of Technology, Germany*

Lithium (Li) is one of the crucial elements for the realization of electric mobility, energy transition and digitization with rising demand and prices over the last decades. However, Europe depends mainly on Li-import from other countries, e.g. Chile, with an import rate of 86% (2010 – 2014; EU, 2018) and a contribution to global Li-production of less than 1% (2017; USGS 2018). This issue is addressed within the Catching Metals project, in which we aim to extract Li in an integrated and environmental friendly way in the Upper Rhine Graben in southern Germany through the processing of geothermal brines produced by geothermal power plants. For the extraction, two manganese oxide adsorbents are investigated in relation to ad- and desorption kinetics, Li-ad- and desorption capacity and the influence of competing dissolved ions on the Li-adsorption capacity.

Two different Li-doped manganese oxides ( $\text{Li}_{1.6}\text{Mn}_{1.6}\text{O}_4$ ,  $\text{Li}_{0.9}\text{Mg}_{0.51}\text{Mn}_{1.55}\text{O}_4$ ) are synthesized and batch experiments with  $\text{Li}^+$  solutions and geothermal brines are conducted to determine ad- and desorption capacity and kinetics. The synthesized manganese oxide adsorbents and batch solutions are examined geochemically and mineralogically using ICP-OES, XRD and SEM.

The mineralogical results show, that both manganese oxide adsorbents have a spinel structure enabling ion-sieve properties and Li-selectivity. Results of the batch experiments show fast ad- and desorption kinetics with a desorption rate of >50% of adsorbed Li within several minutes. Additionally, Li-adsorption capacity increases with increasing temperature. The comparison of batch experiments using pure  $\text{Li}^+$  solutions and natural geothermal brines show a decreased maximum Li-adsorption capacity in the latter due to the presence of competing ions in the brine. While, contrary to our expectation, alkaline elements show little effect on Li adsorption, other elements, e.g. iron, manganese, barium, acted as the most important competing or sorption influencing ions.

The results of our experiments show that Li-extraction from geothermal brines in the Upper Rhine Graben through manganese oxide adsorbents is technologically and economically feasible. Due to the fast kinetics, Li can be extracted in a flow reactor, which can be integrated into the power plant water cycle without the need for separate water storage.

[1] European Commission, 2018: Commission staff working document – Report on Raw Materials for Battery Applications; [2] United States Geological Survey, 2018: Mineral Commodity Summaries: Lithium

10:15am - 10:30am

## Tellurium a strategic metal for green energy technologies: Insights into ore-forming processes

**Manuel Keith<sup>1,2</sup>, Daniel J. Smith<sup>2</sup>, David A. Holwell<sup>2</sup>, Gawen R. T. Jenkin<sup>2</sup>, Joseph Becker<sup>3</sup>, Jason Rampe<sup>3</sup>**

<sup>1</sup>GeoZentrum Nordbayern, Universität Erlangen-Nürnberg, Germany; <sup>2</sup>University of Leicester, School of Geography, Geology and the Environment, UK; <sup>3</sup>Newmont Mining Corporation, USA

Tellurium (Te) is classified by the European Union as an energy critical element of high importance due to its application in the rapidly growing sector of green energy technologies<sup>1</sup>. Currently, most Te is recovered as a by-product from non-ferrous metal mining, principally by Cu ore refining providing little opportunity to increase the Te supply based on current extraction methods<sup>1</sup>. Hence, a shortage in Te is likely to be reached in the near future due to its increasing demand.

Hydrothermal and alkaline magmatic activity in post-subduction environments are suggested to be a critical component in the evolution of Te-rich low-sulphidation epithermal deposits. However, the magmatic-hydrothermal processes leading to the pronounced enrichment of Te in these epithermal districts are still poorly constrained<sup>2,3</sup>. Cripple Creek, Colorado, represents an example for a world-class low-sulphidation epithermal Au-Te anomaly in the continental crust. This area represents a natural laboratory to investigate the processes of ore-formation and Te enrichment in alkaline-hosted epithermal systems.

Petrographic observations combined with *in situ* laser ablation ICP-MS analyses and trace element mapping allow to define key ore-forming processes causing the Au-Te deposition at Cripple Creek. Two main styles of mineralisation can be distinguished: (1) low-grade Au disseminated pyrite-rich ores in brecciated host rocks and (2) high-grade veins with a diverse telluride mineralogy.

Pyrite trace element mapping revealed distinct variations and decoupling of elements (Au-Te) and element pairs (Au-As vs. Co-Ni) in the epithermal district. Fluid boiling at temperatures between 220 and 350°C is interpreted to be the key ore-forming process in the low-grade ore leading to the precipitation of Au, As, Co and Ni from the liquid phase and the preferential partitioning of Te into the vapour phase. Condensation of Te-rich vapours in metal bearing meteoric waters led to the Te precipitation being decoupled from Au in the low-grade ores. In contrast, at lower fluid temperatures (110 to 220°C) fractionation of Au and Te between liquid and vapour, respectively, is suppressed causing the coupled Au-Te enrichment in the high-grade veins. It is suggested that a magmatic volatiles influx leads to the high-grade Te mineralisation.

We propose a two-stage metal fractionation model: (1) magmatic volatile contribution to the hydrothermal system and (2) subsequent fluid boiling causing the Te enrichment in post-subduction epithermal environments.

<sup>1</sup>Moss et al., 2013, JRC Scientific and Policy Reports, 1-241; <sup>2</sup>Keith et al., 2018, Ore Geol. Rev 96, 269-282; <sup>3</sup>Smith et al., 2017, Ore Geol. Rev. 89, 72-779.

## Poster Presentation

Mon: 66

## GeoERA – Geological Survey Organisations contribution to Europe's raw materials sustainability

**Antje Wittenberg<sup>1</sup>, Daniel de Oliveira<sup>2</sup>, Tom Heldal<sup>3</sup>, Francisco Javier González<sup>4</sup>, Lisbeth Flindt Jørgensen<sup>5</sup>**

<sup>1</sup>BGR, Germany; <sup>2</sup>LNEG, Portugal; <sup>3</sup>NGU, Norway; <sup>4</sup>IGME, Spain; <sup>5</sup>GEUS, Denmark

Mineral Raw Materials are essential for societal development and Europe's ambition for economic growth and well-being. Being the front-end of the value chain, secured supply of sustainably produced mineral raw materials is of vital importance to meet the UN Sustainable Development Goals (e.g. for the energy transition of the society in large and the energy demanding industry in particular to be realised locally). With initiatives and actions such as the Raw Materials Initiative, the EIT Raw Materials and the European Battery Alliance the

European Union, Research Organisations and the European Industry focus on:

The security and sustainability of mineral raw materials supply from EU sources; and

The management of competing uses of the European surface and subsurface.

Through the four GeoERA Raw Materials projects EuroLITHOS, FRAME, MINDeSEA and Mintell4EU more than 30 National and Regional Geological Survey Organisations (GSO) from Europe and beyond serving those societal needs mentioned above. Shared expertise and information adds to the EU Raw Materials Knowledge Base by addressing sustainable supply of Mineral Raw Materials from European on- and off-shore resources. EuroLITHOS gives specific attention to ornamental stone resources for which Europe has a long tradition in mining, processing and usage. Increasing demand in maintaining cultural heritage sites and other construction works indicate the specific attention given.

FRAME designed to research the Strategic and Critical Raw Materials (SCRM) in Europe to gain new insights into reserves and resources taking in to account also new technologies and developments. Europe's long-standing tradition in mining and its heaps and dumps will be investigated in view of SCRMs.

MINDeSEA focusses on exploration and investigation of SCRM from seafloor mineral deposits in European waters. GSO and Marine Institutes identifying areas for responsible resourcing and information on management and Marine Spatial Planning in European Seas are in its core of action.

Mintell4EU focusses on harmonizing data, providing spatial data and thematic maps. Updated electronic Minerals Yearbook and the extension of the spatial coverage and quality of data currently in the Minerals Inventory will be the final product.

Increased data quality and data harmonization on Europe's raw material supply potential will provide valuable data publicly accessible through the GeoERA Information Platform and in line with the Raw Materials Information System the EU Science hub of the European Commission.

GeoERA ([www.geoera.eu](http://www.geoera.eu)) is co-funded through the European Union's Horizon 2020 research and innovation programme under grant agreement No 731166.

## **12c) Mineralogy of Ore Deposits – Genesis, Characterization, and Applications**

**Wednesday, 25/Sep/2019: 8:30am - 10:30am**

**Session Chair: Malte Junge** (University Freiburg)

**Session Chair: Lennart A. Fischer** (University of Freiburg)

**Location: Schloss: S8**

### **Session Abstract**

The constant development in technology and the worldwide increasing standard of living, leads to continuous demand for raw materials. The understanding of existing as well as exploration for new ore deposits is therefore an important contribution to our society. Magmatic ore deposits cover a wide range of magmatic settings from dynamic MOR, back-arc systems, granite-related deposits to layered intrusions. These include rock types such as pegmatites, carbonatites and ultramafic-rocks, implying a vast number of ore formation processes. To understand the petrogenesis of magmatic ore deposits it is important to identify and explain ore formation processes including magma mixing, liquid immiscibility, crystal fractionation, partial melting, alteration and interaction with hydrous fluids. The diversity of different magmatic ore deposits provides the opportunity to study field relations, magmatic processes and mineralogy by using analytical tools, such as EPMA, LA-ICP-MS and isotope studies. We invite contributions from studies of natural rocks, experiments and numerical modelling in the field of magmatic ore deposits.

## Lecture Presentations

8:30am - 8:45am

### Using LIBS to detect REE-rich areas in Storkwitz drill cores – A new method for rapid and spatially detailed analysis of geological samples

**Simon Müller, Jeannette Meima, Dieter Rammlmair, Marleen Künker**

*Bundesanstalt für Geowissenschaften und Rohstoffe, Germany*

Fast and innovative space-resolved methods are a key to future exploration of ore deposits. They may provide a quick overview of elements of interest, their concentrations and distribution.

Laser Induced Breakdown Spectroscopy (LIBS) is a new and promising technology that grants fast in situ analysis paired with a high spatial resolution. Sample preparation is reduced to a minimum while the measurement speed maintains high, providing an easy and fast option to measure different kinds of geological samples in a short amount of time. The spatial resolution allows a more selective overview of the sample, precisely indicating the areas that include elements of interest or their indicators. This also supports energy-efficient rock processing by specifically targeting only areas of element enrichment, which is especially relevant for heterogeneous samples. Nevertheless, problems related to different kinds of physical and chemical matrix effects interfere with an interpretation of samples with unknown concentrations, making LIBS analysis a challenging task.

In a BMWi promoted project, we used a stationary LIBS system (Nd:YAG Q-switched 20Hz 1064nm laser and a high-resolution 285-964nm Echelle spectrometer) to analyse different segments of an inhomogeneous drill core from the carbonatite of Storkwitz (Germany) for the occurrence and distribution of Rare Earth Elements (REE). Since the demand of REE is growing year by year, methods and instruments able to detect areas of REE accumulation in a fast and precise way are very important for future exploration projects and the analysis of potential deposits.

Microprobe analysis of thin sections of selected areas indicate a differentiation in fluor and non-fluor bearing phases. REE enrichment is only visible in the former, making it a feasible indicator for these elements. Fluor, mostly hard to detect with methods that are able to maintain a spatial distribution, can be detected with LIBS using molecular CaF bands and potentially serve as reference for REE-enrichment in the samples of Storkwitz.

Validation measurements with  $\mu$ -EDXRF and electron microprobe demonstrate that LIBS is an effective technology for the discovery of light REE in a highly heterogeneous material with respect to their spatial position and their geological surrounding. Data processing in the form of clustering and classification techniques allow a separation between REE-rich phases and other rock forming components. Current research focusses on possibilities for REE quantification with LIBS.

8:45am - 9:00am

### The use of muscovite for B-isotope studies of hydrothermal ores

**Robert Trumbull, Marta Codeco, Johannes Glodny, Rolf Romer, Philipp Weis, Michael Wiedenbeck**

*Helmholtz-Zentrum Potsdam GFZ, Germany*

Boron isotope variations in minerals are useful to constrain the sources and evolution of ore-bearing fluids in hydrothermal ore deposits and in the granites or pegmatites related with them. Because of the complexity of B-distribution in natural ores, in-situ microanalysis is the method of choice, but so far in-situ studies are almost exclusively limited to tourmaline. Muscovite coexists with tourmaline in many ore deposits and it is also common in deposits lacking tourmaline. In those cases, muscovite is commonly the main mineral host for boron, with concentrations of several hundred  $\mu\text{g/g}$ , easily measured by techniques like secondary-ion mass spectrometry (SIMS). Furthermore, muscovite-fluid fractionation of B-isotopes is experimentally established, so the lack of studies using this mineral is a missed opportunity. One reason why muscovite has been neglected in B-isotope studies was the lack of homogeneous reference materials. The Potsdam SIMS lab has now tested and confirmed the B-isotope homogeneity of two widely-available muscovite reference

materials (Harvard 11271 and 98973), and is in the process of establishing them as international reference materials. This contribution gives the results of a test application of in-situ SIMS analysis of muscovite based on the granite-related Panasqueira W-deposit in Portugal. Muscovite in this deposit occurs together with tourmaline in ore-vein selvages and alteration zones, and one goal of the study was to test the utility of B-isotope exchange between muscovite and tourmaline as a geothermometer. Applying the SIMS  $^{11}\text{B}/^{10}\text{B}$  ratios in muscovite-tourmaline pairs with experimental fractionation factors yielded median temperatures of 400 to 460°C from vein selvages and 250°C from a cross-cutting, mineralized fault zone. These values agree with independent temperature estimates from fluid inclusions and Ti-in-quartz thermometry. We conclude that the B-isotope composition of muscovite can be reliably measured by SIMS, and thus it can be used like tourmaline as a fluid monitor and for geothermometry if both minerals coexist.

### 9:00am - 9:30am Session Keynote

#### **Making space for giant Zn deposits in Palaeozoic carbonaceous mudstones: the role of diagenesis**

**Sarah Gleeson<sup>1,2</sup>, Joe Magnall<sup>1</sup>, Merilie Reynolds<sup>3</sup>**

<sup>1</sup>GFZ Potsdam, Germany; <sup>2</sup>Freie Universität Berlin, Germany; <sup>3</sup>University of Alberta, Edmonton, Canada

The North American Cordillera contains a number of large Zn deposits hosted in Palaeozoic biosiliceous, carbonaceous, radiolarian-rich mudstones. Stratabound barite units are associated with the ore deposits, but are also found regionally in barren, correlative sequences. Recent studies have shown that stratabound barite, pyrite and authigenic carbonate formed in the sediment at the sulphate methane transition zone (SMTZ), and are a product of pre-ore diagenesis. Stratabound diagenetic pyrite, preserves positive  $\delta^{34}\text{S}$  values which suggest that the anaerobic oxidation of methane coupled with sulphate reduction (AOM-SR), which was an important source of reduced sulphur during diagenesis.

The hydrothermal systems are superimposed on this diagenetic environment, do not exhale onto the sea-floor and developed in non-euxinic conditions. The  $\delta^{34}\text{S}$  values in ore-stage pyrites suggest reduced S is derived from a number of sources, including recycling of sulphate from the dissolution of diagenetic barite. The radiolarian-rich host rocks, likely dominated by Opal A in the top 100s of metres of the sediment, had high porosities and permabilities that allowed the ore deposits to form in the sub-surface and prevented significant exhalation of the hydrothermal system into the water column. Therefore, the biosiliceous nature of host rock, together with the ability of the hydrothermal fluids to dissolve authigenic barite and carbonate, are major controls on the genesis and size of these important deposits.

### 9:30am - 9:45am

#### **Properties of mineralizing fluids at high-temperature (200 < T < 600 °C): Insights from in-situ spectroscopy**

**Marion Louvel**

WWU Muenster University, Germany

High-temperature aqueous fluids and vapors are key players in the formation of various ore deposits, including world-class porphyry Cu-Au-Mo or rare-earth deposits. These volatile-rich phases however remain elusive, mostly due to difficulties in their sampling. Indeed, neither volcanic fumaroles, nor fluid inclusions can be considered as pristine sample of the high pressure-temperature composition and metal contents.

The development of comprehensive geochemical models describing the effect of magma-fluid-rock interactions on the evolution of magmatic-hydrothermal mineralization hence requires an empirical knowledge of 1) the composition and properties (ie., density) of mineralizing fluids and 2) the nature of metal-ligand complexes that participate to the hydrothermal transport and deposition, directly at the adequate pressure and temperature of formation and circulation. Up to now, such knowledge is mostly limited to temperature below 200 °C and the properties of hydrothermal fluids and behaviour of metals at high P-T hence remain questionable.

Here, I will present the results of *in situ* Raman and X-ray absorption (XAS) measurements that have been conducted in a dedicated hydrothermal autoclave [1,2] to assess the complexation of metals (Cu, REE) with various ligands ( $F^-$ ,  $Cl^-$ ,  $HS^-$ ,  $SO_4^{2-}$ ,  $CO_3^{2-}$ ) up to 600 °C and 1 kbar [3,4]. Additional measurements of the density of  $H_2O$ - $CO_2$ -NaCl fluids up to 500 °C and 1.5 kbar and preliminary experiments that aim to extend our *in situ* studies to melt+fluid systems will also be discussed.

[1] Testemale et al., 2005. Rev. Sci. Instr. 76, 043905-5; [2] Louvel et al., 2015. J. Mol. Liq. 205, 54-60; [3] Louvel et al., 2015. Chem. Geol. 417, 228-237; [4] Louvel et al., 2017. Chem. Geol. 466, 500-511.

**9:45am - 10:00am**

### **From seawater to black smoker vents: Hydrothermal fluids that leach metals from the oceanic crust and generate VMS deposits**

**Lisa Richter, Larry W. Diamond**

*University of Bern, Switzerland*

Metasomatic alteration of basaltic and gabbroic rocks in the deep oceanic crust by heated seawater produces a variety of hydrothermal–metamorphic mineral assemblages including spilites (rocks consisting of chlorite + albite + quartz ± actinolite ± epidote) and epidosites (rocks consisting of epidote + quartz + titanite + Fe-oxides). Epidosites have been proposed as markers of deep upflow in hydrothermal convection cells and as source rocks for the metals in seafloor black-smoker sulfide deposits. Whereas spilitization is attributed to fluid of seawater salinity, the salinity of epidotizing fluids is debated. In addition, the metal contents of the fluids have been constrained by experiments and observations of vent fluids, but no direct analyses are available.

We have analyzed primary fluid inclusions in quartz in spilite assemblages and in coeval epidote and quartz in massive epidosite assemblages in the Semail ophiolite (Oman). The results confirm that the hydrothermal alteration of basaltic dikes, lavas and plagiogranites to spilites and epidosites is due, in both cases, to fluids with salinity close to that of seawater (2.6–4.1 wt.% total dissolved solids). Hypersaline fluid inclusions (>30 wt.% total dissolved solids) in hydrothermally altered plagiogranites are confined to paragenetically earlier hydrothermal–magmatic quartz and hence they are unrelated to spilitization and epidotization. Temperature and pressure reconstructions from the fluid inclusion data reveal that the hydrothermal alteration occurred over a range of *P-T* conditions: 170–430 °C for spilitization and 235–400 °C for epidotization, all at hydrostatic pressures of 27–50 MPa. Laser-ablation-ICP-MS analyses show that the spilitizing fluid is enriched in Fe, Cu and Zn, whereas the epidotizing fluid is metal-depleted. Therefore, in contrast to earlier proposals, we view the spilitizing fluid rather than the epidotizing fluid as the carrier of metals that form volcanogenic massive sulfide (VMS) deposits on the seafloor.

**10:00am - 10:15am**

### **Giant Carlin-type Au deposits formed by coupled partitioning of Au and As into pyrite**

**Christof Kusebauch, Sarah A. Gleeson, Marcus Oelze**

*GFZ Potsdam, Germany*

The giant Carlin-type Au deposits (CTGD) of Nevada (USA) are the second largest accumulation of Au on Earth and currently account for 5-6% of Au produced world-wide. Gold in the CTGDs (and related deposits) is structurally bound in arsenic-rich pyrite. Although, the geodynamic conditions under which these “invisible gold” deposits are formed are well characterized, the geochemical processes controlling the sequestration of Au are poorly understood.

We performed an experimental study at conditions of CTGD formation (T:200°C, *Psat*, w/r:~1000,  $H_2S$ : 0.05 molal) facilitating the replacement of siderite (Fe-carbonate) to form synthetic pyrite. The partitioning of As and Au between hydrothermal fluid and newly formed pyrite was studied at varying fluid compositions

(As: 0-100ppm; Au: 0.05-10 ppm). We find that Au from the fluid strongly partitions ( $D$  values:  $>1000$ ) into newly formed pyrite depending on the As concentration of the pyrite. The coupled partitioning behavior of these two trace elements is key for the enrichment of Au in arsenic-rich pyrite. The newly constrained partition coefficients for As and Au help to explain the observed covariation of these trace elements (on deposit but also micrometer scale) and imply a magmatic-hydrothermal origin of the CTGD ore fluids. We developed a mass balance model based on the derived partition coefficients that shows that simple partitioning (and the underlying process of adsorption) is the major depositional process in the CTGD systems. Our findings help to explain why pyrite in Carlin-type gold deposits can scavenge Au from hydrothermal fluids so efficiently to form giant deposits.

**10:15am - 10:30am**

### **The importance of magmatic processes on the formation of orogenic Au deposits: insight from the Central Lapland Greenstone Belt, Finland**

**Clifford Patten<sup>1</sup>, Jochen Kolb<sup>1</sup>, Ferenc Molnár<sup>2</sup>, Iain Pitcairn<sup>3</sup>**

<sup>1</sup>KIT, Germany; <sup>2</sup>GTK, Finland; <sup>3</sup>Stockholm University, Sweden

Paleoproterozoic greenstone belts are worldwide prospective terranes for orogenic Au deposits. Formation of these deposits require transport of metal-rich hydrothermal fluids from source areas to site of deposition during metamorphism. Recognition of these source areas is an important step in understanding orogenic Au deposit genesis and yet they are not well characterised in Paleoproterozoic greenstone belts. In this study we investigate the role of metavolcanic rocks as the source of orogenic Au deposits in the Paleoproterozoic Central Lapland Greenstone Belt, Finland. The metavolcanic rocks are characterised by mid-oceanic ridge basalts (MORB) and within plate basalts (WPB). MORB greenschist samples have lower Au content (median = 0.29, 0.18-3.97 ppb Au) than the WPB ones (median = 0.92 ppb, 0.83-12.2 ppb) due to different magmatic differentiation processes. Using fresh MORB and WPB data as proxy for protolith composition, mass variation calculation shows that up  $68 \pm 39\%$  of the initial metavolcanic Au content is lost during high grade metamorphism in the upper amphibolite facies ( $>550$  °C). The Kittilä group hosts most of the deposits and up to 1500 km<sup>3</sup> of its base is metamorphosed to upper amphibolite. Mass balance calculation suggests that up to ~2870 t of Au have been mobilised during metamorphism which is significantly higher than the ~280 t Au endowment in the orogenic Au deposits. Metavolcanic rocks appears thus as a fertile source for Au in Paleoproterozoic greenstone belts. Moreover it is important to consider which type of metavolcanic rocks are present within the greenstone belts as WPB are enriched in Au relative to MORB and boost the Au fertility of the source areas.

## **Poster Presentations**

**Tue: 79**

### **Thorium-poor monazite and columbite-(Fe) mineralization in the Gleibat Lafhouda carbonatite and its associated iron-oxide-apatite deposit of the Ouled Dlim Massif, South Morocco**

**Rachid Benaouda<sup>1</sup>, Dennis Kraemer<sup>1</sup>, Maria Sitnikova<sup>2</sup>, Simon Goldmann<sup>2</sup>, Ralf Freitag<sup>2</sup>, Abdelhafid Bouali<sup>3</sup>, Abdellah Mouttaqi<sup>3</sup>, Michael Bau<sup>1</sup>**

<sup>1</sup>Jacobs University, Bremen, Germany; <sup>2</sup>Bundesanstalt für Geowissenschaften und Rohstoffe, Hannover, Germany;

<sup>3</sup>National Office of Hydrocarbons and Mines, Rabat, Morocco

The Gleibat Lafhouda carbonatite is a Paleoproterozoic magnesiocarbonatite which is hosted by Archean gneiss and intruded by massive IOA mineralization. Metasomatized micaceous rocks occur locally at the margin of the carbonatite outcrop and were identified as glimmerite fenite type.

The rare earth element (REE) and Nb mineralization in this intrusion is mainly linked to the associated IOA

and is represented by monazite-(Ce) and columbite-(Fe) as major ore minerals. The IOA forms massive outcrops mainly consisting of magnetite and hematite that usually contain large apatite crystals (up to several centimetres), quartz and some dolomite. Monazite-(Ce) is closely associated with fluorapatite and occurs as numerous inclusions in the altered part of apatite and along apatite cracks. Microprobe investigations of monazite show no zonation patterns and very low Th contents (less than 0.4 wt%), which would be beneficial for commercial extraction of the REE. These features have been interpreted as evidence for the formation of monazite from apatite as a result of hydrothermal volatile-rich fluids interacting with the apatite-rich host rock. Similar monazite-apatite mineralization and chemistry also occurs at depth within the carbonatite, although the outcropping carbonatite is barren and only contains some tiny unidentified secondary Nb-Ta-U phases, synchysite and monazite. Niobium mineralization is commonly represented by anhedral minerals of columbite-(Fe) which occur closely associated with magnetite-hematite and host up to 78 wt% Nb<sub>2</sub>O<sub>5</sub>, 7 wt% Ta<sub>2</sub>O<sub>5</sub> and 1.6 wt% Sc<sub>2</sub>O<sub>3</sub>. This association may suggest that columbite-(Fe) precipitated by an interaction of Nb-rich fluids with pre-existing Fe-rich minerals or as pseudomorphs after pre-existing Nb minerals like pyrochlore.

The composition and textural relationships of the REE and Nb mineralization in the Gleibat Lafhouda intrusion suggests that this deposit was formed by different fluids at multiple stages. The transport of large amounts of REE and Nb suggests that the transporting fluids were highly enriched in complexing ligands (e.g., Cl and/or F) that allowed the rather immobile REE and Nb to be readily transported in solution.

**Tue: 80**

### **As-rich VMS Mineralization at Niuva South, Tonga Arc**

**Jan Johannes Falkenberg, Karsten Haase, Thomas Günther, Manuel Keith**

*GeoZentrum Nordbayern, Universität Erlangen-Nürnberg, Erlangen 91054, Germany*

Hydrothermal systems with black smoker mineralization represent modern analogues to ancient volcanogenic massive sulfides (VMS). Although, the formation processes have been studied extensively at mid-ocean ridges, especially the element transport at hydrothermal fields in active island arc settings is still poorly constrained. Magmatic degassing from volatile-rich parental magmas may be of key importance for the transport and finally the enrichment of elements like As, Au and Cu in black smoker mineralization. Niuva volcano is the northernmost discrete volcanic edifice on the Tofua sector of the Tonga Island Arc and shows extreme degassing. An explosion crater on the southern end hosts the 350-meter wide and 80-meter deep hydrothermal vent field “Niuva South”, which yields massive sulfides mounds, multi-spined- and beehive diffuser black smoker chimneys. Hence, Niuva volcano represents a natural laboratory to better understand the effect of a magmatic volatile flux to subduction zone hydrothermal systems.

Here, we present, for the first time, in-situ analyses of major and trace elements (EPMA/LA-ICP-MS) in a range of metal and metalloid-bearing sulfide phases from the Niuva South seafloor hydrothermal system. The mineralization includes pyrite, chalcopyrite, sphalerite, As-sulfides (Realgar/Orpiment) and barite. Preliminary EPMA propose that As (up to 2,9 wt.%) and Cu (up to 5,0 wt.%) enriched pyrite may be related to a strong magmatic volatile influx to the hydrothermal system. Chalcopyrite shows As contents up to 0,7 wt.%. Sphalerite reveals As and Cu concentrations up to 2,2 wt.% and 3,7 wt.%, respectively. Endmember fluid temperatures (325°C) measured lie on the boiling curve at 1164-m water depth (Gartman et al. 2018). Mineral and fluid data will be used to constrain the influence of different physico-chemical fluid parameters (e.g. temperature, pH, sulfur and oxygen fugacity) on the ore-forming processes. We will constrain the effect of volatile transport and source components in a subduction setting using radiogenic- and stable isotope data (ICP-MS). For example, sediment subduction could lead to an elevated volatile content in the parental magmas and may therefore affect the hydrothermal system. Bulk-ore analyses (LA-ICP-MS and INAA) will reveal local or regional differences regarding metal distribution within the arc-setting. The high As contents may indicate elevated Au values, as known from subaerial Au-rich systems. In combination with the recent finding of colloidal Au particles in black smoker fluids at Niuva South (Gartman et al. 2018) this could raise economic interests.

**Tue: 81****Detection, distribution and speciation of chemical elements with fast XRF mapping and micro X-ray absorption spectroscopy demonstrated for a Tl containing ore**

**Joerg Goettlicher<sup>1</sup>, Thomas Spangenberg<sup>1</sup>, Ralph Steininger<sup>1</sup>, Andreas Voegelin<sup>2</sup>, Gabi Penkert<sup>3</sup>, Peter Penkert<sup>3</sup>**

<sup>1</sup>Institute for Photon Science and Synchrotron Radiation (IPS), KIT, D; <sup>2</sup>Eawag - Swiss Federal Institute of Aquatic Science and Technology, Duebendorf, CH; <sup>3</sup>Fröndenberg, D

Detection, distribution and speciation of chemical elements help understanding rock and ore formation and can give valuable information on critical or hazardous elements. X-ray fluorescence (XRF) mapping is essential to detect and localize such elements in heterogeneous materials for subsequent determination of their structural and chemical-states with X-ray absorption fine structure (XAFS) spectroscopy, but is not time-efficient in the classical step-scan-mode. Continuous sample movement and on-the-fly recording of fluorescence signals with low gate-time-electronics enable mapping of areas large enough to be significant for a geological setting within reasonable time.

On-the-fly (fast) XRF-mapping was applied to Tl-containing rocks showing that Tl  $L\alpha$ -fluorescence-emission is still detectable at 10 ms collection-time per data point with a single-element SDD-detector. Preservation of a typical energy-resolution of about 140 eV at high count-rates when using a SDD-detector enables the recording of Tl  $L_3$ -edge XAFS-spectra on areas of high Fe and As concentrations without the need of filters or a secondary spectrometer. Subject of investigation were samples from the abandoned pyrite-mine in Meggen (NE Rhenish-Massif). The submarine-exhalative Fe-Zn-Pb sulfide-mineralization is of Devonian age with average Tl-concentrations of 193 ppm beneath the orebody, in contrast to typical background-values in the Rhenish-Massif of 0.3–2 ppm Tl [1]. The mine was operational from 1853-1992. Toxicity of Tl came into the public awareness in Germany in 1978/1979 because high levels of Tl were emitted during cement production in Lengerich using pyrite-cinder to regulate hydraulic properties. The used pyrite from Meggen contains 300-400 ppm Tl on average. In an ore-sample of colloform texture, Tl has been detected with fast-XRF-mapping in hot-spots (up to about 2600 ppm) and in low concentrations (about 300 ppm) in bulk Fe-sulfide regions. Point XAFS-spectra from different regions are similar to a TlAsS (lorandite) reference-spectrum, suggesting Tl in pyrite as Tl(I) in irregular S-coordination as has been described recently also in [2].

Measurements of element distributions with on-the-fly-mode gain 2-10 hours for 20000 to 1 Mio data points compared to step-scan-mode. With a 7-element SDD detector and faster signal-processing-electronics, both are now available at the SUL-X beamline of the KIT synchrotron radiation source, a gain in signal of a factor 70 is expected allowing even faster XRF-mappings and better quality of the Tl XAFS data. Verification is under investigation.

Further applications could be for critical metals in ores and their processing residues.

[1] Mueller A.: <https://e-sga.org/de/publications/mineral-deposit-archive/the-meggen-deposit>; [2] George L.L. et al. (2019): *Ore Geology Reviews*, 107, 364-380

**Tue: 82****High resolution mineral-chemical analysis of scheelite from the Felbertal tungsten deposit, Austria**

**Cordula Haupt<sup>1</sup>, Bernhard Schulz<sup>1</sup>, Joachim Krause<sup>2</sup>, Karsten Aupers<sup>3</sup>, Steffen Schmidt<sup>3</sup>**

<sup>1</sup>Technische Universität Bergakademie Freiberg, Institut für Mineralogie, Germany; <sup>2</sup>Helmholtz-Zentrum Dresden Rossendorf, Helmholtz-Institut Freiberg für Ressourcentechnologie, Germany; <sup>3</sup>WOLFRAM Bergbau und Hütten AG, Mittersill, Austria

The Felbertal tungsten deposit is situated in the Hohe Tauern range, near Mittersill, Austria. The ore is hosted in the volcano-sedimentary, polymetamorphic units of the Pre-Permian Habach Complex as disseminated and stockwork mineralisation, mostly associated to quartz. An Eastern and a Western ore zone (EOZ and WOZ), which are spacially divided by the NS oriented valley, have been distinguished. The genetical relation

of different postulated mineralisation events of scheelite in the EOZ and WOZ has not yet been fully resolved. Previous studies reported four different generations, characterised mainly by different fluorescence colour and molybdenum (Mo) content. The first and second generation are characterised by yellow fluorescence and relatively high Mo contents, whereas the later third and fourth generation were observed to have whitish to blue fluorescence colour with low Mo concentration. Processes of remobilisation and recrystallisation have been accepted to be responsible for the different generations (Höll & Eichhorn, 2000).

Formerly less well explored ore bodies have been targeted in the WOZ in the last years. Scheelite in this study was collected in recently worked districts of the mine, namely K8 ore body, K2 Brekzie and scheelite-dotted (SD)-gneiss. Associated scheelites display complex and diverse zonation under 254 nm SW UV light.

To target this, new quantitative and qualitative analysis of scheelites have been made using electron probe micro analysis (EPMA). Qualitative molybdenum distribution maps, quantitative element profiles and cathodoluminescence (CL) images have been combined with microtextural analysis to reveal a new view into the mineralisation history.

Molybdenum distribution maps of scheelite grains between 0.5 and 300  $\mu\text{m}$  are of multiphase character with often sharp, irregular edges between plateaus of even concentration, fractures and peripheral areas contain microscale Mo-sulfides. Profiles show a mostly fluctuating pattern between concentrations of 0.00 to 4.14 wt% Mo oxide. The element maps reveal a more complex microscale distribution of Mo, than can be visualized by UV-light.

Under the microscope scheelite shows undulating extinction, complex fracturing and occasional recrystallisation.

The formation of the scheelite apparently involved multiple dissolution and reprecipitation during a fluid-mineral interaction where relatively Mo-poor scheelite replaced Mo-rich scheelite. This was followed by predominantly brittle deformation but with occasional dynamic recrystallisation of scheelite. These new observations will ultimately influence the genetical interpretation of the Felbertal tungsten deposit.

Höll, R. & Eichhorn R. (2000): Tungsten mineralization and metamorphic remobilization in the Felbertal scheelite deposit, Central Alps, Austria. *Reviews in Economic Geology*, 11: 233–264

## Tue: 83

### Quantification of minerals and valuable metals in drill cores from orogenic gold deposits by LIBS and $\mu$ -EDXRF

**Marko Hornschu, Jeannette Meima**

*BGR Hannover*

Rapid and competitive drill core characterization and quantification of valuable components is a main goal in mineral exploration. Thereto, the development of appropriate drilling core analysis systems offers interesting possibilities. As part of the EU-funded project "ANCORELOG", the state of the art LIBS (Laser Induced Breakdown Spectroscopy) technology is being tested for drill core samples from orogenic gold deposits.

LIBS is a kind of atomic emission spectroscopy using a high-energy laser pulse to form a plasma at the sample surface. The cooling plasma emits light of element specific wavelengths, which can be analyzed in a spectrometer. In general, LIBS is able to detect all elements in all physical states only limited by the sensitivity and wavelength range of the spectrometer system.

It is a broadly used technique for characterization and quantitative analysis of homogenous materials (e.g. steel, scrap), but for heterogeneous samples like drill cores or geologic samples the method needs further development. LIBS analysis of heterogeneous sample material is in particularly complicated by the severe plasma variations that occur due to chemically induced matrix effects. One way to reduce the problems with geologic material is to apply calibration with a carefully selected set of reference samples of known composition and textural structure.

The investigated sample material consists of different lithologies with metamorphic imprints ranging from

greywackes, intermediate metavulcanites, chlorite/sericite schists to amphibolites and skarns. The samples show different levels of complexity, from nearly homogenous to widely heterogeneous with complex structures.

The material was mapped with a resolution of 200µm with a LIBS drill core scanner. The resulting spectra were processed to get the intensity of multiple characteristic emission lines for 25 target elements. Due to limitations in the used spectrometer, direct measurements of gold particles at a µm-scale and some trace elements is unlikely.

Bulk XRF data as well as spatially resolved X-ray fluorescence data (µ-EDXRF) were applied for reference purposes. These were used to build a multivariate calibration model (e.g. PLS Regression) to quantify element contents in LIBS measurements. Because of matrix and plasma effects, correlations between spectral LIBS intensities and element contents are not linear and multivariate calibration is required.

For fast drill core analysis, detailed mappings are time consuming and are not always productive. Therefore, a reduction of the data without loss of fundamental information is necessary. For different samples profiles, reduced and detailed mappings were compared with respect to expenditure of time, validity and accuracy.

**Tue: 84**

### **Lower Group and Middle Group chromitites of the Bushveld Complex – the effect of weathering on the distribution of platinum-group elements**

**Malte Junge<sup>1</sup>, Kai Bachmann<sup>2</sup>, Thomas Oberthür<sup>3</sup>, Nikolay Yu Groshev<sup>4</sup>**

<sup>1</sup>*Institute of Earth and Environmental Sciences, Albert-Ludwigs-University Freiburg, Germany;* <sup>2</sup>*Helmholtz-Zentrum Dresden-Rossendorf, Helmholtz Institute Freiberg for Resource Technology, Germany;* <sup>3</sup>*Federal Institute for Geosciences and Natural Resources (BGR), Germany;* <sup>4</sup>*Geological Institute, Kola Science Centre, Russian Academy of Sciences, 184209 Apatity, Russia*

The Bushveld Complex in South African contains vast resources of Cr, PGE and V. Currently, the Merensky Reef, the Platreef and the UG-2 chromitite seam are the major mining targets for PGE, although chromitites of the Lower Group (LG) and Middle Group (MG) may also contain concentrations up to several ppm PGE.

In a suite of chromitite samples from the Thaba Mine in the western Bushveld Complex it was shown that Pt concentrations in weathered chromitite seams (LG-6 to MG-4) generally exceed those of Pd. However, differences are observed by comparing individual chromitite seams as total PGE concentrations of weathered chromitites from the LG-6 to MG-4 range between 760 and 1300 ppb. Elevated concentrations of Pt and Pd are also present in hanging and footwalls of chromitite seams (median 333 ppb Pt). The PPGE (Rh, Pt, Pd) contents of weathered ores are generally lower than those of the pristine ores. The IPGE (Os, Ir, Ru) are very similar in both pristine and weathered ores. Particularly, Ru concentration is in the same range as the pristine ores.

Platinum concentrations increase from LG-6 to MG-4, whereas Pd remains at near-constant levels, resulting in a strong increase of the Pt/Pd ratio from 2.2 to 15.3. Platinum, largely remains within the chromitite seams and is only locally mobilized within the chromitites and their surrounding hanging and footwalls, whereas a large proportion of the Pd is leached out. Weathering causes mobilization of Pt and Pd out of the chromitites, locally into the hanging and footwall. The general decrease (in particular of Pd) can also be observed by comparing the average Pt/Pd ratio of pristine chromitites from the Thaba Mine. The IPGE are generally less affected by weathering processes which may be explained by the fact that laurite [(Ru,Os,Ir)S<sub>2</sub>] commonly occurs as inclusions in chromite, and PGM incorporated in chromite are largely unaffected by weathering processes.

Tue: 85

### Field observations and mineralogical characterization of magnetite-skarn-occurrences in Isfahan Province, Central Iran

**Nico Kropp<sup>1</sup>, Andreas Kamradt<sup>1</sup>, Hooshang Asadi Haroni<sup>2,3</sup>, Gregor Borg<sup>1</sup>**

<sup>1</sup>Economic Geology and Petrology Research Unit, Martin-Luther-University Halle-Wittenberg, Germany; <sup>2</sup>Department of Mining Engineering, Isfahan University of Technology, Isfahan 8415683111, Iran; <sup>3</sup>Centre for Exploration Targeting, Australian Research Council Centre of Excellence for Core to Crust Fluid Systems, School of Earth and Environment, The University of Western Australia, Crawley, WA 6009, Australia

The Urumieh-Dokhtar-Magmatic-Arc (UDMA), part of the Tethyan Belt, is host to major porphyry-epithermal-skarn related ore deposits. This middle section of this poorly explored arc in central part of Iran comprises two important magnetite-skarn occurrences, associated with different metal content but in a similar geotectonic and plate tectonic setting. The Hashim Abad occurrence between Nain and Isfahan is located in a transition zone between Cretaceous dolomitic marble with a cross-cutting diorite intrusion associated with a NW-SE trending fault. Subsequently, these rocks have undergone greenschist metamorphism. Along the fault the meta-dioritic wall rock was affected by alteration. A hydrothermal influence is indicated by alteration clay minerals and saussuritisation of feldspar. The dolomitic wall rocks controlled the formation of the mineral paragenesis of the skarn, which comprises olivine, phlogopite, and hedenbergite, ideally in Mg-rich systems. Due to intensive weathering, neither olivine nor phlogopite were found, but alteration products such as vermiculite and smectite are present. Lenses of magnetite are associated with green pyroxenes of hedenbergitic composition and show an anomalously high gold content of 520 ppb and is intergrown with chalcopyrite and pyrite. Additionally, colourful secondary copper minerals like malachite and chrysocolla occur along faults. The host rocks, magnetite, and the calc-silicates are cross-cut by different generations of carbonate veins and veinlets, which are partly associated with quartz and minor sphalerite and galena. In contrast, the Golestan mine with its magnetite-skarn occurrence near Kashan town is associated with andesitic dykes, cross-cutting Miocene limestone. Here, the magnetite is associated with yellowish to green andraditic garnet, dark green pyroxene, and wollastonite. The magnetite is associated with chalcopyrite and cobalt-bearing minerals such as cobaltite and pinkish erythrite. The calc-silicate-hosting andesite dykes strike NNW-SSE and show chloritization, indicating a retrograde paragenesis of epidote-chlorite-actinolite. The mineral parageneses of skarns and their metal associations depend strongly on the composition of the host rocks. Both investigated skarns have formed from replacement of carbonate wall rocks resulted in the predominant formation of exo-skarns, locally with small zones of endo-skarns. We propose that the Mg-skarn at Hashim Abad represents a Fe-Cu-Au skarn type, whereas the Ca-skarn at the Golestan mine is rather Fe-Cu-Co skarn type.

Tue: 86

### Geochemical analyses of stream sediments and morphological studies of gold micro-nuggets from the Carnon River Mining District, Cornwall

**Nicolas Meyer, Gregor Borg, Andreas Kamradt**

Economic Geology and Petrology Research Unit, Martin Luther University Halle-Wittenberg, Germany

The Carnon River Mining District is located in Cornwall, between Devoran, Gwennap and Chacewater and is part of the Cornubian Ore Field. During the 18th and 19th century it was an important region for tin and base metal mining. Geologically, the study area is mainly composed of Devonian metasedimentary units, with intercalations of mafic metavolcanic rocks. The sequence has intruded by Late Variscian granites. Mineralised quartz-rich porphyritic dikes and polymetallic, crosscutting veins are characteristic for this area. Tin, copper, and arsenic were the main metals of value, but smaller amounts of lead, zinc and minor wolfram and even smaller quantities of gold have also been produced. Gold nuggets from the region are kept at the Royal Cornwall Museum and the Williams Collection at Caerheys Castle. Ehser et al. (2011)<sup>1</sup> identified placer gold from the Carnon River as the most likely source of the gold of the Bronze Age Sky Disk of Nebra. This study investigates gold micro-nuggets occurrences associated with stream sediment samples taken on

spots of the entire drainage system of the Carnon River. A total of 25 samples were taken from the relatively short Carnon River and its even smaller tributaries. The extraction was accomplished by using a RotaPan for pre-concentrating in the field and a Wilfley-table as well as a pan in the laboratory. Numerous micro-nuggets were photo-documented and morphologically studied using an SEM. Some nuggets show little mechanical abrasion or flattening and at least in one case, slightly flattened, but recognizable bacterioform textures. Other nuggets are more flattened and carry inclusions of K-feldspar and quartz. Gold concentrations range between the lower detection limit up to more than 600 ppb. Samples with high Au concentrations correlate positively with the samples that carry micro-nuggets. Tin concentrations within the pre-concentrates range between 0.2 to more than 1%, whereas the copper contents were partly below 100 ppm, but reached up to 1.3%. Our investigations show that geochemical stream sediment gold concentrations can be grouped into 1<sup>st</sup> order (> 500 ppb), 2<sup>nd</sup> order (< 500 ppb, > 50 ppb), and 3<sup>rd</sup> order (< 50 ppb, > 5ppb) anomalies compared to background values of < 5 ppb Au.

<sup>1</sup>Ehser, A., Borg, G., Pernicka, E. (2011) Provenance of the gold of the Early Bronze Age Nebra Sky Disk, central Germany: geochemical characterization of natural gold from Cornwall. *Eur. J. Mineral*, 23: 895-910.

**Tue: 87**

## **Granitic pegmatites and Nb-, Y-REE- and F-mineralization in the Las Chacras Batholith, Argentina**

**Enrico Ribacki<sup>1</sup>, Uwe Altenberger<sup>1</sup>, Robert Trumbull<sup>2</sup>, Mónica López de Luchi<sup>3</sup>**

<sup>1</sup>University of Potsdam, Institute of Geosciences; <sup>2</sup>Helmholtz Centre Potsdam, GFZ German Research Centre for Geosciences; <sup>3</sup>Instituto de Geocronología y Geología Isotópica, INGEIS (CONICET)

The Devonian Las Chacras Batholith of the Sierra de San Luis in central Argentina intruded into an Ordovician basement, composed of metasediments and S-type granitoids. The batholith is composed of nested granitic intrusions emplaced within a pull-apart structure controlled by major strike slip fault systems (Siegesmund et al., 2004). Coeval intrusions of stocks and syn-plutonic dikes of lamprophyres demonstrate a strong mantle component in the Devonian magmatism. The intrusions show a north to south directed increase in the magmatic differentiation and crustal contamination, as indicated by radiogenic Sr/Nd-isotope ratios (López de Luchi et al., 2017).

Intra-granitic pegmatites occur in all units of the batholith but are most abundant in the south. Some of the pegmatites reveal NYF-type mineralization (Nb-, Y-, REE-, F-rich phases; Lira et al., 2012). In contrast, the pegmatites of the Ordovician basement contain LCT-type mineralization (Li, Cs, Ta).

The present work investigates the mineralogical and geochemical composition of the pegmatites and their granitoid hosts and sources to provide new insights into the evolution of the magmatic system and the development of the NYF mineralization. The focus is on the emplacement and the evolution from primary melts at different structural levels within the crust to a differentiated residual melt as a carrier for high-technology elements. In order to compare the different sources, melt contamination and fractionation processes, such as assimilation and mingling, major and trace element analyses as well as boron isotopes on tourmalines are used. First field and geochemical evidences point to a strong influence of the syn-magmatic mafic mantle-derived melts.

[1] Lira, R. et al. (2012): The Intragranitic Potrerillos NYF Pegmatites and their A-Type Host Granites of the Las Chacras-Potrerillos Batholith, Sierra de San Luis, Argentina. *The Canadian Mineralogist* 50, 1729-1750; [2] López de Luchi, M. et al. (2017): Petrogenesis of the postcollisional Middle Devonian monzonitic to granitic magmatism of the Sierra de San Luis, Argentina. *Lithos* 288-289, 191-213; [3] Siegesmund, S. et al. (2004): The Las Chacras-Potrerillos batholith (Pampean Ranges, Argentina): structural evidences, emplacement and timing of the intrusion. *International Journal of Earth Sciences* 93, 23-43.

Tue: 88

### Fluid-melt partitioning of Sn and W as function of the alumina saturation index of the granitic melt

Christian Schmidt, Rolf L. Romer, Cora C. Wohlgemuth-Ueberwasser, Oona Appelt

Deutsches GeoForschungsZentrum (GFZ), Potsdam, Germany

A basic assumption in traditional models of granite-related hydrothermal Sn-W mineralization is that both Sn and W partition into the magmatic aqueous fluid upon exsolution from a peraluminous or metaluminous granitic melt [1]. However, such deposits typically show predominance of one metal over the other, which may reflect contrasting behavior of these elements during late-stage magmatic processes. Here, we determined the dependence of the fluid-melt partition coefficients of Sn and W on the alumina saturation index (ASI) of the melt. In these experiments, cassiterite and ferberite crystals, 2 molal (Na,K)Cl±0.1 molal HCl solutions, and Macusani glass or synthetic haplogranitic glass (ASI 1.0 or 1.3) were equilibrated at 750 °C, 200 MPa. Fluid-melt partition coefficients were obtained (i) from analyses of fluid inclusions trapped in the glass and of the glass host [2], and (ii) from analyses of quench fluid extracted from the capsules and of the reacted glass.

Our results show different behavior of Sn and W. Tin partitions slightly into the granitic melt at HCl concentrations to 0.1 molal, which is about the maximum in natural magmatic fluids. This is in agreement with the literature, where preference of Sn for the aqueous fluid is reported only at very high HCl molality [3,4]. Tungsten partitions into the aqueous fluid except in the presence of strongly peraluminous granitic melts (ASI >1.3). At constant ASI, fluid-melt partition coefficients of W determined from fluid inclusion analyses are one order of magnitude higher than those from analyses of quench fluid suggesting that values reported in the literature may be underestimates.

Contrasting fluid-melt partitioning and differences in fluid-rock reactions are causes for separation and zonation of Sn and W on the deposit scale and the different style of predominant mineralization. Tin is initially incorporated in oxides and silicates, later mobilized from granite or wall rock of the intrusion by HCl-bearing magmatic fluids, and deposited in greisens upon reaction of the fluid with feldspar. Tungsten is partitioned into the magmatic fluid, can be transported farther away from the intrusion than Sn, and is deposited in scheelite-bearing skarns and upon cooling in quartz-wolframite veins.

[1] Heinrich (1990) *Econ. Geol.* 85, 457–481; [2] Schäfer et al. (1999) *Am. Mineral.* 38, 563–598; [3] Hu et al. (2008) *Geochem. J.* 42, 141–150; [4] Schmidt (2018) *Geochim. Cosmochim. Acta* 220, 499–511.

Tue: 89

### Spectral X-ray CT: A potential new analytical method for a 3-dimensional chemical characterization of ores.

Jonathan Sittner<sup>1</sup>, Jose Ricardo da Assuncao Godinho<sup>1</sup>, Axel Renno<sup>1</sup>, Veerle Cnudde<sup>2</sup>

<sup>1</sup>Helmholtz Institute Freiberg for Resource Technology, Germany; <sup>2</sup>University of Ghent, Belgium

Analytical methods play an indispensable role for the characterization of ore deposits. But most of them lack of a 3-dimensional (3D) information which is important for understanding the structural character of ores. However, X-ray computed tomography (CT) provides this 3D information and has been used in geoscience for the last few decades. It offers several advantages such as its non-destructive character and the low requirements for the sample preparation which make this technique unique. Nevertheless, there are some limitations due to the resolution and the lack of chemical information which is particularly important for the determination of mineral phases in a sample.

The spectral X-ray CT combines a traditional CT scanner with a detector that can resolve the energy specific attenuation from a sample. By using the different positions of the absorption edges in the spectrum the elements can be determine. The detector is able resolve energies between ca. 25 and 160 keV. Thus, elements from Ag up to U can be distinguished in the spectrum.

Compared to classical 2D mineral classification methods the spectral X-ray CT provides a lot of advantages. With the 3D information it is easier and faster to characterize the distribution of ore minerals and to image their 3D structure within the sample. Furthermore, the size and the volume of the mineral phases can be calculated and visualized in 3D. The measured sample volume is also significantly bigger and the method works completely non-destructive.

First tests with gold bearing rocks and single mineral grains such as galena or scheelite show promising results. At the moment it is possible to discriminate Elements respectively different mineral phases and to classify them in a rock. However, further changes are necessary to improve the spectral X-ray CT in the future, but it has a lot of potential.

**Tue: 90**

### **Mn-mineralization in the iron ores from West-Crete (Greece)**

**Georgios Alevizos, Antonios Stratakis, Michael Galetakis**

*Technical University of Crete, Greece*

Significant iron ore occurrences have been identified in many regions of Greece. In Crete these are located in the western part of the island, some of which have been exploited in the past.

The iron ores are placed within the Phyllite-Quartzite-Serie (PQS), a high pressure/low temperature metamorphic subunit of the Phyllite-Nappe of Crete. The PQS consists mainly of phyllites and quartzites in addition to metaconglomerates, marble, calcareous phyllites and metabasalts.

In several occurrences of iron ores small amount of Mn-mineralization has been observed, mainly in the form of manganese oxyhydroxides (cryptomelane, lithiophorite and pyrolusite). These occurrences are located in the areas of Kakopetros, Drakona, Arolithi (cryptomelane), Karanou (lithiophorite and cryptomelane) and Ano Valsamonero (pyrolusite).

Samples from the iron ore occurrence from Kakopetros area, where the highest concentrations of manganese have been observed, were collected and examined. The examined iron ore occurrence is located near to Kakopetros village, about 40 km south-west of Chania town.

The mineralogical composition indicated that the iron ore was consisting mainly of goethite, quartz and cryptomelane with minor quantities of muscovite, lepidocrocite and hematite. The ferruginization occurs mainly in the form of goethite and rarely of lepidocrocite by replacing the groundmass. Goethite is mainly porous but can be also observed in the form of hard crust. Hematite occurs occasionally and has been formed secondarily by goethite dehydration. Quartz grains are allotriomorphic, often fragmented due to the tectonism, while muscovite grains are mostly elongated. The main identified manganese mineral was cryptomelane which with goethite often forms rhythmic concentric cells along the cracks and gaps of the Phyllite-Quartzite formations.

Microanalysis results indicated that the manganese minerals belong to manganomelane group with varying water content. Cryptomelane with relatively low potassium content was the major manganese mineral. Electron probe microanalysis of banded goethite showed a low content of Si, Al and P. The estimated content of water in goethite varied between 12-14.5 wt%.

The ore-microscopic examination in combination with microprobe analyses indicated that iron and manganese rich mineralizing solutions caused the massive replacing mineralization (epigenetic processes) in the native rocks of Phyllite and Quartzites.

The precipitation of Fe and Mn at the boundary between the phyllite-quartzite grains takes place during the change of the redox potentials and is based on the solubility and mobility of these two metals.

**Tue: 91****New insights on Ag-Hg mineralization in the Anti-Atlas Precambrian belt: Case study of the Tassafté ore deposit, NE of the Saghro inlier (Eastern Anti-Atlas, Morocco)****Zakarya Yajjouj<sup>1</sup>, Lakhlifi Badra<sup>1</sup>, Alexandre Lima<sup>2</sup>, Joachim Krause<sup>3</sup>, Brahim Karaoui<sup>4</sup>, Abdelkader Mahmoudi<sup>1</sup>**<sup>1</sup>*Faculty of Sciences, Moulay Ismail University, Meknes, Morocco;* <sup>2</sup>*Departamento de Geociências, Ambiente e Ordenamento do Território, Faculdade de Ciências da Universidade do Porto, Portugal;* <sup>3</sup>*Helmholtz-Zentrum Dresden-Rossendorf, Helmholtz-Institute Freiberg for Resource Technology, Chemnitz Straße 40, D-09599 Freiberg, Germany;* <sup>4</sup>*Department of Geology, Faculty of Sciences and Techniques, Moulay Ismail University, Errachidia, Morocco*

The Moroccan Precambrian Anti-Atlas belt is considered as a large metallogenic province for precious and base metals. These mineralizations systems were assumed to be related to the late Ediacaran volcanic activities (Bouabdellah and Slack, 2016; Tuduri et al., 2018). Here, we present new investigations on the Ag-Hg mineralization in the Tassafté mining area, located in the north edge of the Saghro inlier and about 20 km to the east of the famous Imiter Mine (Ag-Hg).

In the Tassafté mining area, the ore veins correspond to the E-W-trending structures, which are hosted within the Ediacaran volcanic succession and continuing within the Cambrian formations. Paragenetic sequences show that the mineralization evolution occurs in three main stages; i) an early stage with Pb-Zn-As-Fe (galena, sphalerite, pyrite, arsenopyrite) associated with microcrystalline quartz, ii) Cu-Ag stage, coeval with pyramidal quartz. The silver minerals generally crystallized on the corrosion zones and in the fractures affecting pre-existent ore minerals (chalcopyrite, pyrite, and chalcocite). The Ag-mineralizations are represented by sulfosalt (friebergite), silver sulphide (acanthite, argentite), rare native silver and abundant Ag-Hg amalgam. Rare silver minerals are remobilized within calcite veins which were taken place later; iii) the post- Ag mineralization stage (ii) is represented by Cu-Pb sulfide.

The mineralization in the Tassafté shows several similarities with the worldwide (Ag-Hg) Imiter mine. These include; similar volcanic host rocks, ore mineralogy, veins orientations, and gangue minerals.

These preliminary data indicate propose that the Ag-Hg mineralization in the Anti-Atlas belt would be shifted up to younger period than what was supposed by previous studies. It is probably related to the late Variscan - Early Mesozoic episode.

[1] Bouabdellah, M., Slack, J.F., 2016. Mineral Deposits of North Africa. Springer. <https://doi.org/10.1007/978-3-319-31733-5>; [2] Tuduri, J., Chauvet, A., Barbanson, L., Bourdier, J.-L., Labriki, M., Ennaciri, A., Badra, L., Dubois, M., Ennaciri-Leloix, C., Sizaret, S., Maacha, L., 2018. The Jbel Saghro Au(-Ag, Cu) and Ag-Hg Metallogenic Province: Product of a Long-Lived Ediacaran Tectono-Magmatic Evolution in the Moroccan Anti-Atlas. *Minerals* 8, 592. <https://doi.org/10.3390/min8120592>

**Tue: 92****Impact of IRUP on mineralogy and mineral chemistry of the UG2 chromitite in the Thaba mine, Bushveld Complex****Haoyang Zhou<sup>1</sup>, Robert Trumbull<sup>1</sup>, Rik Tjallingii<sup>1</sup>, Ilya Veksler<sup>1,2</sup>**<sup>1</sup>*GFZ German Research Centre for Geosciences, Telegrafenberg, 14473 Potsdam, Germany;* <sup>2</sup>*Institute of Geosciences, University of Potsdam, 14476 Potsdam-Golm, Germany*

Discordant Fe-rich ultramafic pegmatites (IRUPs) are intrusive bodies of diverse size and shape that crosscut the UG2 chromitite and other PGE-bearing layers of the Critical Zone in the Bushveld Complex. IRUP bodies have distinctively coarse grain size and Fe-rich ferromagnesian silicates and Fe-Ti oxides. At the mine scale, IRUPs are known to have a negative impact on the Cr- and PGE ore grades of mineralized layers in the Critical Zone, but the nature of this interaction is unclear in detail. This motivated an ongoing study to investigate drill-core samples of IRUP contacts with the UG2 chromitite from the Thaba mine in the northwestern Bushveld Complex. There, IRUP intrudes the UG2 footwall and also within the ca. 1-meter thick chromitite layer. The IRUPs consist of olivine, clinopyroxene, orthopyroxene, amphibole, phlogopite, ilmenite and Ti-magnetite. Electron microprobe analyses show that these minerals in IRUP are considerably richer in iron than the

same phase in the UG2 chromitite. For example, FeO contents in IRUP vs. UG2 for olivine are 29–42 vs. 14–28 wt.%, for orthopyroxene: 19–27 vs. 7–18 wt.%, for amphibole: 10–16 vs. 4–8 wt.%, and for phlogopite: 12–13 vs. 6–9 wt.%.

Multiple thin sections of the contact zones between IRUP and UG2 chromitite were examined by micro-X-ray fluorescence mapping using a Bruker Tornado M4 instrument. This technique provides continuous element distribution patterns across the IRUP and UG2 contact with a spatial resolution of about 50 microns. The first results show that within about 0.5–2 cm from the IRUP contact the chromitite shows abundant interstitial grains of ilmenite. In addition, chromite in the UG2 layer displays gradual decrease in Cr and Al and increase in Fe and Ti content, and is eventually converted into an unusual Fe-Ti-Cr spinel phase near the contact. Electron microprobe analysis of these Fe-Ti-Cr spinels show a wide range of FeO (53.5–83.9 wt.%), TiO<sub>2</sub> (4.8–13.7 wt.%), Al<sub>2</sub>O<sub>3</sub> (3.0–8.7 wt.%) and Cr<sub>2</sub>O<sub>3</sub> (3.0–28.8 wt.%). We thus suggest that the IRUP intrusions resulted in addition of Ti and Fe into the UG2 layer via interstitial mineral replacements and element diffusion.

## 12d) Reuse Potential of Mining Residues

Wednesday, 25/Sep/2019: 1:00pm - 3:00pm

Session Chair: Jeannette Meima (BGR)

Session Chair: Malte Drobe (BGR)

Location: Schloss: S8

### Session Abstract

This session focusses on mining residues as a potential source for metals and/or industrial minerals. A successful re-use of mining residues depends on several factors including the composition and size of the heap, the availability of appropriate processing technologies, as well as several infrastructural aspects. As the composition of mining heaps is usually very heterogeneous, it is extremely important to obtain a detailed knowledge of the spatial variations in relevant geochemical, mineralogical and textural properties inside a mining heap. Innovative exploration concepts and innovative processing technologies are required to deal with these challenges. We invite contributions that focus on the reuse potential of mining residues, including case studies, the benefits of mining waste cadasters, innovative exploration concepts, as well as innovative processing technologies.

### Lecture Presentations

1:00pm - 1:30pm *Session Keynote*

#### Sourcing of critical elements and minerals from mine waste

**Bernhard Dold**

*Luleå University of Technology, Sweden*

In metal mining, in most cases only a minor percentage of the extracted materials are the target elements (e.g. Fe or Al ores 20-70 %, Zn 2-15%, Pb 1-10%, Cu 0.2-6%, REE 0.1-0.5%, Au 1-20 g/t). Thus, the vast majority of the extracted material is defined as waste, which is deposited in disposal facilities like tailings impoundments, lakes or the sea and in waste dumps, or is backfilled into open pits or underground mines. These mine wastes are the source of environmental pollution (through acid and alkaline drainages; oxidic and reductive dissolution) and catastrophic dam failures like recently in January 2019 in Brumadhino, Brazil. These are the key problems leading directly to the loss of the social license to operate of the mining industry. To minimize the risk from mine waste in the future, its volume has to be reduced. This applies for both, fresh mine waste and historical waste. Latter can still contain important metal contents (specifically the overlooked critical

metals like REE, PGE, and battery metals like Co, Ni, Li, Mn), and have therefore a high potential for successful exploration. From a mineralogical point of view, the material extracted in mining can be differentiated in different mineral groups here ordered with decreasing solubility and increasing volume: 1. Sulphates and chlorides < 2. Fe, Al, Mn hydroxides < 3. oxides < 4. sulphides < 5. silicates. Thus, from an environmental point of view, the first 4 mineral groups are the most critical, but contain also most of the economically valuable elements. The major volumes of silicates are non-hazardous and, if separated accurately, can be used as industrial minerals or for construction material. Important efforts are currently under way to find solution to use tailings as filler and binders like geopolymers, replacing the CO<sub>2</sub> emission intensive Portland cement. But also high-tech applications can be found for these materials as for example quartz for solar cell production and glass industry or micas and pyrite for semi-conductors. Automated Quantitative Mineralogy allows nowadays quantifying accurately the different minerals and combined with micro analytical geochemical techniques the element association to each mineral can be quantified. With this information, a sequential separation can lead to different mineral concentrates, which are the resources for different industrial application, allowing to reduce importantly the final effective waste volume.

**1:30pm - 1:45pm**

### **Re-mining of mine wastes in Germany: Challenges and opportunities**

**Philipp Büttner<sup>1</sup>, Jochen Nühlen<sup>2</sup>, Jeannette Meima<sup>3</sup>, Jens Gutzmer<sup>1</sup>**

<sup>1</sup>Helmholtz Institute Freiberg for Resource Technology, Germany; <sup>2</sup>Fraunhofer Institute for Environmental, Safety, and Energy Technology UMSICHT, Germany; <sup>3</sup>Federal Institute for Geosciences and Natural Resources, Germany

The Fraunhofer Institute for Environmental, Safety, and Energy Technology and the Helmholtz Institute Freiberg for Resource Technology (HIF) have together compiled a mine waste cadaster for Germany on behalf of the Federal Institute for Geosciences and Natural Resources (BGR). For this purpose, a wide variety of data sources was evaluated with the aim to create a national database able to provide an overview about the content of critical raw materials (CRM) in mine waste repositories in Germany. Yet, even though mine wastes containing economically significant amounts of CRM, re-mining these anthropogenic “ore bodies” faces considerable technical and non-technical challenges.

Mine wastes often create environmental problems, such as acid rock drainage with associated high sulfate and heavy metal concentrations. This creates societal pressure for remediation. Remediation, however, is usually achieved by covering the surface with a water impermeable layer, an approach that is not sustainable, because of the required follow-up care and the inaccessibility of the resources that remain contained in the mine wastes. Besides that, legislative barriers are in conflict with recovering CRM and other metals and minerals from historic mine wastes. Many sites have essentially been abandoned since mining ceased in the 20<sup>th</sup> century. High metal contents and acidity released during sulfide oxidation has facilitated the establishment of a very specific flora and fauna. Species on these sites are often rare and strictly protected by environmental legislation. Metal recovery is all but impossible from such sites, despite the fact that acid rock drainage from these sites leads to environmental degradation downstream from the mine waste site.

Another important aspect is the general lack of suitable beneficiation and metallurgical infrastructure in Germany. Large capital investment would thus be necessary to enable the recovery of strategic metals from historic mine waste. Even if high metal concentrations are present in some mine wastes, small volumes will render the set-up of large, stationary plants unfeasible. Instead, flexible and semi-mobile small-scale technologies need to be developed. Such technologies are, at present, not available on the market.

To work at the intersection of society, legislation, remediation and re-mining is the aim of the new rECOMine partnership. This partnership is funded by the Federal Ministry of Education and Research (BMBF) for the next five years within the WIR! Program. It will be coordinated by HIF and build up three test sites in Saxony to develop combined remediation and re-mining technologies under real conditions with local partners.

**1:45pm - 2:00pm****Innovative exploration of mine tailings based on core scanner applications****Jeannette Meima, Dieter Rammlmair, Kerstin Kuhn, Khulan Berkh***Bundesanstalt für Geowissenschaften und Rohstoffe BGR, Germany*

The estimation of the reuse potential of mining residues is not straightforward due to the oft extremely heterogeneous character of mining dumps. Mining residues are often deposited over longer periods. During this deposition period, the origin and composition of the primary ore and/or the applied processing methods may have changed. These variations would result in large-scale spatial variations showing material with clearly different mineralogy and geochemistry in different parts of the mining dump. Furthermore, additional small-medium scale heterogeneity arises due to separation processes during deposition due to differences in grain size and density, as well as due to various supergene processes after deposition. Surface samples, therefore, naturally do not reflect the average composition of mining dumps. Similar to the exploration of primary ores, systematic drilling is required to achieve a 2D/3D compositional overview of a mining heap. Individual drilling cores may reflect the heterogeneity of the mining residues. To be able to differentiate between layers of different reuse-potential, we see a clear advantage in using core scanner applications rather than taking bulk, e.g. meter wise, samples.

This contribution reviews core scanner applications for the characterisation of relevant geochemical and textural properties of drilling cores containing mining residues. Core scanner technologies include imaging technologies, X-ray fluorescence analysis, and Laser Induced Breakdown Spectroscopy (LIBS). Special focus will be on the LIBS-based core scanner, which has been thoroughly tested for a number of different mine tailings.

The LIBS technology is based on atomic emission spectroscopy. The excitation source is a highly energetic pulsed laser, which is focused on the sample surface in order to ablate tiny amounts of material to form a plasma on the sample surface. Analysis of LIBS-spectra, however, is not straightforward due to plasma variations. In particular, chemical variations on the target surface usually lead to severe matrix effects, which could be dealt with using multivariate calibration methods.

**2:00pm - 2:15pm****Next Generation of Tailing Exploration Technologies: XRF-CPT Probe as Real-Time High Resolution Tool for Low Invasive Tailing Characterization****Eugen Martac, Uta Alisch***Fugro Germany Land GmbH, Germany*

Neglected for decades, the tailing bodies may play nowadays a significant role as source of raw materials. To support resource estimation as decision supporting step within potential reprocessing scenarios, Fugro developed a new probe. Its goal is to identify metal-rich horizons in soils and sediments and spatially delineate their architecture as guidance for a reliable and economically efficient tailing reprocessing. With the new XRF-CPT probe, target elements can be measured in real-time and spatially high-resolution and displayed as absolute content in soils and sediments. Moreover, elemental screenings may help to identify potential new targets as unknown elements of interest. The Fugro probe uses the X-ray fluorescence as analysis technology. The element-specific fluorescence radiation is measured by a highly sensitive and finely resolving detector and displayed as energy spectra. Through prior calibration against standards, all detections are tuned into elemental concentrations. Being continuously pushed into the underground by CPT trucks or rigs, the combined XRF-CPT probe allows a simultaneous measurement of geotechnical parameters such as tip pressure and lateral friction and enables a reliable identification of soil lithology and material density.

The presentation points out the added value gained through several exploration experiences on Chilean tailings ranging from field deployments to 3D modeling of elemental spatial distributions with decision key points toward reliable and economically efficient tailing reprocessing. The works were performed within the frame of a research project financed by the German Association for International Cooperation GIZ of the German Ministry of Education and Research (BMBF).

2:15pm - 2:30pm

### Novel approaches to Scandium-species investigation in Bauxite residues by X-ray adsorption near edge structure spectroscopy - Looking for the needle in a haystack

**Marie Christin Hoffmann<sup>1,2,3</sup>, Christian Adam<sup>1</sup>, Christiane Stephan-Scherb<sup>1,2</sup>, Christian Vogel<sup>1</sup>, Lutz Hecht<sup>2,3</sup>**

<sup>1</sup>Bundesanstalt für Materialforschung und -prüfung, Germany; <sup>2</sup>FU Berlin, Institut für Geologische Wissenschaften, Germany; <sup>3</sup>Museum für Naturkunde Berlin, Berlin, Germany

In a rapidly evolving world, the demand on raw materials is increasing steadily and many technologies are dependent on a secure supply of hi-tech metals. Recently, scandium (Sc) has attracted attention since its use in high strength Al-alloys and solid-oxide-fuel-cells strongly improves the performance of those materials.

The element Sc is not exceptionally rare but quite resistant to geochemical enrichment processes, it is scarcely found enriched to high concentrations and is recovered as a by-product. Since Sc enrichment in Greek bauxite residues was shown by Ochsenkühn-Petropoulou et. al (1994), intensive research on this material and development of efficient Sc-recovery methods is ongoing.

This study investigates Sc-bearing species in bauxite residues from alumina production. It aims to provide direct evidence about the Sc-speciation's in those secondary resources and tries to find the link to speciation's in primary resources, e.g. bauxites and laterites.

Therefore, Sc K edge XANES (X-ray absorption near edge structure) spectroscopy is performed using synchrotron radiation to determine the presence of certain Sc-components and distinguish between adsorbed and chemically bonded Sc as was shown for lateritic deposits in Australia by Chassé et al. 2016. For comparison, reference standards of Sc-bearing and Sc-adsorbed species are synthesized. Indirect inferences from leaching behavior of bauxites, in cases supported by analyses with LA-ICP-MS, suggest Sc to be associated with either iron- or aluminum phases (Vind et al. 2017); (Suss et al.). However, it remains unclear how different primary materials influence Sc-speciation in the bauxite residue. Therefore, a comparison between different European bauxite residues is made in this study. The investigations should help to understand Sc chemistry and behavior in different primary and secondary materials and provide fundamentals for metallurgical processing. The research is incorporated in the SCALE project (GA No. 730105) funded by EU Horizon 2020 research and innovation program.

[1] Chassé, M., W. L. Griffin, S. Y. O'Reilly, and G. Calas, 2016: Scandium speciation in a world-class lateritic deposit. *Geochemical Perspectives Letters*, **3**, 105-114; [2] Ochsenkühn-Petropulu, M., T. Lyberopulu, and G. Parissakis, 1994: Direct determination of lanthanides, yttrium and scandium in bauxites and red mud from alumina production. *Analytica Chimica Acta*, **296**, 305-313; [3] Suss, A., N. Kuznetsova, A. Kozyrev, and A. P. a. Sergey: Specific Features of Scandium Behavior during Sodium Bicarbonate Digestion of Red Mud; [4] Vind, J., P. Paiste, A. H. Tkaczyk, V. Vassiliadou, and D. Panias, 2017: The behaviour of scandium in the Bayer process. *Proceedings of 2nd ERES Conference*, 190-192.

2:30pm - 2:45pm

### Bioleaching of Cu/Co-rich mine tailings from the polymetallic Rammelsberg mine, Germany

**Ruiyong Zhang<sup>1</sup>, Sabrina Hedrich<sup>1</sup>, Felix Römer<sup>2</sup>, Axel Schippers<sup>1</sup>**

<sup>1</sup>Federal Institute for Geosciences and Natural Resources (BGR), Germany; <sup>2</sup>Institute of Mineral and Waste Processing, Waste Disposal and Geomechanics, Technical University Clausthal, Germany

Mine tailings that contain considerable amounts of valuable metals are of high interest for reprocessing. Bioleaching is a suitable technique for recovery of various metals from tailings. In this study, different microbial consortia of meso-acidophilic bacteria were applied in shake flasks as well as in 2 L stirred tank reactors (STR) to bioleach cobalt, copper, and other valuable metals from the Rammelsberg mine tailings (polymetallic massive sulfide deposit, Harz mountains, Germany). After succession from low to high solid load, microbial consortia were well adapted to 10% pulp density and showed high leaching efficiency in contrast to the chemical leaching experiments. The community composition seemed to be dependent on solid load irrespective of the initial pH (1.6, 1.8, and 2.0). The adapted mesophilic bacterial consortium at 10 % pulp density contained

mainly *Acidithiobacillus (At.) ferrooxidans* and *At. thiooxidans* which achieved 91 % cobalt (17 mg/L) and 57 % copper (68 mg/L) recovery after 13 days in STR. Comparable data were obtained in shake flask tests. Bioleaching tests with a flotation mine tailings concentrate using the above mentioned bacterial consortium showed that 66 % cobalt (36 mg/L) and 33 % copper (189 mg/L) recovery were achieved at 10 % pulp density in STR. A monolayer biofilm was microscopically observed on surfaces of solid particles of the mine tailings and tailings concentrate. The amounts of ferrous iron and sulfides (mainly pyrite) in the tailings were sufficient to sustain microbial growth and thus no additional substrates were required for tailings bioprocessing.

**2:45pm - 3:00pm**

### **Microbe-mineral interactions during chalcopyrite bioleaching**

**Heike Bostelmann, Gordon Southam**

*The University of Queensland, Australia*

The ubiquitous nature of chalcopyrite in base metal mining residues coupled with its comparative recalcitrance to (bio-)leaching requires a better understanding of the mechanisms governing its interaction with bioleaching microorganisms.

Based on the reactivity of chalcopyrite with both acid and ferric iron, the use of pyrite as a co-substrate was hypothesized to increase copper extraction by providing increased concentrations of both oxidative reagents. Systems possessing pyrite did produce higher soluble iron (and sulphur) concentrations according to their pyrite concentrations, but this did not noticeably improve copper release. The pH, however, did not decrease as expected, but buffered to around pH 1.8 with every feeding, indicating protons were being consumed, although not through acid dissolution of chalcopyrite. Total proton consumption was correlated with the formation of a microbial biofilm on all pyritic surfaces through proton requirements for ATP synthesis. It was further shown that copper concentration of low-grade substrates does not affect leaching rates, rather, copper release is proportional to chalcopyrite surface area.

In order to ascertain the necessity of microbial attachment to enhance the dissolution of chalcopyrite, bacteria were grown separately on sulphur and soluble iron, in order to produce cells of the same species but with different surface characteristics. More hydrophobic, sulphur-grown, cells attached to chalcopyrite readily and subsequently formed microcolonies, whereas iron-grown cells resulted in limited attachment. However, after an initial lag phase, the iron grown cells resulted in improved copper concentrations versus the attached sulphur grown cells. A cross-colonisation study further showed that attachment behaviour was inherent to the cell itself, rather than any surfactants produced and released into the culture fluid, and that the 'original' growth substrate influenced the reactivity of soluble species; high ferric iron concentrations only improved copper recovery in the presence of iron-grown cells, while sulphur-grown cells in spent iron medium did not enhance copper release.

These observations together show that chalcopyrite is not a suitable growth substrate, but rather is catalytically leached by the 'by-products' of other oxidation reactions. It therefore follows that other growth substrates are necessary to grow biomass, with solid substrates out-performing soluble energy sources in terms of bacterial cell counts. Chalcopyrite bioleaching may then occur (be enhanced) during the 'stationary phase' of the culture, where no acidity is consumed for the production of additional biomass, allowing the protons produced during the biooxidation of pyrite or any additional iron added to the system to leach chalcopyrite.

**Poster Presentation****Tue: 93****Interdisciplinary study of mining residues and implications for secondary mining****Wilhelm Nikonow, Dieter Rammlmair, Markus Furche, Jeannet Meima***Federal Institute for Geosciences and Natural Resources (BGR), Germany*

Mining residues are an inevitable consequence of intense mining. After decades or even centuries of mining, these residues may form large bodies with millions of tons of processed material which must be dealt with. Therefore, the idea of secondary mining has evolved and has been pursued with variable degrees of success. In this work, a large tailings impoundment of several millions of tons of material from the flotation of copper sulfides has been examined. The disposal of tailings can be compared to fluvial sediment transport and deposition and therefore is affected by factors like particle size and shape and the basin topography. Due to transport, a physical segregation of particles takes place, which affects the deposition of ore minerals. After deposition, chemical processes like oxidation and re-precipitation take place and produce a re-organization within the tailings impoundment. Therefore, tailings impoundments are complex bodies with internal heterogeneous structures from deposition and weathering. For a reliable exploration and representative sampling, these processes have to be taken into account. In this work, surface sampling with few drillings and geochemical and particle size analyses were carried out. Electrical Resistivity Tomography (ERT) was applied to analyze the impoundment in all three dimensions. The data show systematic variation of particle size and element concentrations. Small particle sizes and high water saturation correspond with areas of low electrical resistivity in the ERT data, which are located in the north and west of the impoundment. Higher electrical resistivity was measured in the south, where the dam was built with coarser material and in the east from where the processed material was deposited. Furthermore, there is a vertical variation, as the upper zone is oxidized and depleted in copper sulfides, while the base is still the originally deposited material.

For possible secondary mining of such kinds of impoundments, a selective recovery is proposed. Since flotation of copper ore is optimal in the region near or below 100  $\mu\text{m}$  particle size, coarser particles need to be milled again, which means high-energy investment. Finer particles, however, are a challenge for the floatation operation and might not be recovered.

Therefore, the proposed approach of considering depositional processes, geochemical reorganization and the process of recovery may be of great assistance for successful tailings exploration including the localization of areas of high-grade material and optimal particle size for selective tailings recovery.

## 13) Open Session

### 13a) 3D Geological Modelling and subsurface potentials

Monday, 23/Sep/2019: 9:00am - 10:30am

**Session Chair: Jennifer Ziesch** (State Authority for Mining, Energy and Geology)

**Session Chair: Stephan Steuer** (Federal Institute for Geosciences and Natural Resources)

**Session Chair: Rouwen Lehné** (HLNUG)

**Location: Vom Stein Haus: Aula / VSH 219**

#### Session Abstract

In the past years, the application of 3D modeling has developed rapidly, and plays an increasing larger role in the geosciences. 3D models are created over a vast range of scales from sub-seismic structures to basin-wide structural 3D models, with a lateral extent of more than 100.000 km<sup>2</sup>. One of the biggest challenges is the construction of consistent complex 3D models (including salt structures and/or fault zones) based on the evaluation and processing of input data from structural/geological maps, wells, and geophysical data, for example, 2D/3D reflection seismic data. Also it is becoming increasingly important to connect (geologic) 3D models of the subsurface with data from other sources and of other scale. To discuss progress, problems and solutions, and to understand the complex interplay of geological 3D models, we offer this session as a platform for professional exchange in the community. Therefore, we are looking for contributions from geological Surveys, academia and the private sector, and all who deal with this topic.

#### Lecture Presentations

9:00am - 9:15am

#### **An overview of current geological modelling activities in the German North Sea by the BGR**

**Frithjof Bense, Heidrun Stück, Stephan Steuer, Fabian Jähne-Klingberg**

*Bundesanstalt für Geowissenschaften und Rohstoffe (BGR), Germany*

The joint project TUNB is a cooperation between the state geological survey organisations of the north German states and the Federal Institute for Geosciences and Natural Resources (BGR). Its aim is to build a harmonized structural 3D model for the entire North German Basin. Apart from the joined 3D modelling tasks, BGR performs several research and modelling tasks in the German North Sea area;

*Seismic interpretation and its visualisation in consideration of uncertainties:*

We used a method to visualise uncertainties in the interpretation of e.g. salt structures along seismic lines based on defining an “uncertainty envelope” around the structure, marking a region of loss in seismic resolution. Through the intersection of these envelopes with the modelled horizon and the salt structure, areas of lower constrain can be detected and visualised.

*Superimposition of structural elements and formation of potential fluid pathways:*

Faults, fault systems and sedimentary structures of different genetic origin (e.g. crestal faults or polygonal fault systems) may form fluid migration network by superimposition, allowing fluids from deeper parts of the sedimentary succession to migrate upwards, even through formations that are considered as barrier formations. We conduct modelling and regional analysis of such features, to identify regions where the barrier integrity might be affected by bypass systems.

*Seismic velocity modelling:*

Based on new interpretation data, a refined velocity model was created in consideration of previous works on seismic velocity. Velocity models are needed to calculate depth and thickness of geological layers interpreted from seismic reflection images. Depth conversion is also a way to remove the structural ambiguity inherent in time interpretation.

*2D/3D backstripping and structural restoration:*

Mesozoic rift structures (e.g. the southern Central Graben and the Horn Graben) played a major role in the structural development of the German North Sea region. Structural and kinematic modelling of those structures provide valuable information for the general understanding of the region (see Müller et al., this volume).

*Harmonisation of geological data across national borders and petroleum system modelling:*

The German North Sea is part of a cross-border pilot area of the project 3DGeo-EU ([www.geoera.eu](http://www.geoera.eu)), where differences in the geological interpretation (e.g. stratigraphy, velocity-model, structural interpretation) between the Netherlands, Germany and Denmark are analysed and harmonized and used for joined petroleum system modelling.

**9:15am - 9:30am**

**3D geological modelling in Saxony-Anhalt - documentation, methods, results and applications towards modern subsurface information systems**

**Alexander Malz, Lars Schimpf**

*Landesamt für Geologie und Bergwesen Sachsen-Anhalt, Germany*

In the past decades, the application of advanced geological tools like 3D modelling gained increasing interest for the spatial planning of the subsurface. First applied to small-scale areas their range successively grew in accordance with high-performance processing equipment and the development of new efficient algorithms. More recently, detailed structural models of larger scales or even country- to basin-wide models were developed by research institutes and state geological surveys. Such modelling campaigns carried out by geological surveys are most often accompanied with huge preparation, management and documentation efforts for the used heterogeneous data sets. Thus, building a countrywide 3D geological model is even a powerful tool for the extension, evaluation and revision of existing data. Its development must be systematically documented and used methods must be evaluated and discussed to ensure the model's conformability.

In this contribution the 3D geological modelling efforts of the Geological Survey of Saxony-Anhalt will be described. We present parts of our large-scale subsurface model built in the framework of the TUNB project (Subsurface Potentials for Storage and Economic Use in the North German Basin). In that context we strongly focus on the digitalisation, evaluation, revision and documentation of data, which is used for structural modelling and model parameterization. These data sets were systematically digitized, attributed by use of hierarchical encryptions and archived in logical documentation systems. By the use of unified modelling techniques it becomes possible to reproduce all information incorporated in our 3D model.

Consequently, generated modelling results in connection with our documentation systems can be used to derive harmonized structural information (e.g. harmonized depth and thickness maps or fault traces) for wide areas of Saxony-Anhalt, which can be provided to a broad public. In our contribution, we would like to present the example of fault information to show how such information can be derived and stored in a hierarchical 'structural information system'. Information will be stored in various levels of detail: (1) a new structural map of Saxony-Anhalt in an approximate scale of 1:200'000 and (2) detailed map sheets (scale of 1:50'000) for single faults strands and selected horizons. Every fault strand contains 3D information for footwall and hanging wall cut-offs and was systematically attributed. As a consequence it became possible to derive geometries, timing and kinematic information for every scale. This shows the enormous potential of 3D modelling in modern geological surveying towards sustainable and comprehensible information.

9:30am - 9:45am

### Producing an improved geological 3D model of Lower Saxony (TUNB) from the 3D tectonic atlas (GTA3D)

**Marcus Helms, Cornelia Wangenheim, Manuela C. Stehle, Sabine Sattler, Jennifer Ziesch**

*1 State Authority for Mining, Energy and Geology (Lower Saxony) LBEG, Germany*

The application of geological 3D models has become more common. They play an increasing role in estimating the potential usability of the subsurface for various applications. For this purpose, we first constructed a 3D model (GTA3D) based on the structural maps of the tectonic atlas of Lower Saxony (Bombien et al. 2012). Since 2014, we have been improving this geological 3D model of the North German Basin (NGB) in Lower Saxony.

Within the joint project TUNB (Deep Subsurface North German Basin), a unified 3D model is being built. This project involves the Geological Survey Organisations (GSOs) of several North German states that cover the NGB. The models from the above-mentioned states were developed individually but thoroughly harmonised along state borders. Here we present the approach that is being taken to improve the Lower Saxony model.

The pre-existing geological 3D model GTA3D serves as the initial basis for the modelling process. As a consequence, this model includes geological inconsistencies and represents primarily geological data processed prior to the early 1990's. The model is now being enhanced using reprocessed 3D depth-migrated seismic data, new borehole data and isopach maps. To begin with, borehole and seismic data require processing. The latter are integrated in the EPOS infrastructure and interpreted in SeisEarth (Emerson E&P Software). Subsequently, the resulting clean datasets are used as input data for the fault and horizon modelling using the Structure and Stratigraphy Workflow of the SKUA-GOCAD software suite (Emerson E&P Software). In border regions towards a neighbouring state, we harmonise the 3D model in cooperation with the GSO involved. Difficulties can arise when stratigraphic horizons were interpreted differently or at places where the quantity of underlying data base differs, which result in contrasting structural interpretations.

The incorporation of new geological data into the previous 3D model has a large impact on geological structures. In particular, prominent faults as well as the geometry of salt structures are now better constrained. Furthermore, the geological inconsistencies of the pre-existing 3D model have been removed in the new 3D model. The improvement of the geological 3D model of Lower Saxony allows new insights into the interplay between salt tectonics, sedimentation and tectonic movement. We demonstrate, for example, that in some places, the volume and the structure of the salt have changed with respect to the original 3D model.

9:45am - 10:00am

### Towards a velocity model of the deep subsurface of Schleswig-Holstein for geological 3D modeling – A part of the joint project TUNB

**Laura Dzieran<sup>1</sup>, Fabian Hese<sup>1</sup>, Katrin Lademann<sup>2</sup>, Thomas Liebsch-Doerschner<sup>1</sup>**

*<sup>1</sup>Landesamt für Landwirtschaft, Umwelt und ländliche Räume Schleswig-Holstein (LLUR SH), Germany; <sup>2</sup>Thüringer Landesamt für Umwelt, Bergbau und Naturschutz (TLUBN), Germany*

The joint project TUNB develops a national coherent geological 3D-model of the deep subsurface of the North German Basin (project partners: BGR and Geological Surveys of Northern Germany). This large 3D-model is constructed on the databases of the Tectonic Atlas of Northwest Germany and the German North Sea Sector (GTA, Baldschuhn et al., 2001), and the Geophysical Map Series of the former German Democratic Republic (GPK, Reinhardt et al., 1991). The project aims to achieve cross-border consistency and integrates the federal state models into a larger and coherent overall 3D model of the subsurface.

The Geological Survey SH focusses on a geological 3D model of the deep subsurface of the onshore part of Schleswig-Holstein; the model includes base surfaces of deposits as old as the Permian Zechstein up to Quaternary strata, faults, and enveloping surfaces of salt diapirs. The dataset of the GTA and the overall understanding of the subsurface of Northern Germany is primarily based on well data and seismic surveys from

oil and gas exploration. An important link between seismic data and the GTA is the velocity model used for time to depth conversion developed by Jaritz et al. (1991). We have successfully reconstructed this velocity model based on original documents. This data can be now used to re-convert geological models based on the GTA from depth to time. A comparison of seismic reflectors and GTA depth maps shows a good fit; however, inconsistencies can be found locally in rather complex areas. In the next step, our velocity model will be further tested to validate its integrity and verify former GTA interpretations. Sonic logs, checkshot data, and seismic processing velocities are investigated and compared to the original velocities to increase the accuracy of future velocity modeling.

**10:00am - 10:15am**

### **3D-Deutschland: a three-dimensional lithospheric-scale density and thermal model of Germany**

**Denis Anikiev<sup>1</sup>, Maria Laura Gomez Dacal<sup>1</sup>, Adrian Lechel<sup>1,2</sup>, Judith Bott<sup>1</sup>, Magdalena Scheck-Wenderoth<sup>1,3</sup>**

<sup>1</sup>Helmholtz Centre Potsdam - German Research Centre for Geosciences GFZ, Department Geosystems, Section Basin Modelling, Potsdam, Germany; <sup>2</sup>Technical University of Berlin, Department Geotechnology, Berlin, Germany; <sup>3</sup>RWTH Aachen University, Faculty of Georesources and Material Engineering, Aachen, Germany

The aim of this study is to integrate previous results on sub-domains – regional three-dimensional models of the Central European Basin System, the Upper Rhine Graben and the Molasse Basin together with the Alpine area – into a lithospheric-scale (up to 133 km in depth) structural model called 3D-Deutschland (3DD) which covers the entire surface of Germany (1000 km in North-South direction and 643 km in East-West direction). The involved regional models were assembled by integration of various published data: geological and geophysical datasets, geological maps, borehole data, seismic profiles, isopach maps and existing smaller-scale models. On top of that, each regional model was independently constrained by gravity and thermal modelling. The lithostratigraphic division of the joint 3DD model resolves sedimentary, crustal and mantle units across the whole territory. Discrepancies between the units were consistently refined using seismic profiles across the boundaries of regional models.

The 3DD model was constrained by 3D gravity modelling (gravity response computed in IGMAS+ was compared to the reference EIGEN-6C4 gravity field). Despite the good fit between modeled and observed gravity in terms of large-scale structures, some ambiguities in low-wavelength part of the gravity field spectrum still remain. These inconsistencies can be overcome by involving higher lithostratigraphic resolution and incorporating more detailed data that became available since publishing of the regional models.

Conductive thermal field modelling (performed using the finite-element simulator GOLEM) showed that heterogeneous distribution of thermal properties associated with the different lithological units causes significant variations of temperature at the same depth level. This distribution is mainly affected by the blanketing effect of sediments with low conductivity, variability in radiogenic heat production in the upper crust (Variscan and Alpine domains) and the depth to the thermal lithosphere-asthenosphere boundary.

The derived 3DD model can serve as a data-consistent background for smaller-scale models, it can be used to improve boundary conditions for local structural, geothermal and stress field studies. The model can be used as a basis for rheological modelling helping to relate observed seismicity with the strength distribution.

**10:15am - 10:30am**

### **A multimodal and multitemporal assessment of mud volcanism in Azerbaijan by drone and remote sensing**

**Lena Merz<sup>1</sup>, Ayten Huseynova<sup>2</sup>, Christoph Hilgers<sup>1</sup>**

<sup>1</sup>Karlsruhe Institute of Technology, Germany; <sup>2</sup>Azerbaijan National Academy of Sciences, Azerbaijan

Understanding the impact of mud volcanism and associated hydrocarbon flow towards the surface is critical for safety of drinking water, agriculture and during hydrocarbons exploration. These natural phenomena are

abundant in Azerbaijan as well as in other countries. Newest developments in drone-based analytical and mapping technologies, as well as freely available high-resolution satellite data, open new possibilities to enhance conventional geological field work. The aim of our project is to map and evaluate migration pathways of fluids from the regional scale down to one mud volcano, and to evaluate the environmental impact of natural seepages of hydrocarbons.

The WNW-trending Greater Caucasus fold- and thrust-belt is characterized by S-SSW verging folds and associated thrusts (e.g. Devlin et al., 1999; Saintot et al., 2006). Horizontal tectonic stress is assumed to be oriented c. 30° with c. 10 mm/year movement velocity (Bonini and Mazzini, 2010). Muds and associated fluids migrate from overpressured shales in up to 5 km depth along faults and fracture networks to the surface and generate constant small seeps and degassing of methane (Guliyev, 2006).

We conducted lineament mapping based on ASTER-data and studied their dilation and slip tendency with 3DStress-software. This fault data is complimented by field measurements of faults and fractures, as well as Structure from motion on outcrops. Additionally, high resolution mapping of mud volcanoes and associated fluid flow by means of drone-based photogrammetry and drone-based methane detection were carried out. Fault orientations along the Greater Caucasus show a majority of faults striking WNW, paralleling the mountain range. Stress analysis of faults show medium to high dilation tendencies for northerly striking faults subparalleling the main horizontal stress and are available for fluid flow. By analysis of mud volcano and fault location we observe that over 50% of mud volcanoes are located over or close to fault intersections.

In our four study areas, fractures strike mainly N-S and W-E in the southeastern part, and NNE-SSW and WNW-ESE in the northwestern part. Drone-based methane detection works at max. flight altitudes of 15 m and a max. speed of 2 m/s. Macro- and mini-seepages away from the main gryphons reveal concentrations of up to 10 ppm per meter air column around mud volcanoes. Digital elevation models and orthophotos of one studied mud volcano before and after one eruption reveal structural details and eruption volume.

## Poster Presentations

Mon: 67

### Step by step: The 3D subsurface model of Mecklenburg-Vorpommern is growing

Karsten Obst, Juliane Brandes, Sabine Matting, Jasmaria Wojatschke, Andre Deutschmann

*Geological Survey of Mecklenburg-Western Pomerania, LUNG M-V, Germany*

Different subsurface uses, e.g. hydrocarbon exploitation, natural gas storage, geothermal energy production, drinking water supply etc. may hamper each other at suitable locations. Therefore, a 3D underground model is needed to visualize the various resources and to support politicians and decision makers in spatial planning of the underground. The Geological Surveys of the north German federal states (SGD) are developing a 3D geological model of the North German Basin (NGB) in the project "Subsurface Potentials for Storage and Economic Use in the North German Basin" (TUNB), which was initiated by the Federal Institute for Geosciences and Natural Resources (BGR) and started in 2014.

The Geological Survey of Mecklenburg-Western Pomerania will model the northeastern part of the project area. The model comprises 13 major lithostratigraphic layers between bases of Zechstein and Rupelian. Besides, numerous tectonic faults and salt diapirs will also be modelled. The model is based on more than 750 deep wells and about 2,500 seismic lines. As the model area is with c. 25,000 km<sup>2</sup> rather large, the modelling is done stepwise.

First, collaborative 3D modelling was applied in the border regions to neighbouring federal states. Typical reflector horizons that mark lithological surfaces close to stratigraphic boundaries were correlated with borehole profiles and modelled using the SNS workflow of SKUA-GOCAD. Salt diapirs and faults were mainly modelled by hand.

The model area of Mecklenburg-Western Pomerania is divided into 11 parts. The first part Ludwigslust was finished in 2017. The parts Waren, Pasewalk and Schwerin were finalized in 2018. In the first half of 2019,

the parts Rostock and Neubrandenburg were completed. This means that more than the half of the project area was modelled. The model includes more than 90 faults at the Zechstein base, 11 diapirs and about 35 supra-salt faults, of which the major fault of Fresendorf-Goritz is the most prominent one with a length of approximately 50 km.

The next steps comprise modelling of the complex Western Pomeranian Fault System (WPFS) in the NE using reprocessed seismic lines and adjustment of the model horizons in the border region to Poland within GEO-ERA using also gravmag data.

**Mon: 68**

### **Tectonic 3D-model of the Berga antiform – Saxo-Thuringian Zone**

**Franz Müller, Uwe Kroner**

*Technische Universität Bergakademie Freiberg, Germany*

The “Bergaer Sattel” of the Saxo-Thuringian Zone of the Central European Variscides constitutes a NE-SW striking antiformal structure. The striking feature of the Berga antiform is the juxtaposition of greenschist facies metamorphic rocks with very low grade lithologies of Paleozoic age. Classically, the entire region is described as a simple southeast-vergent anticline without significant horizontal displacement. However, recent mapping revealed the existence of allochthonous units. To clarify aspects of the architecture, we generated a regional 3D model of the Berga antiform using the SKUA-GOCAD software package. The model results from the incorporation of existing datasets like geological maps and profiles in combination with the extensive acquisition of drilling data as well as the results of a tectonic mapping campaign. The width of the model is 50 km in NE-SW, 15 km in NW-SE direction and the depth is 1 km. Tectonically, we subdivide the Berga antiform in a par-autochthonous and an allochthonous unit, mainly exposed in the SW and the NE part of the antiform respectively. By construction of three stratigraphic horizons the par-autochthonous unit can be modelled as a southeast vergent fold structure. In contrast, the allochthonous unit is characterized by pervasive ductile deformation during low grade metamorphism. Subsequently, the metamorphic layering is affected by NW-SE shortening like the tectonics characteristic for the par-autochthonous unit. We explain the complex architecture of the Berga antiform as follows. Initial NE-SW shortening during the main stage of the Variscan collision led to crustal stacking of the Paleozoic sequence. Separated by NE-SW striking tear faults, the future par-autochthonous domain remained in uppermost crustal levels. Due to dextral tranpression, subsequent exhumation of the allochthonous unit led to overthrusting onto the NE part of the par-autochthonous unit. Late variscan compression culminates in SE vergent thrusting and folding of the entire structure. NW-SE oriented graben structures and N-S oriented strike slip zones resulted from tectonics in post-Variscan time.

**Mon: 69**

### **More data - more Model. Experiences within the project TUNB.**

**Maik Schilling, Christoph Jahnke, Andreas Simon, Thomas Höding**

*Geological Survey of Brandenburg, Germany*

The goal of the project TUNB (Subsurface Potentials for Storage and Economic Use in the North German Basin) is the production of a transnational structural geological 3D model of the North German Basin. Financed by the Federal Institute for Geosciences and Natural Resources, the state geological survey organizations of the federal states of Mecklenburg Western Pomerania, Saxony-Anhalt, Lower Saxony, Schleswig Holstein and Brandenburg are involved. Usually a number of different data are available for the generation of 3D models. In addition to the indispensable borehole data, these are primarily seismic test results in the form of maps and profiles as well as gravimetric investigations and geological maps. All these data were usually collected over a long period of time. Regarding the seismic investigations this period covers more than 50 years in Brandenburg. Within this period, the technique changed which made the measurement results more accurate, but the basics used to interpret the data also changed. Therefore, the stratigraphic assignment of seismic reflectors over time varies, resulting

in discrepancies in the interpreted data between the various study campaigns. Furthermore, older data has been re-processed in recent times, which results in different interpretations compared to the original. All these data cannot be used for modeling without further editing. Based on new insights into the stratigraphic assignment of reflectors, drill holes and reliable seismic results, the entire dataset must be harmonized. Only then the heterogeneous data can be used for modelling purposes. Another aspect of data collection and harmonization is the necessary border matching of models. Within a country or between neighbouring federal states, this is usually possible with manageable effort. This is especially true for the states of the former GDR, since the data base is generally the same here. However, if one wants to compare a model with a model in the neighbouring state or carry out a cross-border modelling, the differences in the interpretation of the seismic data become even clearer. In a first data comparison along the German-Polish border, there are often differences in the assignment of the seismic reflectors. In a first step the seismic data in time domain are compared as well as the different speed models to match the seismic reflectors on both sides of the border.

## Mon: 70

### Experience with the construction of a volumetric model in the German North Sea Sector

**Björn Zehner**

*BGR - Federal Institute for Geosciences and Natural Resources, Germany*

Many projects that deal with the construction of 3D structural models of the subsurface do not model the geological bodies (rock units) directly, but instead describe them indirectly by modeling and rendering the interfaces between these bodies (faults and horizons). Converting these surface-based models into volumetric models is necessary, if they are to be used for process simulation with finite elements or finite differences. Further, this type of model can be used to define and visualize arbitrary cross-sections through the model interactively and to extract important features and subregions in order to provide more intuitive visualizations. In the past, we have described several workflows, involving the use of Skua-Gocad together with the external software packages Gmsh and TetGen, to construct a volumetric tetrahedral representation of the 3D geological subsurface starting from surface based structural models and further to provide a rastered version of the same model. In all these cases, the scenarios presented were structurally fairly simple and where based on an artificial model generated for demonstration purposes. Hence the performance of the suggested workflows needed to be tested using a much more complicated real-world model. The 3D geological model used for this study is a small 10x20 km large sub-region of the "Entenschnabel" in the German North Sea Sector which involves 16 horizons, 43 faults and two salt diapirs. In our contribution we will provide a short discussion on the workflows and share our experience with applying them to the real-world model.

## Mon: 71

### On the visualization of 3D geological models and their uncertainty

**Björn Zehner**

*BGR - Federal Institute for Geosciences and Natural Resources, Germany*

3D visualization is important in order to communicate to customers and stakeholders or to the public the 3D geological models generated. Depending on the anticipated audience, the visualization should be presented in such a way that is easy to understand and intuitive. While this might be worth a discussion in its own right, the issue becomes even more complicated when not only the model itself needs to be shown, but also the certainty with which the subsurface is known. As part of a work package within the GeoERA – 3DGEO-EU project, different options to visualize this uncertainty are evaluated, and example data sets and workflows explaining the use of the suggested methods for 3D geological models will be provided in the near future.

We will briefly discuss the problems we see with the visualization that is currently state of the art for certain geological models and is used by software packages, such as Gocad or Petrel or different Web-Viewers. We will then show how this visualization might be improved and be easier to understand by using volume visual-

ization, a technique that is common in medical visualization and for the visualization of 3D seismic data, but less commonly used for 3D geological models. Further we will discuss how bi-directional transfer functions (color tables) could be used for augmenting the shown 3D geological model with the information on how certain the position and orientation of a shown structural feature is.

Several examples that show how uncertain data could be rendered have been generated and pre-processed using Gocad and have been visualized using the publicly available software Paraview for scientific visualization. Further the open source software Blender for 3D content creation has been used to test the option of providing a more photorealistic rendering, including such effects as shadows and ambient occlusion. The methods and workflows described rely on open source software and are thus available to the 3D modelling community for free. However, in order to really investigate models and data interactively using Paraview and the suggested methods, some extensions would be needed for the visualization software itself.

## 13c) Tectonic Systems (TSK open session)

Tuesday, 24/Sep/2019: 8:30am - 10:00am

**Session Chair: Nikolaus Froitzheim** (Universität Bonn)

**Session Chair: Michael Stipp** (Martin-Luther-Universität Halle-Wittenberg)

**Location: H4**

### Session Abstract

We invite contributions from the fields of tectonics, structural geology, and crystalline geology. Regional and process-oriented studies from all kinds of active or fossil tectonic settings are welcome – rifting, subduction, collision, transform, as well as intra-plate deformation. Studies dealing with the development of methods related to the deformation of crust and lithosphere from the micro-scale to plate scale are also invited.

### Lecture Presentations

**8:30am - 9:00am** *Session Keynote*

#### **Rheology of evaporites at slow deformation rates: integrated understanding of Salt tectonics, Salt caverns and Nuclear waste repositories**

**Janos Urai, Peter A. Kukla**

*RWTH Aachen, Germany*

Reliable modeling of the deformation of rock salt under the very low strain rates characterizing long term engineering conditions and salt tectonic flow requires extrapolation of experimentally - derived flow laws to rates much lower than those attainable in the laboratory. This extrapolation must be based on an understanding of the microscale deformation mechanisms operating under these conditions.

Compared to other rock types, rock salt contains only small amounts of water, but this small amount dramatically enhances fluid-assisted grain boundary processes such as grain-boundary dilatancy, grain-boundary migration and pressure solution. During grain-boundary migration, fluid inclusions interact with the moving grain boundary and this process has a strong effect on rheological properties. This microphysical understanding is missing from current engineering models of the long-term understanding of Salt caverns and Nuclear waste repositories, making predictions of these structures unnecessary uncertain.

We review existing salt engineering, materials science and geoscience literature relevant to this topic, and show that the current controversy on flow laws and fluid flow in evaporites can be solved by focussing on macro- and micro-scale models for deformation, permeation and hydrofracturing, including the role of grain boundary structure, stability of the permeation, problems of extrapolating laboratory data to long-term conditions.

9:00am - 9:15am

### **Microfabrics and composition of brittle faults and veins in Lower Cretaceous claystones (Lower Saxony Basin, Germany): Constraints on the barrier behaviour of clay-rich rock formations**

**Tilo Kneuker<sup>1</sup>, Martin Blumenberg<sup>1</sup>, Harald Strauss<sup>2</sup>, Gernold Zulauf<sup>3</sup>**

<sup>1</sup>Bundesanstalt für Geowissenschaften und Rohstoffe, Stilleweg 2, D-30655, Hannover; <sup>2</sup>Institut für Geologie und Paläontologie, Westfälische-Wilhelms-Universität Münster, Corrensstr. 24, D-48149 Münster; <sup>3</sup>Institut für Geowissenschaften, Goethe-Universität Frankfurt, Altenhöferallee 1, D-60438 Frankfurt/M.

Faults are critical for the evaluation of sealing properties of rock formations, considered as oil and gas storage or for the disposal of heat generating radioactive waste. Even in tight claystone, fluid flow might be supported by brittle fault zones. Our study is focusing on the microfabrics and element mobility of faulted claystone using SEM and optical microscopy combined with various geochemical methods. Apart from lithological variations of Lower Cretaceous clay-rich rock formations, the structure and composition of naturally deformed claystone was investigated in boreholes from the Lower Saxony Basin. Geochemical and phase analyses were carried out using XRD, XRF and LECO analyses. In addition, biomarker signatures and stable isotopes were studied from both fault rock as well as intact claystone.

Synkinematic calcite enrichment and polyphase mineralization of veins as indicators for palaeofluid activity are abundant in certain intervals of the investigated boreholes, where brittle faults with slickensides are present. A scaly fabric with varying strain is common around larger faults. Fine-grained fault gouge in a high-strain domain is depleted in calcite. The low permeability of claystone can lead to periodically high fluid pressures and fracturing along preexisting discontinuities and/or sedimentary heterogeneities, as is documented by mode I veins and crack-seal fabrics in the investigated sections. Enrichment of Mn, Ba and/or Sr in the fault rock is related to calcite enriched zones and tectonic veins. Differences in trace element concentrations of various veins suggest several precipitation phases. Isotope signatures show a local carbonate source for the thin calcite coatings along fault planes, but a more complex palaeofluid interaction in the larger faults and in complex veins, consistent with the microfabrics. Biomarker signatures suggest the occurrence of mature hydrocarbons in sections where steep, only weakly mineralized faults occur, pointing to the presence of migrated hydrocarbons.

From our preliminary results it is concluded that deformation of claystone is largely localized in brittle fault zones including individual fault planes, a scaly fabric and/or incohesive fault gouge. Their position is often controlled by structural or sedimentary heterogeneities. These brittle structures represent inherited damage in the rock mass, they are prone to reactivation, e.g. during rising pore fluid pressure, subsequent tectonic activity or during gallery excavation.

9:15am - 9:30am

### **Two regional tectonic structures - The intersection of Elbe Zone and Eger Rift**

**Ottomar Krentz<sup>1</sup>, Bedrich Mlcoch<sup>2</sup>, Klaus Peter Stanek<sup>3</sup>**

<sup>1</sup>Sächs. Landesamt Umwelt, Landwirtschaft, Geologie, Germany; <sup>2</sup>Czech geological Survey, Prague; <sup>3</sup>TU Bergakademie Freiberg, Germany

The area of North Bohemia and Southern Saxony is characterized by the intersection of two major tectonic structures of different age and behaviour. Variscan, late Cretaceous and Tertiary events created a network of strike-slip, thrusts and normal faults. Related sedimentary basins and volcanic structures preserve the stratigraphic record. The area was investigated by seismic, geoelectric and gravimetric measurements to reconstruct the hidden geological structures below the sediments of the Saxon Bohemian Cretaceous Basin and to summarize the results in a 3D model.

9:30am - 9:45am

**The near surface structure of rift systems****Christoph von Hagke<sup>1,2</sup>, Michael Kettermann<sup>2,3</sup>, Christopher Weismüller<sup>4</sup>, Janos L. Urai<sup>2</sup>, Klaus Reicherter<sup>4</sup>***<sup>1</sup>Institute of Geology & Palaeontology, RWTH Aachen University, Germany; <sup>2</sup>Structural Geology, Tectonics and Geomechanics, RWTH Aachen University; <sup>3</sup>Department of Geodynamics and Sedimentology, Structural Processes Group, University of Vienna; <sup>4</sup>Neotectonics and Natural Hazards, RWTH Aachen University*

Close to the Earth's surface, normal faults can develop massive dilatancy in cohesive rocks, forming major fluid pathways in rift systems. These massively dilatant faults (MDF) are ubiquitous features and well-exposed in Iceland or the East African Rift. Despite their importance for e.g. geohazard assessment or geothermal energy, their detailed geometry at surface and depth is not well understood. We contribute to this understanding by combining data from analog models and field data from unmanned aerial vehicles. Whereas analog models provide insights of the deep structures of MDF, high-resolution digital elevation models on km-scale bridge the gap between aerial/satellite imagery and ground-based fieldwork.

Our study areas on Iceland offer excellent outcrops of MDF, dominantly formed in successive lava flows and different kinematic settings along the exposed Mid Ocean Ridge. We show that fault kinematics and mechanical stratigraphy are important parameters that control fault geometry. We propose that the depth of hybrid failure is much deeper than anticipated in standard models. This has consequences for our understanding of geothermal systems or how we envision the ascent of magma in rift systems. Open fractures form major fluid pathways, and knowing their distribution at depth is vital for fluid flux modeling studies.

**13c) Tectonic Systems (TSK open session)****Tuesday, 24/Sep/2019: 10:45am - 12:30pm****Session Chair: Kamil Ustaszewski** (Friedrich-Schiller Universität Jena)**Session Chair: Armin Dielforder** (GFZ Potsdam)**Location: H4****Lecture Presentations**

10:45am - 11:00am

**Challenges to unravel an abandoned Oligocene rift segment along the River Nile in Egypt****Ali Abdelkhalek, Jonas Kley***Universität Göttingen, Germany*

Interpretation of 2D and 3D seismic combined with high-resolution gravity and magnetic anomaly models reveals structures and crustal thickness variations suggesting that several rift basins occur beneath and around the modern Nile valley. By means of integration with detailed fieldwork, processing of multispectral satellite imagery, digital elevation and digital terrain models (DEMs &DTMs), and SAR radar records, we interpret three main late Paleogene-early Neogene rift segments of NW-NNW orientation. They are exposed on the eastern and western flanks of the modern Nile. The central and northern segments are geometrically well defined and semi-parallel to the Gulf of Suez, while the southern segment has a complex pattern, due to WNW to E-W pre-existing structures. An extensive network of normal faults, related folds, fractures and volcanism accommodated the deformation. Highly oblique, E-W to ENE and WNW-trending, dextral shear zones, basement highs, and basins, which nucleated during Cretaceous rifting and succeeding inversion in southern and central Egypt, were rejuvenated differentially during the Oligocene break-up of the Afro-Arabian plates. These pre-Oligocene inherited structures and sedimentary thickness variations determined the location of accommodation/transfer zones, which controlled the

geometry, segmentation and evolution of the rift, and eventually terminated its northward propagation. The onset of the main rifting phase in the Nile was contemporaneous with the Oligocene Red Sea-Gulf of Suez formation. Rifting is recorded along several grabens within the Eocene plateaus of the Nile by gravity and magnetic anomalies, Oligocene fluvial clastics and red beds, NW-NNW-trending fractures, extensional faults and Oligo-Miocene basalt dikes. Analysis of DTMs in conjunction with processing algorithms of satellite images reveal a network of inverted gravel-filled channels that incised the Eocene shoulders of the Nile. These exhumed channels delineate the fluvial depositional system and flow directions of the channels that fed the rift grabens. The Neogene Nile River in central Egypt evolved along a NW-trending short-lived rift that formed by NE-SW extension during the Oligocene, and was abandoned at an early stage. We suggest four possible reasons for the abandonment: (1) Progressive concentration of extension onto the Red Sea-Gulf of Suez rift, (2) Strain dissipation over wide rift shoulders, (3) rifting confined to thicker (more brittle?) crust along the central part of the Nile, (4) rift abortion in thick sediments of the Tethyan shelf in the north. Additional structural control is suggested by the rift termination coinciding with a belt of ENE-trending “Syrian arc” structures, the WNW-trending Beni-Suef basin and major basalt flows.

**11:00am - 11:15am**

### **High-angle normal faulting at the Tangra Yumco graben (southern Tibet) since ~15 Ma**

**Reinhard Wolff<sup>1</sup>, Ralf Hetzel<sup>1</sup>, István Dunkl<sup>2</sup>, Qiang Xu<sup>3</sup>, Michael Bröcker<sup>4</sup>, Aneta A. Anczkiewicz<sup>5</sup>**

<sup>1</sup>*Institut für Geologie und Paläontologie, Westfälische Wilhelms-Universität Münster, Corrensstraße 24, 48149 Münster, Germany;* <sup>2</sup>*Institut für Sedimentologie und Umweltgeologie, Universität Göttingen, Goldschmidtstr. 3, 37077 Göttingen, Germany;* <sup>3</sup>*Institute of Tibetan Plateau Research, Chinese Academy of Sciences, Lincui Road, Chaoyang District, Beijing 100101, China;* <sup>4</sup>*Institut für Mineralogie, Westfälische Wilhelms-Universität Münster, Corrensstraße 24, 48149 Münster, Germany;* <sup>5</sup>*Institute of Geological Sciences, Polish Academy of Sciences, Senacka 1, 31-002 Kraków, Poland*

Several active graben systems in Tibet and the Himalaya are the expression of ongoing E-W extension, but the significance and history of normal faulting in this large region are still debated (e.g. Ratschbacher et al., 2011). Here, we present geo- and thermochronological data for a granite intrusion in the footwall of an active high-angle normal fault at the Tangra Yumco graben to constrain the onset and history of normal faulting. Crystallization of the granitic rocks occurred  $87 \pm 1$  Ma ago, as revealed by U/Pb zircon dating. Following an initial phase of rapid cooling from magmatic temperatures, a later phase of slow cooling is recorded by Rb/Sr biotite ages between ~72 and ~60 Ma (Wolff et al., 2019). The elevation dependence of the Rb/Sr ages suggests that cooling was controlled by erosion, which proceeded at a rate of ~0.05 km/Ma during the latest Cretaceous and early Paleocene. The subsequent history of normal faulting is recorded by zircon (U-Th)/He ages of  $12.5 \pm 1.1$  and  $9.7 \pm 0.7$  Ma, apatite fission track ages between  $10.8 \pm 1.7$  and  $7.8 \pm 1.2$  Ma, and apatite (U-Th)/He ages from  $4.9 \pm 0.4$  to  $3.0 \pm 0.2$  Ma (Wolff et al., 2019). Thermokinematic modeling of these age data indicates that normal faulting started  $14.5 \pm 1.8$  Ma ago at a rate of ~0.3 km/Ma and accelerated to ~0.7 km/Ma in the Pliocene. Our age constraint for the initiation of faulting supports a widespread onset of rifting in Tibet at ~15–10 Ma, as reported for other graben systems (e.g. Ratschbacher et al., 2011; Sundell et al., 2013; Styron et al., 2015). Finally, we suggest that the distribution of high-angle and low-angle normal faults is controlled by their position relative to the India-Asia convergence vector and by lateral variations in the thermal state of the lithosphere.

[1] Ratschbacher, L.; Krumrei, I.; Blumenwitz, M.; Staiger, M.; Gloaguen, R.; Miller, B. V.; Samson, S. D.; Edwards, M. A.; and Appel, E. (2011) *Geol. Soc. Lond. Spec. Pub.* 353:127–163; [2] Styron, R.; Taylor, M.; and Sundell, K. (2015) *Nature Geosci.* 8:131–134; [3] Sundell, K. E.; Taylor, M. H.; Styron, R. H.; Stockli, D. F.; Kapp, P.; Hager, C.; Liu, D.; and Ding, L. (2013) *Tectonics* 32:1454–1479; [4] Wolff, R.; Hetzel, R.; Dunkl, I.; Bröcker, M.; Xu, Q.; Anczkiewicz, A.A. (2019) *The Journal of Geology* 127:15–36.

**11:15am - 11:30am****The Adriatic slab gap: Regional-scale surface uplift in the Dinarides fold-thrust belt validated by geomorphologic indices****Philipp Balling<sup>1</sup>, Christoph Grützner<sup>1</sup>, Wim Spakman<sup>2</sup>, Kamil Ustaszewski<sup>1</sup>**<sup>1</sup>Friedrich-Schiller-Universität Jena, Germany; <sup>2</sup>Utrecht University, Netherlands

The Dinarides fold-thrust belt on the Balkan peninsula are the result of convergence between the Adriatic and Eurasian plates since Late Cretaceous collision. Double-sided subduction of Adria beneath both Dinarides and Apennines since the Oligocene subjects the associated slabs into a complex four-dimensional setting. We used p-wave tomography (Hall and Spakman, 2015, model UU-P07) to constrain geometries of lithosphere-asthenosphere boundaries underneath the Dinarides in 3D. For almost 600 km along-strike from NW to SE, the leading edge of the subducting slab is nowhere deeper than c. 150 km, forming a very suspicious 'slab gap' underneath much of the Dinarides (Subašić et al., 2017) - in contrast to the northerly adjacent Alps as well as the southeasterly adjacent Hellenides that are unequivocally underlain by slabs. So far, there are no reports of any changes in the geomorphology along-strike the Dinarides that might have formed in response to these contrasting lithospheric geometries.

In the field, we discovered sets of degradational, quasi-horizontal wavecut platforms, which eroded in Mid Eocene to Oligocene faulted and folded rocks. With the help of slope and roughness maps we identified 493 such surfaces, extending c. 600 km along-strike the entire Dinaric coast. Interestingly, the occurrence of these surfaces largely coincides within the extent of the slab gap. Additionally, the Dinaric drainage divide, separating the catchments of the Black Sea and the Mediterranean Sea, coincides with the position of the remaining "missing" Adriatic slab. To verify the minimum amount of surface uplift, we compared the maximum incisions of four river pairs on both sides of the drainage divide from northwest to southeast by river swath profiles.

Our results document very similar amounts of incision to either sides of the drainage divide for all river pairs. The incision gradually increases from 150 m in the northwestern to 300 – 350 m in the southeastern Dinarides. The amount of incision roughly agrees with the elevation of the mapped wave-cut platforms at four prominent elevation peaks at 100 m, 220 m, 470 m and 600 m. Field observations and geological maps document that aggradation of younger post Miocene rocks is absent within the horizontal extent of the Dinaric slab gap. In summary, our results and observations prove that the youngest stage of the Dinaric deformation is dominated by vertical uplift and degradation, which spatially coincides with the position of the Adriatic slab gap.

**11:30am - 11:45am****Forearc growth through background seismicity in Peru-Chile****Andrea Madella, Todd A. Ehlers***University of Tuebingen, Germany*

The geodetically measured uplift signal in coasts adjacent to subduction zones is dominated by the megathrust earthquake cycle, which is the recurrence of stress accumulation through elastic flexure of the overriding plate (interseismic period) and stress release through elastic rebound (coseismic and postseismic periods). Although several cm of interseismic vertical displacement can occur, the net uplift of such flexure-related cycles can be null or even negative, a behavior that questions their significance over longer timescales ( $10^4$ - $10^6$  years) and requires another mechanism to explain continuous rock exhumation and emergence of coasts. In light of this ambiguity, we hypothesize that permanent uplift may be accomplished through non-megathrust background seismicity, here defined as not temporally clustered events of smaller magnitude ( $M_w < 6$ ). This hypothesis is tested by comparing proxies for long-term forearc growth with the background seismicity along the Peru-Chile forearc, a region characterized by strong spatial variability of long-term coastal uplift. We find that along-strike variations of the seismic moment calculated from background seismicity exhibit a significant correlation ( $R=0.7$ ) with both the topographic slope angle, the inferred interplate friction and published es-

imates of million-year-scale coastal uplift. Moreover, the correlation improves when the upper plate events are excluded. We interpret that background seismicity has a significant role in shaping the long-wavelength topography of the forearc and is likely related to processes that cause crustal thickening in the Peru-Chile wedge.

**11:45am - 12:00pm**

### **Hydrothermal monazite dating in the Lepontine Dome between exhumation and shear zone activity**

**Christian A. Bergemann<sup>1</sup>, Edwin Gnos<sup>1</sup>, Alfons Berger<sup>2</sup>, Emilie Janots<sup>3</sup>, Martin J. Whitehouse<sup>4</sup>**

<sup>1</sup>Museum of Natural History Geneva, Switzerland; <sup>2</sup>University of Bern, Switzerland; <sup>3</sup>ISTerre University of Grenoble, France; <sup>4</sup>Swedish Museum of Natural History, Stockholm, Sweden

Central orogenic regions such as the Lepontine Dome of the European Alps experience a complex tectono-metamorphic history. High precision ion probe dating of hydrothermal monazite is an excellent tool to understand the late evolution of such areas. Monazite crystals from open clefts yield <sup>232</sup>Th-<sup>208</sup>Pb crystallization and alteration ages, providing insights into such tectonically active areas at low-grade metamorphic conditions. The mm-sized crystals are a late mineral phase in open, fluid-filled clefts that formed at the brittle-ductile transition and directly date tectonic activity. The spatial distribution of age spots along with chemical zoning in the analyzed monazites suggest a stepwise growth linked with multiple dissolution-reprecipitation processes that occurred when the chemical equilibrium between wall-rock, hydrothermal fluid and crystal was disturbed during cleft deformation.

The 20 analyzed samples, yielding ~480 individual ages, come from an area in the Central Alps comprising the northern half and the western areas of the Lepontine Dome. The study region also includes part of the southern Gotthard Nappe and is bounded to the west by the Rhone-Simplon Fault system. The Lepontine Dome experienced nappe stacking followed by and partly overlapping with greenschist to amphibolite facies metamorphism. Subsequent exhumation, particularly in the central areas and further folding and thrusting, was followed by brittle deformation in combination with hydrothermal fluid flow affecting the entire region that produced the famous mineralized Alpine clefts.

The age data, ranging from 19 to 5.5 Ma over the entire region and 2.5-7.5 Myr within individual grains, records an interplay between exhumation and shear zone activity. The north-eastern and south-western edges of the Lepontine Dome record the oldest monazite ages of 19-12.5 and 16.5-10.5 Ma, respectively. This was followed by crystallization in the central areas around 14.5-9 Ma, largely dating exhumation. Over time the hydrothermal monazite age record moves towards the western region, where ages between 13 and 5.5 Ma are recorded. The later ages after ca. 7.5 Ma are limited to clefts from the westernmost study region and date strike-slip deformation along the Rhone-Simplon fault system.

Hydrothermal monazite crystallization and alteration occur in a temperature window of ca. 350/300 – 200 °C. A comparison with ages derived from cooling based methods such as Ar-Ar in white mica and zircon fission track dating, whose closure temperatures depend on cooling speed, thus allows the identification of areas experiencing low cooling rates at the time of hydrothermal monazite activity.

**12:00pm - 12:15pm**

### **The problem of misconceptions for understanding Phanerozoic collisional orogens**

**Hans-Joachim Massonne**

*China University of Geosciences Wuhan, People's Republic of China*

For Phanerozoic continent-continent collisional orogens such as the Variscan and Alpine ones, countless geodynamic scenarios have been presented over the last decades. If we would better understand the mechanisms of the collision of plates, we could clearly discriminate among these models and abandon almost all of them. At the moment, several misconceptions dominate and hamper the progress in understanding the

geodynamics resulting in collisional orogens. An example is the concept of deep subduction of continental crust which is strongly supported by numerical modelling. Additional support of this concept seems to be provided by reports of diamonds in metamorphic crustal rocks such as micaschists and gneisses. However, such evidence suffers from the negligence to prove that the diamonds were not artificially introduced into thin-sections of these so-called diamondiferous rocks. The penetration of a moderately subducted crustal plate (without the further downgoing mantle lithosphere), called lower continental plate, into the uppermost mantle below the upper continental plate by hydrolytic weakening at the front of the lower continental plate (Massonne, 2016, J. Geodyn. 96) is an alternative to the deep subduction of continental crust at continent-continent collision. This alternative well explains crustal thickening, intracrustal formation of large volumes of granitic melts, and the abundance of medium-grade metamorphic rocks, that had experienced peak pressures between 1.0 and 1.8 GPa, in Phanerozoic orogenic belts.

Another example of a possible misconception is the hypothesis of slab rollback to explain the collision of a major plate (Plate1) with ribbon continents consecutively rifted away from continental Plate2 located at the opposite side of Ocean1 situated between these plates. This hypothesis includes the subduction of this ocean beneath Plate2, the formation of a magmatic arc, and, through slab rollback, a back-arc basin. This basin further develops to Ocean2, the spread of which leads to the travel of the formed ribbon continent to Plate1. However, an alternative scenario exists: still during the subduction of Ocean1, Plate2 is pushed over the upwelling mantle that had generated the spreading centre of Ocean1. This centre is buried beneath the lithosphere of Plate2 and becomes inactive (spreading break - basaltic melts cannot form in the upwelling mantle at depths below 60 km) until it meets with a weak zone in the lithosphere to create the back-arc basin. Thus, it would be more important to locate the zones of upwelling mantle instead of arbitrarily creating oceanic basins in geodynamic models.

## Poster Presentations

Mon: 72

### Seismic reflection study of a regional lines in the Western Desert of Iraq

**Ezzadin Najmadin m. Amin / Baban, Basim R. Al- Hijab, Hamid N. Al-Sadi**

*University of Sulaimani, Iraq*

Nine reflectors (H1-H9) on regional line sections are picked and identified as Jurassic, Triassic, Permian, Carbo/Devonian, Silurian, Ordovician, "Bottom of Ordovician or top of Cambrian", Middle Cambrian and "Basement" rocks respectively. All these reflectors show a dipping configuration and deepening towards east. *Two sequences of reflectors* can be recognized on the regional line sections.

Two major Paleo-highs (*Risha and Anbar uplifts*) were confirmed in the studied area. They are separated by a broad depression (south Rutba depression) filled with post Cambrian deposits. This uplift may be formed during the Hercynian orogeny in Late Devonian-Early Carboniferous. It seems that the Risha uplift is a part of Hail – Rutba arch. The top of the uplift on the regional line Reg121, appear at 290km from the western end of the line, while, lies at a distance 250km from the southwest end of the regional line Reg122. Anbar uplift formed during the Caledonian orogeny at Late Silurian-Early Devonian. The effect of *another uplift* can be seen affecting all geological columns from basement to Cretaceous. This uplift may be formed at Cretaceous time due to the effect of the upwelling hot material coming up from deep source within the mantle. In addition, several local (small) anticlines and synclines are recognized. Also, a number of vertical, sub-vertical faults were delineated. Most of them lie over the top of the two Paleo-highs and over the east of the area. The most prominent one is Abu Jir fault zone, which forms a graben extended from northwest to southeast.

**Mon: 73****Retrograde tectonic activity in the Mont Blanc and Aiguilles Rouges Massifs dated through hydrothermal monazite****Christian A. Bergemann<sup>1</sup>, Edwin Gnos<sup>1</sup>, Martin J. Whitehouse<sup>2</sup>**<sup>1</sup>*Museum of Natural History Geneva, Switzerland;* <sup>2</sup>*Swedish Museum of Natural History, Stockholm, Sweden*

Ion probe dating of mm sized hydrothermal monazite is a promising method for understanding the low-T deformational history of an area. The monazites crystallize in open alpine type fissures (clefths) where they occur as a late crystallization at temperatures of ca. 300/350 °C. The crystals record the age of crystallization without risk of diffusional lead-loss at the prevalent temperatures. Through alteration due to partial dissolution-precipitation/recrystallization, the monazites further have the potential to record several phases of tectonic activity down to ca. 200 °C or somewhat below.

The analysis of hydrothermal monazite from open clefths in the Mont Blanc and Aiguilles Rouges Massifs in the Western Alps reveal three major phases of tectonic activity. These occurred at 11.5–10.5 Ma, 9 Ma and 8–7 Ma, interpreted as (re)crystallization during the onset and continuation of dextral strike-slip faulting. Sub-horizontal clefths formed pre 11.5 Ma in a compressive regime and monazite from the horizontal clefths may thus record all three deformational phases. A comparison of monazite ages with thermochronometers indicates that the clefths along with the network of vertical shear zones in the Mont Blanc Massif became strongly overprinted at 11.5 Ma during a switch from transtensional to pure strike-slip deformation. During these strike-slip movements a younger generation of sub-vertical clefths formed along both sides of the Mont Blanc and in the Aiguilles Rouges Massif. This and associated fluid flow may have been diachronous, as primary monazite crystallization in vertical clefths from the Aiguilles Rouges Massif likely dates their formation to around 9 Ma.

**Mon: 74****Elements of the Osning Fault Zone (NW-Germany) – Key Structures of a Strike-Slip Zone****Manfred Dölling, Günter Drozdowski***Geologischer Dienst Nordrhein-Westfalen, Germany*

The WNW - ESE (hercynian) trending Osning fault zone forms a more than 200 km long strike-slip zone, which separates the Lower Saxony Basin in the north from the Münsterland basin in the south. The structure and kinematics of the Osning fault zone are analyzed on the basis of strike-slip tectonics (Drozdowski & Dölling 2018). This superordinate structuring of the dextral strike-slip zone is carried out by five synthetic, mostly left-kicking oriented sub-segments from the Gronau segment of the Netherlands in the northwest to the Falkenhagen segment of the Hessian Depression in the southeast. Between the individual segments W - E trending en echelon folds developed as connecting structures, such as the Rothenfelde, the Ochtrup and the Waldhügel anticlines, as a result of predominantly narrow crossovers. They can be used as evidence for an N - S oriented palaeostress field during the Late Cretaceous. At the Osning fault zone, the following structural elements are characteristic for the existence of strike-slip tectonics:

- echelon arranged, left-stepping fault elements as synthetic Riedel shears with convergent connection structures. The vertical components of the various strike-slip faults of the Osning fault zone vary between several hundreds and two thousand meters, whereas the horizontal components are much bigger with amounts ranging between 1.5 and 10 km.
- Cross faults as antithetic Riedel shears that were deformed during interaction with the dominant synthetic Riedel shears of the Osning fault zone (e. g. antithetic Bielefeld cross fault).
- Overlap structures (e. g. Ibbenbüren block as push-up, the Grotenburg block as pull-apart), formed between en echelon arranged faults by transpressional and transtensional movements. Occasionally, the overlap structures are associated with block rotations.
- Flower structures with partially low-dipping polar and bipolar faults in the upper floor and steep strike-slip

faults in the lower tectonic level of the northwestern Osning fault zone.

Above all, the close temporal and spatial juxtaposition of compression and extension during Late Cretaceous inversion indicates shearing instead of temporal separate processes, as suggested for instance by Baldschuhn & Kockel (1999). In addition, several other elements of the Osning block and the interpretation of the Münsterland Basin as an asymmetrical strike-slip basin support the strike-slip character of the tectonic structures.

[1] Baldschuhn, R. & Kockel, F. (1999): Das Osning-Lineament am Südrand des niedersachsen-Beckens.- Z. dt. geol. Ges., **150** (4): 673 – 695; [2] Drozdowski, G. & Dölling, M. (2018): Elemente der Osning-Störungzone (NW-Deutschland) – Leitstrukturen einer Blattverschiebungszone.- scriptum-online, **7**: 39 S.

**Mon: 75**

## **The boundary between Eastern and Western Alps as seen from a foreland perspective – an example from the Miocene Molasse Basin**

**Martin Elsner**

*Erdwerk GmbH, Germany*

The boundary between Eastern and Western Alps is commonly assigned to the valley of the Rhine south of Lake Constance. It is documented by the predominance of Helvetic units in the West (Switzerland) and Austroalpine units in the East (Austria and Germany). In the Western Alps and the westernmost part of the Eastern Alps (Vorarlberg, Allgäu), tectonic transport was orogen-normal towards the Foreland basin during the Miocene. In contrast, the Eastern Alps are cross-cut by orogen-parallel to oblique strike-slip faults, leading to an escape of the nappes to the east.

Boundaries in the adjacent North Alpine Foreland Basin (Molasse Basin) are less distinct. Some authors prefer a subdivision in Western, Central and Eastern Molasse Basin, while others classify a Western and Eastern part only. In any case, these are largely geographic definitions, though they do match geological reasonable positions at certain times. However, for the Obere Meeresmolasse (OMM, Ottnangian) and the Obere Süßwassermolasse (OSM, Karpatian to Pannonian), the following features point to a division into a Western and Eastern part, with a transition approximately along the river Lech:

grain size distribution within the OMM shows a minimum here and heavy mineral assemblages indicate different sources to the East and West

the position of the forebulge as indicated by the Albsteinschwelle is present only in the West

the Kirchberger Schichten as transitional member between OMM and OSM are most prominent to the East  
the base of Nördliche Vollschoeterserie/Geröllsandserie, a gravel bearing sequence within the OSM, is distinctly more inclined westward

the thickness of the Nördliche Vollschoeterserie/Geröllsandserie and the presence and duration of hiatuses indicate overall lower subsidence rates eastwards

drainage pattern from the Miocene alpine streams indicate large fan structures westward (Hörnli-, Napf-, Hochgrat-Adelegg-Fan) and much smaller ones to the East

In relation to the boundary between Western and Eastern Alps, this position is shifted for around 80 km to the east, illustrating the relevance of tectonic processes in the orogenic wedge for foreland sedimentation: flexural loading of the orogen and asymmetric, wedge-like subsidence of the foreland in the West (including the westernmost part of the Eastern alps) contrasting lateral extrusion of the piled nappes and almost uniform subsidence of the foreland in the East. Fluvial streams of the OSM showed to be very sensitive to subsidence variations and the distribution of their sediments can be used for basin analysis.

**Mon: 76****Structural geological study of a shear zone at the Stora Le Marstrand formation, island Arndorsholmen (SW Sweden)****Anna Friebe**, Thomas Degen*Economic Geology and Petrology Research Unit, Institut of Geosciences and Geography, Germany*

The geology in SW Sweden is strongly influenced by the Sveconorwegian orogeny (1.1-0.9 Ga). During this deformational event the Idefjorden Terrain was aggregated on the Baltic Shield and large crustal units have been sheared on Baltica and stacked on each other. These crustal units are mainly built up of meta-sediments (ca. 1.67 Ga) which have been intruded by several magmatic suits (1.5-0.9 Ga) of felsic as well as mafic to ultramafic compositions.

During field work northwest of Kungälv (SW Sweden) a north-south trending shear zone on the island Arndorsholmen has been mapped. The lithological units are dominated by migmatized supracrustals of the Stora Le Marstrand formation.

The shear zone has a vertical dip and divides the island in to two different parts. In the western part are high migmatized metasediments and in the eastern part consists of a complex mixture of different lithologies. Additionally, a mafic dyke crops out longside the shear zone. The dyke is 1.5 m thick and while the western rim is deformed and shows a foliation, the eastern rim is nearly undeformed. Furthermore, there are idiomorphic garnets visible in the dyke. The garnets can grow up to 3.5 cm in size. First field observations and microscopically investigations indicate that rocks in the area have been subject to different high metamorphic conditions. Therefor a granulite facies metamorphic overprint was proved in the migmatized metasediments. Additionally, metamorphic characteristic of amphibolite facies conditions, like newly formed biotite with a preferred orientation and growth of garnet, reveal one or more metamorphic overprints under this conditions. This study aims to model the deformation history of this area by tectonic data and cross sections. Furthermore, the different lithologies are analysed microscopically with special focus on shear sense indicators and stretching lineation. Moreover, the grade of metamorphism was determined to reconstruct the p-T-conditions during this deformation.

**Mon: 77****Slab hydration: combining constraints from oceanic plate structure and intraslab seismicity****Jacob Geersen**<sup>1</sup>, Christian Sippl<sup>2</sup>*<sup>1</sup>GEOMAR Helmholtz Centre for Ocean Research Kiel, Germany; <sup>2</sup>Institute of Geophysics, Czech Academy of Sciences*

Most subduction-zones exhibit two bands of intraslab seismicity, the lower one situated at 20-40 km below the plate-interface within the subducting oceanic mantle. This band, which is usually referred to as the lower seismicity plane, runs parallel to the plate-interface and is characterized by rather low magnitude earthquakes showing downdip-extensive mechanisms. The intensity of lower-plane seismicity often varies greatly along a single subduction zone, and can be completely absent in some areas. To date, there is no single accepted physical model which explains the mechanism that drives earthquake occurrence within the lower-plane as well as observed spatial variations over relatively short distances. One hypothesis that has been put forward for explanation of the existence of the lower seismicity plane is that it results from serpentinite dehydration along the 600–650°C isotherm in the oceanic mantle. Serpentinization possibly occurs in the outer rise region of oceanic trenches by water which infiltrates the oceanic crust and mantle along bending-related faults. If this hypothesis is correct, the intensity of lower-plane seismicity should correlate with the amount and penetration depth of water in the slab, and thus with the intensity and the depth extent of bending-related faulting. To test this, we correlate the occurrence and intensity of lower-plane seismicity in the North Chilean, Japan Trench, and Central American subduction-zones with oceanic-plate fault patterns in the outer rise and trench regions. To analyze the intensity of lower-plane seismicity, we compute the ratio

between event numbers in the rather homogeneously active upper seismicity plane and the lower plane in along-strike distance bins. With this approach, we avoid the issue of variable earthquake catalog completeness that would complicate the analysis if absolute event numbers were used. Fault patterns are derived from a compilation of more than 100 ship-based bathymetric surveys complemented by published seismic reflection lines which run perpendicular to the individual margins. First results point towards a higher rate of lower-plane seismicity in regions where plate-bending is expressed in well-developed horst-and-graben structures as well as in regions where topographic features on the oceanic-plate enter the subduction-zone. Future work will further explore this possible correlation.

## Mon: 78

### Pre-Alpine tectonic and sedimentary contacts in the southeastern Ötztal Nappe (Austroalpine, Italy)

**Linus Klug, Nikolaus Froitzheim, Frank Tomaschek, Markus Lagos**

*Rheinische Friedrichs-Wilhelms-Universität Bonn, Germany*

In its southeastern part the Ötztal Nappe comprises the Ötztal Basement s. str., the Schneeberg Complex, the Laas Series and the Texel Complex. The latter is known as the western end of the Eoalpine High-Pressure Belt, for which several subduction and exhumation models exist. For assessing these models, it is essential to clarify the relationships inside the Ötztal Nappe.

Systematic electron-microprobe garnet mapping allows discrimination between different metamorphic histories in the southeastern Ötztal Nappe by zonation patterns. Alpine garnet growth is reported in all units. Variscan high-grade metamorphism is documented by inherited cores of two-phase garnets. While the internal parts of the Schneeberg Complex show only single-phase garnets, the Ötztal Basement s. str., the Laas Series and the Texel Complex show two-phase garnets. The Schneeberg Complex can be divided into the single-phase Schneeberg synforms and the two-phase Schneeberg frame zone (Rahmenzone). The tectonic contact between the Schneeberg synclines and the other units is therefore of pre-Alpine origin. Garnet zonation does not indicate an Alpine contact between the Texel Complex and the Ötztal Basement s. str. This challenges models where the Texel Complex and the Ötztal s. str. represent the footwall and hanging wall of an exhumation-related normal fault (Sölva et al. 2005) or two different nappe systems (Schmid et al. 2004).

To test if the remaining contacts are of sedimentary nature, we used detrital zircon U-Pb dating by laser ablation ICPMS. Previous U-Pb dating of magmatic zircons of granitic intrusions in the southeastern Ötztal Nappe yielded Ordovician (450 – 470 Ma) formation ages. Our set of detrital zircon ages indicates that the Austroalpine basement containing Ordovician magmatites is the source area of the metasediments of the Schneeberg Complex and the Laas Series. We suggest that the Schneeberg and Laas series represent the post-Ordovician, pre-Permian sedimentary cover of the Ötztal/Texel basement. In contrast to the Laas Series and the other units, the rocks presently found in the Schneeberg synclines belonged to a higher structural level of the Variscan orogeny, unaffected by Variscan garnet-grade metamorphism. Therefore, the basal contact of these Schneeberg rocks probably represents a Permian extensional fault or shear zone.

[1] Schmid et al. (2004) *Ecolgae geol. Helv.*, 97, 93-117; [2] Sölva et al. (2005) *Tectonophysics*, 401, 143-166.

## Mon: 79

### Exhumation of a metamorphic core complex: The journey from mid-crust to surface

**Georg Löwe, Kamil Ustaszewski**

*Friedrich-Schiller-Universität Jena, Germany*

Regional-scale extension in the internal Dinarides manifests by the occurrence of several metamorphic core complexes (MCC's) located at the distal Adriatic passive margin and within the Sava Zone. The Sava Zone represents a suturing accretionary wedge juxtaposing Adriatic thrust sheets in a lower-plate position with

European-derived units. In Oligo-Miocene times, the Sava Zone underwent substantial post-collisional extension, triggered by the opening of the Pannonian Basin in response to the NE-directed rollback-motion of the Carpathian slab.

Mt. Cer in western central Serbia represents one of such core complexes and is a key-feature allowing insights into regional-scale extension and associated magmatic and metamorphic processes. Cer MCC is part of the most distal Adriatic Jadar-Kopaonik composite thrust sheet and comprises a central I-Type granitoid of Eo-Oligocene age that was subsequently intruded by an S-Type granite. This multi-phase pluton was exhumed together with amphibolite-facies grade metapelites along a low-angle detachment with top-N transport at approx. 17 Ma as shown by Ar/Ar in-situ geochronology on deformed white mica.

We further used Al-in-hornblende (Hbl) geobarometry to constrain crystallizing pressures for the I-type granitoid. Results ranging from 5 to 6 kbar suggest a mid-crustal depth of intrusion of approx. 16 km while values obtained on Hbl from a lamprophyric dike intruding the I-type granitoid show a maximum at 2 kbar, corresponding to a depth of intrusion at roughly 5 km. Field observations confirm the lamprophyric dikes to be the youngest magmatic feature as they contain pegmatitic xenoliths of S-Type granitic composition.

Our results help to constrain exhumation in a spacio-temporal manner and contribute to a more detailed understanding of the interplay between magmatism and regional-scale extensional tectonics in the internal Dinarides.

**Mon: 80**

### **The Altmark Swell – sedimentary high or uplifted graben shoulder?**

**Alexander Malz**

*Landesamt für Geologie und Bergwesen Sachsen-Anhalt, Germany*

The Altmark Swell in north-western Saxony-Anhalt forms a remarkable structure where sedimentary, facial and tectonic changes occurred during the Mesozoic evolution of the North German Basin. First, it evolved as a structural high in Late Palaeozoic to Early Triassic times, which is proved by several local to regional unconformities in the Buntsandstein Group. Later, i.e. during the Late Triassic, wide areas of the North German Basin area were affected by strong WNW-ESE-directed extension. This event is suspected to have initiated uplift and erosion on top of the Altmark Swell and thus led to the formation of a hiatus spanning the whole Middle to Late Triassic time period (approx. 40 Ma). Most often this is interpreted to have been associated with strong vertical movements in the mechanical basement (sub-salt strata) or was due to the formation of salt pillows.

In the framework of a large-scale 3D modelling campaign carried out at the geological surveys of Northern Germany we re-evaluated a dense network of interpreted reflection seismic sections and several hundreds of boreholes in the vicinity of the Altmark Swell. These data clearly confirm the sedimentological interpretations of earlier researchers and allows for the refinement of distribution outlines in the footwall of unconformities. Nevertheless the structural relationship of sedimentary basins, grabens and bordering faults as well as associated salt structures suggests that the Altmark Swell was rather influenced by huge sub-horizontal, decoupled movements (up to 5 km) along flat normal faults than with vertical, basement-involved faulting. We observed several large, flat faults linked with mechanically weak evaporates. These faults affected the Upper Buntsandstein Group to directly overlay the Zechstein salt. Large horizontal movements resulted in a particular structural configuration, several ramp-flat-ramp geometries and extensional duplexes. In the hanging wall of extensional detachments thick (1.5 km) Late Triassic strata was deposited while large salt pillows grew in the footwall of flat faults exposed on the Late Triassic surface.

In this contribution we present our observations and provide a tectonic-sedimentary model of the Altmark Swell, which helps to explain the distribution and extent of unconformities in relationship to fault and fold geometries observable over a distance of approximately 100 km along the western border of the Altmark Swell.

**Mon: 81****Stress rotation due to discontinuities and material transitions****Karsten Reiter***TU Darmstadt, Germany*

The in-situ stress state in the upper crust is an important issue for economic purposes and scientific questions as well. Several methods have been established in the last decades to indicate the present-day orientation of the maximum compressive horizontal stress ( $S_{Hmax}$ ). It was assumed, that the  $S_{Hmax}$  orientation on a regional scale is governed by the same forces that drive plate motion. The  $S_{Hmax}$  orientation data, compiled by the World Stress Map (WSM) project, confirmed that for many regions in the world. Also due to the increasing amount of data, it is now possible to identify clearly several areas in the world, where stress orientation deviates strongly from the expected orientation due to plate boundary forces (first order stress sources), or the plate wide pattern. In some of this regions a gradual rotation of  $S_{Hmax}$  can be observed.

Several second and third order stress sources have been identified in the past that can explain the stress rotation. For example, these are lateral heterogeneities in the crust, such as density, petrophysical or petro-thermal properties and discontinuities, like faults. Apparently, there is no study, which quantifies the potential amount of stress rotation depending on these second and third order stress sources in detail. For that reason, generic geomechanical numerical models have been set up, consisting of several sloping units, with variable elastic material properties such as Young's modulus, Poisson ratio and density. An almost identical model geometry allows additionally to separate the units by contact surfaces allowing a slip along the faults, depending on a chosen friction coefficient.

The model results indicate, that a density contrast or variation of the Poisson's ratio alone is only able to rotate the horizontal stress orientation sparsely. In contrast to that a lower or higher Young's modulus as well as low friction on the faults allows significant stress rotations. Not only the area near a discontinuity or the material transition is affected by the stress rotation, whole blocks can be affected. This indicates that significant material contrasts and low friction discontinuities are able to generate significant stress rotation for larger areas in the crust.

**Mon: 82****Salt pillow growth in the Bay of Mecklenburg, SW Baltic Sea: Timing and regional tectonic link****Niklas Ahlrichs<sup>1,2</sup>, Elisabeth Seidel<sup>2</sup>, Christian Hübscher<sup>2</sup>, Vera Noack<sup>1</sup>***<sup>1</sup>Federal Institute for Geosciences and Natural Resources (BGR), Berlin, Germany; <sup>2</sup>University of Hamburg, Institute of Geophysics, Germany*

We study salt pillow growth at the northeastern North German Basin margin (part of the Central European Basin System) by means of seismic imaging. New high-resolution gapless seismic sections from the BalTec project illuminate the stratigraphic and tectonic pattern of the subsurface from the base of the Zechstein salt to the seafloor. This allows a complete reconstruction and timing of salt movement from deposition to present day. We present key profiles across three adjacent salt pillows in the central area of the Bay of Mecklenburg (SW Baltic Sea). Stratigraphic correlation with onshore wells rests upon additional marine profiles as well as vintage land seismic surveys. We identify and compare phases of salt movement within the regional tectonic framework with emphasis on the nearby Glückstadt Graben and Tornquist Zone.

Salt pillow growth initiated in the Late Triassic with ongoing movement until the Jurassic. After a phase of cessation, salt movement rejuvenated in the Late Cretaceous and Tertiary. Contemporaneous tectonic activity in the Tornquist Zone allows a linkage of regional tectonics and salt movement. The rejuvenation of pillow growth in the Late Cretaceous correlates to the regional tectonic reorganization of the North German Basin and Tornquist Fan area and the change from an extensional to compressional setting alongside basinwide graben inversion and thrust faulting.

**Mon: 83****Strain analysis of the Zervreila Orthogneiss of the northern Adula Nappe, eastern Switzerland, Central Alps****Burcu Tasdemir, Ruth Keppler, Nikolaus Froitzheim, Jacek Kossak-Glowczewski***IGM, Rheinische Friedrich-Wilhelms-Universität, Bonn, Germany*

The Adula Nappe of the Central Alps mainly comprises pre-Mesozoic basement rocks which were overprinted by eclogite facies metamorphism during the Alpine cycle. The metamorphic peak conditions increase from 1.0-1.3 GPa/450-550°C in the north to 3.0 GPa/800°C in the south. The complex internal structure of the Adula Nappe is the consequence of intense deformation. According to Löw (1987) the northern Adula Nappe experienced at least four ductile alpine deformation events. The first Sorreda Phase (D1, 45-40 Ma) is attributed to isoclinal folding and thrust imbrication. The Zapport Phase (D2, 40-35 Ma) occurred during isothermal decompression (nappe emplacement) near peak conditions, leading to N-S orientated stretching lineations, mylonitic fabrics, isoclinal folding, and top-N shearing of the nappe. The Leis Phase (D3, 35-30 Ma) post-dates D2 and is still related to isothermal exhumation. It is characterized by coaxial deformation, WSW-ENE stretching lineations (orogen-parallel), and open to isoclinal folding. The formation of the Northern Steep Belt and N-vergent antiforms at the front of the Adula Nappe are attributed to the youngest Alpine deformation phase, the Carassino Phase (D4, 30-20 Ma). The sum of all these deformation phases is responsible for the complex present-day geometry of the Adula Nappe. However, the exhumation mechanism of the nappe is still in debate, since the models face kinematic problems through the absence of top-S shear sense indicators at the roof of the nappe.

In this study, we performed thin section analysis and applied the Fry method (center-to-center method) to determine deformation structures and the finite bulk strain of the northern part of the Adula Nappe, south of the Zervreila Lake. The method depends on competence difference of matrix and clasts. Thus, estimated finite strains are matrix strains at outcrop scale. Over thirteen Zervreila Orthogneiss outcrops within the study area were measured for finite strain.

Thin section analysis revealed a Sorreda Phase (D1) foliation defined by inclusions in feldspar grains. Fry analysis shows a high concentration in the flattening field of the Flinn diagram, and two samples plotting in the constrictional field. This slightly scattered pattern indicates an overprint of penetrative N-shearing Zapport structures (D2; mostly plane strain with some constrictional strain) by the younger coaxial Leis deformation phase (D3; flattening strain). The finite strain resulted from the addition of the effects of the two deformation phases.

Löw, S. 1987. *Beiträge zur Geologischen Karte der Schweiz N.F.*, **161**, 1-84.

**Mon: 84****On the indispensability of haptic sensations with hand specimens – a plea for integrating rock collections into structural geology and tectonics teaching in the digital era****Kamil Ustaszewski, Madeline Richter***Friedrich-Schiller Universität Jena, Germany*

Experience from 5 years of teaching various structural geology and tectonics classes at both the Bachelor and Master level at the University Jena shows that the maintenance of an ample rock collection with hand specimens, which illustrate a large gamut of deformational fabrics, and its integration into 'hands-on' exercises forms a very welcome addition to traditional (and in the view of students sometimes soporific) classroom teaching. Vivid and convincing teaching necessitates the illustration of the numerous natural deformation processes with representative hand specimens rather than mere photographs of outcrops, samples or thin sections.

We started building a collection of rock specimens shortly after appointment of the first (senior) author at

the Institute of Geosciences in Jena in 2013. Back then, the institute was hardly in possession of any hand specimens illustrating the broad gamut (as well as the aesthetics) of deformation fabrics. At present, the collection contains c. 150 specimens of samples, showing various types of tectonically induced strain fabrics (e.g. brittle vs. ductile fabrics, numerous types of foliations and lineations), igneous fabrics (magmatic flow textures, cumulate textures, intrusive contacts, migmatites) as well as examples of rock-fluid interaction (e.g. serpentinized peridotites or multiply veined carbonates). Specimens were mostly collected during student field trips and own research campaigns across Germany, the Alps and Carpathians, the Balkan peninsula and Taiwan.

The sample collection now portrays the rich spectrum of deformation fabrics acquired at both shallow-crustal conditions by dominantly frictionally controlled mechanisms (such as extension and shear fractures, catclasites or dilational breccia) or during creep (crack-and-seal fabrics, various stylolites) as well as mid- to lower-crustal conditions by dominantly viscous mechanisms (numerous greenschist- to granulite-facies mylonites) or subordinately also frictional mechanisms (pseudotachylites).

Testimonies of our students suggest that studying traditional handouts during lectures along-side with hand specimens is a very welcome, more vivid addition to teaching, providing the students with much sought optic and haptic sensations that illustrate the large number of tectonic processes way better than field photographs (e.g. Outcropedia, outcropedia.tectask.org) or virtual 3D outcrops (e.g. eRock, www.e-rock.co.uk) can.

We hence conclude that the maintenance of a collection of hand specimens, displaying the spectrum of strain fabrics across a large range of both temperatures and strain rates is an indispensable (and well affordable) addition to traditional classroom teaching and not at all obsolete in the digital era.

## Mon: 85

### Extensional continental basins: Feedbacks between the tectonic and thermal history

**Katharina Vogt<sup>1</sup>, Attila Balázs<sup>2</sup>, Taras Gerya<sup>3</sup>**

<sup>1</sup>International Geothermal Centre, Bochum University of Applied Sciences, Bochum, Germany; <sup>2</sup>Laboratory of Experimental Tectonics, Department of Sciences, Università degli Studi Roma Tre, Rome, Italy; <sup>3</sup>Geophysical Fluid Dynamics Group, Institute of Geophysics, ETH, Zurich, Switzerland

Extension of continental lithosphere may result in a wide range of different crustal architectures, fault geometries, sediment patterns and thermal histories. These variations were shown to be strongly controlled by the rheological and thermal structure of the lithosphere, the kinematic history of the system, the existence of heterogeneities in the crust and/or mantle and surface processes. Understanding the geodynamic evolution of the system, and, in particular feedbacks between the tectonic and thermal history of the system has direct implications for the assessment of potential petroleum systems and geothermal applications. In order to better understand the time-dependent evolution of these key aspects, we conduct a series of numerical, thermo-mechanical models in 3D. These models are based on the thermo-mechanical code I3VIS, which solves the mass, momentum, and energy conservation equations for incompressible media. The code uses non-Newtonian viscoplastic rheologies to simulate flow and is specifically designed to study lithospheric extension. First results indicate the importance of rheological heterogeneities in the crust and/or mantle on the overall geometry and tectonic evolution of extensional continental basins. Reactivation of nappe contacts and fossil suture zone localizes deformation and results in asymmetric basins that exhibit along-strike variability in terms of fault geometries, basement structures, subsidence, and thermal evolution.

## 13d) Communicating (geo-)science

Monday, 23/Sep/2019: 9:00am - 10:30am

**Session Chair: Rebecca Bast** (Westfälische Wilhelms-Universität Münster)

**Session Chair: Vera Laurenz-Heuser** (S.-H. Eiszeitmuseum)

**Session Chair: Julia Roszjar** (Natural History Museum Vienna)

**Location: Schloss: S 055**

### Session Abstract

Making science accessible for everybody, and shaping discussions about key geoscience issues such as climate change, natural hazards or biodiversity helps rebutting fake news and answering the question “Why do we need fundamental research?”. In times where the effects of man-made climate change are scientifically sound but publicly in doubt, the communication of scientific results to policy makers, journalists, and the general public becomes increasingly important. This session aims at bringing together various and innovative strategies to communicate science to a broad audience. How do you communicate your scientific work? Tell us for example about your citizen science project(s), science-related social media or public outreach activities. We especially invite unconventional contributions such as multimedia reports, public exhibits, press releases, etc. Please indicate in your abstract what you intend to present, and in which form (e.g. poster, exhibit, digital report, etc.).

### Lecture Presentations

9:30am - 10:00am *Serge-von-Bubnoff Medal*

#### **More Geosciences in German Schools: Opportunities for Geoscientists to Support the Training and Selection of Students for the Annual Competition „International Earth Science Olympiad (IESO)“**

**Sylke Hlawatsch**

*Richard-Hallmann-Schule, Germany*

German national teams have taken part in the IESO since 2012. The DGGV (Fachsektion Geodidaktik) coordinates the training and selection process of secondary school students ([/www.die-deutsche-olympiade-der-geowissenschaften.de/](http://www.die-deutsche-olympiade-der-geowissenschaften.de/)). While Earth sciences generally are not part of German school education, participating schools implement clubs, courses which can be selected among others as well as extracurricular activities in order to prepare their students. This procedure allows synergy effects of otherwise isolated outreach activities of geoscience research centres and museums and can enhance quality and quantity of geoscience education in schools all over Germany.

The IESO is an annual competition for secondary school students. It tests their skills in all major areas of geosciences, including geology, mineralogy, geophysics, meteorology, terrestrial astronomy and environmental sciences. The theoretical examination covers problems which are supposed to measure the participants' knowledge and understanding, while the practical examination consists of tasks which are designed to assess participants' abilities to carry out scientific investigations in geoscience inquiries. The main aim of the IESO is to encourage students' interest and public awareness of geosciences and to enhance Earth science learning. Last but not least, the IESO has developed in pursuit of encouraging friendly relationships among young learners from different countries and promoting international cooperation in exchanging ideas and materials on Earth sciences education. ([www.ieso-info.org](http://www.ieso-info.org))

Geoscience research institutions have offered hands-on workshops for students who wish to take part in the selection process. A successful program consisting of modules which offer basic knowledge and others which offer insight into recent research programmes and analytical methods will be presented.

**10:00am - 10:15am****Der Mineralogische Lehrkoffer im MINT-Unterricht – eine Brücke von Natur zu Naturwissenschaft und Technik****Maria Mrosko<sup>1</sup>, Bastian Joachim-Mrosko<sup>2</sup>, Lennart A. Fischer<sup>1</sup>, Gilla Simon<sup>3</sup>, Lutz Hecht<sup>4</sup>, Malte Junge<sup>1</sup>, Magdalena Blum-Oeste<sup>4</sup>, Roland Stalder<sup>2</sup>**<sup>1</sup>University of Freiburg, Germany; <sup>2</sup>University of Innsbruck, Austria; <sup>3</sup>Museum Mensch und Natur, München, Germany; <sup>4</sup>Museum für Naturkunde, Berlin, Germany

Geowissenschaften spielen trotz ihrer enormen Bedeutung für viele gesellschaftsrelevante Themen in den meisten Lehrplänen nur eine untergeordnete Rolle und sind daher im Unterricht von der Grundschule bis hin zur gymnasialen Oberstufe kaum sichtbar. Ein vorrangiges Ziel des Projektes "Mineralogischer Lehrkoffer (MiLeKo)" ist daher, Schülerinnen und Schüler sowie Lehrerinnen und Lehrer für mineralogische Themen im Hinblick auf rohstoff- und umweltrelevante Fragestellungen zu sensibilisieren. In den Jahren 2014 bis 2018 wurden zwei Projektphasen finanziell durch die Alexander Tutsek-Stiftung gefördert. Dadurch konnten fünf verschiedene Lehrkoffer-Module entwickelt werden, die Themen wie „Vielfalt der Gesteine: Fenster zur Erde“, „Rohstoffe: Vom Erz zum Metall“ oder „Symmetrie: Farben und Formen der Natur“ behandeln. Die Koffer werden im gymnasialen Unterricht eingesetzt und fordern die Schülerinnen und Schüler über das Begreifen und Erforschen der Handstücke auf, selbst die Mineralogie zu entdecken. Bisher wurden über 300 Koffer hergestellt und deutschlandweit an Lehrerinnen und Lehrer verteilt. Dies hat vor allem dazu beigetragen, ein Netzwerk an engagierten Lehrkräften zu knüpfen. Die große Nachfrage hat jedoch gezeigt, dass der Bedarf noch lange nicht gedeckt ist. Nach dem erfolgreichen Abschluss der zweiten Projektphase hat sich die Alexander Tutsek-Stiftung nun bereit erklärt, eine dritte Phase im Zeitraum 2019-2021 zu unterstützen.

In dieser Phase ist geplant, die Lehrkräfte, die den Koffer schon jetzt im Unterricht einsetzen, nachhaltig zu binden. Hierfür sollen weiterführende Unterrichtsmaterialien entwickelt und tiefer greifende Informationen zur Verfügung gestellt werden. Außerdem sollen für einen Einsatz im interdisziplinären Unterricht neue fächerübergreifende Module konzipiert werden. Ein weiteres Ziel ist es, ein Netzwerk an Ausleih- und Auffüllstationen an Universitäten, Museen und geowissenschaftlichen Institutionen im gesamten Bundesgebiet aufzubauen. Ein "Rent a Scientist"-Programm und Fortbildungsangebote für Lehrerinnen und Lehrer sowie Referendare sollen zusätzlich etabliert werden.

**10:15am - 10:30am****Geology in a nutshell – A rock-cycle game created during a geology course for elementary school students****Vera Laurenz-Heuser***S.-H. Eiszeitmuseum, Germany*

Within the "Enrichment programme" of the German State of Schleswig-Holstein, particularly gifted students are given the opportunity to attend extracurricular courses, which go beyond the normal topics and methods of school education.

In the framework of this programme I organized a geology course for grades 3-5, with the goal of making the pupils understand Earth as a system with interdependent processes, which is particularly important in the current discussion on climate change.

The course is based on the occurrence of a variety of rocks at the German Baltic coast deposited during the last glacial maximum in Northern Europe, with rocks comprising all major rock types, including magmatic, metamorphic and sedimentary rocks. The pupils got to collect their own set of rocks during an initial excursion to a cliff, which were then used to demonstrate the different rock types, their formation, and their relation within the geological rock cycle. In addition, the "DMG Lehrkoffer" is used during the course, especially to show Minerals and rocks not found during the excursion.

Central to the course are student activities, in order to support students in gaining knowledge on the rocks and processes themselves. Examples of activities are investigating the rocks with “geologist’s tools” such as magnet, magnifying glasses and vinegar as well as creating fact sheets on the different rocks. Science experiments are another integral part to demonstrate processes usually occurring on time scales and in depths not accessible to us. Examples are melting a wax model of the mantle or extracting Cu from malachite.

As a final result of the course, the pupils created a game of dice demonstrating the different stations of the rock cycle and the underlying processes, which will be presented at the conference.

## Monday, 23/Sep/2019: 11:15am - 1:00pm

### 11:15am - 11:30am

#### Teaching Science Communication to Geoscience students

##### Rebecca Bast

*Westfälische Wilhelms-Universität Münster, Germany*

The skill to reduce scientific knowledge to the relevant points and communicate those to a lay audience is becoming increasingly important. However, science communication has not been included in many classical curricula yet, and young scientists are often unable to cope with society’s demands.

How does communication between experts and lay people work? Why does it fail from time to time? What are the expectations of the individual stakeholders, scientists and citizens? How can they even work together, and why would they?

Which platforms and media channels are available to scientists? Who are the recipients? What is special about giving a public talk? How can scientists make use of the press? And what are the benefits of such efforts?

All those questions can (and should) be discussed in a science communication class to help science finally emerge from the ivory tower (e.g., Schäfer et al., 2015). I would like to encourage academic staff to enrich the curricula with interdisciplinary courses such as science communication to train the students’ general competences.

I will therefore present my concept for teaching science communication to Bachelor students, provide an exemplary module description and literature resources (mostly in German, though). The main topics covered are:

Expert-Lay-Communication

Science and Society

Citizen Science Projects

Museums and Science Centers

Science Journalism

Blogs and Social Media

TED Talks and Science Slams

The class includes visiting a museum and a science center. As a final assignment, the students write an article for an (imaginary) popular scientific journal. In cooperation with the university’s press office, one of the articles may be published in the university newspaper (“wissen|leben”).

**11:30am - 11:45am****Minerals in Thin Section ('MINTS'): An open-access, interactive website for transmitted-light petrographic microscopy****Jürgen Reinhardt<sup>1</sup>, Michael Raith<sup>2</sup>, Tanja Reinhardt<sup>3</sup>, Hans-Peter Schertl<sup>4</sup>**<sup>1</sup>University of the Western Cape, South Africa; <sup>2</sup>Universität Bonn, Germany; <sup>3</sup>University of KwaZulu-Natal, South Africa; <sup>4</sup>Ruhr-Universität Bochum, Germany

Polarized-light microscopy remains an indispensable tool for the mineralogical analysis of geological samples. It is commonly the critical (and inexpensive) step before taking mineral and rock analysis to the next level (such as electron microprobe, XRF, ICP-MS analyses). The importance of microscopic mineral and rock analysis is also reflected in the large variety of textbooks available on the subject that range from pure data compilations to printed atlases of photomicrographs. A drawback of the former is the lack of photographic reference material, and a drawback of the latter is the high cost of colour printing, which limits the scope of any image collection in book form.

The obvious way ahead is a web-based approach providing easy access from wherever an internet connection is available. As long as there is provision of large storage space, there is practically no limit to the amount of images in the database. Image size needs to be restricted only to ensure quick downloading. While the open-access e-book 'Guide to Thin Section Microscopy' by Raith, Raase & Reinhardt (2012) focuses on the methodical-practical approach, the new website is essentially an optical-mineralogical database, sorted by minerals and mineral groups, with emphasis on thin section images.

The website involves the following elements:

- (1) A mineral index with links to data pages and image sets
- (2) A graphical presentation of crystallographic-morphological properties combined with optical indicatrix geometry
- (3) A graphical overview of refractive index ranges in combination with a crystal-plate thickness versus birefringence plot using a novel interference colour chart
- (4) A condensed listing of optical and morphological mineral properties
- (5) An extensive archive of photomicrographs involving multiple image sets for each mineral species. These image sets include plane-polarized-light and crossed-polarizers modes showing critical grain sections and orientations as well as lambda-plate overlays. The variation of optical and/or morphological properties within a mineral group (such as a solid solution series) can be given sufficient coverage by adding appropriate image sets.
- (6) A search facility is included that allows input of own observations

The web-based approach has the advantage that the database can be modified by the authors at any time to upgrade, add and delete material as desired. While the initial release focuses on the more common minerals and mineral groups, the website will move towards a more extensive coverage. Input from "outside" will also be encouraged. The website will be hosted by the Deutsche Mineralogische Gesellschaft (DMG).

**11:45am - 12:00pm****OutcropWizard - A modern access to the classic themes of geoscience****Martin Monschau, Edouard Grigowski, PD Dr. Gösta Hoffmann***University of Bonn, Germany*

Here we present the project OutcropWizard, an innovative mobile solution to access and explore geology. The App was initially launched in 2017 and we document a continuous rise in user numbers. The approach is based on crowdsourcing and we expect the amount of information to grow rapidly in a non-linear fashion. Our target group of content generators are experts and students alike. OutcropWizard is a not-for-profit project.

The study of outcrops is a main part of geological surveying and therefore, collecting information beforehand is key to understanding each outcrop in the field. However, information on outcrops is often connected with extensive research or static content, such as print media and info panels. Hence, the centralisation of digital outcrop information in a database accessible with mobile devices improves the information acquisition and is therefore attractive, especially for students who use smartphones as primary information sources. Additional benefits in contrast to traditional media are the implementation of latest research results, the ease of use of mobile navigation and the possibility of multilingual and international datasets. The blended learning aspect becomes increasingly important as a connection between traditional media and modern technology in the field. Therefore, we have developed the blended learning application OutcropWizard as a modern access to the classic themes of geoscience.

OutcropWizard displays outcrops, museums and points of geoscientific interest categorised on a map. A detailed description with images, as well as stratigraphic and lithological information is provided on each outcrop. Professionals, students and interested users can share their impressions via pictures and comments and can also upload their own outcrops in the most common languages. A translation tool allows the allocation of outcrop information by the users. 3D-models and videos give a first impression of an outcrop in the classroom and allow the exploration of Earth's history everywhere. With the creation of own excursion routes the virtual excursion guide can be self-compiled, supporting teachers field trip plans. This enables point to point navigation for each individual user. Additionally, the upcoming virtual professor tool will facilitate blended learning even more by experts videos.

The benefit of a digitised and centralised database is the possibility of up-to-date data, implementing new publications and information on each outcrop. OutcropWizard is an impressive method for sharing cross-language information with professionals, institutions, students and interested users. Thus, OutcropWizard will improve blended learning within educational institutions and connect the geoscientific community in a modern way.

**12:00pm - 12:15pm**

### **Why PDFs are not suitable for communicating (geo)scientific results**

**Markus Konkol**

*University of Muenster, Germany*

Many geoscientific articles are based on computational methods, e.g. a spatiotemporal analysis. It is common practice to describe the analysis as part of the methodology section in a paper. Nevertheless, it is less common to make these materials publicly accessible. Besides issues such as the time needed to prepare code and data, a key issue is that the "classic" way of publishing a paper (i.e. as a PDF file) is not suitable for describing and publishing computational research. It is challenging (if it is even possible) to describe the computational steps in such a detail that others can understand and reuse the analysis and the data. However, even if the materials, i.e. the source code and data, are attached to the paper, they are largely disconnected from the actual text. Besides the lack of connections between the paper, the source code, and the data, a further issue is that PDFs are static. To solve this issue, interactive geoscientific papers could help to better understand how the results were achieved. For example, an interactive paper could show which source code lines and which data subsets were used to produce a specific result. Besides the possibility to inspect the materials underlying the results in the paper, a further benefit is the creation of interactive results. We found a number of papers in which the authors suggested alternative values for parameters that were used in the analysis but they were not able to show the effects on the results in a static PDF file. This talk describes the concept of a binding which assists authors in creating interactive geoscientific papers by creating links between the paper, the analysis code and the data. Based on these links, the authors can specify controls (e.g. a slider) allowing readers to manipulate analysis parameters within a certain range. Giving readers the possibility to inspect and explore the results might facilitate a reader's, reviewer's, or journalist's understanding of the reported results - a key goal of researchers who publish papers. An essential requirement for this alternative way of publishing research is open reproducible research, i.e. code and data underlying the results in the paper are

publicly available and executable. Hence, interactive geoscientific papers not only help authors to communicate their research but also to follow good scientific practice.

**12:15pm - 12:30pm**

### **Asteroid Day: Communicating the danger from impacts on Earth and the relevance of meteorites and their parent bodies**

**Julia Roszjar<sup>1</sup>, Ludovic Ferrière<sup>1</sup>, Christian Koeberl<sup>1,2</sup>**

<sup>1</sup>Natural History Museum Vienna, Austria; <sup>2</sup>Department of Lithospheric Research, University of Vienna, Althanstrasse 14, 1090 Vienna, Austria

The international Asteroid Day takes place annually and worldwide on June 30<sup>th</sup> in remembrance of the Tunguska explosion event over Siberia in 1908. It was co-founded in 2014 by astrophysicist and lead guitarist of Queen Dr. Brian May, Apollo 9 astronaut Rusty Schweickart, the German filmmaker Grig Richters, and Danica Remy, president of the non-profit B612 foundation, which is dedicated to planetary science and defense against asteroid impacts on Earth. In 2016, the United Nations General Assembly declared June 30<sup>th</sup> the international Asteroid Day, an official day of education to raise public awareness about asteroid impact hazards. The NHM Vienna is a founding member of the international Asteroid Day and actively contributes as an official partner to transfer our knowledge and scientific work on meteorites and their parent bodies, as well as of impact craters and events. On this occasion, the NHM Vienna organizes a dedicated and varying program and events that are open to the public and attract a broad audience. Participation in this global awareness program allows to communicate fundamental science in the field of space science and to transfer groundbreaking knowledge, new findings, and state-of-the-art research in the field of solar system research. Some examples of activities that were held at the NHM Vienna in participation of the international Asteroid Day are: podium discussions with well-known international experts, dedicated movie presentations, special guided tours in the world-largest display of meteorites, invited public talks on specific aspects of meteorites and space missions, such as the hunt for micrometeorites, the DAWN mission, building blocks of life, the threat from Near-Earth objects, and various interactive activities such as the 3D printing of a meteorite and a drawing contest for pupils, as well as the installation of a “meteor radar station”. The latter provides not only a visualization, but also an acoustic display, implemented in the permanent exhibition of the museum, to transfer knowledge about the influx of extraterrestrial material on Earth in an interactive station and is also available online ([www.nhm-wien.ac.at/forschung/mineralogie\\_\\_petrographie/meteor](http://www.nhm-wien.ac.at/forschung/mineralogie__petrographie/meteor)). These activities have been widely reported in the Austrian media, generating further public awareness. We would like to promote more exchange with other institutions to discuss innovative public outreach strategies and possibilities to contribute in such global awareness programs and look forward to discussing original ideas and concepts.

## 13e) Building a Global Network of Geochemical Data

Monday, 23/Sep/2019: 11:15am - 1:00pm

Session Chair: Kirsten Elger (GFZ German Research Centre for Geosciences)

Session Chair: Friedhelm von Blanckenburg (GFZ Potsdam)

Location: Vom Stein Haus: Aula / VSH 219

### Session Abstract

Future science endeavours in geochemistry, petrology, mineralogy, and volcanology will increasingly rely on access to and analysis of large volumes of data as data science is emerging as a new research paradigm in these fields. Data systems such as EarthChem and GEOROC have provided access to global, though thematically focused data syntheses. More geochemical data systems are emerging at national, programmatic, and subdomain levels in response to Open Access policies and science needs, and many other repositories manage geochemical data. There is an urgent need to develop and implement global standards and best practices for geochemical data to become FAIR (Findable, Accessible, Interoperable, Re-usable), and to establish standard protocols for exchanging geochemical data among distributed data systems. This session aims at engaging relevant communities and groups in the Earth sciences to present their data facilities and to explore ideas and opportunities for a global geochemical data network that facilitates and promotes discovery and access of geochemical data through coordination and collaboration among international geochemical data providers.

### Lecture Presentations

11:15am - 11:30am

#### Big Data in Geochemistry? Examples, needs and outlook

Gerhard Wörner<sup>1</sup>, Bärbel Sarbas<sup>2</sup>, Jens Nieschulze<sup>3</sup>, Albrecht Hofmann<sup>4</sup>

<sup>1</sup>Universität Göttingen, Geowissenschaftliches Zentrum, Germany; <sup>2</sup>MPI für Chemie, Mainz, Germany; <sup>3</sup>Abt. Forschung, Universität Göttingen, Germany; <sup>4</sup>MPI für Chemie, Mainz, Germany, Lamont-Doherty Earth Observatory, Columbia University, New York

The global database GEOROC (Geochemistry of Rocks of the Oceans and Continents; <http://georoc.mpch-mainz.gwdg.de/>) is maintained by the Max Planck Institute for Chemistry in Mainz. The database is a comprehensive collection of published analyses of igneous rocks (volcanic rocks, plutonic rocks, and mantle xenoliths). It is complemented by PetDB, which covers primarily mid-ocean ridge basalts. GEOROC contains major and trace element concentrations, radiogenic and nonradiogenic isotope ratios as well as age data for whole rocks, glasses, minerals and inclusions. Samples come from 11 different types of geological settings. Metadata include, among others, geographic location with latitude and longitude, rock class and rock type, alteration grade, analytical method, laboratory, reference materials and references.

GEOROC has provided geochemistry with a tool to analyse large data sets in geochemistry with a focus on igneous processes. Applications of the database GEOROC are numerous in the study of volcanic rocks but also in sedimentary, palaeo-oceanographic, as well as atmospheric research. Datasets in GEOROC are cross-linked with GeoRem, an MPI database for reference materials of geological and environmental interest, such as rock powders, synthetic and natural glasses as well as minerals, isotopic, biological, river water and seawater reference materials. GEOROC presently holds data for 530.740 samples comprising 21.564.700 single data values and gets around 100 citations per year.

A range of old and new research questions can now be addressed by systematically and statistically analysing and exploring this data base: Are there secular variations in igneous rock compositions or the major and trace element inventory of the continental crust throughout Earth history? Can certain widely-used trace element signatures, such as Sr/Y be calibrated and confidentially used to extract crustal thickness of magma process-

ing in arcs worldwide and in the past ? Are there geochemical systematics in arc magmas on our planet that allow predictions about their fertility to form, and constrain genetic processes of, rich Cu deposits ?

This contribution reviews and explores recent examples of “Big Data” approaches to igneous and planetary geochemistry and identifies the needs and modes to further advance the field of “digital geochemistry” using GEOROC 2.0.

**11:30am - 11:45am**

### **An online research platform for cosmochemistry**

**Dominik C Hezel<sup>1</sup>, Premkumar Elangovan<sup>2</sup>, Andreas Morlok<sup>3</sup>, Jörn Koblitz<sup>4</sup>**

<sup>1</sup>University of Cologne, Germany; <sup>2</sup>Royal Surrey County Hospital NHS Foundation Trust, England; <sup>3</sup>University of Münster, Germany; <sup>4</sup>MetBase Library, Germany

We built a platform for cosmochemistry that combines three key components and tools for cosmochemical research, reference data, publication blog, and teaching. The three components are: (i) a bulk meteorite, meteorite component and comprehensive literature database, called MetBase. MetBase has been established more than 30 years ago and is a well-known by and important tool for many meteoriticists. This database has been outfitted with a new technical foundation. For example, it is now possible to quickly, intuitively and immediately plot data. (ii) A resources database. This contains key data such as average chondrite group element abundances, meteorite mineral information, a glossary, etc. Importantly, this database contains about 150 videos explaining key figures, tables, equations, concepts, etc. in cosmochemistry, including rich supplemental information, review tools, etc. Thereby, this resources database not only a reference tool, but also a tool for teaching. These resources are the newest addition to the platform, and still in a state of being set-up. (iii) A daily blog collecting all new relevant cosmochemical literature into one single stream. This blog (cosmochemistry-papers) exists since about 5 years, with still growing view-numbers (>50.000 per year).

The combination of these three key ingredients allow access and visualisation of many data, understanding and refreshing knowledge, and up-to-date literature information. Researchers and students who are new to the field can quickly catch-up by selecting and completing tailored assignments. The assignments can already include the full database, i.e., existing, but importantly also new hypotheses and ideas can directly be tested.

The entire platform can only be a start. We are currently in talks with the various meteorite societies to explore possibilities to make this a more official and even more comprehensive platform.

The platform is online and accessible vial [metbase.org](http://metbase.org). The MetBase database is (still) partly commercial, while the Resources and Cosmochemistry-Papers sections are free.

**11:45am - 12:00pm**

### **Medusa: A Metadata System for Samples analysed in the Geo- and Environmental Sciences**

**Schlegel Jutta<sup>1</sup>, Ulbricht Damian<sup>2</sup>, Elger Kirsten<sup>2</sup>, Friedhelm von Blanckenburg<sup>1</sup>**

<sup>1</sup>GFZ German Research Centre for Geosciences, Potsdam, Section Geochemistry of the Surface; <sup>2</sup>GFZ German Research Centre for Geosciences, Potsdam, Library and Information Services

In the age of Big Data, an increasing amount of data is being generated and used across disciplines, which is developing increasingly into a prerequisite of modern science. The need for easily accessible databases to reuse this data is growing in importance. The starting point of any analytical (geo- and hydrochemical, inorganic- and organic chemical, mineralogical, ecological, microbiological) database is the complete documentation of sample metadata, such that origin, locations, type, sampling method, storage place and unambiguous sample names can be traced.

We adopted the open source database Medusa that was originally developed for high-temperature and cosmochemical geochemical samples by a research group from Okayama University (Japan) [1]. Medusa is

designed as a web application written in Ruby and can be used with all common web browsers. Data security and access are ensured through the implementation of intelligent group management. The original source code [2] was modified at the GFZ German Research Centre for Geosciences [3] to meet the requirements of samples in a higher variety of scientific fields (i.e. biology, geomorphology, geochemistry, geology, ecology, hydrology and soil science) and to enable data exchange within scientific frameworks, such as the Earth-Shape project (DFG-SPP 1803). The metadata stored in Medusa provides the full provenance of a sample: the path of a sample from sampling in the field, its exact geo-location, sampling campaigns and -methods, depth profiles and time series, storage, laboratory, to subsequent preparations and analyses can be traced. In addition, Medusa allows to link publications, images, files with laboratory protocols, and data tables, simplifying communication and data exchange within collaborative projects. Medusa is fully searchable and uses a hierarchical parent-child scheme for sample splitting- and distribution. Samples and subsamples are uniquely identified with IGSNs, which are persistent identifiers for physical samples [4]. Medusa is now capable to import and export metadata via CSV files, generate and publish IGSNs, QR sample codes, and visualize and filter the sampling sites in an interactive map. In this presentation we will present successes and challenges of almost 3 years of Medusa development and user experience.

[1] Yachi, Y., Kitagawa, H., Kunihiro, T., Nakamura, E., 2014. Software Dedicated for the Curation of Geochemical Data Sets in Analytical Laboratories. *Geostandards and Geoanalytical Research*, 38, 95-102. <https://doi.org/10.1111/j.1751-908X.2013.00205.x>; [2] <http://github.com/misasa/medusa>; [3] <http://github.com/ulbricht/medusa>; [4] <http://www.igsn.org/>

**12:00pm - 12:15pm**

### **EPOS Multi-scale laboratories: a network of European laboratories**

**Kirsten Elger<sup>1</sup>, Jose-Luis Fernandez-Turiel<sup>2</sup>, Richard Wessels<sup>3</sup>, Damian Ulbricht<sup>1</sup>, - EPOS MSL Team<sup>3</sup>**

<sup>1</sup>GFZ German Research Centre for Geosciences, Germany; <sup>2</sup>Institute of Earth Sciences J. Almera - CSIC, Bracelona, Spain; <sup>3</sup>Utrecht University, Department of Earth Sciences, The Netherlands

The Multi-scale laboratories (MSL) represent a community of European solid Earth sciences laboratories including high temperature and pressure experimental facilities, rock physics, analogue tectonic and geodynamic modelling, paleomagnetism, and geochemical and other analytical and microscopy laboratories that have been formed within EPOS, the European Plate Observing System within the European Strategy Forum on Research Infrastructures (ESFRI).

Laboratory facilities are an integral part of Earth science research. The diversity of methods employed in such infrastructures reflects the multi-scale nature of the Earth system and is essential for the understanding of its evolution, for the assessment of geo-hazards and for the sustainable exploitation of geo-resources. Experimental and analytical data from these laboratories often provide the backbone for scientific publications, but are often available only as supplementary information to research articles. Moreover, much of the collected data remain unpublished, inaccessible, and often not preserved for the long term.

MSL are committed to make data Findable, Accessible, Interoperable, and Reusable (FAIR). This includes the development or adoption of data and metadata standards for the different subdomains and the DOI-referenced data publication as best practice for data sharing that are accessible via the EPOS - Multi-scale laboratories data catalogue (<https://epos-msl.uu.nl/>).

The MSL strategy promotes the collaboration with existing international databases (e.g., MagIC for paleomagnetic data and EarthChem for geochemical data) and scientific institutional or domain repositories, for example, GFZ Data Services [1], Digital.CSIC [2] and NERC-BGS [3]. These workflows involve the use of controlled vocabularies (geoSciML, NASA GCMD) for better representing MSL datasets and the development and use of data templates with the aim to enable seamless data ingest to international databases after the data are published with a DOI in the repositories.

The Project EPOS Implementation Phase (EPOS IP) was funded by the European Commission (Grant Agreement no: 676564-EPOS IP, Call H2020-INFRADEV-2014-2015/H2020-INFRADEV-1-2015-1).

**12:15pm - 12:30pm****GEOROC - a Global Geochemical Database****Baerbel Sarbas<sup>1</sup>, Albrecht Hofmann<sup>1,2</sup>**<sup>1</sup>Max Planck Institute for Chemistry, Germany; <sup>2</sup>Lamont-Doherty Earth Observatory, Columbia University, New York

GEOROC (Geochemistry of Rocks of the Oceans and Continents; <http://georoc.mpch-mainz.gwdg.de/>) is a database of published analyses of volcanic rocks and mantle xenoliths. Since recently, data for plutonic rocks are added. The analyses include major and trace element concentrations, radiogenic and non-radiogenic isotope ratios as well as analytical ages for whole rocks, glasses, minerals and inclusions. Samples come from ten tectonic settings and span the whole geological age scale from Archean to Recent. Metadata include, among others, geographic location with latitude and longitude, rock class and rock type, geological age, degree of alteration, analytical method, laboratory, and reference. The GEOROC web page allows selection of samples by geological setting, geography, chemical criteria, rock or sample name, and bibliographic criteria. In addition, it provides a large number of precompiled files for individual locations, minerals and rock classes. The actual version of GEOROC contains almost 1,500,000 analyses with about 21,500,000 single data values for 531,000 samples from 17,640 references.

Since its introduction about 20 years ago, together with the database PetDB, GEOROC became a crucial tool for geochemists. It is used worldwide, mainly by hard-rock geochemists but also in biogeochemistry, climate geochemistry and other earth sciences. In addition to routine applications citing GEOROC (currently about 100 papers per year), the database is increasingly being used as a primary source for an entirely new scientific approach, namely to address questions concerning the global chemical evolution of Earth's crust. This research involves statistical analysis of thousands of geological samples. This research also addresses questions whether the tectonic processes responsible for creating and destroying continental crust have fundamentally changed over Earth history and impacts our understanding of the evolution of Earth's atmosphere.

The database is maintained by the Max Planck Institute for Chemistry in Mainz. It was established in the former geochemistry department of Albrecht Hofmann. Currently it is hosted by the climate geochemistry department. However, funding by the Max Planck Community will end in the near future and a new location is needed.

**12:30pm - 1:00pm Session Keynote****Building on the Success of Geochemical Databases: Toward a Global Research Infrastructure of Geochemical Data****Kerstin Annette Lehnert, Annika Johansson***Lamont-Doherty Earth Observatory, Columbia University, United States of America*

Geochemical data impact virtually all Earth and space science (ESS) disciplines and discovery in many fields, from the study of global climate change, to present and past biogeochemical cycles, to magmatic processes and mantle dynamics, to responsible exploitation of natural resources, to the origin of life on Earth, to the origin of the universe, benefits from geochemical data that are accessible and reusable in a convenient and meaningful way. More than 2 decades ago, the emergence of web-enabled databases gave rise to large-scale geochemical data syntheses such as GEOROC and PetDB. These databases have revolutionized access to geochemical data, inspiring and making possible a vast range of studies and new discoveries, not only within the defined domains they cover but also in new and unexpected scientific and educational applications. The EarthChem facility further supported the analysis and mining of these databases by developing a web portal, which provides a single point of access to the combined content of these databases that now exceeds 30 million analytical data points and increasingly enables 'Big Data science'.

While the success of the afore mentioned geochemical databases is convincingly demonstrated by the number, diversity, and relevance of studies that use them and publications that cite them, they have not attained the status of a sustained and global research infrastructure. Coverage of geochemical databases is still limited

to mostly igneous rocks from specific tectonic settings. Funding for the maintenance of the data systems is mostly project-based and short term, without the sustainability necessary for trustworthy services. And incorporation of new data remains a mostly manual process executed by data curators, who extract data from publications, reformat them for ingestion into the databases, and try to add metadata as far as available. In order to build a comprehensive and sustainable data infrastructure for geochemical data, globally endorsed conventions for documenting geochemical data and standard protocols for exchanging these data among systems will need to be developed, implemented, and governed. Such data standards will enable more automated aggregation of data into databases, and will facilitate networking and interoperability among existing databases and new data systems that are emerging at national, programmatic, and subdomain levels (e.g. EPOS, AuScope, Critical Zone Network) in response to Open Access policies and science needs, to accelerate and broaden the availability of FAIR (Findable, Accessible, Interoperable, Reusable) geochemical data across all areas of geochemistry and internationally.

## 13f) Research data and software management in times of FAIR and Open Data

Wednesday, 25/Sep/2019: 8:30am - 10:30am

**Session Chair: Andreas Hübner** (GFZ German Research Centre for Geosciences)

**Session Chair: Dirk Fleischer** (Christian-Albrechts-Universität)

**Location: Vom Stein Haus: Aula / VSH 219**

### Session Abstract

Demands for integrity, transparency and reproducibility of today's research are increasing, posing new challenges for research data and software management in all science communities. The demands do arise from various directions within the scientific community, as it is growing together in scientific networks. Bottom-up driven initiatives like the Research Data Alliance (RDA) and national and international funding organizations bringing forward the German Alliance for Marine Science (DAM), the German National Research Data Infrastructure (NFDI) or the European Open Science Cloud (EOSC), all call for frictionless interoperability from the top-level side. All of this is supported by the intermediate activities like the Coalition for Publishing Data in the Earth and Space Sciences (COPDESS) and FAIR initiatives, promoting the cultural change in publishing and citation of data, samples and software in journal articles towards more transparent research. This session invites contributions that present novel approaches, best practices and community efforts in geoscience research data and research software management to enable open access and reuse of data and related code.

### Lecture Presentations

**8:30am - 9:00am** *Session Keynote*

#### Wasn't "open" FAIR enough? The future of data and software publication

**Jens Klump**

*Commonwealth Scientific and Industrial Research Organisation, Australia*

The value of making research data available is broadly accepted. Policies concerning the open access to research data and software tried to implement new norms calling for researchers to make their data more openly available. These policies either appealed to the common good or focused on publication and citation as an incentive to bring about a cultural change in how researchers share their data with their peers. The Berlin Declaration on Open Access to Knowledge in the Sciences and Humanities already recognised data and software as integral parts of the record of science that should be made accessible alongside the publication.

But when we compare the total number of publications in the fields of science, technology and medicine with the number of data publications from the same time period, the number of openly available datasets is rather small. This indicates that policies on data sharing were not effective in changing behaviours and bringing about the wanted cultural change.

The FAIR principles take a different approach by recognising the potential value of data and the barriers making it hard to realise this potential value. Making data findable, accessible, interoperable, and reusable (FAIR) adds value to data beyond mere open access. Agreements such as the “Commitment to Enabling FAIR Data in the Earth, Space, and Environmental Sciences” by the Coalition on Publishing Data in the Earth and Space Sciences (COPDESS) developed guidelines for researchers, data repositories, and publishers regarding best practices around open data.

Inspired by the activities of the FORCE11 working group focused on data citation, the FORCE11 Software Citation Working Group developed a set of citation principles to encourage broad adoption of a consistent policy for software citation across disciplines. The aim was to make software a citable entity in the scholarly ecosystem.

This presentation will discuss how the FAIR principles and the FORCE11 Software Citation Principles, although not yet perfectly aligned, go beyond the Berlin Declaration. By setting out to researchers, data repositories, and publishers how to integrate data and software into the record of science as first-class citizens this will define new standards for the quality and intellectual merit of scientific publications.

**9:00am - 9:15am**

### **Increasing the visibility of data and samples: publishing services of GFZ Data Services**

**Kirsten Elger, Damian Ulbricht, Boris Radosavljevic, Andreas Hübner, Roland Bertelmann**

*GFZ German Research Centre for Geosciences, Germany*

There is an increasing international demand for free and open access to publicly funded scientific research products ranging from “classical” textual manuscripts to data, samples and software underlying scholarly publications. Data and software publications with assigned digital object identifier (DOI), comprehensive metadata and documentation readable for humans and machines are best practice for FAIR data. Initiatives like the Coalition on Publishing Data in the Earth and Space Sciences ([www.copdess.org](http://www.copdess.org)) and the AGU-lead Enabling FAIR Data Project (<http://www.copdess.org/enabling-fair-data-project/>) have reached milestones for FAIR data publishing and explicitly recommend domain repositories for research data publications.

GFZ Data Services is a research data repository for the Geosciences domain, hosted at the GFZ German Research Centre for Geosciences in Potsdam. Datasets published via GFZ Data Services range from large dynamic datasets from data intensive global monitoring networks and observatories with real-time acquisition, to satellite data, to the full suite of highly heterogeneous datasets collected by individual researchers or small teams (“long-tail data”). Data and software are published with DOI and complemented by descriptive documents or Data Reports.

GFZ Data Services is partner repository of FID GEO the Specialised Information Service for Solid Earth Geosciences (Fachinformationsdienst der Geowissenschaften der Festen Erde, <http://www.fidgeo.de/>). FID GEO offers information and advice on the publication of research data for the geoscience community and data publishing services via GFZ Data Services.

Furthermore, GFZ is allocating agent for the International Geo Sample Number (IGSN), the globally unique persistent identifier for physical samples with discovery functionality of digital sample descriptions via the internet.

A major focus for the data curation is to provide a comprehensive data description via standardised and machine-readable metadata, including the use of controlled vocabularies and to carefully cross-reference the different research products and people/ institutions involved via their metadata using Persistent Identifier (DOI, IGSN, ORCID, Fundref). The embedding of Schema.org in DOI Landing Pages allows discovery through search engines like the Google Dataset Search and Scholix allows to link data publications and scholarly literature, even when the data were published years after the article.

**9:15am - 9:30am**

### **Visual Project Summary, Bull-Eye Chart, Task Bingo and Work Package Chess - graphical tools for a data management workshop within the Horizon 2020 MEET project**

**Bianca Wagner<sup>1</sup>, Birgit Schmidt<sup>2</sup>, Timo Gnad<sup>2</sup>, MEET Team<sup>3</sup>**

<sup>1</sup>University of Göttingen, Germany; <sup>2</sup>Göttingen State and University Library; <sup>3</sup>ES Géothermie Strasbourg (Project Coordinator)

Four types of geometrical and gaming-like visualizations which were recently developed for a data management workshop within the Horizon 2020 MEET project as well as a summary of the workshop outcomes will be presented.

The “Graphical Project Summary” shows in a simple and clear way the key information of the project structure, such as work package leaders, duration, person months, countries or involved partners. The audience of the workshop was informed about this structure and the main responsibilities in a very short amount of time by these thematic figures

The “Bull-Eye Chart” visualizes the involvement of all partners according to their background in certain work packages and allows the identification of key partners for the communication of data-related topics.

The “Task Bingo” was designed as a tool for group work, which was performed in small teams of each involved project partner institution or company. With the help of this game-like figure all participating persons could be motivated to specify within 15 minutes their general types of data-related tasks that will be performed by them within the lifetime of the project.

The “Work package Chess”, another game-like figure, was created for the second part of the group work. This time, the data flow between one and all other work packages had to be marked for each task-related type of data within 15 minutes.

The main goals of the deployment of these tools were the creation of awareness for data management, the advent of more challenging data management tasks, the identification of data-related subgroups of partners and their needs as well as the specification of data types and data flows within each work package and the facilitation of data-related communication between project partners.

The EU-funded MEET project (**M**ultidisciplinary and multi-context demonstration of **E**GS exploration and **E**xploitation **T**echniques and potentials) started on 1<sup>st</sup> of May 2018 and brings together 16 partners from 5 countries with different scientific and technical backgrounds (Industry, SME - small and medium enterprises, Universities, Geological Surveys and research institutions). The main objective of the project is to address the increase of the usage of the deep geothermal potential all over Europe. The project is subdivided into eight work packages, which are dedicated to such topics as management and ethics, analysis, construction and demonstration or upscaling, dissemination & communication.

**9:30am - 9:45am**

### **Publication of the Content of BGR's Information Systems to the Semantic Web**

**Andreas-Alexander Maul, Andreas Pasewaldt, Tanja Wodtke**

*Bundesanstalt für Geowissenschaften und Rohstoffe, Germany*

Just before the rise of the Web 2.0 Tim Berners-Lee, James Hendler, and Ora Larissa published an article on “The Semantic Web”, which is also known as “Web 3.0” or the “Web of Data”. It contains a general description of how to express the meaning of data and to present knowledge in the World Wide Web in order to make it more interoperable and machine-friendly. Several W3C standards on an appropriate data model (RDF), the declaration of vocabularies (RDFS and OWL), and a versatile query language (SPARQL) were up to follow. Since then it is possible to work with standardized formats and vocabularies, such that computer programs do not need to learn too much in order to understand the meaning of the data and to follow the linkages between them. Therefore, machines, software agents or computer programs should be able to search data on the WWW for a given purpose and present more concise and more complete results.

At the Federal Institute for Geosciences and Natural Resources (BGR) a number of information systems have been reworked during the past three years. In this context, RDF/SPARQL interfaces will be added to these systems in order to increase their interoperability. This will be achieved by using a software applying W3C's R2RML, the RDB to RDF Mapping Language. Problems we are facing are poorly normalized relational schemas, for which this kind of mapping is not well-defined (e. g. the database of the "Lithostratigraphic Dictionary"). Other problems not yet solved are the stable online publication of large amounts of data as in case of the "Geoscientific Collections" database with millions of entries. Some of these problems can be addressed by database normalization. Others will be solved by changing from transient (in-memory) to persistent Linked Data Views.

The setup of RDF/SPARQL interfaces for BGR Information Systems is still in progress but seems to be a good preparation for data discovery by using standardised exchange formats and vocabularies and by resolving the linkages between the resources.

**9:45am - 10:00am**

### **A Roadmap for Research Data Management in the Geosciences: Responding to Community Needs**

**Boris Radosavljevic, Kirsten Elger, Damian Ulbricht, Christian Haberland, Javier Quinteros, Roland Bertelmann**  
*GFZ German Research Centre for Geosciences, Potsdam, Germany*

Many researchers are overwhelmed by challenges of FAIR data requirements by journal publishers, institutional guidelines or legacy data. The GeoDataNode project, funded by the Federal Ministry for Research and Education (BMBF), conducted a survey of data management practices at the Helmholtz Centre Potsdam GFZ German Research Centre for Geosciences (GFZ). The aim was to assess the state of current practices and needs, and their alignment to institutional and national guidelines for data management. The target audience included scientific and technical employees at all levels. A response rate of 24% of the demographic target was achieved.

The survey revealed a general need for improvement and structuring of research data handling. This includes the provision of adequate storage space, back-up schedules, and the familiarization of young researchers with good scientific practice.

Using the knowledge gathered by the survey, we present the next steps for the project and the GFZ. This includes more intuitive ways for researchers to orient themselves at any stage of the data life cycle. Key element in addressing this challenge is the development of a "FAIR Data Roadmap" including an online data readiness "decision tree" as a central guidance for researchers at every stage of data management activities. Additional activities are the promotion of data publications, IGSN and other PIDs as best practice for data sharing. For example, databases listing information regarding scientific instruments used in a study (including persistent identifiers; PID's) ensure globally unique identification of instruments and provide important metadata (e.g., calibration information).

**10:00am - 10:15am**

### **Enhancing FAIRness of global air quality data: The Tropospheric Ozone Assessment Report database**

**Sabine Schröder, Sander Apweiler, Rajveer Saini, Björn Hagemeyer, Martin G. Schultz**  
*Forschungszentrum Jülich, Germany*

In a community effort involving more than 200 scientists from over 60 countries, the Tropospheric Ozone Assessment Report (TOAR) [1, 2] has recently produced the first comprehensive analysis of global tropospheric ozone changes. A major factor of its success and widespread reception is the extensive database of global surface observations, which has been built with multi-faceted metadata and user-friendly web services in the spirit of Open Data and the FAIR principles. TOAR data are made available via a graphical web interface [3], a

REST service [4] and as aggregated products on PANGAEA [5] together with software tools for data analysis. In preparation of the 2<sup>nd</sup> phase of TOAR we are now revising the database schema to further enhance FAIRness of this global air quality data holding and to align the TOAR data services with principles defined by the RDA [6] and EOSC-hub [7]. The new structure of the database seeks to enhance data documentation especially with respect to traceability and provenance. By blending controlled vocabulary and ontologies with less constrained fulltext fields we will be able to preserve any metadata supplied to us without the need to reach a broad community consensus about metadata standardisation (which would be impossible to accomplish). The redesign of the TOAR data infrastructure also includes further standardisation of the web service infrastructures and automated data quality control tools. In this context, AAI (Authentication and Authorization Infrastructure) and data licensing are important aspects of consideration. Last not least, providing TOAR data users with a flexible and powerful infrastructure for data access and online analysis raises some performance issues, which require the exploration of modern concepts and tools for distributed workflows.

[1] <http://www.igacproject.org/activities/TOAR>; [2] <https://collections.elementscience.org/toar>; [3] <https://join.fz-juelich.de/>; [4] <https://join.fz-juelich.de/services/rest/surfacedata/>; [5] <https://doi.pangaea.de/10.1594/PANGAEA.876108>; [6] <https://rd-alliance.org/>; [7] <https://www.eosc-hub.eu/news/guidelines-scientific-content-providers-eosc-hub>

**10:15am - 10:30am**

### **NFDI4Earth: current state and goals for the future**

**Roland Bertelmann<sup>1</sup>, Hildegard Gödde<sup>1</sup>, Gunnar Lischeid<sup>2</sup>, Sören Lorenz<sup>3</sup>, Adrian Krolczyk<sup>2</sup>, Karsten Peters<sup>4</sup>, Martin Schultz<sup>5</sup>, Hannes Thiemann<sup>4</sup>, Gauvin Wiemer<sup>6</sup>**

<sup>1</sup>GFZ German Research Centre for Geosciences, Germany; <sup>2</sup>Leibniz Centre for Agricultural Landscape Research (ZALF), Germany; <sup>3</sup>GEOMAR Helmholtz Centre for Ocean Research Kiel, Germany; <sup>4</sup>German Climate Computing Center, Germany; <sup>5</sup>Forschungszentrum Jülich, Germany; <sup>6</sup>MARUM – Center for Marine Environmental Sciences, Germany

The national research data infrastructure (NFDI) in Germany [1] aims to systematically manage scientific and research data, provide long-term data storage, backup and accessibility, and network the data both nationally and internationally. Within this framework, NFDI4Earth [2], an emerging consortium with many participating institutions, strives to serve researchers within Earth System Research.

The strategy of the NFDI4Earth is to further identify the demands for digital changes in German Earth System Science community in a structured community consultation process, to establish a set of common principles, rules and standards, to establish experimental prototype platforms, operating on distributed resources, and to provide tools and mechanisms for data integration and analysis.

NFDI4Earth is aware that the objectives of NFDI and in particular NFDI4Earth can only be achieved on a consortia basis anchored in the broader scientific community. For this reason, NFDI4Earth aims to create awareness right from the beginning and initiate collaborations also beyond Germany's borders. This presentation introduces the current state of consolidation of the NFDI4Earth and its goals to the scientific community.

[1] [https://www.dfg.de/en/research\\_funding/programmes/nfdi/index.html](https://www.dfg.de/en/research_funding/programmes/nfdi/index.html)

[2] <https://www.nfdi4earth.de/>

**Wednesday, 25/Sep/2019: 1:00pm - 3:00pm**

**1:00pm - 1:15pm**

### **Next Generation of Interoperable Information Systems for Spatial Data**

**Thorsten Agemar**

*LIAG, Germany*

Public geo-information systems are playing an increasingly important role in geoscientific research and sub-surface spatial planning. Geologic data can be provided and visualised via the Internet using various web

technologies. Modern map servers can handle user requests and coordinate systems. OGC-services like Web Feature Service or Web Map Service enable users to insert remote map data into their own GIS products. Other OGC-services such as 3D-Portrayal-Service or Web Coverage Service could be used for 3D data. However, for geologic 3D objects interoperability issues like common data formats are not yet resolved. Transferring 3D models via web-based information systems in a convenient and interoperable way requires new concepts. Currently available 3D viewers in the Internet offer nice visualisation but they lack important features for scientific work like for instance cropping interactively volume parts, adding parameters, doing calculations or obtaining data downloads.

The Leibniz Institute for Applied Geophysics looks back on a long history of developing and operating information systems for georeferenced data that are used by geologists, geophysicists and engineers. This presentation will give an overview of new achievements, current developments and visions for the future in the field of scientific geo-information systems.

**1:15pm - 1:30pm**

### **Research software - landscape and actors**

**Bernadette Fritsch**

*Alfred Wegener Institut, Helmholtzzentrum für Polar- und Meeresforschung, Germany*

Software plays a crucial role in the whole lifecycle of most of scientific data and must be considered in all discussions about openness of data and reproducibility of science. Consequently, some interest and working groups in RDA are dealing with software code.

The spectrum of research software ranges from packages driven by large teams of developers and used by a broad community, to small scripts that scientists almost casually write for their own work. The knowledge of modern software development practice is very different, as well as individual skills in programming and documentation. The quality levels are often correspondingly different. In order to reduce such differences in the medium term, general policies can be helpful.

Policies can provide a framework for a defined way of dealing with software. In Germany, some coordinated activities are delving into this topic. For example in the Helmholtz Association, the working group Open Science expanded its perspective from initially only data, and has now set up a Taskgroup. Research software was also anchored as an issue in the Priority Initiative Digital Information of the Alliance of Science Organisations in Germany. The panels have already published some recommendations on the development, use, and provision of research software. At present, they are working on guidelines that can serve as a basis for daily work at the institutions. The documents cover different facets, ranging from development practice and quality assurance to publication of software and licensing. The talk will give an overview about the status of these activities. It will also shed light on the players in the software development. Starting from the UK, people are increasingly organizing themselves, working at the interface between science and computer science. In Germany too, there has been an association de-RSE since 2018, which campaigns for the interests of research software engineers.

**1:30pm - 1:45pm**

### **Promoting cultural change in data publishing**

**Andreas Hübner, Kirsten Elger, Roland Bertelmann**

*GFZ German Research Centre for Geosciences, Germany*

The citable publication of research data with a Digital Object Identifier (DOI) is a key element in the current cultural change of scientific publishing: a research publication today is much more than a printed or electronically available manuscript. Data, software, experimental protocols, and physical samples associated with a scientific article meet the increasing demands for more integrity, transparency, and reproducibility of research. In addition, the reusability of data by others opens up extensive research options.

FID GEO [1], the Specialised Information Service for Solid Earth Geosciences (Fachinformationsdienst Geowissenschaften der Festen Erde) is a German key player for the promotion of data publications in the geosciences and offers data publication services with their partner repository GFZ Data Services, the domain repository for geosciences data, hosted at GFZ German Research Centre for Geosciences. With regular workshops and conference presentations, FID GEO informs researchers and infrastructure units alike about both technical aspects on data publications and international developments in the data curation landscape.

This presentation focuses on recent recommendations for publishers, repositories and funders, developed within the “Enabling FAIR Data in the Earth and Space Sciences” Project (funded by the Laura and John Arnold Foundation and led by AGU, [2]). Building on the work of The Coalition on Publishing Data in the Earth and Space Sciences (COPDESS, [3]), Earth Science Information Partners (ESIP), and the Research Data Alliance (RDA), the Enabling FAIR Data in the Earth, Space, and Environmental Sciences project has issued recommendations, standards, and tools to meet the challenges associated with state-of-the-art data publication and sample identification. Researchers play a vital role in changing the data publication culture towards a future in that data is no longer published as supplements to journals, but in data repositories, data citations are executed with DOIs (Digital Object Identifiers), and data citations in reference lists of the articles will be the standard. Publishers will honour increasingly the citation of DOI-referenced data publications, actively promote the use of domain repositories and request a data availability statement. Funders will promote open and FAIR data principles and practices in their core Earth, space, and environmental science activities and policies and align data management plans accordingly.

[1] [www.fidgeo.de](http://www.fidgeo.de); [2] <https://copdess.org/enabling-fair-data-project/>; [3] <https://copdess.org>

**1:45pm - 2:00pm**

### **Computational reproducibility in the geoscientific publication cycle**

**Edzer Pebesma, Daniel Nüst, Markus Konkol, Christian Kray**

*University of Muenster, Germany*

Computational reproducibility is possible when the data, procedures and software involved in a study is shared along with a scientific publication. When this can be done, it is still an open problem how this should be done: journals often mention the option, but give no hints to authors what they should provide and how they should wrap data, scripts and software. Mutual expectations from reviewers and readers on one side, and author on the other side, are largely missing. The project “Opening Reproducible Research” (<http://o2r.info/>), of which the second phase is now funded by the DFG, has the ambition to formalise these expectation, and develops a workflow for journals such that it becomes easy for authors and reviewers to verify completeness (“one-click reproduce”), and easy for readers to re-execute the computational aspects of a publication. In addition, potential extensions are explored that include searching reproducible publications for data and procedures, and interaction with the settings of particular parameters resulting in updated figures, so that readers can experience a richer view than the classical fixed non-interactive pdf publication. In the second phase of this project, this infrastructure will be put into action by running special issues with journals at existing publishers (Copernicus, Elsevier).

## **Poster Presentations**

**Tue: 94**

### **Building a Portal for Interdisciplinary Planetary Data**

**Elfrun Lehmann, Harry Becker**

*Institute of Geological Sciences, FU Berlin, Germany*

In 2010, the Alliance of Science Organisations (Allianz der Wissenschaftsorganisationen) in Germany responded to the increasing amount of research data by adopting ‘*Principles for the Handling of Research Data*’ (Alliance of Science Organisations, 2010). In 2015, the German Research Foundation followed suit and

aligned its '*Guidelines on the Handling of Research Data*' (DFG, 2015) with these '*Principles*'. In accordance with DFG's '*Guidelines*', the collaborative research center TRR 170 (*Late Accretion to Terrestrial Planets*) has adopted a policy how to manage long-term archiving and accessibility of its research data.

Research data generated in TRR 170 subprojects are diverse reflecting the range of methods used, including laboratory and other instrumental data on planetary samples, remote sensing data, geological maps and model simulations. Accordingly, the strong interdisciplinary alignment of the TRR 170 research network comprises heterogeneous data and different data formats.

During the first funding period, we built a file management and database system, *TRR 170-DB*, to manage data of TRR 170. *TRR 170-DB* is operated on the open source data management software *Dataverse* and can be accessed via a web portal, the *Planetary Data Portal*. *TRR170-DB* and *Dataverse's* functionalities ensure that each step in the data lifecycle of research data is met. The *Planetary Data Portal* is hosted on a VM server and provides storage for published and unpublished TRR 170 data for access within the TRR 170 network. We use up-to-date programming standards and languages (JavaScript, PHP, HTML, CSS, SQL) to customize interactions between users and *TRR 170-DB*. The file management and database software *Dataverse* provides standard-compliant metadata to ensure that metadata can be mapped easily to several standard metadata schemas (Dublin Core, Worldmap, DDI, VO, etc.).

Research data stored in *TRR170-DB* can take advantage of a *Dataverse* functionality that provides digital object identifiers (DOI) through *DataCite* services. DOI assigned research data are traceable and thus facilitates reproducible research.

The landscape of repositories in the planetary sciences is highly fragmented and dispersed between different scientific disciplines. A key aspect of the future development of the *Planetary Data Portal* is to bring together data and relevant information from different planetary communities. The *Planetary Data Portal* will serve as a single access point to various communities, including planetary sample data and experimental studies, planetary missions, geophysical modeling and astrophysics/astronomy.

**Tue: 95**

### **V-FOR-WaTer – a virtual research environment to access and process environmental data**

**Marcus Strobl<sup>1</sup>, Elnaz Azmi<sup>1</sup>, Sibylle K. Hassler<sup>2</sup>, Mirko Mälicke<sup>2</sup>, Jörg Meyer<sup>1</sup>, Erwin Zehe<sup>2</sup>**

<sup>1</sup>Steinbuch Centre for Computing, Karlsruhe Institute of Technology (KIT), Germany; <sup>2</sup>Institute for Water and River Basin Management, Karlsruhe Institute of Technology (KIT), Germany

Thanks to the growth and automation of observational networks and sensors that are more sophisticated, the amount and diversity of data in hydrology is increasing rapidly. These data form the basis for a better understanding of ecological systems and for the development and application of models to describe and forecast changes within these systems. The need of sharing data is widely acknowledged today, though many datasets are still stored on local computers with the corresponding meta information spread over field and lab books. Such data is hardly reusable for other researchers. This makes the collection of data from different sources very time consuming and the necessary additional pre-processing of data enormously slows down the scientific work.

In V-FOR-WaTer we develop a web portal to access, scale, and process data, to simplify the gathering of data, speed up the scientific workflow and improve reproducibility of analyses. Our workflow manager facilitates in combination with a detailed documentation the reproducibility of processes and analyses. In addition, we will offer the transfer of data to an established repository, thus encourage publications of data. Today we have a working prototype of the V-FOR-WaTer portal consisting of a customisable metadata model that corresponds to international standards with a focus on hydrological data, a sophisticated data filter, and a toolbox containing basic processes and specialised tools. The portal is being developed in close collaboration between the hydrology group and the computing centre of the Karlsruhe Institute of Technology. This way we maximise performance and usability of the portal, which will create a significant benefit for the environmental science communities.

**Tue: 96****The Metadata Editor of GFZ Data Services****Damian Ulbricht, Kirsten Elger***GFZ German Research Centre for Geosciences, Potsdam, Germany*

Following the FAIR principles, research data should be Findable, Accessible, Interoperable and Reuseable. Publishing research output under these principles requires to generate machine-readable metadata and to use persistent identifiers for cross-linking with research articles, related software for processing or physical samples that were used to derive the data. In addition, research data should be indexed with domain keywords to facilitate discovery. Software solutions are required that help scientists in generating metadata, since metadata models tend to be complex and the serialisation into a format for metadata dissemination is a challenging task.

For the publication activities of 'GFZ Data Services' we developed a metadata editor that assists scientists to create metadata in different metadata schemas (ISO19115, NASA GCMD DIF, DataCite) that are popular in the earth sciences, while being at the same time usable by and understandable for scientists. Emphasis is placed on removing barriers in particular, the editor is publicly available on the internet [1] without registration, a copy of the metadata can be saved to and loaded from the local hard disk and scientists are not requested to provide information that may be generated automatically. To improve usability, form fields are translated into the scientific language and we offer a facility to search structured vocabulary lists. Vocabulary terms originate from GCMD Science Keywords, Instruments, and Platforms, the International Chronostratigraphic Chart, the CGI Simple Lithology and the INSPIRE GEMET Thesaurus. Related research products that improve understanding and reuse can be linked through persistent identifiers. In addition, multiple geospatial references can be entered via an interactive mapping tool, which helps to minimize problems with different conventions to provide latitudes and longitudes.

The metadata editor exists in different instances that are tailored to the needs of particular research projects or research infrastructures, e.g. the 'Multi-scale Laboratories' Thematic Core Service of the European Plate Observing System (EPOS-IP) or the Geophysical Instrument Pool Potsdam (GIPP).

[1] <http://dataservices.gfz-potsdam.de/panmetaworks/metaedit>



We cordially would like to thank our exhibitors and sponsors:

**ThermoFisher**  
SCIENTIFIC

 **Springer Spektrum**

  
**Schweizerbart**  
Science publishers

Freie Universität  Berlin

**EAGE**  
EUROPEAN  
ASSOCIATION OF  
GEOLOGISTS &  
ENGINEERS

**VU**  **VRIJE  
UNIVERSITEIT  
AMSTERDAM**

  
**BRUKER**

 **NATIONALER  
GEO PARK**

<http://www.geomuenster2019.de>

